ISBN 978-2-87355-030-1

Proceedings of the International Meteor Conference

Egmond, the Netherlands

2–5 June, 2016

INTERNATIONAL METEOR CONFERENCE 2016

Published by the International Meteor Organization

Edited by Adriana Roggemans and Paul Roggemans

Proceedings of the International Meteor Conference

Egmond, the Netherlands

2–5 June, 2016

Published by the International Meteor Organization

Edited by Adriana Roggemans and Paul Roggemans

Proceedings of the International Meteor Conference

Egmond, the Netherlands, 2–5 June 2016

International Meteor Organization

ISBN 978-2-87355-030-1
EAN 9782873550301

Copyright notices
© 2016 The International Meteor Organization.
The copyright of papers submitted to the IMC Proceedings remains with the authors.

It is the aim of the IMO to increase the spread of scientific information, not to restrict it. When material is submitted to the IMO for publication, this is taken as indicating that the author(s) grant(s) permission for the IMO to publish this material any number of times, in any format(s), without payment. This permission is taken as covering rights to reproduce both the content of the material and its form and appearance, including images and typesetting. Formats may include paper and electronically readable storage media. Other than these conditions, all rights remain with the author(s). When material is submitted for publication, this is also taken as indicating that the author(s) claim(s) the right to grant the permissions described above. The reader is granted permission to make unaltered copies of any part of the document for personal use, as well as for non-commercial and unpaid sharing of the information with third parties, provided the source and publisher are mentioned. For any other type of copying or distribution, prior written permission from the publisher is mandatory.

Editing and printing
Front cover picture: Shrimp fishing boat excursion on the Waddenzee (Photo by *Casper ter Kuile*).
Publisher: The International Meteor Organization
Printed: The International Meteor Organization
Design IMC logo: Dušan Bettonvil
Typesetting: MS Word template prepared by Vincent Perlerin
Editors: Adriana Roggemans, Paul Roggemans
Proofreaders : Lucie Heywood, Bob Lunsford, Tony Markham, Michael O'Connell, Vincent Perlerin, and Jean-Louis Rault
Selection of photographs and captions: Felix Bettonvil, from photographs submitted by Eva Bojurova, Malcolm J. Currie, Casper ter Kuile, Marc Neijts, Dragana Okolić, Dušan Pavlović, Adriana Roggemans, Irmgard Schmidt, and Arnold Tukkers
Bibliographic records: all papers are listed with the SAO/NASA Astrophysics Data System (ADS) – http://adsabs.harvard.edu with publication code *2016pimo.conf* .

Distribution
Further paper copies of this publication may be ordered from the International Meteor Organization, through the IMO website (http://www.imo.net).
Legal address: International Meteor Organization, Jozef Mattheessensstraat 60, 2540 Hove, Belgium

Cautionary Note
from the Publisher and
the Chairs of the Local and Scientific Organizing Committees

The International Meteor Conference (IMC) is the annual conference of the International Meteor Organization (IMO). It is open to members and non-members alike, under the same conditions. Besides ensuring that the IMC format is respected, the IMO oversees the registration process, and provides logistic support, while the local organization is entrusted to a dedicated group of meteor workers active in the region where that year's conference is taking place. For the 35th IMC, the IMO Council selected the proposal of the Meteor Section of the Royal Dutch Association for Meteorology and Astronomy (KNVWS, by its Dutch abbreviation) to have this conference in Egmond, the Netherlands, from June 2 to 5, 2016, and this for three reasons: (1) the KNVWS Meteor Section has experience with the successful local organization of previous IMCs; (2) the KNVWS Meteor Section celebrates its 70th anniversary in 2016; and (3) their offer allowed us to have the IMC 2016 in conjunction with the Meteoroids conference, which would allow for strong cross-fertilization between the professional and amateur meteor communities. As is the case usually, the local organization was taken care of by the Local Organizing Committee (LOC), consisting of key members of the KNVWS Meteor Section and the Dutch Meteor Society. New this year was the installation of a Scientific Organizing Committee (SOC), to which the IMO Council appointed Jean-Louis Rault (chair), Felix Bettonvil, and Paul Roggemans. (The SOC extended itself with some experts to ensure that all subject domains were covered). In view of the administrative support from the IMO Treasurer on the one hand and the scientific support from the new SOC on the other hand, the IMO Council deemed the function of IMC Liaison Officer no longer necessary and canceled it.

The success of the 35th IMC, with a record number of participants and presentations, proved that the IMO had made the right choice, much to the credit of all the LOC and SOC members involved. This success would be very volatile, however, if the rich scientific output of the conference would not be documented for future reference. Within the IMO, this awareness has always been strongly present, and therefore the IMO publishes the IMC proceedings in its publication series, identified by a dedicated ISBN number. The editing of these proceedings is a huge undertaking, which in the past was taken care of by either the LOC, or the IMO directly, or a combination of both. In the new structure, the SOC delegated this task to Paul Roggemans, who was found prepared to take this task upon himself, this time with the aid of his wife Adriana as co-editor.

Paul and Adriana Roggemans did a great job and accomplished this formidable task in a record time, but with the finish line in view, strange things started to happen. A draft version sent to Paul's fellow SOC members and some proofreaders only mentioned the appropriate ISBN number, but did not acknowledge the IMO as publisher, being the case for many years. And his editorial contained a strange, contorted story about the relationship between the IMO and the IMCs, apparently—as it soon became clear—to justify his unilateral actions. Indeed, while SOC chair Jean-Louis Rault expressly asked Paul to delay the preparation of the final version a few days to allow the SOC to evaluate what was going on, Paul Roggemans ignored this request, published what is rightfully an IMO publication without consent on his own non-IMO-related blog *MeteorNews* and subsequently sent the link to all participants. Needless to say, this very personal action is an unacceptable infringement of the IMO's rights. While all of us acknowledge the great effort Paul and Adriana Roggemans have put into these proceedings, there is no justification for the abuse of Paul's function to accommodate his personal agenda.

For some time, all of us pondered on the course of action to be taken, but after deliberation, we decided for a conservative approach in the interest of transparency: the cover and front material was modified to conform to the standards of an IMO publication, but the numbered pages were left unaltered with respect to the version Paul Roggemans published in his personal name. At the same time, we added this statement to make clear that the viewpoints expressed by Paul Roggemans in his editorial are his and his only. In particular, his statement that the IMC is not an IMO conference, is blatantly untrue.

Of course, this should not prevent you from enjoying this publication and its rich content, which reflects the success and the high level of the 35th IMC.

We wish you happy reading!

Cis Verbeeck, IMO President
Jürgen Rendtel, IMO Vice-President
Bob Lunsford, IMO Secretary-General
Marc Gyssens, IMO Treasurer
Felix Bettonvil, Chair of the LOC of the 35th IMC
Jean-Louis Rault, Chair of the SOC of the 35th IMC

Contents

Contents 1

Foreword
Felix Bettonvil 6

From the editor – about the IMC Proceedings
Paul Roggemans 8

Program of the 35th International Meteor Conference, Egmond , 2 – 5 June, 2016 13

Artificial meteor test towards: On-demand meteor shower
Shinsuke Abe*, Lena Okajima, Hironori Sahara, Takeo Watanabe, Yuta Nojiri and Tomohiko Nishizono* 17

Asteroidal meteors detected by MU radar head-echo observations
Shinsuke Abe*, Johan Kero, Takuji Nakamura, Yasunori Fujiwara, Daniel Kastinen, Jun-ichi Watanabe and Hiroyuki Hashiguchi* 18

On the age and parent body of the daytime Arietids meteor shower
Abedin Abedin, *Paul Wiegert, Petr Pokorny and Peter Brown* 19

A Monte-Carlo based extension of the Meteor Orbit and Trajectory Software (MOTS) for computations of orbital elements
Thomas Albin*, Detlef Koschny, Rachel Soja, Ralf Srama and Bjoern Poppe* 20

An antenna, a radio and a microprocessor: which kinds of observation are possible in meteor radio astronomy?
Lorenzo Barbieri 26

Accurate Geminid velocities with CHIPOlAtA
Felix Bettonvil 31

Photographic spectra of fireballs
Jiří Borovička 34

The 2016 Quadrantids
Brando Gaetano 39

Recent shower outbursts detected by the Canadian Meteor Orbit Radar (CMOR)
Peter Brown 42

The Radio Meteor Zoo: a citizen science project
Stijn Calders*, Cis Verbeeck, Hervé Lamy and Antonio Martínez Picar* 46

Results from the Canadian Automated Meteor Observatory
Margaret Campbell-Brown 50

Ablation of small Fe meteoroids – first results
David Čapek *and Jiří Borovička* 53

FRIPON network status
François Colas*, Brigitte Zanda, Sylvain Bouley, Jérémie Vaubaillon, Chiara Marmo, Yoan Audureau, Min Kyung Kwon, Jean-Louis Rault, Pierre Vernazza, Jérôme Gattacceca, Stéphane Caminade, Mirel Birlan, Lucie Maquet, Auriane Egal, Monica Rotaru, Laurent Jorda, Cyril Birnbaum, Cyril Blanpain, Adrien Malgoyre, Julien Lecubin, Alberto Cellino, Daniele Gardiol, Mario Di Martino, Christian Nitschelm, Jorje Camargo, M. Valenzuela, Ludovic Ferrière, Marcel Popescu and Damien Loizeau* 55

The dimension added by 3D scanning and 3D printing of meteorites
Sebastiaan J. de Vet 56

Status of the Desert Fireball Network
***Hadrien A. R. Devillepoix**, Philip A. Bland, Martin C. Towner, Martin Cupák, Eleanor K. Sansom, Trent Jansen-Sturgeon, Robert M. Howie, Jonathan Paxman and Benjamin A. D. Hartig* 60

Data processing of records of meteoric echoes
Peter Dolinský 63

Calibration of meteor spectra
***Martin Dubs** and Koji Maeda* 65

Investigation of meteor shower parent bodies using various metrics
***Bogdan Alexandru Dumitru**, Mirel Birlan, Alin Nedelcu and Marcel Popescu* 69

The challenge of meteor daylight observations
***Auriane Egal**, Min-Kyung Kwon, François Colas, Jérémie Vaubaillon and Chiara Marmo* 73

PRISMA, Italian network for meteors and atmospheric studies
***Daniele Gardiol**, Alberto Cellino and Mario Di Martino* 76

The evolution of ROAN 2016 - Radio surveillance of meteors and determination of reflection points through calculation of the radio path, based on times
***Tudor Georgescu,** Ana Georgescu and Cezar Lesanu* 80

Video meteor light curve analysis of Orionids and Geminids and developing a method for obtaining the absolute light curves of shower meteors from the single station data
***Ljubica Grašić**, Nikolina Milanović and Dušan Pavlović* 83

Consequences of meteoroid impacts based on atmospheric trajectory analysis
Maria Gritsevich 87

Synthetic spectra of meteors
***Meryem Guennoun**, Michel-Andres Breton, Nicolas Rambaux, Jérémie Vaubaillon and Zouhair Benkhaldoun* 91

Meteoroid streams and comet disintegration
Ayyub Guliyev 94

A fast meteor detection algorithm
Pete Gural 96

The occurrence of interstellar particles in the vicinity of the Sun An overview – 25 years of research
Maria Hajdukova, jr 105

A tale of two fireballs
***Mike Hankey** and Vincent Perlerin* 111

Results from the CAMS video network
Peter Jenniskens 113

Hemispherical radiating pattern antenna design for radio meteor observation
Jakub Kákona 114

Meteor trajectory estimation from radio meteor observations
Jakub Kákona 117

The multi technique meteor observations in 2014
***Anna Kartashova**, Galina Bolgova, Yurij Rybnov, Olga Popova and Dmitry Glazachev* 120

A statistical approach to the temporal development of orbital associations
***Daniel Kastinen** and Johan Kero* 123

The role of population in tracking meteorite falls in Africa
***Fouad Khiri**, Abderrahmane Ibhi, Thierry Saint-Gerant, Mohand Medjkane and Lahcen Ouknine* 127

Height computation of a fireball
Detlef Koschny 131

Simultaneous analogue and digital observations and comparison of results
Pavel Koten, *Rostislav Štork, Petr Páta, Karel Fliegel and Stanislav Vítek* 133

Meteors and meteorites spectra
Jakub Koukal, *Jiří Srba, Sylvie Gorková, Libor Lenža, Martin Ferus, Svatopluk Civiš, Antonín Knížek, Petr Kubelík, Tereza Kaiserová and Pavel Váňa* 137

Retrieving meteoroids trajectories using BRAMS data: preliminary simulations
Hervé Lamy *and Cédric Tétard* 143

Easy way to estimate meteor brightness on TV frames
Vladislav A. Leonov *and Alexander V. Bagrov* 148

Photometric stellar catalogue for TV meteor astronomy
Vladislav A. Leonov *and Alexander V. Bagrov* 151

ROAN Remote radio meteor detection sensor
Cezar Eduard Lesanu 155

Calibration of occasionally taken images using principles of perspective
Esko Lyytinen *and Maria Gritsevich* 159

The KUT meteor radar: An educational low cost meteor observation system by radio forward scattering
Waleed Madkour *and Masa-yuki Yamamoto* 164

Meteor spectra using high definition video camera
Koji Maeda *and Yasunori Fujiwara* 167

Effects of meteor head plasma distribution on radar cross sections and derived meteoroid masses
Robert A. Marshall, *Sigrid Close, Peter Brown and Yakov Dimant* 171

Numerical simulation of the BRAMS interferometer in Humain
Antonio Martínez Picar, *Christophe Marqué, Cis Verbeeck, Stijn Calders, Sylvain Ranvier, Emmanuel Gamby, Michel Anciaux, Cédric Tetard and Hervé Lamy* 175

Construction of a meteor orbit calculation system for comprehensive meteor observation
Satoshi Mizumoto, *Waleed Madkour and Masa-yuki Yamamoto* 179

Flux density, population index, perception coefficient, and the Moon
Sirko Molau 185

Current progress in the understanding of the physics of large bodies recorded by photographic and digital fireball networks
Manuel Moreno-Ibáñez, *Maria Gritsevich, Josep Ma. Trigo-Rodríguez and Esko Lyytinen* 192

Large meteoroid's impact damage: review of available impact hazard simulators
Manuel Moreno-Ibáñez, *Maria Gritsevich and Josep Ma. Trigo-Rodríguez* 197

Measurements of CCD optical linearity for magnitude determination during meteor observations
Andrey Murtazov *and Alexander Efimov* 202

Astronomy through the microscope: A workshop during the opening night of the 2016 IMC
Gert Jan Netjes *and Sebastiaan de Vet* 205

PaDe - The particle detection program
Theresa Ott, *Esther Drolshagen, Detlef Koschny and Bjoern Poppe* 209

Evaluating video digitizer errors
Chris Peterson 214

Sungrazing comets and meteoroids
Eduard Pittich *and Nina Solovaya* 217

Werkgroep Meteoren – 70 Years and counting
Urijan Poerink *and Sebastiaan J. de Vet* 222

Novel methods for 3D numerical simulation of meteor radar reflections
Jukka Räbinä*, Sanna Mönkölä, Tuomo Rossi, Johannes Markkanen, Maria Gritsevich and Karri Muinonen* 227

Meteor detections at the Metsähovi Fundamental Geodetic Research Station (Finland)
Arttu Raja-Halli*, Maria Gritsevich, Jyri Näränen, Manuel Moreno-Ibáñez, Esko Lyytinen, Jenni Virtanen, Nataliya Zubko, Jouni Peltoniemi and Markku Poutanen* 230

An attempt to explain VLF propagation perturbations associated with single meteors
Jean-Louis Rault *and Jean-Jacques Delcourt Dr. Sc.* 235

65 years of meteor radar research at Adelaide
Iain M. Reid *and Joel Younger* 242

Minor meteor shower activity
Jürgen Rendtel 247

The radio meteor signal path from transmitter to spectrogram: an overview
Tom Roelandts 250

Status of the CAMS-BeNeLux network
Paul Roggemans*, Carl Johannink and Martin Breukers* 254

eMeteorNews: website and PDF journal
Paul Roggemans*, Richard Kacerek, Jakub Koukal, Koen Miskotte and Roman Piffl* 261

An overview of the CILBO spectral observation program
Regina Rudawska*, Joe Zender and Detlef Koschny* 265

ESA/ESTEC Meteor Research Group – behind the scenes
Regina Rudawska 266

Meteor reporting made easy- The Fireballs in the Sky smartphone app
Eleanor Sansom*, Jay Ridgewell, Phil Bland and Jonathan Paxman* 267

Croatian Meteor Network: Ongoing work 2015 – 2016
Damir Šegon*, Denis Vida, Korado Korlević and Željko Andreić* 270

Fireballs from Australian Desert Fireball Network – search for similar orbits
Lukáš Shrbený*, Pavel Spurný and Phil A. Bland* 275

On the accuracy of orbits from video meteor observations
Ivica Skokić*, Damir Šegon and Goran Kurtović* 280

Collisional lifetimes of meteoroids
Rachel Halina Soja*, G. J. Schwarzkopf, Maximilian Sommer, Jérémie Vaubaillon, Thomas Albin, Jens Rodmann, Eberhard Grün and Ralf Srama* 284

EN091214 Zdar – one of the most precisely documented meteorite fall
Pavel Spurny*, Jiri Borovicka, Jakub Haloda, Lukas Shrbeny and Tomas Zikmund* 287

The Swedish Allsky Meteor Network: first results
Eric Stempels *and Johan Kero* 288

No sign of the 2015 Daytime Sextantids through combined radio observations
Giancarlo Tomezzoli *and Lorenzo Barbieri* 291

AMOS - trajectory and orbital data from SVMN and Canary Islands
Juraj Tóth*, Leonard Kornoš, František Ďuriš, Pavol Zigo, Štefan Gajdoš, Dušan Kalmančok, Jozef Világi, Jaroslav Šimon, Marek Buček, Jaroslav Šimon, Miquel Serra-Ricart, Juan Carlos Perez, Javier Licandro, Ovidiu Vaduvescu and Jürgen Rendtel* 294

Expedition Atacama - project AMOS in Chile
Juraj Tóth *and Stanislav Kaniansky* 295

AMOS-Spec - meteor spectra from Modra Observatory
Juraj Tóth*, Pavol Matlovič, Regina Rudawska, Pavol Zigo and Dušan Kalmančok* 297

Rediscovery of Polish meteorites
Zbigniew Tymiński*, Marcin Stolarz, Przemysław Żołądek, Mariusz Wiśniewski and Arkadiusz Olech* 298

A (revised) confidence index for the forecasting of meteor showers
Jeremie Vaubaillon 302

Software for Analysis of Visual Meteor Data: R package MetFns – Workshop report
Kristina Veljković 304

Summary of the Open Session at the IMC 2016
Cis Verbeeck*, Megan Argo, Peter Brown, Sirko Molau, Jürgen Rendtel and Antonio Martínez Picar* 305

Open-source meteor detection software for low-cost single-board computers
Denis Vida*, Dario Zubović, Damir Šegon, Peter Gural and Robert Cupec* 307

Big data era in meteor science
Dejan Vinković*, Maria Gritsevich, Vladimir Srećković, Bojan Pečnik, Gyula Szabó, Victor Debattista, Petr Škoda, Ashish Mahabal, Jouni Peltoniemi, Sanna Mönkölä, Areg Mickaelian, Esa Turunen, Jakub Kákona, Jarkko Koskinen and Victor Grokhovsky* 319

Statistical approach to meteoroid shape estimation
Vladimir Vinnikov*, Maria Gritsevich, Daria Kuznetsova, Olga Krivonosova, Dmitry Zhilenko and Leonid Turchak* 330

Catalogue of representative meteor spectra
Vlastimil Vojáček*, Jiří Borovička, Pavel Koten, Pavel Spurný and Rostislav Štork* 333

2014 Southern δ-Aquariid observing campaign – carried out from Crete
Thomas Weiland 338

Current status of Polish Fireball Network
Mariusz Wiśniewski*, Przemysław Żołądek, Arkadiusz Olech, Zbigniew Tyminski, Maciej Maciejewski, Karol Fietkiewicz, Mariusz Gozdalski, Marcin Przemysław Gawroński, Tomasz Suchodolski, Maciej Myszkiewicz, Marcin Stolarz and Krzysztof Polakowski* 341

Space fireworks for upper atmospheric wind measurements by sounding rocket experiments
Masa-yuki Yamamoto 344

Exploring the relationship between meteor parameters based on photographic data
Yulia Yancheva*, Simona Hristova and Eva Bojurova* 348

Radar observations of the Volantids meteor shower
Joel Younger*, Iain Reid, Damian Murphy* 352

Taurids 2015
Przemysław Żołądek*, Arkadiusz Olech, Mariusz Wiśniewski, Regina Rudawska, Marcin Bęben, Tomasz Krzyżanowski, Maciej Myszkiewicz, Marcin Stolarz, Marcin Gawroński, Mariusz Gozdalski, Tomasz Suchodolski, Walburga Węgrzyk and Zbigniew Tymiński* 358

International Meteor Conference 2017, Petnica, Serbia, September 21–24, 2017
Dušan Pavlović*, Snežana Todorović and Miroslav Živanović* 361

Participants list 364

Author index 372

Foreword

It is always an honor to write the introduction of this meteor-specific booklet: the proceedings of the International Meteor Conference. This year, it was held in the village of Egmond (Netherlands) from June 2nd until June 5th, 2016, and organized by the Meteor Section of the Dutch Association for Astronomy and Meteorology KNVWS, on the occasion of her 70th anniversary.

This IMC was a big one, with 158 participants, making it the largest so far. That is why the memories of this conference resulted in such an extensive work: the papers of 60 oral presentations and 31 posters.

This IMC had the specialty that it was combined with Meteoroids. This professional conference took place immediately after the IMC and created an excellent opportunity to attract many professionals to the IMC and also amateurs to Meteoroids. Both did attend in large numbers, and our fear that the timing of having the conference in June, in competition with many other conferences in this busy conference month, as well as the problematic timing for students due to examinations, did not become true at all. As often, the IMC turned out to be a bowl full of energizing liquid, enabling cross fertilization between amateurs, and this year between many amateurs and professionals as well.

This time the IMC had, for the first time, a Scientific Organizing Committee (SOC), and despite it doing most of its work in the background, it helped ensure that a program that was both interesting and high quality was created. The most demanding 'hurdle' to be taken was how to handle the enormous amount of contributions in the limited time available. The decision was made to limit all talks to 10 minutes (plus 2 minutes for discussion) in order to allow for speaking time for all oral presenters. In addition, the SOC chose to reserve extra time on request in the evening, for those topics that benefitted from deeper discussion.

There was also another novelty: this year the conference accommodated an open session, in which questions could be asked to a panel of specialists. A report of this exciting event is included in these proceedings. Also for the first time a poster prize was handed out for the author with the best poster, as well as a photo competition, also with a nice trophy for the winner, based on selection by an 'expert' panel and votes. Furthermore, we actively invited participants to bring equipment along, which brought on show two new All-sky cameras of the Desert Fireball Network and a working 3D-printer for printing meteorite replicas.

Although we feel thankful that the conference was much appreciated, we did realize beforehand that due to the enormous amount of participants, we would run into physical limits. Not only did the hostel itself reach its maximum capacity, we also felt that this was also the case for the format of the conference. Luckily all went well, but some rethinking of the future conference format may be required. The many satisfaction forms that we received (more than half of the participants) will surely help.

Of course there were many aspects that were not of concern at all because they ran very smoothly. Thanks to Marc Gyssens, the registration process was no burden for us by any means. Vincent Perlerin took care of all website related issues and in the background –not visible for most of us but of enormous help- a super sophisticated database. Backstage the IMO council members were there, always open for suggestions and feedback where needed during all preparation work. A special thanks there is also for Jean Louis Rault, who offered at the last minute to take on the not easy task of giving the summary talk. And last, but not least, Paul Roggemans, who once again offered to be main editor of the(se) proceedings, and used all efforts to complete them as soon as possible.

In addition to the support from the meteor community, we got also fantastic support from the hostel staff, who did always all we asked for, and gladly accepted that we practically took over almost the entire hostel. Of course, the conference could never have been a success without the participants. Applause is deserved for how well everyone (without a single exception!) kept to the tight schedule. Very well done.

Exhausted, but satisfied, on Sunday afternoon after 3 intensive days and nights, it was also time for the LOC to leave the hostel. Each member flooded with their own intense, unforgettable memories. We all saw that the field of meteoroids – meteors – meteorites is a very exciting one, and every year more and more so. The specialization of visual observations, the initial goal of IMO in gathering these worldwide, is accompanied now by many other techniques, best maybe video, but also spectroscopy, radio, simulations, software, lab experiments. Modelling and forecasts improve year after year, and rather than making observational results less important, all these models and theory actually ask for yet more – and better – observational work. The specialism of meteors touches an ever increasing number of other disciplines:

meteorites, comets, asteroids, hazards for spacecraft. And last, but not least, technical innovations, like almost everywhere, truly become interdisciplinary.

‘Meteors’ is also a field where the contribution of amateurs still is highly appreciated. And not to be forgotten: visual work remains valuable, for the calibration of other techniques and for the continuation of the only long-term record of the monitoring of activity.

Far outside our field, the discovery of exoplanets, dust and accretion around other stars (the current big hype in astronomy) is already being linked to the dust and meteoroids in our own solar system. In the same way as the study of the sun in solar physics is relevant to stars in stellar astronomy, our own solar system is the only place in which we can currently study in detail what will be seen in the future around other stars. How exciting it is. Meteors are fun.

And IMCs are fantastic!

Of course we hope to see you all next year again.

Thanks to all!

The LOC of the IMC 2016,

Felix, Joost, Arnold, Casper, Elise, Jos, Marc, Roy, Sebastiaan and Urijan

‘*Organizing an IMC again was extremely exciting, but the fact to realize how vivid our field of meteors is, even more*’

Felix Bettonvil

‘*It is amazing to see how many people with such different backgrounds and cultures can be connected by a magical natural phenomenon. Being able to make possible that all these people can meet is fantastic!*’

Joost Hartman

From the editor – about the IMC Proceedings

Paul Roggemans

Pijnboomstraat 25, 2800 Mechelen, Belgium
paul.roggemans@gmail.com

At the occasion of the 25th IMC in Roden, the Netherlands in 2006, the history of the IMCs was put in the spotlight with a dedicated presentation. Meanwhile we are 10 years later and many new faces appeared at the conference as regular participants. An update on the history of the IMCs is given. One of the first time participants at the 35th International Meteor Conference was the 1000nd officially registered participant according to the final effective participants' lists since 1979. In total 1033 different individuals have participated at one or more IMCs since 1979. The 35th IMC broke a few records: the largest total number of participants, the largest number of presentations, both talks and posters and the thickest IMC Proceedings ever. The International Meteor Conference got a splendid reputation worldwide as unique event among all international meetings of amateur astronomers. As far as the author is aware of, there is no other amateur conference in any astronomy domain comparable to the IMC. Some statistics about the conference and its history are presented.

1 Introduction

With a record number of participants the IMC at Egmond, the Netherlands, offered plenty of time for informal chats. I was a little bit surprised to hear how few people know about the origin of the conference and its purpose. The roots of the IMC are 10 years older than the IMO and this early history has been documented before (Roggemans, 2006; Roggemans and ter Kuile, 2007). The IMO has grown out of a personal network of meteor correspondents and the early IMCs happened to be the place where correspondents could meet in person long before the IMO got founded. The journal WGN is older than the IMCs and served as journal to exchange observing reports between correspondents when the earliest IMCs were organized.

When the IMO was founded in 1988, WGN became the journal of the IMO, but the IMCs kept an independent status and never became the IMO conference. Pro's and contra's to establish a formal international meteor organization provided animated debates at each IMC until 1990. The main concern against the founding of an IMO was that any 'too large' society risked degenerating into some kind of bureaucratic institute. When IMO got created a significant group of meteor observers did not want to see 'their' IMC being taken over by IMO. As a kind of gentlemen agreement, it was decided that the IMC would keep its independent status while IMO would provide some logistic support to the event and could have its yearly General Assembly at the IMC. This explains why the IMC is being organized by a LOC and not by the IMO staff and why several of the IMC Proceedings were produced independently from IMO. After the 1990 IMC where the topic was discussed (Koschny, 1991) the discussions ceased and the IMC remained an open event without any membership requirements.

2 The evolution since 2006

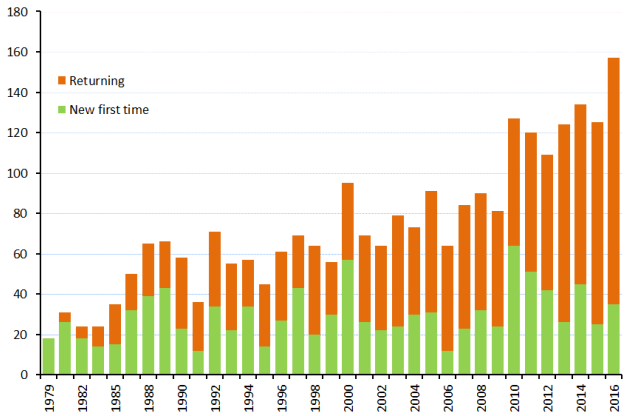

Figure 1 – The evolution of the number of registered, effectively present participants for all 35 meetings. New first time participants are marked in green, returning participants who had been at some previous IMC are marked in orange.

The history of the IMCs shows a steady growth in number of participants over a 38 year period. The first five meetings involved a rather small group with only few regular participants. Most participants were first time participants in the early years and it took a while to get a regular returning public. *Figure 1* shows the evolution of the number of IMC participants, with the number of first time participants marked in green and returning participants in orange. The interest to participate remained many years very stable from 1986 till 2002, with outliers in 1991, with a rather small group due to a lack of publicity, and 2000, with many local amateurs being on the participants' list. From 2003 till 2009 a growing number of regular returning participants mark another period with more people involved than before, 2006 being an outlier due to fewer first time registrations. Since 2010 the totals were significant higher than ever before.

The success of the IMC depends on how many people experience their participation as useful and sufficient motivating to return to a next conference. *Figure 2* shows the proportion of people who quit participation after the IMC (red at bottom) and those who return at some future conference (green at top). Some people stay away for several years and do return after a long period of absence. The proportions for recent years will change as more IMCs will be organized in the future and see more people return after being absent in recent years. Some years have a remarkable large proportion of participants who quit attending IMCs after the meeting of that year. These events were known as excellent IMCs, there must be some explanation why so many did not go to next IMCs.

If we make a query to check how many first time participants never go to any next conference and how many 'regular' participants quit at each IMC, it is obvious that in 2000, 2010 and 2011 an exceptional large number of people attending just this single event had no interest in going to any future meeting. In total 646 individuals (63%) attended just a single event. Depending on the publicity and the policy of the Local IMC organizer more local amateurs take the opportunity to attend an IMC as a once in a lifetime event. These single event participants are marked in orange in *Figure 3*. The number of people who quit having attended previous IMCs is rather small (marked in red in *Figure 3*). The number of new, first time participants who return at some future meetings (green in *Figure 3*) in general is larger than the loss of 'regular' attendants who quit at a given year. As a result there is a steady growth in regular participants who had attended previous events and who continue going to future meetings (blue in *Figure 3*).

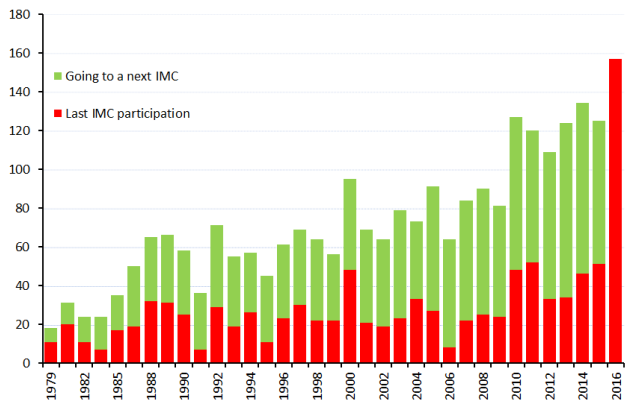

Figure 2 – Trying to scope the interest of the participants at each IMC. The red bars represent the number of participants that never returned to any later IMC, the green bars indicate the the number of participants going to some later IMC.

There is a very obvious evolution in the international character of the IMC over 38 years. Until 1991 residents from the hosting country made up a large portion of the participants. A few peculiar years are 1993 when the IMC took place in France while interest in meteor work at that time was almost nonexistent in France. Also 2015 seduced rather few Austrian participants for the IMC in Austria. On the other hand 1994 (Bulgaria), 1997 (Serbia), 2000 (Romania), 2004 (Bulgaria) and 2011 (Romania) had remarkable many local residents participating. For Romania these two years also coincide with a rather large number of single event participants who never returned at any future meeting.

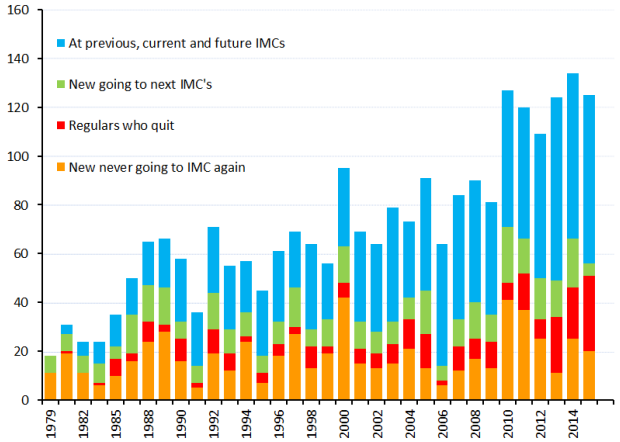

Figure 3 – Same as *Figure 2*, but with the number of continuing participants and those who quit at a given IMC, splitted in new and returning participants (not relevant for recent years).

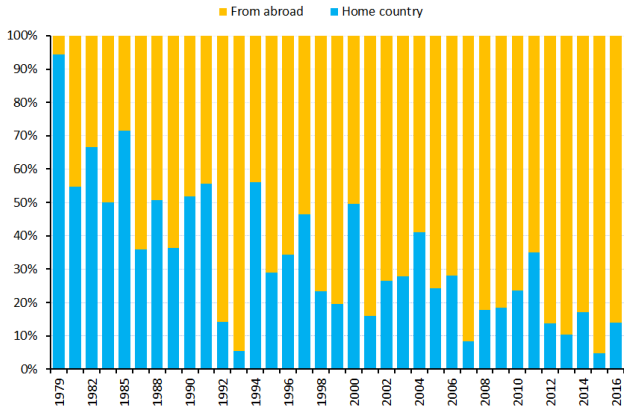

Figure 4 – The evolution of the international composition of the IMC participants lists. Blue (bottom) indicates the percentage individuals with their domicile in the hosting country. In yellow (top) the percentage of people coming from abroad, regardless nationality but according to their legal domicile at the moment of the IMC.

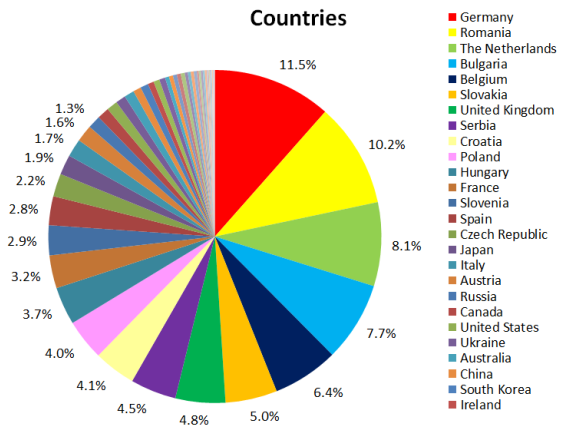

Figure 5 – The 1033 participants of all 35 conferences came from 50 different nations on all continents. The overall distribution for 38 years of IMCs is shown with the percentages in a pie graph.

Looking at the origin of all 1033 IMC participants most

participants came from Germany which is no surprise as the first IMCs were in Germany and meteor observing has been very popular among German amateurs past 40 years. The Netherlands and Belgium were strongly involved with the IMC tradition and have a long tradition of amateur meteor observing. The large numbers of Bulgarian and Romanian participants come from two IMCs in each of these countries with a large number of local amateurs participating at these specific events, also visible in *Figure 4*.

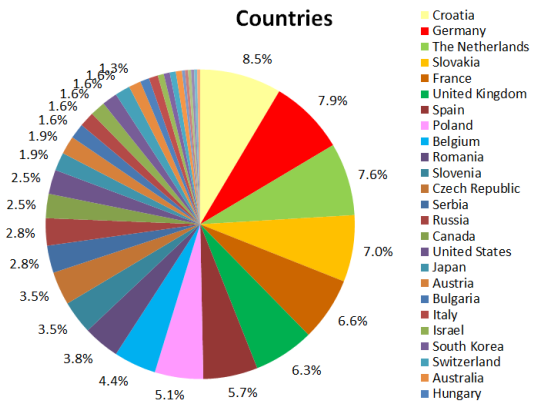

Figure 6 – The 316 participants of the 5 last IMCs (2012–2016) according to the country where participants had their domicile during the IMC.

Of course there is an evolution in the interest in meteor astronomy which is to some extend influenced by the IMCs. Looking at more recent times, taking only past 5 years a complete different picture occurs. Croatia happens to have the strongest representation at the recent IMCs, followed by Germany and the Netherlands. The presence of British and Slovak meteor workers increased while French meteor workers made a spectacular progress in recent years. Romania, Belgium and Bulgaria were much less present at recent IMCs, Belgium because of a general decrease in interest in meteor work, Romania and especially Bulgaria as no IMC took place during past 5 years in these countries.

3 The role of IMC Proceedings

Except for the very first meeting in 1979 which had its Proceedings, four meetings remained undocumented without Proceedings, although the intention to make Proceedings existed, lack of time prevented a successful completion for the 1980, 1982, 1983 and 1985 Proceedings. In the early years the Meteor Seminars or Meteor Weekends like the IMC was then called, inspired rather few participants to return at a next meeting. To listen to interesting presentations is enjoyable for a dedicated meteor worker, but it remains no more than pleasant entertainment as most details are quickly forgotten once the conference is finished. Why to spend a few days, costs and efforts to attend a conference if nothing is left from all interesting presentations in a written form? At the 1986 Meteor Weekend in Belgium, the author insisted to have Proceedings again in order to assure a more stable interest for future conferences. A Belgian amateur, Luc Vanhoeck (°1959 – †2005), volunteered to edit the 1986 Proceedings. Having complete conference Proceedings on time dramatically improved the popularity of the International Meteor Weekend after 1986. The uninterrupted availability of Proceedings had a positive effect on the interest in the conference and definitely played a major role in the current success of the IMCs.

Although that the importance to have all relevant content in Proceedings is obvious, the making of IMC Proceedings has often proved to be a challenging task that scarce off any volunteers to accept the challenge. Except for the very first (1979) Proceedings, a text editor has been used to produce the Proceedings since 1986. The advantage of any text processor is that the author can deliver his text saving the time for the editor to typewrite all content like what happened until the 1970s. Both the text editing software as the printing hardware improved a lot over past 30 years. For the first Proceedings content was still delivered on floppy disks that were sent by post services. Communication by e-mail enabled another significant improvement to submit content and to solve editorial issues. Imagine that until 1993 most of the communication about Proceedings happened with letters sent by post!

In spite of all these technical advantages the Proceedings took unreasonable long time to get ready, something that discouraged authors from making the effort to write a paper. In the early years Proceedings were ‘home made’ using some privately owned text editor and were relatively soon available. However collecting the papers has been the most difficult aspect ever since the beginning. Since poor communication was often the reason why some author failed to deliver any paper for the Proceedings, it was decided that the IMO Secretary General, having a very efficient network of contacts in the meteor world, would take care to collect all papers and to edit the IMC Proceedings. That proved to work very well as the 1993 Proceedings covered the complete content of the presentations. It was also decided to use the same style as WGN for the Proceedings which meant that these had to be prepared in LaTeX. Only very few people in IMO were able to use LaTeX and just like WGN in that time the Proceedings got a huge delay just because all edited articles had still to be converted into LaTeX code which was a time consuming job that had to be done by the WGN editors.

I collected systematically all the papers and prepared the editing work and André Knöfel took care about the LaTeX aspects. The 1994, 1995 and 1996 IMC Proceedings appeared pretty complete. When I decided to quit my mandate as IMO Secretary-General in 1998, I also quit taking care about the IMC Proceedings. André Knöfel continued as editor for the 1997 and 1998 IMC Proceedings. Without an extensive network of contacts it became impossible to collect papers for all the IMC presentations and as a result the IMC Proceedings contained only a partial coverage of all presentations. Several other editors got involved with the IMC

Proceedings. Only papers that were spontaneously submitted were included in the Proceedings and editors gave up trying to get the Proceedings more complete. To make things worse, some Proceedings appeared with huge delays such as the 2001 IMC Proceedings that appeared as late as end 2002.

The 2007 IMC Proceedings almost failed to get produced, and luckily Jürgen Rendtel took care to resume the editing work in order not to have an IMC without Proceedings. The 2007 IMC proceedings were very incomplete and appeared as late as in 2010, in the same year as the also delayed and incomplete 2008 IMC Proceedings and the more on time 2009 IMC Proceedings. The 2010 IMC in Armagh was a very successful IMC with a large number of presentations. Unfortunately only less than half of the presentations got documented in the Proceedings.

The poor performance with the IMC Proceedings made some people wondering if Proceedings were necessary at all. Incomplete and very late Proceedings made indeed very little sense while the role of the Proceedings in the success of the IMC was overlooked. The organizing of the 2011 IMC suffered from the general failure of the IMO to back up the IMC organizer. The author decided to help when too few registrations and too few lectures were announced for the 2011 IMC in Sibiu, Romania. When also no preparations were made to deal with the 2011 IMC Proceedings, the author decided to take care about the 2011 IMC Proceedings. With the experience achieved with the 1993, 1994, 1995 and 1996 IMC Proceedings, I started collecting papers. It was rather sad to see how reluctant most authors were to submit any paper. The reputation of the IMC Proceedings had got a serious blow after several years of very poor editions, with the 2007 and 2010 IMC Proceedings being the most problematic. It costed a lot of time and effort to motivate everybody to make an effort to submit a paper and to give the IMC Proceedings a last chance to prove that we could manage such publication. A strict and open editing procedure was implemented so that everybody could see the progress made with the editing work. We started in October 2011 and it took until June 2012 before the last papers were collected. Most papers were delivered in *MS Word* format and after editing the content I had to prepare the LaTeX files with a simple text editor (*Notepad)*. Editing an article is time consuming, on average about 3 hours per paper. Some need just 1 hour, others need extensive rewriting and take more than 6 hours. Transferring all the content into LaTeX files, inserting all the LaTeX syntax by hand, without any LaTeX editor is a very inefficient way to work. When ready the LaTeX version had to be compiled and bugs removed to obtain a printable version. Marc Gyssens volunteered to act as co-editor and the 2011 IMC Proceedings appeared right before the 2012 IMC at La Palma, saving postage by distributing printed copies at the 2012 IMC.

Doing the 2012 and the 2013 IMC Proceedings in the same way, year after year I experienced more goodwill among the authors to deliver a paper on time. The IMC Proceedings were taken serious again.

Still one aspect caused unjustifiable delays: the LaTeX conversion and compilation which happened to get again postponed by many months. In my opinion the usage of LaTeX in IMO and all the delay that occurred with this extraordinary time wasting LaTeX code, was an unfortunate mistake in IMO and caused a lot of damage to the organization because of the chronic delays on each and every publication. For the 2014 IMC Proceedings I decided to try out *MS Word* as 90% of all papers were delivered in Word. Vincent Perlerin offered to help with a template in Word for the IMC Proceedings. Thanks to the help and assistance of Vincent Perlerin, I managed to get the 2014 IMC Proceedings done together with Jean-Louis Rault as co-editor, in just a couple of months. In fact The 2014 IMC Proceedings were ready only a couple of months after the 2013 IMC Proceedings which had been distributed at the 2014 IMC.

A fast and efficient editing procedure generated more goodwill among all people involved and the 2015 IMC Proceedings went even smoother and faster. Although I was very keen to continue my tasks with the IMCs, I was very surprised and sadly disappointed with the initiative to cancel my task as IMC coordinator end 2015. It remained uncertain if I would do any more IMC Proceedings as dealing with the IMC Proceedings without being involved with the organizing of the IMC creates a serious handicap, not being able to anticipate on the requirements for Proceedings during the preparations for an IMC. The 2016 IMC Proceedings were expected to be exceptional in volume due to the connection with the Meteoroids conference. Felix Bettonvil involved me in the SOC and asked me if I could still take care of the 2016 IMC Proceedings. I had serious doubts because of the difficult work circumstances imposed by the IMO staff. Shortly before the IMC I decided to accept the challenge, together with my wife Adriana as co-editor.

One advice for the future: IMC papers should be submitted *before* the IMC, it is too bad to require delivery after the conference as that has nothing but disadvantages for everybody. A SOC can only function properly if it has papers at hand to consider proposed presentations.

Acknowledgment

I thank *Felix Bettonvil* for keeping me informed about ongoing IMC matters, for his help to collect the papers from many authors and for his assistance with various other aspects. I also thank the proofreaders, *Bob Lunsford*, *Vincent Perlerin* and *Jean-Louis Rault* for their time and patience to check many papers. *Tracy Heywood*, *Tony Markham* and *Michael O'Connell* for proofreading and rewriting a number of papers. Thanks to *all the authors* for delivering their paper(s) on time and for proofreading the edited version. Last but not least I thank my wife *Adriana* who helped as co-editor to get papers in the right format and to solve specific issues with MS Word.

Table 1 – Overview of all IMC Proceedings available online. Click on the name of the Proceedings you want to consult at the *ADS Abstract Service*, then click "Send query" to see the list of available content (ADS = number of papers, PP = number of pages).

IMC Proceedings edition	Editors	ADS	PP
IMC Proceedings Königswinter (Bonn) - Germany, 8-10 June 1979	Schmitz B., Becker H. J.	11	24
IMC Proceedings Pullach (Munich) - Germany, 21-23 November 1980	No Proceedings	-	-
IMC Proceedings Hasselt - Belgium, 26-28 February 1982	No Proceedings	-	-
IMC Proceedings Brecklenkamp - Netherlands, 13-15 May 1983	No Proceedings	-	-
IMC Proceedings Violau (Augsburg) - Germany, 22-24 February 1985	No Proceedings	-	-
IMC Proceedings Hingene - Belgium, 3-5 October 1986	Vanhoeck L.	19	80
IMC Proceedings Oldenzaal - Netherlands, 25-27 March 1988	Lanzing J.	24	84
IMC Proceedings Balatonföldvár - Hungary, 5-8 October 1989	Spányi P., Tepliczky I.	24	84
IMC Proceedings Violau (Augsburg) - Germany, 6-9 September 1990	Heinlein D., Koschny D.	26	64
IMC Proceedings Potsdam - Germany, 19 - 22 September 1991	Rendtel J., Arlt R.	26	90
IMC Proceedings Smolenice - Slovakia, 2-5 July 1992	Ocenas D. , Zimnikoval P.	23	93
IMC Proceedings Puimichel - France, 23-26 September 1993	Roggemans P.	35	113
IMC Proceedings Belogradchik - Bulgaria, 22-25 September 1994	Knöfel A., Roggemans P.	19	89
IMC Proceedings Brandenburg - Germany, 14-17 September 1995	Roggemans P., Knöfel A.	24	133
IMC Proceedings Apeldoorn - Netherlands, 19-22 September 1996	Knöfel A., Roggemans P.	24	143
IMC Proceedings Petnica - Yugoslavia, 25-28 September 1997	Knöfel A., McBeath A.	21	109
IMC Proceedings Stará Lesná - Slovakia, 20-23 August 1998	Arlt R., Knöfel A.	25	117
IMC Proceedings Frasso Sabino - Italy, 23-26 September 1999	Arlt R.	26	156
IMC Proceedings Pucioasa - Romania, 21-24 September 2000	Arlt R., Triglav M., Trayner C.	31	132
IMC Proceedings Cerkno - Slovenia, 20-23 September 2001	Triglav M., Knöfel A., Trayner C.	22	109
IMC Proceedings Frombork - Poland, 26-29 September 2002	Olech A., Zloczewski K., Mularczyk K.	30	175
IMC Proceedings Bollmannsruh - Germany, 19-21 September 2003	Triglav-Cekada M., Trayner C.	36	194
IMC Proceedings Varna - Bulgaria, 23-26 September 2004	Triglav-Cekada M., Kac J.; McBeath A.	24	115
IMC Proceedings Oostmalle - Belgium, 15-18 September 2005	Bastiaens L., Verbert J., Wislez J.-M., Verbeeck C.	33	195
IMC Proceedings Roden - Netherlands, 14-17 September 2006	Bettonvil F., Kac J.	36	190
IMC Proceedings Barèges - France, 7-10 June 2007	Rendtel J., Vaubaillon J.	20	83
IMC Proceedings Šachtička, Slovakia, 18-21 September 2008	Kaniansky S., Zimnikoval P.	17	120
IMC Proceedings Poreč, Croatia, 24 - 27 September 2009	Andreic Z., Kac J.	20	105
IMC Proceedings Armagh, Northern Ireland (UK), 16 - 19 September 2010	Asher D. J., Christou A. A., Atreya P., Barentsen G.	28	106
IMC Proceedings Sibiu, Romania, 15 - 18 September 2011	Gyssens M., Roggemans P.	47	148
IMC Proceedings La Palma, Spain, 20 - 23 September 2012	Gyssens M., Roggemans P.	65	236
IMC Proceedings Poznan, Poland, 22 - 25 August 2013	Gyssens M., Roggemans P., Zoladek P.	63	222
IMC Proceedings Giron, France, 18 - 21 September 2014	Rault J.-L., Roggemans P.	58	225
IMC Proceedings Mistelbach, Austria, 27 - 30 August 2015	Rault J.-L., Roggemans P.	62	239
IMC Proceedings Egmond, the Netherlands, 2 - 5 June 2016	Roggemans A., Roggemans P.	100	374

References

Koschny D. (1991). "Preface". In Heinlein D. and Koschny D., editors, *Proceedings of the International Meteor Conference*, Violau, Germany, 6-9 September, 2006. IMO, page iv.

Roggemans P. (2006). "The 25th International Meteor Conference". *WGN, Journal of the IMO*, **34**, 115–118.

Roggemans P. and Ter Kuile C. (2007). "25 edition of the International Meteor Conference since 1979". In Bettonvil F. and Kac J., editors, *Proceedings of the International Meteor Conference*, Roden, The Netherlands, 14-17 September, 2006. IMO, pages 129–133.

Program of the 35th International Meteor Conference
Egmond , 2–5 June, 2016

Thursday, 2 June, 2016

14:00 – 19:00	Arrival and registration IMC participants.
19:00 – 20:00	Welcome reception & speeches.
20:00 – 21:00	Dinner.
21:00 – …	Parallel Program.
	Option A - Free entertainment.
	Option B – Workshops.
21:00 – 21:45	Meteor Spectroscopy.
21:45 – 22:30	Microscopic view inside meteorites.

Friday, 3 June, 2016

07:30 – 08:30	Breakfast.
08.55 - 09.00	Local announcements.
	SESSION 1 – Meteor showers & sporadic background I: video & radio. (Chair: *Damir Šegon*).
09:00 – 09:12	*Peter Jenniskens*: "Results from the CAMS video network".
09:12 – 09:24	*Joel Younger*: "Radar Observations of the Volantids Meteor Shower".
09:24 – 09:36	*Giancarlo Tomezzoli*: "No sign of the 2015 Daytime Sextantids through Combined Radio Observations".
09:36 – 09:48	*Paul Roggemans*: "Update CAMS Benelux 2015-2016".
09:48 – 10:00	*Przemysław Żołądek*: "Taurids 2015".
10:00 – 10:12	*Ljubica Grašić*: "Video Meteor Light Curve Analysis of Orionids and Geminids".
10:12 – 10:24	*Ivica Skokić*: "On the accuracy of orbits from video meteor observations".
	SESSION 2 – Meteor showers & sporadic background II: visual. (Chair: *Sirko Molau*).
10:24 – 10:36	*Juergen Rendtel*: "Minor meteor shower activities".
10:36 – 10:48	*Thomas Weiland*: "2014 Southern Delta-Aquariid Observing Campaign - carried out from Crete".
10:48 – 11:24	**Coffee break & Poster Session.**
	SESSION 3 – Fireballs and meteorite recovery. (Chair: *Sebastiaan de Vet*).
11:24 – 11:36	*Pavel Spurny*: "EN091214 Zdar - one of the most precisely documented meteorite fall".
11:36 – 11:48	*Vincent Perlerin*: "The tale of two fireballs".
11:48 – 12:00	*Daniele Gardiol*: "Italian Network for Meteors and Atmospheric Studies (PRISMA)".
12:00 – 12:12	*Lukas Shrbeny*: "Fireballs from Australian Desert Network".
12:12 – 12:24	*Jiri Borovicka*: "Photographic spectra of fireballs".
12:24 – 12:36	*Manuel Moreno-Ibáñez*: "Current progress in the understanding of the physics of large bolides recorded by photographic and digital fireball networks".
12:36 – 12:48	*Ana Georgescu*: "The evolution of ROAN 2016 - Radio surveillance of meteors and determination of reflexion points through calculation of the radio path, based on times".
12:48 – 13:00	*François Colas*: "FRIPON Network Status".

13:00 – 14:00 **Lunch.**

SESSION 4 – Observing techniques.
(Chair: *Dušan Pavlović*).

14:00 – 14:12 *Auriane Egal*: "The challenge of meteors daylight observations".

14:12 – 14:24 *Sirko Molau*: "Flux density, population index, perception coefficient, and the Moon".

14:24 – 14:36 *Pavel Koten*: "Simultaneous analogue and digital observations and comparison of results".

14:36 – 14:48 *Alexander Bagrov*: "Easy way to estimate meteor brightness on TV frames".

14:48 – 15:00 *Tom Roelandts*: "The radio meteor signal path from transmitter to spectrogram: an overview".

15:00 – 15:12 *Lorenzo Barbieri*: "An antenna, a radio, a microprocessor: which observations in amatory meteor radio astronomy?".

SESSION 5 – Parent bodies, meteoroids, meteorites, planets and their relation.
(Chair: *Denis Vida*).

15:12 – 15:24 *Abedin Abedin*: "On the age and parent body of the daytime Arietids meteor shower".

15:24 – 15:36 *Peter Brown*: "Recent Canadian Meteor Orbit Radar detected meteor shower outbursts".

15:36 – 16:24 **Coffee break & Poster Session.**

SESSION 6 – Numeric modelling.
(Chair: *Rachel Soja*).

16:24 – 16:36 *Daniel Kastinen*: "A statistical approach to the temporal development of orbital associations".

16:36 – 16:48 *Jérémie Vaubaillon*: "A confidence index for the forecasting of the meteor showers".

16:48 – 17:00 *Robert Marshall*: "Interpretation of Meteor Radar Head Echoes".

SESSION 7 – Atmospheric processes and phenomena
(Chair: *Jean-Louis Rault*).

17:00 – 1712 *Masa-yuki Yamamoto*: "Space fireworks for upper atmospheric wind measurements by sounding rocket experiments".

17:12 – 17:24 *David Čapek*: "Ablation of small Fe meteoroids".

17:24 – 17:36 *Vlastimil Vojacek*: "Catalogue of meteor spectra".

17:36 – 17:48 *Shinsuke Abe*: "Artificial Meteor Test towards On-demand Meteor Shower".

17:48 – 18:00 *Simona Hristova*: "Exploring the relationship between meteor parameters based on a photographic data".

18:00 – 18:12 *Jean-Louis Rault*: "An attempt to explain VLF propagation perturbations associated with single meteors".

18:12 – 19:12 **Poster session with all poster authors.**

01. *Francois Colas*. "FRIPON acquisition, detection and reduction pipe line".
02. *Eduard Pittich*. "Sungrazing comets and meteoroids".
03. *Felix Bettonvil*. "CHIPOlAtA results".
04. *Regina Rudawska*. "An overview of the CILBO spectral observation program".
05. *Johan Kero*. "First results of the Swedish Allsky Meteor Network".
06. *Zbigniew Tymiński*. "Polish Meteorites".
07. *Rachel Soja*. "Lifetimes of meteoroids".
08. *Peter Dolinsky*. "Data processing of records of meteoric echoes".
09. *Gaetano Brando*. "The 2016 Quadrantids".
10. *Juraj Toth*. "AMOS - trajectory and orbital data from SVMN and Canary Islands".
11. *Pavel Zigo*. "AMOS-Spec - meteor spectra from Modra Observatory".
12. *Meryem Guennoun*. "Synthetic spectra of meteors".
13. *Maria Hajdukova*. "The occurrence of interstellar meteoroids. Overview - 25 years of research".
14. *Paul Roggemans*. "Meteor News".

15. *Alexander Bagrov*. “Photometric Stellar Catalogue for TV meteor Astronomy”.
16. *Ljubica Grašić*. “Video Meteor Light Curve Analysis of Orionids and Geminids”.
17. *Ibhi Abderrahmane*. “The role of population in tracking meteorite falls in Africa”.
18. *Shinsuke Abe*. “Asteroidal Meteors Detected by MU Radar Head-echo Observations”.
19. *Jakub Koukal*. “Meteors and meteorites spectra”.
20. *Sebastiaan de Vet*. “The added dimension of 3D scanning and printing of meteorites”.
21. *Antonio Martinez Picar*. “Numerical simulation of BRAMS interferometer in Humain”.
22. *Yasunori Fujiwara*. “Meteor spectra using high definition video camera in 2015”.
23. *Jakub Kákona*. “Hemispherical radiating pattern antenna design for radio meteor observation”.
24. *Maria Gritsevich*. “Novel methods for 3D numerical simulation of meteor radar reflections”.
25. *Maria Gritsevich*. “Statistical approach to meteoroid shape estimation”.
26. *Maria Gritsevich*. “Meteor detections at the Metsähovi Fundamental Geodetic Research Station (Finland)”.
27. *Tudor Georgescu*. “ROAN 2016 - Progress”.
28. *Bogdan Dumitru*. “Investigation of meteor shower parent bodies using various metrics”.
29. *Urijan Poerink*. “70 years KNVWS Werkgroep Meteoren”.
30. *Manuel Moreno-Ibáñez*. “Large meteoroids’ impact damage: review of available impact hazard simulators”.
31. *Andrey Murtazov*. “Measurements of CCD optical linearity for magnitude determination in meteor observations”.

19:12 – 20:12	**Dinner.**
20:12 – 21:12	28th IMO General Assembly.
	Parallel Program.
	Option A – Free entertainment.
	Option B – Open session with discussion panel.
	Option C - Extended-talk Session I (21:30 – 23:30).
21:30 – 22:30	*Pavel Spurny*: Recent instrumentally documented meteorite falls.
22:30 – 23:00	*Maria Gritsevich*: Calibration of occasionally taken images using principles of perspective.
23:10 – 23:30	*Maria Gritsevich*: Consequences of meteoroid impacts based on atmospheric trajectory analysis.

Saturday, 4 June 2016

07:30 – 08:30	Breakfast.
08:55 – 09:00	Local announcements.
	SESSION 8 – Data pipelines & Software. (Chair: *Christian Steyaert*).
09:00 – 09:12	*Thomas Albin*: “A Monte-Carlo based extension of the Meteor Orbit and Trajectory Software (MOTS) for computations of orbital elements”.
09:12 – 09:24	*Denis Vida*: “Open-source meteor detection software for low-cost single-board computers”.
09:24 – 09:36	*Pete Gural*: “A Fast Meteor Detection Algorithm”.
09:36 – 09:48	*Theresa Ott*: “PaDe - The Particle Detection Program”.
09:48 – 10:00	*Stijn Calders*: “The BRAMS Zoo, a citizen science project: current status”.
10:00 – 10:12	*Hervé Lamy*: “Automatic detection of meteor echoes in BRAMS data: towards a final decision”.
10:12 – 10:36	**Coffee break & Poster Session.**
	SESSION 9 – Ongoing work, History & Miscellaneous. (Chair: *Antonio Martinez Picar*).
10:36 – 10:48	*Damir Šegon*: “Croatian Meteor Network: ongoing work 2015-2016”.
10:48 – 11:00	*Juraj Toth*: “Expedition Atacama - project AMOS in Chile”.

11:00 – 11:12	*Regina Rudawska*: "ESA/ESTEC Meteor Research Group – behind the scenes".
11:12 – 11:24	*Iain Reid*: "60 years of radio meteor studies at Adelaide University".
11:24 – 11:36	*Detlef Koschny*: "Height computation of a fireball".
11:36 – 11:48	*Eleanor Sansom:* "Meteor Reporting Made Easy- Fireballs in the Sky's smartphone app".
11:48 – 12:00	*Maria Gritsevich*: "Big Data Era in Meteor Science".
12:30	Departure for excursion to the world heritage site the Waddenzee.
19:00 – 20:00	**Closing dinner.**
20:00 – 21:00	Parallel Program.
	Option A – Free entertainment.
20:00 – 20:45	Option B – Workshop: Software for analysis of visual meteor data.
	Option C - Extended-talk Session II (20:00 – 21:00).
20:00 – 20:20	*Sirko Molau*: "Flux density, population index, perception coefficient, and the Moon".
20:20 – 20:40	*Pete Gural*: "A Fast Meteor Detection Algorithm".
20:40 – 21:00	*Daniel Kastinen*: "A statistical approach to the temporal development of orbital associations".
21:00 – ...	Last night of the IMC in the bar, free entertainment.

Sunday, 5 June 2016

08:30 – 09:30	Breakfast.
09:55 – 10:00	Local announcements.
	SESSION 5A – Parent bodies, meteoroids, meteorites, planets and their relation. (Chair: *Denis Vida*).
10:00 – 10:12	*Ayyub Guliyev*: "Meteor streams and comet disintegration".
	SESSION 10 – Instruments. (Chair: *Pete Gural*).
10:12 – 10:24	*Mariusz Wiśniewski*: "Current status of Polish Fireball Network".
10:24 – 10:36	*Hadrien Devillepoix*: "Status of the Desert Fireball Network".
10:36 – 10:48	*Chris Peterson*:: "Evaluating video digitizer errors".
10:48 – 11:00	*Martin Dubs*: "Calibration of meteor spectra".
11:00 – 11:12	*Waleed Madkour*: "The KUT meteor radar: An educational low cost meteor observation system by radio forward scattering".
11:12 – 11:24	*Cezar Lesanu:* "ROAN Remote Radio Meteor Detection Sensor".
11:24 – 12:00	**Coffee break & Poster Session.**
	SESSION 11 – Observing techniques II. (Chair: *Francesco Ocaña*).
12:00 – 12:12	*Anna Kartashova*: "The complex meteor observations in 2014".
12:12 – 12:24	*Satoshi Mizumoto*: "Comprehensive observation of meteors combining with infrasonic, optic and radio scattering signals".
12:24 – 12:36	*Jakub Kákona*: "Meteor trajectory estimation from radio meteor observations".
12:36 – 12:48	*Margaret Campbell-Brown*: "Results from the Canadian Automated Meteor Observatory".
12:48 – 13:00	*Jean-Louis Rault*: "Conference summary".
13:00 – 13:10	Closing of the 35th IMC.
13:10 – 14:00	**Lunch.**
14:30	Departure of participants, Bus transfer to Schiphol, Bus transfer to Meteoroids 2016.

Artificial meteor test towards On-demand meteor shower

Shinsuke Abe, Lena Okajima, Hironori Sahara, Takeo Watanabe, Yuta Nojiri and Tomohiko Nishizono

shinsuke.avell@gmail.com

An arc-heated wind tunnel is widely used for ground-based experiments to simulate environments of the planetary atmospheric entry under hypersonic and high-temperature conditions. In order to understand details of a meteor ablation such as temperature, composition ratio and fragmentation processes, the artificial meteor test was carried out using a JAXA/ISAS arc-heated wind tunnel. High-heating rate around 30 MW/m^2 and High-enthalpy conditions, 10000 K arc-heated flow at velocity around 6 km/s were provided. Newly developed artificial metallic meteoroids and real meteorites such as Chelyabinsk were used for the ablation test. The data obtained by near-ultraviolet and visible spectrograph (200 and 1100nm) and high-speed camera (50 μs) have been examined to develop more efficient artificial meteor materials. We will test artificial meteors from a small satellite in 2018.

Sinsuke Abe (Photo Irmgard Schmidt).

Asteroidal meteors detected by MU radar head-echo observations

Shinsuke Abe, Johan Kero, Takuji Nakamura, Yasunori Fujiwara, Daniel Kastinen, Jun-ichi Watanabe and Hiroyuki Hashiguchi

shinsuke.avell@gmail.com

The recent development of the technique carried out using the middle and upper atmosphere radar (MU radar) of Kyoto University at Shigaraki (34.9N, 136.1S), which is large atmospheric VHF radar with 46.5 MHz frequency, 1 MW output transmission power and 8330 m^2 aperture array antenna, has established very precise orbital determination from meteor head echoes. A tremendous number, more than 150000, of observed precise orbits of meteoroids by the MU radar meteor head-echo observation will shed light on new discoveries of meteoroids. Here we report some interesting features related with asteroids or distinct comets.

Wednesday evening: the LOC meets for the last time before the start, latest details are discussed. From left to right Roy Keeris, Casper ter Kuile (hidden), Arnold Tukkers, Jos Nijland, Elise Ijland, Mark Neijts, Joost Hartman and Sebastiaan de Vet.

On the age and parent body of the daytime Arietids meteor shower

Abedin Abedin, Paul Wiegert, Petr Pokorny and Peter Brown

Dept. of Physics and Astronomy, University of Western Ontario, London, Ontario, N6A 3K7, Canada
aabedin@uwo.ca

The daytime Arietid meteor shower is active from mid-May to late June and is among the strongest of the annual meteor showers, comparable in activity and duration to the Perseids and the Geminids. Due to the daytime nature of the shower, the Arietids have mostly been constrained by radar studies. The Arietids exhibit a long-debated discrepancy in the semi-major axis and the eccentricity of meteoroid orbits as measured by radar and optical surveys. Radar studies yield systematically lower values for the semi-major axis and eccentricity, where the origin of these discrepancies remain unclear. The proposed parent bodies of the stream include comet 96P/Machholz and more recently the Marsden's group of sun-skirting comets. In this work, we present detailed numerical modelling of the daytime Arietid meteoroid stream, with the goal to identifying the parent body and constraining the age of the stream. We use observational data from an extensive survey of the Arietids by the Canadian Meteor Orbit Radar (CMOR), in the period of 2002–2013, and several optical observations by the SonotaCo meteor network and the Cameras for All-sky Meteor Surveillance (CAMS).

Our simulations suggest that the age and observed characteristics of the daytime Arietids are consistent with cometary activity from 96P, over the past 12000 years. The sunskirting comets that presumably formed in a major comet breakup between 100 – 950 AD (Chodas and Sekanina, 2005), alone, cannot explain the observed shower characteristics of the Arietids. Thus, the Marsden sunskirters cannot be the dominant parent, though our simulations suggest that they contribute to the core of the stream.

References

Sekanina Z. and Chodas P. W. (2005). "Origin of the Marsden and Kracht Groups of Sunskirting Comets. I. Association with Comet 96P/Machholz and Its Interplanetary Complex". *The Astrophysical Journal Supplement Series*, **161**, 551–586.

A Monte-Carlo based extension of the Meteor Orbit and Trajectory Software (MOTS) for computations of orbital elements

Thomas Albin[1,2], Detlef Koschny[3,4], Rachel Soja[1], Ralf Srama[1] and Bjoern Poppe[2]

[1] **Institute for Space Systems, University of Stuttgart, Pfaffenwaldring 29, 70569 Stuttgart, Germany**
albin@irs.uni-stuttgart.de

[2] **Universitaetssternwarte Oldenburg, Institute of Physics and Department of Medical Physics and Acoustics, Carl von Ossietzky University, 26129 Oldenburg, Germany**

[3] **European Space Agency, ESA/ESTEC, Keplerlaan 1, 2201 AZ Noordwijk ZH, Netherlands**

[4] **Chair of Astronautics, Technical University Munich, Boltzmannstrasse 15, 85748 Garching, Germany**

The Canary Islands Long-Baseline Observatory (CILBO) is a double station meteor camera system (Koschny et al., 2013; Koschny et al., 2014) that consists of 5 cameras. The two cameras considered in this report are ICC7 and ICC9, and are installed on Tenerife and La Palma. They point to the same atmospheric volume between both islands allowing stereoscopic observation of meteors. Since its installation in 2011 and the start of operation in 2012 CILBO has detected over 15000 simultaneously observed meteors. Koschny and Diaz (2002) developed the Meteor Orbit and Trajectory Software (MOTS) to compute the trajectory of such meteors. The software uses the astrometric data from the detection software MetRec (Molau, 1998) and determines the trajectory in geodetic coordinates. This work presents a Monte-Carlo based extension of the MOTS code to compute the orbital elements of simultaneously detected meteors by CILBO.

1 Introduction

The Canary Islands Long-Baseline Observatory (CILBO, Koschny et al., 2013; 2014) has been in continuous operation since January 2013. One part of CILBO consists of two camera systems installed on Tenerife (ICC7) and La Palma (ICC9) that observe an overlapping area in the sky at an altitude of approximately 100 km between both islands. Meteors that cross both Field-of-Views (FOV) simultaneously are observed stereoscopically. This allows a precise reconstruction of the trajectory and orbit. *Figure 1* shows the position and pointing of the so called boresight of both CILBO cameras. The red and green skewed pyramids indicate the FOVs of ICC9 and ICC7, respectively. Additionally, an example of a stereoscopically observed meteor between both islands is shown. Each dot of the meteor represents the determined geodetic coordinates from each recorded video frame.

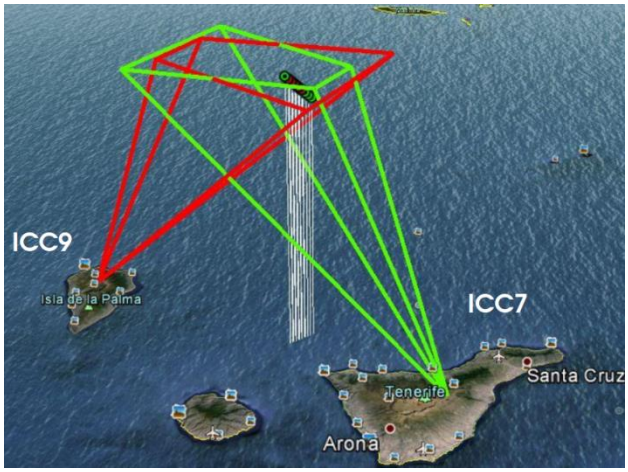

Figure 1 – Location and camera pointing of the CILBO cameras ICC7 and ICC9 on Tenerife and La Palma, respectively. The skewed pyramids represent the field-of-views of the cameras. The data points of a recorded meteor are drawn within the overlapping observation volume.

Based on the meteor data set of around 15000 simultaneously observed meteors, a pointing and velocity bias analysis has been completed (Albin et al., 2015a; 2015b) as well as an un-biasing of the velocity distribution and mass influx based on the ECSS model (Drolshagen et al., 2014; Ott et al., 2014; Drolshagen et al., 2015; Kretschmer et al., 2015).

The complete data recording and processing pipeline consists of miscellaneous software packages. The software *MetRec* (Molau, 1999) has been chosen for the meteor detection. Both cameras are operated with a frame rate of 25 fps and a video frame length of 40 ms, respectively. *MetRec* determines the photometric center of each meteor it detects on the video frames. The center's position is computed in a relative CCD coordinate system as well as in equatorial coordinates using the background stars as a reference. All information are then saved in a so-called *inf*-file. *Figure 2* shows the content of an *inf*-file. Finally, the individual video frames are saved in a stacked image for visual verification in order to exclude false detections. *Figure 3a and b* show a meteor detected simultaneously by both CILBO cameras. The meteor shows a double-peak feature and has been

```
AppearanceDate 03.05.2014
AppearanceTime 00:15:31
ReferenceStars \dev\metrec\config\20130831.ref
FrameCount 10
#   time  bright   x      y      alpha     delta   c_x    c_y    c_alpha  c_delta  use
01  31.565 ----  0.289  0.328   10.9126   27.232  -----  -----  --------  -------  no
02  31.605 ----  0.288  0.323   10.9053   27.186  -----  -----  --------  -------  no
03  31.646 ----  0.287  0.318   10.8975   27.139  -----  -----  --------  -------  no
04  31.686  3.2  0.287  0.314   10.8901   27.093  -----  -----   10.8913   27.098  yes
05  31.726  2.7  0.286  0.309   10.8823   27.046  -----  -----   10.8807   27.039  yes
06  31.766  3.3  0.285  0.301   10.8701   26.982  -----  -----   10.8701   26.979  yes
07  31.806  3.8  0.284  0.294   10.8589   26.916  -----  -----   10.8595   26.920  yes
08  31.846 ----  0.283  0.287   10.8477   26.850  -----  -----  --------  -------  no
09  31.886 ----  0.282  0.281   10.8364   26.783  -----  -----  --------  -------  no
10  31.926 ----  0.281  0.274   10.8257   26.716  -----  -----  --------  -------  no
```

Figure 2 – Example of an inf file. The first four rows provide the meta data (appearance time, data, reference file). The fifth row provides the table column headers for the measurement data. Column 1 is a consecutive number, column 2 lists the detection time in seconds and column 3 shows the determined brightness. In addition to the detected meteor frames, *MetRec* saves 3 frames before and after the meteor detection, for which no brightness values are given. The next four columns provide the position of the photometric center in relative CCD coordinates and in right ascension and declination. c_x and c_y are currently not used. c_alpha and c_delta are corrected astrometric right ascension and declination (by fitting the position measurements to a great circle). The last column indicates whether a meteor has been detected in the video frame.

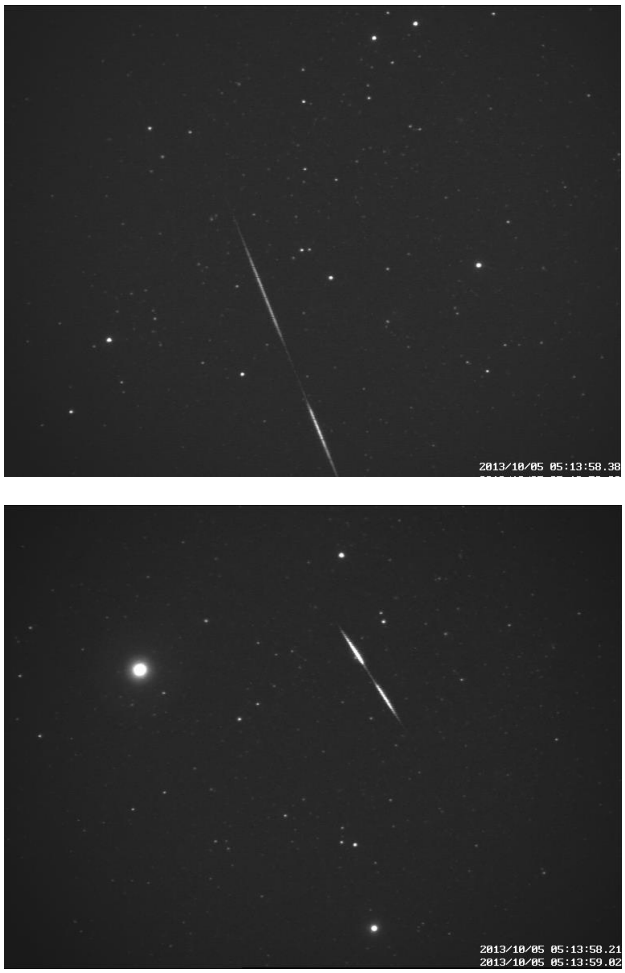

Figure 3 – A meteor detected simultaneously by ICC7 (top) and ICC9 (bottom). The meteor appears shorter in the ICC9 image because there the radiant is closer to the camera boresight.

detected on 5 October 2013 at $05^h13^m59^s$ UTC. The different lengths of the meteor and brightness are due to the flight direction and distance to the camera. Furthermore, the smaller angular velocity of the meteor on the ICC9 frames leads to less illuminated pixels compared to ICC7. The result is that the meteor appears brighter on the ICC9 frames than on the ICC7.

For each CILBO camera individual directories contain the information for each detected meteor. A Python-based routine then checks the camera directories and identifies simultaneously detected meteor candidates. The Meteor Orbit and Trajectory Software (Koschny and Diaz, 2002) is then used to determine the trajectory for each meteor candidate in geodetic coordinates. These coordinates are shown in *Figure 1* for a stereoscopically observed meteor. The geodetic information of the meteor as well as the detection time and time distance of 40 ms allows a precise trajectory reconstruction. The final positions are indicated as circles within the FOV of both cameras. An overview of the *MOTS* algorithm is shown in *Section 2*.

The orbit of the meteors can be computed with the geodetic trajectory information. The methods and algorithms as well as the Monte-Carlo based approach to determine the aforementioned errors are described in *Section 3*.

2 The Meteor Orbit and Trajectory Software (MOTS)

Koschny and Diaz (2002) developed the *Meteor Orbit* and *Trajectory Software* (*MOTS*) which is used in this work to compute the trajectory of a meteor in geodetic coordinates. Here a short overview of the *MOTS* algorithm is given. A complete mathematical description can be found in the corresponding paper.

Figure 4 shows the computation procedure schematics. S1 and S2 are two double-stationary meteor cameras, here ICC7 and ICC9. The meteor appears at point B and ends at the point E. Both points describe a thick black line that indicates the actual flight path of the meteor. Using the geographical coordinates of station S1 and the observation data of the meteor, a plane can be found

crossing the camera station and the flight path of the meteor. $\vec{n}$ defines the plane normal. Hereafter, this plane is called support plane.

A directional vector can be defined with the astrometric data from the station S2 (example: vector ($\overrightarrow{M2}$)). The intersection point between the support plane and the defined vector from S2 can then be computed. The height and projected geographical coordinates are then computed in order to obtain final geodetic state vector of the meteor. This requires also time information.

To verify the data the same plane and vector crossing computation can be done with respect to station S2, where the astrometric data and geographical position of S2 defines the support plane.

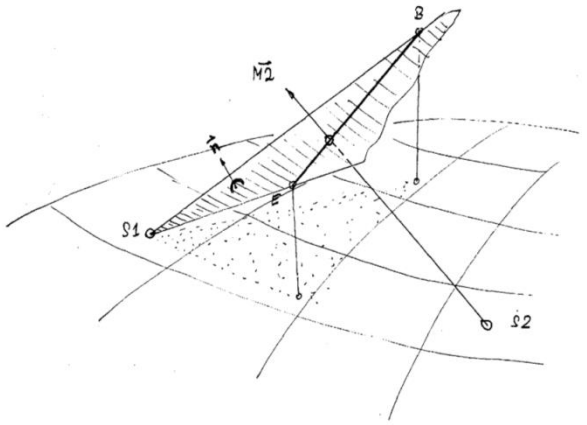

Figure 4 – Schematic diagram of the computation routine of MOTS. S1 and S2 indicate the two camera locations. The meteor is a thick black line with the starting and ending point B and E respectively. n is the normal vector of the drawn plane between meteor and S1. M2 is a direction vector of a determined meteor position as seen from S2. The intersection point between M2 and the plane determines a geodetic coordinates point for the meteor. From Koschny and Diaz (2002).

Albin et al. (2015b) have shown that continuously operated meteor cameras have a velocity determination bias for meteors detected on 3 frames. The velocity determination cannot use the first and last frames because the meteor appears and disappears in the frames, respectively. The following methods are applied for this work:

- Meteor on 3 frames: No suitable velocity determination. Can be used to compute the support plane.
- Meteor on 4 frames: Only one velocity value can be computed, between frame 2 and 3.
- Meteor on > 4 frames: All values from the second to the second-to-last frame can be used. Depending on the total number of frames a linear, quadratic or higher polynomial fit function can be used to determine an accurate velocity function. The velocity of the meteor is then computed using the function at the initial position.

3 The Monte-Carlo (MC) based extension

This chapter presents the orbit code algorithm and an MC-based-extension to compute an accurate error for the orbital elements based on the astrometric accuracy.

Orbit Determination

The developed orbit code is based on the existing *MOTS* routines. It determines the orbital elements of a meteor in the following way. As a visual guideline, the computation steps 3 to 5 are illustrated schematically in *Figure 5*:

1. **Identification of simultaneously detected meteors:** A routine compares the inf-files in the data directories of ICC7 and ICC9 and searches for simultaneously detected meteors. Approximately 30 % of all meteors have been observed at the same time from both cameras. The identified inf-files are then loaded and sent to the *MOTS* computation routine.
2. **Trajectory determination:** The inf-files are then used to determine the trajectory of the meteor in geodetic coordinates. Two geodetic state vectors are computed with respect to each camera (see *Section 2*). The velocity of the meteor is computed if it has been recorded on at least 4 video frames. Meteors with a length of 3 frames are only used to compute the support plane.
3. **Determination of the initial state vector in an Earth-Centric coordinate system (ECCS):** The trajectory vectors and the time information are now used to generate two Cartesian state vectors $\vec{s}_{ICC7}$ and $\vec{s}_{ICC9}$ of the meteor in an Earth-Centric coordinate system. NASA's *SPICE* software package is used for the computation of orbital elements and other astro-dynamical properties[1]. Furthermore, a Python wrapper needs to be used since currently no native Python support is available[2].

   First, the orbital elements of the two state vectors are computed in ECCS. If the determined initial meteor velocity does not exceed 11.2 km/s (escape velocity of the Earth), the corresponding eccentricity is between 0 and 1, which corresponds to a bound orbit around the Earth. The reasons for these bound meteoroids could be:

   - The meteor decelerated already in the atmosphere before it was detected by CILBO.
   - The meteor was a piece of a space debris on an Earth-bound orbit.
   - The meteor was a meteoroid which has been captured by Earth following a "mini-moon" orbit with a decreasing velocity due to close encounters with Earth and friction with its exosphere.
4. **Backward propagation:** If the eccentricity is $e \geq 1$ the corresponding meteoroid was on a para- / hyperbolic orbit in ECCS. In this case the initial state

[1] http://naif.jpl nasa.gov/naif/index html
[2] https://github.com/AndrewAnnex/SpiceyPy

vectors are computed backwards in time until the state vectors reaches Earth's Sphere-of-Influence (SOI) within a certain threshold (e.g. with an accuracy of 1^s, so called threshold time).

The SOI is the approximate spheroid-shaped region around a planetary body where the dominant gravitational force comes from the body. Influences and perturbations such as other planets or by the Sun can be neglected. This simplification allows a quicker trajectory computation since the orbit computation becomes a 2-body problem. The radius of a simplified spherical SOI r_{SOI} can be computed by the following equation, where a is the semi-major axis and m is the mass of the Earth. M is the mass of the Sun. This leads to a SOI radius for Earth of approximately 900000 km.

$$r_{SOI} = a \cdot \left(\frac{m}{M}\right)^{\frac{2}{5}}$$

An adaptive algorithm has been developed to compute the meteoroid's state vector at Earth's SOI. Initially, the backwards time steps are set to 1000 s. With an initial velocity of e.g. 30 km/s this leads to a propagation step of 30000 km. After crossing the SOI border, the propagation time is inverted and decreased by an order of magnitude until the meteoroid crosses the SOI again. This iterative approach is repeated until the threshold time is reached.

5. **Computing orbital elements in heliocentric coordinates:** After reaching Earth's SOI the state vector is transformed to the heliocentric coordinate system in J2000 (ECLIPJ2000). This requires that the state vector of the Earth is added to the meteoroid's one. With the final state vector the orbital elements can be computed. Additionally, further astro-dynamical properties can be computed like e.g. the radiant in an Earth-Centric Sun-Pointing coordinate system to identify sporadic background sources like e.g. the Apex- or Anti-Helion-Source.

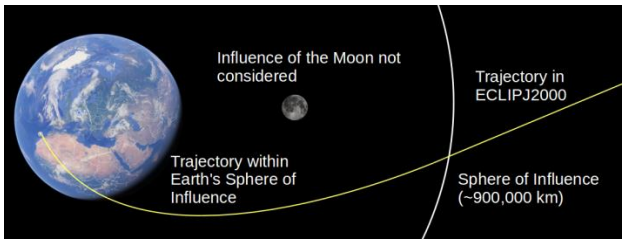

Figure 5 – Schematic overview of the computation procedure within Earth's vicinity (graph not in scale). The initial meteor state vector is computed above the Canary Islands and computed back in time until it reaches the Sphere of Influence of Earth (SOI, approx. 900000 km). For this computation the gravity of the Moon and other celestial bodies is not considered. At the SOI the state vector of the meteoroid is transformed to a heliocentric coordinate system (ECLIPJ2000). Meteors that have a bound orbit around Earth cannot reach Earth's SOI. In this case, the final ECLIPJ2000 transformation is not applied.

Error propagation and computation

The described orbit determination procedure computes the orbital elements and further properties of the trajectory with respect of ICC7 and ICC9. However, it does not contain the astrometric accuracy as an input error source. Here, an MC-based approach is presented that has been developed for the described orbit determination algorithm. *Figure 6a to 6d* show schematically the procedure for a meteor with a length of 5 frames, projecting the MC-generated astrometric data on a support plane.

Figure 6a shows the determined astrometric data of the 5 photometric centers of the observed meteor. Due to the optical distortion and the quantization of the measurements these position values do not follow a perfect trajectory path. The white arrow indicates the flight direction of the meteor and represents the determined flight direction vector by *MOTS*.

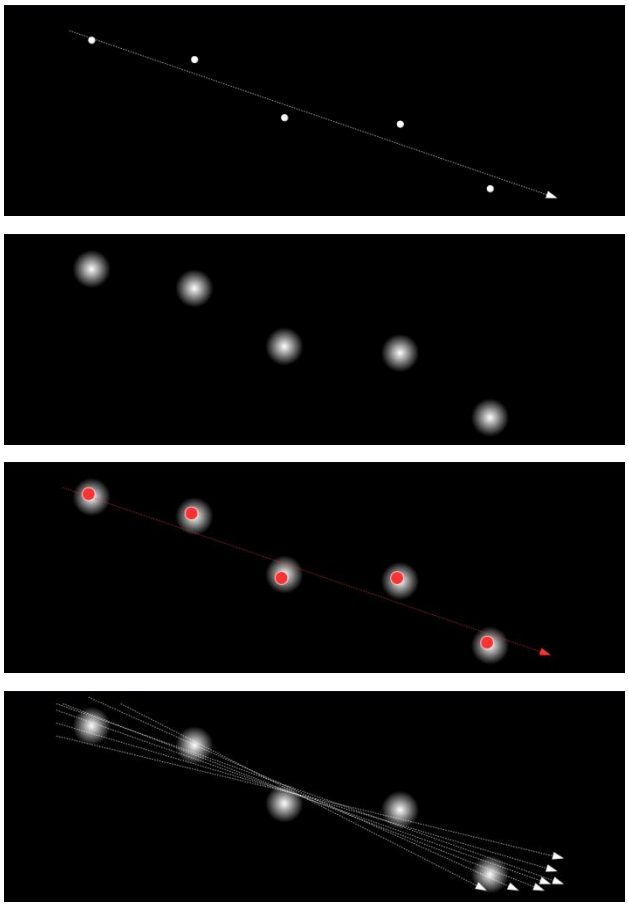

Figure 6a,b,c,d – Graphical representation of the Monte-Carlo algorithm as explained in the text.

Each observation night *MetRec* saves a log file that contains the astrometric accuracy data of each meteor observation. The accuracy is derived from the variance of the astrometric data that are fitted on a great circle. These entries are used for the extension of the existing code to a Monte_Carlo version. The calculated astrometric positions of the meteor, (*Figure 6a*) are replaced by 2-D Gaussian distributions (*Figure 6b*). The standard deviation of the functions is the corresponding astrometric accuracy. These Gaussian distributions are assumed to represent the *Probability Density Function*

(PDF) of each determined photometric center. Since the angular distance between two right ascension values decreases for higher declinations, the Gaussian functions need to be scaled according to their corresponding declination.

A set of possible virtual observations can be generated, based on these PDFs. *Figure 6c* shows an example of a possible meteor flight path and position determination based on the measurement uncertainty. The red dots represent the newly generated photometric centers based on the Gaussian PDFs. The new flight direction path is computed, using the trajectory software *MOTS* (red arrow).

This re-sampling procedure is done several times, to generate an ensemble of possible flight direction paths (*Figure 6d*). This ensemble is then used to compute the orbital elements, using computation steps 3 to 5. To obtain sufficient statistical results the number of re-samples depends on the number of frames and the astrometric accuracy. However, a re-sampling size of at least 100 appears sufficient.

Unbiased Descriptive Statistics

The MC approach provides a set of possible solutions. The final statistical analysis links each solution with a probability. To obtain statistical conclusions out of the resulting data set, the correct descriptive statistical parameters must be chosen. Distributions are often described by a mean and standard deviation. However, these parameters apply only for Gaussian and symmetric distributions. Since the outcome of a MC computation is unknown and likely not Gaussian or symmetric, different parameters are required. *Figure 7* shows an example of an MC-result. The distribution shows possible argument of periapsis solutions of a meteor detected at 2014-08-01T22:54:26, visualized as a histogram with evenly spaced bars. The red (dotted) and blue (solid) vertical lines indicate the mean and median (separation between lower and upper half of the distribution) respectively. The blue dashed lines show the upper and lower boundaries of the quartiles of the data (quartiles: separate the data in lowest 25 % and highest 75 % and and vice versa). The plot provides information on the mean and standard deviation, median and median absolute deviation, interquartile range and the lower and upper quartile. The IQR, by definition contains 50% of the entire dataset. The *Median Absolute Deviation* (MAD) is a descriptive parameter for the scattering and variation of the data around the median and is defined by (where X_i is an element of the data array X of length n):

$$MAD = median(|X_i - median(X_i)|)$$

Due to the skewness of the distribution the mean is shifted by about 4 % with respect to the median. Outliers do not affect the median if the total number of re-samples is large compared to the number of outliers. Since the shape of the distributions from the MC code is unknown, we recommend using the following entries per each orbital element and further astro-dynamical calculations:

- Median;
- Median Absolute Deviation;
- Interquartile Range;
- Lower and Upper Quartile (and also additional data separations at 15 % and 85 %).

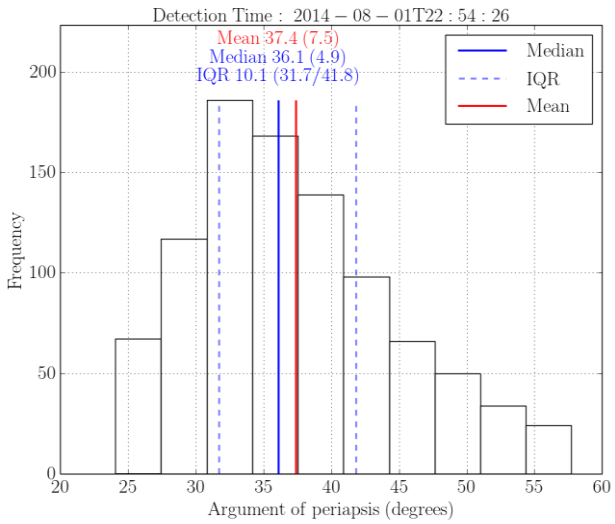

Figure 7 – Argument of periapsis distribution (Meteor detection time: 2014-08-01T22:54:26) to visualize different descriptive statistical parameters. The dotted red and blue line show the mean and median, respectively. The blue dashed lines show the quartiles of the distribution. Above the distribution the corresponding values are shown. The standard deviation and median absolute deviation are given in parenthesis next to the mean and median values. The last row shows the width of the interquartile range, with the lower and upper quartile range given within the parenthesis. The re-sampling size is 1000.

Saving the mean and standard deviation helps to estimate the shape of the final distributions. Assuming a distribution is Gaussian shaped, the MAD scales with the standard deviation σ by a constant factor. The conversion is:

$$\sigma \approx 1.4826 MAD$$

If the determined standard deviation and scaled MAD value are comparable, the final distribution is likely to be symmetrically shaped or even Gaussian.

Additionally, the covariance matrix between the orbital elements is saved in order to have a quantitative measure of the dependencies between each orbital element.

4 Conclusion

In this work we presented a Monte-Carlo based extension of the *MOTS* software. The developed algorithm considers the astrometric accuracy and previous works on the velocity determination bias, as well as un-biased descriptive statistical parameters to compute possible meteor orbit solutions.

Reference

Albin T., Koschny D., Drolshagen G., Soja R., Srama R. and Poppe B. (2015a). “Influence of the pointing direction and detector sensitivity variations on the detection rate of a double station meteor camera”. In Rault J.-L. and Roggemans P., editors, *Proceedings of the International Meteor Conference*, Mistelbach, Austria, 27-30 August 2015. IMO, pages 225–231.

Albin T., Koschny D., Drolshagen G., Soja R., Srama R. and Poppe B. (2015b). “De-biasing of the velocity determination for double station meteor observations from CILBO”. In Rault J.-L. and Roggemans P., editors, *Proceedings of the International Meteor Conference*, Mistelbach, Austria, 27-30 August 2015. IMO, pages 214–219.

Drolshagen E., Ott T., Koschny D., Drolshagen G. and Poppe B. (2014). “Meteor velocity distribution from CILBO double station video camera data”. In Rault J.-L. and Roggemans P., editors, *Proceedings of the International Meteor Conference*, Giron, France, 18-21 September 2014. IMO, pages 16–22.

Drolshagen S., Kretschmer J., Koschny D., Drolshagen G. and Poppe B. (2015). “Mass accumulation of Earth from interplanetary dust, meteroids, asteroids and comets”. In Rault J.-L. and Roggemans P., editors, Proceedings of the International Meteor Conference, Mistelbach, Austria, 27-30 August 2015. IMO, pages 220–225.

Kretschmer J., Drolshagen S., Koschny D., Drolshagen G., Poppe B. (2015). “De-biasing CILBO meteor observational data to mass fluxes”. In Rault J.-L. and Roggemans P., editors, *Proceedings of the International Meteor Conference*, Mistelbach, Austria, 27-30 August 2015. IMO, pages 209–213.

Koschny D. and Diaz del Rio J. (2002). “Meteor Orbit and Trajectory Software (MOTS) - Determining the Position of a Meteor with Respect to the Earth Using Data Collected with the Software MetRec”. *WGN, the Journal of the IMO*, **30**, 87–101.

Koschny D., Bettonvil F., Licandro J., v. d. Luijt C., Mc Auliffe J., Smit H., Svedhem H., de Wit F., Witasse O. and Zender J. (2013). “A double-station meteor camera setup in the Canary Islands – CILBO”. *Geosci. Instrum. Method. Data Syst.*, **2**, 339–348.

Koschny D., Mc Auliffe J., Bettonvil F., Drolshagen E., Licandro J., van der Luijt C., Ott T., Smit H., Svedhem H., Witasse O. and Zender J. (2014). “CILBO - Lessons learnt from a double-station meteor camera setup in the Canary Islands”. In Rault J.-L. and Roggemans P., editors, *Proceedings of the International Meteor Conference*, Giron, France, 18-21 September 2014. IMO, pages 10–15.

Molau S. (1999). “The Meteor Detection Software MetRec”. In Arlt R. and Knoefel A., editors, *Proceedings of the International Meteor Conference*, Stara Lesna, Slovakia, 20-23 August 1998. IMO, pages 9–16.

Ott T., Drolshagen E., Koschny D., Drolshagen G. and Poppe B. (2014). “Meteoroid flux determination using image intensified video camera data from the CILBO double station”. In Rault J.-L. and Roggemans P., editors, *Proceedings of the International Meteor Conference*, Giron, France, 18-21 September 2014. IMO, pages 23–29.

An antenna, a radio and a microprocessor: which kinds of observation are possible in meteor radio astronomy?

Lorenzo Barbieri

[1] **RAMBo meteor group, AAB, Associazione Astrofili Bolognesi, Bologna, Italy**
barbieriofiuco@gmail.com

Radio meteors are usually investigated by professional radars. Amateur astronomers cannot have transmitters, so usually they can only listen to sounds generated by a radio tuned to a TV or military transmitter. Until recently, this kind of observation has not produced good data. The experience of "RAMBo" (Radar Astrofilo Meteorico Bolognese) shows which data can be extracted from an amateur meteor scatter observatory and the results which can be achieved.

1 The meteor scatter observatory

Meteor shower observations, traditionally carried out by visual observers, have for several years also used automatically recorded images captured by TV cameras and can also be carried out using radio waves.

At an altitude of around 100 km in the upper atmosphere, the bremsstrahlung begins by the friction of meteoric particles intercepted by the Earth in its movement around the Sun. It is here that meteors appear. The bremsstrahlung by friction leads to extensive overheating of the corpuscle (ablation), the result of which is the vaporization of the material entering the atmosphere, the generation of light, and the ionization of a large number of atmospheric molecules in a radius of some meters along its trajectory. This generates a long, narrow cylinder of ionized molecules of a very short time duration (the time required for recombination of the ionized molecules) which behaves like a reflective object for radio waves, in the same way as aircraft and satellites.

"Radio meteor" observation is not affected by the presence of the Sun or Moon, or by cloud, and can thus be carried out continuously. Meteor observing via radio waves is usually achieved by "traditional" radar, which consists of a transmitter and a receiver. Normally these pieces of apparatus are spaced hundreds of kilometers apart and the antennas point towards the layers of the atmosphere around the 100 km altitude in the midway position between transmitter and receiver. The transmitted signal is directed upwards so it can only be received when a reflective object is placed along the radio electric emission optical path. When this occurs, the signal is reflected and the receiver picks up the presence of the object.

Professional radars, thanks to the fact that they transmit pulsed signals and that they use complex antenna arrays to analyze the reflected signal, are able to calculate the size, speed, direction and position of meteors at the sky. Since amateur observers cannot own transmitters, they commonly use other people's transmitters, e.g. transmitters on VHF (Very High Frequency), possibly on air day and night, with high power and at a great distance. They may be radio or television transmitters, or equipment installed for military aircraft and satellite control.

This situation has two great drawbacks.

Firstly, the exact technical characteristics of the transmitter and its behavior are unknown.

Secondly, the absence of multiple arrays of antennas and the lack of pulsed signals greatly reduce the capabilities of an amateur setup compared to a professional one. The experience of RAMBo (Radar Astrofilo Meteorico Bolognese) shows which data can be extracted from such observations and the results which can be achieved.

2 "RAMBo" set up

The transmitter

Like other European observatories, RAMBo uses a military radar transmitter, GRAVES, that is continuously on air in VHF at great power. Located near Dijon, in France, it is built for spacecraft orbit determination.

Its transmission is directed upwards and due to the Alps, it is not receivable from Bologna directly.

Technical data:

- Frequency 143.050 MHz
- Polarization: circular
- Power = 1MW (RF)
- Irradiation = south ± 90 °
- Height oscillating in an angle of about 25 °

The receiver setup

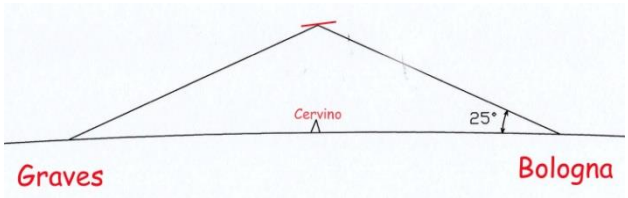

Figure 1 – Calculation of the zenithal angle of view.

The RAMBo receiving set up is composed of a Yagi directive antenna (10 elements) pointed in azimuth in the direction of the transmitter (300°), and in declination about 25 degrees above the horizon (*Figure 1 and 2*), the direction in which we have calculated the reflection point in the upper atmosphere.

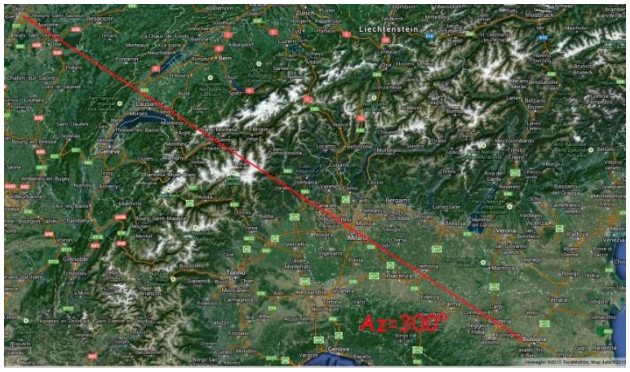

Figure 2 – Calculation of the angle of view in azimuth.

Its polarization is vertical. The choice of this polarization is based on the belief that there could be more meteors with horizontal rather than vertical traces.

Since the polarization of the transmitter is circular, and the polarization emerging from the reflection is orthogonal to the plane of reflection, we can expect a greater number of vertically polarized echoes than horizontal ones. In fact, a week of measurements specifically performed with horizontal polarization gave a two-thirds lower result compared to the vertical configuration.

Given the characteristics of the antenna (large directivity), the area of sky that should be investigated consists of an area of twenty to thirty square degrees above the Alps, roughly vertically above the Matterhorn.

The receiver is a Yaesu 897 tuned in SSB (Single Side Band) about 1000 Hz below the Graves carrier. Thanks to the SSB technique, the difference between these two frequencies means that the Graves carrier (not modulated) may be heard as a signal of frequency equal to the difference between the two frequencies. As we will see, this rate is actually affected by the Doppler Effect, both for the body speed when entering the atmosphere and for the speed of movement of the ionized cylinder due to high altitude winds.

The purpose of RAMBo is the analysis of the audio signal generated by the receiver.

3 Sound analysis

Sound is picked up from the direct audio output of the receiver, avoiding the potentiometer controlled headset output, and with the automatic gain control (AGC) disabled.

Normally the audio signal is a continuous rustle (chaotic noise). Over this signal we can occasionally hear three different types of sound:

- Discharge;
- Aircraft and satellites;
- Meteoric echoes.

The discharges are transient pulses: very short in time and of high amplitude, sometimes individual and sometimes in rapid sequences of variable length. These impulses, if measured and counted, represent “false positives” which will affect meteoric data.

There are a lot of causes of discharge: they may come from storms, even far away, or from ionization due to solar activity. Other causes are human activities: combustion engines in the receiver proximity, electric motors or other power transients on the power line feeding the radio receiver, such as neon lighting. These last problems can be overcome by using a power supply with a daytime battery charged by a solar panel. However, this does not completely solve the problems caused by discharges received in the antenna.

Discharges are the biggest problem of meteor scatter receivers. The RAMBo experience led to six different trials with various techniques to avoid this problem. Only the sixth attempt finally solved the problem.

Aircraft and satellite echoes are similar to those generated by meteors, but are generally of lower level, their frequency varies slowly and their duration is high. These echoes could be numerous if we receive with omnidirectional antennas and if the receiver is close to large urban areas with an airport nearby. The use of high-gain antennas (i.e. directive) solves this problem. In our case, aircraft and satellites are almost never received, and the sound level of their echoes is lower than that of meteors.

Meteors produce clear sound characterized by a frequency near 1000 Hz. This frequency, in theory, is generated by the beat between the transmitter’s carrier (in our case the Graves Tx) and the frequency of the radio receiver, tuned in at SSB 1000 Hz below the transmission carrier. The exact value of the echo frequency is not easy to predict, due to both possible instability or radio receiver tolerances, as well as to the speed of high altitude winds which propel and distort the ionization cylinder caused by the meteor’s entry into the atmosphere. Finally, the speed and direction of the meteor could also affect this frequency (Doppler Effect).

Our experience leads us to say that this variability is almost always confined inside a window of approximately 300 Hz centered on the mean frequency.

The sound analysis and data recording are both made with Arduino, the well-known low-cost microprocessor of the “Internet of Things” (IoT) through a program which we have written (*Figure 3*).

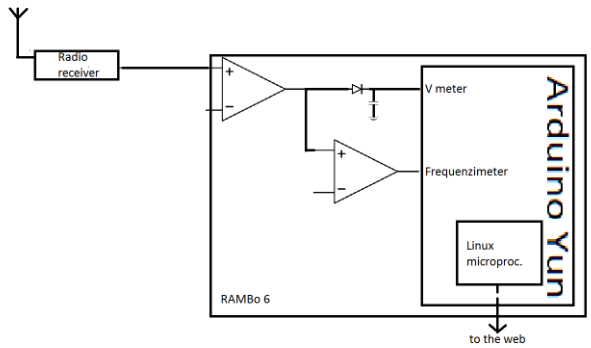

Figure 3 – Block diagram.

RAMBo 6 acts as a preamplifier for the signal coming from the radio output and then splits it into two different channels. After a further amplification, the signal is rectified and integrated. This allows Arduino to measure the received signal amplitude (*Figure 4*).

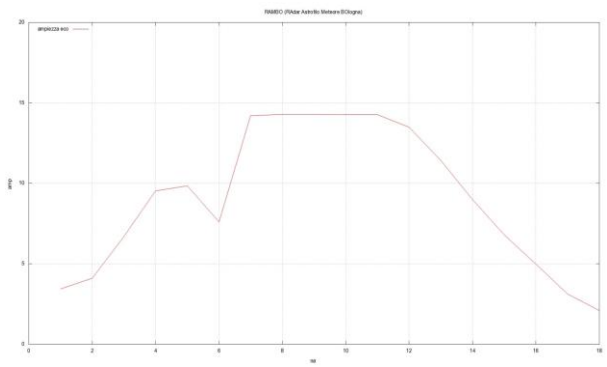

Figure 4 – An overdense meteor profile generated by "Rambo".

In this graph we can see an overdense meteor echo analyzed by RAMBo. In *Figure 5* there is another overdense meteor profile found in literature.

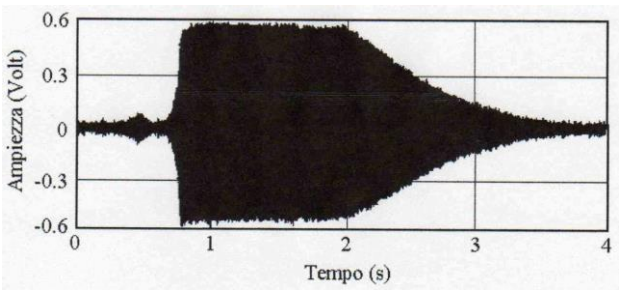

Figure 5 – An overdense meteor profile coming from a professional radar.

As can be seen, the profile is roughly the same.

At the same time, the signal is measured by using Arduino as a frequency meter. Normally, the signal of chaotic noise contains random frequencies. As soon as a meteoric echo arrives, the measured frequency tends to be confined inside a window centered about the mean frequency previously set. When this occurs, RAMBo starts counting time. At the end of this process, when the measured frequency comes back chaotic, Arduino has recorded both the echo duration (in milliseconds) and day and time of the event.

For each echo, RAMBo assigns a serial number. In addition at the zero minute of every hour, Arduino zeroes the meteor/hour count and then starts again from one.

The analysis of the rise time of the initial impulse gives us a figure that is proportional to the meteor speed coming into the atmosphere. The shorter the rise time, the faster the meteor speed, and vice versa.

4 The data logger

The data we now have included:

- Progressive event number;
- Hourly number;
- Date and time (UT);
- Echo length (milliseconds);
- Echo amplitude (millivolts);
- A number proportional to the rise time.

For each echo RAMBo6 creates a CSV-type (common separated values) data string containing the six listed items of information.

Every row generated by an echo is added to a log file.

Every night at 18^h U.T. Arduino sends the file via internet to a cloud site, so it can be analyzed at home.

Graphic layout

The log file is normally represented in a graphic form using math graphic software (e.g.: *gnuplot*). In this graph (*Figure 6*) we can see the result of a weekly recording.

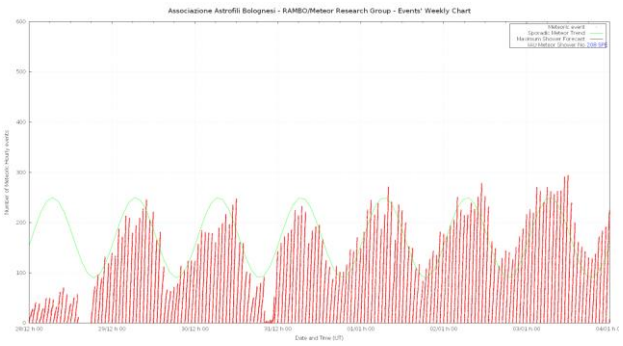

Figure 6 – A weekly "Rambo" hourly rate (HR) layout.

Each red dot represents a meteor echo; on the x-axis there is time, on the y-axis the number of events. In this manner, the height of each column represents the number of meteors per hour (hourly rate). The dot size is proportional to the echo duration logarithm.

The sinusoidal trend is clear, approximated in green, due to the diurnal variation of the apparent speed with which the Earth impacts the meteors. Day 29/12 was the first day in which Rambo6 began to run. The comparison with the previous day shows the sensitivity increase compared to the previous version (RAMBo5).

5 How much it costs

Here is a summary of the cost of RAMBo in Euros:

- Antenna 74;
- Cable 10;
- Connectors 5;
- Radio (2nd hand) 500;
- Sound card 40;
- Arduino Yun 68;

Total 697

As can be seen, a meteor scatter observatory of this kind is well within the reach of many amateur groups.

6 The results

Rambo 6 registers more than 2500 meteorological echoes a day, with an hourly average of about 100.

- Overdense meteors (echoes longer than 800 ms) account for about 1%, according to data in literature.

- In the days without meteor showers, we can recognize the typical sinusoidal sporadic meteor trend, with the maximum at 6 and the minimum at 18 (Local Time).

- In the case of meteor showers we can easily see the beginning time, the maximum and the end.

- We can also evaluate the shower intensity, with reference to the standard sporadic trend (Hourly Rate).

$$ZHR = \frac{\overline{HR} \cdot F \cdot r^{6.5-lm}}{\sin(hR)}$$

For this purpose we have developed a special program (in Python) for meteor shower analysis. With this program, we first subtract the average value of sporadic days immediately before and after the meteor shower containing only sporadic activity, then we adjust the hourly rate with a number proportional to the tangent of the radiant height on the horizon. We thus obtain a value very similar to the ZHR (Zenith Hourly Rate) commonly used in visual observations. An example of such processing (*Figure 7*) comes from the "RZHR" program, i.e. RAMBo ZHR.

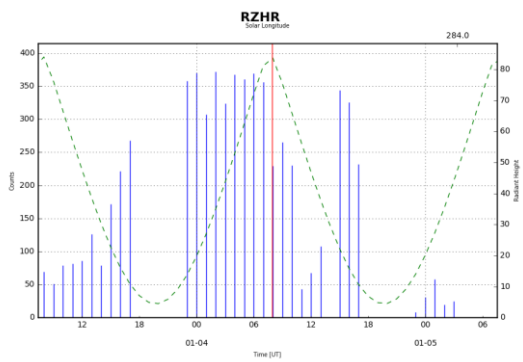

Figure 7 – An RZHR graph.

In this graph we can notice the beginning of the transit of the Earth through the Quadrantids cylinder and the Rzhr value. We can still see that also in this case the Quadrantids have a bipolar structure, similarly to other streams (e.g. Geminids).

The dotted green line shows the radiant height on the horizon. The red line shows the moment in which the shower maximum was expected. RAMBo is thus able to indicate with great accuracy the time difference between predictions and observations.

- RAMBo also allows us to carry out a meteor mass evaluation. Since the echo duration is proportional to the meteor dimension, we can see the mass trend over time.

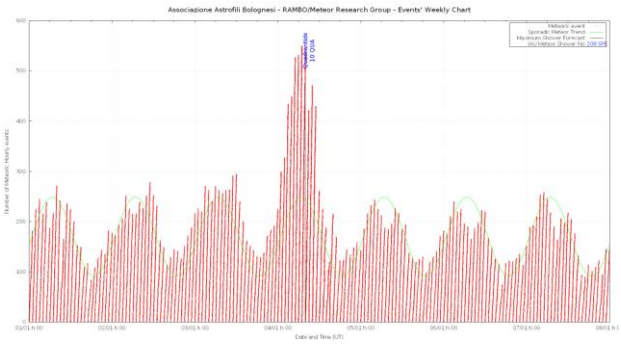

Figure 8 – The 2016 Quadrantids HR.

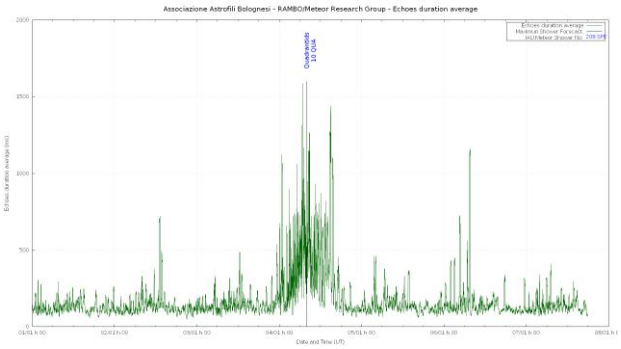

Figure 9 – The 2016 Quadrantids mass trend.

Figures 8 and 9 show the same period of time (a week). In the former we can see an activity increase in the number of echoes (hourly rate) due to the meteor shower. In the latter we note a meteor mass increase due to the echo duration average. Although the time period is the same, the two ordinate values are completely different. So the trend analogy is impressive. In the mass trend graph, the bipolar structure of the swarm is clearly visible, just as can be seen in the hourly rate graph.

7 Future developments

The image of the RZHR graph in the previous chapter concerning the Quadrantids swarm partially shows the shower. Most of the beginning and end of the shower is lacking. This is due to the fact that during the phenomenon the radiant was not always above the horizon.

In essence: if it is true that a meteor scatter observatory can observe night and day, with and without the Moon, in good and bad weather, it is equally true that it can

observe a meteor shower if and only if its radiant is above the horizon. It follows therefore that any observer coverage, as with any other type of observation, is partial.

Like visual or video observations, meteor radar observation should also create a global network able to achieve total coverage.

What is primarily needed is a small network of a few observers strategically placed almost 120° apart in the same hemisphere so as to create complete coverage for each radiant.

8 The "Marsadl"

(Meteor Analyzer by Radio receiver, Sound Analyzer and Data Logger)

The RAMBo6 experience was conceived as an example of the "Internet of Things" (IoT) that simplifies the feasibility of many projects in various fields. So this leads us to propose this low-cost, simple project as an idea to set up a meteor scatter observer network. What is needed for every observer can be summarized as follows:

1) The existence hundreds of kilometers away of a VHF transmitter continuously *on air*, whether it is military or television whose carrier can be tuned in amplitude modulation;
2) A Yagi directive antenna (from 6 to 10 elements) with a vertical polarization mount in a fairly unobstructed area, pointing in azimuth in the direction of the transmitter and with a declination pointing above the midpoint of the line between T_x and R_x at about 100 km altitude;
3) A receiver with good input sensitivity tuned in SSB mode 1000 Hz over the carrier (USB: Upper Side Band), with the audio output independent to the squelch and the volume potentiometer, and with automatic gain control (AGC) disabled;
4) An ANALOG power supply (and therefore not a switcher) able to feed all the apparatus 24 hours a day;
5) A network cable with web access for the data uploading.

The circuit diagram, the Arduino software and our data analysis script are available to anyone interested in this experience. The data of all those who join MARSADL will be shared, so to create a network that not only stores data but allows us all to analyze the information together.

With 157 IMC participants, the lecture room always was well filled. (Photo Casper ter Kuile).

Accurate Geminid velocities with CHIPOlAtA

Felix Bettonvil

Sterrewacht Leiden, Universiteit Leiden, Niels Bohrweg 2, 2333 CA Leiden, the Netherlands

NOVA Optical and Infrared Instrumentation Division at ASTRON, Oude Hoogeveensedijk 4, 7991 PD Dwingeloo, the Netherlands

KNVWS Meteor Section, the Netherlands
bettonvil@strw.leidenuniv.nl

For several years, the high-resolution photographic camera CHIPOlAtA has been used to acquire precise orbits for Geminid and Perseid meteor shower members. In this paper I analyze the first set of data obtained during the Geminids 2014.

1 Introduction

CHIPOlAtA (Bettonvil, 2014, 2015) is a photographic camera system that is equipped with a precise and fast chopping shutter, enabling precise measurement of the velocity of a meteor. This is the most critical parameter in the determination of its orbit, hence accurate measurement is crucial.

The camera comprises a Liquid Crystal (LC) optical chopper (Bettonvil, 2010), which periodically switches between dark and transparent state up to several hundred cycles/sec[1], much faster than traditional meteor photography, and comparable with the – somewhat slower (100Hz), but more sensitive – CABERNET system as operated in the French Pyrenees area by IMCCE (Vaubaillon, 2014).

High resolution orbit determination is valuable as it permits detection of fine structures in meteoroid streams and provides accurate input for meteoroid stream modelling.

This paper focuses on the reduction of obtained data, in particular the Geminids 2014. In the next Section first a brief description of the instrument setup is given.

2 Instrument description

CHIPOlAtA consists of two Canon 550D 18Mpxl DSLR cameras mounted on the same tripod and aligned such that one long FoV is obtained. With a relatively long focal length of 50mm a field of 18x50 deg^2 is formed, which is always aligned such that the long axis points to the radiant. Each camera has a built-in LC shutter, which are operated synchronously. All data is stored in jpeg format. The sensitivity is set to ISO 6400, exposure time 14s.

CHIPOlAtA is always operated in double station mode, the second station being a wider field, lower resolution system, mostly video, depending on the location of the observations. The two stations together enable trajectory and orbit calculation.

Technical details on the instrumental setup is given in (Bettonvil, 2014, 2015).

3 Data

So far, 4 observing campaigns have been carried out, covering the Perseids and Geminids in 2014 and 2015. Geminids are always observed with chopper frequencies of 200Hz, Perseids -due to their higher velocity- with 300Hz. Preliminary results have already been reported earlier (Bettonvil, 2014, 2015). *Table 1* gives an overview of the collected data. So far ~66 meteors have been captured, of which ~75% were double station.

In this paper I will focus on the data of the Geminids 2014. This campaign was carried out in The Netherlands, as weather in other parts of Europe was too unstable to justify a trip elsewhere. Fortunately, the conditions in The Netherlands turned out to be rather good. Klaas Jobse (Oostkapelle), with his CAMS Benelux cameras, served as the second station (Roggemans et al., 2016).

4 Analysis

Depending on the brightness, trail lengths vary between ~40 and over 200 breaks, and can extend over 2500 pixels long. Bright meteors have easily measurable breaks; the weakest tend to fade out in the background noise. This noise varies from image to image and cannot be subtracted by taking dark fields.

For the analysis presented here, we focus on the three brightest captures, having (visual) brightness's of resp. +1, 0 and –2:

- December 14, 2014, $00^h54^m55^s$ UT, magnitude +1
- December 13, 2014, $23^h40^m26^s$ UT, magnitude 0
- December 14, 2014, $00^h22^m44^s$ UT, magnitude -2

[1] http://www.lc-tec.com/optical-shutter (LC-Tec, 2015)

Table 1 – Overview of all collected data so far during Perseid and Geminid observing campaigns in 2014 and 2015. Shown are location, optics, chopper frequencies, resolution, total number of trails captured, and double station captures. The results of CABERNET (Geminids 2015) are not known yet, and as such the number of double station captures is pending.

Shower	Location	Lens	Cycl/s	Resolution	2nd cam	# trails	# double station
Perseids 2014	Bosnia	50/F2.8	50–200 Hz	21"	none	5	none
Geminids 2014	Netherlands	2x50/F2.8	200 Hz	21"+17"	video	17	13
Perseids 2015	Croatia	2x50/F2.8	200–300 Hz	17"+17"	12M + video	13	10
Geminids 2015	France	2x50/F2.8	200 Hz	17"+17"	CABERNET*	31	?

(*) See Vaubaillon (2014).

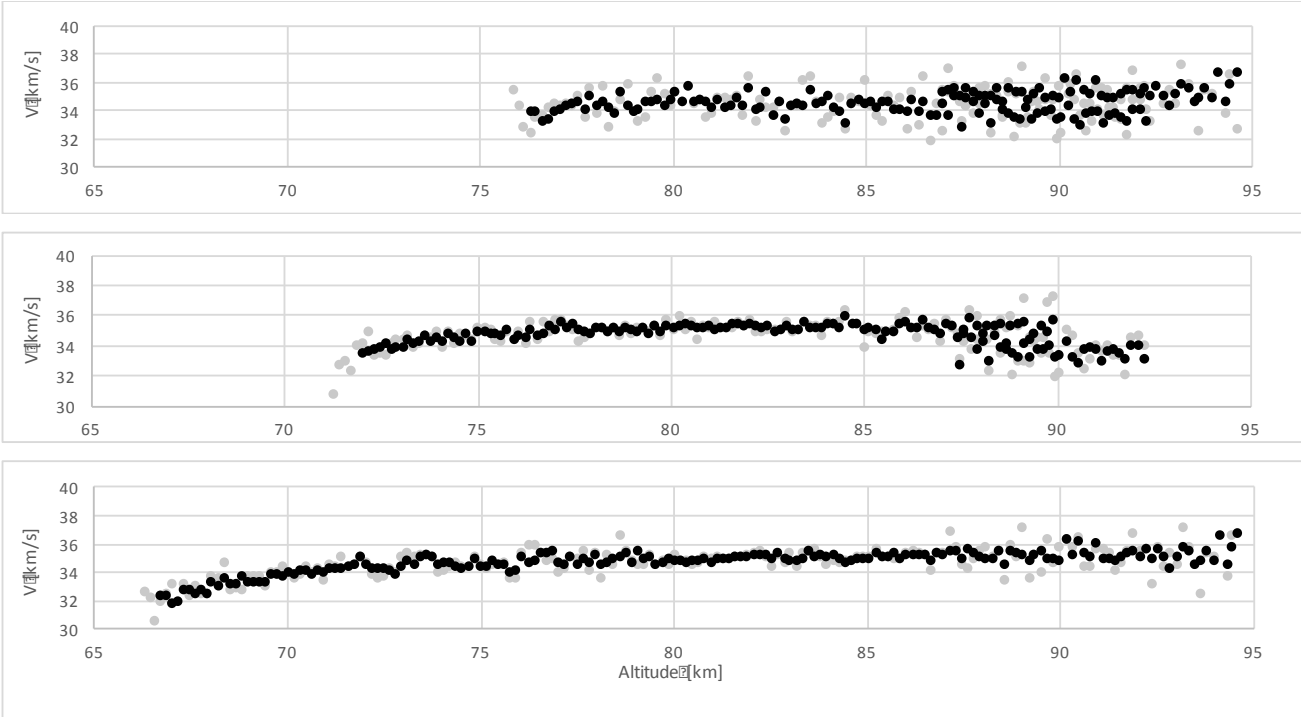

Figure 1 – Velocity profiles for all analyzed Geminids. Top: Geminid +1; Center: Geminid 0, Bottom: Geminid –2. Vertical and horizontal scale for all plots is the same. Grey dots represent a 3pt running average, black dots a 6pt running average.

The data reduction largely follows the method described in (Bettonvil, 2015). Astrometry is done with SAO Image DS9[2], and both the positions of reference stars and meteor breaks measured with the help of the centroid function, which works reasonable well as both stars and meteor breaks are quasi-circular dots. The reproducibility of an individual measurement is typically in the range of 0.2 – 0.5 pxl, which depends largely on the brightness: bright dots are less affected by the background noise.

Plate reduction is carried out with own software[3] and, due to the lack of distortion, is straightforward. Astrometric solutions are typically precise to a couple of arc seconds.

Following the astrometry, the atmospheric trajectory is calculated, again with own software, and based on the method of intersection of planes. The line of intersection represents the meteor trajectory and finally all meteor break measurements are projected on to this line. As a result, the length of the individual breaks in kilometers and also the velocity in km/sec become known.

5 Discussion

Figure 1 illustrates the measured velocity of the three analyzed Geminids. We will now look more closely at this velocity.

First of all, we can conclude that the weakest part of the trail (always the initial part) does indeed give a larger spread in velocities than the brighter parts. In addition, the +1 Geminid trail shows more variation than the brighter 0 and –2 Geminids.

The bright central parts of the 0 and –2 Geminids show stable and constant velocity.

All three meteors, but most strikingly the brightest Geminids, show a deceleration. The brighter Geminids tend, as expected, to reach lower altitudes.

From the distribution of the velocities we are able to say more about the accuracy obtained, which is illustrated in *Table 2*. The average velocity is computed from all data

[2] http://ds9.si.edu/site/Home html
[3] Meteor35 – Software package for reduction of meteor orbits, including astrometry, atmospheric trajectory calculation and orbital elements, developed by the KNVWS Meteor Section.

in the first half of the trail (and thus the part with the evident deceleration is left out). In first order it is assumed that the velocity of this first part represents V_∞. Over the entire first part the standard deviation amounts from 0.3 to 0.6 km/s per measured dot, or 1–2% of the computed velocity, which amounts to ~0.1–0.2 pxl uncertainty per measured dot. If we assume a constant velocity, the average velocity can be determined with an accuracy better than 0.01 km/s in all cases.

Table 2 – Average apparent velocity and obtained accuracies for the three Geminids.

	+1	0	-2
Average V [km/s]	34.01	35.18	35.05
STDV [km/s]	0.63	0.32	0.41
Error avg [km/s]	0.008	0.005	0.004
Accuracy [km/s]	–	0.05	0.08

The question that then pop ups is if we are allowed to assume that the velocity in the first part is indeed constant? For this reason, the velocity in the brightest central part of the two brightest parts is analyzed a bit more closely: these parts have been split in two and for each of them the average velocity has been computed. The conclusion is clear: in both of these cases the velocity in the first part is higher than for the second half, with a difference of respectively 0.05 and 0.08 km/s for the two brightest Geminids. This allowed us to conclude that deceleration is already present in the brightest part.

6 Conclusions

The above results indicate that rather than averaging the first half of the trail to obtain an estimate for V_∞, a fit based on a deceleration model (e.g. exponential, Gompertz or other) is required. We can conclude that the true V_∞ is therefore slightly higher than the average velocity computed so far until now (with an approx. amount indicated with 'Accuracy' in *Table 2*). Exact calculation of V_∞ is to be done and planned for the near future.

7 Future

Until now, Canon 550D DSLRs have been used for CHIPOlAtA. Nowadays much better cameras are available, with both higher sensitivity and lower noise, allowing for a more rapid collection of a large data sample.

References

Bettonvil F. (2010). "Digital All-sky cameras V: Liquid Crystal Optical Shutters". In Andreic Z., and Kac J., editors, *Proceedings of the International Meteor Conference*, Poreč, Croatia, 24-27 September, 2009. IMO, pages 14–18.

Bettonvil F. C. M. (2014). "High resolution photographic imaging". In Rault J.-L. and Roggemans P., editors, *Proceedings of the International Meteor Conference*, Giron, France, 18-21 September 2014. IMO, pages 30–33.

Bettonvil F. C. M. (2015). "High resolution orbits of Perseids and Geminids with CHIPOlAtA". In Rault J.-L. and Roggemans P., editors, *Proceedings of the International Meteor Conference*, Mistelbach, Austria, 27-30 August 2015. IMO, pages 78–82.

Roggemans P., Breukers M. and Johannink C. (2016). "Status of the Benelux CAMS network". In Roggemans A. and Roggemans P., editors, *Proceedings of the International Meteor Conference*, Egmond, the Netherlands, 2-5 June 2016. Pages 254–260.

Vaubaillon J., Egal A., Clovirola A., Colas F., Bouley S., Atreya P., Reffet B. and Rudawska R. (2014). "The "CAmera for BEtter Resolution" (CABERNET): First scientific results". In Muinonen K. et al., editors, *Proceedings Asteroids, Comets, Meteors 2014*, Helsinki, Finland, 30 June - 4 July, 2014. Page 549.

Photographic spectra of fireballs

Jiří Borovička

Astronomical Institute of the Czech Academy of Sciences, 251 65 Ondřejov, Czech Republic
jiri.borovicka@asu.cas.cz

Two methods of spectroscopy of meteors using image intensified video cameras and classical photographic film cameras are compared. Video cameras provide large number of low resolution spectra of meteors of normal brightness, which can be used for statistical studies. Large format film cameras have been used through the history and provide high resolution spectra, which can be used to derive temperature, density and absolute abundances of various elements in the radiating plasma. The sensitivity of films is, however, low and only spectra of bright meteors (fireballs) can be studied. Examples of photographic fireball spectra are provided.

1 Introduction

Spectroscopy of meteors becomes increasingly popular among both amateur and professional astronomers. Nowadays, mostly low resolution video spectroscopy is being used. Meteor spectroscopy, however, has a long history in which photographic techniques using classical photographic plates and films played a major role. But photographic spectra have not only historical value. In some respects, in particular resolution, they are superior in comparison with video spectra. Classical spectrographs are still in use at the Ondřejov Observatory. In this paper I will compare both techniques and their advantages. I will also present some examples of photographic spectra. In the future, nevertheless, high resolution digital cameras will be probably fundamental for meteor spectroscopy.

2 Brief history of instrumental meteor spectroscopy

The first meteor spectrum was photographed by chance on June 18, 1897, during the objective prism stellar spectroscopy program performed by the Harvard College Observatory in Arequipa, Peru (Pickering, 1897a;b;c). The first systematic photographic meteor spectroscopy program was set up in Moscow (Blajko, 1907). The first spectra were obtained with objective prisms on blue sensitive emulsions. Later, panchromatic and even infra-red emulsions as well as transmission diffractive gratings become available. Nevertheless, the number of obtained spectra increased only slowly and reached 122 worldwide in 1952 (Millman, 1952). The early history and the knowledge about meteor spectra around 1960 were described in Millman and McKinley (1963). At that time, large format photographic cameras with rather long focal length started to be used and detailed spectra of bright meteors containing over a hundred of emission lines were obtained (e.g. Halliday, 1961; Ceplecha, 1971; Borovička, 1993; 1994a). Of course, long term systematic observations were needed to capture a good fireball spectrum.

Later, spectra of fainter meteors were photographed by Maksutov cameras with large aperture (Harvey, 1973).

Television techniques started to be used for meteor spectroscopy as early as 1969 (Hemenway et al., 1971). Originally, it was necessary to film the TV monitor with a motion picture camera to analyze the spectra. Later it became possible to transform the video image to a hard copy. The full development of video spectroscopy started in 1990's with the advancement of computer technology. CCD spectrographs have been also occasionally used (Jenniskens, 2007).

3 Video spectra

An example of meteor spectrum obtained with video camera equipped with image intensifier is shown in *Figure 1*. Image intensifiers or very sensitive television cameras enable people to obtain also spectra of meteors fainter than magnitude zero. The wavelength coverage is quite wide, typically 400–900 nm, i.e. covering both visible and near infrared regions. On the other hand, the resolution of classical video signal, when digitized, is relatively low (768 x 576 pixels for PAL system). The resulting spectral resolution depends on the used lens and grating but is low in any case, typically 1 nm/pixel. The FWHM (full width at half maximum) of spectral lines in *Figure 1* is 5.8 nm, so lines spaced less than about 5.5 nm cannot be resolved.

A catalog of representative low resolution video spectra of meteors was recently published by Vojáček et al. (2015). Meteor spectra consist of a relatively faint continuum, emission atomic lines and molecular bands. Nitrogen and oxygen lines and nitrogen molecular bands are of atmospheric origin (i.e. are produced by heated atmosphere in the vicinity of the meteoroid). Atmospheric emissions are particularly prominent in fast meteors and dominate the red and infrared part of the spectrum (see *Figure 1*). To study the composition of meteoroids, meteoric lines are important. Only Mg, Na, Fe, and in some cases Ca, can be usually resolved in video spectra. Lines of Ca^+, Mg^+, Si^+, and H from the hot spectral component (Borovička, 1994b) are present in spectra of bright and fast meteors only.

Fortunately, the observable elements proved to be interesting and a number of meteor spectral classes could be identified by Borovička et al. (2005) when simply

plotting the Mg, Na, and Fe line intensities in a ternary diagram. This kind of analysis was repeated more recently by other authors, e.g. Madiedo (2015), Vojáček et al. (2015) or Rudawska et al. (2016). Mg represents silicates, Na the volatile part of the meteoroid, and Fe is contained in both metal and silicates (and sulfides). Ca, if observed, can be used to track the refractory part.

The advantage of video spectroscopy is its sensitivity. It can be used to study small (millimeter to centimeter) sized meteoroids, which proved to be chemically more diverse than larger bodies observed photographically. Since small meteoroids are numerous, good statistics can be obtained within reasonable period of time.

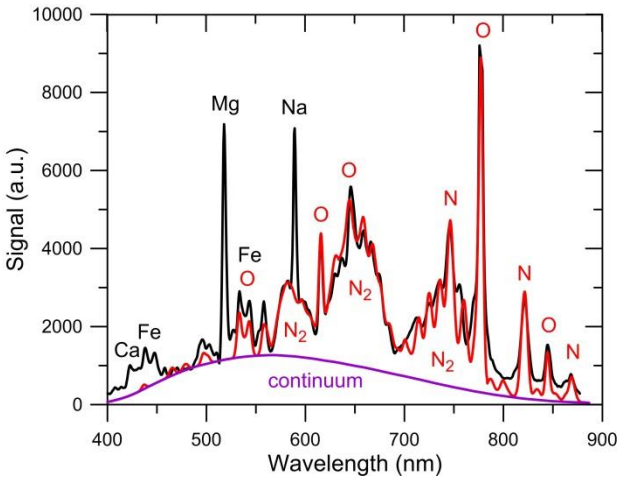

Figure 1 – Video spectrum (SZ 1308) of a sporadic meteor of velocity 69 km/s and approximate magnitude -2 captured on November 11, 2000. Measured signal summed along the meteor path and not corrected for spectral sensitivity of the instrument is plotted as a function of wavelength (black curve). Approximate continuum level is given in violet. The estimated contribution of atmospheric emissions of N, N_2, and O above the continuum level is plotted in red. Important emissions are identified; meteoric emissions in black and atmospheric emissions in red.

4 Photographic spectra

Examples of two photographic spectra obtained at the Ondřejov Observatory are presented in *Figures 2 and 3*. The used spectrographs are equipped with the 4.5/360 mm Tessar lenses and blazed objective gratings with 400 and 600 grooves per mm, respectively. Whole night exposures are recorded on large format sheet film 18x24 cm (Fomapan 200 ASA) providing a field of view of 28x36°. An underpressure system is used to keep the films flat. Six spectrographs are in use in all clear moonless nights. A rotating shutter interrupts the exposure 15 times per second. The system has been used in Ondřejov since 1960 (Ceplecha and Rajchl, 1963), when it replaced older spectrographs with a smaller format, and was upgraded several times since then (e.g. prisms were replaced by gratings and glass plates, which are no longer available, were replaced by films).

The spectrum in *Figure 2* is an example of the spectrum of relatively faint (–5 mag) and slow (20 km/s) fireball. The spectrum in *Figure 3* was produced by a brighter (–9 mag) and faster (48 km/s) fireball. Both fireballs were sporadic. The identification of 125 spectral lines in the latter spectrum was published by Mozgova et al. (2015). The resolution of the spectrum is 4.5 nm/mm. The spectrum was scanned in 14 bits by the photogrammetric scanner Ultrascan 5000 with the step of 10 μm (i.e. with resolution 2540 dpi). The typical FWHM is 0.25 nm; it is worse in the violet part of the spectrum, which is out of focus due to imperfection of the lens. On the other hand, the violet part of the second order spectrum of the Leonid spectrum S 30132 studied by Borovička (2004) was very sharp with FWHM 0.1 nm.

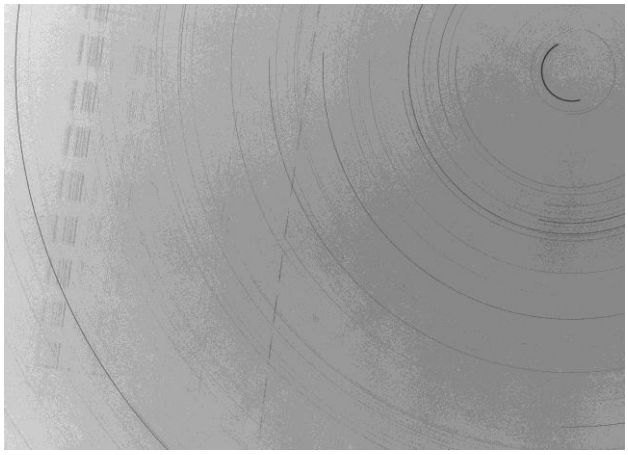

Figure 2 – Reproduction of the photographic spectrum (plate S 38301) of a –5 magnitude sporadic fireball captured near the celestial pole on February 20, 2012. The fireball velocity was 20 km/s and maximum brightness was reached at a height of 44 km. The fireball moved from top to bottom. Wavelengths increase from left to right. The brightest line belongs to sodium.

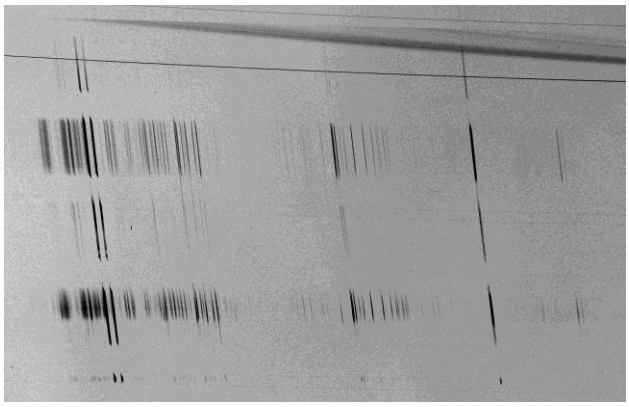

Figure 3 – Reproduction of the first order photographic spectrum (plate S 37724) of a –9 magnitude sporadic fireball captured on August 2, 2011. The fireball velocity was 48 km/s and maximum brightness was reached at a height of 83 km. The fireball moved from top to bottom. Wavelengths increase from left to right. The brightest lines belong to ionized calcium (two lines on the left) and sodium (on the right).

A large number of spectral lines resolved in photographic spectra enable detailed analysis of the radiating region to be performed. Most spectral lines belong in almost all cases to neutral iron. Measuring intensities of a large number of Fe lines with different excitation potentials and transition probabilities makes it possible to determine plasma temperature and Fe column density (see e.g. Borovička, 2005). Lines of more elements than in video spectra can be resolved and their relative abundances can

be determined. *Figure 4* shows the magnesium triplet (seen as single line in video spectra) at 516.7–518.4 nm, numerous lines of Fe I multiplet 15 between 527–546 nm, which can be only partly resolved in video spectra, and a chromium triplet at 520.5–520.8 nm, which is usually hidden between Mg and Fe lines in video spectra. Three bright Cr lines (Cr I multiplet 1) lie at 425.4, 427.5 and 429.0 nm, respectively (*Figure 5*), but are mixed with nearby Fe lines in video spectra. The same is valid for Mn I multiplet 1 at 403.1–403.4 nm. The Ca I line at 422.7 nm is the only non-Fe line in this crowded part of the spectrum, which can be bright enough to be measured with confidence in video spectra. Very difficult is the Si I line at 390.6 nm, which is located close to Fe lines and can be resolved only in the best photographic spectra (see Borovička, 2004). It is the only silicon line in the main spectral component. There are Si II lines in the hot spectral component; this component is, nevertheless, present only in fast fireballs (Borovička, 1994b).

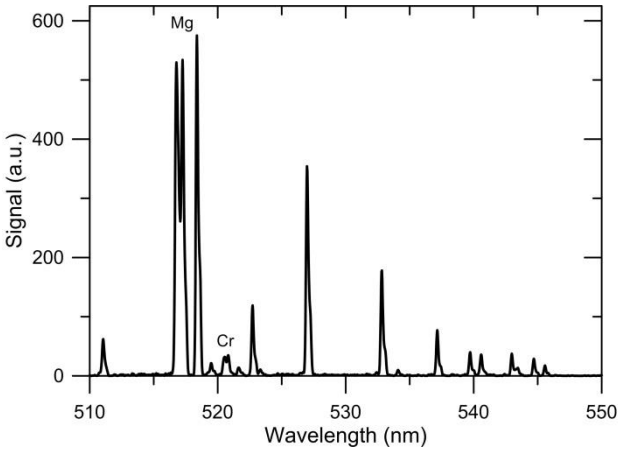

Figure 4 – Part of the spectrum S 37724 (see *Figure 3*) at the maximum brightness containing magnesium and chromium lines. The other (non-identified) lines belong to iron.

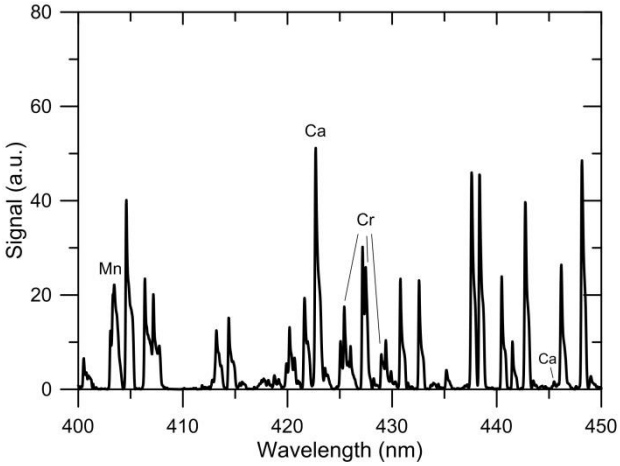

Figure 5 – Part of the spectrum S 37724 (see *Figure 3*) at the maximum brightness containing manganese, calcium, and chromium lines. The other (non-identified) lines belong to iron.

A long term photographic program can occasionally provide unique spectra as was the case on May 7, 1991, when two spectra of the very bright Benešov superbolide were obtained in Ondřejov. The bolide had an initial velocity of 21 km/s and reached an absolute magnitude of –19.5. Four small meteorites were recovered 20 years after the fall (Spurný et al., 2014). The meteorites were of various types, including ordinary chondrite LL3.5 with achodritic clast and H5 ordinary chondrite. The bolide spectrum was described by Borovička and Spurný (1996). *Figures 6 and 7* show part of the spectrum at the height of 57 km. Among others, lines of Ni, Ti, and Ba are present.

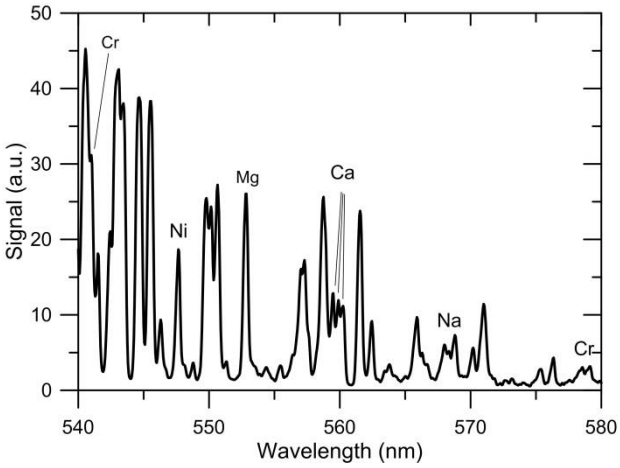

Figure 6 – Part of the spectrum of the Benešov superbolide at a height of 57 km containing a nickel line. Some other lines are also identified; the non-identified lines belong to iron.

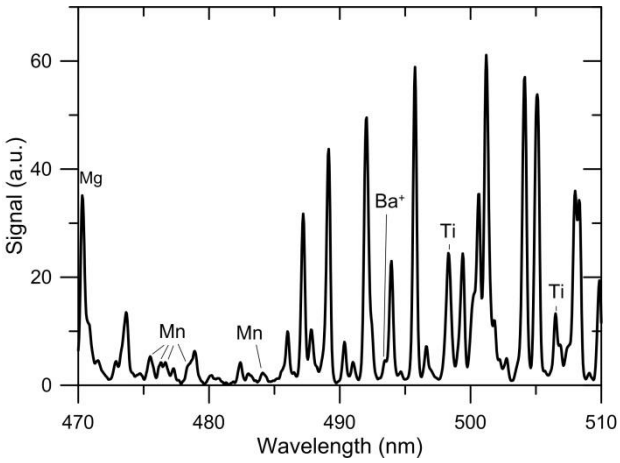

Figure 7 – Part of the spectrum of the Benešov superbolide at a height of 57 km containing titanium lines and possibly also a line of ionized barium. Some other lines are also identified; the non-identified lines belong to iron.

High resolution photographic spectra are usually not very suited for the detection of continuous radiation and diffuse molecular bands. If the resolution is high, diffuse radiation is spread over a large area. In low resolution, on the other hand, it is concentrated into few pixels. This is the reason why the continuum and N_2 bands are so prominent in video spectra. The Benešov bolide was, nevertheless, so bright that it provided the opportunity to study molecular radiation in a high resolution meteor spectrum. The beginning of the bolide clearly shows FeO radiation in the yellow and red part of the spectrum, especially in the vicinity of the sodium line (*Figure 8*). FeO can be seen in photographic spectra of slow fireballs quite regularly (see e.g. Borovička, 1994a; 2005). In Benešov, however, other oxides were also detected, namely CaO, AlO, and MgO. They are present at lower

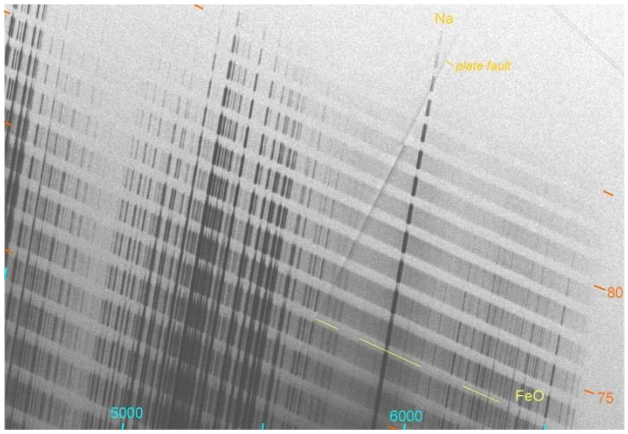

Figure 8 – Reproduction of a part of the Benešov spectrum near the beginning of the bolide. The bolide altitude in km is indicated by orange marks in the interval of 5 km. Wavelength in Å (1 Å = 0.1 nm) is indicated by cyan marks in the interval of 500 Å. Yellow lines indicate the position of three diffuse FeO bands at one particular altitude.

altitudes, especially in the wake and in the radiating cloud persisting at the position of the main flare at the height of 25 km (Borovička and Spurný, 1996). The radiating cloud spectrum is reproduced in *Figure 9*. In a recent paper (Borovička and Berezhnoy, 2016), we analyzed the molecular radiation in the Benešov bolide in detail, studying dependence on altitude and deriving vibrational and rotational temperatures of AlO. N_2 radiation was also marginally detected as a red continuum in the bolide spectrum at heights around 50 km. N_2 is a stable molecule, which can be present at temperatures around 5000 K. CN and TiO were not detected. For more details see Borovička and Berezhnoy (2016).

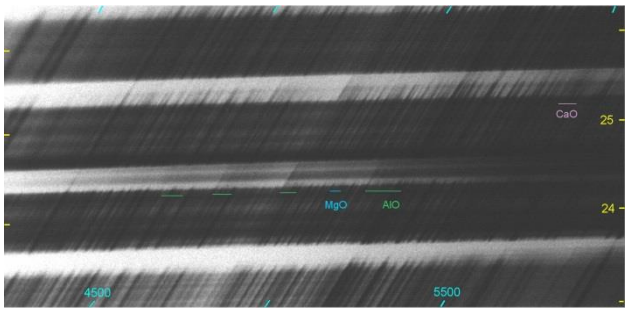

Figure 9 – Reproduction of a part of the Benešov spectrum at heights around 25 km including the radiating cloud at ~ 24.5 km. The bolide altitude in km is indicated by yellow marks in the interval of 1 km. Wavelength in Å (1 Å = 0.1 nm) is indicated by cyan marks in the interval of 500 Å. The presence of the brightest molecular bands is indicated by horizontal lines: AlO in green, MgO in blue, and CaO in purple.

5 Conclusions

The advantage of image intensified video spectroscopy is its high sensitivity allowing to probe small (millimeter sized) meteoroids. Since video spectra are of low resolution, only few meteoric elements can be studied, namely only Mg, Na, and Fe in most cases. On the other hand, the possibility of obtaining large numbers of spectra is convenient for statistical studies. Different populations of small meteoroids with varying content of Na and Fe were revealed this way. Temporal evolution of the spectrum can be also studied. In particular, Na sometimes behaves differently than other elements (Borovička et al., 1999).

Classical film spectroscopy has low sensitivity and only spectra of bright meteors can be obtained. Nevertheless, high resolution can be achieved and much more lines can be resolved than from video spectroscopy. Photographic spectra can be used to investigate physical conditions in the radiating plasma such as temperature and density and absolute abundances of various elements, such as Fe, Mg, Na, Ca, Cr, Mn, Al, Si, Ni or Ti (depending on the quality of the spectrum). Existing photographic archives have not been fully exploited, yet.

The advancement of digital imaging technology is, nevertheless, changing the situation described in this paper. High definition or even 4K videos provide nice spectra of resolution intermediate between analog video and film spectrographs as demonstrated at this conference by Maeda and Fujiwara (2016). The sensitivity is also intermediate between the two earlier systems. In the near future, high resolution video cameras or DSLR cameras will certainly open new chapter in the history of meteor spectroscopy.

Acknowledgment

This work was supported by grant no. 16-00761S from GAČR and the institutional project RVO:67985815.

References

Blajko S. (1907). “On the spectra of two meteors”. *Astrophysical Journal*, **26**, 341–347.

Borovička J. (1993). “A fireball spectrum analysis”. *Astronomy and Astrophysics*, **279**, 627–645.

Borovička J. (1994a). “Line identifications in a fireball spectrum”. *Astronomy and Astrophysics Supplement Series*, **103**, 83–96.

Borovička J. (1994b). “Two components in meteor spectra”. *Planetary and Space Science*, **42**, 145–150.

Borovička J. (2004). “Elemental Abundances in Leonid and Perseid Meteoroids”. *Earth, Moon, and Planets*, **95**, 245–253.

Borovička J. (2005). “Spectral Investigation of Two Asteroidal Fireballs”. *Earth, Moon, and Planets*, **97**, 279–293.

Borovička J. and Berezhnoy A. A. (2016). “Radiation of molecules in Benešov bolide spectra”. *Icarus*, **278**, 248–265.

Borovička J. and Spurný P. (1996). “Radiation study of two very bright terrestrial bolides and an application to the comet S-L 9 collision with Jupiter”. *Icarus*, **121**, 484–510.

Borovicka J., Stork R. and Bocek J. (1999). “First results from video spectroscopy of 1998 Leonid meteors”. *Meteoritics and Planetetary Science*, **34**, 987–994.

Borovička J., Koten P., Spurný P., Boček J. and Štork R. (2005). “A survey of meteor spectra and orbits: evidence for three populations of Na-free meteoroids”. *Icarus*, **174**, 15–30.

Ceplecha Z. (1971). “Spectral data on terminal flare and wake of double-station meteor No. 38421 (Ondřejov, April 21, 1963)”. *Bulletin of the Astronomical Institutes of Czechoslovakia*, **22**, 219–304.

Ceplecha Z. and Rajchl F. (1963). “The meteor spectrum with dispersion from 11 to 38 Å/mm”. *Bulletin of the Astronomical Institutes of Czechoslovakia*, **14**, 29–48.

Halliday I. (1961). “A Study of Spectral Line Identifications in Perseid Meteor Spectra”. *Publications Dominion Observatory Ottawa*, **25**, 3–16.

Harvey G. A. (1973). “NASA-LRC faint meteor spectra”. In Hemenway C. L., Millman P. M. and Cook A. F., editors. *Evolutionary and physical properties of meteoroids*. NASA SP 319, pages 131–139.

Hemenway C. L., Swider A. and Bowman C. (1971). “Meteor spectroscopy using an image orthicon”. *Canadian Journal of Physics*, **49**, 1361–1364.

Jenniskens P. (2007). “Quantitative meteor spectroscopy: Elemental abundances”. *Advances in Space Research*, **39**, 491–512.

Madiedo J. M. (2015). “The rho-Geminid meteoroid stream: orbits, spectroscopic data and implications for its parent body”. *Monthly Notices of the Royal Astronomical Society*, **448**, 2135–2140.

Maeda K. and Fujiwara Y. (2016). “Meteor spectra using high definition video camera in 2015”. In Roggemans A. and Roggemans P., editors, *Proceedings of the International Meteor Conference*, Egmond, the Netherlands, 2-5 June 2016. Pages 167–170.

Millman P. M. (1952). “Meteor news (Photographic meteor spectra)”. *Journal of the Royal Astronomical Society of Canada*, **46**, 121–124.

Millman P. M. and McKinley D. W. R. (1963). “Meteors”. In Kuiper G. P. and Middlehurts B., editors. *The Moon Meteorites and Comets*. The University of Chicago Press, pages 674–773.

Mozgova A. M., Borovicka J., Spurny P. and Churyumov K. I. (2015). “Identification of emission lines in a meteor spectrum obtained on August 2, 2011”. *Odessa Astronomical Publications*, **28**, 289–291.

Pickering E. C. (1897a). “Spectrum of a meteor”. *Harvard College Observatory Circulars*, No. 20, 1–2.

Pickering E. C. (1897b). “Spectrum of a meteor”. *Astronomische Nachrichten*, **145**, 77–78.

Pickering E. C. (1897c). “Spectrum of a meteor”. *Nature*, **57**, 101.

Rudawska R., Tóth J., Kalmančok D., Zigo P. and Matlovič P. (2016). “Meteor spectra from AMOS video system”. *Planetary and Space Science*, **123**, 25–32.

Spurný P., Haloda J., Borovička J., Shrbený L. and Halodová P. (2014). “Reanalysis of the Benešov bolide and recovery of inhomogeneous breccia meteorites – old mystery revealed after 20 years”. *Astronomy and Astrophysics*, **570**, A39.

Vojáček V., Borovička J., Koten P., Spurný P. and Štork R. (2015). “Catalogue of representative meteor spectra”. *Astronomy and Astrophysics*, **580**, A67.

The 2016 Quadrantids

Brando Gaetano

RAMBO/Meteor Research Group - Associazione Astrofili Bolognesi (AAB) – Bologna, Italy
brandogae@gmail.com

A report is presented on the observation of the Quadrantid shower recorded by RAMBO early January 2016. The data analysis – done by calculating the RZHR (Radar ZHR) – shows the complexity of the shower, in which the presence of multiple filaments is verified. A meteoroids mass profile is also made. Finally a comparison is made between the RAMBO radar data and the IMO visual data.

1 Introduction

The Quadrantid shower (10 QUA in the IAU Meteor Data Center[1]) is probably one of the greatest of all meteor showers that crosses the Earth's orbit each year, generating a visible increase in the number of "shooting stars" (Weiland, 2012). Its fame is lower than that for other meteor streams because of the adverse weather conditions of the first nights of the year. For this reason, radar observations take a greater importance since the radio systems are free from visibility conditions.

2 Quadrantids meteor shower

The shower duration is generally short - between 8.5 and 12 hours (Shelton, 1965; Hughes and Taylor, 1977; Baggaley, 1979) – and this is probably due to its very recent origin: the first sighting seems to have been around 1835. Only in 1862 there is a first document that mentions "shooting stars of January". In 1864 Alexander Herschel identifies the radiant point near the star c Quadrantis Muralis (coordinates $\alpha = 230°$, $\delta = +49°$): the name "Quadrantids" comes from this. Since 1929, following the redefinition of the system of constellations accomplished by the International Astronomical Union, the constellation was abolished and now the radiant lies in Boötes. Some astronomers call this shower the "Bootids" (Jenniskens, 2006).

A lot has been done to find its parent body. Since 2003, the year of the discovery of the asteroid *2003 EH_1*, numerical simulations tend to discard a cometary origin and now it is assumed that this stream of debris may indeed have been generated by that asteroid (Porubcan and Kornos, 2005). Until now astronomers are not sure that this parent body is actually a "classically understood" asteroid or instead it is the core of an extinct comet, the *C/1490 Y_1*.

The orbit of the Quadrantids is much tilted ($I > 70°$). The particles' velocity relative to the Earth (41 Km/h) is a medium value in the meteor velocity range. Different filaments were detected within this stream (Jenniskens, 2006).

[1] IAU MDC, http://www.ta3.sk/IAUC22DB/MDC2007/

3 The 2016 observation

For 2016 the forecast[2] of its peak was January, 4 at $8^h\ 00^m$ ($\lambda_\odot = 283°.18$).

The observations of the Quadrantids performed by RAMBO (Radar Astrofilo Meteorico Bolognese) - built by the Meteor Research Group[3] of Associazione Astrofili Bolognesi[4] show that the phenomenon started when the radiant is decreasing in the afternoon of January 3 (*Figure 1*). It drops to below 10° of altitude for six hours and then starts to rise in elevation, at about 23^h UT, when the phenomenon is already in full swing. At about 6^h UT on January 4, it gets at its maximum before decreasing again.

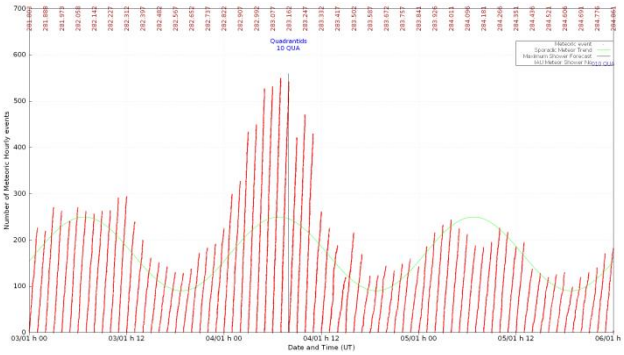

Figure 1 – 2016 Quadrantids Hourly Rate: green line represent the sporadic meteors trend.

The radiant culminates at 8^h UT. Its descending elevation did not allow us to record two peaks at 9^h UT and 15^h UT on January 4.

4 Data analysis

The data analysis shows the presence of at least three filaments, two very close and one spaced of about 8 hours from the first peak.

The statistical analysis and the calculation (McKinley, 1961; Sandri, 2003) of the RZHR (*Figure 2*) – performed with *RZHR3*, a software program written in Python

[2] Data taken from the *IMO 2016 Shower Calendar*, pages 4-5.
[3] The RAMBO/Meteor Research Group has an email address (rambometeorgroup@gmail.com) and a web site (http://www ramboms.com) - in Italian and in English - where all the data and publication are collected.
[4] AAB web site: http://www.associazioneastrofilibolognesi.com

version 3 by the author (*Figure 7*) – highlights more effectively the hourly rate trend corrected for the height of the radiant point and for the sporadic meteors contribution.

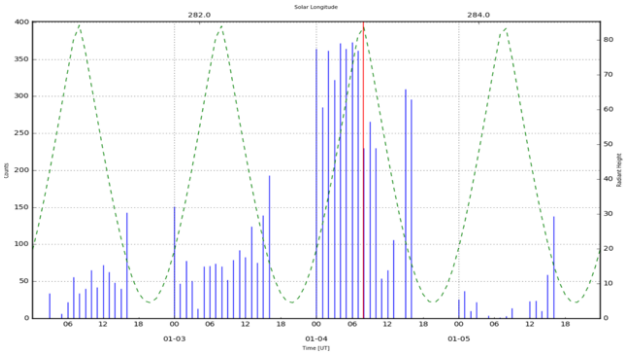

Figure 2 – Radar ZHR (RZHR): blue lines are RZHR values, the red line is the forecasted peak and the green dotted line is the radiant point position.

In addition to the hourly rate, the evidence of the stream's complexity is illustrated by the meteoroids mass profile. *Figure 3* shows the trend of the meteor echoes duration. As the echo duration is proportional to the meteoroid mass, I can obtain an indication on the mass variation during the meteoric shower. Although the data are not related, I can see that this trend is perfectly comparable with the hourly rate profile.

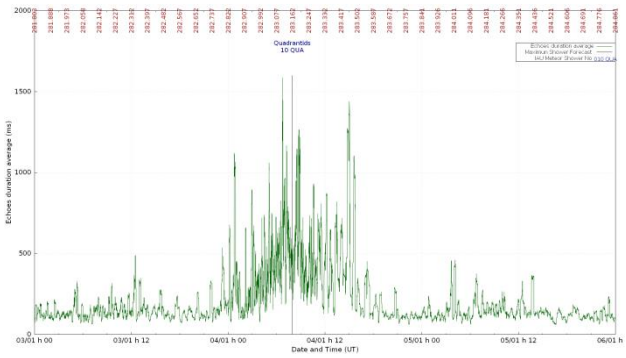

Figure 3 – Meteoroids mass variation in the echoes analysis.

I can say that the 2016 Quadrantids shower recorded by RAMBO has seen a succession of three peaks: two very close at solar longitude of 283.12 ($6^h\ 58^m$ UT) and 283.19 ($8^h\ 37^m$ UT) and a third at 283.45 ($14^h\ 44^m$ UT).

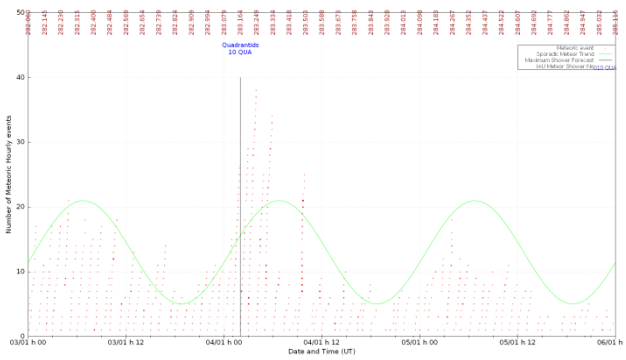

Figure 4 – 2015 Quadrantids Hourly Rate.

5 Data comparison

RAMBO data

The 2015 RAMBO registration (*Figure 4*), accomplished with a less reliable version, and the RZHR calculation (*Figure 5*) shows a trend similar to those of 2016: a maximum composed of two closely spaced peaks and an extra peak about 8 hours later.

IMO data

It may be interesting to compare RAMBO radar data with the IMO visual data.

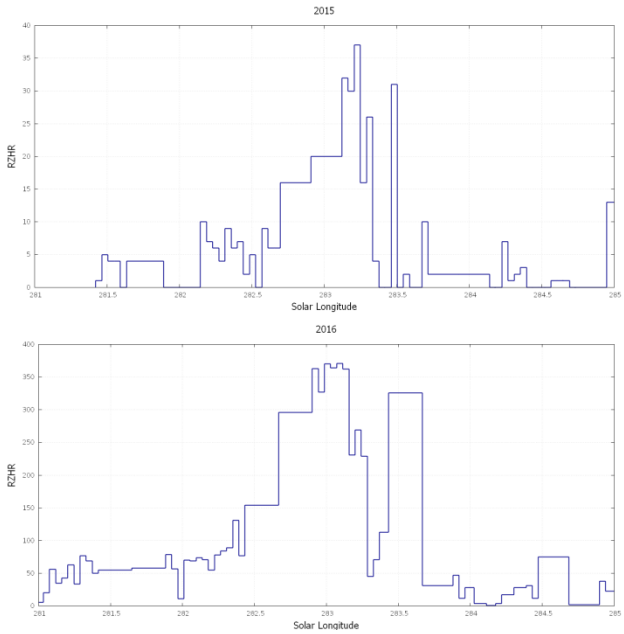

Figure 5 – 2015 (top) and 2016 (bottom) RZHR comparison.

Table 1 – Peaks of the Quadrantids from visual and radar observations.

Year	$\lambda_\odot$ peak	Source
2008	283.28	*IMO*
2009	283.08	*IMO*
	283.17	*IMO*
2011	283.23	*IMO*
	283.45	*IMO*
2012	283.07	*IMO*
	283.11	*IMO*
	283.62	*IMO*
2013	283.45	*IMO*
	283.62	*IMO*
2014	283.18	*IMO*
2015	283.22	*RAMBO*
	283.30	*RAMBO*
	283.50	*RAMBO*
2016	282.88	*IMO*
	283.05	*IMO*
	283.20	*IMO*
	283.12	*RAMBO*
	283.19	*RAMBO*
	283.45	*RAMBO*

In *Table 1*, I summarize the solar longitude of the peaks observed by IMO[5] and by RAMBO. *Figure 6* is a graphical representation of *Table 1*. It is clear that the radio data displays the same time pattern.

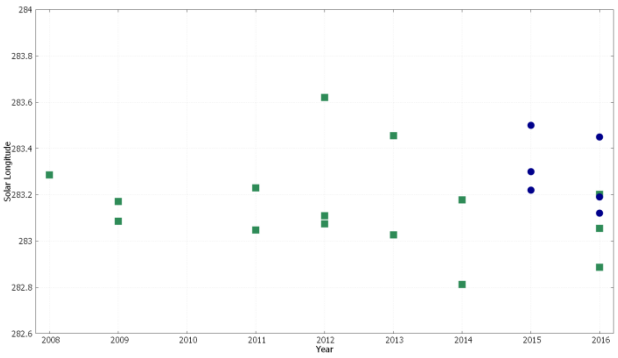

Figure 6 – Solar longitudes of the Quadrantids' peaks in 2008–2016 from visual observations (IMO, green squares) and 2015–2016 RAMBO data (blue dots).

6 Future development

Looking at the IMO data represented in *Figure 6*, It looks as if a few years are not present. This may be due to unfavorable night weather conditions (widespread cloud cover, rain, snow, etc.) or the presence of light disturbances (the Moon in its various phases, light pollution). These are the limits of visual observation. On the other hand, the strength of visual observations is the possibility of observing the phenomenon on a global level.

Radar observations do not suffer from weather conditions or the presence of light pollution and they can be made throughout the day, but they need a well-built and calibrated system of registration and a subsequent statistical analysis to eliminate the part of sporadic meteors.

This is RAMBO: a system built and well calibrated that works seven days a week, twenty-four hours a day. For the moment it is limited to a single observing station (the seat of our association in Bologna) and the necessity to have the radiant point above the horizon.

These problems can be overcome if, as in visual observing, a global radio network is created. As research group, we hope for the future that other similar setups could be installed all around the world, in order to achieve a global coverage.

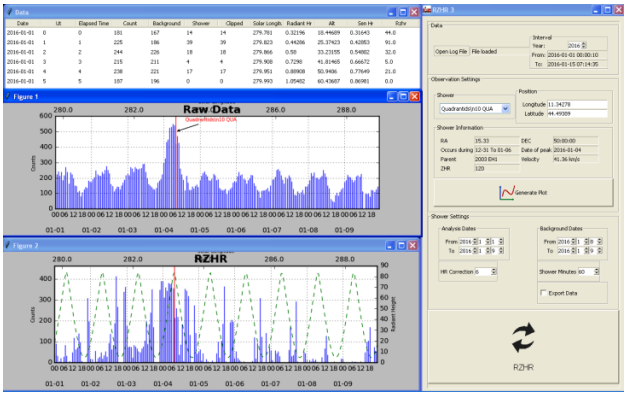

Figure 7 – *RZHR3* screenshot.

References

Baggaley W. J. (1979). "The interpretation of overdense radio meteor echo duration characteristics". *Bulletin of Astronomical Institutes of Czechoslovakia*, **30**, 184–189.

Hughes D. W. and Taylor I. W. (1977). "Observations of overdense Quadrantids radio meteors and the variation of the position of stream maxima with meteor magnitude". *Monthly Notices of the Royal Astronomical Society*, **181**, 517–526.

Jenniskens P. (2006). "Meteor Showers and their Parent Comets". *Cambridge University Press*, pages 357–376.

McKinley Q. W. R. (1961). "Meteor Science and Engineering". *McGraw-Hill Book Company.*

Porubcan V. and Kornos L. (2005). "The Quadrantids meteor stream and 2003 EH1 V". *Contributions Astronomical Observatory Skalnate Pleso*, **35**, 5–16.

Sandri M. (2003). "Analisi di sciami meteorici di origine cometaria attraverso tecniche radar e visuali". *Master Degree at Università di Padova. (In Italian).*

Shelton J. W. (1965). "Photographic Quadrantid meteors". *The Astronomical Journal*, **70**, 337–345.

Weiland T. (2012). "A rare opportunity: Observing the 2011 Quadrantid maximum from Austria". *WGN, Journal of the IMO*, **40**, 171–175.

[5] IMO – ZHR Live Graphs, http://www.imo net/zhr

Recent shower outbursts detected by the Canadian Meteor Orbit Radar (CMOR)

Peter Brown

Dept. of Physics and Astronomy, University of Western Ontario, London, Ontario, N6A 3K7, Canada
pbrown@uwo.ca

We present recent detections of short-duration shower outbursts as measured by the Canadian Meteor Orbit Radar (CMOR) between 2013–2016. In this interval, CMOR detected two strong shower outbursts unlinked to known showers. These included an outburst of the Kappa Cancrids (KCA – IAU 793) on January 5, 2015 and from the Gamma Lyrids (GLY – IAU 794) on February 7, 2015. Both have an orbit consistent with a Halley-type comet (HTC) or nearly isotropic-comet. Analysis of GLY activity also revealed a previously unreported annual shower, the September Ursae Majorids, (SUR – IAU 795).

1 Introduction

The Canadian Meteor Orbit Radar (CMOR) is a 12 kW multi-static backscatter radar operating at 29.85 MHz. Details of the system and operations are given in Jones et al. (2005) and Brown et al. (2008; 2010).

CMOR measures approximately 5000 meteoroid orbits per day. Through an automated data acquisition and analysis pipeline, all meteor echo trajectories and radiants are computed and then searched for "clumpiness" in sun-centered radiant space ($\lambda - \lambda_o, \beta, V_g$) using a 3D wavelet transform to isolate probable meteor showers. The data reduction analysis procedure is described in detail in Brown et al. (2008) and Brown et al. (2010). An update to the wavelet shower detection process has been described in Pokorný et al. (2016) and this procedure is what is used in the following analysis.

2 CMOR outburst survey

As part of normal wavelet processing, CMOR regularly detects and identifies ~150 annual meteor showers which can be linked to those appearing in the IAU Meteor Data Center catalogue. To assess significance of shower activity in any one degree of solar longitude at any given radiant location, individual wavelet coefficients are computed and an annual time series is generated. The resulting activity-time profile provides a metric for the overdensity of radiants over any given year per day at the chosen radiant location.

Figure 1 shows an example of this process. The xsig value (y-axis) is the number of standard deviations the wavelet coefficient in any one solar longitude bin is above the median value for the entire year. It is a proxy for relative activity. Note that for *Figure 1* all data gathered by CMOR from 2002–2016 have been stacked into a virtual year to improve signal-to-noise for annual showers.

From earlier work (Brown et al., 2010) it was found empirically that xsig values for CMOR above 3 are the minimum needed to reasonably identify "local maxima" which may be part of true showers. In general, the majority of such weak "clumps" are still false-positives, but a string of similar radiant locations spread over time are likely to be part of a shower. As the xsig value grows, the probable existence of a shower becomes greater.

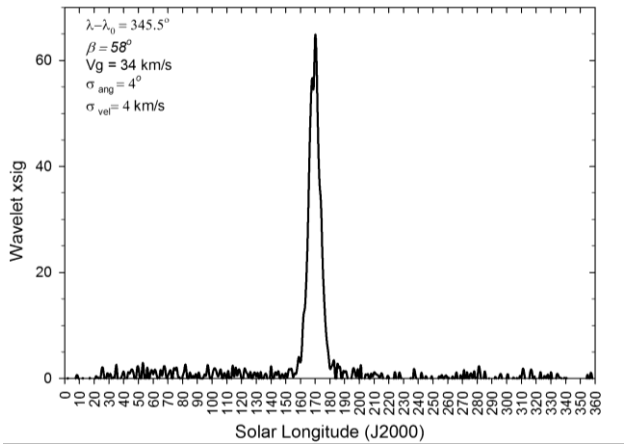

Figure 1 – The relative strength of the wavelet coefficent in units of standard deviations above the median background throughout the year from CMOR measurements. The sun-centred radiant location and probe sizes (angular radiant and speed) are shown in the inset.

In the example of *Figure 1* it can be seen that the xsig value is in excess of 60. This is an indication of a strong shower. *Figure 2* shows a plot of all radiants measured by CMOR for $\lambda = 171°$ (the location of maximum in *Figure 1*) over all years (38720 radiants) in sun-centered coordinates. Each radiant is represented as a blue circle 1° in radius, a median estimate of individual radiant measurement uncertainty. Regions of higher radiant density (radiants deg^{-2}) are shown in redder/yellow colors.

To locate meteor shower outbursts (short-lived – typically much less than a day in duration showers) we examined all CMOR wavelet maxima for each year from 2013–2016. Our search was designed to find wavelet radiant maxima not linked to any showers in the IAU catalogue. We required the xsig values to be larger than 10 and the activity to occur in no more than two solar longitude bins.

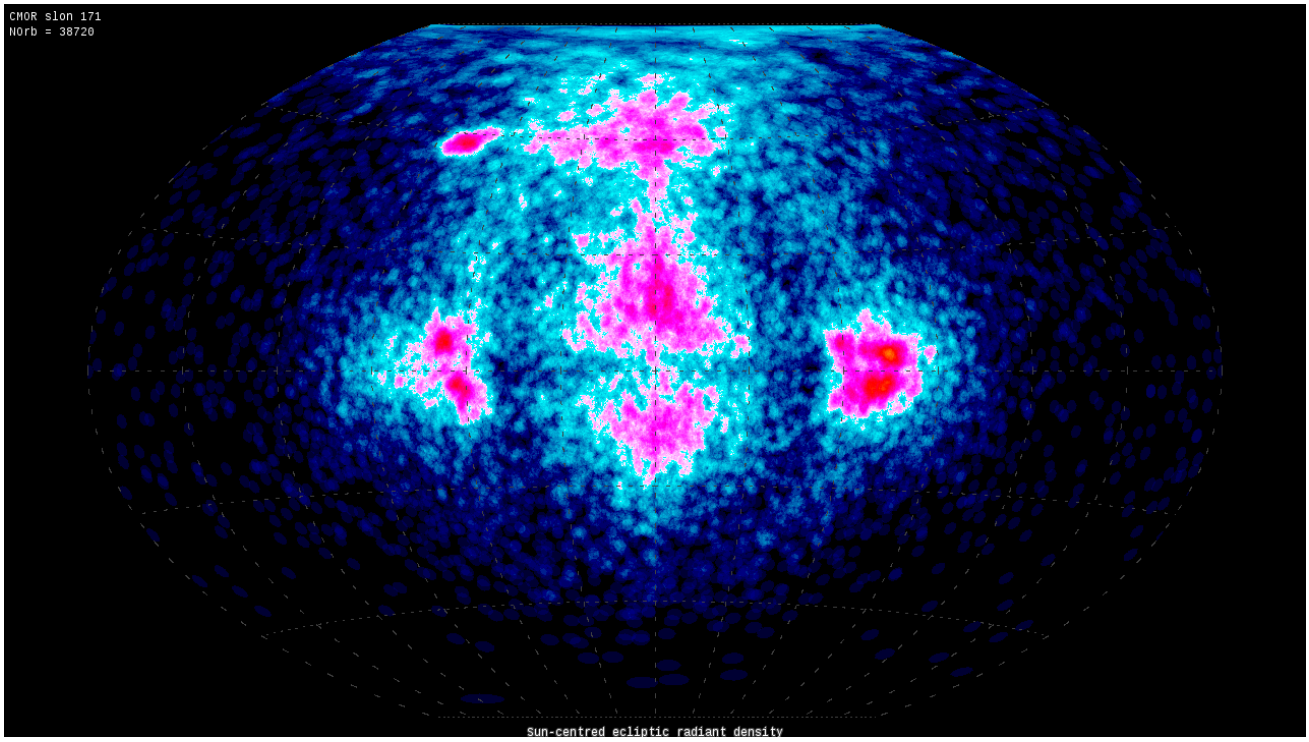

Figure 2 – The distribution of radiants measured by CMOR at λ=171° for data stacked from all years between 2002–2015 in sun-centred ecliptic coordinates. The thick red arrow points to the radiant location corresponding to *Figure 1*.

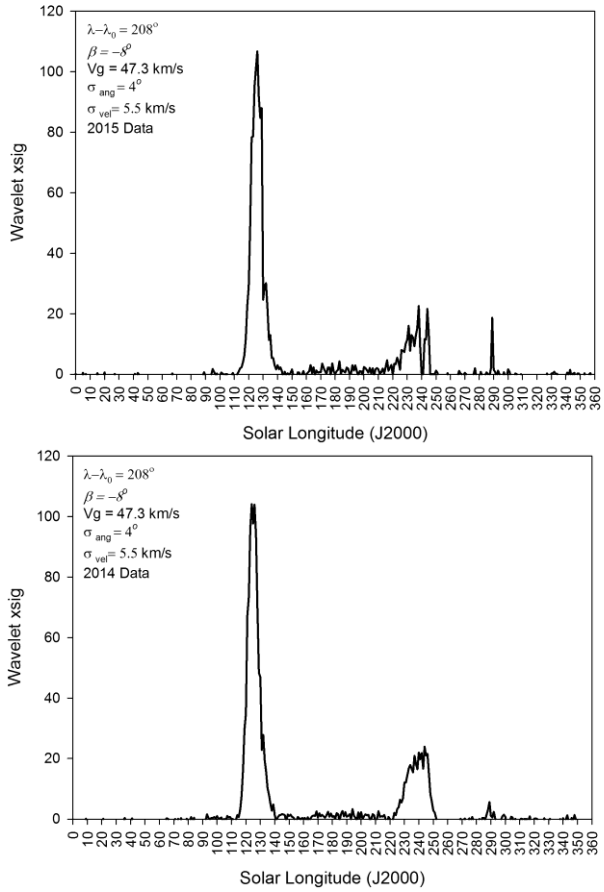

Figure 3 – The xsig value of the wavelet coefficient at the radiant coordinates shown in the figure insets for 2014 (bottom) and 2015 (top). The first peak near λ=125° is the South Delta Aquariid (SDA) shower, while the broader activity near λ=240° is from the November Omega Orionids (NOO). The KCA outburst is apparent at λ=289° in 2015. Weak annual activity from the KCA is also visibe in some earlier years (such as 2014), but at much lower levels than detected by CMOR in 2015.

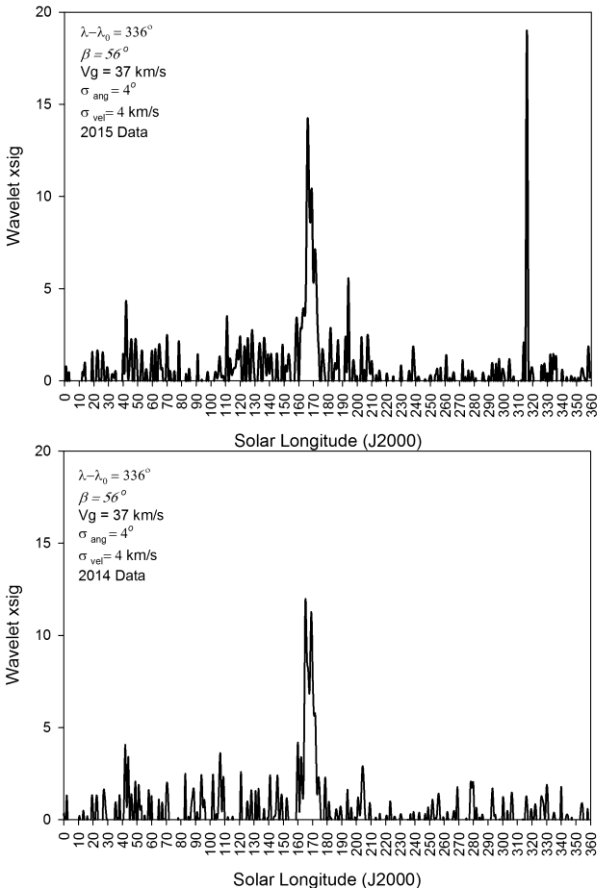

Figure 4 – The xsig value of the wavelet coefficient at the radiant coordinates shown in the figure insets for 2014 (bottom) and 2015 (top). The peak near λ=171° is the newly recognized annual September Ursae Majorids (SUR), found during the outburst search and isolated more completely in *Figure 1*. The GLY outburst is apparent at λ=316° in 2015 with an xsig of 19. No earlier evidence for this shower is visible in any year from 2002–2014 in CMOR data.

Table 1 – Sun-centred radiant locations, geocentric speeds and orbital elements for the Kappa Cancrid outburst (Jan 9–10, 2015) and the Gamma Lyrid outburst (February 5, 2015). The number of individual CMOR orbits associated with each outburst (N_{orb}) is also shown. All angular coordinates are J2000.0.

λ-λ_o	β	V_g (km/s)	a (AU)	e	q (AU)	Q (AU)	i	ω	Ω	N_{orb}	Shr
208	-8	47.3	∞	1.00	0.055	∞	35	152.6	109.5	40	KCA
336.2	56	37	100	0.992	0.78	3000	54.6	125.7	316.5	32	GLY

Table 2 – Sun-centred radiant locations, geocentric speeds and orbital elements for the annual September Ursae Majorid (SUR) shower. The number of individual CMOR orbits detected during all of 2002–2015 associated with the shower (N_{orb}) is also shown. All ansgular coordinates are J2000.0.

λ-λ_o	β	V_g (km/s)	a (AU)	e	q (AU)	Q (AU)	i	ω	Ω	N_{orb}	Shr
345.3	58	34	21	0.961	0.84	42	48.6	131.3	170.5	9096	SUR

3 Results and discussion

Using these criteria we found two outbursts over the three year survey period. Note that CMOR detected enhanced activity and/or other shower outbursts during this time (for example outburst activity from the STAs in 2015, the KCG in 2014 (Moorhead et al., 2015) and the ETA in 2013). However, all were associated with known showers and lasted more than 2 days in duration so are not included in the results from this survey.

Table 1 summarizes radiant and mean stream orbits for these two outbursts. We do not show uncertainties in these values as the error in mean speed and radiant location for isolated single-day wavelet maxima are difficult to establish, as the wavelet transform is a non-local measure. Isolating individual orbits for each outburst we can approximately estimate uncertainties. We find a standard deviation of 1.6 km/s in speed and 1.3° in radiant spread for the KCA from a sample of 40 individually measured orbits. Similarly, we find an uncertainty in V_g of 2 km/s and 2.7° spread for the much broader shower radiant of the GLY outburst among 32 measured orbits. The corresponding xsig profiles for 2015 (and 2014 for comparison) are given in *Figures 3 and 4* respectively.

The associated orbits are typical of Halley-type comets and/ or nearly isotropic comets (NICs). However, a search of existing comet and NEOs did not find any object with a similar orbit (D-criteria < 0.1). Hence these two outbursts may be indications of as yet-undiscovered HTCs/NICs or that the original parents have disintegrated entirely.

In examining the GLY wavelet time series, an earlier recurring shower of ~2 weeks duration peaking near λ=171° was serendipitously detected. Manual examination of the IAU shower catalogue showed no reported shower with these characteristics, despite the strong activity in CMOR measurements. Closer examination of the CMOR shower wavelet pipeline showed that this was one of only a handful of annual showers detected by CMOR but as yet not reported in the IAU catalogue (and not detected in the earlier CMOR surveys by Brown et al. (2010)). The associated wavelet time series and radiant plot were previously shown in *Figure 1 and 2*.

Details of the new shower (the September Ursae Majorids - SUR) are summarized in *Table 2*. As with the previously discussed two outburst showers, the SUR has an HTC/NIC-like orbit and no obvious parent. This is a common feature for showers located near the North Toroidal sporadic source (Pokorny et al., 2014). However, the SUR shows similarly strong activity each year, a long duration and broad, diffuse radiant, all indications of an old (many ka) stream.

4 Conclusions

Using CMOR orbital data gathered between 2013–2016 we performed a dedicated search for unlinked, brief (<2 day) shower outbursts. Our survey found two outburst showers. The first, occurring on January 9–10, 2015 (with radiant in Cancer) is now called the Kappa Cancrids (KCA). The second on February 5, 2015 (with a radiant in Lyra) is the Gamma Lyrids (GLY). Each outburst has an HTC/NIC-like orbit. Both outbursts consisted of several dozen measured radiants in regions of the sky with relatively low radiant density. The resulting wavelet excursions of the showers were more than 10σ above the median background wavelet level at the same radiant locations recorded over the previous year.

As part of the GLY detection, an annual shower, the September Ursae Majorids (SUR), was also recognized in CMOR data with activity extending back to as early as 2002.

None of the streams has a known parent body. This demonstrates the utility of meteoroid streams for tracing either unknown or recently disintegrated HTC/NIC comets with nodes near the Earth.

Acknowledgment

Funding for operation of CMOR is provided by the NASA Meteoroid Environment Office (MEO) through NASA co-operative agreement NNX15AC95A.

References

Brown P. G., Weryk R. J., Wong D. and Jones J. (2008). "A meteoroid stream survey using the Canadian Meteor Orbit Radar I. Methodology and radiant catalogue". *Icarus*, **195**, 317–339.

Brown P. G., Wong D. K., Weryk R. J. and Wiegert P. (2010). "A meteoroid stream survey using the Canadian Meteor Orbit Radar II: Identification of minor showers using a 3D wavelet transform". *Icarus*, **207**, 66–81.

Jones J., Brown P. G., Ellis K. J., Webster A., Campbell-Brown M. D., Krzemenski Z. and Weryk R. J. (2005). "The Canadian Meteor Orbit Radar : system overview and preliminary results". *Planetary and Space Science*, **53**, 413–421.

Moorhead A. V., Brown P. G., Spurný P., Cooke W. J. and Shrbený L. (2015). "The 2014 Kcg Meteor Outburst: Clues to a Parent Body". *The Astronomical Journal*, **150**, id. 122, 13 pp.

Pokorný P., Vokrouhlický D., Nesvorny D., Campbell-Brown M. D. and Brown P. G. (2014). "Dynamical Model for the Toroidal Sporadic Meteors". *The Astrophysical Journal*, **789**, id. 25, 20 pp.

Pokorný P., Janches D., Brown P. G. and Hormaechea J. L. (2016). "An Orbit Meteoroid Stream Survey using the Southern Argentina Agile Meteor Radar (SAAMER) based on a wavelet approach". To be submitted.

Peter Brown: a real ambassador for the small bodies in our solar system (Photo Eva Bojurova).

The Radio Meteor Zoo: a citizen science project

Stijn Calders[1], Cis Verbeeck[2], Hervé Lamy[1] and Antonio Martínez Picar[2]

[1] **Royal Belgian Institute for Space Aeronomy**
Stijn.Calders@aeronomy.be

[2] **Royal Observatory of Belgium**

Scientists from the BRAMS radio meteor network have started a citizen science project called Radio Meteor Zoo in collaboration with Zooniverse in order to identify meteor reflections in BRAMS spectrograms. First, a small-scale version of the Radio Meteor Zoo was carried out with a sample of meteor identifications in 12 spectrograms by 35 volunteers. Results are presented here and allowed us to define a method that reliably detects meteor reflections based on the identifications by the volunteers. It turns out that, if each spectrogram is inspected by 10 volunteers, hit and false detection percentages of 95% respectively 6% are expected. The Radio Meteor Zoo is online at https://www.zooniverse.org/projects/zooniverse/radio-meteor-zoo. Citizen scientists are kindly invited to inspect spectrograms.

1 Introduction

The BRAMS (Belgian RAdio Meteor Stations) network consists of ~30 receiving stations spread all over the Belgian territory and a single radio transmitter installed at the Geophysical Centre of the Royal Meteorological Institute (RMI) in Dourbes (Calders et al., 2014; Lamy et al., 2015). This radio transmitter emits a sine wave with circular polarization at a frequency of 49.97 MHz and with a constant power of 150 W. At each receiving station, the signal is sampled with a frequency of 5512 Hz, providing a bandwidth of ~2.5 kHz. Data are saved as WAV (sound) files every 5 minutes. BRAMS data are usually presented as spectrograms, which provide the frequency content of the signal as a function of time. Spectrograms are built from raw data using the FFT on 16384 samples and with an overlap of 90%. Only 200 Hz of the whole bandwidth, centered on the direct signal of the transmitter, are usually shown as the majority of the meteor echoes appear there. Spectrograms are very useful because the spectral signatures of meteor echoes are very different from those due to "spurious" signals such as e.g. reflections on airplanes or broad-band interferences.

Each BRAMS receiving station is recording continuously, producing each day 288 WAV files and detecting ~ 1500–2000 meteors. This huge amount of data requires the use of automatic detection algorithms. Several attempts were made to identify meteor reflections either in raw data or in spectrograms by using automatic detection algorithms, with varying degrees of success as discussed in detail in (Calders and Lamy, 2014; Lamy et al., 2015). The automatic detection of overdense radio meteor echoes in particular remains a difficult task due to the various and complex shapes they produce in spectrograms. This problem is particularly striking during meteor showers where these types of meteor echoes are observed abundantly. In this paper, a new strategy for the identification of meteor reflections in the spectrograms is explored. Instead of detecting meteor reflections automatically by means of software, we propose to rely on the best detector which is the (trained) human eye. This is a well-established method nowadays in observational science, known as crowdsourcing or citizen science (Lintott, 2008).

2 The Radio Meteor Zoo

The authors have started collaboration with the scientists at Zooniverse to use their platform to host a project called *Radio Meteor Zoo*.

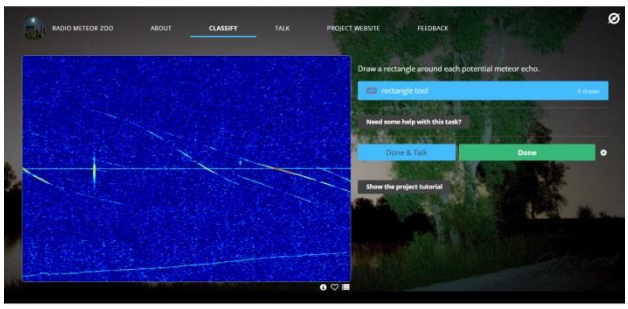

Figure 1 – The Radio Meteor Zoo website.

In order to be able to analyze the *Radio Meteor Zoo* contributions, we must be able to answer the two following important questions:

- What is the minimum number of volunteers we need to inspect a given spectrogram such that we can statistically be confident in the results?
- In a given spectrogram, how can we accurately derive the number and position of meteor echoes based on individual contributions?

In order to answer these questions, a test was performed with 12 spectrograms and 35 users.

3 A small-scale version of the Radio Meteor Zoo

Description of the test data set

We used 12 spectrograms from the BRAMS receiving station in Ottignies obtained on 15 March 2015 between 0^h and 1^h UT. The authors carefully inspected the spectrograms together. In total 120 meteor reflections

were identified in the 12 spectrograms. These detections represent the reference dataset.

Composition of the test group

The test group consisted of 35 volunteers with a strong physics background, and most of them are interested in meteor research but not necessarily familiar with radio observations.

Meteor identification interface

Both the authors and the test group used the same interactive web tool to inspect the spectrograms and to identify meteor reflections. This tool is accessible online[1]. With this tool a user can draw a rectangle around each feature in the spectrogram that he considers to be a meteor. Once the user has identified all meteor reflections in the spectrogram, he can navigate to the next spectrogram. He can also navigate back to check his identifications in a previous spectrogram.

The coordinates of the rectangles, both in pixels coordinates and in frequency/time coordinates, are saved in a comma-separated values (CSV) file. A CSV file was created for each user.

Training

The volunteers of the test group were asked to read first a tutorial. This tutorial explains what a spectrogram looks like and provides examples of typical signatures of meteor reflections and common distortions (like reflections on airplanes or broad-band interferences). Finally the tutorial explains what is expected from the volunteer: drawing rectangles around potential meteor echoes and how to do it correctly.

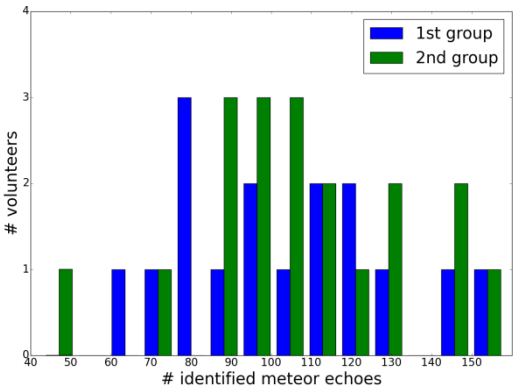

Figure 2 – Total number of meteor echoes identified by the different volunteers in the 12 spectrograms.

From the results of a first group of volunteers (16 people in the test group of 35), the authors learned that the median volunteer identified 99 meteor reflections (median absolute deviation MAD=19). This is far less than the 120 meteors that the authors had identified. The difference between the counts from the test group and the reference dataset was mostly due to the faintest meteor echoes. Therefore the tutorial was updated asking the users to draw a rectangle even when they have a doubt about a faint meteor. After all, it is easier to filter out a false detection than to retrieve a missed meteor detection. The median volunteer of the second group identified 107 meteor reflections in the spectrograms (MAD=17). A histogram of the individual counts is given in *Figure 2*.

Challenges

It was soon realized that there is a large spread on the number of meteors identified by the 35 persons. For instance, one volunteer identified 7 meteor reflections in the spectrogram in *Figure 3*, while another volunteer identified 17 meteor reflections, and the reference dataset yielded 15 meteor reflections.

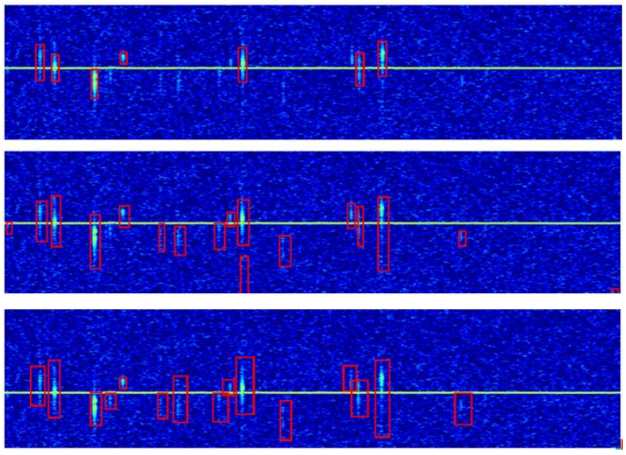

Figure 3 – Meteor reflection identifications by different volunteers in the same spectrogram. Top: volunteer 1 identifies 7 meteor reflections; middle: volunteer 2 identifies 17 meteor reflections; bottom: the reference detection identifies 15 meteor reflections.

4 How to interpret the *Radio Meteor Zoo* identifications?

First let us try to answer the second question from *Section 2*: in a given spectrogram, how can we accurately derive the number and position of meteor echoes based on individual contributions? In order to investigate this closer, we performed for every of the 12 spectrograms the following analysis for all values of *i* between 1 and 35.

- Create a binary version of the spectrogram called $image_0$ which has pixel value 1 for pixels identified as a meteor pixel in the reference spectrogram, and pixel value 0 for all other pixels.
- Create a binary version of the spectrogram called $image_1$ which has pixel value 1 for pixels which were identified as a meteor pixel by at least *i* volunteers, and pixel value 0 for all other pixels.
- Calculate the number *D(i)* of pixels for which $image_0$ and $image_1$ have different pixel values.

This allowed us to determine the value of *i* which minimizes *D*(*i*).

It turns out that the number *D(i)* of pixels where "at least *i* volunteers" and the reference spectrogram disagree, has a minimum at $i_{optimal}$ = 12 volunteers. This means that in order to best reconstruct the reference spectrogram, we should consider as meteor pixels those pixels that have been identified as meteor pixels by at

[1] http://brams.aeronomie.be/zoo

least 12 of the 35 volunteers. The corresponding spectrogram is called the optimal identification spectrogram.

Now let us try to answer the first question of *Section 2*: what is the minimum number of volunteers we need to inspect a given spectrogram? Indeed, in the *Radio Meteor Zoo* project, it would be better to have a number of volunteers n that have to inspect a single spectrogram well below 35. For example, if 2000 spectrograms have to be investigated (corresponding to approximately one week of data for one receiving station), that would already amount to 70000 individual inspections for 35 users. So we repeated the analysis above for each number of volunteers n between 1 and 35. For every n we randomly selected 1000 combinations of n volunteers out of 35 to have a significant number of simulations without making it too CPU intensive.

Figure 4 provides for every n the optimal number of volunteers $i_{\text{optimal}}(n)$ which minimizes D(i). For instance, $i_{\text{optimal}}(35) = 12$ for $n = 35$, as was explained before. As expected, $i_{\text{optimal}}(n)$ increases with n.

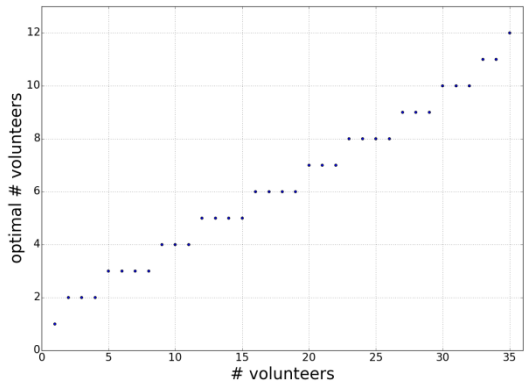

Figure 4 – For every number of volunteers n on the x-axis, the y-axis shows the optimal number of volunteers $i_{optimal}(n)$ that minimizes D(i).

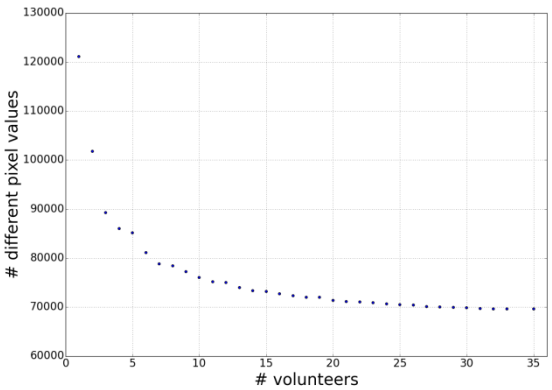

Figure 5 – The number of pixels D(i) for which the optimal identification spectrogram for n volunteers and the reference spectrogram have different pixel values, as a function of number n of volunteers considered.

For every value of n (number of volunteers), we can now derive an optimal identification spectrogram of meteor reflections by considering a pixel as a meteor pixel if it is identified as such by at least $i_{\text{optimal}}(n)$ volunteers. In *Figure 5*, the number of pixels D(i) where the optimal identification spectrogram disagrees with the reference spectrogram is plotted as a function of number of volunteers n. Note that each spectrogram contains 595 × 864 pixels in the 200 Hz range shown to the volunteers. For 12 spectrograms the total amount of pixels is therefore larger than 6×10^6. The values of D(i) shown in *Figure 5* represents thus maximum ~2% of the total number of pixels in the worst case. This curve varies smoothly as a function of n, and of course has a minimal (best) value at $n = 35$.

Figure 5 allows us to select a value for the number of volunteers n which is much smaller than 35 but yet still delivers accurate meteor reflection identifications. For the *Radio Meteor Zoo*, we selected $n = 10$ volunteers per spectrogram. Indeed, using 10 volunteers instead of 35, corresponds only to an increase of 9% of D(i), i.e. 9% more pixels with different values in the optimal identification spectrogram and in the reference spectrogram.

5 Results

When we apply the identification method described above on the spectrogram from *Figure 6* (with number of volunteers $n = 12$), the same 15 meteors are identified as in the reference spectrogram.

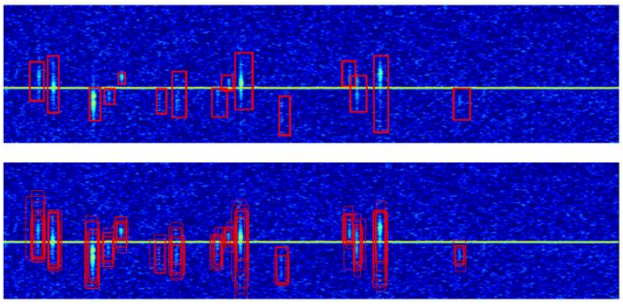

Figure 6 – Comparison of the reference meteor spectrogram (top) and optimal identification spectrogram by the method described above with 12 volunteers (bottom). The same meteors were identified in both cases.

Until now, we have only considered meteor pixels instead of meteor reflections as a whole. To which extent does meteor reflection identification by the above method correspond to the meteor echoes in the reference dataset? In order to investigate this, we have applied a minimum bounding box algorithm to group meteor pixels into individual meteor echoes.

For every value of n between 1 and 35, 1000 random combinations of $i_{\text{optimal}}(n)$ out of n volunteers are considered. For each combination, the number of hits (meteor reflections identified by both the reference and the proposed method) and the number of false detections (meteor reflections identified by the proposed method but not by the reference) are calculated.

In *Figure 7*, the medians of the percentage of hits and false detections over these 1000 iterations are plotted as a function of the number of volunteers n. For the *Radio*

Meteor Zoo, we will employ 10 volunteers per spectrogram, which amounts to a median percentage of hits of 95% and a median percentage of false detections of 6%. The median percentage of false detections is quite low because we have very few airplane echoes at night.

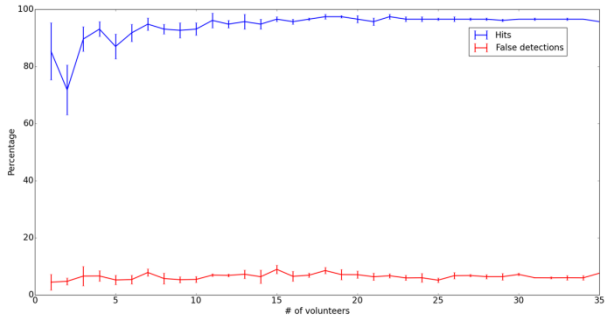

Figure 7 – Median percentage of hits and false detections of the proposed method as compared to the reference detection, as a function of number of volunteers *n*.

6 Discussion

Employing the meteor reflection identifications of 12 spectrograms by 35 volunteers, we were able to define a statistical method to identify meteor reflections. Based on $n = 10$ volunteers inspecting each spectrogram, a median percentage of hits of 95% and a median percentage of false detections of 6% is obtained. Note that post-processing (e.g. looking at the power profile) can be invoked to analyze and reject false detections after detection.

Since the population of *Radio Meteor Zoo* volunteers may differ systematically from the population of 35 volunteers in the test (in particular with regard to their physics background), a similar test will be performed in order to validate our approach with the *Radio Meteor Zoo* volunteers.

These manual identifications will prove to be extremely useful during meteor showers because these contain many complex overdense meteor echoes. They will also be of great use to calibrate and test the pre-existing and potential new automatic detection algorithms.

We are ready to start analyzing *Radio Meteor Zoo* data. It is accessible via the following URL: https://www.zooniverse.org/projects/zooniverse/radio-meteor-zoo. We kindly invite all readers to help us by identifying meteor reflections and promoting this website!

Acknowledgments

BRAMS is a project of the Royal Belgian Institute for Space Aeronomy (BIRA-IASB[2]) funded by the Belgian Solar - Terrestrial Centre of Excellence (STCE[3]). This project is carried out in collaboration with many radio amateurs from Belgium: without whose voluntary contribution we would have no observations. We thank them for their sustained effort. The identification of radio meteors by 35 volunteers was compared with our reference detection set. They were contacted by the authors during the Meteorendag 2015 in Heesch, The Netherlands and the IMC 2015 in Mistelbach, Austria. Also some colleagues from the Royal Belgian Institute for Space Aeronomy but unfamiliar with the BRAMS project were participating. We would therefore like to thank all the participants of our test panel. Gratitude is also expressed towards the Zooniverse team for hosting the *Radio Meteor Zoo* and for their valuable advice.

[2] http://www.aeronomy.be
[3] http://www.stce.be

References

Calders S., Lamy H., Gamby E. and Ranvier S. (2014). “Recent developments in the BRAMS project”. In Gyssens M., Roggemans P. and Zoladek P., editors, *Proceedings of the International Meteor Conference*, Poznan, Poland, 22-25 August 2013. IMO, pages 170–172.

Calders S. and Lamy H. (2014). “Automatic detection of meteors in BRAMS data”. In Rault J.-L. and Roggemans P., editors, *Proceedings of the International Meteor Conference*, Giron, France, 18–21 September 2014. IMO, pages 194–196.

Lamy H., Anciaux M., Ranvier S., Calders S., Gamby E., Martinez Picar A. and Verbeeck C. (2015). “Recent advances in the BRAMS network”. In Rault J.-L. and Roggemans P., editors, *Proceedings of the International Meteor Conference*, Mistelbach, Austria, 27-30 August 2015. IMO, pages 171–175.

Lintott C. J., Schawinski K., Slosar A., Land K., Bamford S., Thomas D., Raddick M. J., Nichol R. C., Szalay A., Andreescu D., Murray P. and Vandenberg J. (2008). “Galaxy Zoo: Morphologies derived from visual inspection of galaxies from the Sloan Digital Sky Survey”. *Monthly Notices of the Royal Astronomical Society*, **389**, 1179–1189.

Results from the Canadian Automated Meteor Observatory

Margaret Campbell-Brown

Department of Physics and Astronomy, University of Western Ontario, London, Canada
Margaret.campbell@uwo.ca

Some recent results from the Canadian Automated Meteor Observatory (CAMO) are presented. Comparing the begin heights and speeds of meteors between the two CAMO systems shows that the two populations, which differ by approximately an order of magnitude in mass, are quite different, with the more sensitive system recording many more slow meteors than the less sensitive system. At slow speeds for the more sensitive camera system, light curve shapes do not behave as expected, with stronger meteors having early-peaked light curves. Most meteoroids captured by the CAMO tracking system fragment in one way or another, and current ablation models are poor at predicting the nature of the fragmentation. The narrow field system is proving useful in many areas of meteor physics.

1 Introduction

While radio observations of meteors have the advantage of being independent of weather and daylight, there are many ways in which optical observations can provide more information about individual meteors. The errors in trajectories for multi-station meteors tend to be lower for optical than for radar meteors. Radars tend to scatter off one or a few points along the meteor trail, while optical observations can provide a more complete light curve and therefore constraints on meteor ablation. Optical observations have different observing biases than radar, and comparing speed and flux measurements in the two systems can help to determine if these are being adequately corrected.

The Canadian Automated Meteor Observatory (CAMO) consists of two sets of cameras for observing meteors optically. Here we present some of the recent work done with these systems.

2 The CAMO systems

Overview

The CAMO systems are described in detail in (Weryk et al., 2013). Cameras are placed at two sites, one near Tavistock, Ontario, Canada and the other near Elginfield, Ontario, Canada. They have been in operation since 2010. The two systems operate automatically when the sky is dark, clear and moonless.

The influx system

The first CAMO system consists of a single intensified video camera at each site. The cameras are Cooke pco.1200 CCD cameras, with 1600 by 1200 pixels and 14-bit optical depth, and run at 20 frames per second. They are lens coupled to 25 mm Gen III ITT image intensifiers with 50 mm objective lenses for a field of view of 20 degrees. The system can detect meteors as faint as +7.5 magnitude, but most of the meteors detected are around magnitude +5, since fainter meteors generally do not have enough frames to be useful.

Meteors are detected automatically, not in real time, with MeteorScan (Gural, 1997), and manually reduced.

The tracking system

The tracking, or mirror system, is inspired by the AIM-IT system (Gural et al., 2004), which was the first instrument to track meteors in real time. It consists of two intensified video cameras at each site. All four have ImperX VGA-120L CCD cameras (640 by 480 progressively scanned pixels, 12-bit optical depth) lens coupled to 18 mm image intensifiers. One camera at each site has a 25 mm f/0.85 lens, with a field of view of 28 degrees, and runs at 80 frames per second. Meteors in this system are detected in real time using Asgard; after four frames, a predicted trajectory is calculated and used to direct light from the meteor, with a pair of orthogonal mirrors, onto the second camera. This camera has a 545 mm f/11, 80 mm refractor as on objective lens. It runs at 120 frames per second, and has a field of view of 1.5 degrees. The cameras can detect meteors down to +5 magnitude, but most of the reduced meteors area around magnitude +3.

About one in three meteors observed with the tracking system are well tracked in the narrow field camera.

3 Results

Heights, speeds and sensitivity

Once the trajectories and speeds are obtained from two station meteors, one of the simplest and most useful ways to analyze the data is with a plot of begin height against speed. *Figure 1* shows these plots with more than 3000 meteors obtained with the tracking system (*Figure 1a*) and the influx system (*Figure 1b*).

Both systems show the expected trend of increasing begin height with increasing speed, and both show two approximate populations of meteoroids. More fragile or more volatile particles ablate higher at the same speed, while stronger or more refractory particles begin lower in the atmosphere. It is obvious from the plot that the influx

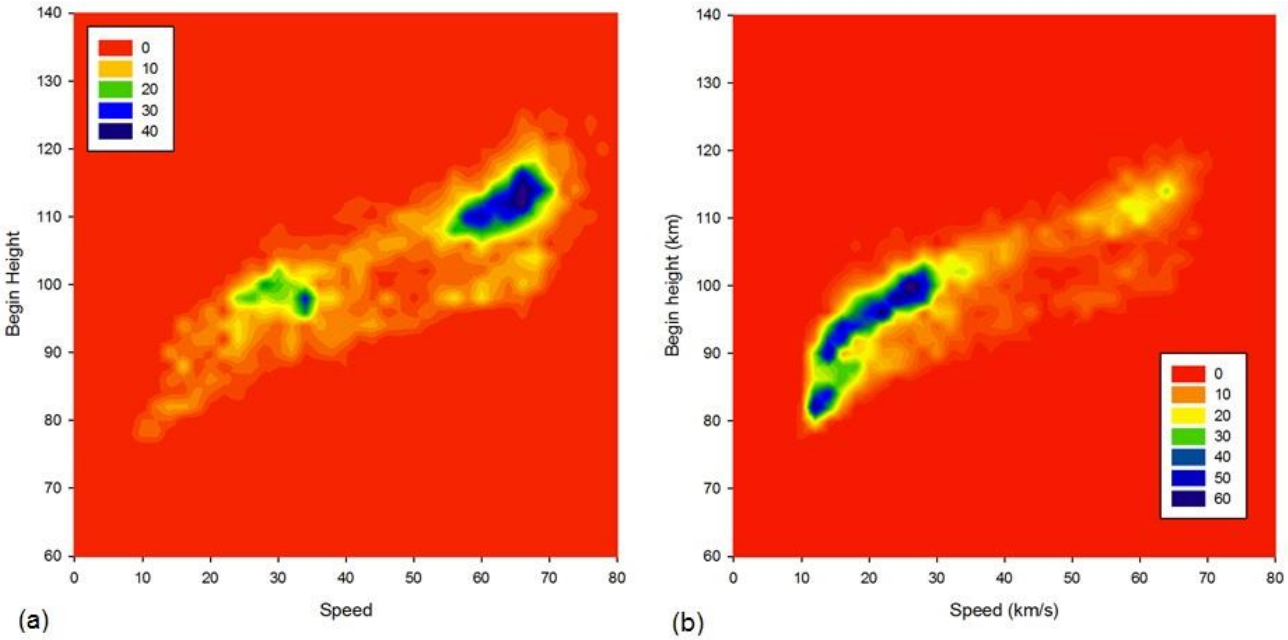

Figure 1 – Begin height vs. speed for the (a) tracking system and (b) influx system.

system sees many more slow meteors than fast ones, while the tracking system sees more fast meteors than slow ones. The reason for this is the difference in the limiting magnitudes between the two systems: the average mass at 30 km/s for the tracking system is about 1 mg, while the average for the influx system is 0.1 mg. The presence of the lowest speed, lowest begin height meteors is unexpected, and explored in Campbell-Brown (2015).

Light curves and strengths

The light curves of optical meteors are often used to determine the structure of meteoroids. In particular, a light curve with the peak toward the end of the curve is usually associated with a strong meteoroid, while a symmetric light curve with the peak in the middle is assumed to be produced by a weak, fragmenting meteoroid.

We can describe the shape of a light curve with the F parameter, which is the ratio of the difference between the height at peak magnitude and the end height to the difference between the begin and end heights. An F parameter less than 0.5 indicates an early-peaked light curve, and greater than 0.5 indicates a late-peaked light curve.

We can compare the F parameter to a measure of the meteoroid's strength. The K_b parameter was developed by Ceplecha (1967) to describe the energy needed to start intensive evaporation, taking into account the speed and zenith angle. Small K_b parameters indicate fragile or volatile material, while large ones indicate strong or refractory particles. We can separate the two populations seen in the begin height / speed plots above with a K_b parameter of about 7.1.

Figure 2 shows the F parameter of meteors from the influx system as a function of speed, with the black points showing all meteors and the red triangles only the strongest meteoroids, with K_b >7.1. At speeds over 30 km/s, all meteors have, on average, symmetric light curves. At low speeds, however, strong meteoroids have early-peaked light curves, the opposite of what we would expect.

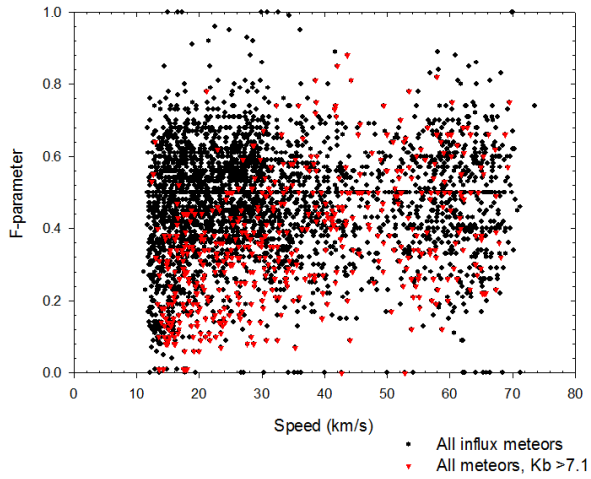

Figure 2 – Light curve skew as a function of meteor speed. The red triangles indicate the strongest meteoroids.

Meteoroid fragmentation

The CAMO tracking system has a resolution as high as 3 meters per pixel, though at usual ranges 5 meters per pixel is typical. This allows the system to observe fragmentation even in very faint meteors, which in lower resolution video appear not to fragment at all.

Figure 3 shows several examples of discrete and continuous fragmentation observed with the CAMO tracking system. Subasinghe et al. (2016) studied a large sample of tracking camera meteors, and found that about 85% had long tails, indicating some sort of continuous fragmentation into very small particles. Another 5% showed fragmentation into a few large pieces, and the

remainder showed almost no spread at all, implying that little or no fragmentation was taking place.

The same paper studied the connection between light curve shape and fragmentation behavior. It was found that, for fragmenting meteors, the light curves were generally symmetric, as expected. However, meteors showing very little fragmentation also had symmetric light curves: classical meteor theory suggests that their light curves should be late peaked, but this was not the case. The reason may be differential ablation of an inhomogeneous body, or small amounts of fragmentation not visible in the narrow field camera.

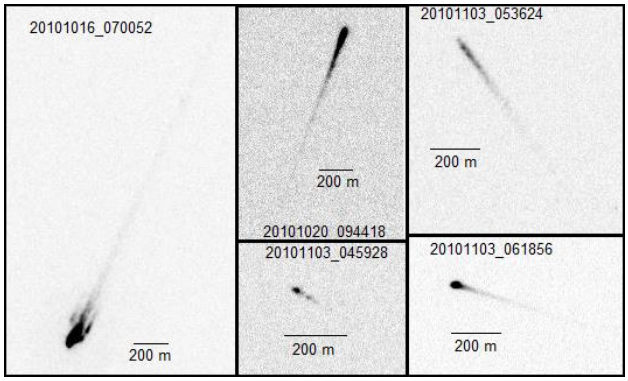

Figure 3 – Narrow field meteors observed with the CAMO tracking system.

The light emitted by fragments of meteoroids can also be used to constrain ablation models. Recently, two meteoroid ablation models (one by M. Campbell-Brown, the other by J. Borovička) were used to predict the appearance of ten meteors in the narrow field system, and both failed (Campbell-Brown et al., 2013). Both models predicted wakes which were both too long and too bright, indicating that the fragmentation models used were incorrect.

4 Conclusion

The difference in populations between the two CAMO systems of different sensitivities emphasizes the importance of observing meteors in different mass ranges. The origin and history of meteoroids is very different for particles of differing sizes and observations at all sizes provide interesting constraints in understanding how meteoroids formed and how their orbits evolve.

Data from the CAMO system show that light curve shape is not the simple indicator of meteoroid strength and fragmentation behavior it is sometimes assumed to be. Strong meteoroids may have symmetric or even (particularly for slow meteoroids) early-peaked light curves, and fragmentation behavior observed in the tracking system was not predictable from the wide field light curves.

Fragmentation is known to be important in the ablation of small meteoroids, and the CAMO system confirms that about 90% of meteoroids show obvious fragmentation.

In the future, data from the CAMO optical systems will be used to investigate debiased speed distributions of the sporadic meteoroid complex, to calculate optical meteor fluxes, and to look for meteoroids on hyperbolic orbits. The very precise spatial measurements possible with the narrow field camera will help to get very precise orbits. The narrow field measurements will also provide strong constraints to ablation models, with fragmentation and deceleration both much more tightly characterized.

Acknowledgments

CAMO was build thanks to a grant from the Canada Foundation for Innovation and support from the NASA Meteoroid Environment Office (NASA Cooperative Agreement NNX11AB76A).

References

Campbell-Brown M. D. (2015). “A population of small refractory meteoroids in asteroidal orbits”. *Planetary and Space Science*, **118**, 8–13.

Campbell-Brown M. D., Borovička J., Brown P. G. and Stokan E. (2013). “High-resolution modelling of meteoroid ablation”. *Astronomy and Astrophysics*, **557**, A41.

Gural P. (2007). “An operational autonomous meteor detector: Development issues and early results”. *WGN, Journal of the IMO*, **25**, 136–140.

Gural P., Jenniskens P. M. and Varros G. (2007). “Results from the AIM-IT meteor tracking system”. *Earth, Moon, and Planets*, **95**, 541–552.

Subasinghe D., Campbell-Brown M. D. and Stokan E. (2013). “Physical characteristics of faint meteors by light curve and high-resolution observations, and the implications for parent bodies”. *Monthly Notices of the Royal Astronomical Society*, **457**, 1289–1298.

Weryk R. J., Campbell-Brown M. D., Wiegert P. A., Brown P. G., Krzeminski Z. and Musci R. (2013). “The Canadian Automated Meteor Observatory (CAMO): System overview”. *Icarus*, **225**, 614–622.

Ablation of small Fe meteoroids – first results

David Čapek and Jiří Borovička

Astronomical institute of the Czech Academy of Sciences, Ondřejov, Czech Republic
capek@asu.cas.cz

A numerical model describing atmospheric flight of small iron meteoroids is presented. Several ablation scenarios are considered and it is discussed if these can explain a population of faint, short duration meteors with low beginning height and quick increase of brightness.

1 Introduction

A population of faint meteors with low velocities, low beginning heights and short duration has been described by Borovička et al. (2005) and Campbell-Brown (2015). Most of them have unusual light curves with rapid increase of brightness and maxima near the beginning of their luminous trajectory. A possible explanation is that the meteoroids are composed from iron; due to high thermal conductivity they are melted throughout before the beginning of ablation, which is then relatively rapid.

2 Model

We tried to check this hypothesis and developed a numerical model which considers spherical meteoroid with radial temperature field. The temperature of the meteoroid is determined from the heat diffusion equation with appropriate initial and boundary conditions. On the surface, the conservation of energy is considered – the incoming energy from the air flow is balanced by losses due to radiation, conduction and evaporation. The moving boundary between liquid and solid phase is described by Stefan's condition. The model uses thermophysical parameters for pure iron, most of which depend on temperature. Three alternative processes of ablation were studied:

Evaporation of liquid iron

When temperature reaches 1811 K, a layer of liquid iron appears on the surface. The evaporation rate of liquid iron is computed according to the *Hertz-Knudsen* formula (also called *Langmuir* evaporation). The melting of solid iron inside the meteoroid continues. At the same time the temperature of the melt further increases until it reaches boiling temperature, which depends on dynamic pressure. The evaporation from the surface causes a decrease of the meteoroid radius. The kinetic energy of the evaporated mass is transformed into radiation.

Liquid iron drop breakup

Liquid iron drop is subject to aerodynamic loading. If it is sufficiently intensive, the drop can deform and finally break up into many smaller droplets. This process increases the effective cross section and it would lead to a rapid increase of brightness. The condition for breakup is described by the critical *Weber* number.

Immediate removal of liquid layer

As soon as the liquid iron appears, it is immediately removed (blown off) from the surface by air flow and its kinetic energy is transformed into radiation.

In all these cases we considered luminous efficiency to be 1 percent and the heat transfer coefficient to be equal to 1.

3 Results

For the comparison with the model predictions we took light curves, pre-atmospheric masses and velocities determined for eight meteors by Borovička et al. (2005).

We found that the ablation caused by evaporation of the liquid iron layer is a too slow process and it would produce much longer meteors than observed ones. The second ablation process – a breakup of liquid iron drop would take place about ten kilometers below the terminal heights of the observed meteors. In some cases it would not take place at all. This process is therefore not able to explain the observed meteors. The ablation caused by immediate removal of the layer of liquid iron would produce (in most cases) slightly shorter meteors with slightly higher beginning and terminal heights.

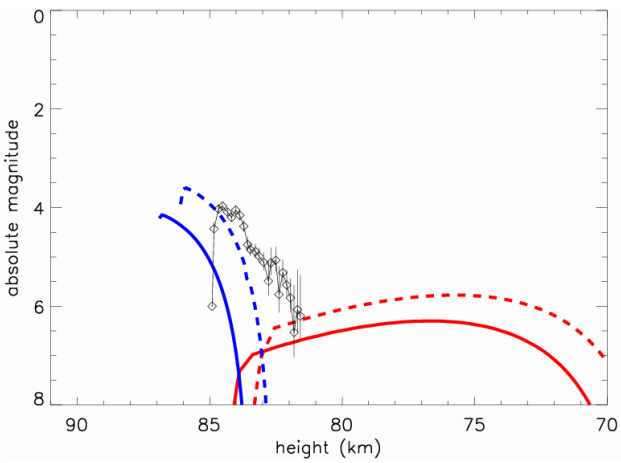

Figure 1 – Comparison of the measured light curve (black) with theoretical ones. The immediate blow off of the liquid layer would produce blue curves and the boiling of the liquid layer would produce red ones. Dashed and solid curves correspond to two different photometric masses deduced from the observation (3.3×10^{-5}g and 2.0×10^{-5}g).

Nevertheless, the model with this process leads to results which are much more similar to the observations than in the case of the previous two ablation processes.

The model considering vaporization of the layer of liquid iron predicts light curves completely different from the observed ones as it can be seen in *Figure 1*. On the other hand, the immediate removal of the liquid iron layer produces light curves, which are more similar to the observed ones. They have rapid increase of the brightness, the maxima near the beginning height and a slower decrease.

4 Conclusion

Our simple model shows that the ablation of small iron meteoroids cannot be described by the melting of the whole meteoroid volume and its consequent vaporization. Such process is too slow. The breakup of the liquid iron drop by aerodynamic loading is also inconsistent with observations since the breakup is expected at too low heights. The most probable ablation process is a fast blow off of the melted layer forming small droplets which then ablate rapidly.

Our next research will be devoted to a more precise description of this process, the variation of model parameters and several other improvements (use of thermophysical parameters for iron-nickel alloy, taking the oxidation of the liquid into account, etc.).

Acknowledgment

This work was supported by GAČR grant 16-00761S.

References

Borovička J., Koten P., Spurný P., Boček J. and Štork R. (2005). “A survey of meteor spectra and orbits: evidence for three populations of Na-free meteoroids”. *Icarus*, **174**, 15–30.

Campbell-Brown M. (2011). “A population of small refractory meteoroids in asteroidal orbits”. *Planetary and Space Science*, **118**, 8–13.

FRIPON network status

François Colas[1], Brigitte Zanda[2], Sylvain Bouley[3], Jérémie Vaubaillon[1], Chiara Marmo[3], Yoan Audureau[3], Min Kyung Kwon[1], Jean-Louis Rault[7], Pierre Vernazza[4], Jérôme Gattacceca[5], Stéphane Caminade[3], Mirel Birlan[1], Lucie Maquet[1], Auriane Egal[1], Monica Rotaru[6], Laurent Jorda, Cyril Birnbaum, Cyril Blanpain, Adrien Malgoyre, Julien Lecubin, Alberto Cellino[8], Daniele Gardiol[8], Mario Di Martino, Christian Nitschelm, Jorje Camargo, M. Valenzuela, Ludovic Ferrière, Marcel Popescu and Damien Loizeau

[1] **IMCCE, Observatoire de Paris, Paris, France**
francois.colas@imcce.fr

[2] **DIMPMC, Muséum National d'Histoire Naturelle, Paris, France**
Zanda@mnhn.fr

[3] **GEOPS, Université Paris Sud, Orsay, France**
sylvain.bouley@gmail.com

[4] **LAM, Institut Pytheas, Marseille, France**
pierre.vernazza@lam.fr

[5] **CEREGE, Institut Pytheas, Marseille, France**
gattacceca@cerege.fr

[6] **Universciences, Paris, France**
Monica.Rotaru@universcience.fr

[7] **IMO, Radio Commission**
f6agr@orange.fr

[8] **INAF, Osservatorio Astrofisico di Torino**
gardiol@oato.inaf.it

The FRIPON network (Fireball Recovery and Interplanetary observation Network) will be fully operational in 2016 (www.fripon.org). This “open source” project includes several new features that will be described in detail. We also discuss the opportunities for expansion outside France.
The main innovation is the connectivity of cameras enabling better efficiency for meteors detection, and the possibility of computing orbits in real time to organize an observation campaign within 24 hours.
Another innovation is the ability to daytime detections. Statistics show that there are more meteorites in late afternoon than during the rest of the day because of their low speed.
As the project has been designed from the start to handle a large number of cameras it is easy to extend it to increase its effectiveness. I will show the next extension of the network and its operation.

The dimension added by 3D scanning and 3D printing of meteorites

Sebastiaan J. de Vet

Meteor Section, Royal Netherlands Association for Meteorology and Astronomy
Sebastiaandevet@gmail.com

An overview for the 3D photodocumentation of meteorites is presented, focussing on two 3D scanning methods in relation to 3D printing. The 3D photodocumention of meteorites provides new ways for the digital preservation of culturally, historically or scientifically unique meteorites. It has the potential for becoming a new documentation standard of meteorites that can exist complementary to traditional photographic documentation. Notable applications include (i.) use of physical properties in dark flight-, strewn field-, or aerodynamic modelling; (ii.) collection research of meteorites curated by different museum collections, and (iii.) public dissemination of meteorite models as a resource for educational users. The possible applications provided by the additional dimension of 3D illustrate the benefits for the meteoritics community.

1 Introduction

The rapid technological and software developments in the 'maker community' have resulted in accessible means for 3D scanning and additive manufacturing, often competitive with industrial of scientific versions of similar technology. These developments also provide new means for amending scientific studies and documentation efforts of meteorites. For the meteoritics community, possible niches exist where 3D scanning and 3D printing may contribute to existing research, or even allow for new fields of science to be explored. Within the framework of this paper, I focus in particular on the digital 3D documentation and replication of objects, where the workflow itself may be broken down into three steps.

The first step involves the digitization of the object's shape and surface texture. In this case 'texture' refers to the image file that is projected on the polygons of a model, rather than the small-scale topography of its surface. One approach involves projection of a light pattern to aid the digitization of an object's shape. Examples of the method include laser scanners from a variety of commercial vendors and open source projects (i.e. using a 1D light pattern), while more advanced methods use a spatially differing light pattern (i.e. a 2D pattern) branded as 'structured light'. This term will be used hereafter as a generic term to refer to all methods where the distortion of a separate light source is used to quantify the geometry of an object. A contrasting approach relies on photogrammetry to derive a shape model from a multitude of photographic images. This approach has been widely used in various applications, e.g. for producing digital terrain models of landscapes in geosciences. Photogrammetry can be used to render 3D models of objects when they are covered from multiple angles. Several software programs are available that can facilitate this approach for digitizing objects in 3D models.

The second step requires the processing of the model using dedicated 3D software suites. Some commercial scanning hardware comes with its own model processing software, while other freely-available software programs offer similar functionality. As these functions are indigenous and may vary between various software suites, users seeking specific details are referred to the wealth of online tutorials and work flows described by the user communities. Typically these workflows encompass steps such as the clean-up of the mesh by removing artefacts and noise, the closing of holes in the mesh, and the stitching and merging of two or more meshes. These steps allow for the fusion of the 3D scans into one single 'watertight' shape model of the meteorite.

The final step is *Additive Manufacturing* (AM), commonly known as '3D printing', which aims at converting the digital model into a physical object. AM technology meanwhile involves many types of technologies based on extrusion, powder bed or light polymerization. As the materials portfolio has expanded rapidly the past few years, physical 3D models can now be produced using a variety of materials such as thermoplastics, polymers and ceramic powders. The innovative concept of the 3D printing approach is the additive nature of the manufacturing process, which contrasts the commonly used subtractive approach where material is removed (by e.g. drilling, milling etc.). For objects with complex organic geometries, such as meteorites, additive manufacturing offers sufficient degrees of freedom for fabrication of these types of objects. A popular method is *Fused Filament Fabrication* (FFF), also known as *Filament Deposition Modelling* (FDM), which is based on the extrusion of molten thermoplastics. This fabrication method lends itself well for the production of geometric facsimilia of meteorites. Due to the monochrome nature of the filament, models printed using FFF can only convey geometric characteristics. Other AM methods such as *Powder Bed* printing provide full-color printing capabilities and may render models into nearly photorealistic facsimilia of the

original meteorite. However, before the 3D model can be printed it has to be converted into a file format that is suitable for the printer to use, often this is the *Standard Tessellation Language* or STL file format. Subsequently this file needs to be 'sliced' into discrete printable layers that can be deposited by a 3D printer, using e.g. the *Fused Filament Fabrication* method. This final step in the 3D replication of a meteorite lies within reach of many, as 3D printer costs are reducing and access to 3D printing infrastructure is provided at 'maker spaces', via online commercial 3D printing services, or via online printing networks. In support of the workflow described above, this paper aims to (i.) qualitatively compare two different approaches to the 3D scanning of meteorites and (ii.) explore the unique potential of 3D scanning and 3D printing for the meteoritics community.

2 Methods and materials

For the proof of concept presented here, 3D scans and models were produced of an arbitrary meteorite; a Sayh al Uhaymir 001 meteorite that is classified as an ordinary chondrite (L5) and has been recovered from a remote desert region in Oman. Two contrasting methods for the digitization of the SaU001 were selected and compared, with user-friendliness and accessibility in mind. The first and most advanced method involves a *David 3D SLS-2* scanning system with an automated scanning platform (*Figure 1a*). This method uses a monochrome camera to measure the distortion of a light pattern projected by a projector onto an object, in order to triangulate points. Scan resolution can be as high as 0.1% of scanned object size, with a maximum of 0.06 mm, which renders an object into a high-fidelity digital model. The scanning algorithm also uses an RGB-color protocol to simultaneously obtain images in three color bands that are combined to produce a photographic texture file for draping over the shape model. Scans of the top and bottom of the SaU001 were made and semi-automatically (i.e. user-driven) merged in a manufacturer supplied software program to obtain a single shape model of the meteorite.

The second method that was evaluated did not require any special scanning hardware, other than a digital photo camera. Models were produced using Autodesk's *123D Catch*. This freeware software program finds a photogrammetric solution of many overlapping photos to produce a 3D model of the photographed object. The accuracy of the model is dependent on parameters such as image focus, scene background and lighting conditions, and therefore requires a structured approach during photographing (*Figure 1b*). Similar to the other method, a model covering the entire shape of a meteorite requires several digital models from two or more orientations to be made, which subsequently need to be merged into one single shape model using software programs such as *MeshLab*.

Figure 1 – The two methods that have been compared for digitizing a SaU001 meteorite. (a) The set-up as used for scanning with the structured light approach using the David 3D SLS-2 (product images from www.david-3d.com). In (b) the structured approach required for photographing an object when using photogrammetric software such as Autodesk's 123D Catch.

3 Results and discussion

Digitization of the SaU001 meteorite using the two methods is shown in *Figure 2*. The 3D model comprises a surface composed of triangles (faces) that collectively form the model's so-called 'mesh'. The mesh's face counts of the two models was found to differ significantly; 3954344 for structured light scanning vs. 29900 for the photogrammetric solution. This difference reflects the difference in resolution that can be achieved with each technique. In practice for 3D printing this difference may be nullified by the printing resolution (*Figure 3*). The two methods compared in this study therefore illustrate the range of options, but also the quality available to users interested in the 3D digitization of objects. Based on resolution criteria, structured light scanning offers a high-resolution approach to producing 3D models. This comes, however, at the cost of investing in the required hardware. This is contrasted by the photogrammetry approach that only requires a minimum of a photo camera, but at a tradeoff of a more extensive workflow to obtain the final 3D model. The resolution requirements of the final model and the intended application should therefore drive the method selection. For example, the 123D Catch software renders a model in arbitrary units and needs additional scaling to render a model at true size for printing (*Figure 3*), albeit that this is not a stringent requirement for e.g. online applications. The high-resolution models obtained by structured light

Earth' orbit at 2015 June 6.5, after the comet's perihelion passage, again. Mass of the black particle was not changed. Its value is equal to our model mass $M = 1.78 \times 10^{-11}$ kg.

The examples showed that the considered non-gravitational forces can guide an ejected particle from the Kreutz sungrazers to the Earth's crosser orbit. This process is more sensitive to the mass of a particle than to its ejection velocity. To receive an Earth crossing particle from a comet belonging to the Kreutz group a high ejection velocity is needed. The ejection velocity in our example, 15 km s^{-1}, is higher than the supposed ejection velocity of 0.6−1 km s^{-1} derived from observations of the Perseids by Harris et al. (1995) and Wu and Williams (1996) or the significantly higher values according to Williams (1996).

4 Conclusion

The spatial distribution of model particles ejected with zero velocity from the comet with mean orbital elements of the Kreutz group can be used for the estimation of the possibility for such source of Earth crossing particles. Orbital elements of comets from the Kreutz group are not very different. Therefore, the structure of hyperbolic and near parabolic dust streams of the Kreutz comets at their apparition near the Sun must be very similar. The width and length of such streams depends on the activity of a parent comet and its perihelion distance. We can conclude that the resulting distribution of the investigated particles is more or less common for all comets of this group.

In spite of a number of simplifications involved, some interesting inferences are possible. Since the dust tail occupied a thin layer around the plane of a cometary orbit, the point of its crossing by a detector determines uniquely the size and time release of the particles encountered. Essentially most of the dust released from comets belonging to the Kreutz sungrazers leaves the solar system on near-parabolic or hyperbolic orbits, because the radiation pressure limit is high.

A particle with favorable mass, ejection time, and velocity can cross the Earth's orbit. Due to the orbit of a parent comet, with very small perihelion distance, the probability for an Earth crossing particle is higher for the pre-perihelion ejections than for those, after the perihelion. Time interval for post-perihelion ejections is very short and does not exceed several days.

Generally, to obtain the Earth crossing particle at a given mass and ejection time, a very high ejection velocity, of several km s^{-1} is needed. On the other hand, if a particle has a suitable mass, the Earth crossing orbit of the particle is created with zero or a very small ejection velocity. Therefore, comets belonging to the Kreutz sungrazers may be considered as a source of the Earth-crossing small dust particles.

Acknowledgment

The authors thank the Local and Scientific organizing committee of the IMC 2016 for the conference in Egmond and its Proceedings 2016.

References

Everhart E. (1985). “An efficient integrator that used Gauss-Radau spacing”. In Carusi A. and Valsecchi G. B., editors, *Dynamic of Comets, their Origin and Evolution*. Reidel, Dordrecht, pages 185–202.

Giorgini J. D., Yeomans D. K., Chamberlin A. B., Chodas P. W., Jacobson R. A., Keesey M. S., Lieske J. H., Ostro S. J., Standish E. M. and Wimberly R. N. (1996). “CJPL’s on-line solar system data service”. *Bull. Am. Astron. Soc.*, **28**, 1158.

Guliyev A. C. (2010). “Origin of short-period comets”. Baku, 1–151.

Harris N. W., Yau K. K. C. and Hughes D. W. (1995). “The true extent of the nodal distribution of the Perseid meteoroid stream”. *Monthly Notices of the Royal Astronomical Society*, **273**, 999–1015.

Klačka J. and Pittich E. M. (1994). “Long-term orbital evolution of dust particles ejected from comet Encke”. *Planetary and Space Science*, **42**, 109–112.

Kreutz H. C. F. (1888). “Undersuchungen Über das Cometensystem 1843 I, 1880 I und 1882 II”. Publication der Sternwarte in Kiel, Druck von C. Schaidt, C. F. Mohr, 3, 111.

Marsden G. B. and Williams I. P. (2008). “Catalogue of Cometary Orbits”. 17th ed. Minor Planet Center/ Central Bureau for Astronomical Telegrams, Cambridge, MA.

Sekanina Z. (2000). “Solar and Heliospheric Observatory Sungrazing Comets with Prominent Tails: Evidence on Dust-Production Peculiarities”. *The Astrophysical Journal*, **545**, L69–L72.

Sekhar A. and Asher D. J. (2014). “Meteor showers on Earth from sungrazing comets”. *Monthly Notices of the Royal Astronomical Society*, **437**, L71–L75.

Verniani F. (1973). “An Analysis of the Physical Parameters of 5759 Faint Radio Meteors”. *Journal of Geophysical Research*, **78**, 8429–8462.

Williams I. P. (1996). “What Can Meteoroid Streams Tell Us about the Ejection Velocities of Dust from Comets”. *Earth, Moon, and Planets*, **72**, 321–326.

Wu Z. and Williams I. P. (1996). “Leonid meteor storms”. *Monthly Notices of the Royal Astronomical Society*, **280**, 1210–1218.

Yasunori Fujiwara, Jiri Borovicka and Pete Gural.

In the evening there was time for workshops. Here the workshop by Kristina Veljkovic on software for the analysis of visual meteor data.

Werkgroep Meteoren – 70 Years and counting

Urijan Poerink[1,2] and Sebastiaan J. de Vet[1]

[1] **Meteor Section, Royal Netherlands Association for Meteorology and Astronomy**

[2] **Esdoornlaan 12, NL-5263 GE Vught, The Netherlands**

poerinku@planet.nl

In 2016 the Meteor Section of the Royal Netherlands Association for Meteorology and Astronomy celebrated its 70 year jubilee. In this paper we provide a brief historical narrative that incorporates the main developments and events of the Meteor Section, spanning seven decades of meteor observations in The Netherlands.

1 Introduction

Dutch amateur astronomy has a long tradition in meteor observations. Meteor research in The Netherlands truly began the 1860's, just like in other countries. The spectacular Leonid storms of 1833 and the years 1866-1868 have had a major effect on the development of the scientific study of meteors, which had previously been thought to be atmospheric phenomena. In 1866 observers counted hundreds of Leonids per minute/a few thousand per hour in Europe.

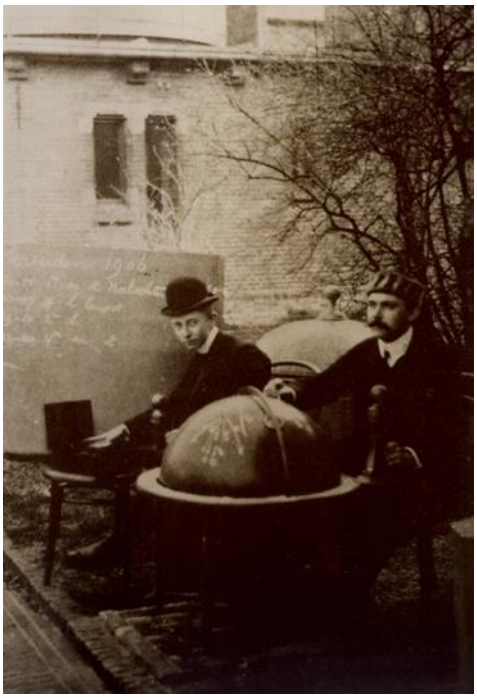

Figure 1 – Perseids, August 1906. Dr. Jan van der Bilt (r.) and Dr. Adriaan van Maanen and their big black sphere, on which they chalked the meteors (Sonnenborgh Observatory, Utrecht).

In 1943, during World War II, three young amateur astronomers, Hugo van Woerden, Sidney van den Bergh and Lammert Huizing established the Astroclub, the predecessor of the present-day Meteor Section. Their club of meteor observers comprised brothers, friends, mathematic teachers and other amateur observers and grew steadily in 1943–1944 to a group of about 35 members. They set up a national network of meteor observers and organized observing campaigns. In their first steps in meteor observations they experienced many practical difficulties. One of those difficulties was related to the ongoing ware time conditions; during World War II the occupying force confiscated most radio sets and therefore the observers could not receive time signals in order to correct their clockworks. The members of the Astroclub edited the monthly magazine 'De Meteoor', which in 1946 would become the section's astronomical magazine. Observers publish their reports and results of their observations in 'De Meteoor' and the monthly magazines of the Netherlands Association for Meteorology and Astronomy ('Hemel en Dampkring' and later in 'Zenit'). After WWII in August 1946, the 'Werkgroep Meteoren van de Nederlandse Vereniging voor Weer- en Sterrenkunde (NVWS)' was formally founded at the suggestion of Dr J.J. Raimond Jr., the President of the NVWS. Internationally the group became known as the Meteor Section of the Netherlands Association for Meteorology and Astronomy.

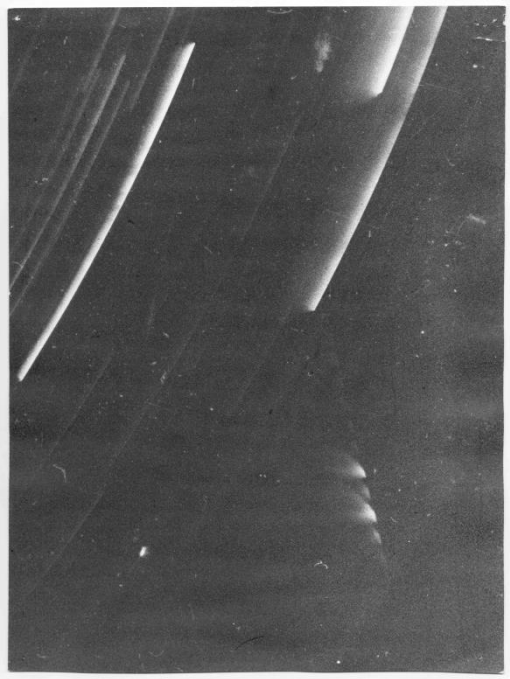

Figure 2 – First 'Dutch' meteor photograph was taken on 7 August 7 1953 during a Perseid observation campaign by amateur-astronomer Mr. M. Alberts.

2 Highlights from 70 years of the Meteor Section

The 1950's

On 7 August 1953, during the Perseid Campaign, amateur astronomer Mr. Machiel Alberts obtained a very first photograph of a 'Dutch' meteor (see *Figure 2*).

The 1960's

- In the 1960's amateurs made photographic plates of meteors with large cameras originally intended for aerial photography. ('upside-down aerial photography', *Figure 3*).
- The Meteor Section presented a catalogue, containing observations of anomalous sounds for fireballs from 1947-1958.

Figure 3 – Amateurs make photographic plates of meteors with cameras originally intended for aerial photography.

- In 1966 amateurs photographed the spectrum obtained of a Lyrid meteor (*Figure 4*) and in 1967 they observed radar echoes of the Leonid outburst, using the transmitter of a radar station at the University of Eindhoven (*Figure 5*).

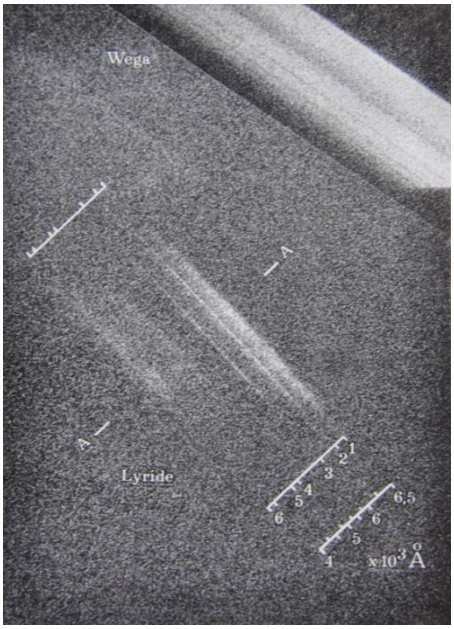

Figure 4 – Spectrum of a Lyrid meteor taken in the skies above The Netherlands in 1966.

Figure 5 – Member of the Meteor Section listening to the echoes of meteors via radio meteor scatter. the radio waves, reflected by the meteor, on paper. A Yagi antenna "catches" the radio signal reflected from a meteor ionization trail and a pen recorder captures it on paper.

- In 1969 amateurs used spectrographs for the imaging of meteors with a glass prism to simultaneously obtain the meteor's spectrum (*Figure 6*).

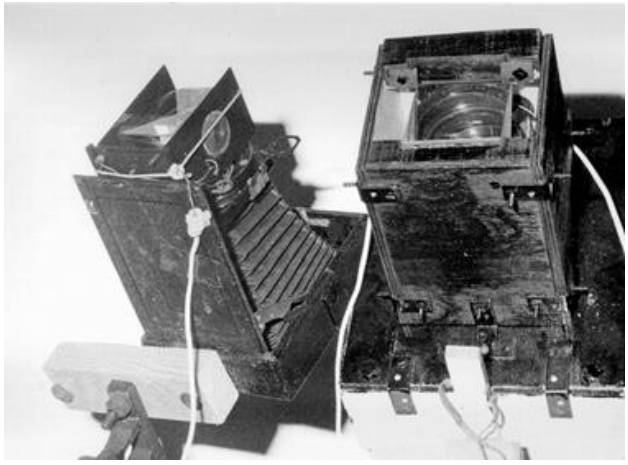

Figure 6 – Meteor spectrographs, used by members of the Meteor Section in the late 1960s.

Figure 7 – A Perseid campaign in the '90's. On the front the first all sky camera of Felix Bettonvil.

The 80's and early-90's

- During annual meteor campaigns amateurs made visual and photographic observations using batteries

of two or more cameras and increasingly sophisticated equipment (*Figure 8*).

Figure 8 – Photo batteries of six and eigth single-lens reflex cameras (MECAT's), built by Felix Bettonvil (1980's, 1990's). MECAT is the acronym of 'MEteor CATcher'.

- A successful Perseid observation campaign in 1993 took a large group of members to observation sites in The Netherlands and France, where they witnessed a ZHR of more than 300 during the outburst on 11–12 August 1993 (*Figure 10*).
- Batteries of six and eight single-lens reflex cameras (MECAT = MEteor CATcher), built by Felix Bettonvil, were used extensively for all-sky meteor observations in the 1980's and 1990's (*Figure 7*).

The90's and -2000's

- The Meteor Section carried out various successful international observations, e.g. to monitor the Leonid outbursts of 1998, 1999, 2001 and 2002. Members travelled to observation sites in The Netherlands, Jordan, South Korea, China, Denmark, Spain, France and Portugal. They photographed thousands of Leonids.
- The Meteor Section and its members introduced more and more meteor observing methods and developed sophisticated photographic and video equipment. A growing number of all-sky cameras cover the Dutch airspace and thanks to that, searching for meteorites takes on a new dimension. In 2013 and 2015 two fireballs led to search campaigns for meteorites. Meteorite events were organized for local inhabitants, alas with no recovery of new meteorites.
- The Meteor Section continues to expand digitally; the website and social media are used to collect fireball reports and an effective public outreach program takes place via popular social media.

3 Involvement in the recovery of 'Dutch' meteorites

Several meteorites have fallen in The Netherlands. On 12 June 1840, a big stone fell in front a group of peat cutters near de Dutch village of Uden. Not long thereafter on 2 June 1843, this meteorite impact was followed by the fall of two masses near the city of Utrecht. Years later those stones were recognized as meteorites. No meteorite falls have been documented in The Netherlands in the period predating 1840, with the exception perhaps of an event that took place in the city Dordrecht. On 6 August 1650, a glowing stone was strew down "with the lightning" and broke the windows and burned the woodwork of the Mayor's house in the city of Dordrecht. In 1807 this stone was lost in the explosion of a ship stocked with gunpowder in the city Leiden, and was lost without being studied in detail to establish its nature.

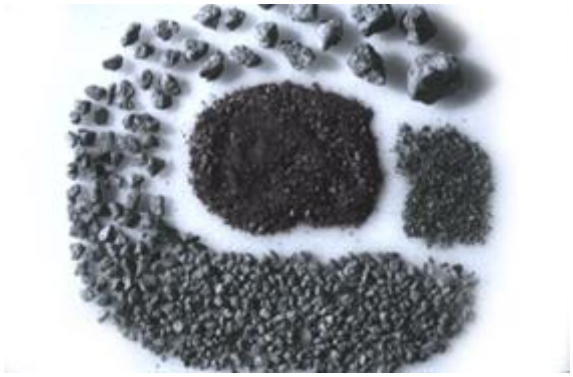

Figure 9 – All fragments of the Glanerbrug meteorite which hit a house on 7 April 1990.

The Meteor Section played a notable role in the recovery of the Glanerbrug meteorite. In the evening of 7 April 1990 a meteorite crashed through the roof of a house in the Dutch village of Glanerbrug, near the German border (*Figure 9*). The Meteor Section and other Dutch and German astronomical and meteorological observatories and institutes received hundreds of reports of the fireball. A team of researchers of the Meteor Section and the Dutch Meteor Society interviewed witnesses and managed to reconstruct the trajectory. The fall of the Glanerbrug (LL4-6, 855 g) and the subsequent investigations and research, plus its publication, mark one of the highlights in the 70 years history of the Meteor Section.

In 2012 a meteorite (CM2-an, 65g) was rediscovered with the help from Meteor Section members. Historical research showed that on 27 October 1873 a farmer witnessed the fall of the meteorite in his field near the village of Diepenveen.

The Uden (1840), Utrecht (1843), Diepenveen (1873), Ellemeet (1925) and Glanerbrug (1990) are currently the only meteorites recovered in The Netherlands. They are considered to be items of natural historical heritage and fragments are curated in various national and international university and museum collections.

Figure 10 – The Perseid Campaign in August 1993 in Southern France. Members of the Meteor Section and other Dutch amateur astronomers witnessed the Leonid outbursts in several countries (e.g.. The Netherlands, Jordan, South Korea, China, Denmark, Spain, France, Portugal). They photopgraphed thousands of Leonids in November 1998, 1999, 2001 and 2002

4 International Meteor Conferences in the Netherlands

Figure 11 – The first IMC in The Netherlands, May 1983.

As part of its international outlook on meteor observations, the Meteor Section has continuously invested itself in organizing international events, such as the International Meteor Conferences (IMC's) of the International Meteor Organization (IMO). Since the 1980's the Meteor Section and the International Meteor Organization have organized four International Meteor Conferences in The Netherlands, which include:

- *Lattrop, Brecklenkamp, May 1983*: 24 amateurs from Belgium, Germany and the Netherlands, organized the 4th International Meteor Weekend (*Figure 11*).
- *De Lutte (Oldenzaal), March 1988*: 65 amateurs and professionals from 9 countries participated in the 7th International Meteor Conference (*Figure 12*).
- *Apeldoorn, September 1996*: The Meteor Section hosted the 15th International Meteor Conference with 61 participants from 12 countries in Apeldoorn (*Figure 13*).
- *Roden, September 2006*: The Meteor Section hosted the 25th International Meteor Conference with 68 participants from 16 different countries. The participants paid a visit to the Westerbork Synthese Radio Telescope and LOFAR (LOw-Frequency ARray) (*Figure 14*).
- *Egmond, June 2016*: 157 participants from 30 countries from five continents gathered at this 35th meeting. It was the first time that so many professionals and amateurs came together at an IMC.

Figure 12 – The second IMC in The Netherlands, March 1988, with Dr. Bertil Lindblad giving his lecture.

Figure 13 – Hugo Van Woerden, one of the founding members of the Meteor Section during his talk at the 1996 IMC in Apeldoorn.

5 Awards for members of the Meteor Section

In recognition of their contribution to the field of meteor science, several members of the Meteor Section have been laureate for their efforts in the advancement of the field of meteor science. The most notable award is bestowed by the Royal Netherlands Association for Meteorology and Astronomy (KNVWS). This award – named after the Dutch astronomer Dr. Jan van der Bilt (1876–1962) – was established in 1944 to honor amateurs who either contributed significantly to the popularization of astronomy, or as an amateur contributed to astronomy on a professional level. The ten Meteor Section members are recipients of the 'Van der Bilt Prize' include Thomas van Dijk (1957), Johan Degewij (1966), Ben Apeldoorn (1971), Machiel Albers (1974), Felix Bettonvil en Urijan Poerink (1991), Simon van Leverink (1995), Herman ten Haaf (2000) and Koen Miskotte and Casper ter Kuile (2008).

6 Conclusion

Meteor and meteorite research in The Netherlands has evolved and diversified significantly during the seventy years gone by since the founding of the Meteor Section. While many meteor observers are currently involved in high-tech forms of meteor observations, using all-sky cameras or automated camera systems, others are involved in computational aspects of orbits, dark flights and strewn fields; the study meteorites; or just enjoy themselves observing meteors with the unaided eye. Even after 70 years, meteor observations in The Netherlands are still a flourishing activity with dozens of active amateurs and professionals.

Figure 14 – The 2006 IMC participants on excursion at Westerbork.

Novel methods for 3D numerical simulation of meteor radar reflections

Jukka Räbinä[1], Sanna Mönkölä[1], Tuomo Rossi[1], Johannes Markkanen[2], Maria Gritsevich[3,4,5] and Karri Muinonen[2,3]

[1] **University of Jyvaskyla, Department of Mathematical Information Technology, P.O.Box 35 (Agora), FI-40014 University of Jyvaskyla, Finland**

[2] **Department of Physics, P.O. Box 64, FI-00014 University of Helsinki, Finland**

[3] **Finnish Geospatial Research Institute, P.O. Box 15, FI-02431 Masala, Finland**

[4] **Dorodnicyn Computing Centre, Federal Research Center "Computer Science and Control" of the Russian Academy of Sciences, 119333 Moscow, Russia**

[5] **Institute of Physics and Technology, Ural Federal University, 620002 Ekaterinburg, Russia**

We use two novel methods for numerical simulation of meteor radar reflections. The one is based on the discrete exterior calculus, time-dependent simulations, and a control-based approach for accelerating the time evolution. The other is implemented as a time-harmonic solver based on the volume integral equation method for electric current. Despite the different framework, both methods give the solution in frequency domain. We model the radar reflections in a three-dimensional space as time-harmonic electromagnetic scattering from plasmatic obstacles. This makes our study different from the more conventional numerical simulations concerning scattering by a solid obstacle without a plasma model.

1 Introduction

The meteor head echo feature has been studied by high power large aperture (HPLA) radars since 1960's (Evans, 1965). Based on the observations conducted by the different radar systems and post-processing techniques, there exist several models for the meteor head echo simulations. One reason for this is the characteristics of the radar system, e.g., in terms of frequency and antenna geometry (Kero et al., 2012). It is also worth mentioning that there are differences in the meteor sizes. According to the observations reported by, e.g., Vertatschitsch et al. (2011) and Wannberg et al. (2011), the head echo can be modeled as overdense scatter from a plasma layer, surrounding the meteor, with a certain density distribution. In these models, the plasmatic object is assumed to be a conducting spherical object, and the electromagnetic phenomenon can be presented by partial differential equations coupling the electric and magnetic fields. The traditional way of solving electromagnetic problems, presented in the space-time domain as partial differential equations, is to use the Yee's finite difference time domain (FDTD) method (Yee, 1966). In this study, we use more generalized finite differences by applying the discrete exterior calculus (DEC) for the numerical simulation of meteor radar reflections. We also compare the method with another recently introduced efficient method that is based on the volume integral equation method for the electric current (J-VIE).

2 Numerical models and simulation methods

With numerical techniques, it is possible to test how changes in the atmospheric conditions affect the meteor radar reflections and explain unexpected results in the measurements. To get reliable simulation outputs, the appropriate models, methods and input information all need to be defined. We apply the partial differential equation model, in which the source of the scatter is presented as a plasmatic obstacle, and the dielectric tensor is derived from the equation of motion presenting charged, non-magnetized cold plasma (Nickisch and Franke, 1992). Numerical simulations based on the model are presented with the FDTD for 2D layers by Dyrud et al. (2008) and for 3D domains by Yu and Simpson (2010). The recent method development and enhanced computational resources provide possibilities to improve the accuracy of the numerical simulations or solve more demanding problems. We present two numerical methods that have recently shown to be efficient for 3D simulations.

3 Discrete exterior calculus

The properties and calculus of differential forms is provided in a natural way at the discretization stage. Hence, with the discrete exterior calculus (DEC), constructed with discrete differential forms, we associate the degrees of freedom of the electric and magnetic fields to the primal and dual mesh structures, respectively. The connection between the primal and dual forms is obtained by the discrete Hodge operator, the quality of which depends on the mesh construction. Our generalized formulation of the DEC for Maxwell's equations (Pauly and Rossi, 2011) works on unstructured grids, and it covers both the classical Yee's FDTD scheme and the Bossavit-Kettunen approach (Bossavit and Kettunen, 1999). The method has shown to give promising results with time-dependent problems (Räbinä et al., 2015).

4 Accelerated convergence for time simulation

The time-harmonic solution can be reached by asymptotic time simulation. However, the method is computationally inefficient, especially for scattering problems with non-convex or inhomogeneous obstacles. We improve the method by accelerating the convergence of the time-domain simulation to the steady-state solution. The concept is earlier applied and compared to other methods in acoustics (Airaksinen and Mönkölä, 2010), elastodynamics (Mönkölä et al., 2008), and electromagnetics (Räbinä et al., 2014). With the DEC space discretization, only matrix-vector multiplications are needed for explicit time-stepping which provides efficient time evolution. The first results considering three-dimensional electromagnetics coupled with the meteor plasma dynamics are presented by Räbinä et al. (2016).

5 Volume integral equation method for the electric current

In the volume integral equation method for the electric current (J-VIE), the unknown equivalent electric current density is expanded with piecewise constant basis functions (Markkanen et al., 2012). The resulting system is solved iteratively by the generalized minimal residual method restarted after every 50 iterations (GMRES(50)). The matrix-vector multiplication in each iteration step is accelerated by the pre-corrected-FFT algorithm.

6 Conclusions

For both methods, only sparse matrices are stored. With the DEC, most of the matrices are diagonal, and the solution procedure is realized by the conjugate gradient method. Only the current and previous gradient and search vectors and scalar-valued weights must be stored at each iteration. For the VIE-based method, a large but sparse pre-correction matrix for the FFT is assembled, and the solution method (GMRES) uses the results of the earlier iterations. The DEC-based controlled time integration is found to be more efficient, and its performance is not sensitive to the level of discretization and the values of the material parameters.

Acknowledgments

This project has been funded by the Academy of Finland, grants 259925, 257966, 260027, and 260076, the ERC Advanced Grant No 320773, ”Scattering and Absorption of Electromagnetic Waves in Particulate Media” (SAEMPL), and the Act 211 of the Government of the Russian Federation, agreement No 02.A03.21.0006. The authors acknowledge being a part of the network supported by the COST Action MP1104 ”Polarization as a tool to study the Solar System and beyond” and by the COST Action TD1403 ”Big Data Era in Sky and Earth Observation”.

References

Airaksinen T. and Mönkölä S. (2010). “Comparison between the shifted-Laplacian preconditioning and the controllability methods for computational acoustics”. *Journal of computational and applied mathematics*, **234**,1796–1802.

Bossavit A. and Kettunen L. (1999). “Yee-like schemes on a tetrahedral mesh, with diagonal lumping”. *International Journal of Numerical Modelling*, **12**, 129–142.

Dyrud L., Wilson D., Boerve S., Trulsen J., Pecseli H., Close S., Chen C. and Lee Y. (2008). “Plasma and Electromagnetic Simulations of Meteor Head Echo Radar Reflections”. *Advances in Meteoroid and Meteor Science*. Springer New York, pages 383–394.

Evans J. V. (1965). “Radio-echo studies of meteors at 68-centimeter wavelength”. *Journal of Geophysical Research*, **70**, 5395–5416.

Kero J., Szasz C., Nakamura T., Terasawa T., Miyamoto H. and Nishimura K. (2012). “A meteor head echo analysis algorithm for the lower VHF band”. *Annales Geophysicae*, **30**, 639–659.

Markkanen J., Ylä-Oijala P. and Sihvola A. (2012). “Discretization of volume integral equation formulations for extremely anisotropic materials”. *IEEE Trans. Ant. and Propag.* **60**, 5195–5202.

Mönkölä S., Heikkola E., Pennanen A. and Rossi T. (2008). “Time-harmonic elasticity with controllability and higher-order discretization methods”. *Journal of Computational Physics*, **227**, 5513–5534.

Nickisch L. J. and Franke P. M. (1992). “Finite-difference time-domain solution of Maxwell’s equations for the dispersive ionosphere”. *IEEE Antennas and Propagation* **34**, 33–39.

Pauly D. and Rossi T. (2011). “Theoretical considerations on the computation of generalized time-periodic waves”. *Advances in Mathematical Sciences and Applications*, **21**, 105–131.

Räbinä J., Mönkölä S. and Rossi T. (2015). “Efficient time integration of Maxwell’s equations by generalized finite differences”. *SIAM Journal on Scientific Computing*, **37**, B834–B854.

Räbinä J., Mönkölä S., Rossi T., Markkanen J., Gritsevich M. and Muinonen K. (2016). “Controlled time integration for the numerical simulation of meteor radar reflections”. *Journal of Quantitative Spectroscopy and Radiative Transfer*, **178**, 295–305.

Räbinä J., Mönkölä S., Rossi T., Penttilä A. and Muinonen K. (2014). “Comparison of discrete exterior calculus and discrete-dipole approximation for electromagnetic scattering”. *Journal of Quantitative Spectroscopy and Radiative Transfer*, **146**, 417–423.

Vertatschitsch L. E., Sahr J. D., Colestock P. and Close S. (2011). “Meteoroid head echo polarization features studied by numerical electromagnetics modeling”. *Radio Science*, **46**, RS6016.

Wannberg G., Westman A. and Pellinen-Wannberg A. (2011). “Meteor head echo polarization at 930 MHz studied with the EISCAT UHF HPLA radar”. *Annales Geophysicae*, **29**, 1197–1208.

Yee K. S. (1966). “Numerical solution of initial boundary value problems involving Maxwell’s equations in isotropic media”. *IEEE Transactions on antennas and propagation*, **14**, 302–307.

Yu Y. and Simpson J. J. (2010). “An EJ collocated 3-D FDTD model of electromagnetic wave propagation in magnetized cold plasma”. *IEEE Transactions on Antennas and Propagation*, **58**, 469–478.

Also kind of a tradition nowadays: table soccer. Dušan Pavlovic, Uroš and Dušan Bettonvil versus Ljubica Grašić and Javor Kac, with Snežana Todorović as supporter.

Meteor detections at the Metsähovi Fundamental Geodetic Research Station (Finland)

Arttu Raja-Halli[1], Maria Gritsevich[1,2,4], Jyri Näränen[1], Manuel Moreno-Ibáñez[1,3], Esko Lyytinen[4], Jenni Virtanen[1], Nataliya Zubko[1], Jouni Peltoniemi[1,5] and Markku Poutanen[1]

[1] **Finnish Geospatial Research Institute (FGI), Masala, Finland**
firstname.lastname@nls.fi

[2] **Institute of Physics and Technology, Ural Federal University, Ekaterinburg, Russia**
gritsevich@list.ru

[3] **Institute of Space Sciences (IEEC-CSIC), Barcelona, Spain**
mmoreno@ice.csic.es

[4] **Finnish Fireball Network, Helsinki, Finland**
esko.lyytinen@jippii.fi

[5] **University of Helsinki, Helsinki, Finland**
jouni.peltoniemi@helsinki.fi

We provide an overview and present some spectacular examples of the recent meteor observations at the Metsähovi Geodetic Research Station. In conjunction with the Finnish Fireball Network the all-sky images are used to reconstruct atmospheric trajectories and to calculate the pre-impact meteor orbits in the Solar System. In addition, intensive collaborative work is pursued with the meteor research groups worldwide. We foresee great potential of this activity also for educational and outreach purposes.

1 Introduction

The Metsähovi Geodetic Research Station of the Finnish Geospatial Research Institute (FGI) of the National Land Survey of Finland (NLS) (before 1.1.2015 Finnish Geodetic Institute) is one of the Global Geodetic Observation System (GGOS) core sites and is equipped with all the fundamental space geodetic techniques (e.g., satellite laser ranging – SLR and Global Navigation Satellite System – GNSS) together with superconducting and absolute gravimeters. Satellite laser ranging is a space geodetic technique where the flight time of short laser pulses to, e.g., Earth orbiting satellites is used to range the objects with an accuracy that is a couple of mm for low Earth orbit targets. SLR can be used, e.g., to calculate the orbits of satellites, to study the changes in the low harmonics of Earth's gravity field, and to determine the movement of the Earth's center of mass. There are currently approximately 50 operational SLR-stations worldwide. Metsähovi is one of the northernmost SLR stations of the International Laser Ranging Service (ILRS). First SLR observations in Finland were made at the Metsähovi research station already in 1978. To enrich efficiency of the station, recently we have acquired a modern kHz-capable SLR system, as well as auxiliary instrumentation like the Vaisala weather station and an Alcor OMEA 2Mpx all-sky camera devoted to continuous observations. The later enables us an efficient collaboration with the Finnish Fireball Network (FFN) and the SPanish Meteor Network (SPMN[1]), both in terms of meteor registrations and subsequent data analysis (Gritsevich et al., 2014; Trigo-Rodríguez et al., 2015; Lyytinen and Gritsevich, 2016; Dmitriev et al., 2015; Moreno-Ibáñez et al., 2015; Moreno-Ibáñez et al., 2016; Blanch et al., 2016; Trigo-Rodríguez et al., 2016; Kohout et al., 2015).

2 Observatory building

To establish a new and modern SLR station the first SLR building in Metsähovi, erected in 1975, was torn down in 2014 and a new observatory was built. The observatory building was designed to house all the sensitive electronics of the SLR system in an almost clean-room environment on the first floor. Also the temperature of the electronics room is kept stabile within one degree. An operator controls everything remotely from a second room to keep the temperature stable in the electronics room and to avoid dust entering the room. The SLR-telescope system stands on a concrete pillar in the center of the building, which is anchored to bedrock and separated from the building to avoid all vibrations. The pillar is 3.5 m high and hollow to allow the laser to be guided from the electronics room downstairs to the transmitting telescope (Coudé path). The telescope is shielded from weather conditions by a 5.3 m fast-moving slit-type dome manufactured by *Baader Planetarium GmbH*.

Externally, we have installed a high-end Vaisala weather station[2] equipped with temperature, humidity, pressure, wind, precipitation, global radiation and snow height sensors. In addition the dome has its own humidity and precipitation sensor for automatic closing at raining

[1] http://www.spmn.uji.es

[2] www.vaisala.com

conditions. In order to image the whole sky we have installed an all-sky camera (Näränen et al., 2014), which allows cloud and meteor detections. Together with the camera we have two ADS-B antennas which register the velocity and position information broadcasted by airplanes.

Figure 1 – The new SLR observatory of the Metsähovi Fundamental Geodetic Research Station: on the left the mast with two ADS-B antennas and the 2Mpx all-sky camera for meteor observation.

3 Instrumentation of the SLR Station

The Metsähovi station is equipped with key items needed in an SLR system: a telescope for transmitting and receiving laser pulses; a time interval counter / event timer for timing the flight time; a detector for receiving the laser pulse; a time reference; a laser with a stable repetition rate (Hz-kHz), energy level and pulse length (few picoseconds). The main instruments of the SLR system of Metsähovi consist of: a very fast and accurately tracking (> 10deg/s, < 1") *Cybioms/OMI* 50cm SLR telescope with a separate 10 cm telescope for transmitting the laser, and a 15 cm telescope for visual observations; a *HighQ GmbH* laser, capable of 2kHz repetition rate with a 0.8 W average power and a few picosecond pulse length, and a Single Photon Avalanche Diode – detector (*C-SPAD*). For more details on the SLR system see: Näränen et al., 2014; Raja-Halli et al., 2014; Raja-Halli et al., 2015.

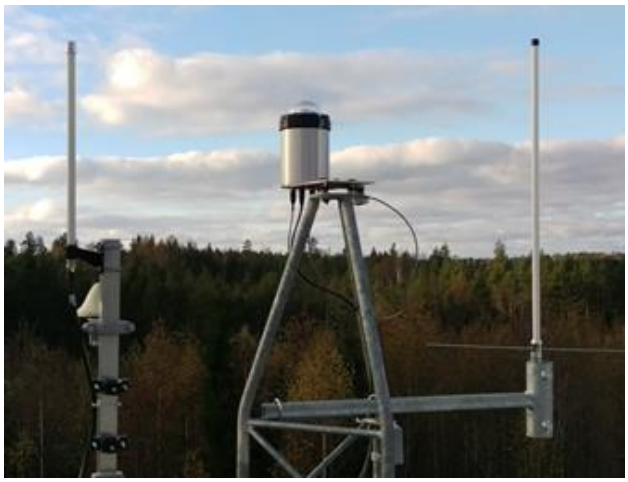

Figure 2 – Meteor detection system: 2Mpx all sky camera and ADS-B antennas.

For visualizing the sky during SLR observations we have installed an *Alcor OMEA 2Mpx* all-sky camera on a 6 m height mast. The camera has a field of view of 185° × 185° and the wavelength range is 350 – 750 nm. It has an automatic iris with maximum aperture F1.8 and an automatic exposure control with exposure times ranging from 0.1 ms to one hour, which allows correcting exposure at any time. In addition, a library of dark images and a hot pixel list is created to remove noise from the images. The camera dome is provided with a heating system to remove any water condensation and ice formation; this allows us imaging even during winter nights when frosting is likely to happen. During daytime we take images every five minutes to visualize clouds. During night the camera takes the next exposure immediately as it has readout the last one. Therefore the deadtime of the camera remains small, usually less than few seconds between exposures.

Figure 3 – The new SLR telescope. The 15cm refractor is not shown in the image.

4 Meteor detection

From the images taken by the camera we have detected multiple aurora borealis events as well as a number of meteors. In *Figures 4 and 5* we present some examples of the recent Metsähovi all-sky camera observations. In conjunction with the Finnish Fireball Network (FFN) the images recorded by this camera are used to reconstruct atmospheric trajectories and to calculate the pre-impact meteor orbits in the Solar System (Dmitriev et al., 2015).

The Finish Fireball Network (FFN) was established in 2002 as a result of growing interest to continuous meteor and fireball monitoring using dedicated equipment initiated by Ilkka Yrjölä in 1998[3]. In the current state the network consists of the 24 active stations with permanent instrumental setup and monitors a surface over Finland and neighboring areas of about 400000 km^2 (Gritsevich

[3] http://www.kolumbus.fi/oh5iy/

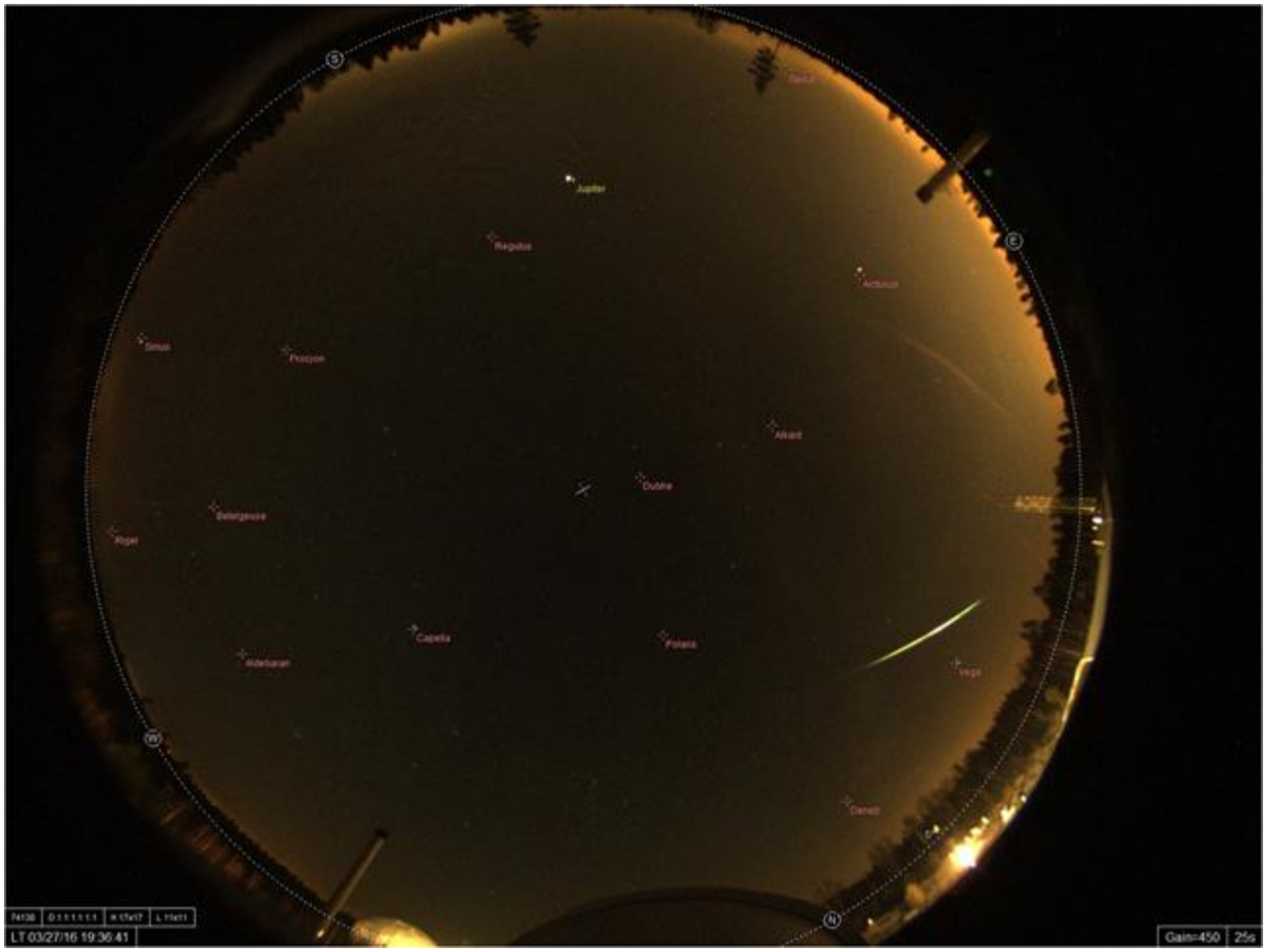

Figure 4 – Recent fireball examples recorded by the Alcor OMEA 2Mpx all-sky camera at the Metsähovi Geodetic Research Station.

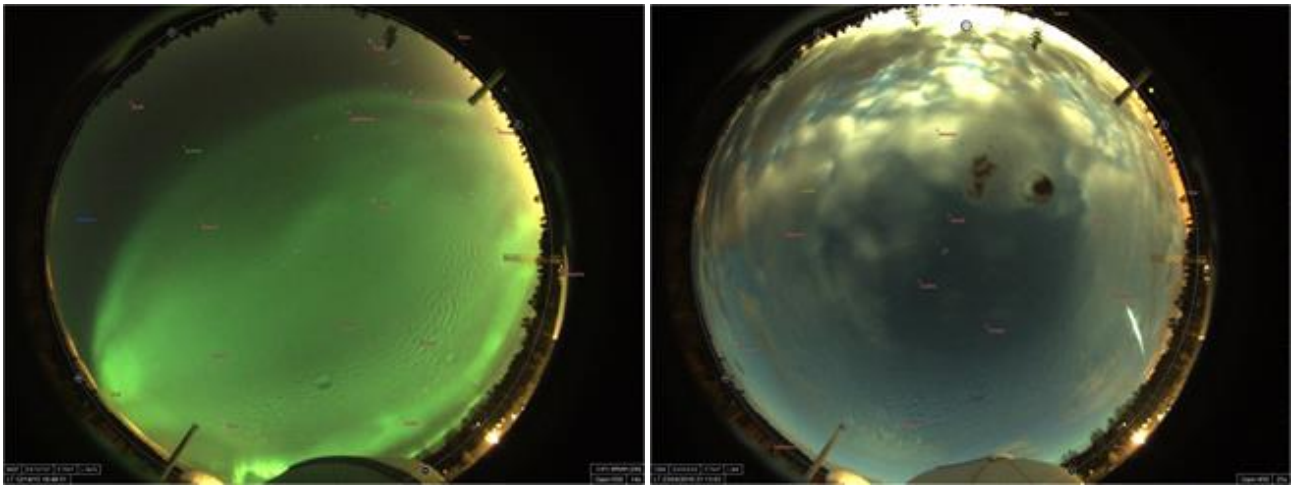

Figure 5 – Aurora borealis and recent fireball examples recorded by the *Alcor OMEA 2Mpx* all-sky camera at the Metsähovi Geodetic Research Station.

et al., 2014; Trigo-Rodríguez et al., 2015; Lyytinen and Gritsevich, 2016). Most of the active stations are run by amateur astronomers. A majority of interesting events are reduced the following days after the registration and the atmospheric trajectories corresponding to the visual path of fireballs are reproduced using the *fb_entry program* (Lyytinen and Gritsevich, 2013). The program uses atmospheric trajectory parametrization described in (Gritsevich 2007, 2009; Gritsevich and Koschny, 2011; Bouquet et al., 2014). Selected cases – e.g. the ones matching meteorite-producing criteria introduced in (Gritsevich et al., 2012; Turchak and Gritsevich, 2014) – are studied more thoroughly including mass computation, dark flight simulations, and pre-impact orbit estimate with account for the real atmospheric conditions corresponding to the time and location of a fireball (Lyytinen and Gritsevich, 2016).

The all-sky camera installation at the Metsähovi Geodetic Research Station and the ongoing meteor work were largely inspired by the recovery of the Annama meteorite (Gritsevich et al., 2014; Trigo-Rodríguez et al., 2015; Dmitriev et al., 2015; Kohout et al., 2015; Lyytinen and Gritsevich, 2016). This was the first meteorite recovered by the FFN. The data recorded provided enough information to determine its atmospheric trajectory which allowed to eventually simulate its dark flight and enabled prompt meteorite recovery. Furthermore, the accuracy of the data available permitted the derivation of its orbital parameters and parental relationship (Trigo-Rodríguez et al., 2015; Dmitriev et al., 2015).

5 Conclusion and future prospects

The Metsähovi Fundamental Geodetic Research Station is adequately equipped with all the necessary instrumentation for detailed meteor detection. Thus, its use for further cooperation with fireball networks is suitable and it would largely help in meteor observation campaigns.

There is increasing interest in using SLR systems to observe also non-cooperative targets (i.e., objects with no reflectors such as space debris (Virtanen et al., 2016) in low orbits. Recently, our team has investigated the new Metsähovi system's feasibility for space debris observations in a *MATINE*-funded research project.

The new SLR system is designed from the beginning as a flexible platform for future development. This will ensure that the Metsähovi SLR system is easily upgraded in the future and also that it can be modified to participate in state-of-the-art research such as space-debris tracking and time transfer over optical satellite link.

Acknowledgments

Our work has been supported by the Finnish Ministry of Agriculture and Forestry, the European Space Agency (ESA), the Academy of Finland (project 260027), the Finnish Scientific Advisory Board for Defence (MATINE), and by the Magnus Ehrnrooth Foundation.

References

Blanch E., Trigo-Rodríguez J. M., Madiedo J. M., Lyytinen E., Moreno-Ibáñez M., Gritsevich M., and Altadill D. (2016). "Detection of nocturnal and daylight bolides from Ebre Observatory in the framework of the SPMN fireball network". In Trigo-Rodríguez J. M., Gritsevich M. and Palme H., editors, *Assessment and Mitigation of Asteroid Impact Hazards*, Springer, New York. In print.

Bouquet A., Baratoux D., Vaubaillon J., Gritsevich M. I., Mimoun D., Mousis O. and Bouley S. (2014). "Simulation of the capabilities of an orbiter for monitoring the entry of interplanetary matter into the terrestrial atmosphere". *Planetary and Space Science*, **103**, 238–249 . http://dx.doi.org/10.1016/j.pss.2014.09.001.

Dmitriev V., Lupovka V. and Gritsevich M. (2015). "Orbit determination based on meteor observations using numerical integration of equations of motion". *Planetary and Space*

Science, **117**, 223–235, http://dx.doi.org/10.1016/j.pss.2015.06.015

Gritsevich M. and Koschny D. (2011). "Constraining the luminous efficiency of meteors". *Icarus*, **212**, 877–884. http://dx.doi.org/10.1016/j.icarus.2011.01.033.

Gritsevich M., Lyytinen E., Moilanen J., Kohout T., Dmitriev V., Lupovka V., Midtskogen V., Kruglikov N., Ischenko A., Yakovlev G., Grokhovsky V., Haloda J., Halodova P., Peltoniemi J., Aikkila A., Taavitsainen A., Lauanne J., Pekkola M., Kokko P., Lahtinen P. and Larionov M. (2014). "First meteorite recovery based on observations by the Finnish Fireball Network". In Rault J.-L. and Roggemans P., editors, *Proceedings of the International Meteor Conference*, Giron, France, 18-21 September 2014. IMO, pages 162–169.

Gritsevich M. I. (2007). "Approximation of the Observed Motion of Bolides by the Analytical Solution of the Equations of Meteor Physics". *Solar System Research*, **41**, 509–514. http://dx.doi.org/10.1134/S003809460706007X.

Gritsevich M. I. (2009). "Determination of Parameters of Meteor Bodies Based on Flight Observational Data". *Advances in Space Research*, **44**, 323–334. http://dx.doi.org/10.1016/j.asr.2009.03.030.

Gritsevich M. I., Stulov V. P. and Turchak L. I. (2012). "Consequences for Collisions of Natural Cosmic Bodies with the Earth Atmosphere and Surface". *Cosmic Research*, **50**, 56–64. http://dx.doi.org/10.1134/S0010952512010017.

Kohout T., Gritsevich M., Lyytinen E., Moilainen J., Trigo-Rodríguez J. M., Kruglikov N., Ishchenko A., Yakovlev G., Grokhovsky V., Haloda J., Halodova P., Meier M. M. M., Laubenstein M., Dimitrev V. and Lupovka V. (2015). "Annama H5 Meteorite Fall. Orbit, Trajectory, Recovery, Petrology, Noble Gases, and Cosmogenic Radionuclides". *Meteoritics and Planetary Science*, **50**, MetSoc 2015 special issue, # 5209.

Lyytinen E. and Gritsevich M. (2013). "A flexible fireball entry track calculation program". In Gyssens M. and Roggemans P., editors, *Proceedings of the International Meteor Conference*, La Palma, Canary Islands, 20-23 September 2012. IMO, pages 155–167.

Lyytinen E. and Gritsevich M. (2016). "Implications of the atmospheric density profile in the processing of fireball observations". *Planetary and Space Science*, **120**, 35–42. http://dx.doi.org/10.1016/j.pss.2015.10.012.

Moreno-Ibáñez M., Gritsevich M. and Trigo-Rodríguez J. M. (2015). "New methodology to determine the terminal height of a fireball". *Icarus*, **250**, 544–552. http://dx.doi.org/10.1016/j.icarus.2014.12.027.

Moreno-Ibáñez M., Gritsevich M. and Trigo-Rodríguez J. M. (2016). "Measuring the terminal heights of bolides to understand the atmospheric flight of large asteroidal fragments". In Trigo-Rodríguez J. M., Gritsevich M. and Palme H., editors, *Assessment and Mitigation of Asteroid Impact Hazards*, Springer, New York. In print.

Näränen J., Lankinen J. and Raja-Halli A. (2014). "A New Toolset for Passive Monitoring of Air Traffic and Sky Conditions at Metsähovi Station, Finland (3073)". *Proceedings of the 19th International Workshop on Laser Ranging*, Annapolis MD, Oct. 27-31, 2014.

Raja-Halli A., Näränen J., Poutanen M., Kloth A. and Steinborn J. (2014). "Progress Report on the New SLR System of GGOS'S Core Site Metsähovi, Finland (3090)". *Proceedings of the 19th International Workshop on Laser Ranging*, Annapolis MD, Oct. 27-31, 2014.

Raja-Halli A. and Näränen J. (2015). "Progress report on the new satellite laser ranging system of Metsähovi Geodetic Research Station". *Conference abstract book of the XXVII Geophysics Days* at the University of Oulu on 26-27 May, 2015, pages 60–62.

Trigo-Rodríguez J. M., Lyytinen E., Gritsevich M., Moreno-Ibáñez M., Bottke W. F., Williams I., Lupovka V., Dmitriev V., Kohout T. and Grokhovsky V. (2015). "Orbit and dynamic origin of the recently recovered Annama's H5 chondrite". *Monthly Notices of the Royal Astronomical Society*, **449**, 2119–2127. http://dx.doi.org/10.1093/mnras/stv378.

Trigo-Rodríguez J. M., Palme H. and Gritsevich M. (2016). "Barcelona Asteroid Day 2015: revisiting the threat by asteroid and comet impact". In Trigo-Rodríguez J. M., Gritsevich M. and Palme H., editors, *Assessment and Mitigation of Asteroid Impact Hazards*, Springer, New York. In print.

Turchak L. I and Gritsevich M. I. (2014). "Meteoroids Interaction with the Earth Atmosphere". *Journal of Theoretical and Applied Mechanics*, **44**, 15–28. http://dx.doi.org/10.2478/jtam-2014-0020.

Virtanen J., Poikonen J., Säntti T., Komulainen T., Torppa J., Granvik M., Muinonen K., Pentikäinen H., Martikainen J., Näränen J., Lehti J. and Flohrer T. (2016). "Streak detection and analysis pipeline for space-debris optical images". *Advances in Space Research*, **57**, 1607–1623. doi:10.1016/j.asr.2015.09.024.

An attempt to explain VLF propagation perturbations associated with single meteors

Jean-Louis Rault[1] and Jean-Jacques Delcourt Dr. Sc.[2]

[1] **IMO Radio Commission, 16, rue de la Vallée, Epinay sur Orge, France**
f6agr@orange.fr
[2]ionosphere.d23@skynet.be

A first evidence of sudden changes in the amplitude of distant VLF radio transmissions related to single meteors was found during GEM 2010 meteor shower radio observations. Based on many similar observations gathered during different meteor showers, this paper is dedicated to the corresponding physical phenomena involved at the level of the D layer of the Earth ionosphere.

1 Introduction

Various phenomena such as UV and X rays bursts radiated by the Sun, γ rays radiated by distant stars, electrons precipitations induced by wave-particle interactions within the magnetosphere, nuclear explosions, etc., create transient VLF propagation disturbances by modifying the electron content of the D layer of the ionosphere (Barr, 2000).

A first evidence for sudden amplitude changes induced by single meteors on signals received from distant VLF transmitters was found during a Geminids 2010 observation campaign (Rault, 2013).

This paper is aimed to clarify the causes of such VLF propagation modifications induced by meteors.

2 Observations

In the frame of studies related to interactions between meteors and Earth ionosphere, 29 meteors showers (Perseids, Geminids, Draconids, Leonids, Quadrantids, η-Aquariids and Lyrids) and some sporadic activity have been observed simultaneously on VHF and VLF radio frequencies since 2008. A dedicated autonomous portable radio setup was developed for that purpose and used in several remote and radio electrically quiet areas.

During each observation campaign, the ELF/VLF band and the VHF forward scatter echoes produced by the meteors illuminated by the French military radar GRAVES meteors were recorded 24h a day.

A first VLF propagation disturbance associated to a single meteor was discovered in 2010 on the amplitudes of the FTA and DHO38 transmissions (see *Figure 2*).

3 Instrumentation and data reduction

Observation setup

The setup (see *Figure 3*) consists in a Zoom H4N digital stereo audio recorder connected to the output of an AOR AR5000+3 communication receiver tuned on 143.050 MHz (frequency of the Graves radar) and to a wide band E-field ELF/VLF preamplifier (5 Hz to 24 kHz bandwidth). The VHF aerial consists in a 5/8th lambda vertical whip and the ELF/VLF sensor is made of a 1.5 m high vertical mesh cylinder (diameter: 50 mm). A 12 V car battery and a 16 gigabytes SD memory card allow the system to run remotely and continuously for more than 24h (Rault, 2010).

Figure 1 – Locations of some of the observation sites and of the radio transmitters used for simultaneous VLF and VHF observation campaigns.

VLF transmitters: ● GBZ 19,6 kHz & GQD 22,1 kHz ■ DHO38 23,4 kHz ▲FTA 20,9 kHz ▬ HWU 21,75 kHz ○ICV 20,27 kHz.

VHF radar used for meteor scatter detection: **GRV**

Observation locations: ▌Baraque de l'Air (Lozère) ★Pic du Midi observatory.

Data processing

The stereo audio records allow searching for possible correlations between any ELF/VLF events and the meteor forward scatter VHF echoes.

The data reduction consists in performing a spectral analysis (thanks to Fast Fourier Transformations) of the two data channels and in searching visually for any correlated events.

The VLF transmitters use a MSK (Minimum Shift Keying) modulation scheme, so the amplitude of their transmissions is measured and plotted by performing an average of the power delivered by each of the bins of the FFT output, which is centred on the mean transmission frequency of each transmitter under study.

The FFT analysis and plotting are performed thanks to the Spectrum Lab software developed by Wolfgang Büscher[1] (Büscher, 2016).

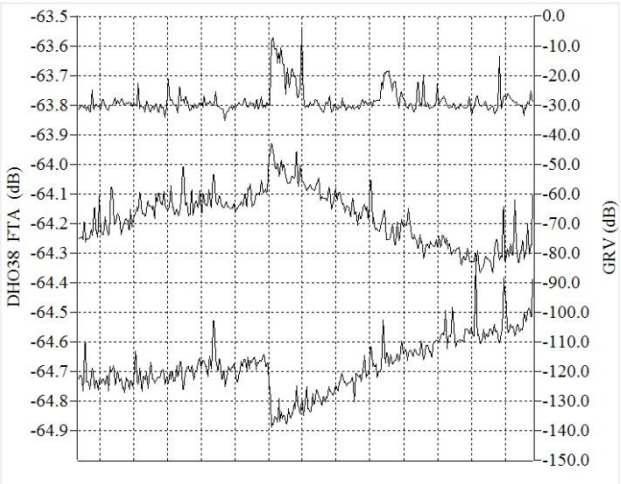

Figure 2 – First observation at Pic du Midi observatory of a constructive interference on FTA (middle trace) and of a destructive interference on DHO38 (lower trace) triggered by a single meteor (meteor VHF echo on upper trace). Time scale: 10s/square.

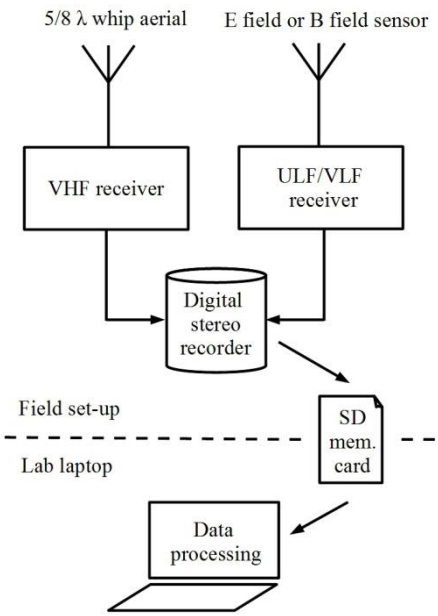

Figure 3 – Diagram of the radio VHF and ELF/VLF setup.

The original stereo data are sampled at 48 kHz by the digital recorder, but are processed at 384 kHz during the data reduction phase. Fooling the analysis software in such a way allows processing the data 8 times faster than the real time, thus saving a lot of time during analysis.

4 Discussion

Interference patterns

In this chapter are successively examined: the geometry of the VLF radio paths (see *Figure 1*), the reasons why a meteor can induce VLF constructive or destructive interferences at the observation location and the duration of the events.

VLF transmitter-receiver radio paths

Regarding the VLF paths, we must consider three different channels: the ground wave, the sky wave (Delcourt)[2] and the *reflected* wave from the meteor trail (*Figure 4*). In fact, there are no *reflected* waves, neither for the ionospheric D layer circuit, nor for the *pseudo reflection* on the trail. The D region is not a sharp boundary layer but a graded index medium. There is no singularity at the virtual height of reflection (*V*) but a bended path, which is an ionospheric mirage around the actual refracting height (*R*). The beam is thus always transmitted but never reflected and the Fresnel's coefficients exhibit no phase opposition between the incident and the transmitted waves. The interference figure at the receiving site depends only on three parameters: wave length, length of ground path and length of virtual sky path. The real wave and the virtual wave are in phase when leaving the D layer. The difference in length for the real and virtual paths is balanced by the real and virtual propagation velocities which are linked through the refractive index.

The Transmitter-Receiver ground / sky distances difference is described as follows (see *Figure 5*):

$$d_c - d_s = 2\sqrt{2R\,[R+h]\left[1-\cos\frac{d_s}{2R}\right] + h^2} - d_s \qquad (1)$$

$$\varepsilon = \frac{2\sqrt{2R\,[R+h]\left[1-\cos\frac{d_s}{2R}\right] + h^2} - d_s}{\lambda} = f_{[h,\,d_s,\,\lambda]}$$

where d_s is the ground wave path length, d_c is the sky path length, h the virtual height of reflection, λ the wavelength and R the Earth radius which is equal to 6378 km. The interference pattern is described as:

$$I = \cos(2\pi \,.\, \varepsilon) \qquad (2)$$

As shown on *Figure 6*, aerial airborne measurements known as *Hollingworth's pattern* (Hollingworth, 1926) give results consistent with the equation (2).

[1] http://www.qsl.net/dl4yhf/spectra1 html

[2] "Basse ionosphère, région D. Les fondamentaux". (2015) http://www.coucheD.be

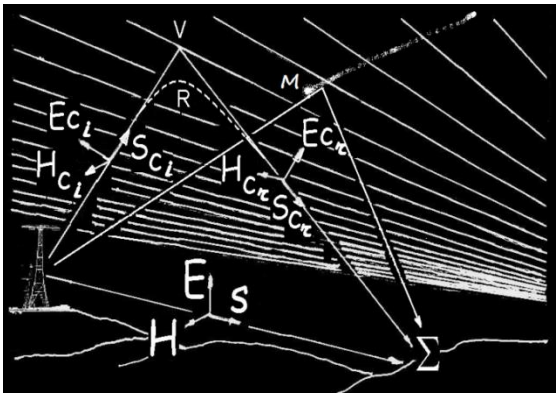

Figure 4 – VLF interference components. E and H are the electric and magnetic field vectors, S is the Pointing vector, "i" and "r" mean incident and reflected.

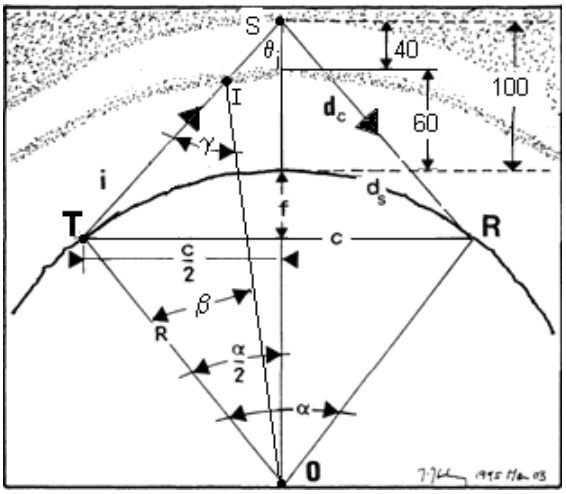

Figure 5 – Geometry of a VLF circuit involving the D layer.

The evolution of the ionosphere ionization vs altitude depends on the sun illumination in the UV and X rays wavelengths, and thus with solar time. During day time, the "*reflection"* altitude, in the range 60 – 70 km, is lower than the meteor trails average altitude, therefore restricting the recordings to night time when the D layer altitude reaches 90 to 100 km, which, in first approximation, is the range of altitudes area of most of the meteor trails (*Figure 7*).

The wavelengths of the signals radiated by the VLF transmitters are around 15 km, a value which is comparable to the length of the meteor trails. The diameter of a trail can reach 10 to 20 m, making any VLF specular reflection not possible. If we translate this in the visible domain, this would be similar to an attempt to visualize a 0.5 µm long and 5 atoms large wire with a microscope. So another explanation has to be found. After midafternoon, the D layer bottom climbs up to the mesopause region, inducing an interference pattern evolution. The concentration of electrons increases with the altitude. The localized enhancement of the electron content within a meteor trail – 10^{14} m^{-3} instead of 10^{9} – (Belkovich, 2005) should counterfeit an altitude increase, and therefore a modification of the amplitude of the received signal. This modification depends on the phase φ between the ground wave and the sky wave, as follows:

- higher signal level if $-\pi/2 < \varphi < +\pi/2$ rd
- lower signal level if $+\pi/2 < \varphi < +3\pi/2$ rd

But the trail is a closed medium presenting a small ohmic resistance in the range of a few tens of ohms, so the Maxwell laws apply.

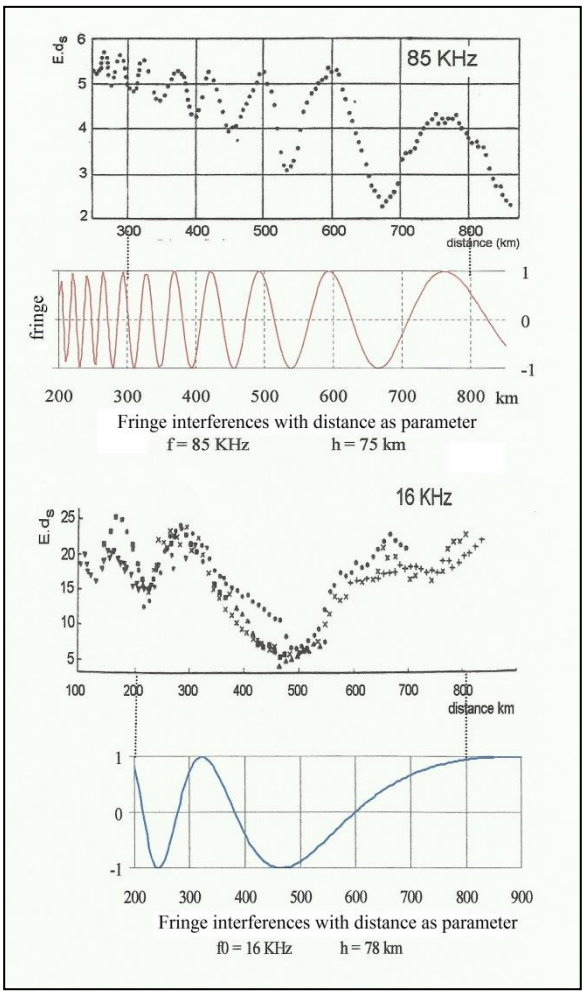

Figure 6 – Interference evolution pattern depending on d_s.

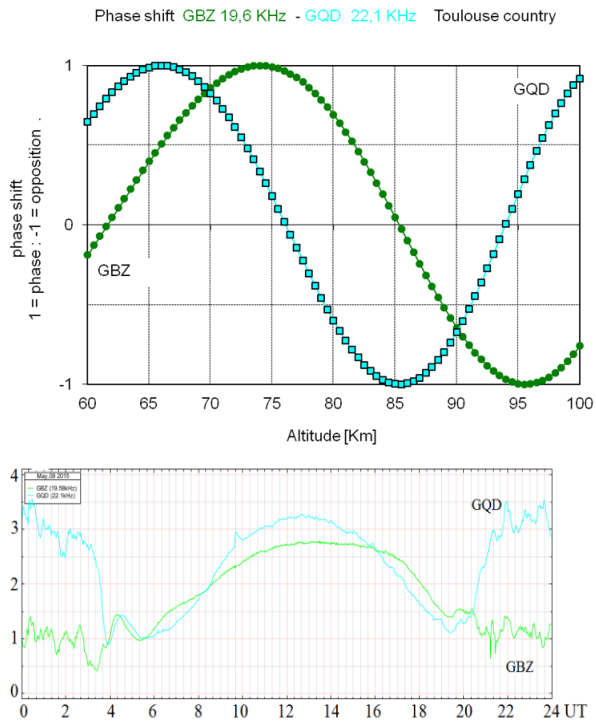

Figure 7 – Interference pattern of UK VLF transmissions due to ionospheric D layer altitude changes, as seen from Toulouse.

The local induced electric field is therefore opposed to the incident electric field, implying the following variations on the received signal:

- lower signal level if $-\pi/2 < \varphi < +\pi/2$ rd
- higher signal level if $+\pi/2 < \varphi < +3\pi/2$ rd

A similar result can be obtained thanks to a more general law which is applicable in the propagation plane: the incident sky wave induces an electron motion in the meteor trail population, which is thus developing a work (i.e. force x displacement). The most important part of this work is lost in collisions as heat, and after "penetrating" in the meteor trail, the sky wave Poynting vector becomes smaller than before the interaction. So the influence of the sky wave in the interference pattern becomes lower during the meteor trail expansion and diffusion.

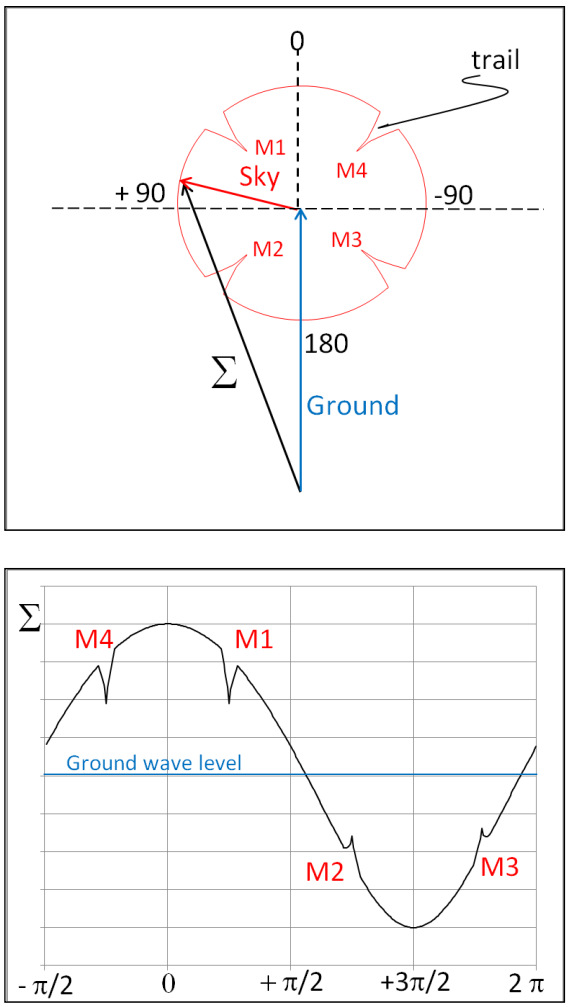

Figure 8 – Evolution of the reception level Σ with phase . M1 to M4 are the trail effect . The sky wave is assumed to be constant in amplitude except during trail effect. The reading can be done in the two directions counterclockwise or clockwise, from left to right or inverse.

A question arises: are these interactions a fortunate combination of circumstances? In fact, the 2D (2 dimensional) sky wave paths shown on *Figures 4 and 5* are over simplified. In the real world, many different sky paths are possible, all of them being included inside an ellipsoidal cavity which is more or less overlapping the D layer, and all of them are converging in the receiver area.

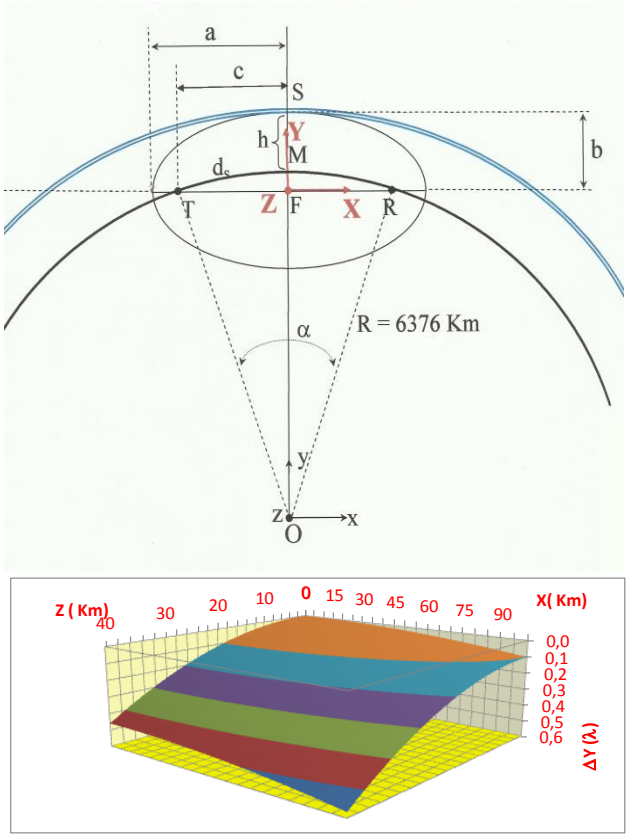

Figure 9 – Geometry of the overlapping of the elliptical cavity insuring a multipath skywave with the D region at night.

Let's have the following configuration shown on *Figure 9*:

- transmitter – receiver distance: d_s = 1000 km
- night ionospheric D layer altitude : 100 km
- Earth radius : 6376 km
- λ : 15 km
- $\alpha/2$ = 0.078 rd
- *FM* = 19.594 km
- *TR* = 998.975 km
- *a* (semi major axis) = 513.605 km
- *b* (semi minor axis) = 119.594 km
- translation of Earth → ellipse axis system:

$$x = \mathbf{X}$$

$$y = \mathbf{Y} + (6376 - 19.594)$$

$$z = \mathbf{Z}$$

The Cartesian equation of the D layer at 100 km altitude is:

$$x^2 + y^2 = (6376 + 100)^2$$

The Cartesian ellipse equation is:

$$\frac{X^2}{a^2} + \frac{Y^2}{b^2} = 1$$

For a deviation ΔX of 10 km, with S being the discordance, ΔY between the ellipse of propagation and the D layer is 15m or 0.001 λ, 0.025 λ for ΔX = 50 km, 0.1 λ for ΔX = 100 km and 0.42 λ for ΔX = 200 km.

So, beyond 100 km, the *reflected* beam creates a diffraction pattern on the reception site.

The problem is more crucial on the plane which is orthogonal to the propagation plane. At a distance of 100 km and for a lateral deviation of 20 km, the gap between the D layer and the ellipsoid is a little bit more than 3 km or 0.2 λ. However the ellipsoid influences only the focalization on the receiver site and not the energy exchanged between the incident beam and the meteor trail in the 90 – 100 km altitude range.

If we accept the criteria of $\Delta Y \leq \lambda/10$ for a reasonable diffraction pattern on the site of reception for $d_s = 1000$ km and for a few millimeters large meteor, we can expect a meteor VLF signature if the meteor decay occurs in a volume of the ionosphere 200 km long, 40 km wide ($S = 8000\ km^2$), 20 km wide and 10 km thick and centered on the virtual point of reflection the meteor.

Analysis of the events durations

If we consider a siderite meteor having a 1 mm diameter and a velocity of 40 km/s, the electron concentration in its trail is a function of time and distance of the trail heart according to equation (3):

$$[N_{d,t}] = \frac{[N_l]}{\pi\,[R_0^2 + 4\,D\,t]} . e^{-\frac{d^2}{R_0^2 + 4\,D\,t}} = \frac{[N_l]}{\pi\,R_t^2} . e^{-\frac{d^2}{R_t^2}} \qquad (3)$$

where $[N_l]$ is the linear electrons concentration, d the coaxial distance, R_o the initial radius of the trail, D the ambipolar diffusion coefficient and R_t the radius at which the electron concentration is the part e^{-1} of the initial concentration, and t is time (see *Figure 10*).

The trail consists of concentric quasi neutral layers of electrons and ions which are coming either from the ionized mesosphere or from the ionization of the meteor core. The mesospheric electrons and ions diffuse more promptly than those of meteoritic origin but are at least ten times less numerous (Lebedinec and Sosnova, 1967).

After 60 s which is the average duration observed for the VLF meteor signatures, the electron density of mesospheric origin is around 2.10^9 m^{-3}, i.e. the same as the mesospheric background, while the meteoritic free electron density is in the range of 2.10^{10}, thus always discernible by the incident VLF wave.

Geminids 2010 (from Pic du Midi Observatory)

Analysis of some VLF meteor events

Many VLF propagation perturbations correlated with single meteors have been identified among the 1.5 terabytes of data collected during 29 observation campaigns. It is worth noting that no VLF meteor disturbances at all were observed during day time.

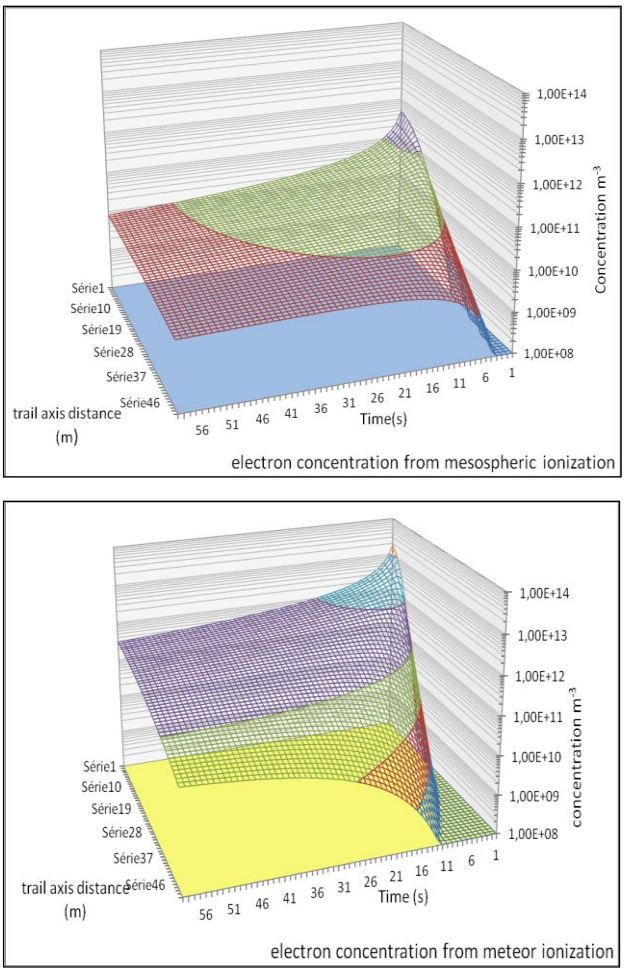

Figure 10 – Evolution of the mesospheric and meteoric and electron concentrations vs time and distance computed from R_0.

This is explained by the fact that when the Sun is illuminating the upper atmosphere, the altitude of the ionosphere D layer decreases and its free electrons density increases dramatically, thus masking any influence of the meteor trails on the VLF propagation.

A sample of 4 night events is described below. The distances (in km) between the VLF transmitters and the observation location were as follows:

	FTA	HWU	DHO38
GEM 2010	651	429	1256
LYR 2013	466	316	1006
GEM 2014	466	316	1006

The event occurred around midnight (see *Figure 2*). The D layer bottom was at an altitude of about 95 to 100 km. The phase pattern evolution is shown by the coloured rectangle on the right of *Figure 11*. The reception level of DHO38 was on the rise while that of FTA was on the decline. On the graph we are moving from the left to the right. In accordance with what was explained above, the DHO38 level should drop and that of FTA should increase with a meteor decay at h > 95 Km, which was the case.

Lyrids 2013 (from Baraque de l'Air, Lozère)

The date of the observing records is important. We are one month after the equinox and during night, the ceiling of the D layer is lower than in december at Le Pic du Midi Observatory.

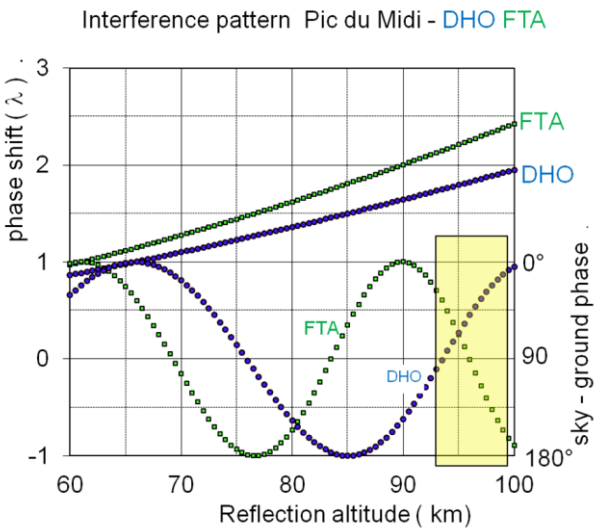

Figure 11 – Evolution of the interference fringes with altitude at Pic du Midi Observatory.

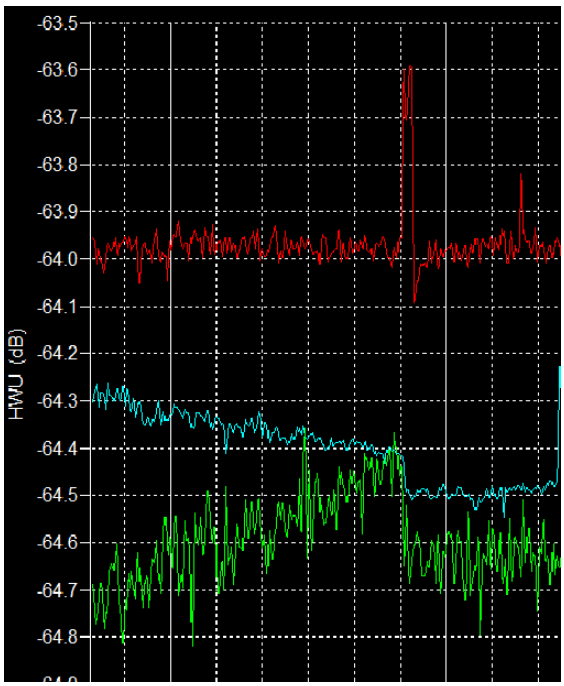

Figure 12 – Top in red: Graves radar signal. In blue: DHO38, in green HWU. Recorded at Baraque de l'Air / Lozère on 2013 April 21, $23^h24^m54^s$UTC.

The evolution of the interference figure is from left to right at rise for both DHO38 and HWU, which finally leads to a dip on the reception level (*Figures 12 and 13*). In the present case, *h* is greater than 93 km.

Figure 14 shows the record of a trail appearing 4 ½ hours later, with an amplitude peak instead of a dip.

At 04^h UTC, at the ionospheric mid *reflective* point we are just in the middle of the sunrise phase at the level of the mesopause. Within ten minutes, all the D layer is wholly illuminated and in an half hour the D layer floor has collapsed down to an altitude of 70 km. Thus the declining HWU interference pattern is followed from right to left, producing an amplitude peak for HWU.

Geminids 2014 (from Baraque de l'Air, Lozère)

During this December campaign, the receiving site was the same as in April 2013.

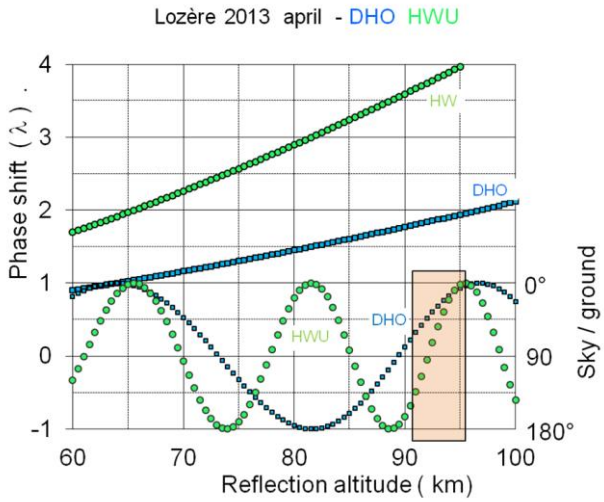

Figure 13 – Evolution of the interference fringes with altitude at Baraque de l'Air / Lozère.

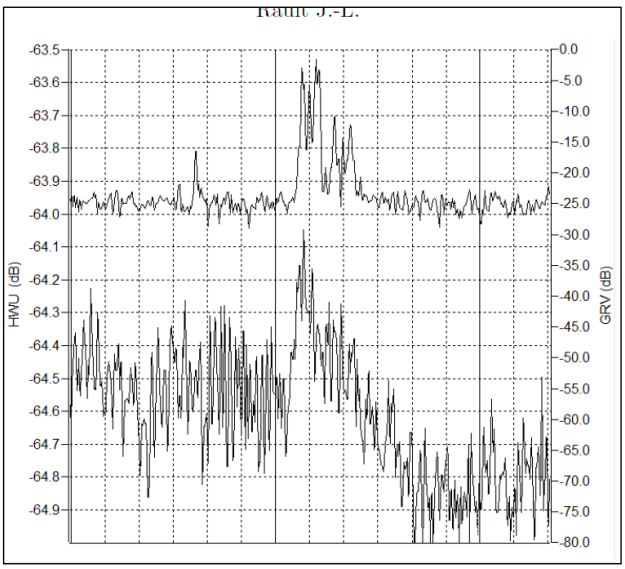

Figure 14 – Top: Graves radar echo, bottom: HWU amplitude recorded at Baraque de l'Air / Lozère on 2013 April 22, 04^h 03^m29^s UTC, 10s/div.

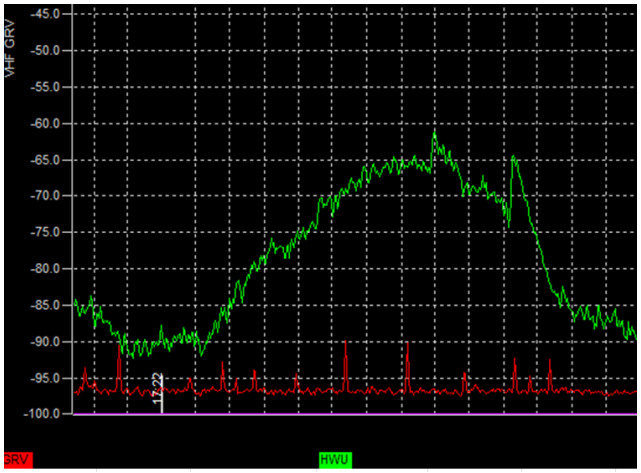

Figure 15 – HWU amplitude (green) and Graves signal (red). 0,1 $dB_{(V)}$ / vertical division, 32 s / horizontal division. Recorded at Baraque de l'Air / Lozère.

During night the reception level is not totally erratic and we can observe fluctuating trends moving up or down with a period of a few minutes to a half hour (see *Figure 15*). The reception levels are the result of a wandering along the interference pattern. In the middle of the winter nights, the cause is exclusively aeronomic and even meteorological. The fluctuations in the interference figure are approximately 6 minutes long, including two meteor interference events probably of the M3 type (see *Figure 8*) at an altitude of 90 km < h < 93 km.

5 Conclusion

Hundred hours of observation of various meteor showers and sporadic meteor activity and manual analysis have led to the evidence of multiple VLF amplitude disturbances directly correlated with single meteors during night time. A coherent theoretical explanation of these observations has been elaborated in this paper. In the next future, a statistical study of the shapes, amplitudes and durations of a large batch of VLF meteor events should allow to improve the detailed understanding of these phenomena.

References

Barr R., Jones D. L. and Rodgers C. J. (2000). "ELF and VLF radio waves". *Journal of Atmospheric and Solar-Terrestrial Physics*, **62**, 1689–1718.

Bel'Kovich O. I. (2005). "The physics of meteoroid ablation and the formation of ionized meteor trails". In Verbeeck C. and Wislez J.M, editors, *Proceedings of the Radio Meteor School*, Oostmalle, Belgium, 10–14 September 2005. IMO, pages 21–26.

Büscher W. (2016). Spectrum Laboratory software.

Hollingworth J. (1926). "The propagation of radio waves". *IEE Journal*, **64**, 579–589.

Lebedinec V. N. and Sosnova A. K. (1967). "Radio reflections from meteor trails". In Kresak L. and Millman P. M, editors, *Physics and dynamics of meteors IAU symposium n°33*, Tatranska Lomnica, Czecoslovakia, 4–9 september 1967, pages 27–44.

Rault J. L. (2013). "Evidence for VLF propagation perturbations associated with single meteors". In Gyssens M., Roggemans P. and Zoladek P., editors, *Proceedings of the International Meteor Conference*, Poznan, Poland, 22-25 August 2013. IMO, pages 345–351.

Rault J. L. (2010). "Searching for ELF/VLF meteor signatures". *WGN, Journal of the IMO*, **38**, 67–75.

65 years of meteor radar research at Adelaide

Iain M. Reid[1,2] and Joel Younger[1,2]

[1] **ATRAD Pty Ltd, Adelaide, Australia, 5031**
ireid@atrad.com.au

[2] **School of Chemistry and Physics, University of Adelaide, Australia, 5005**

Over 65 years of radar research using meteor radar at Adelaide University in Australia is very briefly reviewed.

1 Early days

Radio studies of meteors began at Adelaide in 1949, and like many radio and radar based research efforts of that era, grew out of wartime radar research. Lenard Huxley arrived at Adelaide University from the University of Birmingham in 1948 to take the Elder Chair of Physics, and began revitalizing the Department, and establishing a number of research areas (Crompton, 2007)[1]. He was supported in this by the new Vice Chancellor, A.P. Rowe. Both Rowe and Huxley had been at the Telecommunications Research Establishment (TRE) during the Second World War. Rowe had been Chief Superintendent, and Huxley had established and headed the radar training school for both civilian and service personnel in the TRE. In another interesting connection to wartime research, Adelaide graduate Sir Mark Oliphant had drawn Huxley's attention to the advertisement for the position (Blake, 2010)[2].

One of the new research areas to be initiated in physics was radar meteor astronomy, and Huxley asked Graham Elford to pursue this topic. After the first measurements of upper atmosphere winds inferred by the drift of meteor trails were reported by Manning et al. (1950) at Stanford, the Adelaide effort was broadened out to include the study of the upper atmosphere. This became Graham Elford's main research area. In 1950, two Honors students, Des Liddy and Alan Weiss, joined the group, followed by PhD student David Robertson at the beginning in 1951. Robertson had previously worked with Oliphant at Birmingham, and brought considerable technical expertise to the group (Blake, 2010)[2].

Robertson was an amateur radio ham, and it was his personal 500W transmitter located at his home at Mount Lofty, together with receivers in Adelaide, Burra and Kulpara, that was used to make the first observations of meteor trails by the group in 1951. Subsequently, he developed the Adelaide meteor wind radar together with Elford and Liddy, the basic design concepts of which continued to be used at Adelaide until the mid-1970's, and which were also used later for the meteor radar at Atlanta by Bob Roper (Roper, 1984). This system operated at 27 MHz and used a 240 W continuous wave (CW) approach. Robertson submitted his PhD thesis on 'Reflection of radio waves from meteor trails, with applications to the measurement of upper atmosphere winds', in August 1953. Graham Elford followed late in 1954 with his thesis on the investigation of winds in the upper atmosphere. Robertson and Elford (1953) published the first

Figure 1 – the Upper Atmosphere Group 1962. Back row: R. Roper, J. Welsby, C. Nilsson, A. Bastian, B. Stone. Front row: Dr. E. Murray, Miss J. Allister, Miss M. Chapman, Dr. G. Elford.

observations of upper atmosphere winds using the meteor technique after those of Manning et al. (1950). In March 1955, this version of the Adelaide Meteor wind radar was decommissioned.

Beginning in early 1954, with funding from the Australian Antarctic Division, effort was directed to the development of a new radar to measure upper atmosphere winds in the Antarctic. The new pulsed radar system for this work (see *Figure 2*) was developed by Eric Murray. In December 1956, Carl Nilsson, a very recent BSc graduate, took the equipment to Mawson Base and operated it there during the International Geophysical year. Murray analyzed the data for his PhD thesis.

The work on meteor astronomy continued along with the upper atmosphere winds work. Nilsson later completed a PhD on meteor orbits which used some of the Mawson radar data. With support in the form of radar equipment

[1] http://adb.anu.edu.au/biography/huxley-sir-leonard-george-holden-516/text22851
[2] https://physsci.adelaide.edu.au/about/physics/history/documents/physics-in-adelaide-the-1950s.pdf

provided by Sir Bernard Lovell at the University of Manchester, Alan Weiss set up an independent radar system to study meteor showers. This work formed part of his PhD thesis, which he submitted in May 1954. He published his work on the distribution of the orbits of sporadic meteors in Weiss (1957).

2 New field sites

St Kilda

The Mawson meteor radar was very difficult to maintain, and it was decommissioned in 1959. Effort had shifted to

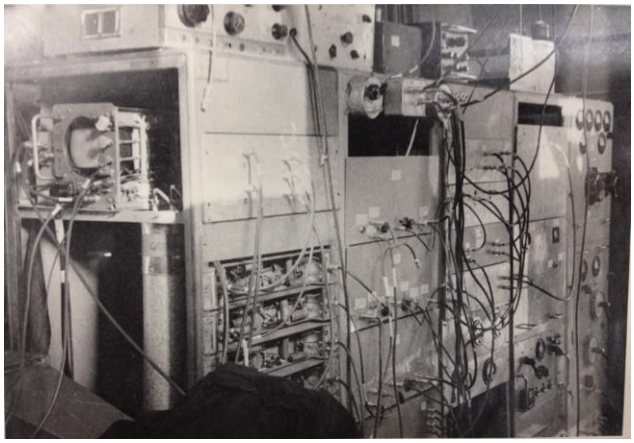

Figure 2 – The Mawson meteor radar. The first upper atmosphere wind measurements on the Antarctic Continent were made using this equipment.

the development of a new dedicated field site at St Kilda, north of Adelaide, and a new radar, with the transmitter located in Adelaide, and the main receiving station at St Kilda was completed in 1958. The arrangement is shown in *Figure 3*, and one of the remote receiving sites is shown in *Figure 5*. The Upper Atmosphere Group in 1962 is shown in *Figure 1*.

Highlights of the work produced using this radar included the determination of meteor orbits, measurements of 'turbulence' intensity, and long term measurements of upper atmosphere winds. Nilsson's work (Nilsson, 1964) resulted in the first set of measurements of meteor orbits in the southern hemisphere (2200 in total). Most orbits were found to lie close to the plane of the ecliptic. Bob Roper was the first person to measure upper atmosphere variability at small scales (< 2 km). His measurements were interpreted as being related to the turbulent dissipation rate at 93 km, but are more likely due to small scale wave motions rather than actual turbulence. Nevertheless, they were a valuable contribution to better understanding the dynamics of this region. Interferometric measurements of the mean wind field (see *Figure 4* and *Figure 6*) continued using this radar until the mid-1970's, although it was run in campaign mode after 1972. Work at the St Kilda field site ceased in the mid-1970's and was relocated to the nearby Buckland Park field site.

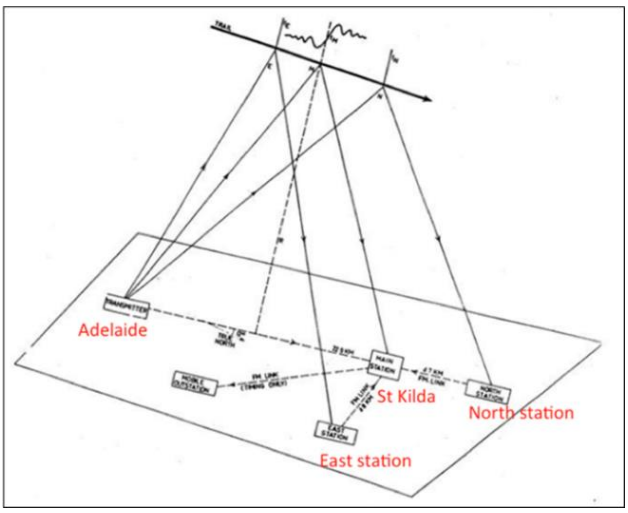

Figure 3 – The multi-station system in 1958. The receiving main site at St Kilda had two supplementary receiving sites about 5 km East and North and the data were sent to the main station via FM links.

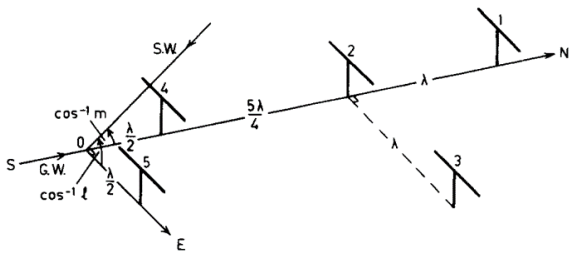

Figure 4 – The interferometer used for wind measurements at the St Kilda field site. Each antenna was a half-wave dipole and the direction cosines of the sky wave were deduced from the relative phases on the five antennas.

Buckland Park

Basil Briggs joined the Department in 1962. He had been a Junior Scientific Officer at the TRE between 1942 and 1946 before joining the Radio Research Group at the Cavendish Laboratory, Cambridge, where he worked from 1946 to 1961. Together with Graham Elford, he developed the large MF/HF radar array at Buckland Park (Briggs et al., 1969). This versatile array was used for investigations of the ionosphere, the neutral atmosphere and of meteors observed at both 2 and 6 MHz. Examples of the latter work include observations of 2 MHz meteor echoes (Brown, 1976), their height distribution (Olssen-Steel and Elford, 1987), and the measurements of winds using 2 MHz meteor trails (Tsutsumi et al., 1999).

3 Decline and rebirth of meteor wind radars

Figure 5 – Bob Roper and Carl Nilsson with receiving equipment at one of the St Kilda remote receiving sites.

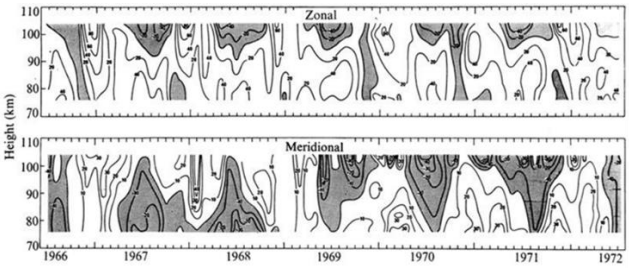

Figure 6 – Six years of upper atmosphere winds measured using the St Kilda radar.

Decline of meteor wind radars

The closure of the St Kilda site and the dedicated meteor radar in the mid-1970's was typical of a general decline of radar meteor upper atmosphere wind research around the world, and the measurement of upper atmosphere winds became more common by using partial reflection radars (see e.g., Reid, 2015). But some new meteor radars were developed in this period. For example, in the early 1970's, the Soviet VETA radars were developed by the Kharkov Institute of Radio Electronics. These formed the basis of an extensive network, albeit one with no height information. This is briefly discussed by Roper (1984). A new meteor radar was also developed in Kyoto by Aso et al. (1979), but generally the technique fell from favor until the late 1990's.

Rebirth of meteor wind radars

Increased interest in using meteor trails for the measurements of upper atmosphere winds came following the advent of ST and MST radars. These powerful radars operating in the lower VHF band were designed to measure winds using the Doppler technique in the Stratosphere and Troposphere (ST), and for the most powerful radars, the Mesosphere (M) as well. By piggybacking a dedicated data acquisition system onto these pulsed radars, their narrow beams could be used for meteor studies. One such system, MEDAC, was developed at the University of Colorado (e.g., Valentic et al., 1996) and used with a number of ST radars.

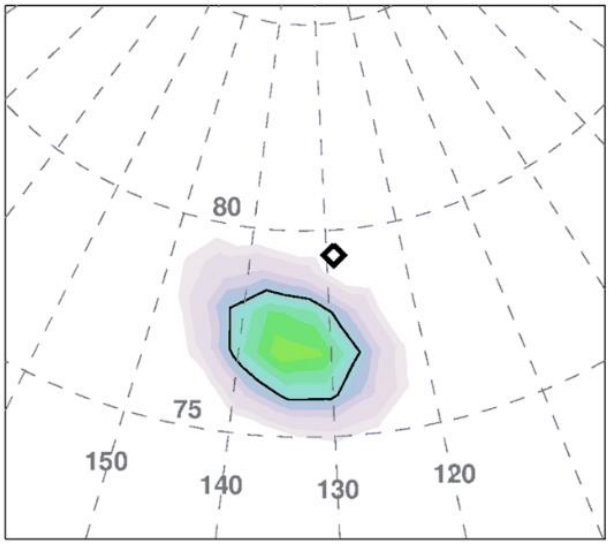

Figure 7 – The Camelopardalids 2014 Activity Map. The diamond is the pre-infall radiant, the solid contour is the full width half maximum (further details in Younger et al., 2015a).

One issue with this approach is that because most meteor trails occur low in the sky, most meteor trails are detected in the radar sidelobes, and without interferometry, their actual location is indeterminate. At Adelaide, the main beam of the radar was directed at 60° off–zenith, successfully avoiding this issue (e.g., Cervera and Reid, 1995).

A variation of this approach using an additional receiving only interferometer together with an MST radar was pioneered on the MU MST radar in Japan (e.g., Tsutsumi et al., 1994). This was followed by the development of a new class of dedicated all-sky meteor radars using an interferometric approach and producing real-time winds in the late early 1990's (e.g., Holdsworth et al., 2004). This development was made possible by the ready availability of cheap powerful computers, and development of solid state transmitters and better data acquisition systems. These radars have now largely displaced the previously more common partial reflection radars used for measuring upper atmosphere winds.

4 Recent work

The 21st centrury has seen meteor radar become a standard tool for the routine measurement of upper atmospheric winds, with radars developed by ATRAD achieving detection rates in excess of 30000 meteors per day. Ongoing wind observations continue to provide deep insights into the structure and dynamics of the

atmosphere and how the motions of air masses are coupled between the upper and lower atmosphere (Bossert et al., 2015). The ability to measure atmospheric conditions in the meteor region at higher temporal resolutions has facilitated the studies of mesospheric meteorology, exotic plasma behaviours, and detailed astronomical observations. A substantial breakthrough has been the implementation of the Fresnel transform technique, which provides high-accuracy meteoroid speeds, in addition to producing images of radar reflectivity along meteor trails (Elford, 2004; Holdsworth et al., 2007).

Astronomy has followed a similar path to atmospheric observations, as broad surveys of shower activity (Younger et al., 2009) have given way to detailed investigations of individual showers. Individual showers have enabled the performance of radar techniques to be tested with known populations, further refining established practices (Younger et al., 2012). The unprecedented detection of the Camelopardalids shower of 2014 (Younger et al., 2015b) was the first time that a new shower had been predicted prior to its first occurrence and demonstrated the ability of meteor radar data to be rapidly analysed in response to unusual events (see also Younger et al., 2016).

New fields of research have been opened, as old assumptions have given way to a better understanding of meteor trail plasma. Meteor radar echo durations have been found to be strongly affected by plasma neutralization at lower altitudes (Lee et al., 2013; Younger et al., 2014), which allows observation of the chemistry of the D-region of the ionosphere. Inconsistent temperature estimates can now be explained (Cervera and Reid, 2000; Holdsworth et al., 2006), and new methods of using meteor radar to measure atmospheric density have been developed (Younger et al., 2015a).

Moving forward, the future of meteor radar lies in the establishment of networks of radars to observe not just the conditions above a single site, but the motions of the atmosphere across large areas. Together with Chinese colleagues, the utility of small meteor radars to investigate non-specular echoes and some aspects of plasma irregularities has been explored (Li et al., 2013). Advances in radar sensitivity and echo interpretation are allowing meteor radars to also be used to study the lower portion of the ionosphere, including sporadic E layers. The use of remote receiving sites, such as those used in the St Kilda radar is being reinvestigated using GPS locking, and is a promising new development for the measurement of wind fields over large regions. Astronomical applications will also benefit, as complete coverage of the celestial sphere is achieved, with the observations of multiple sites being assimilated into large-scale virtual observatories.

5 Conclusion

We have very briefly reported on more than 65 years of meteor radar research at Adelaide University. A feature of the work has been observations both in Australia and Antarctica over that period, and of continuing innovation. The group is continuing to exploit the observations for measurements of temperature, density and scale heights in the upper atmosphere, and the use of remote GPS-locked receiving sites. The Adelaide all-sky meteor radars have been commercialized, and there are an increasing number of meteor radars in China.

Acknowledgments

We have relied in part on notes made and conversations with Graham Elford to form part of the background to this work. Graham is the authority and any errors are of course ours.

References

Aso T., Tsuda T. and Kato S., (1979). “Meteor radar observations at Kyoto University”. *Journal of Atmospheric and Terrestrial Physics*, **41**, 517–525.

Blake A. (2010). “Physics at Adelaide, the 1950’s – A decade of Change”. 22 pages.

Bossert K., Fritts D. C., Pautet P. D., Williams B. P., Taylor M. J., Kaifler B., Dörnbrack A., Reid I. M., Murphy D. J., Spargo A. J. and MacKinnon A. D. (2015). “Momentum flux estimates accompanying multiscale gravity waves over Mount Cook, New Zealand, on 13 July 2014 during the DEEPWAVE campaign”. *Journal of Geophysical Research: Atmospheres*, **120**, 9323–9337.

Briggs B. H., Elford W. G., Felgate D. G., Golley M. G., Rossiter D. E. and Smith J. W. (1969). “Buckland Park aerial array”. *Nature*, **223**, 1321–1325.

Brown N. (1976). “Radio echoes from meteor trains at a radio frequency of 1.98 MHz”. *Journal of Atmospheric and Terrestrial Physics*, **38**, 83–87.

Crompton R. W. (2007). “‘Huxley, Sir Leonard George Holden (1902–1988)’”. *Australian Dictionary of Biography*, National Centre of Biography, Australian National University.

Cervera M. A. and Reid I. M. (1995). “Comparison of simultaneous wind measurements using colocated VHF meteor radar and MF spaced antenna radar systems”. *Radio Science*, **30**, 1245–1261.

Cervera M. A. and I. M. Reid (2000). “Comparison of atmospheric parameters derived from meteor observations with CIRA”. *Radio Science*., **35**, 833–843.

Elford W. G. and Robertson D. S. (1953). “Measurements of winds in the upper atmosphere by means of drifting meteor trails II”. *Journal of Atmospheric and Terrestrial Physics*, **4**, 271–284.

Elford W. G. (2004). “Radar observations of meteor trails, and their interpretation using Fresnel holography: a new tool in meteor science”. *Atmospheric Chemistry and Physics*, **4**, 911–921.

Holdsworth D., Elford W., Vincent R., Reid I., Murphy D. and Singer W. (2007). “All-sky interferometric meteor radar meteoroid speed estimation using the Fresnel transform”. *Annales Geophysicae*, **25**, 385–398.

Holdsworth D. A., Reid I. M. and Cervera M. A. (2004). “Buckland Park all-sky interferometric meteor radar”. *Radio science*, **39** (5), 12 pages.

Holdsworth D. A., Morris R. J., Murphy D. J., Reid I. M., Burns G. B. and French W. J. R. (2006). “Antarctic mesospheric temperature estimation using the Davis mesosphere-stratosphere-troposphere radar”. *Journal of Geophysical Research: Atmospheres*, **111**(D5), DOI 10.1029/2005JD006589.

Lee C. S., Younger J. P., Reid I. M., Kim Y. H. and Kim J. H. (2013). “The effect of recombination and attachment on meteor radar diffusion coefficient profiles”. *Journal of Geophysical Research: Atmospheres*, **118**(7), 3037–3043.

Li G., Ning B., Hu L., Chu Y. H., Reid I. M. and Dolman B. K. (2012). “A comparison of lower thermospheric winds derived from range spread and specular meteor trail echoes”. *Journal of Geophysical Research: Space Physics*, **117**(A3), DOI 10.1029/2011JA016847.

Manning L. A., Villard Jr O. G. and Peterson A. M. (1950). “Meteoric echo study of upper atmosphere winds”. *Proceedings of the IRE*, **38**, 877–883.

Nilsson C. S. (1964). “A Southern Hemisphere radio survey of meteor streams”. *Australian Journal of Physics*, **17**, 205–256.

Olsson-Steel D. and Elford W. G. (1987). “The height distribution of radio meteors: observations at 2 MHz”. *Journal of Atmospheric and Terrestrial Physics*, **49**, 243–258.

Reid I. M. (2015). “MF and HF radar techniques for investigating the dynamics and structure of the 50 to 110 km height region: a review”. *Progress in Earth and Planetary Science*, **2**, 1–34.

Roper R. G. (1984). “MWR, Meteor Wind Radars”. In International Council of Scientific Unions Middle Atmosphere Handbook, **13**, 124–134 (SEE N85-17452 08-46).

Tsutsumi M., Tsuda T., Nakamura T. and Fukao S. (1994). “Temperature fluctuations near the mesopause inferred from meteor observations with the middle and upper atmosphere radar”. *Radio Science*, **29**, 599–610.

Tsutsumi M., Holdsworth D., Nakamura T. and Reid I. (1999). “Meteor observations with an MF radar”. *Earth Planets Space*, **51**, 691–699.

Valentic T. A., Avery J. P., Avery S. K., Cervera M. A., Elford W. G., Vincent R. A. and Reid I. M. (1996). “A comparison of meteor radar systems at Buckland Park”. *Radio Science*, **31**, 1313–1329.

Weiss A. A. (1957). “The incidence of meteor particles upon the earth”. *Australian Journal of Physics*, **10**, 77–102.

Younger J. P., Reid I. M., Vincent R. A., Holdsworth D. A. and Murphy D. J. (2009). “A southern hemisphere survey of meteor shower radiants and associated stream orbits using single station radar observations”. *Monthly Notices of the Royal Astronomical Society*, **398**, 350–356.

Younger J. P., Reid I. M., Vincent R. A. and Murphy D. J. (2012). “Meteor shower velocity estimates from single-station meteor radar: accuracy and precision”. *Monthly Notices of the Royal Astronomical Society*, **425**, 1473–1478.

Younger J. P., Lee C. S., Reid I. M., Vincent R. A., Kim Y. H. and Murphy D. J. (2014). “The effects of deionization processes on meteor radar diffusion coefficients below 90 km”. *Journal of Geophysical Research: Atmospheres*, **119**, 10027–10043. Doi:10.1002/2014JD021787.

Younger J. P., Reid I. M., Vincent R. A. and Murphy D. J. (2015a). “A method for estimating the height of a mesospheric density level using meteor radar”. *Geophysical Research Letters*, **42**, 6106–6111.

Younger J. P., Reid I. M., Li G., Ning B. and Hu L. (2015b). “Observations of the new Camelopardalids meteor shower using a 38.9 MHz radar at Mohe, China”. *Icarus*, **253**, 25–30.

Younger J. P., Reid I. M. and Murphy D. J. (2016). “Radar Observations of the Volantids Meteor Shower”. In Roggemans A. and Roggemans P., editors, *Proceedings of the International Meteor Conference*, Egmond, the Netherlands, 2-5 June 2016. Pages 352–357.

Minor meteor shower activity

Jürgen Rendtel

Leibniz-Institut für Astrophysik Potsdam, An der Sternwarte 16, 14482 Potsdam, Germany

International Meteor Organization, Eschenweg 16, 14476 Potsdam, Germany
jrendtel@web.de

Video meteor observations provide us with data to analyze structures in minor meteor showers or weak features in flux profiles. Samples obtained independently by other techniques allow to calibrate the data sets and to improve the confidence of results as demonstrated with a few results. Both, the confirmation of events predicted by model calculation and the input of observational data to improve the modelling results may help to better understand meteoroid stream evolution processes. Furthermore, calibrated data series can be used for studies of the long-term evolution of meteor shower activity.

1 Introduction

Over the recent years, a substantial number of minor meteor showers have been detected using video meteor data. Most of the new entries to the IAU meteor shower database have been found from orbital data obtained by multiple station observations. The data also allow deriving physical parameters such as the flux or particle size distribution for weak sources. In this paper we discuss optical observations. Radio techniques can contribute to several of the raised points as well.

A large sample is expected to include a sufficient number of meteors from weak sources and thus allows us to deal with details of low activity showers. Nevertheless, at some point the question of the reliability of short-term or weak features in ZHR or flux profiles arises. In such cases it is useful to have an independent data sample at hand.

Over the previous decades, a huge amount of data has been collected by other techniques, mainly visual observations. In some cases, additional activity information can be retrieved from publications which give sufficient details back over decades. This allows investigating long-term evolution of meteor shower activity, particularly for major and well established showers such as the Geminids (Rendtel, 2004) or the Orionids (Rendtel, 2008). It has also been shown that in case of a large continuous sample, minor features in rate profiles can be resolved, for example a short pre-maximum peak of the Orionids in 1993 (Rendtel and Betlem, 1993).

Currently, observational data obtained with different methods is available for the activity periods of many meteor showers. By combining these data it is possible to detect and confirm weak features and to be more confident with the results. Furthermore, such dual samples allow calibrating data sets obtained by different methods. This way it is possible to later combine old visual and recent video data to extend the covered period for long-term studies.

2 Some results

In order to check the possibilities for detection of weak features in minor showers, we may first look at details in major shower activity profiles which are usually well covered by observations obtained with different techniques. In a next step, we can then analyze data of minor showers in the same way.

The Quadrantid (010 QUA) maximum 2016 was expected around January 4, 8^h UT. A possible rate enhancement between 22^h UT and 2^h UT (corresponding to $\lambda_\odot$ 282.74° and 282.91°) was suggested from calculations of Vaubaillon given in the IMO Meteor Shower Calendar for 2016. Both, the video and visual data show a slight enhancement at $\lambda_\odot$ = 282.88° (*Figure 1*). The coincidence in position and level as well as the slightly later occurring dip at 282.94° provide confidence that the features are real.

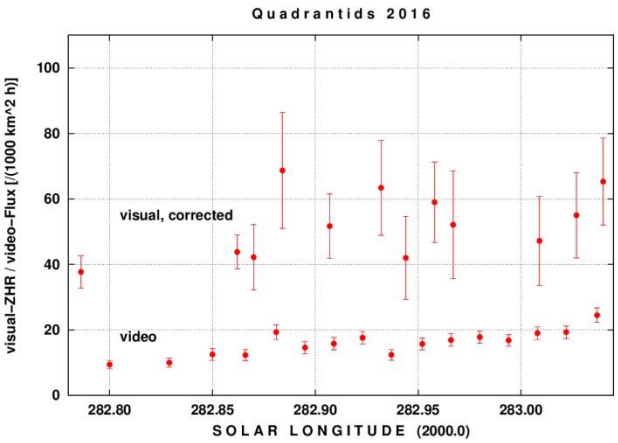

Figure 1 – Detail from the ascending branch of the 2016 Quadrantids observed visually (ZHR) and by video (flux). Two minor features can be found in both data samples: a minor peak at $\lambda_\odot$ = 282.88° and an also very minor dip at $\lambda_\odot$ = 282.94°. Each data set alone would not provide confidence that this may be a real structure in the stream.

A similar short peak was found in the Perseid (007 PER) ZHR and flux profiles of 2015 obtained by visual and video observers (see *Figure 8* in Molau et al., 2015a). As

the peak occurs just in one data bin, a single data set would have left a large uncertainty about the reliability. Detecting the short peak in coinciding bins of independent samples obtained by different techniques increases the confidence significantly.

In the case of most minor showers the amount of data is much smaller than for near-maximum periods. So it may happen that different samples provide us with no conclusive information about the activity profiles. The information about a possible activity of the kappa-Cepheids (751 KCE) on 2015 September 21 was scarce (Šegon et al., 2015) and the activity derived from a very small visual meteor sample (Rendtel, 2015) is not confirmed by video data (Molau et al., 2016).

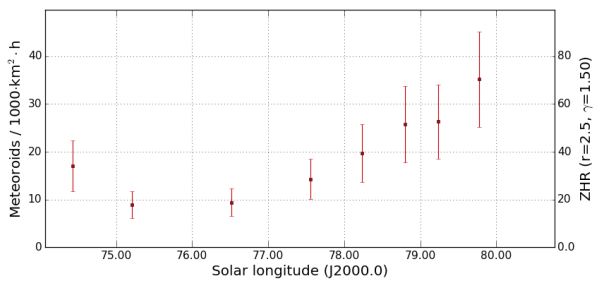

Figure 2 – Flux of the 171 ARI calculated from video data of the IMO VMN from 2011 to 2015 using the tool provided by meteorflux.io on the net. (Parameters: minimum sample 10 shower meteors per bin, minimum radiant elevation 5°.) The activity is well detectable, but no profile with a maximum occurs.

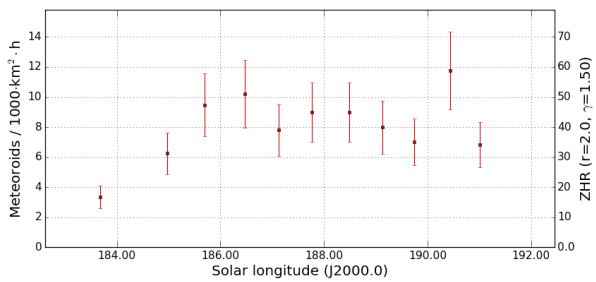

Figure 3 – Flux of the 221 DSX calculated from video data of the IMO VMN from 2011 to 2015. The profile shows slightly higher flux values around the middle of the period, but no clear maximum. (Parameters: minimum sample 20 shower meteors per bin, minimum radiant elevation 5°.)

Extending the observing period into the twilight, some attempts are made to collect data of the Daytime Arietieds (171 ARI) in early June and the Daytime Sextantids (221 DSX) around end of September. Certainly, radio and radar data would be best to establish flux profiles, these are not yet available. Both showers can easily be found in video data, but do not allow deriving a reliable flux profile yet. The observing conditions are close to the limits particularly for the Arietids (*Figure 2*) due to the twilight at northern locations but are slightly better for the Sextantids near the autumnal equinox (*Figure 3*). Currently we find that the fluxes increase only after the listed maximum positions at 77° and 184°, respectively. In both cases the corrections due to rapidly changing radiant elevation and observing conditions need to be improved – likely a case for combining radio and video data.

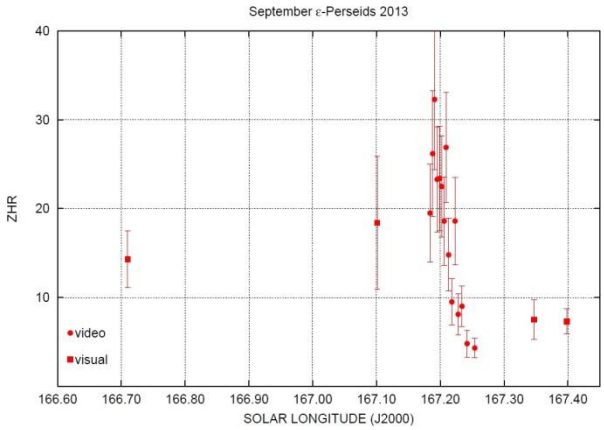

Figure 4 – The combination of visual and video observations around the peak of the September epsilon Perseids in 2013 allows to complete the profile and to calibrate the values obtained by the different methods.

The situation was much better in the case of the September epsilon-Perseids 2013. Here the data of the visual and video observations can be perfectly used to complete the information about the ZHR/flux and the population index (*Figure 4*, from Rendtel et al., 2014).

Extending the length of data series is not only possible for major or medium level showers as mentioned in the Introduction. It can also be applied to minor showers, provided that the radiant position used for the shower association remained consistent over the period under study. This, for example, is the case for the northern radiant of the kappa-Cygnids. Its position is far away from other active radiants at the same time and their velocity is obviously low. This allowed searching for suspected periodicities in rate enhancements back over 41 years. A wavelet analysis was applied to the data set to check whether there are signs of periodicities within the 41 years covered by the data (*Figure 5*). The available data includes no hints at periods lower than 20 years in the kappa-Cygnid appearance (for details refer to Rendtel and Arlt, 2016).

3 Conclusions

Improved technical equipment and collaboration allow us to detect and analyze minor showers and weak features in the flux profiles.

Almost complete coverage of the observable time with video meteor networks seems to make visual observation obsolete. But there are several good reasons to continue using various techniques.

Independent samples of one target are useful to calibrate the data and to obtain better information about the reliability of observed features and quantities in flux

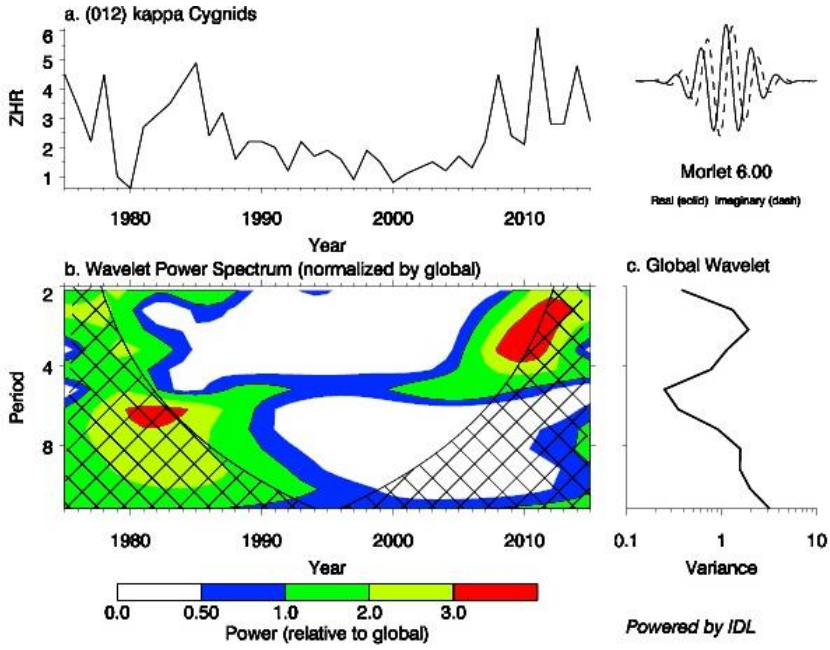

Figure 5 – Wavelet analysis of the kappa Cygnid ZHR data from 41 years. Panel (a) shows the ZHR, (b) the wavelet power spectrum. The cross-hatched region is the cone of influence and (c) gives the global wavelet power spectrum. Details are given in (Rendtel and Arlt, 2016).

profiles. Since visual observers often concentrate to major shower activity periods, it is worth to alert them in periods with possible meteors from usually weak or unknown sources. This is one purpose of the annual IMO Meteor Shower Calendar.

Activity of meteor showers may vary considerably from one return to the next. Therefore, in many cases an average activity profile of a given shower does not provide appropriate information about the meteoroid stream. Well calibrated video and visual data may be used to establish long time series. So we may for example look for a pattern in the occurrence of the high northern showers in September-October (Rendtel and Molau, 2010). The currently very weak delta-Aurigids (224 DAU) might have been more prominent in the past since Drummond (1982) referred to photographic data.

Another important field is the interaction between observers and authors of model calculations which should optimally work in both directions: observers check the periods with predicted possible rate anomalies, but provide information which may help to improve the models, eventually understanding the meteoroid release processes from their parent better.

References

Drummond J. (1982). “A note on the Delta Aurigid meteor stream”. *Icarus*, **51**, 655–659.

Molau S., Crivello S., Goncalves R., Saraiva C., Stomeo E. and Kac J. (2015). “Results of the IMO Video Meteor Network - August 2015”. *WGN, Journal of the IMO*, **43**, 188–194.

Molau S., Crivello S., Goncalves R., Saraiva C., Stomeo E. and Kac J. (2016). “Results of the IMO Video Meteor Network - September 2015”. *WGN, Journal of the IMO*, **44**, 21–26.

Rendtel J. (2004). “Evolution of the Geminids observed over 60 years”. *Earth, Moon, and Planets*, **95**, 27–32.

Rendtel J. (2008). “The Orionid meteor shower observed over 70 years”. *Earth, Moon, and Planets*, **102**, 103–110.

Rendtel J. (2015). “Minor kappa-Cepheid (751 KCE) activity on 2015 September 21”. *WGN, Journal of the IMO*, **43**, 177–178.

Rendtel J. and Arlt R. (2016). “Kappa Cygnid rate variations over 41 years”. *WGN, Journal of the IMO*, **44**, 62–66.

Rendtel J. and Betlem H. (1993). “Orionid meteor activity on October 18, 1993”. *WGN, Journal of the IMO*, **21**, 264–268.

Rendtel J., Lyytinen E., Molau S. and Barentsen G. (2014). “Peculiar activity of the September epsilon-Perseids on 2013 September 9”. *WGN, Journal of the IMO*, **42**, 40–47.

Rendtel J. and Molau S. (2010). “Meteor activity from the Perseus-Auriga region in September and October”. *WGN, Journal of the IMO*, **38**, 161–166.

Šegon D., Andreić Ž., Korlević K. and Vida D. (2015). “Croatian meteor network: ongoing work 2014-2015”. In Rault J.-L. and Roggemans P., editors, *Proceedings of the International Meteor Conference*, Mistelbach, Austria, 27-30 August 2015. IMO, pages 51–57.

The radio meteor signal path from transmitter to spectrogram: an overview

Tom Roelandts

Impulse Response, Beerse, Belgium
tom@impulseresponse.eu

In this paper, we present an overview of the radio meteor signal path, from the sinusoidal carrier wave that is initially transmitted, to the spectrogram that is typically used as the final result in the receiving chain. We describe the amplitude modulation and Doppler shift that is caused by the meteor, the combination of the reflected with the directly received signal at the antenna, the down conversion in the receiver, the sampling, and the down sampling in software. A simulation of the complete process results in detailed plots at each of these steps.

1 Introduction

The results of the *Belgian RAdio Meteor Stations (BRAMS)* network (Calders and Lamy, 2011), (Ranvier et al., 2015) are often analyzed through *spectrograms*. In this paper, we provide an overview of the complete radio meteor signal path that leads to these spectrograms at the very end of the receiving chain.

Starting from the knowledge that the transmitted signal is a simple sinusoidal carrier wave, the conceptual picture is clear. A BRAMS spectrogram represents the reflection of that carrier off a number of meteor trails, together with a relatively low amplitude directly received signal (and plane echoes, which we ignore in this paper). However, in practice, several things happen to the signal in addition to it being reflected off the meteor trail.

In this paper, we describe all the major effects that the signal encounters before it is finally plotted as a spectrogram. Additionally, we have implemented a simulation of the complete signal path, which allows showing detailed plots at each step. Both the description and the simulation are meant to demonstrate the major effects that happen, without necessarily capturing every last detail of each process.

2 Signal path

Overview

Figure 1 shows an overview of the signal path. The initial carrier is modified by the interaction with the meteor trail, by being combined with the directly received signal at the antenna, by being down converted in the receiver, by being sampled, and by being down sampled in software. In the remainder of this paper, each of these steps is described in more detail.

The different effects are illustrated by plots that were generated through a simulation of the complete signal path. This simulation was performed at a radio frequency (RF) of 100 kHz. This is equivalent to using the true RF, since the down conversion step is independent of that RF.

Transmitter

The transmitter produces a simple sinusoidal carrier wave at a frequency of $f_T = 49970000$ Hz. Hence, the carrier wave can be defined as

$$\sin(2\pi f_T t),$$

where t is the time in seconds.

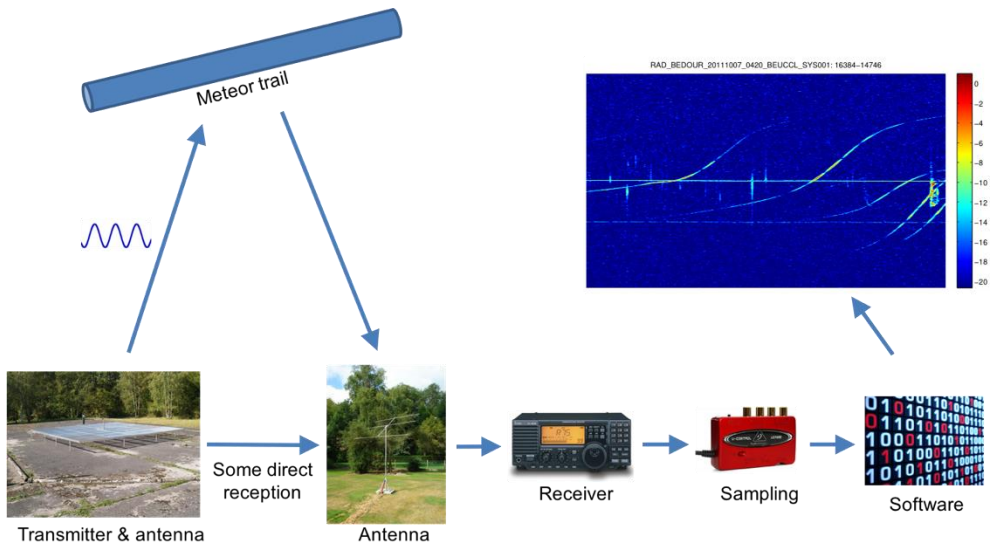

Figure 1 – Overview of the signal path.

Meteor trail

If a meteor trail with a geometrically favorable orientation is present, it will reflect the carrier wave towards the antenna. The effect of this reflection is a modulation of the *amplitude* of the carrier. In the simulation, a simple meteor amplitude profile was used, consisting of a fast linear rise followed by an exponential decay (*Figure 2*). We write this amplitude profile as $A(t)$. The fast linear rise models the quick formation of the trail, while the exponential decay models its diffusion.

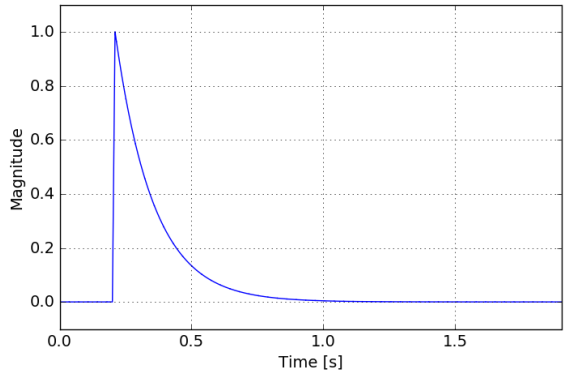

Figure 2 – Meteor amplitude profile.

In addition to the amplitude modulation, the reflection off the trail also causes a Doppler shift of the carrier frequency, if the trail is moving due to high altitude winds. Such a Doppler shift is observed very often in practice. If the reflection off the trail causes a Doppler shift of f_D Hz, then the received frequency will be $f_T + f_D$ Hz.

Combining the amplitude profile of the meteor with the Doppler shift, the reflected wave that is received by the antenna is

$$A(t)\sin(2\pi(f_T + f_D)t).$$

This amplitude-modulated carrier is illustrated in *Figure 3*. The graph is solid blue because of the very high frequency of the carrier.

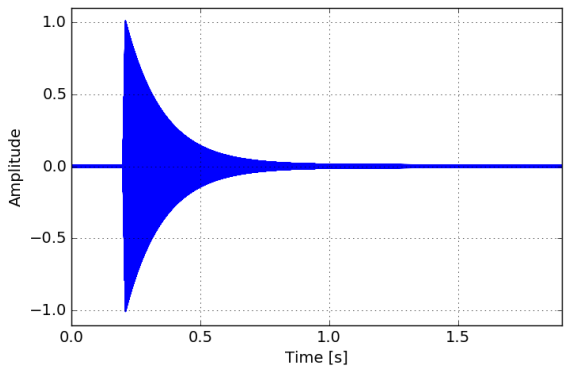

Figure 3 – Amplitude-modulated carrier after reflection off the meteor trail.

Receiver Antenna

At most of the BRAMS stations, the antenna picks up a low-amplitude signal directly from the transmitter. When a meteor appears, its signal is combined with it. The directly received signal has a much lower amplitude than many of the meteor reflections. However, this does not imply that it can be ignored. In the simulation, we have set the amplitude of the directly received signal to 1% of the maximum level of the simulated meteor.

Due to the Doppler shift that the reflected signal contains, the two signals that are combined at the antenna have a different frequency. At a direct reception level of D, the combined signal can be written as

$$D\sin(2\pi f_T t) + A(t)\sin(2\pi(f_T + f_D)t).$$

Summing two sinusoids with a slightly different frequency produces *beats*, which are variations in the amplitude of the signal due to alternating constructive and destructive interference. In the simulation, we have used a Doppler rate of 25 Hz. *Figure 4* shows how the resulting beats are superimposed on the received amplitude profile as small "bumps". The frequency of 25 Hz can be recognized in the period of the amplitude variations.

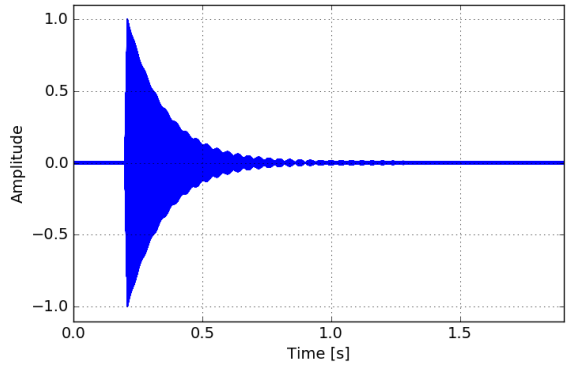

Figure 4 – The combined reflected and directly received signal at the antenna.

The corresponding power profile, which is simply the signal of *Figure 4* squared, is shown in *Figure 5*.

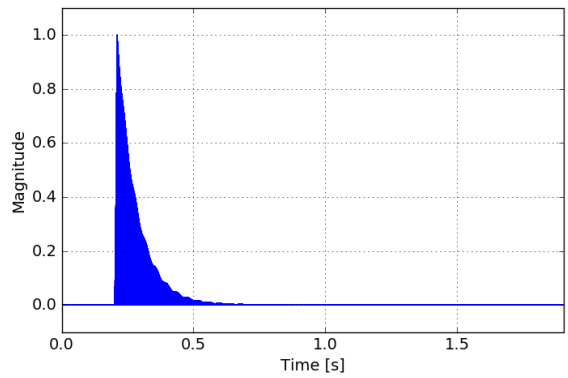

Figure 5 – Power profile of the received signal.

Although the Doppler shift of the reflection might be deduced from the period of these beats, it can easily be determined more directly from a spectrum or a spectrogram. Hence, it might be better to remove the directly received signal from the data, and avoid these beats altogether, since they might be obscuring the properties of the reflection itself. Removing the directly

received signal is relatively easy, since the received carrier is quite constant, both in frequency and in power.

Receiver

The signal of *Figure 4* is the input to the receiver. This implies that the received spectrum can now be computed. *Figure 6* shows a part of the complete spectrum, centered at the original carrier frequency of, in the simulation, 100 kHz. There is a small peak at 100 kHz and the larger peak of the meteor reflection at an offset of 25 Hz (the Doppler offset).

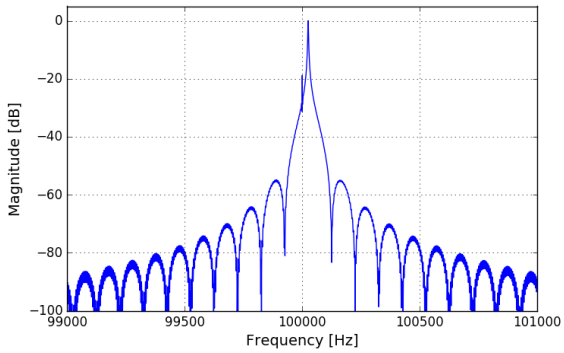

Figure 6 – The spectrum that is received at the receiver.

At the receiver, this signal is *mixed*, i.e., *multiplied*, with a local oscillator (LO) at a small frequency offset of 1 kHz. This is done simply by tuning the receiver to a frequency of 49969000 Hz instead of the exact value of f_T. Note that this multiplication of signals is completely different from what happens at the antenna, where two signals are *added*. Moreover, the offset of the LO is on purpose. The effect of mixing the received signal with an LO that is offset is that the frequency contents of the meteor reflection is *down converted*, i.e., its frequencies are *shifted* from its original RF frequencies around $f_T + f_D$ to a range of frequencies around 1 kHz.

When sinusoids at two frequencies f_1 and f_2 are multiplied, we have that

$$\sin(f_1)\sin(f_2) = \cos(f_1 - f_2) - \cos(f_1 + f_2),$$

from the well-known *product-to-sum* trigonometric identities. This means that, for an ideal mixer, the result of mixing is a first frequency component at the difference $f_1 - f_2$ and a second frequency component at the sum $f_1 + f_2$ of the original frequencies.

With the LO frequency $f_{LO} = f_T - 1\,\text{kHz}$, the two components of the directly received signal will be at $f_T - f_{LO} = 1\,\text{kHz}$ and at $f_T + f_{LO} = 2f_T - 1\,\text{kHz}$. The two components of the meteor reflection, with its additional Doppler shift, will be at $f_T + f_D - f_{LO} = f_D + 1\,\text{kHz}$ and at $f_T + f_D + f_{LO} = 2f_T + f_D - 1\,\text{kHz}$. The complete spectrum is shown in *Figure 7*. In that figure, there is clearly a first peak at 1 kHz and a second one just below 200 kHz (again, the simulation uses 100 kHz instead of f_T). To illustrate that these peaks are indeed two copies of the original spectrum, compare the detailed version of the spectrum that shows the component at 1 kHz (*Figure 8*) with *Figure 6*.

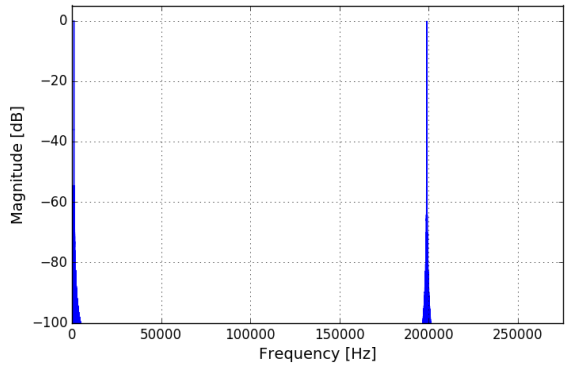

Figure 7 – The full spectrum of the input signal mixed with the local oscillator.

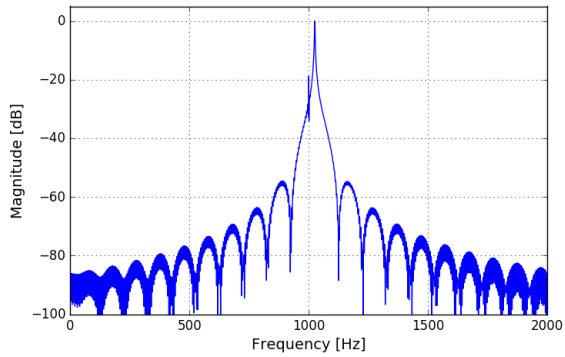

Figure 8 – The spectrum of the input signal mixed with the local oscillator, centered at 1 kHz.

Because of this frequency shift, the signal can be sampled at much lower sampling rates than would be necessary to sample directly at the RF.

Sampling

The Behringer UCA222 sampling device is programmed to sample the down converted signal at 22050 Hz. As is to be expected, the CODEC chip in the sampling device correctly low-pass filters the incoming signal, i.e., it removes frequencies above 11025 Hz, which is half the sampling rate (Texas Instruments, 2008).

The sampling process is the only place where the simulation is not exactly like the real setup. In the simulation, the complete signal path is digital, so there is no actual sampling step at this point. However, that step is replaced with a *down sampling* step that takes the sampling rate of the simulation, which is 551200 Hz, and reduces it to 5512 Hz. A proper low-pass filter with a cutoff frequency of 2756 Hz is included. The spectrum of the down sampled signal is shown in *Figure 9*.

Software

The two operations in the software that are relevant for the signal path are a further down sampling from 22050 Hz to 5512 Hz and the generation of the spectrogram itself. For the down sampling, an additional low-pass filter is included, to remove the frequency contents between 11025 Hz to 2756 Hz. This makes the

output of the simulation equivalent to the output of the software.

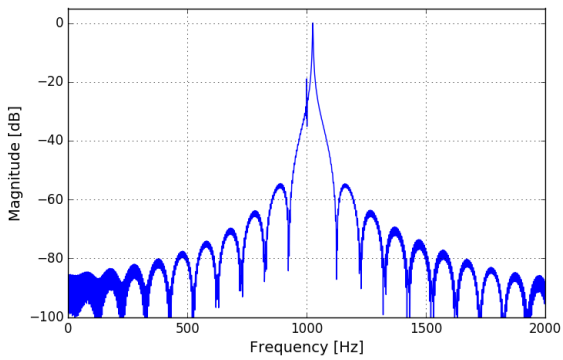

Figure 9 – Spectrum of the sampled signal.

Comparison with the original spectrum

The spectrum at the final sampling rate of 5512 Hz (*Figure 9*) is very close to the originally received spectrum of *Figure 8*. Moreover, it is also quite close to the *bandpass* spectrum of *Figure 6*, confirming that down converting and down sampling the received signal is a valid methodology.

To further explore this, we can also compare the spectrum of *Figure 9* with the spectrum of the original meteor profile. A *two-sided* spectrum, i.e., with 0 Hz in the middle, corresponding to the profile of *Figure 2*, is shown in *Figure 10*. Typically, a spectrum such as this would be shown *one-sided*, i.e., with a frequency range between 0 Hz and some appropriate maximum, since it is symmetrical. However, for easier comparison with the spectrum of *Figure 9*, we have chosen to plot it two-sided here.

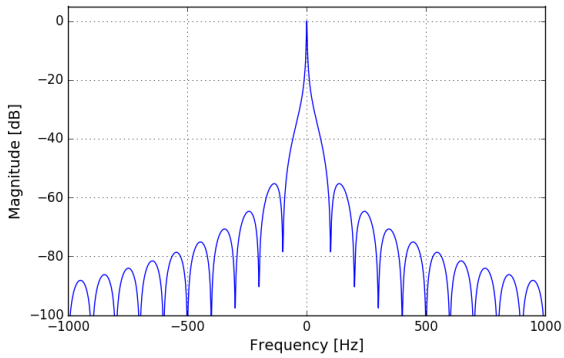

Figure 10 – Spectrum of meteor profile.

The main differences between *Figure 9* and *Figure 10* are the Doppler shift and the small secondary peak caused by the directly received carrier. However, apart from these small changes, both spectra are quite similar.

Spectrogram

Although spectra are a very insightful way to compare the signal at the different stages of processing, they do not provide insight in the time component of the received signal. For that, a spectrogram is generated (*Figure 11*).

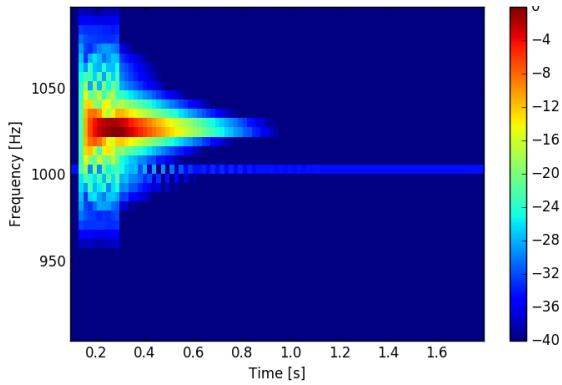

Figure 11 – Spectrogram of the sampled signal.

For comparison with the spectrograms as they are usually presented for BRAMS, *Figure 12* shows the same spectrogram as *Figure 11*, but then for the usual time period of 5 minutes.

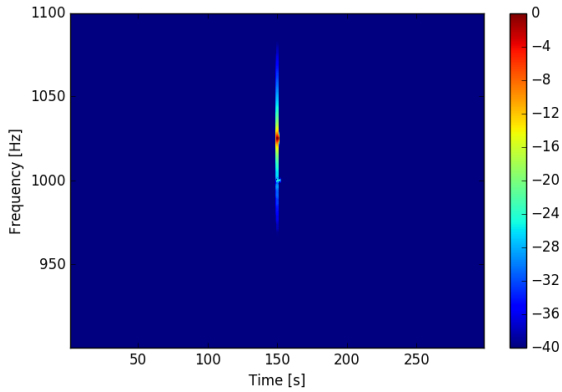

Figure 12 – Spectrogram of the sampled signal, rescaled to a time axis of 5 minutes.

The reflection in *Figure 12* is close to a typical short meteor in an actual BRAMS spectrogram.

3 Conclusion

We have provided an overview of the complete signal path of a radio meteor, from the transmitter to the spectrogram as it is typically generated by a BRAMS station.

References

Calders S. and Lamy H. (2011). “Brams : status of the network and preliminary results”. In Gyssens M. and Roggemans P., editors, *Proceedings International Meteor Conference*, 15-18 September 2011, Sibiu, Romania. IMO, pages 73–76.

Ranvier S., Lamy H., Anciaux M., Calders S., Gamby E. and De Keyser J. (2015). “Instrumentation of the Belgian RAdio Meteor Stations (BRAMS)”. *International Conference on Electromagnetics in Advanced Applications (ICEAA)*, Turin, Italy, 7-11 September 2015, pages 1345–1348.

Texas Instruments (2008). “PCM2902 Stereo Audio CODEC w/USB Interface” datasheet.

Status of the CAMS-BeNeLux network

Paul Roggemans[1], Carl Johannink[2] and Martin Breukers[2]

[1]**MeteorNews.org, Pijnboomstraat 25, 2800 Mechelen, Belgium**
paul.roggemans@gmail.com

[2]**Dutch Meteor Society & KNVWS Werkgroep meteoren, the Netherlands**
c.johannink@t-online.de, breukers@wxs.nl

An overview is being given of the further expansion of the CAMS@BeNeLux network since previous IMC, July 2015 until May 2016. The weather proved less favorable than in the year before, but thanks to a number of new cameras and extra observing stations, the overall performance of the network remained at the same level in spite of the often poor weather circumstances.
This paper compares the Kappa-Cygnids performance of 2015 with the analyses made for the 2014 data, following the same methodology. In 2015 the Kappa Cygnids were remarkable absent which confirms the periodic nature of the abundant Kappa-Cygnids display in 2014.
The CAMS@BeNeLux network was the first to draw attention to enhanced activity of the newly discovered Chi Cygnids meteor shower with 5 accurate orbits in the night of 14–15 September 2015. A search through a selection of all orbits of September 2015 yield 71 possible Chi Cygnid orbits of which 18 were selected to calculate the average orbital elements.

1 Introduction

CAMS or *Cameras for All Sky Meteor Surveillance*[1] is a project financed by NASA, coordinated by Peter Jenniskens. The purpose of the project is to validate the IAU Working List of Meteor Showers[2]. CAMS uses small field of view optics covering the complete sky as a mosaic, and this since end 2010 from three different observing sites in California, US. The concept has been applied by amateur astronomers since 2012 in the Netherlands and since 2014 in Florida and at the Mid Atlantic coast. A complete professional system has been installed at two stations in New Zealand since 2014 and another one is being installed in the United Arab Emirates in 2016. The build-up of the CAMS network has been described in detail in different publications (Bettonvil et al., 2014; Gural 2011; Jenniskens et al., 2011; Roggemans et al., 2014, 2015).

2 Evolution of the CAMS@BeNeLux

At the previous IMC end of August 2015 the status of the CAMS@BeNeLux network was described until June 2015. Between July 2015 and April 2016, 8 new cameras became operational, 4 of these at the new CAMS stations Gent, Uccle and Dourbes in Belgium (*Figure 1*). The station Lieshout (NL) has suspended its participation due to lack of time by the operator, Paul Lindsay. The extra cameras and stations permitted to increase the density of the network and to expand the collection area in the atmosphere with two new regions over the West of Belgium and the North of France (*Figure 2*).

Regardless the number of available cameras, the rather unfavorable climate offers no more than about a couple of clear nights per month throughout the year in the North West of Europe. Most of the nights during which our network collects orbits are just partial clear nights with a very variable cloud cover at each CAMS-station. Overall we can say that the past 10 months were monitored under less favorable weather circumstances than previous year, with exceptions for the period from end July, August, September October 2015 and first half of May 2016 which had better weather circumstances compared to these months in a year before.

Figure 1 – The positions of the 15 cameras at 7 stations in Belgium, the 34 cameras at 9 stations in the Netherlands and the 7 cameras at one station in Germany.

[1] http://cams.seti.org/
[2] http://www.astro.amu.edu.pl/~jopek/MDC2007/index.php

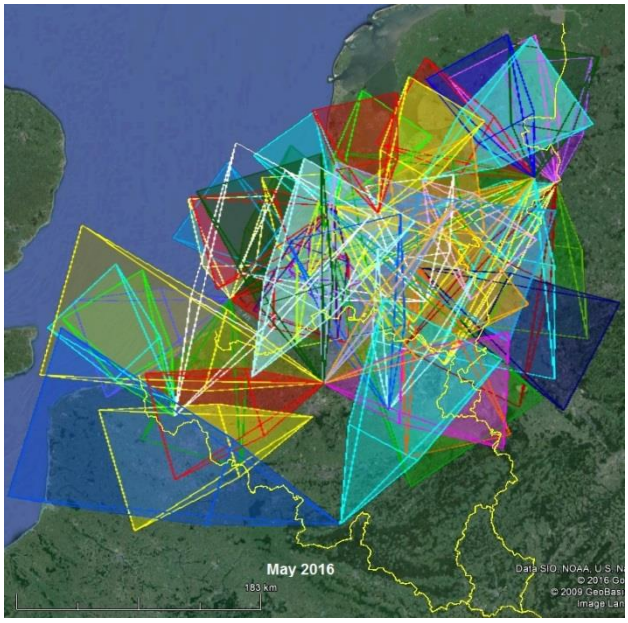

Figure 2 – The coverage of the atmosphere of all operational cameras, intersected at 90 km elevation.

The rather poor weather could be compensated to a large extend by the installation of Auto-CAMS at several stations. Auto-CAMS has been adapted and tested for Europe by Steve Rau and assures that the cameras run each night as long as the Sun is 8° below the horizon. This way no unexpected periods with clear skies are lost during the nights while manual CAMS operators may decide not to run their cameras because of a too bad weather forecast. The general poorer weather circumstances of past 10 months explain why the average number of cameras with successfully collected orbits per month (red line in *Figure 3*) did not increase with the increasing number of active cameras (green line in *Figure 3*). The number of clear or partial clear nights with orbits improved slightly (blue bars in *Figure 3*).

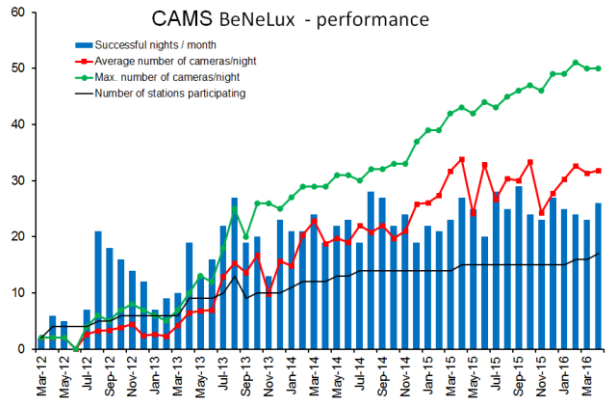

Figure 3 – The performance of the CAMS@BeNeLux network.

Figure 4 shows the monthly yield in orbits while *Figure 5* displays the growth of the database of collected orbits. On 25–26 May 2016, the 40000th orbit was obtained. August, September and October 2015 added significant numbers of orbits. 4 years after the start of our CAMS network only 4 nights of the calendar year remain without any orbits. *Figure 6* shows a significant progress made in past 10 months with as many as 140 nights with 100 or more orbits available per night. Datasets with over 100 orbits per night should allow for shower association searches. Since the CAMS@BeNeLux results are only a subset of the global CAMS dataset of orbits, significant larger numbers of orbits are available for global CAMS shower searches.

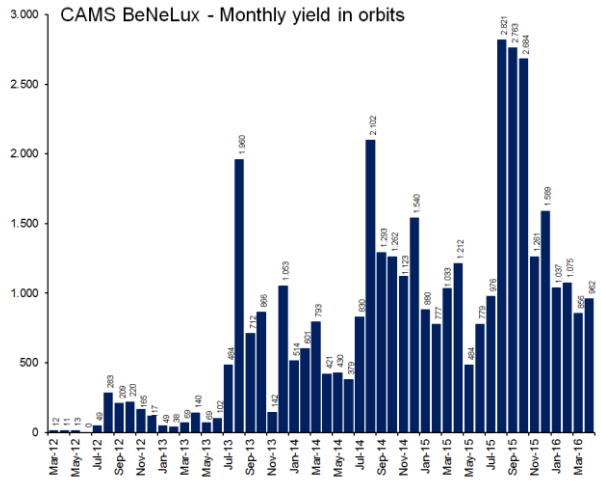

Figure 4 – Monthly distribution of the heliocentric orbits obtained by the CAMS@BeNeLux-network.

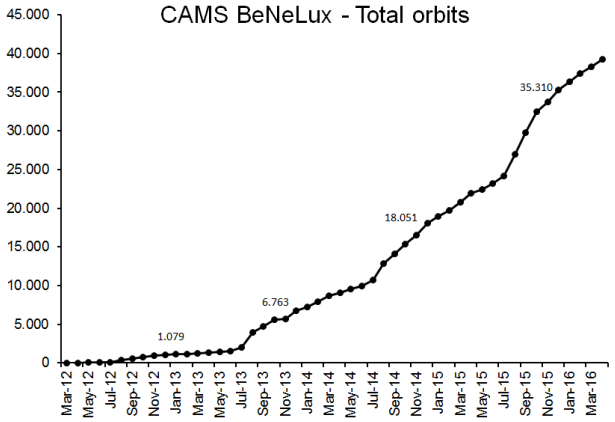

Figure 5 – The evolution of the total number of heliocentric orbits accumulated by the CAMS – BNL network.

TOTAAL	01-02	02-03	03-04	04-05	05-06	06-07	07-08	08-09	09-10	10-11	11-12	12-13	13-14	14-15	15-16	16-17	17-18	18-19	19-20	20-21	21-22	22-23	23-24	24-25	25-26	26-27	27-28	28-29	29-30	30-31	31-01	
Januari	2	53	493	97	2	60	142	106	57	137	65	21	104	7	116	151	181	129	7	38	167	59	5	52	22	43	27	69	13	47	8	2.480
Februari	68	138	90	92	65	134	9	43	18	57	74	169	43	21	234	147	72	39	12	5	89	55	146	173	26	73	189	130	80	0	0	2.491
Maart	28	45	147	122	89	80	179	96	134	157	231	240	169	61	44	155	94		29	1	37	115	48	49	117	55	96	43	53	2	67	2.763
April	58	35	7	64	68	128	38	128	54	130	93	46	96	90	77	97	184	79	232	284	105	101	137	27	31	4	142	83	11	117	0	2.746
Mei	14	33	63	34	65	16			34	27	2	77	66	25	43	48	65	48	59	49	2	6	64	30	24	15	7	32	14	29	5	996
Juni	25	29	64	60	60	86	64	40	49	51	90	56	18	30	77	64	27	1		11	13	33	12	5	28		76	8	73	110	0	1.260
Juli	115	23	92	18	97	111	42	34	131	18	52		18	58	49	51	88	69	74	63	66	113	140	100	121	40	3	34	117	237	165	2.339
Augustus	350	308	96	331	367	282	158	299	173	417	446	1447	255	213	162	16	43	22	216	202	200	212	111	37	47	168	159	176	53	30	152	7.166
September	156	260	165	119	137	29	60	140	175	244	234	107	42	237	86	103	253	73	76	123	17	82	47	100	242	284	365	357	325	339	0	4.977
Oktober	337	335	237	149	27	135	62	48	93	272	280	66	73	1	33	34	36	213	98	128	132	31	114	24	108	405	332	34	267	421	507	5.032
November	203	197	115	50	34	84	199	37	17	297	38	92	119	39	5	24	25	16	8	74	107	215	45	231	117	150	19	107	26	1	0	2.691
December	2	40	14	146	109	113	329	183	298	241	304	241	677	116	23	16	23	17	139	103	3	31	107	98	86	30	208	83	294	17	208	4.299
																																39.240
0 orbits:	6																															
>0 orbits:	360																															
>100 orbits	140																															
>1000 orbits	1																															

Figure 6 – Total number of orbits per calendar date (~1° in Solar Longitude) accumulated 2012–2016 (until April 2016).

The CAMS@BeNeLux network is operated by a team of motivated amateurs. The success of each station depends a lot on the commitment of the other stations to run their cameras in order to enable simultaneous registrations of meteors at different stations. Running one up to 8 cameras per station during successive nights all year round and calibrating, confirming and reporting the data on a day-by-day bases without any problematic delays, altogether represents a lot of work. The CAMS team is

running with a mixture of new and veteran meteor observers, all very dedicated to assure the continuity and efficiency of the network.

3 Highlights July 2015 – May 2016

The rather average weather in July 2015 produced only few 100% clear nights for the network. Weather improved in August and although that 11–12 August was overcast without any orbits, 12–13 August produced as many as 713 orbits in a single night! After a poor last week of August, September was blessed with more than usual clear nights with over 200 orbits per night. The Chi Cygnids displayed enhanced activity on 14–15 September and were first reported by the CAMS network and later confirmed by other networks.

October still counted a fair number of clear nights although most of the Orionid activity period was lost due to cloudy weather. November confirmed its reputation to be rather unfavorable for astronomical observations in the Low Lands of North Western Europe. No winter weather in December but also rather few clear nights and no luck with the best Geminid nights.

2016 started with poor circumstances for the Quadrantids, but overall January 2016 was just a normal month as were February and March with less clear nights than in 2015 when these months were doing better than usual for the winter season. April was again a normal month with a good coverage of the Lyrid activity. The exceptional series of clear nights in the first part of May allowed monitoring the Eta Aquariids, but the second half of May was again rather poor.

4 What about the κ–Cygnids in 2015?

A selection of 149 orbits was made with a radiant position within the range $\alpha \approx$ [220° to 310°] and $\delta \approx$ [+39° to +74°], the geocentric velocity Vg ≈ [12 to 34 km/s], with as inclination i ≈ [16° to 46°] and as argument of perihelion $\omega \approx$ [150° – 216°] for the period $\lambda_\odot$ [115°–158°] (*Figure 7*). These criteria were chosen on bases of the known information available on the κ-Cygnids and related showers. For a single station visual observer each of these meteors, regardless where these would be spotted at the sky, would fulfil the criteria available for visual observers to identify a meteor as a κ-Cygnid.

In 2014 as many as 250 possible Kappa Cygnids were listed, while 2015 produced only 149 such meteors. We applied the same method as for the 2014 Kappa Cygnid analyses. Each orbit was compared to the reference orbits of the Kappa Cygnids (12 KCG) and four meteor showers associated with the Kappa Cygnids: the γ–Draconids (184 GDR), the ι–Draconids (703 IOD), the August Draconids (197 AUD) and the August μ–Draconids (470 AMD) (*Table 1*). The shower association was done using the D criterion according to Drummond (1981), indicated as D'. Some of the orbits fulfil the criteria for more than one of the reference showers.

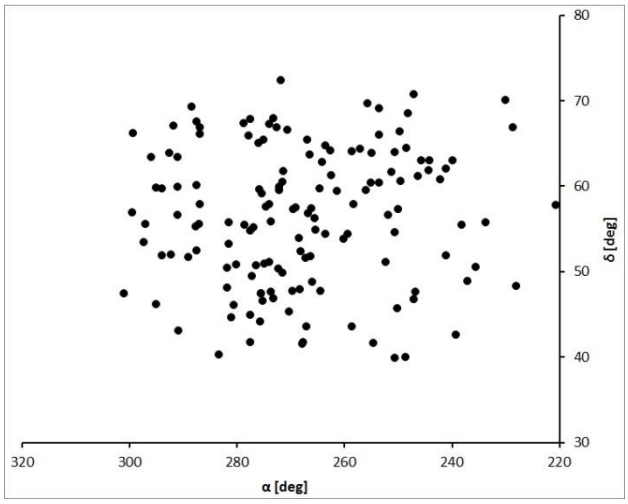

Figure 7 – Radiant plot of selected 'possible' κ-Cygnid orbits.

If the same orbit fulfilled the criteria for two or more of the reference orbits, the orbit was associated with the reference orbit which produced the best fit. The procedure was followed for both the results using the criterion according to Drummond and according to Southworth & Hawkins. As threshold we took as upper limit D' < 0.105 for Drummond and $D_{SH} < 0.25$ for Southworth and Hawkins. For most associations this results in the same association, but not for all. The orbits are all somehow related and question is how to determine the right association?

In *Figure 8a* we reproduce the plot of the 2014 radiants in ecliptic coordinates and in *Figure 8b* we do the same for the 2015 radiants. It is very obvious that the Kappa Cygnids which were very abundant in Figure 8a do not appear at all in *Figure 8b*. Only 69 out of the 149 possible Kappa Cygnid meteors qualify for shower association according to the D-criterion of Drummond and only 53 according to Southworth and Hawkins. In 2014, 189 orbits out of the 250 candidates fulfilled the D' criterion, among as many as 131 orbits confirmed as Kappa Cygnids. In 2015 only 6 orbits were identified as Kappa Cygnids based on D' (also 6 if we use D_{SH} as criterion).

For the 2014 analyses we had removed all the radiants that did not associate with any of the reference orbits, for 2015 we included these as orange dots in *Figure 8b*. Only 2 associate with the γ–Draconids (10 in 2014), 20 with the ι–Draconids (6 in 2014), 28 with the August Draconids (22 in 2014) and 7 with the August μ–Draconids (20 in 2014).

The distinguishing between associations of a single orbit with multiple candidate reference orbits is rather confusing and not at all well determined. Either another methodology is required to distinguish between different related sources, or the relevance of the existence of the various related showers should be questioned. Does it make sense to consider closely related concentrations within a rather dispersed complex? The Kappa Cygnids and its associated showers are probably comparable with the Taurid complex.

Table 1 – Reference orbits obtained by CAMS (Jenniskens et al., 2016a, 2016b, 2016c and 2016d) used to identify the possible Kappa Cygnids with the D criterion of Drummond and the D-criterion according to Southworth and Hawkins.

Shower	N Orbits	RA_{geo} (°)	DEC_{geo} (°)	V_{geo} km/sec	q AU	a AU	e	i (°)	ω (°)	Ω (°)
184 GDR	40	280.1	50.3	27.5	0.977	16.42	0.967	40.3	202.5	124.7
703 IOD	12	232.3	53.3	17.8	0.990	2.93	0.664	26.1	161.5	157.2
12 KCG	25	277.5	52.8	20.9	0.995	2.95	0.662	32.5	196.9	140.0
197 AUD	17	271.7	58.9	21.1	1.008	2.82	0.644	33.8	188.7	142.6
470 AMD	53	256.4	62.5	21.3	1.009	2.87	0.648	33.8	175.5	149.5

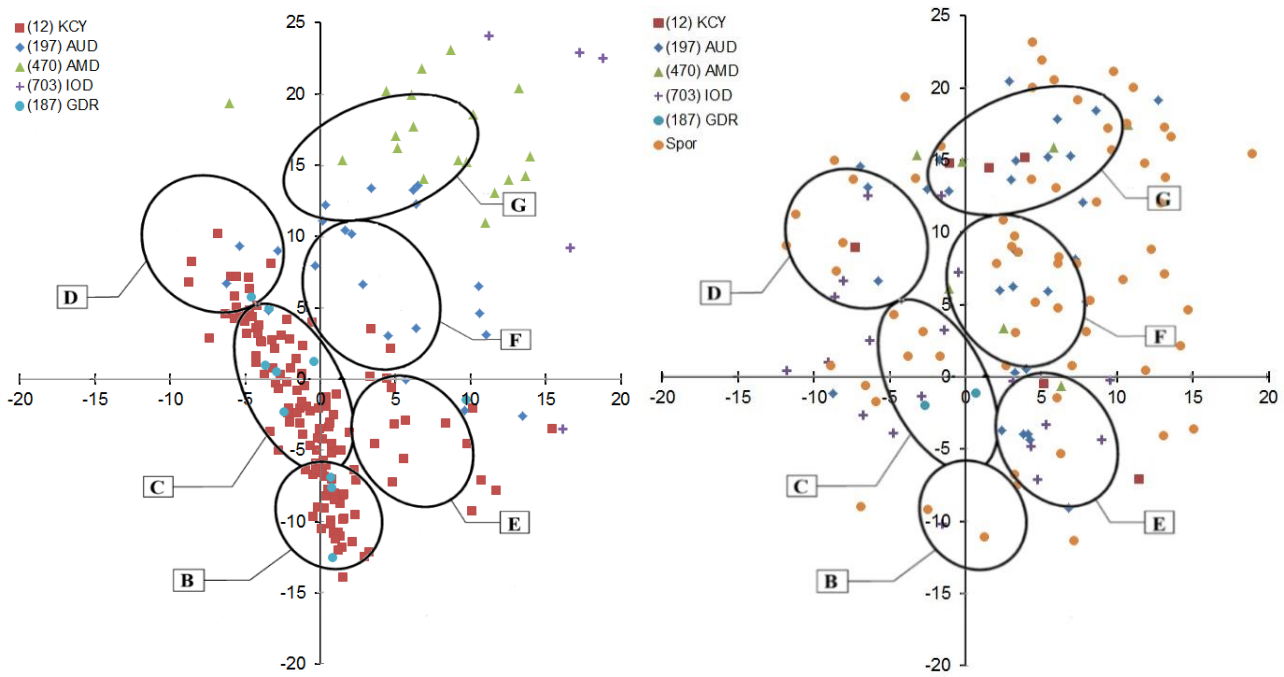

Figure 8a – The radiant plot in ecliptic coordinates according to the D criterion of Drummond (D' < 0.105) in 2014. *Figure 8b* – The radiant plot in ecliptic coordinates according to the D criterion of Drummond (D' < 0.105) in 2015. The shapes in both figures refer to the radiant associations as described in a previous paper (Roggemans et al., 2015) in order to compare with an analyses of Masahiro Koseki (2014).

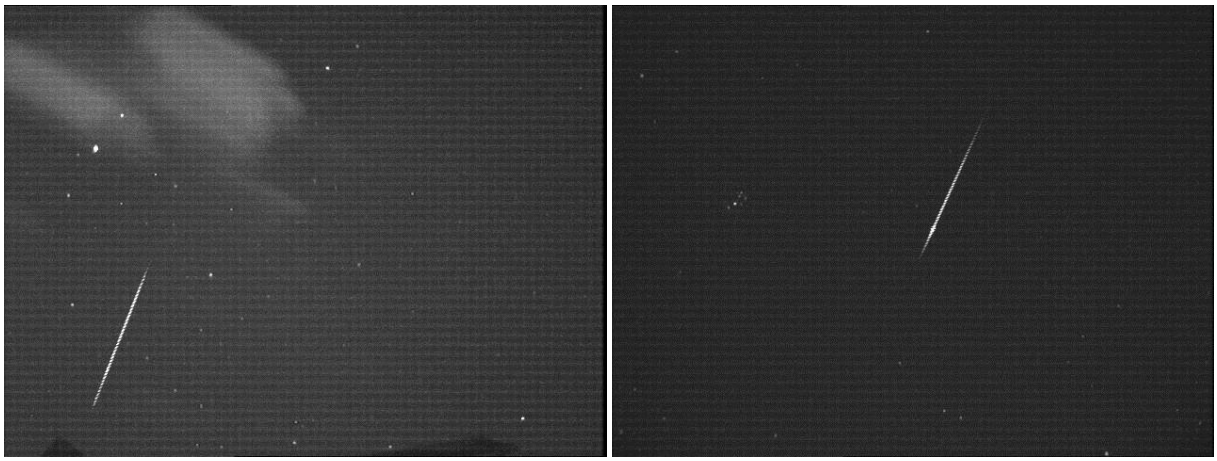

Figure 9a – (left) Chi-Cygnid recorded by Martin Breukers (CAMS 321) at 14 Sep. 2015, $19^h50^m08.51^s$ UT.

Figure 9b – (left) Chi-Cygnid recorded by Hans Betlem (CAMS 372) at 15 Sep. 2015, $00^h05^m31.76^s$ UT.

5 Discovery of the χ–Cygnids (757 CCY)

During the night of 14–15 September 2015, visual observers Koen Miskotte and Michel Vandeputte suspected some activity from a radiant region in Cygnus. Martin Breukers could confirm this very quickly from the CAMS-data of this night and also Peter Jenniskens could add a few more orbits obtained by CAMS California. On September 17 Daniel Green issued CBAT 4144 (2015) to announce the 'new' meteor shower.

Yasuo Shiba verified the records of the SonotaCo network and found 5 similar orbits recorded between 13 and 21 September 2015. Four more orbits were found in the 2010 dataset of SonotaCo (Shiba, 2015). Jakub Koukal checked the EDMOND database and selected 16 orbits for the period 8–17 September (Koukal et al., 2016). He also could select 49 orbits from the entire EDMOND database with the earliest orbits for the Chi Cygnids found in 2007.

After the initial discovery of the shower, Martin Breukers and Carl Johannink selected 450 orbits from the 2763 orbits collected in September 2015 for further investigation. The D criterion according to Drummond (Drummond, 1981) was applied and 71 orbits collected between 1 and 29 September fulfilled the criterion D' < 0.1. The nature of this shower with its very low velocity produces a very large scattered radiant. To eliminate suspected outliers an additional filter was applied with α ≈ [296° to 306°], δ ≈ [+27.6° to +37.6°] and the geocentric velocity Vg ≈ [12.5 to 17.5 km/s]. This selection left 21 orbits to fit all the selection criteria during a period from 10 to 28 September. Considering the radiant plot, there is no trace of any radiant drift (*Figure 10*).

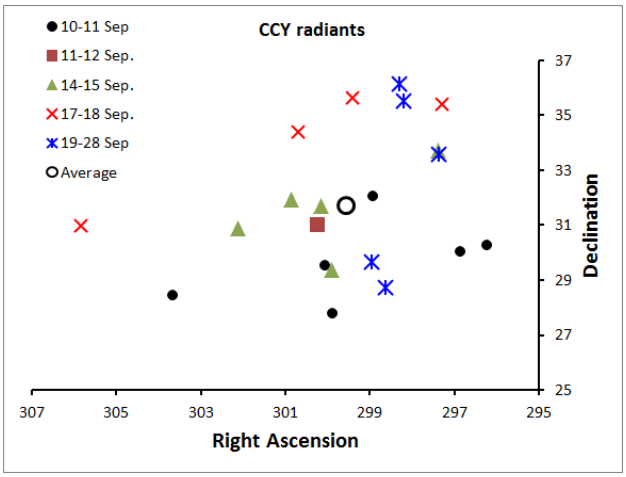

Figure 10 – Radiant plot of the orbits associated with the Chi Cygnids (757 CCY), for different dates: no trace of a radiant drift can be seen in this plot.

Table 2 – The final 21 orbits which fulfil the D criterion of Drummond (D'_{EDM}) using the orbit obtained from EDMOND data as reference and the D criterion of Drummond (D'_{CAMS}) using the initial orbit obtained by CAMS as reference.

Observed	Beg Time	α_{geo}	δ_{geo}	V_{geo}	q	a	e	i	ω	Ω	D'_{EDM}	D'_{CAMS}
10/09/2015	19:11:36.67	303.7	+28.4	14.2	0.9347	2.39	0.609	16.5	215.87	167.56	**0.05**	**0.06**
10/09/2015	19:31:04.40	296.8	+30.0	14.6	0.95651	2.85	0.664	17.4	209.01	167.57	**0.04**	**0.03**
10/09/2015	20:27:53.48	296.2	+30.3	13.8	0.95989	2.53	0.621	16.7	208.59	167.61	**0.04**	**0.05**
10/09/2015	20:50:57.82	300.1	+29.5	14.4	0.94697	2.61	0.637	17.1	212.12	167.62	**0.01**	**0.02**
10/09/2015	20:55:49.90	298.9	+32.0	14.6	0.95124	2.56	0.628	18.0	211.07	167.62	**0.02**	**0.03**
10/09/2015	23:47:35.13	299.9	+27.8	13.8	0.94848	2.52	0.624	16.0	211.90	167.74	**0.03**	**0.04**
11/09/2015	22:02:34.86	300.2	+31.0	14.9	0.94781	2.77	0.658	18.0	211.49	168.64	**0.03**	**0.02**
14/09/2015	21:18:22.83	302.1	+30.9	14.2	0.94883	2.55	0.627	17.1	211.48	171.53	**0.02**	**0.03**
14/09/2015	21:21:19.62	300.9	+31.9	14.7	0.95192	2.74	0.653	17.9	210.22	171.53	**0.02**	**0.01**
14/09/2015	21:21:59.04	297.4	+33.7	14.9	0.96206	2.88	0.666	18.6	207.01	171.53	**0.04**	**0.03**
14/09/2015	22:23:21.14	299.9	+29.4	13.4	0.95672	2.47	0.612	15.9	209.39	171.58	**0.05**	**0.06**
15/09/2015	00:05:31.76	300.2	+31.7	13.9	0.95573	2.48	0.614	17.0	209.66	171.65	**0.04**	**0.05**
17/09/2015	19:27:51.74	297.3	+35.4	14.6	0.96705	2.72	0.644	18.6	205.39	174.38	**0.02**	**0.01**
18/09/2015	00:30:10.44	299.4	+35.6	15.6	0.96064	3.11	0.692	19.7	206.88	174.59	**0.08**	**0.07**
18/09/2015	00:43:21.81	300.7	+34.4	14.8	0.95807	2.74	0.650	18.5	208.20	174.60	**0.02**	**0.01**
18/09/2015	01:35:19.02	305.8	+31.0	15.4	0.94028	3.07	0.694	18.0	212.57	174.63	**0.08**	**0.07**
19/09/2015	23:30:26.49	298.3	+36.1	14.6	0.96746	2.71	0.643	18.7	205.07	176.50	**0.02**	**0.02**
20/09/2015	22:38:34.19	298.6	+28.7	13.2	0.96896	2.77	0.651	15.2	204.37	177.44	**0.03**	**0.02**
24/09/2015	21:06:26.01	298.9	+29.6	13.9	0.97225	3.29	0.704	15.9	202.24	181.29	**0.10**	**0.09**
27/09/2015	20:27:52.87	297.4	+33.6	14.2	0.97819	3.29	0.703	17.3	199.64	184.20	**0.09**	**0.09**
28/09/2015	02:15:15.57	298.2	+35.5	13.5	0.97753	2.63	0.628	17.1	200.57	184.44	**0.04**	**0.04**

Table 3 – Comparing the first released orbit (CAMS) with EDMOND 2015, EDMOND 2007–2015 and this analysis.

	α_{geo}	δ_{geo}	V_{geo}	q	a	e	i	ω	Ω
CBET	301.0±2.2	32.6±1.6	15.1±0.9	0.949±0.003	2.75±0.40	0.655±0.041	18.6±1.6	209.9±1.9	171.64±0.23
E-2015	300.5±2.1	31.7±2.3	14.2±0.6	0.953±0.009	2.56±0.25	0.627±0.036	17.4±1.0	210.1±2.9	171.43±2.11
EDMOND	300.6±2.9	31.5±3.1	14.5±0.8	0.951±0.011	2.64±0.24	0.640±0.032	17.6±1.4	210.6±3.2	170.71±2.44
This (18)	299.8±2.3	31.5±2.5	14.4±0.6	0.955±0.009	2.69±0.20	0.644±0.024	17.5±1.1	209.5±2.9	171.35±3.30

Table 2 Lists all 21 orbits that fulfilled all criteria. Note that most of the 50 eliminated orbits are very likely related to this shower but the current methodology does not allow an unambiguous identification.

In *Table 3* the initial orbit obtained from the first CAMS data is compared to the data obtained from the EDMOND database, the 2015 EDMOND data and the long term EDMOND data. The average orbit for CAMS@BeNeLux has been considered for the 18 orbits in the range of 10 to 20 September. The χ-Cygnids (757 CCY) displayed enhanced activity in 2015 but the display wasn't short lived but covering at least a couple of weeks. Orbits from this meteor shower can be detected at least during two weeks. It may be too early to draw any conclusions about any periodicity in the occurrence of enhanced activity, but the shower probably displayed enhanced activity in 2010 too, which was not detected by any network as far as we know. The very slow velocity and large scatter on the radiant area may explain why the shower escaped from the attention of meteor surveys before.

6 Meteorite hunt for fireball 2015 March 25, $23^h00^m45^s$ UT

In May 2016 several CAMS operators participated in field searches for meteorites dropped by the fireball of 25 March 2015. This fireball passed close to the fields of view of several cameras of our network but managed to slip in between the camera fields, illustrating the need for an even more dense coverage by cameras.

Figure 11 – The ongoing field searches in May 2016 here with Adriana Roggemans, Paul Roggemans and Tim Polfliet.

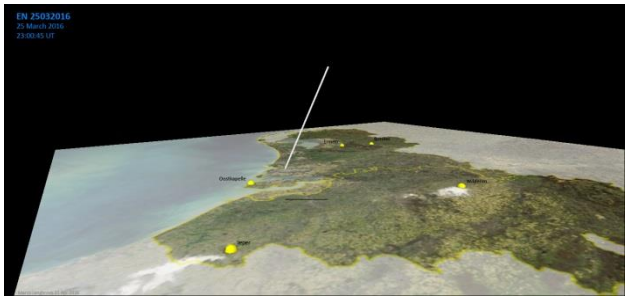

Figure 12 – The 2015 March 25, $23^h00^m45^s$ UT fireball that managed to slip in between the coverage of our CAMS network without being captured (Credit Marco Langbroek).

7 Conclusions

The CAMS@BeNeLux network expanded further since the last IMC, with extra cameras, extra stations and more volume in the atmosphere being covered. Since the last IMC more than 17000 orbits were collected and the total number of orbits obtained by the network reached over 40000 orbits since 25–26 May 2016. The weather in general was less favorable during the considered period than the year before.

The Kappa Cygnids were remarkable absent in 2015 after their abundant display in 2014. CAMS@BeNeLux was the first to draw attention to the enhanced activity of the Chi Cygnids with a sample of 5 accurate orbits obtained in the night of 14–15 September 2016, after a hint from visual observers Koen Miskotte and Michel Vandeputte. In this paper we could list 21 orbits associated with the new shower 757 CCY.

Acknowledgment

The authors wish to thank all participants for their efforts and discipline to submit the CAMS data shortly after each observing night. We also emphasize that all the efforts of the CAMS@BeNeLux team are done as volunteers and that all equipment is being financed privately by each participant without any kind of subsides. The current (May 2016) CAMS@BeNeLux team:

Hans Betlem (Leiden, operating CAMS 371, 372 and 373), *Felix Bettonvil* (Utrecht, operating CAMS 376 and 377), *Jean-Marie Biets* (Wilderen, operating CAMS 381 and 382), *BISA – Hervé Lamy* (Dourbes, operating CAMS 394 and 395, Uccle, operating CAMS 393), *Martin Breukers* (Hengelo, assistant coordinator and

operating CAMS 320, 321, 322, 323, 324, 325, 326 and 327), *Franky Dubois* (Langemark, operating CAMS 386), *Luc Gobin* (Mechelen, operating CAMS 390 and 391), *Robert Haas* (Alphen aan de Rijn, operating CAMS 360, 361, 362, 363, 364 and 365), *Klaas Jobse* (Oostkapelle, operating CAMS 331, 332, 337, 338 and 339), *Carl Johannink* (Gronau, coordinator and operating CAMS 311, 312, 313, 314, 315 and 316), *Paul Lindsay* (Lieshout, operating CAMS 356 and 357), *Koen Miskotte* (Ermelo, operating CAMS 351 and 352), *Piet Neels* (Ooltgenplaat, operating CAMS 341, 342, 343 and 344), *Tim Polfliet* (Gent, operating CAMS 396), *Steve Rau* (Zillebeke, operating CAMS 385 and 387), *Paul Roggemans* (Mechelen, operating CAMS 383, 384, 388 and 389) and *Erwin Van Ballegoij* (Heesch, operating CAMS 347 and 348).

The authors also wish to thank *Pete Gural*, *Peter Jenniskens* and *Denis Vida* for their continuous support with CAMS related questions, software solutions and updates.

References

Bettonvil F., Johannink C. and Breukers M. (2014). “CAMS BeNeLux”. In Rault J.-L., and Roggemans P., editors, *Proceedings of the International Meteor Conference*, Giron, France, 18–21 September 2014. IMO, pages 55–58.

Drummond J. D. (1981). “A test of comet and meteor shower associations”. *Icarus*, **45**, 545–553.

Green D. W. E. (2015). “New chi Cygnids meteor shower”. Central Bureau Electronic Telegram No. 4144.

Gural P. S. (2011). “The California All-sky Meteor Surveillance (CAMS) System”. In Asher D. J., Christou A. A., Atreya P. and Barentsen G., editors, *Proceedings of the International Meteor Conference*, Armagh, Northern Ireland, 16–19 September 2010. IMO, pages 28–31.

Jenniskens P., Gural P. S., Dynneson L., Grigsby B. J., Newman K. E., Borden M., Koop M. and Holman D. (2011). “CAMS: Cameras for Allsky Meteor Surveillance to establish minor meteor showers”. *Icarus*, **216**, 40–61.

Jenniskens P., Nénon Q., Albers J., Gural P. S., Haberman B., Holman D., Morales R., Grigsby B. J., Samuels D. and Johannink C. (2016a). “The established meteor showers as observed by CAMS”. *Icarus*, **266**, 331–354.

Jenniskens P., Nénon Q., Gural P. S., Albers J., Haberman B., Johnson B., Holman D., Morales R., Grigsby B. J., Samuels D. and Johannink C. (2016b). “CAMS confirmation of previously reported meteor showers”. *Icarus*, **266**, 355–370.

Jenniskens P. and Nénon Q. (2016c). “CAMS verification of single-linked high-threshold D-criterion detected meteor showers”. *Icarus*, **266**, 371–383.

Jenniskens P., Nénon Q., Gural P. S., Albers J., Haberman B., Johnson B., Holman D., Morales R., Grigsby B. J., Samuels D. and Johannink C. (2016d). “CAMS newly detected meteor showers and the sporadic background”. *Icarus*, **266**, 384–409.

Koseki M. (2014). “Various meteor scenes II: Cygnid-Draconid Complex (κ-Cygnids)”. *WGN, Journal of the IMO*, **42**, 181–197.

Koukal J., Srba J. and Toth J. (2016). “Confirmation of the χ Cygnids (CCY, IAU#757)”. *WGN, Journal of the IMO*, **44**, 5–9.

Roggemans P., Betlem H., Bettonvil F., Biets J. M., Breukers M., Haas R., Jobse K., Johannink C., Langbroek M., Miskotte K., Neels P., Nijland J. and ter Kuile C. (2014). “The Benelux CAMS Network – status July 2013”. In Gyssens M., Roggemans P. and Zoladek P., editors, *Proceedings of the International Meteor Conference*, Poznan, Poland, 22-25 August 2013. IMO, pages 173–175.

Roggemans P., Breukers M. and Johannink C. (2015). “Status of the CAMS-BeNeLux network”. In Rault J.-L. and Roggemans P., editors, *Proceedings of the International Meteor Conference*, Mistelbach, Austria, 27-30 August 2015. IMO, pages 41–50.

Shiba Y. (2015). “χ Cygnids observation in Japan”. *WGN, Journal of the IMO*, **43**, 179–180.

Southworth R. R. and Hawkins G. S. (1963). “Statistics of meteor streams”. *Smithsonian Contributions to Astrophysics*, **7**, 261–286.

eMeteorNews: website and PDF journal

Paul Roggemans[1], Richard Kacerek[2], Jakub Koukal[3], Koen Miskotte[4] and Roman Piffl[5]

[1] **Pijnboomstraat 25, 2800 Mechelen, Belgium**
paul.roggemans@gmail.com

[2] **19 Comet Close, Ash Vale, Surrey, GU125SG, United Kingdom**
rickzkm@gmail.com

[3] **Valašské Meziříčí Observatory, Vsetínská 78, 75701 Valašské Meziříčí, Czech Republic**
j.koukal@post.cz

[4] **De la Reystraat 92, 3851 BK Ermelo, the Netherlands**
k.miskotte@upcmail.nl

[5] **astrofoto.sk, Azalková 28, 90042 Dunajska Luzna, Slovakia**
ceres@global.sk

Amateur meteor workers have always been interested to exchange information and experience. In the past this was only possible via personal contacts by letter or by specialized journals. With internet a much faster medium became available and plenty of websites, mailing lists, Facebook groups, etc., have been created in order to communicate about meteors. Today there is a wealth of meteor data circulating on internet, but the information is very scattered and not directly available to everyone. The authors have been considering how to organize an easy access to the many different meteor related publications. The best solution for the current needs of amateur meteor observers proved to be a dedicated website combined with a PDF journal, both being free available without any subscription fee or registration requirement. The authors decided to start with this project and in March 2016 the website meteornews.org has been created. A first issue of eMeteorNews was prepared in April 2016. The year 2016 will be a test period for this project. The mission statement of this project is: "Minimizing overhead and editorial constraints to assure a swift exchange of information dedicated to all fields of active amateur meteor work."

1 Introduction

Amateur meteor work is booming since video meteor observing became easily accessible for a large number of amateurs. However it is very difficult to follow all the developments as there are too many different sources to check. Some journals impose time-consuming editing procedures and require a semiprofessional level. Most amateurs don't have the time for that and therefore seek alternatives in social media such as Facebook and Twitter, various online Newsgroups and blogs. So far internet and social media in particular prove to be a jungle of information and it became impossible to keep track of all interesting news. The traditional media like specialized journals serve mainly as reference source for ongoing research. These journals are not suitable for amateurs who just wish some 'easy reading' information about the meteor community. Something is missing and the question is if and how amateurs can improve the situation.

2 Meteor publication history

Amateur meteor astronomy has been for a long time a marginal domain within astronomy compared to planetary, variable or double star observing. The first attempts for a methodologic approach of meteor observations were made by professional astronomers and explorers as a kind of hobby in the first part of the 19th century. Systematic meteor observing by amateur astronomers started around mid-19th century and has been marked by ups and downs. Meteor astronomy has been sadly neglected by professional astronomers for a long time as astrophysics offered better career options. Who could be interested to spend a professional career to deal with no more than just the dust in our solar system? In the first half of the 20th century, the domain has been left over to a large extend to amateur astronomers with only a few exceptions of professional astronomers dealing with meteor work. The options to publish about meteor observations were limited to a few popular astronomy journals. A few amateur meteor observers centralized observing reports and published these. Thanks to their efforts we have some information about meteor stream activity in the late 19th and early 20th century. People like F. Denning in the UK, C.P. Olivier in the USA and C. Hoffmeister in Germany left a treasure of observational data with their regular meteor reports.

Things improved around mid-20th century with a new generation of astronomy students and future professional astronomers who caught interest in meteor observing. The development of radio and radar observations offered a complete new tool while the upcoming research for aerospace triggered important investments in risk assessment for spaceflights in the 1950s. Publications about meteor research boomed and amateur meteor work flourished. Unfortunately, once the risk assessments proved save for spaceflights, major meteor research programs were shut down. The popularity of amateur meteor observers got a nasty blow begin 1960's and

professional meteor research remained limited to a few specialized institutes across the globe.

Figure 1 – Frederick William Denning, one of the most productive authors of meteor reports and news ever.

End 60ies, early 70ies the moon landings and space exploration inspired many young amateur astronomers. Meteor observing didn't require any expensive equipment and proved an ideal activity for clubs to explore the constellations and to enjoy the ever surprising meteor phenomena. Some young amateurs got fascinated by the poorly known nature of the major meteor showers and specialized into meteor observing. This new generation of meteor observers was confronted with one major drawback: lack of information. The books "*Meteor astronomy*" (Lovell, 1954) and "*Meteor Science and engineering*" (McKinley, 1961) were sold out and only available at some libraries. Research papers published in professional journals remained inaccessible for most young amateurs. The gap in the market was solved with a number of amateur meteor journals and newsletters: "Meteor News" (quarterly, USA), "Meteoros" (quarterly, UK), "NVWS Bulletin" (bi-monthly, Netherlands), "Meteor" (monthly, Hungary), "Radiant" (bi-monthly, Netherlands), "Werkgroepnieuws" (monthly, Belgium), etc. These homemade journals helped amateurs to read about each other's results and experiences and inspired for more international cooperation. The content covered easy reading reports about visual observing campaigns, basic analyses of data, fireball descriptions, some peculiar meteor phenomena, etc. Although these journals were very basic in lay out and quality, active observers looked forward to read about each other's work.

Typically amateur achievements often depend on the work and commitment of one or few volunteers. Most of the popular journals of the 70ies and 80ies disappeared. To save printing and mailing costs the journal Radiant of the Dutch Meteor Society became "eRadiant" and still continues as popular reading in PDF format among Dutch speaking amateurs. WGN published meteor work from amateurs worldwide and became the Journal of the IMO in 1988. WGN evolved into a semiprofessional journal which is very valuable as source for references for future research. Originally WGN was distributed as a newsletter free of charge. When printing and mailing costs increased a modest subscription fee was charged, for instance in 1981 the annual subscription fee to WGN was 2 Euro. The cheap price was possible thanks to the efforts of volunteers to avoid all sources of costs. Also in that time any content was edited and published within two months after receipt of a contribution. The subscription fee increased when the printing wasn't done any longer by volunteers, but by a commercial service and also other overhead costs had to be covered by the subscription fee.

3 Back to the roots?

The success of most amateur meteor newsletters was due to the rapid publication of observing reports at a very low fee if it was not just for free. Too complicated editing procedures and or too high subscription fees may explain why active meteor observers decide not to subscribe or to quit their subscription. Amateurs got plenty of alternatives to exchange their observing experiences via internet, such as on Facebook, Twitter, News Groups, blogs, etc. Internet offers the possibility to share meteor news without any costs, which was the purpose in the 1970's and 1980's.

It is obvious that there is a gap between the swift publication on line and the advanced paper publications. Could a new meteor platform fill the gap in the market? eRadiant as online journal in PDF is still very popular among Dutch speaking amateurs. Would it be useful to set up something similar for the international community of amateur meteor observers? Discussions with several leading amateur meteor workers in recent months proved very positive. The idea was suggested to consider a new online publication with as name eMeteorNews which is straightforward for what it stands for. The first idea was to produce an online journal as PDF, inspired by eRadiant. But another brilliant idea was to set up a dedicated website to publish meteor news as soon as possible when it becomes available. The main purpose is to share meteor news, quickly and easy, with a minimum of editing constraints. Thanks to the new technology we can get rid of overhead costs and get back at the working conditions of over 30 years ago: rapid sharing of information free of charge. The authors very quickly reached a consensus to set up the MeteorNews project.

4 A new project: MeteorNews

Combining the advantages of a Meteor News website with these of a PDF journal, we can 'eat from two bags of food' and have something as fast as social media, combined with a PDF journal for archiving and reference purposes. Some of the advantages would be:

- Free of charge as the production would require zero costs;
- No membership and no registration required being independent from any society;
- Fast publication on the website;
- Flexibility in volume and periodicity for the PDF journal;
- Archiving as PDF for storage with the ADS Abstract service;
- Ease of use with no editing constraints to submit content;
- Printable as PDF format ready for local printing;
- Searchable content on both the website and in the PDF archive;
- Full color publication on the website and in the PDF;
- Boost outreach in this field being unlimited free available to anyone interested.

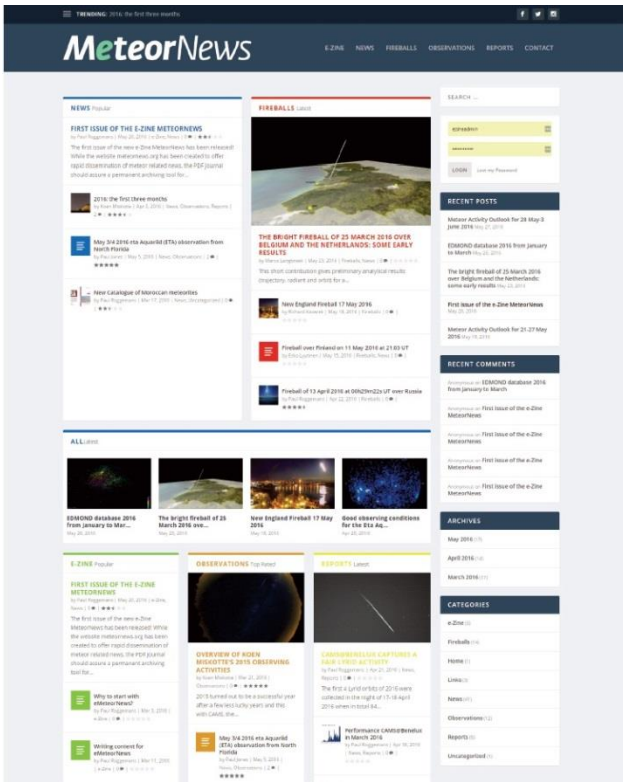

Figure 2 – The MeteorNews.org website with the layout designed by the website administrator, Roman Piffl, has been created and put online in just a few days.

With eMeteorNews we hope to bring the essential information together accessible from a single source. The new eMeteorNews should be complementary and not compete with any existing publications. There is no restriction to the type of content but it should remain dedicated to the active amateur meteor workers for quick and efficient dissemination of meteor news without any bureaucratic overhead.

The mission statement of this project is: "*Minimizing overhead and editorial constraints to assure a swift exchange of information dedicated to all fields of active amateur meteor work*."

5 Practical aspects

Who will take care of this? Beyond the authors of this paper some more people volunteered to become MN-editor. Meteor workers interested to join the editorial board are welcome to join the current editorial board:

- Salvador Aguirre (*Mexico*)
- Karl Antier (*France*)
- François Colas (*France*)
- Antal Igaz (*Hungary*)
- Paul Jones (*USA*)
- Richard Kacerek (*U.K.*)
- Jakub Koukal (*Czech Republic*)
- Marco Langbroek (*Netherlands*)
- Bob Lunsford (*USA*)
- Jose Maria Madiedo (*Spain*)
- Koen Miskotte (*Netherlands*)
- Roman Piffl (*Slovakia*)
- Paul Roggemans (*Belgium*)
- Your name here?

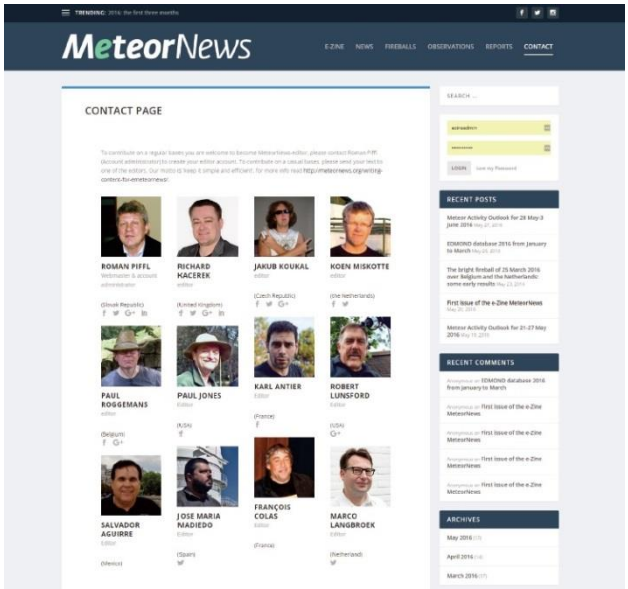

Figure 3 – The MeteorNews editorial board.

When? Discussions about this project started begin of 2016. The response to the idea was very positive. Several people offered to help and are interested to participate. Since we start from scratch, we'll work out a prototype as experiment and use the rest of 2016 as a test period. We hope to collect news on the website meteornews.org and to compile a few online issues in PDF format. If the test period proves successful we'll register an ISSN number and start archiving with ADS abstract service in 2017.

What to publish? We welcome input from all meteor workers: reports on visual observations, reports from camera networks, reports on radio observations, fireball and particular meteor sightings, anything related to meteor work. The content should focus on practical aspects, the style should be informal easy reading text.

Figure 4 – The first issue of the eZine appeared in May 2016.

How to submit content? Send your text and pictures by mail to one of the MeteorNews.org editors. Short announcements can be published easily in WordPress without any layout requirements. To keep MeteorNews.org easy reading, submit the following as text without bothering about editing aspects:

- A short title (mandatory);
- Name(s) of author(s) (mandatory);
- Contact address(es) of the author(s) (optional);
- Abstract (optional for news but recommended for articles);
- Body text (mandatory);
- Pictures (optional, but if pictures are submitted a caption is mandatory);
- References (optional).

If you have a relative long and elaborated contribution it may be worth the effort to prepare this as a Word document. In such case we recommend to use the Word template which can be downloaded from MeteorNews.org. Save this dotx file on your computer. In Word you find under 'File' – 'Options' – 'Add ins', here at the bottom you see 'Manage' select 'Templates' and click 'Go' in the tab 'Templates browse to select the eMeteorNews dotx file. Make sure to mark 'Automatically update document styles'.

6 Publication policy

As soon as some content is received by an editor, it will be published as soon as possible on the MeteorNews.org website.

Every now and then a selection of articles collected on the website will be assembled as a journal in PDF which will be reported and archived with the ADS abstract service (from 2017 onwards). All papers published in MeteorNews.org and its PDF journal eMeteorNews will be archived for consultation and reference purposes.

The website will include short news flashes which refer to other publications and these items will not be included in the PDF Journal for the simple reason that these are being published elsewhere. The PDF version of eMeteorNews will certainly cover all orginal and elaborated submissions from the MeteorNews website. In particular observing reports from visual observers and activity reports from camera networks will be included in the PDF Journal.

An overview of the CILBO spectral observation program

Regina Rudawska, Joe Zender and Detlef Koschny

European Space Agency, Noordwijk, the Netherlands
rrudawska@cosmos.esa.int

The video equipment can be easily adopted with a spectral grating to obtain spectral information from meteors. Therefore, in recent years spectroscopic observations of meteors have become quite popular. The Meteor Research Group (MRG) of the European Space Agency has been working on upgrating the analysis of meteor spectra as well, operating image-intensified camera with objective grating (ICC8). ICC8 is located on Tenerife station of the double-station camera setup CILBO (Canary Island Long-Baseline Observatory). The pipeline software processes data with the standard calibration procedure (dark current, flat field, lens distortion corrections). While using the position of a meteor recorded by ICC7 camera (zero order), the position of the 1st order spectrum as a function of wavelength is computed Moreover, thanks to the double meteor observations carried by ICC7 (Tenerife) and ICC9 (La Palma), trajectory of a meteor and its orbit is determined. Which merged with simultaneously measurement of meteor spectrum from ICC8, allow us to identify the source of the meteoroid. Here, we report on preliminary results from a sample of meteor spectra collected by CILBO-ICC8 camera since 2012.

Jérémie Vaubaillon and Regina Rudawska.

ESA/ESTEC Meteor Research Group – behind the scenes

Regina Rudawska

European Space Agency, Noordwijk, The Netherlands
rrudawska@cosmos.esa.int

The ESA/ESTEC Meteor Research Group consists of a team people with one goal: understand the effects of meteoric phenomena on planetary atmospheres and surfaces, as well as on spacecraft. The team carries out observational and theoretical studies in order to increase our knowledge of the small particle complex in the solar system. This talk addresses a number of tasks within the group seen from a perspective of a research fellow.

Joost Hartman, spotted in the back office, early in the morning.

Meteor reporting made easy- The Fireballs in the Sky smartphone app

Eleanor Sansom[1], Jay Ridgewell[2], Phil Bland[1] and Jonathan Paxman[3]

[1] **Dept. Applied Geology, Curtin University, Perth, Australia**
eleanor.sansom@postgrad.curtin.edu.au

[2] **Science Outreach, School of Science, Curtin University, Perth, Australia**

[3] **Dept. Mechanical Engineering, Curtin University, Perth, Australia**

Using smartphone technology, the award-winning 'Fireballs in the Sky' app provides a new approach to public meteor reporting. Using the internal GPS and sensors of a smartphone, a user can record the start and end position of a meteor sighting with a background star field as reference. Animations are used to visualize the duration and characteristics of the meteor. The intuitive application can be used in situ, providing a more accurate eye witness account than after-the-fact reports (although reports may also be made through a website interface). Since its launch in 2013, the app has received over 2000 submissions, including 73 events which were reported by multiple users. The app database is linked to the Desert Fireball Network in Australia (DFN), meaning app reports can be confirmed by DFN observatories. Supporting features include an integrated meteor shower tool that provides updates on active showers, their visibility based on moon phase, as well as a tool to point the user toward the radiant. The locations of reports are also now shown on a live map on the Fireballs in the Sky webpage.

1 Introduction

The International Meteor Organization received 19082 reports of fireballs via their web-form between Jun 01, 2015 and May 31, 2016 (IMO, 2016). In order to use eyewitness reports to reconstruct meteor/fireball trajectories, the key elements required are the position of the observer and the start and end direction (both altitude and azimuth) of the event. The duration, brightness, color, fragmentation events and any associated sounds (sonic booms) are additional useful information. Accurately estimating start and end directions, in particular the altitude, can be difficult. The Fireballs in the Sky smartphone app, developed by *Thoughtworks Inc*., in collaboration with Curtin University, uses the technology of smartphones to allow users to report on the spot. Updated features include an integrated meteor shower tool that provides updates on active showers, their visibility based on moon phase, as well as a tool to point the user toward the radiant. This app is freely available through Google Play and the iTunes App stores.

2 Reporting made easy

To submit a report of either a meteor or a fireball, users will be guided through the following steps (illustrated in *Figure 1, 2, 3 and 4*):

1. Note whether any sonic booms were heard. This can be modified if a delayed boom was later heard.
2. Aim phone at location where fireball started, aided by a background star field to more accurately report orientation (*Figure 2*).
3. Aim phone at location where fireball ended, again using reference star background (*Figure 3*).
4. Describe additional details such as duration, brightness, color and any flare/fragmentations (as well as number of fragments seen). The responsive animation allows the user to adjust the simulation to accurately reflect their sighting (*Figure 4*).
5. Report summary is presented and additional notes, including contact details in case of further investigation, may be provided.

Figure 1 – Screenshots of the Fireballs in the sky reporting procedure. a) homepage- report a sighting, or checkout meteor shower tool.

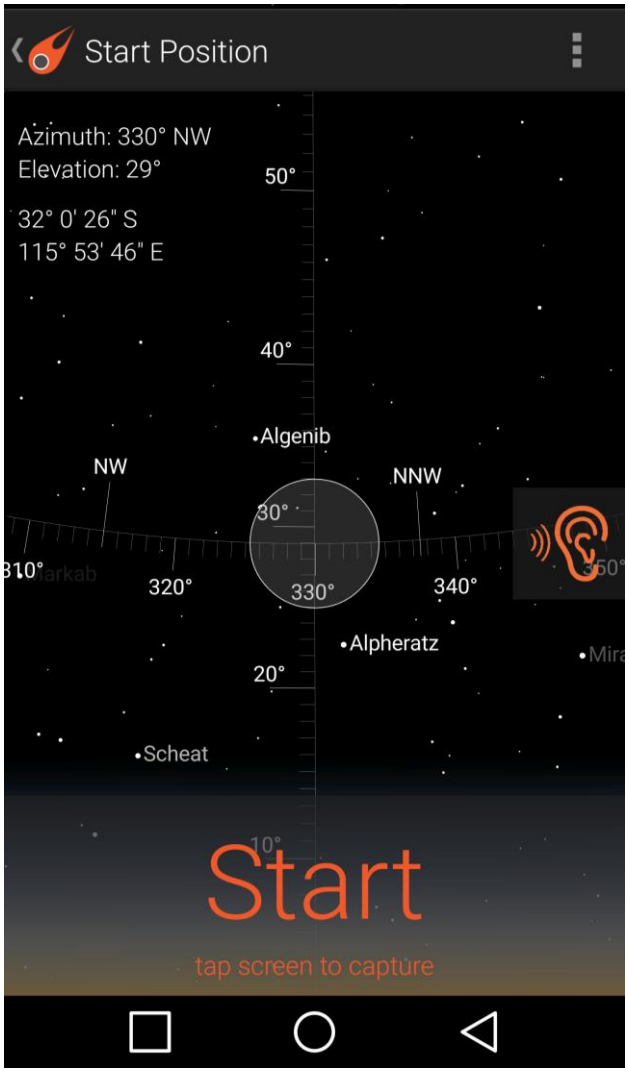

Figure 2 – Screenshots of the Fireballs in the sky reporting procedure. b) step 2- record where fireball started.

The app uses the internal GPS, accelerometers, magnetometers and gyroscopes to record the orientation of the phone when reporting a fireball. When a report is submitted, it will include the GPS location of the observer, the altitude and azimuth of both start and end points recorded by the internal phone sensors, as well as all the other fireball information. If phone signal is unavailable at the time of submission, as long as the phone GPS is still active, the report will be saved until the user returns to an area with network coverage. Users can also report a fireball at a later time on the webpage[1]. Report locations can be seen on the Fireballs in the Sky webpage[2]. Reports made within close proximity at similar times are automatically grouped and users will receive a message saying their sighting has been "corroborated". Reports that have been verified by photographic records are marked as "confirmed". Reporting via the app is simple and accessible to all members of the public to report an event, even children.

The app database is linked to the Desert Fireball Network in Australia (DFN), meaning app reports can be confirmed by DFN observatories. Corroborated reports are automatically triangulated, using a straight line trajectory assumption, in a similar workflow to that used by the DFN. When app users report an event that is observed by multiple DFN observatories, an assessment of app report reliability can be made. . Since its launch in 2013, the app has received over 2000 submissions, including 73 events which were reported by multiple users. Some reports are for daytime events which are unable to be captured by DFN observatories that run only during the night. App reports are therefore able to provide data on fireballs that may not otherwise be recorded.

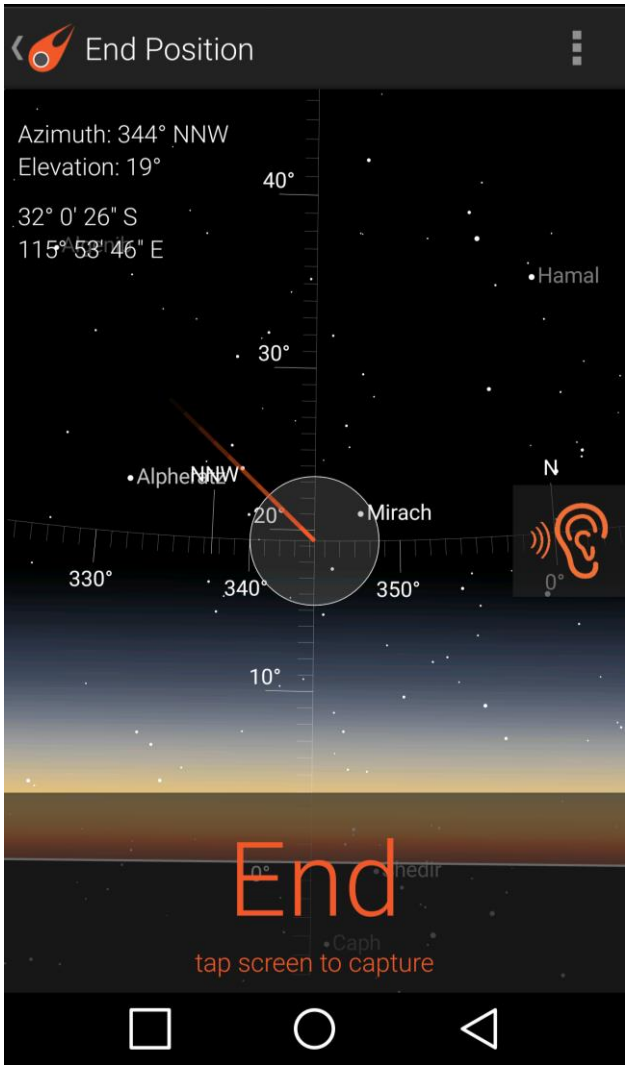

Figure 3 – Screenshots of the Fireballs in the sky reporting procedure. c) step 3- record where fireball ended.

Improved error estimation

Eyewitness reports can provide fireball trajectories, though errors in both altitude and azimuth can be greater than 30° (Tatum, 1998). The use of smartphone sensors can increase the accuracy of reported observations, aided by the star background and fireball animation for user reference. As the report is made on-the-spot this will help improve the quality of the report while it is fresh in the observer's mind.

3 Meteor shower tool

A recent addition to the app is a meteor shower information tool. The next shower peak will appear on the home screen. 69 showers are separated into major and

[1] http://fireballsinthesky.com
[2] http://fireballsinthesky.com.au/maps/app-sightings/

minor depending on zenithal hourly rate. Their peak day is given along with their expected viewing dates. After selecting a shower, an introduction is given, including the viewing conditions based on the phase of the moon during shower peak. The tool also points the user toward the radiant.

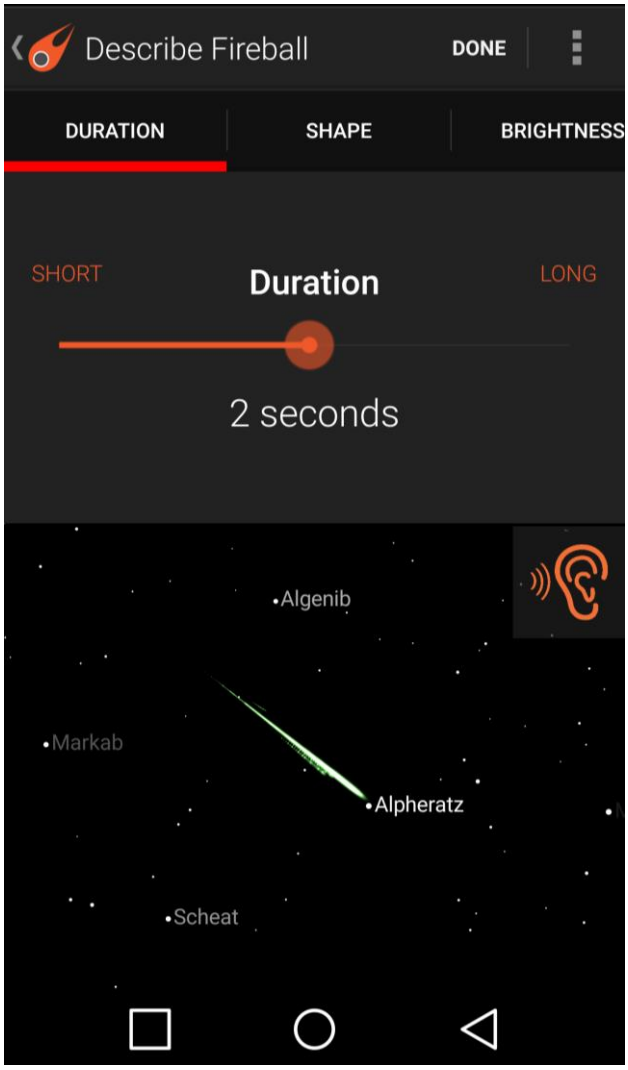

Figure 4 – Screenshots of the Fireballs in the sky reporting procedure. d) describe characteristics with help of fireball animation.

4 Conclusion

The easy-to-use Fireballs in the Sky smartphone app encourages and enables users around the world to report scientifically useful fireballs on the spot. The use of smartphone technology and animations aims to increase the accuracy of meteor and fireball reports. Through the app, users can also access an interactive meteor shower finder with an augmented reality radiant indicator, information on current and upcoming meteor showers and their estimated visibility.

Acknowledgments

The app was conceived as part of the Fireballs in the Sky outreach project, funded by *Inspiring Australia* and developed by *Thoughtworks Inc*.

References

IMO (2016). “Fireball Reports”. URL: fireballs.imo net accessed: 13 June 2016.

Tatum J. B. (1998). “Tracking a fireball from eyewitness accounts with reference to the west coast event of 1995 December 22”. *Journal of the Royal Astronomical Society of Canada*, **92**, 78–82.

Croatian Meteor Network: Ongoing work 2015 – 2016

Damir Šegon[1], Denis Vida[2], Korado Korlević[3] and Željko Andreić[4]

[1] **Astronomical Society Istra Pula, Park Monte Zaro 2, 52100 Pula, Croatia**
Višnjan Science and Education Center, Istarska 5, 51463 Višnjan, Croatia
damir.segon@pu.htnet.hr

[2] **Astronomical Society "Anonymus", B. Radića 34, 31550 Valpovo, Croatia**
Faculty of Electrical Engineering, University of Osijek, KnezaTrpimira 2B, 31000 Osijek, Croatia
denis.vida@gmail.com

[3] **Višnjan Science and Education Center, Istarska 5, 51463 Višnjan, Croatia**
korado@astro.hr

[4] **University of Zagreb, Faculty of Mining, Geology and Petroleum Engineering, Pierottijeva 6, 10000 Zagreb**
zeljko.andreic@oblak.rgn.hr

Ongoing work of the Croatian Meteor Network (CMN) between the 2015 and 2016 International Meteor Conferences is presented. The current sky coverage is considered, software updates and updates of orbit catalogues are described. Furthermore, the work done on meteor shower searches, international collaborations as well as new fields of research are discussed. Finally, the educational efforts made by the CMN are described.

1 Introduction

In this paper we present the ongoing work of the Croatian Meteor Network (CMN) between the 2015 and 2016 IMCs, as well as the results from previous years' analysis. Topics covered by this paper contain information on the current sky coverage of CMN cameras, improvements done on CMN software, status of the CMN orbit catalogues, results from international collaborations, a brief overview of new fields of research and efforts made on educating young people interested in meteor astronomy.

2 CMN sky coverage

During the period between the two IMCs, the number of active cameras has remained at 22. As pointed out in our 2015 IMC proceedings paper (Šegon et al., 2015), there is a significantly smaller coverage over the southern part of Croatia. However, we managed out to reinstall one camera (CMN Čiovo) and regain at least partial coverage over that part of Croatia. The sky coverage at 100 km height can be seen in *Figure 1*.

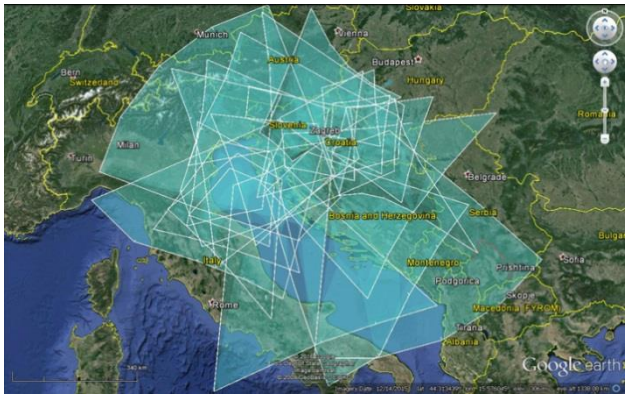

Figure 1 – CMN sky coverage at the height of 100 km.

As far as the coverage at 20 km height is concerned, a significant part of the sky in the mid-Adriatic coastal part of Croatia has been regained again thanks to the Čiovo camera. Our intention is to have a complete coverage over Croatia at 20 km height, by at least by one camera. This is of the highest importance for recording meteorite-dropping fireballs and estimating their terminal point dynamics, which combined with other trajectory dynamics and light curve data should provide information about a possible meteorite fall.

Figure 2 – CMN sky coverage at the height of 20 km.

3 CMN orbit catalogues and software updates

All data up to 2016 has been processed and it is ready for final review and orbit catalogue production. Only three stations remained in an unautomated processing mode, due to hardware limitations and unavailability of internet connection at those locations.

Since 2014, most of the CMN stations operate in an almost completely automatic mode (Vida et al., 2014), meaning almost no manual effort is needed to reduce the

data. As such, all incoming data are ready for orbit pairing. However, prior to the introduction of the automation procedures, up to the year 2014, there was still a considerable number of stations which required some degree of manual data reduction. That is the reason why only one catalogue, the one for 2013, has been published between the two IMCs. The catalogues for 2014 and 2015 should be completed and published during this year as their preparation is mostly complete.

Furthermore, significant improvements were done on the *CMN_BinViewer* software (Vida et al., 2014) which allowed many CMN and CAMS camera operators to recheck and visualize their observations in a more convenient way. As noted by the software's users, the Confirmation feature used by CAMS camera operators proved to be most useful and timesaving.

4 International collaboration and results

In the paper published in WGN43:5 we presented our last results from the 2013 CMN shower search which used the SonotaCo and CMN meteor orbit databases, presenting the last four candidate meteor showers possibly connected to four asteroidal parent bodies (Šegon et al., 2015). Jérémie Vaubaillon did the dynamical modeling for all potential meteor shower associations to parent bodies, results of which are being analyzed in a paper to be published soon.

At the last year's IMC at Mistelbach, we announced the possibility of an enhanced activity by Kappa Cepheids on September 21st. This activity had been only observed visually by Jürgen Rendtel (Rendtel, 2015) observing from the island of La Palma in Spain. However, there are no confirmations from video or radar observations up to this date about any enhanced activity of the shower. We do not have any announcements for 2016, according to the modeling done by Jérémie Vaubaillon there are no predicted direct intersections of meteoroid orbits with the Earth's orbit in 2016 for that shower.

A very strong Taurid activity has been observed during 2015 by the CMN as well as by other meteor observers (Molau, 2016). One very interesting event recorded by the CMN was a Taurid fireball which produced a long lasting meteor train (more than 45 minutes). The fireball itself has been observed by three CMN video cameras, as well as four Slovenian Meteor Network all-sky and DSLR cameras. Thanks to members of the Slovenian Meteor Network, the propagation of the train is currently being investigated from combined observations, and will be presented in a separate paper.

5 New technology and fields of research

Low-cost radiometer – an improved version

The low-cost radiometer project presented at the 2015 IMC (Vida et al., 2015) has been continued and an improved version has been developed. While the first version used a single operational amplifier and only one *BPW34* photodiode, the new version uses a quad operational amplifier and a total of 9 photodiodes. Groups of 3 *BPW34* photodiodes have their signal summed and fed into one of the channels of the amplifier. The amplified signal of all 3 groups is summed. There is an option to feed the resulting signal into the fourth channel of the amplifier for additional amplification. This approach resulted in a larger signal to noise ratio. The encountered issue was a ~50 Hz noise caused by the light pollution in urban areas, thus it was decided to develop a standalone system powered by the *Raspberry Pi* single-board computer which can run on batteries charged by a solar panel and be installed in a remote location.

The system has been tested from several urban locations. The recordings were found to be very noisy because of the present light pollution. A simple noise filtering procedure was implemented, but it was discovered the system is also sensitive to the very slight frequency drift (±0.01 Hz) present in the electrical grid. This frequency drift causes issues during filtering as one cannot assume a constant frequency during the observed time. Thus a more advanced procedure has been developed which models the noise on a short segment of the recording during which it assumes a linear frequency drift. The noise model is then subtracted from the raw data to obtain a clean signal. This approach is limited as the frequency drift is a stochastic process which can sometimes cause a bad model fit. We continue the work to solve this issue. As the system was not directly paired to a video camera and we encountered issues with keeping a proper time on the *Raspberry Pi*, we cannot confidently claim that the system recorded any meteors or fireballs yet. There are many candidates in the recorded data but no direct correlation can be made at this moment. Nevertheless, many fireworks were recorded during the New Year's celebration in Pula, Croatia. The total cost of the system (not counting the *Raspberry Pi 2* computer) is about 10€. Next steps are to install the system in a non-light polluted location, paired with an all-sky camera running on the same *Raspberry Pi* computer. This combination is possible as the radiometer recording procedures are not computationally intensive, while the meteor capture and detection software for the *RPi* exists. (Vida et al., 2015; 2016).

Open-source low-cost meteor station

During last year's IMC, (Zubović et al., 2015) presented a low-cost video meteor station. This year, (Vida et al., 2016) provided an update on this project. In summary, a complete solution for video meteor capture and detection has been developed for a price of about 150 USD. Some minor work on testing and documentation still needs to be done, but the system is close to being fully functional. The developed system is compatible with CAMS standards and represents an opportunity for a cheap way to create new and expand existing meteor networks. Furthermore, the price of the system makes it suitable for educational purposes – one of the long term goals of the CMN is to give high school and university students an opportunity to have their own meteor station at home and

to learn about astronomy, computer and data science with their own equipment and data.

Telescopic meteors

One of the most common issues when dealing with video meteor orbit data is the lack of astrometrical precision. The work of (Skokić et al., 2016) has shown that even most reliable video orbits made by CAMS software show significant dispersion in D-critera.

Initial tests done by the Slovak Video Meteor Network (Koukal et al., 2015), Sirko Molau (Molau, 2015) and the CMN during 2014 have shown that telescopic meteors are not elusive. We have conducted parallel tests using a 55mm F/1.0 *Kowa* lens and a 4mm F/1.2 lens during the night of December 12–13, the pre-maximum night of the 2014 Geminids. The moderate field of view lens (4mm) yielded a total of 118 meteors, while the 55mm *Kowa* lens yielded 42 meteors. Regarding the *Kowa* lens, due to its significantly longer focal length and a significantly higher on-chip meteor velocity, we have concluded that the camera's geometry (FOV center in respect to radiant position) plays an important role in terms of the number of recorded meteors.

As the initial results in regard to the number of recorded meteors were encouraging, it was decided to pursue the matter further. To maximize the number of recorded telescopic meteors, a system of 8 *Kowa* lenses in a 4x2 configuration was built. 8 *Sony ICX672* (*NTSC Exview HAD II*) *NTSC* board cameras are used for imaging with the lenses. The developed system covers a FOV of about 15.6°×10.4° and records a live video with stars visible down to magnitude 10. A second such system is being built and both with be operational in the near future.

Questions which we want to discuss here are how many meteors would such setup record compared to a moderate FOV lens, and could the system be useful for flux and ZHR estimations? Thus, in order to have a grasp of the numbers involved, Peter Gural performed simulations using the *MeteorSim* software (Gural, 2001), and the results are presented below.

As the used lenses have a much higher focal length than moderate FOV systems, ground separation of the stations can be much closer due to a higher astrometrical precision. A smaller distance between the stations thus means a higher sky volume overlap between the stations, which in turn could yield a higher number of recorded common events. These events could therefore be of similar apparent magnitudes as the distance between meteors and the stations is much larger than the distance between the stations themselves.

Fainter limiting magnitude should allow capturing more sporadic meteors as the population index for sporadic sources is about 3 or more (Rendtel, 2004). All these factors can be accounted for in the simulation. Furthermore, one important point to consider are weather conditions for both stations as it rarely occurs they are ideal. In the case of the telescopic setup, weather conditions should be more or less the same for both due to their proximity to each other.

MeteorSim simulations were done using three entrance velocities, paired with population indices: 72 km/s (r = 2.5), 35 km/s (r = 2.5) and 12.5 km/s (r = 3.0). Two types of output were analyzed: meteor limiting magnitude and meteor count, for different radiant distances (i.e. the distance between the center of the FOV and the radiant). The resulting graphs are shown in *Figures 3 and 4*. From *Figure 3* can be noticed that meteor counts strongly depend on the radiant distance, but this dependence is less pronounced for slower meteors.

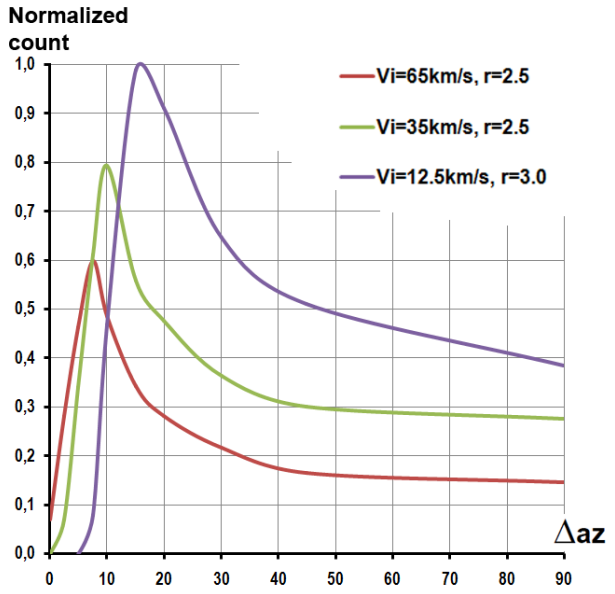

Figure 3 – CMN Normalized meteor counts versus radiant distance for three entrance velocities: 72, 35 and 12.5 km/s, according to *MeteorSim* results.

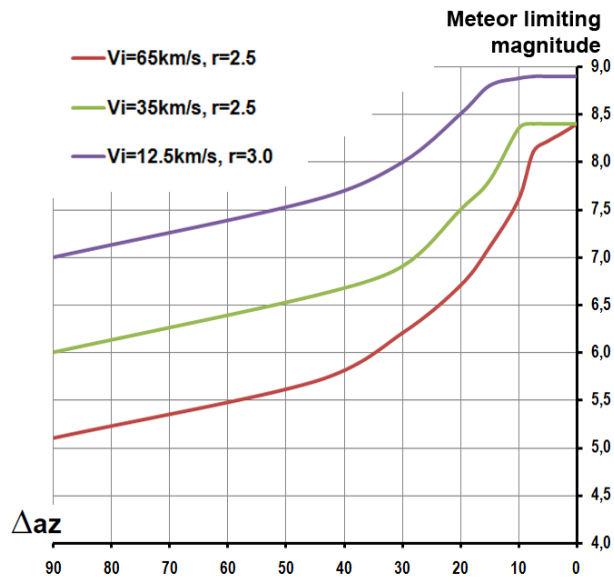

Figure 4 – CMN Limiting meteor magnitude versus radiant distance for three entrance velocities: 72, 35 and 12.5 km/s, according to MeteorSim results.

Figure 4 shows that regardless the entrance velocity, the setup should be able to detect all meteors down to the 5th magnitude, and all meteors down to magnitude 6 for meteors with the entrance velocity of 35 km/s. These

results mean that the system should have acceptable ZHR estimations for e.g. Geminids, regardless of the radiant distance.

One of the primary goals of this project is to obtain high-precision deceleration data of the recorded meteors which would yield very precise orbits. Furthermore, as the meteor's on-chip velocity is large and the frame rate of the used camera is not all that high (60 Hz per field with the *NTSC* camera after deinterlacing, i.e. ~16.7 ms per field), meteors appear as streaks on individual fields. During the testing we have found many meteors that have streaks longer than 50 pixels per one field. If one looks at the profile of each streak and extracts its light curve with 1 pixel steps, that process would allow converting spatial information of meteor's brightness to temporal information. Effectively, that would mean that the light curve of a telescopic meteor could be sampled with thousands of samples per second.

Finally, the data generated by this system could be used for other purposes, such as analysis of star scintillations and occultations.

6 Education

From the very beginnings of the Croatian Meteor Network, one of our main goals is education of students, ranging from elementary school to university students.

One of the students' groups at the Višnjan School of Astronomy (which takes place for more than 25 years) is always dedicated to meteor work. Each group has about 4 to 5 students who are led by a mentor. Such approach allows for a higher individuality and a deeper concentration on the matter, but still requires much teamwork. Most importantly, students are being introduced to the scientific method through original (very often their own) observations which adds value to their work.

During the 2015/16 academic year, the CMN deepened contacts with teachers interested in astronomy and provided data for Croatian astronomy contests and other educational projects. Two of the new CMN cameras are situated on schools in Koprivnica and Rovinj. Our goal is to spread this collaboration further and deploy more meteor stations on schools.

Workshops and lectures about the CMN and meteor astronomy in general were held at the Physics Department of the University of Osijek and at the Fran Galović high school in Koprivnica.

7 Conclusion

Ongoing work of the Croatian Meteor Network between the two IMCs has been presented. The current status of the network was described, results of scientific endeavors were discussed, and the status of ongoing projects was given.

The discussed projects have enough material to be elaborated in separate papers, as this was done for a chosen set of projects. The others were described here in a shorter format to minimize the required time for their description, while still providing some information about them. Any reader interested in a particular project is encouraged to contact the authors for more information.

Acknowledgments

Our acknowledgments go to all members of the Croatian Meteor Network, in alphabetical order (by first name): Alan Pevec, Aleksandar Borojević, Aleksandar Merlak, Alen Žižak, Dalibor Brdarić, Damir Matković, Dario Klarić, Dario Zubović, Dejan Kalebić, Denis Štogl, Dorian Božićević, Filip Lolić, Filip Novoselnik, Gloryan Grabner, Goran Ljaljić, Ivan Gašparić, Ivica Ćiković, Janko Mravik, Josip Belas, Krunoslav Vardijan, Luka Osokruš, Maja Crnić, Mark Sylvester, Mirjana Malarić, Reiner Stoos, Saša Švagelj, Sonja Janeković, Tomislav Sorić, Zvonko Prihoda, Željko Arnautović, Željko Krulić and most of all, Peter Gural. This work was partially supported by the Faculty of Mining, Geology and Petroleum Engineering, University of Zagreb, Višnjan Science and Education Center and by private funds of CMN members.

References

Gural P. (2002). "Meteor Observation Simulation Tool". In Triglav M., Knöfel A. and Trayner C., editors, *Proceedings of the International Meteor Conference*, Cerkno, Slovenia, 20-23 September 2001. IMO, pages 29–35.

Koukal J., Srba J. and Gorková S. (2015). "NFC - Narrow Field Camera". In Rault J.-L. and Roggemans P., editors, *Proceedings of the International Meteor Conference*, Mistelbach, Austria, 27-30 August 2015. IMO, pages 91–93.

Molau S., Kac J., Crivello S., Stomeo E., Barentsen G., Goncalves R., Saraiva C., Maciejewski M. and Maslov M. (2015). "Results of the IMO Video Meteor Network – October 2014". *WGN, Journal of the IMO*, **43**, 33–38.

Molau S., Crivello S., Goncalves R., Saraiva C., Stomeo E. and Kac J. (2016). "Results of the IMO Video Meteor Network – November 2015". *WGN, Journal of the IMO*, **44**, 46–50.

Šegon D., Andreić Ž., Korlević K. and Vida D. (2015). "Croatian Meteor Network: ongoing work 2014 – 2015". In Rault J.-L. and Roggemans P., editors, *Proceedings of the International Meteor Conference*, Mistelbach, Austria, 27-30 August 2015. IMO, pages 51–57.

Šegon D., Gural P., Andreić Ž., Vida D., Skokić I. and Novoselnik F. (2015). "Four possible new high-declination showers". *WGN, Journal of the IMO*, **43**, 147–150.

Rendtel J. (2004). “The population index of sporadic meteors”. In Triglav-Čekada M. and Trayner C., editors, *Proceedings of the International Meteor Conference*, Bollmannsruh, Germany, 19-21 September 2003. IMO, pages 114–122.

Rendtel J. (2015). “Minor kappa-Cepheid (751 KCE) activity on 2015 September 21”. *WGN, Journal of the IMO*, **43**, 177–178.

Skokić I., Šegon D. and Kurtović G. (2016). “On the accuracy of orbits from video meteor observations”. In Roggemans A. and Roggemans P., editors, *Proceedings of the International Meteor Conference*, Egmond, the Netherlands, 2-5 June 2016. Pages 280–283.

Vida D., Turčinov R., Šegon D. and Silađi E. (2015). “Low-cost meteor radiometer”. In Rault J.-L. and Roggemans P., editors, *Proceedings of the International Meteor Conference*, Mistelbach, Austria, 27-30 August 2015. IMO, pages 180–184.

Vida D., Šegon D., Gural P. S., Martinović G. and Skokić I. (2014). “CMN_ADAPT and CMN_binViewer software”. In Rault J.-L. and Roggemans P., editors, *Proceedings of the International Meteor Conference*, Giron, France, 18-21 September 2014. IMO, pages 59–63.

Vida D., Zubović D., Šegon D., Gural P. and Cupec R. (2016). “Open-source meteor detection software for low-cost single-board computers”. In Roggemans A. and Roggemans P., editors, *Proceedings of the International Meteor Conference*, Egmond, the Netherlands, 2-5 June 2016. Pages 307–318.

Zubović D., Vida D., Gural P. and Šegon D. (2015). “Advances in the development of a low-cost video meteor station”. In Rault J.-L. and Roggemans P., editors, *Proceedings of the International Meteor Conference*, Mistelbach, Austria, 27-30 August 2015. IMO, pages 94–97.

Damir Šegon.

Fireballs from Australian Desert Fireball Network – search for similar orbits

Lukáš Shrbený[1], Pavel Spurný[1] and Phil A. Bland[2]

[1] **Interplanetary matter department, Astronomical Institute of the Czech Academy of Sciences, Ondřejov, Czech Republic**
shrbeny@asu.cas.cz

[2] **Department of Applied Geology, Curtin University, Perth, Australia**

We studied the fireball activity from the Desert Fireball Network records from 2006 to 2014 and identified a couple of time periods with increased number of fireballs. We searched for orbital similarities among the fireballs in these time periods and have found members of 10 individual meteor showers and two groups of similar orbits that do not correspond to any known meteor shower.

1 Introduction

The multi-station photographic observation of fireballs using fireball networks represents a very efficient and precise method of recording the atmospheric interactions of larger meteoroids. During the short moment of meteoroid ablation we can determine its atmospheric trajectory, orbit, light curve and basic physical properties. The only one photographic fireball network in the Southern Hemisphere is the *Desert Fireball Network* (DN) in Australia. The DN was designed to recover number of meteorites with accurate orbits, and thus bright fireballs with possibility of meteorite fall were processed preferentially. The published data cover two successful recoveries of Bunburra Rockhole and Mason Gully meteorites (e.g. Bland et al., 2009; Spurný et al., 2011; 2012; Welten et al., 2012), observation of the HAYABUSA spacecraft reentry (Borovička et al., 2011), and atmospheric trajectories and orbits of other 30 bright fireballs presented at Asteroids, Comets, Meteors 2008 conference in Baltimore (Bland et al., 2008).

We used already measured fireballs to search for similarities in their radiant positions and heliocentric orbits with meteor showers or with other DN fireballs. We present five time periods during a year of increased fireball activity, fireballs belonging to five individual meteor showers from the IAU MDC working list of meteor showers, and two groups of similar orbits that do not correspond to any known meteor shower.

2 Instrumentation, observations and data processing

One of the most advanced fireball networks was the Desert Fireball Network (Bland et al., 2004), where each station was equipped with a modern and sophisticated Autonomous Fireball Observatory (AFO) (Spurný et al., 2007). The AFO imaging system consists of a Zeiss Distagon fish-eye objective (f/3.5, f = 30 mm) and a large-format sheet film (9 × 12 cm emulsion ILFORD FP4 125 with panchromatic spectral sensitivity approximately between 360 and 650 nm). All AFOs are equipped with a rotating shutter close to the focal plane to determine the fireball velocity. Each AFO also includes an all-sky brightness sensor (radiometer) with a sampling rate of 500 measurements per second. Therefore, along with an accurate time of the fireball passage and duration, we also obtain a very detailed light curve. The multi-station operation of the network started in December 2005 and the last film was exposed in April 2015. Altogether, more than 260 multi-station fireballs were recorded. The network has been changed in last few years and the number of cameras has increased to 30 digital fireball observatories (ADFO) equipped by Nikon D800 still cameras and Watec 902H video cameras (Bland et al., 2014; Towner et al., 2015). Over the next few months, the DN should establish over 50 new ADFOs (Sansom et al., 2015).

We predominantly search for shower fireballs in time intervals with increased fireball activity. Only about 90 fireballs were measured and calculated so far so it is very probable that other meteor shower members will be identified after processing of the whole DN data set.

All the presented fireballs were measured and processed using our standard procedures (Borovička et al., 1995; Ceplecha, 1987). The Fishscan software, created by Dr. Jiří Borovička, serves for positional and photometric measuring of fireballs on scanned copies of films. Therefore, all the fireballs here, along with precise atmospheric trajectories, also have precise Fishscan photometry (for details see Shrbený, 2009 or Shrbený and Spurný, 2009).

3 Activity of DN fireballs and proposed shower membership

Fireball activity

After developing and processing of all the DN films we were interested if there are time periods during a year with increased fireball activity. We took dates of 853 fireball occurrences (single-station events also included) of nine complete years from 2006 to 2014 and plotted the

histogram with 9–11 days bins (depending on the month length, 3 bins per month). The number of fireballs was corrected to 10 days for all the bins (*Figure 1*). The average value of fireballs observed per 10 days is 23. Five most prominent activity periods and meteor showers active in these periods are the beginning of March (σ-Hydrids, γ-Normids), end of May (α-Scorpiids, S ω-Scorpiids), end of July/beginning of August (Piscis Austrinids, S δ-Aquariids, α-Capricornids, S ι-Aquariids, η-Eridanids), end of October/beginning of November (S and N Taurids), and beginning of December (Phoenicids, December Monocerotids, N χ-Orionids, γ-Puppids, Geminids).

Working list of meteor showers

Seven fireballs belonging to five individual meteor showers from the IAU MDC working list of meteor showers were identified. The meteor showers are N μ-Sagittariids, June ε-Ophiuchids, κ-Aquariids, N χ-Orionids, and γ-Puppids. Atmospheric trajectories of the fireballs are presented in *Table 1*, physical data in *Table 2*, and orbital elements in *Table 3*.

The dynamic pressures, *p*, in *Table 2* are determined from the high resolution light curves from AFO radiometers and correspond to the first significant outburst. If we assume that these significant outbursts correspond to fragmentation points, the dynamic pressures in *Table 2* are the highest ones reached without fragmentation. Thus a comparison with the tensile strength of the material can be made. The dynamic pressures are a function of the velocity, *v*, and the air density, *ρ*, at the fragmentation point ($p = \rho v^2$).

N μ-Sagittariid fireballs are according to the PE criterion the most fragile and probably of cometary origin. The orbital association of DN210606A and DN240606 with the shower is not very confident, since the D_H criterion (Jopek, 1993) between the fireballs and fireballs and the mean shower orbit is 0.1. The shower is also part of the antihelion source so the orbital similarities could be incidental.

The atmospheric trajectory and the dynamics of DN120907 were determined with accuracy high enough to apply the fragmentation model of Ceplecha et al., 1993 and determine precise values of initial velocity, ablation coefficient, and product $Km^{-1/3}$. The terminal height of 50 km was reached by this meteor with a terminal velocity of only 6 km/s and with an absolute brightness of –1.8 ± 0.8 mag, which corresponds to an almost completely decelerated object. The model provides a solution with one fragmentation point at a height of 56.5 km, and the ablation coefficient of 0.110 s^2/km^2. This corresponds to a velocity of 15.3 km/s and a dynamic pressure of 0.118 MPa. The results of the model can also help to constrain the meteoroid bulk density, ρ_d. We can separate ρ_d from the definition of the shape-density coefficient, *K*, if we know m_{inf} and the value of product ΓA. The same procedure was applied on one Leonid fireball (Spurný et al., 2000), and in our case (m_{inf} = 58 g and assuming ΓA = 1.1) this provides an estimate of bulk density of 3.2 g/cm^3. A couple of significant outbursts of the brightness of the DN120907 are visible in its light curve. The outbursts correspond to heights of 60 and 52.5 km, or to dynamic pressures of 0.082 and 0.146 MPa respectively, which is in good agreement with the fragmentation model. According to the PE criterion (Ceplecha and McCrosky, 1976) the DN120907 is of type II, which is between the classifications based on the ablation coefficient and the bulk density. However, if we take the unknown shape of the body (ΓA) and the accuracy of m_{inf} into account the spread of possible bulk densities is large: from 1.9 to 3.5 g/cm^3.

The second fireball with the fragmentation model solution is DN061207A. The model provides a solution without fragmentation. The results of the model can also provide an estimate of the meteoroid bulk density. If we apply the same procedure as described above and use m_{inf} = 40 g, we arrive at a bulk density of 0.6 g/cm^3. No significant outbursts of the brightness of DN061207A are visible in its light curve. This is in good agreement with a no-fragmentation solution of the fragmentation model.

Table 1 – Atmospheric trajectories of the fireballs belonging to the working list of meteor showers. *H* is the height above sea level, the subscript "*B*" denotes values at the beginning point of the atmospheric trajectory, the subscript "*E*" at the end point.

Fireball name	Time (UT)	H_B (km)	H_E (km)	IAU No. and code
DN210606A	17:17:40	81.23	64.60	067 NSA
DN240606	15:10:24	88.75	76.02	067 NSA
DN210606B	12:21:41	78.93	68.47	459 JEO
DN120907	14:32:11	74.38	50.00	076 KAQ
DN021207	14:56:25	87.07	73.51	256 ORN
DN071205B	12:17:36	93.38	80.50	301 PUP
DN061207A	18:09:55	92.00	61.74	301 PUP

Table 2 – Physical data on the fireballs belonging to the working list of meteor showers. ZD_E is the zenith distance of the radiant at the end point of the atmospheric trajectory, v_{inf} is the initial velocity, M_{max} is the maximum absolute magnitude, m_{inf} is the initial photometric mass, the *PE* coefficient describes the empirical end height criterion and designates the type of fireball (Ceplecha and McCrosky, 1976), and *p* is the dynamic pressure at the height of the first fragmentation (high resolution light curve is not available for DN071205B due to Moon that was brighter than the fireball).

Fireball name	ZD_E (deg)	v_{inf} (km/s)	M_{max} (mag)	m_{inf} (g)	PE type	p (MPa)
DN210606A	28.9	25.39	-8.8	250	IIIA	0.055
DN240606	15.7	26.32	-5.8	30	IIIB	0.008
DN210606B	28.65	17.96	-8.2	420	IIIB	0.023
DN120907	17.68	16.49	-4.3	58	II	0.082
DN021207	60.01	30.76	-5.9	27	II/IIIA	0.044
DN071205B	73.95	43.53	-5.4	10	II	-
DN061207A	21.67	44.06	-7.8	40	II	0.117

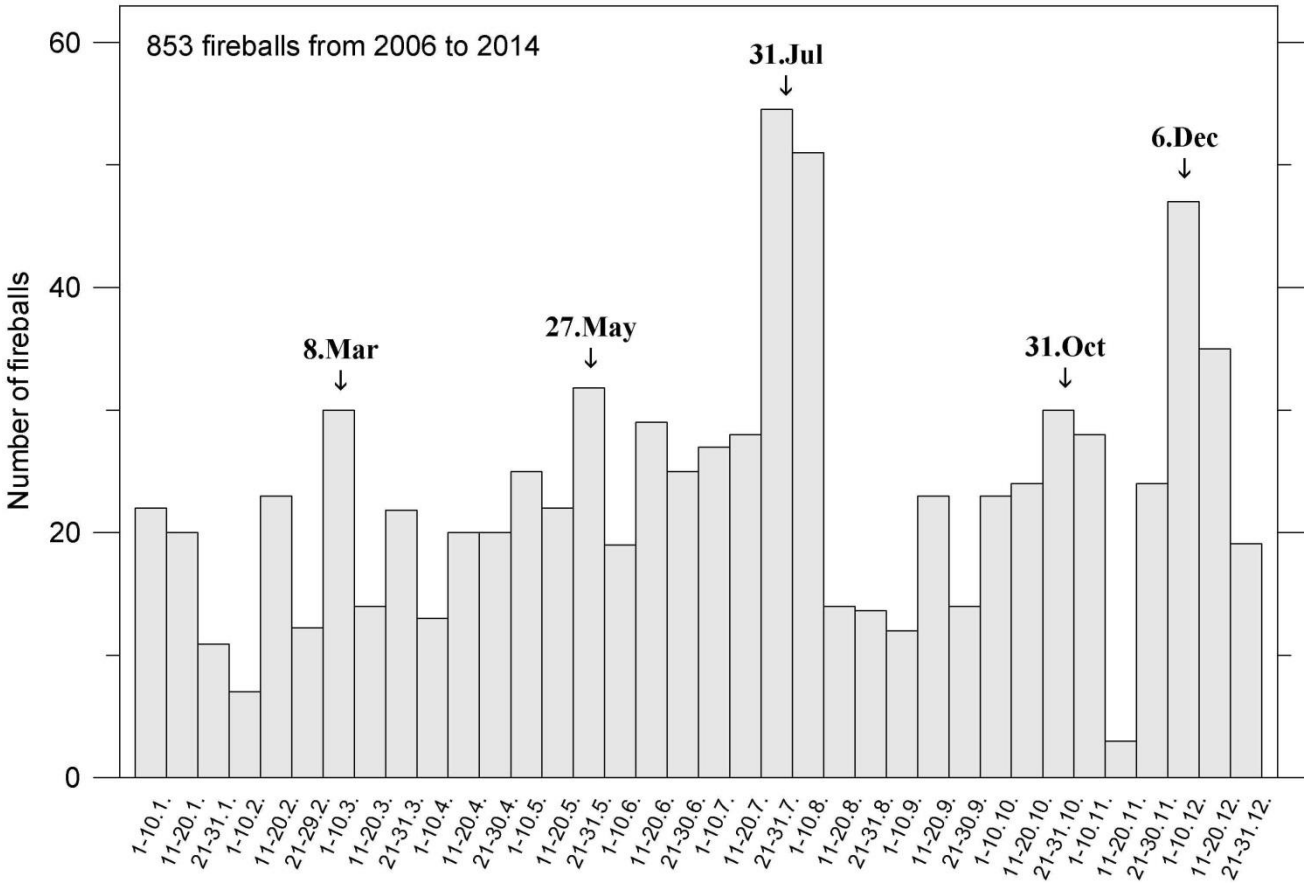

Figure 1 – Activity of DN fireballs from 2006 to 2014. The five most prominent activity periods are marked.

Table 3 – Radiants and orbital elements (J2000.0) of the presented fireballs. (α_G, δ_G) is the geocentric radiant and v_G is geocentric mean velocity without atmospheric drag (not measurable on our records).

Fireball name	α_G (deg)	δ_G (deg)	v_G (km/s)	a (AU)	e	q (AU)	ω (deg)	Ω (deg)	i (deg)	IAU No. and code
DN210606A	267.39	-12.0	22.8	2.87	0.789	0.615	264.1	90.1143	8.5	067 NSA
DN240606	271.46	-16.67	23.83	3.09	0.8121	0.5805	267.52	92.8962	5.35	067 NSA
DN210606B	245.27	-8.44	14.11	2.54	0.655	0.8750	229.53	89.9219	5.11	459 JEO
DN120907	319.55	-15.96	12.30	2.64	0.6582	0.9012	42.63	349.287	0.08	076 KAQ
DN021207	82.03	26.86	28.55	2.002	0.8292	0.3419	296.17	249.9206	4.33	256 ORN
DN071205B	129.76	-47.62	41.81	2.88	0.661	0.97741	11.39	75.4213	73.60	301 PUP
DN061207A	131.79	-47.15	42.55	2.78	0.647	0.98169	7.83	74.1286	75.44	301 PUP
DN220506	259.33	-22.80	35.64	2.79	0.931	0.191	312.90	61.36	0.55	-
DN270506	264.21	-25.62	35.78	2.98	0.935	0.195	132.22	246.1525	4.54	-
DN240509	263.7	-15.1	35.14	2.33	0.915	0.197	313.2	63.5607	16	-
DN200606B	294.9	-16.7	39.97	3.14	0.968	0.099	326.5	88.9844	14	-
DN230606	296.88	-21.27	35.17	1.96	0.924	0.149	141.13	271.98	0.3	-

Only two minor outbursts are presented and correspond to heights of 79 and 72 km, or to dynamic pressures of 0.042 and 0.118 MPa respectively. According to the *PE* criterion both the γ-Puppids are of type II, which is not in good agreement with the estimate of the bulk density. This discrepancy can be only partially explained by the unknown shape of the body and the accuracy of m_{inf}. In all the cases, the bulk density is no higher than 1 g/cm^3, and such an overestimation of m_{inf} to increase the density is not probable (m_{inf} of 3 g gives 2.2 g/cm^3).

We are aware that any association of a small number of orbits with any meteor shower is doubtful without modelling of the dynamical evolution of the orbits, which would confirm the shower membership. To prove the proposed associations this kind of modelling is needed.

Similarities without any shower membership

Two groups of similar orbits that do not correspond to any known meteor shower were identified among DN fireballs using the D_H criterion (Jopek, 1993). Their

radiants and orbital elements are in *Table 3* and we can see that both groups belong to the antihelion source, which increase the probability that the orbital similarities are incidental. Atmospheric trajectories of the fireballs are presented in *Table 4* and physical data in *Table 5*.

Table 4 – Atmospheric trajectories of the fireballs not belonging to known meteor showers. *H* is the height above sea level, the subscript "*B*" denotes values at the beginning point of the atmospheric trajectory, the subscript "*E*" at the end point.

Fireball name	Time (UT)	H_B (km)	H_E (km)
DN220506	14:34:26	94.66	80.36
DN270506	16:28:13	96.08	67.65
DN240509	17:49:27	83.29	48.58
DN200606B	12:56:39	78.26	42.58
DN230606	20:51:10	76.34	49.48

Table 5 – Physical data on the fireballs not belonging to known meteor showers. ZD_E is the zenith distance of the radiant at the end point of the atmospheric trajectory, v_{inf} is the initial velocity, M_{max} is the maximum absolute magnitude, m_{inf} is the initial photometric mass, *PE* coefficient describes the empirical end height criterion and designates the type of fireball (Ceplecha and McCrosky, 1976), and *p* is the dynamic pressure at the height of the first fragmentation.

Fireball name	ZD_E (deg)	v_{inf} (km/s)	M_{max} (mag)	m_{inf} (g)	PE type	p (MPa)
DN220506	30.90	37.33	-6.5	6	IIIA/IIIB	0.011
DN270506	5 95	37.50	-8.6	50	II/IIIA	0.026
DN240509	22.2	36.85	-10.5	1300	II	1.045
DN200606B	57.4	41.48	-11.6	1600	I	1.68
DN230606	49.14	36.88	-8.1	120	I	0.44

The first group was observed in the end of May. There were three fireballs observed with similar radiant position and shape of heliocentric orbit (especially the two ones in 2006). These fireballs belong to the antihelion source, so the orbital similarities may be incidental. Also the distinct atmospheric behavior of these fireballs prefers rather an incidental connection than a common origin. PE types differ from type II to IIIB and also the dynamic pressures cover a wide range from 0.01 to 1.0 MPa. A heterogeneous nature of a possible parent object is not impossible but incidental orbital similarities are more probable.

The second group was observed in the end of June. There were two fireballs with similar radiant position and shape of heliocentric orbit, especially a small perihelion distance. Both the fireballs performed similar atmospheric behavior, both showed significant deceleration, a small value of the ablation coefficient (0.001 and 0.003 s^2/km^2), and both penetrated deep into the atmosphere (PE type I). The orbital similarity can be incidental also in this case. A very similar atmospheric behavior can be caused by a close approach to the Sun where a change of the material nature takes place due to thermal desorption of Na (Čapek and Borovička, 2009). Na is almost lost when $q \leq 0.2$ AU and the meteoroid is smaller than 10 cm.

4 Conclusion

We have searched for orbital similarities among DN fireballs and meteor showers in time periods during a year with increased fireball activity. We have identified fireball members of five individual meteor showers from the IAU MDC working list of meteor showers. We have also identified two groups of similar orbits that do not correspond to any known meteor shower. On the basis of their radiant positions, heliocentric orbits, and atmospheric behavior it is probable that these associations are incidental.

External sources of shower elements are needed to identify shower members in DN fireballs due to the small number of fireballs in our data set belonging to one shower. Once identified, DN fireballs can provide precise data on meteor showers, since the majority of DN fireballs have a precise atmospheric trajectory and heliocentric orbit, detailed light curve, dynamic pressure in the first fragmentation point and modelling of some of them can provide ablation coefficient and bulk density.

Acknowledgment

This work was supported in part by Preamium Academiae from the Czech Academy of Sciences and by the institutional project RVO:67985815.

References

Bland P. A. (2004). "Fireball cameras: The Desert Fireball Network". *Astronomy and Geophysics*, **45**, 5.20–5.23.

Bland P. A., Spurný P., Shrbený L., Borovička J., Bevan A. W. R., Towner M. C., McClafferty T., Vaughan D. and Deacon G. (2008). "The Desert Fireball Network: First Results of Two Years Systematic Monitoring of Fireballs over the Nullarbor Desert of South Western Australia". Asteroids, Comets, Meteors 2008. *LPI Contribution No. 1405*, id. 8246.

Bland P. A., Spurný P., Towner M. C., Bevan A. W. R., Singleton A. T., Bottke W. F., Greenwood R. C., Chesley S. R., Shrbený L., Borovička J., Ceplecha Z., McClafferty T. P., Vaughan D., Benedix G. K., Deacon G., Howard K. T., Franchi I. A. and Hough R. M. (2009). "An Anomalous Basaltic Meteorite from the Innermost Main Belt". *Science*, **325**, 1525–1527.

Bland P. A., Towner M. C., Paxman J. P., Howie R. M., Sansom E. K., Cupak M., Benedix G. K., Tingay S. J., Harrison J. A., Dyl K. A., Bevan A. W. R. and Galloway M. J. (2014). "Digital Expansion of the Desert Fireball Network". *LPI Contribution No. 1800*, id.5287.

Borovička J., Spurný P. and Keclíková J. (1995). “A new positional astrometric method for all-sky cameras”. *Astronomy and Astrophysics Supplement*, **112**, 173–178.

Borovička J., Abe S., Shrbený L., Spurný P. and Bland P. A. (2011). “Photographic and Radiometric Observations of the HAYABUSA Re-Entry”. *Publications of the Astronomical Society of Japan*, **63**, 1003–1009.

Ceplecha Z. (1987). “Geometric, dynamic, orbital and photometric data on meteoroids from photographic fireball networks”. *Bulletin of the Astronomical Institutes of Czechoslovakia*, **38**, 222–234.

Ceplecha Z. and McCrosky R. E. (1976). “Fireball end heights - A diagnostic for the structure of meteoric material”. *Journal of Geophysical Research*, **81**, 6257–6275.

Ceplecha Z., Spurný P., Borovička J. and Keclíková J. (1993). “Atmospheric fragmentation of meteoroids”. *Astronomy and Astrophysics*, **279**, 615–626.

Čapek D. and Borovička J. (2009). “Quantitative model of the release of sodium from meteoroids in the vicinity of the Sun: Application to Geminids”. *Icarus*, **202**, 361–370.

Jopek T. J. (1993). “Remarks on the meteor orbital similarity D-criterion”. *Icarus*, **106**, 603–607.

Sansom E. K., Bland P. A., Paxman J. A. and Towner M. (2015). “A novel approach to fireball modeling: The observable and the calculated”. *Meteoritics and Planetary Science*, **50**, 1423–1435.

Shrbený L. (2009). “Meteor Shower Fireballs”. PhD thesis.

Shrbený L. and Spurný P. (2009). “Precise data on Leonid fireballs from all-sky photographic records”. *Astronomy and Astrophysics*, **506**, 1445–1454.

Spurný P., Betlem H., van’t Leven J. and Jenniskens P. (2000). “Atmospheric behavior and extreme beginning heights of the thirteen brightest photographic Leonid meteors from the ground-based expedition to China”. *Meteoritics and Planetary Science*, **35**, 243–249.

Spurný P., Borovička J. and Shrbený L. (2007). “Automation of the Czech part of the European fireball network: equipment, methods and first results”. In Valsecchi G. B., Vokrouhlický D. and Milani A., editors, *Near Earth Objects, our Celestial Neighbors: Opportunity and Risk*, Proceedings of IAU Symposium 236. Cambridge: *Cambridge University Press*, pages 121–130.

Spurný P., Bland P. A., Shrbený L., Towner M. C., Borovicka J., Bevan A. W. R. and Vaughan D. (2011). “The Mason Gully Meteorite Fall in SW Australia: Fireball Trajectory and Orbit from Photographic Records”. 74th Annual Meeting of the Meteoritical Society. *Published in Meteoritics and Planetary Science Supplement*, id.5101.

Spurný P., Bland P. A., Shrbený L., Borovička J., Ceplecha Z., Singelton A., Bevan A. W. R., Vaughan D., Towner M. C., McClafferty T. P., Toumi R. and Deacon G. (2012). “The Bunburra Rockhole meteorite fall in SW Australia: fireball trajectory, luminosity, dynamics, orbit, and impact position from photographic and photoelectric records”. *Meteoritics and Planetary Science*, **47**, 163–185.

Towner M. C., Bland P. A., Cupak M. C., Howie R. M., Sansom E. K., Paxman J. P., Inie M., Galloway M., Deacon G., Dyl K. A., Benedix G. K., Tingay S. J., Harrison J. A. and Bevan A. W. R. (2015). “Initial Results from the Desert Fireball Network”. *LPI Contribution No. 1832*, 1693.

Welten K. C., Meier M. M. M., Caffee M. W., Laubenstein M., Nishizumi K., Wieler R., Bland P. A., Towner M. C. and Spurný P. (2012). “Cosmic-ray exposure age and preatmospheric size of the Bunburra Rockhole achondrite”. *Meteoritics and Planetary Science*, **47**, 186–196.

On the accuracy of orbits from video meteor observations

Ivica Skokić[1], Damir Šegon[2] and Goran Kurtović[1,3]

[1] **Astronomical Society "Anonymus", B. Radića 34, 31550 Valpovo, Croatia**
ivica.skokic@gmail.com

[2] **Astronomical Society Istra Pula, Park Monte Zaro 2, 52100 Pula, Croatia**
damir.segon@pu.htnet.hr

[3] **Faculty of Electrical Engineering, University of Osijek, Kneza Trpimira 2B, 31000 Osijek, Croatia**
goran.kurtovic@gmail.com

The velocity limits of the meteor shower's geocentric velocity distribution from the CAMS meteoroid database were determined and used to calculate perturbed orbits. These were compared with the mean stream orbit using the D_{SH} dissimilarity criterion. It was found that for the slow meteor showers (Alpha Capricornids and Geminids), the resulting orbits are within the generally accepted cutoff values for stream associations, while for the faster showers (Perseids, Orionids and Quadrantids) the resulting orbits differ significantly from their mean stream orbit.

1 Introduction

In recent years we witnessed a fast growth and development of video meteor networks providing accurate multi-station measurements of atmospheric meteoroid trajectories and determination of their heliocentric orbits. As a result, several video meteor databases have been compiled, e.g. CAMS, Cameras for Allsky Meteor Surveillance (Jenniskens et al., 2016), SonotaCo (SonotaCo, 2009), EDMOND, European Video Meteor Network Database (Kornoš et al., 2013) and CMN, the Croatian Meteor Network database (Korlević et al., 2013). The wealth of data in these databases improved parameters of established meteor showers and enabled discoveries of many new possible showers.

Several different methods are used to determine error propagation from the measured meteor path to the calculated radiant and heliocentric orbit parameters. Ceplecha (1987) used a convergence angle between the intersecting planes containing the meteor as observed from two or more stations, as a measure of quality of the determined orbit. Better error estimation is achieved by least-squares fitting and a covariance matrix calculation (e.g. Borovička, 1990; Gural, 2012; Dmitriev et al., 2015), by Monte Carlo type simulations (e.g. SonotaCo, 2016) or a combination of the two (e.g. Bettonvil, 2006). These methods assume that observational errors are well known, which is mostly the case for positional measurements, but might not be true for velocity measurements, which are very important for the pre-atmospheric orbit determination. Among other factors that may influence the velocity measurement, we mention the frame rate of the video systems (Albin et al., 2016) and the meteor deceleration profile.

In this paper, as our first step in the analysis of the accuracy of video meteoroid orbits, we check how the spread in velocity distribution affects the mean orbit, for a given meteor shower.

2 Method and data

We used the CAMS v2.0 meteoroid database (Jenniskens et al., 2016), which contains more than 110000 orbits from the period 2010–2013 with detailed information about atmospheric and pre-atmospheric orbits and even shower associations. The speed accuracy of the catalog data is stated to be <10% (median 0.9%).

First, a geocentric velocity (V_g) distribution of all meteoroids of a particular shower is plotted and the mean velocity and velocity spread are estimated. This is done visually to account for a possible asymmetry in the distribution. Next, the mean geocentric velocity of the shower is perturbed by the velocity range determined earlier, and the resulting orbit is compared with the mean shower orbit.

For the comparison of orbits we used an orbit dissimilarity criterion, a numerical value which tells us by how much two orbits differ from each other. Several criteria have been proposed and all have their strengths and weaknesses (Moorhead, 2016). Different authors give or use slightly different cutoff values for the criteria, for the two orbits to represent the same meteoroid stream (e.g. Galligan, 2001; Rudawska et al., 2012). Here we use the D_{SH} criterion, introduced by Southworth and Hawkins (1963), with a typically used cutoff value of 0.15.

3 Results

We performed an analysis of the five established meteor showers, Alpha Capricornids (CAP), Geminids (GEM), Quadrantids (QUA), Perseids (PER) and Orionids (ORI), that were selected on the basis of the increasing geocentric velocity and large number of recorded

meteors. The shower details and calculation results are presented in *Table 1*.

Alpha Capricornids

This is a shower with slow meteors whose geocentric velocity distribution shows a range between 20–27 km s^{-1} with a typical velocity around 23 km s^{-1} (*Figure 1*). As can be seen from *Table 1*, the orbits of the minimum and maximum V_g are indeed within our $D_{SH} < 0.15$ limit for association with the mean orbit of this shower.

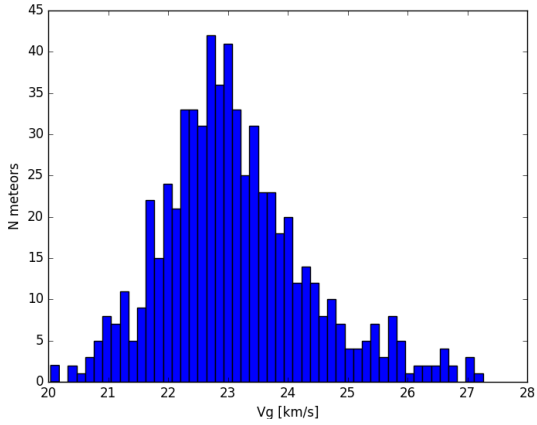

Figure 1 – Alpha Capricornids V_g distribution.

Geminids

A well-known slow shower originating from the asteroid 3200 Phaethon shows a typical geocentric velocity of 34 km s^{-1} (*Figure 2*). Most Geminid meteors have a velocity between 30–40 km s^{-1} with a small number of fast meteors going up to 45 km s^{-1}. Nevertheless, all of them have a strong orbit similarity with D_{SH} ~0.07. The calculation shows that to reach the limiting $D_{SH} = 0.15$ value, mean V_g can be perturbed by -8 up to +16 km s^{-1}.

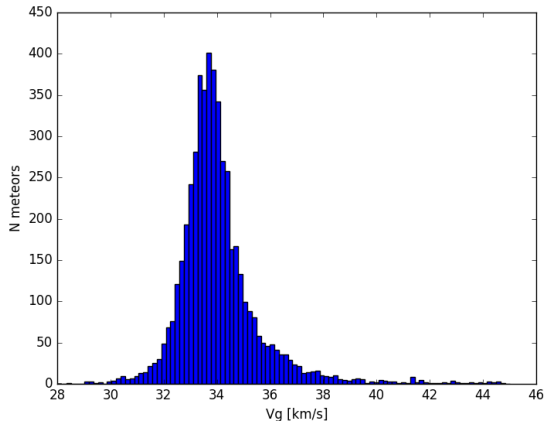

Figure 1 – Geminids V_g distribution.

Quadrantids

Quadrantids are somewhat faster than Geminids with a typical velocity of 41 km s^{-1} and range of 37–48 km s^{-1} with several meteors even going down to 35 and up to 50 km s^{-1} (*Figure 3*). These slower and faster than mean meteors have a high D_{SH} of 0.2–0.5, well over the limit of 0.15 as cutoff value for shower association. To be within this D_{SH} value, QUA meteors should fall in the 39–43 km s^{-1} V_g range.

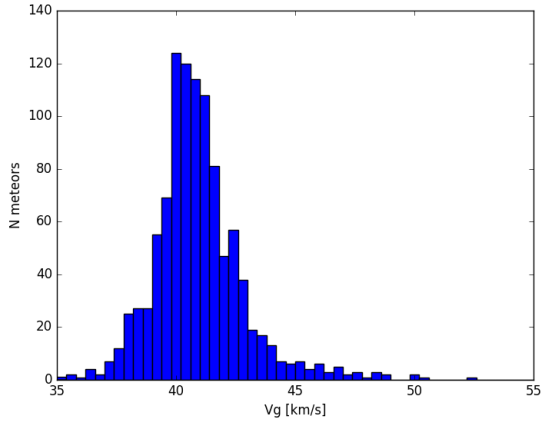

Figure 3 – Quadrantids V_g distribution.

Perseids

Perseids are fast meteors with a mean V_g of 59 km s^{-1} (*Figure 4*). Most PER meteors have velocities within ±4 km s^{-1} from the mean, but there is a hint of a small bump in the 65–70 km s^{-1} range. These V_g values result in high $D_{SH} = 0.6 – 1.0$ indicating that they might not be members of PER shower.

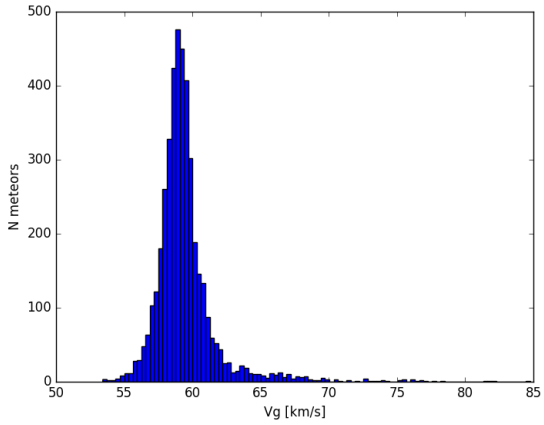

Figure 4 – Perseids V_g distribution.

Table 1 – Shower V_g values and resulting D_{SH}

Shower	N	V_g [km s^{-1}]	V_g (min–max) [km s^{-1}]	D_{SH} (min–max)	ΔV_g (D_{SH} = 0.15) [km s^{-1}]
CAP	640	23	20-27	0.11-0.14	±4
GEM	5064	34	30-40	0.06-0.07	-8 +16
QUA	1028	41	37-48	0.22-0.48	±2.5
PER	4258	59	55-70	0.62-1.01	±2
ORI	3002	66	62-75	0.18-0.62	±3

Orionids

The final and fastest shower in this analysis, Orionids, has a typical V_g of 66 km s^{-1} with most meteors in 62–75 km s^{-1} range (*Figure 5*). Almost all slower meteors satisfy the D_{SH} 0.15 limit, but faster meteors do not. There is even a small number of meteors between the 76–80 km s^{-1} range which might not at all be part of this shower. The D_{SH} limit of 0.15 gives a velocity range 63–69 km s^{-1}, so all meteors faster than 70 km s^{-1} possibly do not belong to the Orionids.

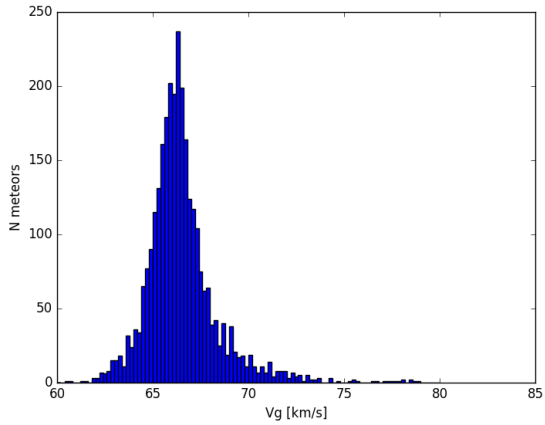

Figure 5 – Orionids Vg distribution.

4 Discussion and conclusions

All showers show an asymmetric geocentric velocity distribution with an excess of higher velocity meteoroids. The meteors from the V_g distribution tail show a good similarity with the mean orbit for slow showers (CAP and GEM) and can be reliably associated with the shower, but for faster showers (QUA, PER and ORI), this is not the case. The $D_{SH} = 0.15$ condition limits the V_g to within 2–3 km s^{-1} of the mean value for these faster showers, and yet they all display a much larger velocity spread. If these meteors from the distribution tail belong to the same shower is hard to tell without detailed dynamical analysis. It may be that the large D_{SH} value in some of these cases is not due to the V_g spread, but linked to some other parameter influencing the result. For example, it is known that the orbit inclination has an effect on the D criteria limits (Galligan, 2001). Due to the small statistical sample of only five analyzed showers, it is impossible to tell if this is the case here and it will be a topic of further investigation.

The meteors in the tails of V_g distribution might also just be outliers due to the method used to associate them with the certain shower. One possible explanation is that the velocity fit of the observational data is sensitive to small perturbations and can result in these outliers (Jenniskens, personal communication; Albin et al., 2016). Another possibility might be the fact that D criteria do not have a single fixed threshold value that fits all the cases (Rudawska et al., 2012).

This paper is only a preliminary first step in a more detailed analysis in preparation. The plan is to check the influence of measurement errors on different parameters, such as errors in the radiant position, velocity and meteoroid orbits. Also, we plan to check more showers, use all available meteoroid databases, other D criteria and extensive simulations with a final goal of quantifying the accuracy of meteoroid orbits determined from video observations.

Acknowledgment

We thank the CAMS network for publishing the CAMS v2.0 meteoroid orbit database. We also thank Denis Vida (CMN) for his constructive comments and Paul Roggemans for his patience while preparing this paper.

References

Albin T., Koschny D., Soja R., Srama R. and Poppe B. (2016). “A Monte-Carlo based extension of the Meteor Orbit and Trajectory Software (MOTS) for computations of orbital elements”. In Roggemans A. and Roggemans P., editors, *Proceedings of the International Meteor Conference*, Egmond, Netherlands, 02–05 June 2016. Pages 20–25.

Bettonvil E. J. A. (2006). “Least squares estimation of a meteor trajectory and radiant with a Gauss-Markov model”. In Bastiaens L., Verbert J., Wislez J.-M. and Verbeeck C., editors, *Proceedings of the International Meteor Conference*, Oostmalle, Belgium, 15–18 September 2005. IMO, pages 63–73.

Borovička J. (1990). “The comparison of two methods of determining meteor trajectories from photographs”. *Bulletin Astronomical Institutes of Czechoslovakia*, **41**, 391–396.

Ceplecha Z. (1987). “Geometric, dynamic, orbital and photometric data on meteoroids from photographic fireball networks”. *Bulletin Astronomical Institutes of Czechoslovakia*, **38**, 222–234.

Dmitriev V., Lupovka V. and Gritsevich M. (2015). “Orbit determination based on meteor observations using numerical integration of equations of motion”. *Planetary and Space Science*, **117**, 223–235.

Galligan D. P. (2001). “Performance of the D-criteria in recovery of meteoroid stream orbits in a radar data set”. *Monthly Notices of the Royal Astronomical Society*, **327**, 623–628.

Gural P. S. (2012). “A new method of meteor trajectory determination applied to multiple unsynchronized video cameras”. *Meteoritics and Planetary Science*, **47**, 1405–1418.

Jenniskens P., Nénon Q., Albers J., Gural P. S., Haberman B., Holman D., Morales R., Grigsby B. J., Samuels D. and Johannink C.

(2015). “The established meteor showers as observed by CAMS”. *Icarus*, **266**, 331–354.

Korlević K., Šegon D., Andreić Ž., Novoselnik F., Vida D. and Skokić I. (2013). “Croatian Meteor Network Catalogues of Orbits for 2008 and 2009”. *WGN, Journal of the IMO*, **41**, 48–51.

Kornoš L., Koukal J., Piffl R. and Toth J. (2013). “Database of meteoroid orbits from several European video networks”. In Gyssens M. and Roggemans P., editors, *Proceedings of the International Meteor Conference*, La Palma, Canary Islands, Spain, 20–23 September 2012. IMO, pages 21–25.

Moorhead A. V. (2016). “Performance of D-criteria in isolating meteor showers from the sporadic background in an optical data set”. *Monthly Notices of the Royal Astronomical Society*, **455**, 4329–4338.

Rudawska R., Vaubaillon J. and Atreya P. (2012). “Association of individual meteors with their parent bodies”. *Astronomy and Astrophysics*, **541**, A2, 1–5.

SonotaCo (2009). “A meteor shower catalog based on video observations in 2007-2008”. *WGN, Journal of the IMO*, **37**, 55–62.

SonotaCo (2016). “Observation error propagation on video meteor orbit determination”. *WGN, Journal of the IMO*, **44**, 42–45.

Southworth R. B. and Hawkins G. S. (1963). “Statistics of meteor streams”. *Smithsonian Contributions to Astrophysics*, **7**, 261–285.

Robert Haas and Mirel Birlan.

Collisional lifetimes of meteoroids

Rachel Halina Soja[1], G. J. Schwarzkopf[1], Maximilian Sommer[1], Jérémie Vaubaillon[3], Thomas Albin[1,4], Jens Rodmann[2], Eberhard Grün[5] and Ralf Srama[1]

[1] **Institute of Space Systems, University of Stuttgart, Pfaffenwaldring 29, 70569 Stuttgart, Germany**
soja@irs.uni-stuttgart.de

[2] **Institute for Astrophysics, University of Göttingen, Germany**

[3] **IMCEE, Paris, France**

[4] **Universitätssternwarte Oldenburg, Carl von Ossietzky University, Oldenburg, Germany**

[5] **Max Planck Institute for Nuclear Physics (MPIK), Saupfercheckweg 1, 69117 Heidelberg, Germany**

Collisions of meteoroids with interplanetary dust grain fragments particles, dispersing larger particles amongst lower mass intervals. Here we use the method of Grün et al. (1985) and the IMEM interplanetary dust model to calculate the collisional lifetimes for different orbits, and for particles in different meteor showers. The timescales are usually long – of order 10^4 years for 1mm grains on Jupiter-family and Hally-type comet orbits. However, near-sun orbits particles suffer more frequent collisions and therefore have much shorter lifetimes. We discuss factors that affect the accuracy of these calculations.

1 Introduction

Meteoroids ejected from their parent bodies are dispersed from their original orbits by various gravitational and non-gravitational forces, including the gravity of the Sun and planets, radiation pressure and Poynting-Robertson effect. The very smallest sub-micron particles are blown out of the solar system by radiation forces. Other small grains spiral into the sun as a result of the Poynting-Robertson drag force. However, the dynamics of larger visual-meteor-forming particles are not strongly affected by these processes. It is therefore likely that their lifetimes are dominated by collisions with other particles in the interplanetary dust cloud (Grün et al., 1985) or by other processes.

Understanding the timescale on which a given meteoroid is likely to be destructed by a collision is important for understanding the evolution of streams and the sporadic background. Currently available estimations of the collisional lifetime of meteoroids rely on old models of the interplanetary dust flux and velocity distribution (Tokhtas'ev,1982; Grün et al., 1985; Steel and Elford, 1986). Here we use ESA's Interplanetary Meteoroid Environment Model (IMEM) (Dikarev et al., 2005) to recalculate the collisional lifetimes, and discuss consequences for meteor showers resulting from low-perihelion parent bodies.

2 Calculation of collisional lifetimes

Here we describe the calculation of the collisional lifetimes for meteoroids in interplanetary space. This is dependent on the number of impactor particles (the interplanetary dust cloud), and the size and properties of the meteoroid, which determines how often it is hit, and what energy is required to disrupt the particle. The relative velocity of the collision is also necessary, in order to determine the energy of the collision.

The lifetime is not a fixed quantity, because the collisional probability varies along the orbit of the particle – nearer the Sun, the flux of interplanetary particles is higher, and the probability of impact increases. It will also vary as the orbit of the particle changes due to gravitational perturbations and Poynting-Robertson drag. We therefore evaluate the collisional probability at 100 points along one orbit of the meteoroid, and sum the contributions. This provides us with the collisional lifetime for a particular type of orbit. It describes the collisional lifetime of a specific object only when the orbit is stable.

We calculate the rate of catastrophic collisions – those for which the largest fragment is half the size of the original mass. We assume that the meteoroid is disrupted by the smallest size of particle able to do so. We then require (1) a formalism to describe the size of this projectile, and (2) a model to describe the flux of particles of this size.

A target particle with mass m_1 is catastrophically disrupted by a projectile of mass m_2 when $m_1 \leq \Gamma m_2$. Here Γ depends on particle properties (target particle density ρ (g/cm^3) and unconfined compressive strength S_c (kbar)) and the impact speed v (km/s). As derived from results of Gault (1973) and Hörz et al. (1975), and given by Grün et al. (1985):

$$\Gamma = 9.76 \times 10^2 S_c^{-0.45} (m_1/\rho_1)^{0.075} v^2$$

These equations are used to calculate the mass of a particle that can cause catastrophic disruption for a given impact velocity. The collisional probability is calculated by determining the number of particles with this mass that impact the meteoroid. Grün et al. (1985) use fluxes at 1 AU derived from Pegasus and HEOS-2 measurements, and assumes an impact velocity of 20 km/s at 1 AU, applying a factor $(r/r_0)^{-1}$ to account for the speed dependent with heliocentric distance r (AU).

We take projectile particle fluxes and impact velocities from IMEM. The number of impacts is the sum of the flux of particles from six different impact directions and five different impactor populations (two cometary, two asteroidal, and interstellar dust) (Dikarev et al., 2005). This allows us to calculate the collisional lifetime along any orbit in the inner solar system.

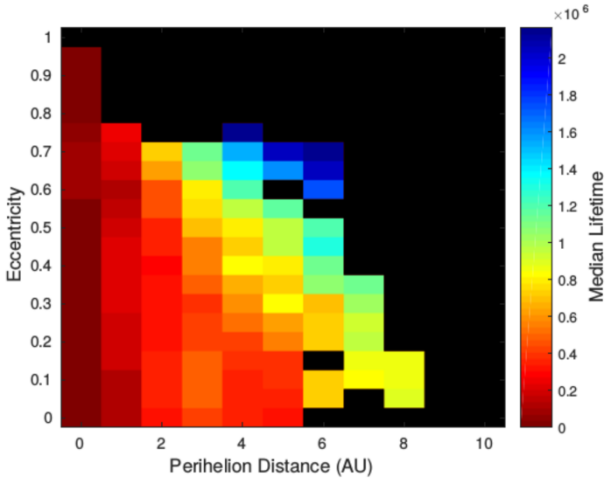

Figure 1 – Median collisional lifetime for particles with a radius of 100μm and a bulk density of 2000 kg/m^3, as a function of perihelion distance and eccentricity, for a sample of 4000 solar system objects.

The collisional lifetimes at Earth orbit agree with the results of Grün et al. (1985), as expected. We then calculate the lifetimes along the current orbits of more than 4000 solar system bodies: asteroids, comets, and planets, and evaluate the median lifetime for prograde orbits for each combination of perihelion distance and eccentricity (*Figure 1*). This demonstrates that lifetimes are longest for orbits with high perihelion distance and eccentricity, and shortest for low perihelion orbits.

3 Results for meteor showers

In *Figure 2* we show the collisional lifetime as a function of mass for different meteor shower parent bodies, for a bulk density of 2000 kg/m^3. The collisional lifetimes of visual-meteor-sized (~1–10mm) meteoroids are generally long (10^4 or 10^5 years). In addition, meteoroids from Jupiter family comets can survive longer because their orbits are frequently altered by Jupiter. However, for some comets with low perihelion and low-moderate eccentricity, the collisional lifetimes can be short (*Figure 2*). These lifetimes are also dependent on the bulk density and the compressive strength of the particles. These calculations find that Geminid meteoroids of size 5 mm (10^{-3} kg) survive 500–1000 years, for densities 1000–3500 kg/m^3, respectively. 100 μm particles survive roughly 10 times longer. Thus, large particles in the Geminids and other near-sun streams might be removed by collisions on timescales shorter than the expected lifetimes of the shower particles.

These results are dependent on the accuracy of the IMEM interplanetary dust model and our collisional model. The equations given in *Section 2* arise from experiments made with a narrow range of materials that may not well describe the composition, structure or velocities of meteoroids.

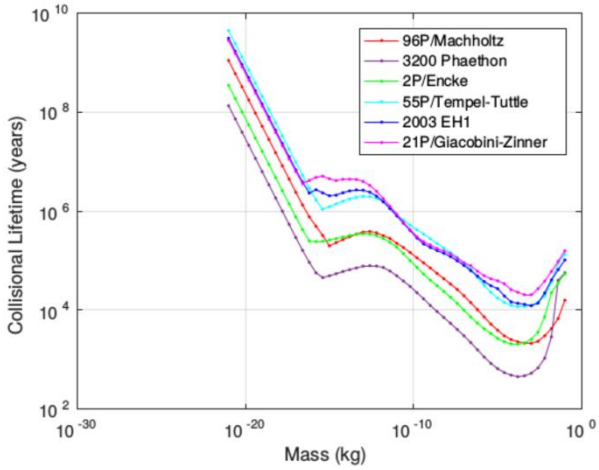

Figure 2 – Collisional lifetime as a function of mass for six probable meteor shower parent objects, for meteoroids with a bulk density of 2000 kg/m^3.

Meteor shower studies and other investigations of the dust cloud might provide additional constraints to the model. For instance, no lack of large particles was found in the mass distribution of the Geminids, which might be indicative of short lifetimes, and dynamical models indicate that this meteor shower is unlikely to be able to form over only a few hundred years (Ryabova, 1999). Ryabova (1999) also estimates the age of the Geminids at about 2000 years. Additionally, other authors find meteoroid modeling requires higher collisional lifetimes, at least for some particle sizes, than those given by the model of Grün et al. (1985) (Nesvorný et al., 2012; Pokorný et al., 2014).

4 Conclusion

We present calculations of the collisional lifetimes of meteoroids using the formalism of Grün et al. (1985) and meteoroid fluxes and velocities from the IMEM model. We find low lifetimes for meteoroid streams with low perihelion distances.

However, further work is required to define the collisional lifetimes of large meteoroids. The lifetime depends strongly on the physical parameters of the meteoroid, including the bulk density and compressive strength. It also depends on the definition of the Γ parameter. Existing experimental results may not well describe the materials and impact velocities of meteoroids in interplanetary space. We are therefore investigating if the results of simulations of collisions of interplanetary particles can be used to constrain this parameter, and provide more relevant lifetime estimates.

It has also been suggested that additional mechanisms may cause large grains to break up on very short timescales (Jenniskens, 2015). It is clear that questions remain about the dominant mechanisms for removing interplanetary meteoroids as a function of size.

Acknowledgments

This work is funded under ESA contract 4000114513/15/NL/HK.

References

Dikarev V., Grün E., Baggaley J., Galligan D., Landgraf M. and Jehn R. (2005). “The new ESA meteoroid model”. *Advances in Space Research*, **35**, 1282–1289.

Giese R. H. and Grün E. (1976). “The compatibility of recent micrometeoroid flux curves with observations and models of the zodiacal light”. *Interplanetary Dust and Zodiacal Light*, **48**, 135–139.

Grün E., Zook H. A., Fechtig H. and Giese R. H. (1985). “Collisional balance of the meteoritic complex”. *Icarus*, **62**, 244–272.

Hörz F., Schneider E., Gault D. E., Hartung J. B. and Brownlee D. E. (1975). “Catastrophic rupture of lunar rocks - A Monte Carlo simulation”. *The Moon*, **13**, 235–258.

Jenniskens P. (2015). “Meteoroid Streams and the Zodiacal Cloud”. In Michel P., DeMeo F. E. and Bottke W. F., editors, *Asteroids IV*. University of Arizona Press, Tucson, pages 281–295.

Nesvorný D., Jenniskens P., Levison H. F., Bottke W. F., Vokrouhlický D. and Gounelle M. (2010). “Cometary Origin of the Zodiacal Cloud and Carbonaceous Micrometeorites. Implications for Hot Debris Disks”. *The Astrophysical Journal*, **713**, 816–836.

Pokorný P., Vokrouhlický D., Nesvorný D., Campbell-Brown M. and Brown P. (2014). “Dynamical Model for the Toroidal Sporadic Meteors”. *The Astrophysical Journal*, **789**, id. 25, 20 pages.

Ryabova G. O. (1999). “Age of the Geminid Meteor Stream (Review)”. *Solar System Research*, **33**, 224–238.

Tokhtas’ev V. S. (1982). “Influence of collisions of meteor bodies on the evolution rate of meteoroid streams”. (Russian Title: Влияние столкновений между телами на скорость эволюции метеорных потоков), *Meteor matter in the interplanetary space*, In Bel'kovich O. I., Babadzhanov P. B., Bronshten V. A. and Sulejmanov N. I., editors, Proceedings of the All-USSR symposium held in Kazan, USSR, Sept. 9-11, 1980. Moskow-Kazan, pages. 162–174.

Galina Ryabova and Rachel Halina Soja.

EN091214 Zdar – one of the most precisely documented meteorite fall

Pavel Spurny, Jiri Borovicka, Jakub Haloda, Lukas Shrbeny and Tomas Zikmund

Astronomical Institute of the Czech Academy of Sciences, 251 65 Ondřejov, Czech Republic
pavel.spurny@asu.cas.cz

This contribution will provide an overview of the current status of fireball observations conducted by the Astronomical Institute of the Czech Academy of Sciences in Ondrejov and will bring a detailed analysis of the Zdar nad Sazavou meteorite fall in the Czech Republic on 9 December 2014, which is one of the most precisely determined and predicted meteorite fall in history.

Pavel Spurny giving his lecture.

The Swedish Allsky Meteor Network: first results

Eric Stempels[1] and Johan Kero[2]

[1] **Department of Physics & Astronomy, Uppsala University, Sweden**
Eric.Stempels@physics.uu.se

[2] **Swedish Institute of Space Physics, Kiruna, Sweden**
kero@irf.se

The Swedish Allsky Meteor Network started operations with two cameras in early 2014 and has since grown steadily. Currently, seven stations are active and several more will come online in the near future. The network to a large degree relies on low-cost stations run by private individuals or small societies of amateur astronomers. Originally based on the Danish meteor network Stjerneskud, the central node of Uppsala University provides the network with the necessary infrastructure, such as a continually updated software distribution and automatic processing of data from all stations. Although covering a very large land mass with relatively low resources is challenging, there have up to now been several well-observed events, often in collaboration with observations from neighboring countries. We give a short overview of the network's current status, chosen technical solutions, and some results.

1 Introduction

The Swedish Allsky Meteor Network was initiated as a response to the need of objective and empirical references for (often exaggerated) reports of meteors and meteorites in popular media. It has since grown to a fully integrated network of self-reporting all-sky camera stations that deliver data for in-depth analysis of meteors and fireballs.

Starting from a single camera at Uppsala University in early 2014, the network currently consists of seven active stations, of which four are run by amateur astronomers. Another four stations are expected to come online during 2016, and a few more stations are in an early planning stage. See also *Figure 1*.

Very similar networks have been implemented in Denmark[1] (currently eight cameras) and Norway[2] (three cameras). There is a close collaboration among these networks, and we have established a common data format for easy exchange of observations.

Detailed information on activities and results of the Swedish Allsky Meteor Network can be found online[3] (albeit in Swedish).

2 Implementation

In terms of surface area Sweden is the third largest country in Europe (after France and Spain), but has a relatively small population mainly concentrated in urban areas in the south and east. It is therefore challenging to plan for a dense network with small baselines. Instead, the network is constructed as a "citizen science" project, where interested individuals, schools and amateur astronomer societies can contribute. Central support to the network is offered by Uppsala University, providing central computing resources, software development and webpages. Because of this format, the chosen implementations for software and hardware are deliberately kept simple, flexible and at low cost. A typical station costs €500 – €1000, depending on the exact choice of components, and there is hardly any maintenance required.

Hardware solutions

A dedicated software package has been developed for this project. This package only requires a moderately fast CPU, and is able to run on recycled computers or small card-based Linux devices (ODROID, Raspberry Pi2 or better). The software implements the *Video4Linux (V4L)* library and therefore supports any V4L video device. While typical webcams cannot provide the sensitivity necessary for capturing meteors, V4L also supports framegrabbers, which makes it possible to combine these with high-sensitivity analog video cameras such as the popular WATEC 902H2 Ultimate (ca 0.4 Mpix) video camera. Currently four out of seven active stations use this solution, together with small f/2 180-degree fisheye lenses.

Recently, several affordable digital camera chips with fast readout have become available through the ZWO ASI brand of cameras, for which also a Linux-based API is available. Experiments with a 1/3" ASI120MC (1.2 Mpix) and the low-noise 1/1.9" ASI185MC (2.3 Mpix) led us to add support for these cameras to our software. With these new cameras routine detection of meteors down to ca $V = 1^m$ is possible, gaining about 1–2 magnitudes compared to a WATEC 902H2 Ultimate, as well as a strong improvement in the astrometric solution due to the increased resolution. ZWO ASI cameras will be implemented in at least two stations during 2016.

Software solutions

Software for all stations is distributed by Uppsala University through the *Subversion* version control package. Each station monitors the sky at a rate of

[1] "Stjerneskud", see http://www.stjerneskud.info
[2] "Norsk Meteornettverk", see http://norskmeteornettverk no
[3] http://www.astro.uu.se/meteorwiki

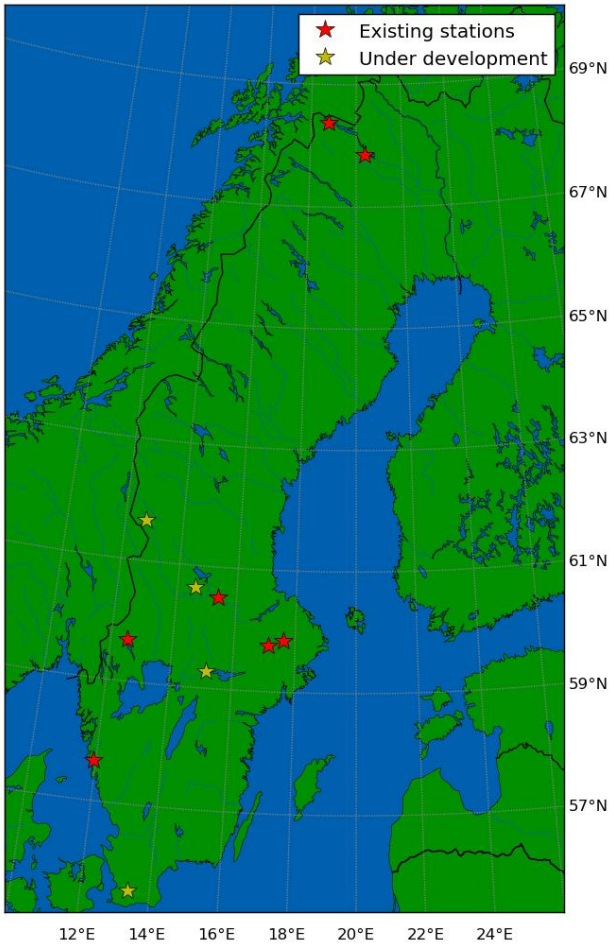

Figure 1 – An overview of the current extent of the Swedish Allsky Meteor Network.

10–25 fps, and performs on-line motion analysis and only saves video data when significant meteor-like events are detected. In addition, each node archives one-minute stacked frames for future reference. Data from each station is available on a webpage in near real-time.

Recorded events are processed at each station, calculating an astrometric solution for the observed trajectory at the sky. Events are then handed over to the central node in Uppsala, where an automatic triangulation and speed analysis of common events is performed. Events with deep atmospheric penetration are analyzed in further detail with a dark-flight code developed in Uppsala, based on the formulation of Pecina and Ceplecha (1983) and Ceplecha and Revelle (2005 – single body solution), including wind shift. The code is able to reproduce the dark flight and impact locations of other well-studied meteor falls, such as Neuschwanstein (2002), Benešov (1991) and Maribo (2009).

3 Results

During two years of operation the Swedish Allsky Meteor Network has detected a wide range of events. During prominent meteor showers, such as the Perseids or the Geminids, several hundreds of meteors were recorded. For about half of these events triangulated trajectories are available. Sporadic and bright fireballs that require dark-flight modelling are detected at a rate of about once to

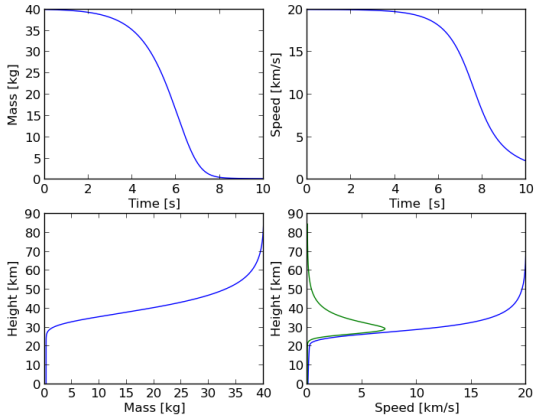

Figure 2 – Four graphs showing the simulated evolution of the meteoroid body of the August 13, 2015 fireball. The green line on the bottom right shows the deceleration of the meteoroid in km s^{-2}.

twice per month. Any bright event that might trigger public interest is published online through the network's homepage.

A good example of what the network can achieve is the potentially meteorite-dropping fireball that was observed in the early morning of August 13, 2015. Since the fireball occurred on the same night as the Perseid meteor shower, many casual observers witnessed this event, and some even caught the luminous trail on camera. The event itself is not related to the Perseids, as is evident from its reconstructed infall trajectory.

The fireball was about as luminous as the full moon (at a distance of about 100 km), and was visible for more than 7 seconds. Five automated stations recorded the fireball, two near Uppsala, one almost below the track in Arvika, as well as two stations of the Norwegian network. The combined video data suggest an infall velocity of 20.0 km/sec, and the meteoroid appears to have come from an Aten-type orbit. As can be seen from the infall and dark-flight simulation in *Figure 2* the body most likely fragmented at a height of about 35-40 km, when the meteoroid experienced a large deceleration, corresponding to a dynamic pressure of about 1 MPa. The final mass of the meteoroid fragment that reached the ground is estimated to be about 0.5 kg. Although the luminous path of the fireball is completely within Swedish territory, the predicted fall area is 10 km into Norway, close to the town of Aremark. Searches for meteorites have been conducted in this area, but no finds have been reported. These results are in agreement with independently calculated solutions by the Finnish URSA Fireball Network (Lyytinen, priv. comm.).

Another notable event detected by the Swedish network was an explosive and very luminous and slow fireball south of Stockholm in the early evening of October 23, 2015. Although simulations indicate a very high probability for this event to generate meteorites the impact area was over the Baltic Sea.

Although central Sweden now is reaching an adequate coverage of stations with baselines of 300 – 400 km, several fireballs were detected at great distances. Currently, the most distant events detected were recorded from Uppsala, at 650 km (Copenhagen) and 700 km (St Petersburg). Even though the accuracy of detections at such distances is not very large, these observations make it possible to confirm or deny that fireballs occurred, thereby providing valuable feedback to local media.

4 Future plans

Apart from integrating new camera models in software, most development efforts are currently in improving the collaboration with neighboring countries, if possible through automatic exchange of data. In addition, we plan to continue the expansion of the Swedish network in terms of a "citizen science" project. While this is likely to improve coverage in central and southern Sweden, it will be more challenging to monitor northern Sweden, with a relatively low population density. Depending on the available funding, we are therefore also considering to design "packaged" stations, where a prospective user only needs to assemble the station and make it available online.

Acknowledgments

We acknowledge support from the *Märta and Erik Holmberg endowment*, which financed the first allsky meteor camera in Sweden.

References

Pecina P. and Ceplecha Z. (1983). "New aspects in single-body meteor physics". *Bulletin of the Astronomical Institutes of Czechoslovakia*, **34,** 102–121.

Ceplecha Z. and Revelle D. O. (2005). "Fragmentation model of meteoroid motion, mass loss, and radiation in the atmosphere". *Meteoritics and Planetary Science*, **40,** 35–54.

Reception manned by Dragana Okolić and Dušan Bettonvil.

No sign of the 2015 Daytime Sextantids through combined radio observations

Giancarlo Tomezzoli[1] and Lorenzo Barbieri[2]

[1] **EurAstro Association, Zeppelinstrasse 43, D-81669 Munich, Germany**
gt@gmx.de

[2] **Associazione Astrofili Bolognesi, Via Sebastiano Serlio 25/2, c/o Parco DLF, I-40100 Bologna, Italy**
barbieriofiuco@gmail.com

To investigate the presence or absence of the daytime Sextantids in the year 2015, the EurAstro Radio Station (EARS) in Munich (DE) performed a combined radio observation campaign together with the Radio Astronomy and Meteor Bologna (RAMBO) radio station located in Bologna (IT). The combined radio observations of EARS and RAMBO are in mutual agreement and confirm that, as in the year 2014, also in the year 2015 no evidence has existed of a meteor activity due the 2015 daytime Sextantids.

1 Introduction

DSX 221[1] also indicated as Sextantids is a daytime meteor shower having features not well-known. It was discovered by Weiss in September 1957, who recorded 30 meteors per hour. No more Sextantids were reported until 1961. The next shower was observed in 1969, so the hypothesis has been advanced that DSX 221 is a four year periodic meteor shower.

Following the invitation made by Rendtel at the IMC 2014 in Giron, France (Rendtel, 2014) to observe DSX 221 in the period 30 September – 05 October 2014 by any possible means, the EurAstro Radio Station (EARS) in Munich, Germany (48°07'58,0”N, 11°34'47.3”E) performed radio observation of DSX 221 in the recording period 30/09/2014, 07h00m UT – 05/10/2014, 16h00m UT (Tomezzoli and Verbeeck, 2015). The conclusion was that the meteor activity of DSX 221, if present at all, was at a much lower level than the sporadic meteor activity.

In order to investigate the presence or absence of the daytime Sextantids in the year 2015, EARS performed a combined radio observation campaign together with the Radio Astronomy and Meteor Bologna (RAMBO) radio station located in Bologna, Italy (44°30'28,9”N, 11°21’12,0”E).

2 EARS and RAMBO combined radio observation

EARS, based on the forward scattering principle and operated by Giancarlo Tomezzoli, adopted the same observation configuration adopted in the year 2014: radio beacon from the GRAVES radar (emitter at Broyes-lès-Pesmes, 47°20’51.72”N, 05°30’58.68”E, about 500 km from Munich), vertical antenna J-Pole 144, receiver ICOM 1500 (USB mode, 143.049 MHz), computer Pavillion dv6 (processor Intel Core Duo T2500) and SpecLab V26 b10 as recording software. The EARS radio observation in the recording period from 27/09/2015, 08h15m UT – 03/10/2015, 07h30m UT proceeded smoothly without problems. Meteor radio echoes were counted visually by Giancarlo Tomezzoli by looking at the JPG images recorded by SpecLab every 5 minutes.

RAMBO, based on the forward scattering principle and operated by Lorenzo Barbieri and others, adopted the following observation configuration: radio beacon from the GRAVES radar (about 500 km from Bologna), Yagi 7 elements antenna, Yaesu 897 receiver, Arduino microcontroller and homemade recording software. The RAMBO radio observation in the recording period from 28/09/2015, 00h00m UT – 04/10/2015, 00h00m UT proceeded smoothly without problems. Meteor radio echoes were counted by an ad hoc developed RAMBO software and plotted n graphic form by using Gnuplot[2].

The EARS observed hourly meteor radio echo rates in the EARS observing period are summarized in the diagrams of *Figure 1*. Evidently the meteors of DSX 221, if any, were superposed on the ever present sporadic meteors. To better characterize the meteor radio echoes in the recording period, an underdense radio echo from the images recorded by EARS was assumed as underdense reference radio echo to distinguish between recorded underdense strong and faint radio echoes. The results of

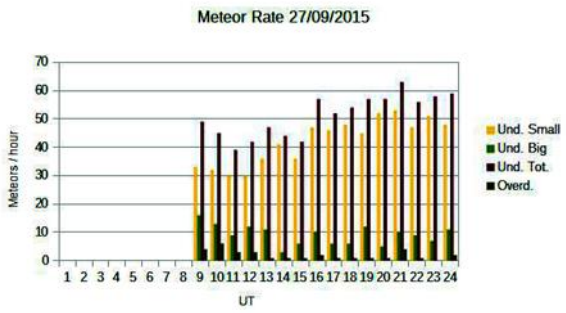

Figure 1a – EARS observed hourly meteor radio echo rates during the EARS recording period: 27 September 2015.

[1] http://www.bbc.co.uk/dna/ptop/plain/A40721212

[2] http://www.gnuplot.info/

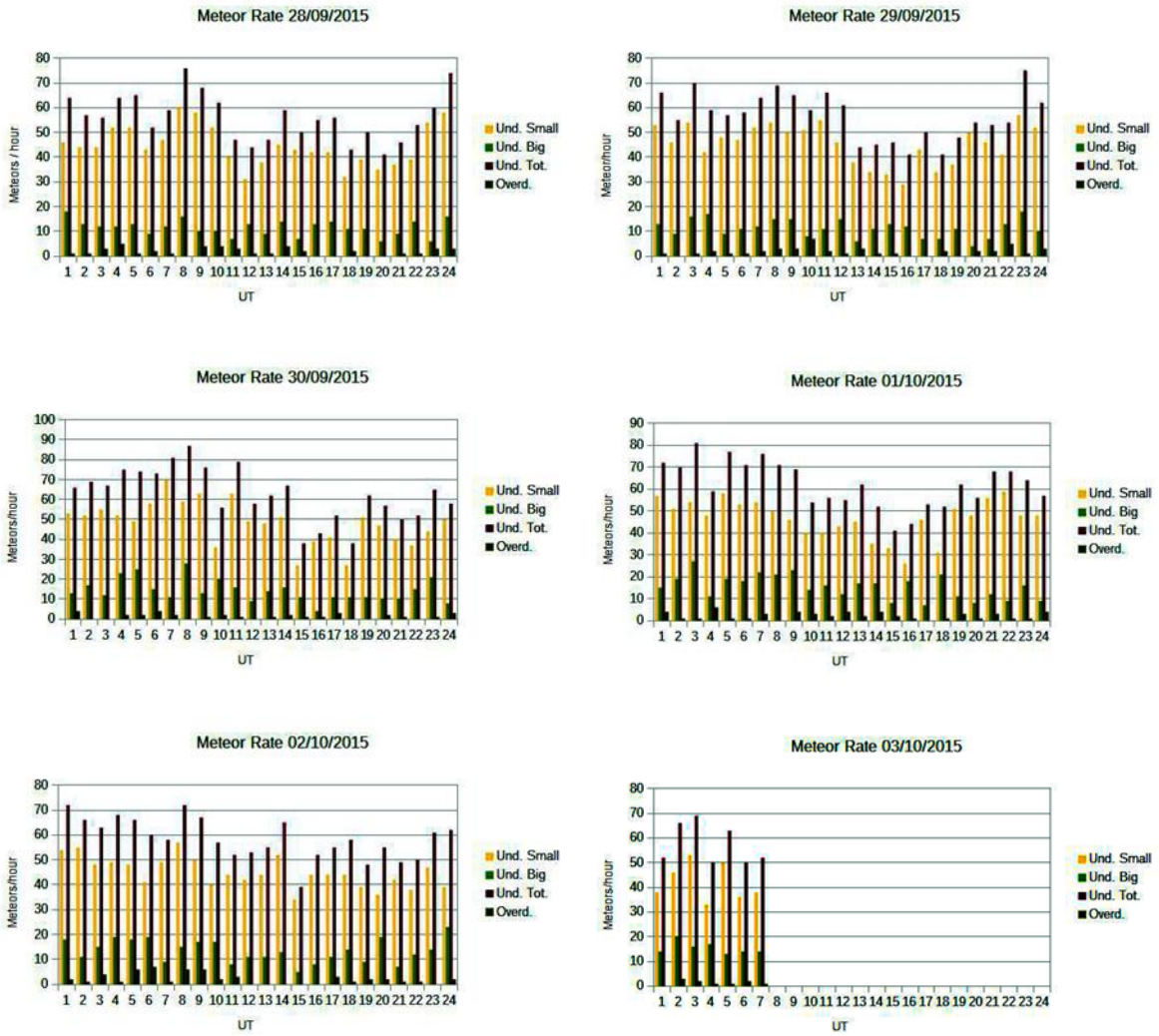

Figure 1b, 1c, 1d, 1e, 1f, 1g – EARS observed hourly meteor radio echo rates during the EARS recording period: 28 September – 3 October 2015.

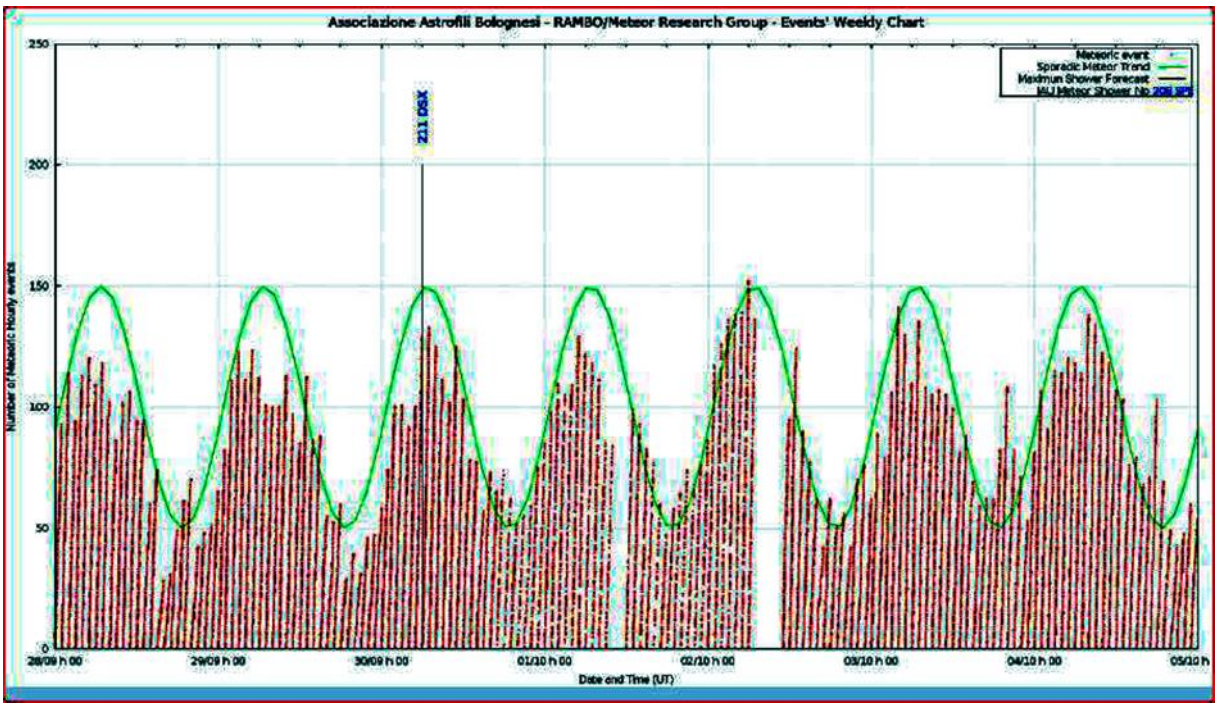

Figure 2 – RAMBO observed hourly meteor radio echo rates during the RAMBO recording period – the position of the expected maximum of DSX 221 is indicated.

the comparison are shown in *Figure 1*. Looking at the diagrams in *Figure 1*, it is possible to recognize that during the EARS recording period no maximum attributable to DSX 221 was detected.

The RAMBO observed hourly meteor radio echo rates in the RAMBO observing period are summarized in the diagram of *Figure 2*. Looking at the diagram in *Figure 2*, it is possible to recognize that during the RAMBO recording period no maximum attributable to DSX 221 was detected.

3 Conclusions

The combined radio observations of EARS and RAMBO are in mutual agreement and confirm that, as in the year 2014, also in the year 2015 no evidence has existed of a meteor activity due the 2015 daytime Sextantids.

References

Rendtel J. (2014). "Daytime meteor showers". In Rault J.-L. and Roggemans P., editors, *Proceedings of the International Meteor Conference*, Giron, France, 18-21 September 2014. IMO, pages 93–97.

Tomezzoli G., Verbeeck C. (2015). "No sign of the 2014 Daytime Sextantids and mass indexes determination from radio observations". In Rault J.-L. and Roggemans P., editors, *Proceedings of the International Meteor Conference*, Mistelbach, Austria, 27-30 August 2015. IMO, pages 165–170.

Mirel Birlan and Tudor Georgescu in a silent corner in the restaurant.

AMOS - trajectory and orbital data from SVMN and Canary Islands

Juraj Tóth[1], Leonard Kornoš[1], František Ďuriš[1], Pavol Zigo[1], Štefan Gajdoš[1], Dušan Kalmančok[1], Jozef Világi[1], Jaroslav Šimon[1], Marek Buček[1], Jaroslav Šimon[1], Miquel Serra-Ricart[2], Juan Carlos Perez[2], Javier Licandro[2], Ovidiu Vaduvescu[2] and Jürgen Rendtel[3]

[1] **Dept. of Astronomy, Physics of the Earth and Meteorology, Faculty of Mathematics, Physics and Informatics, Comenius University in Bratislava, Slovak Republic**
toth@fmph.uniba.sk

[2] **Instituto de Astrofísica de Canarias, Canary Islands, Spain**

[3] **International Meteor Organization**

The Slovak Video Meteor Network based on four stations from October 2013 (double station from 2009) and two cameras on the Canary Islands from March 2015 have recorded several tens of thousands meteors by the end of 2015. Naturally, only a part (about 20%) was observed simultaneously. Using precise all-sky astrometry (Borovička, 1995) and our own trajectory and orbit program based on Ceplecha (1987), we gained the reliable video meteors database for further meteor studies.

1 Introduction

Observations are performed every clear night, even in partly cloudy sky and during all Moon phases. The optical system is identical in all four Slovakian stations (camera resolution 1280 × 960 pixels, 15 frames per second, Tóth et al., 2011; Zigo et al., 2013). The only difference with the Canary Islands and Atacama Desert stations in Chile is the camera resolution 1600 x 1200 pixels, 20 frames per second (Tóth et al., 2015). All together from March 2016, 8 AMOS cameras are working from both hemispheres.

Currently, the UFOAnalyzer software (SonotaCo) provides us the identification of stars and meteors on individual frames. Astrometry from the all-sky reduction method of Borovička (1995) is used for special events following the atmospheric trajectory and orbit calculation by our own program MT 2.4 based on Ceplecha (1987). Automatization and more precise photometric reduction of data reduction will be done in the near future.

The database will be publicly available with all atmospheric and orbital parameters including uncertainties from the Monte Carlo error propagation (Kornoš et al., 2015).

2 Conclusion

We have successfully developed, tested and installed AMOS cameras in Slovakia, on the Canary Islands and in the Atacama Desert in Chile. The data will be available soon.

Acknowledgment

This work was supported by APVV-0517-12, and VEGA 1/0225/14.

References

Borovička J., Spurný P. and Keclikova J. (1995). “A new positional astrometric method for all-sky cameras”. *Astronomy and Astrophysics Supplement*, **112**, 173–178.

Ceplecha Z. (1987). “Geometric, dynamic, orbital and photometric data on meteoroids from photographic fireball networks”. *Bulletin of the Astronomical Institutes of Czechoslovakia*, **38**, 222–234.

Kornoš L., Ďuriš F. and Tóth J. (2015). “Astrometric precision and orbit determination by AMOS”. In Rault J.-L. and Roggemans P., editors, *Proceedings of the International Meteor Conference*, Mistelbach, Austria, 27-30 August 2015. IMO, pages 101–104.

Tóth J., Kornoš L., Vereš P., Šilha J., Kalmančok D., Zigo P. and Világi J. (2011). “All-Sky Video Orbits of Lyrids 2009”. *Publications of the Astronomical Society of Japan*, **63**, 331–334.

Tóth J., Zigo P., Kalmančok D., Simon J., Kornos L., Világi J., Rudawska R., Serra-Ricart M., Perez J. C. and Licandro J. (2015). “5 months of AMOS on the Canary Islands”. In Rault J.-L. and Roggemans P., editors, *Proceedings of the International Meteor Conference*, Mistelbach, Austria, 27-30 August 2015. IMO, pages 63–65.

Zigo P., Tóth J. and Kalmančok D. (2013). “All-Sky Meteor Orbit System (AMOS)”. In Gyssens M. and Roggemans P., editors, *Proceedings of the International Meteor Conference*, La Palma, Canary Islands, Spain, 20-23 September 2012. IMO, pages 18–20.

Expedition Atacama - project AMOS in Chile

Juraj Tóth[1] and Stanislav Kaniansky[2]

[1] **Dept. of Astronomy, Physics of the Earth and Meteorology, Faculty of Mathematics, Physics and Informatics, Comenius University in Bratislava, Slovak Republic**
toth@fmph.uniba.sk

[2] **Hvezdáreň v Banskej Bystrici, organizačná súčasť Krajskej hvezdárne a planetária M. Hella v Žiari nad Hronom**

The Slovak Video Meteor Network operates since 2009 (Tóth et al., 2011). It currently consists of four semi-automated all-sky video cameras, developed at the Astronomical Observatory in Modra, Comenius University in Bratislava, Slovakia. Two new generations of AMOS (All-sky Meteor Orbit System) cameras operate fully automatically at the Canary Islands, Tenerife and La Palma, since March 2015 (Tóth et al., 2015). As a logical step, we plan to cover the southern hemisphere from Chile. We present observational experiences in meteor astronomy from the Atacama Desert and other astronomical sites in Chile. This summary of the observations lists meteor spectra records (26) between Nov.5–13, 2015 mostly Taurid meteors, single and double station meteors as well as the first light from the permanent AMOS stations in Chile.

1 Introduction

The main aim of the expedition was to select two sites for the new AMOS cameras in Chile. Sites need to have a local infrastructure and good observing condition. Moreover, the responsible persons need to agree with such installation.

2 Sites selection and installation

In this paper, we present observational experiences in meteor astronomy from the Atacama Desert and other astronomical sites in Chile. The summary of the observations lists meteor spectra records (26) between Nov. 5–13, 2015 mostly from Taurid meteors (*Figure 2*). We also present fish-eye views from selected sites with ideal astronomical conditions as well as sky brightness observations. We measured the mean sky background at SpaceObs (*Figure 1*) of 21.75 mag./sq.arsec influenced by strong airglow emission.

Finally, we have selected two sites for location and installation of the AMOS cameras at SpaceObs near San Pedro de Atacama and Paniri Caur observatory near Calama. The distance between these two stations is 83.5 km and is ideal for trajectory and orbit calculations depending on the meteor plane with respect to both stations. The small private observatory Paniri Caur is situated in the village Chiu-Chiu 30 km North-East from Calama city. The altitude of the observatory is at 2533 m above sea level. The second site was selected after the agreement with Alain Maury in SpaceObs, which is 6 km South of San Pedro de Atacama at 2400 m altitude.

The installation of the two AMOS systems was performed successfully in March 2016 by Pavol Zigo and Jaroslav Šimon.

3 Conclusion

We have successfully selected and installed AMOS cameras in the Atacama Desert in Chile. The cameras are working fine in the desert conditions.

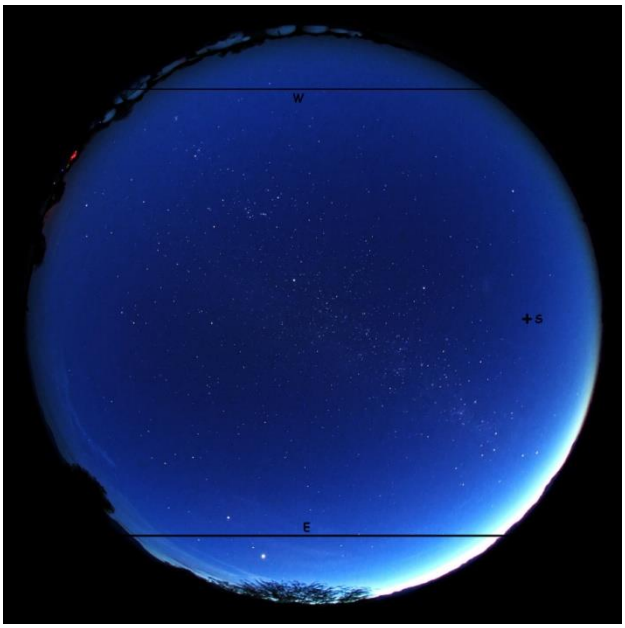

Figure 1 – Fish-eye view of the sky from San Pedro de Atacama (SpaceObs). The actual field of view of AMOS is depicted by black lines on the West and East side.

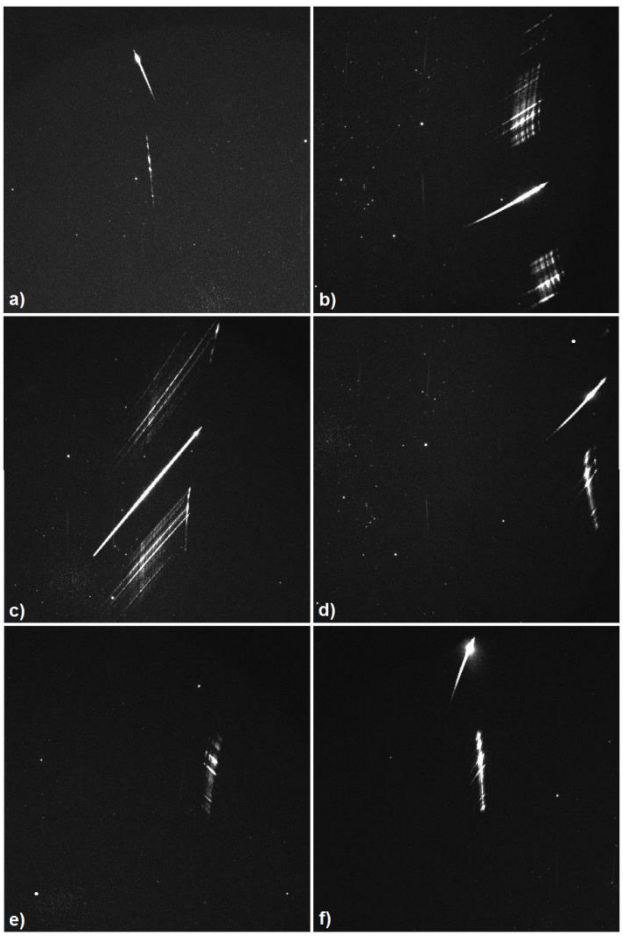

Figure 2 – Meteor spectra of Taurids by the AMOS camera with 500 lp/mm gratings. The observation was performed from San Pedro de Atacama on November 5–12, 2015.

Acknowledgment

This work was supported by APVV-0517-12, and VEGA 1/0225/14. We would like to thank Ján Mäsiar, R. Piffl, I. Majchrovič for the photographic techniques we used during the expedition and the local staff in SpaceObs, Paniri Caur and Pangue Observatory.

References

Tóth J., Kornoš L., Vereš P., Šilha J., Kalmančok D., Zigo P. and Világi J. (2011). "All-Sky Video Orbits of Lyrids 2009". *Publications of the Astronomical Society of Japan*, **63**, 331–334.

Tóth J., Zigo P., Kalmančok D., Simon J., Kornos L., Világi J., Rudawska R., Serra-Ricart M., Perez J. C. and Licandro J. (2015). "5 months of AMOS on the Canary Islands". In Rault J.-L. and Roggemans P., editors, *Proceedings of the International Meteor Conference*, Mistelbach, Austria, 27-30 August 2015. IMO, pages 63–65.

AMOS-Spec - meteor spectra from Modra Observatory

Juraj Tóth[1], Pavol Matlovič[1], Regina Rudawska[2], Pavol Zigo[1] and Dušan Kalmančok[1]

[1] **Dept. of Astronomy, Physics of the Earth and Meteorology, Faculty of Mathematics, Physics and Informatics, Comenius University in Bratislava, Slovak Republic**
toth@fmph.uniba.sk

[2] **ESA/ ESTEC, Noordwijk, the Netherlands**

We present results from the meteor spectra program at Modra observatory, Slovakia (Comenius University in Bratislava) in the period November 2013 – April 2016. The advantage of the program is the presence of the Slovak Video Meteor Network and close collaboration with the European Fireball Network and CEMENt and EDMONd networks which provide trajectory and orbital data for almost all observed meteor spectra.

1 Introduction

The primary aims of our research are focused on determining the spectral and physical differences between cometary and asteroidal bodies, the role of sodium abundance in meteoroids, and the spectral characteristics of different shower and sporadic meteors. We utilize the observations of the spectral All-sky Meteor Orbit System (AMOS-Spec), which provides a systematic survey of meteor spectra since November 2013. The system is installed at the Modra observatory with the setup based on the standard AMOS system (Tóth et al., 2011) equipped with a 30 mm f/3.5 lens (FOV ~ 140° × 100°), and 1000 grooves/mm grating yielding a spectral resolution of ~ 1.3 nm/pix. The absolute limiting magnitude of a meteor with spectrum is around -2.

First results (Rudawska et al., 2016) demonstrated the capability of the system and showed promise in pursuing our scientific goals. Here, we report the results of 131 meteor spectra collected during 11/2013 – 04/2016.

The analyzed spectral events were corrected for dark current, flat-fielded, and divided by the spectral response curve of the system. Before evaluating the relative intensities of studied emission lines of the meteoroid atoms and ions, the continuum radiation and atmospheric lines were subtracted from the spectrum.

2 Conclusion

The presence of the Slovak Video Meteor Network (SVMN) consisting of 4 additional AMOS stations in Slovakia enabled multi-station observations of studied meteors. Additional observations were kindly provided by Pavel Spurný (European Fireball Network) and Jakub Koukal (Central European Meteor Network). Of the 131 meteors captured with spectra, 103 were observed by multiple stations, which allows us to determine heliocentric orbits and additional physical properties of meteoroids such as the photometric mass, material strength parameters Kb and PE (Ceplecha, 1988) and dynamical pressure causing the meteoroid fragmentation (Popova et al., 2011). Results will be available in another publication.

Acknowledgment

This work was supported by APVV-0517-12, and VEGA 1/0225/14.

References

Borovička J., Koten P., Spurný P., Boček J. and Štork R. (1995). “A survey of meteor spectra and orbits: evidence for three populations of Na-free meteoroids”. *Icarus*, **174**, 15–30.

Ceplecha Z. (1988). “Earth's influx of different populations of sporadic meteoroids from photographic and television data”. *Bulletin of the Astronomical Institutes of Czechoslovakia*, **39**, 221–236.

Rudawska R., Tóth J., Kalmančok D., Zigo P. and Matlovič P. (2016). “Meteor spectra from AMOS video system”. *Planetary and Space Science*, **123**, 25–32.

Tóth J., Kornoš L., Vereš P., Šilha J., Kalmančok D., Zigo P. and Világi J. (2011). “All-Sky Video Orbits of Lyrids 2009”. *Publications of the Astronomical Society of Japan*, **63**, 331–334.

Popova O., Borovička J., Hartmann W. K., Spurný P., Gnos E., Nemtchinov I. and Trigo-Rodríguez J. M. (2011). “Very low strengths of interplanetary meteoroids and small asteroids”. *Meteoritics and Planetary Science*, **46**, 1525–1550.

Rediscovery of Polish meteorites

Zbigniew Tymiński[1,2], Marcin Stolarz[1], Przemysław Żołądek[1], Mariusz Wiśniewski[1] and Arkadiusz Olech[1,3]

[1] **Polish Fireball Network, Comets and Meteors Workshop, ul. Bartycka 18, 00-716 Warszawa, Poland**
pkim.inbox@gmail.com

[2] **National Centre for Nuclear Research RC POLATOM, ul. Sołtana 7, 05-400 Otwock, Poland**
Zbyszek.tyminski@gmail.com

[3] **Copernicus Astronomical Center, Polish Academy of Sciences, ul. Bartycka 18, 00-716 Warszawa, Poland**
olech@camk.edu.pl

The total number of Polish registered meteorites (by July 2016) including the meteoritical artifacts as Czestochowa Raków I and II is 22. Most of them are described by the pioneer of Polish Meteoritics Jerzy Pokrzywnicki who also identified the meteorite fall locations. In recent years prospectors found impressive specimens of known Polish meteorites such as Morasko: 34 kg, 50 kg, 164 kg, 174 kg and 261 kg or Pultusk: 1578 g, 1576 g, 1510 g, 610 g and 580 g expanding and determining precisely the known meteorite strewn fields.

1 Introduction

The history of meteoritics in Poland dates back to the early nineteenth century due to Vilnius Log (Dziennik Wileński) which was the only science bulletin at that time in Polish language publishing the information about the meteorites especially about the falls. The large historical meteorite drops such as Białystok (1827) and Pułtusk (1868) didn't allow the scientists to leave this extraordinary subject. In 1894 Ernest F. Chladni, German physicist, published a groundbreaking essay about falling rocks from space but decades earlier in 1825, Feliks Drzewiński presented in Polish the article "Of meteoritic stones and the reasons that could create them", unfortunately with the explanation out of truth. During today's the keen interest in the subject continues but it seems that is more by amateurs than by scientists. A very large group of Polish enthusiasts dealing with meteorites but people associated with meteorites professionally forms a small community. The phenomenon of a sizeable group of meteorite hunters in our country is supported also by the law which fortunately does not prohibits to collect meteorites (but one needs the permission of the Environment Ministry for abroad transportation), unlike archaeological sites, where searching with a metal detector can lead to serious consequences not only in Poland.

2 Most famous meteorite falls

Pułtusk, chondrite fall 1868

The largest meteorite fall observed in the modern history, before February 2013 when the superbolide Chelyabinsk appeared, was the Pułtusk meteorite. In Chelyabinsk, the bolide dropped a huge number of meteorites from which a large part is still lying in the fields around the village of Pervomaisky. The fall of Pułtusk was similar and both falls are classic examples of "meteorites shower". Pieces from the Pułtusk meteoroid (type H4/5) felt at least in the area of the village Obryte to St. Rosalie and Rzewnie (15 km long) forming a strewn field divided into two relatively equal parts by the Narew river. Around this river prospectors try their luck hunting for meteorites with a much better effect than the lottery win. Because the area was flooded in the time of the fall, some meteorites have not been picked up there. Nowadays the fact that the riverbed of the Narew is shifted and the drainage was done in the fields it gives high chances to find meteorites. Today seekers equipped with specialized detectors (for stony meteorites type VLF is recommended) bring a few to several new meteorites each year from fields in Pułtusk. The biggest masses of finds during last years were 1578 g (Bingoraj, 2008), 1510 g (Smuła, 2009), 580g (Stolarz, 2010), and 1576 g (Kosmowski, 2015). The biggest pieces discovered just after the fall were about 9 kg and two pieces of about 8 kg (one meteorite is kept by the Earth Museum of the Polish Academy of Sciences and the others are in the Natural History Museums in London and in Berlin). Pułtusk is also known from many small meteorites called "pultusk peas" – the total number was estimated to 70000 pieces (Samsonowicz, 1952). The main supplier of this meteorite for Europe was German mineral dealer F. Krantz (he sold about 7000 pieces). Thanks to him the Pultusk meteorites are in all the famous museum collections in the world. They are also in many private collections.

Białystok, eucrite fall 1827

The second famous meteorite in Poland is Białystok because of its observed fall in a time when people didn't believe that stones can originate from the "sky". The prove was about 4 kg of meteorites collected after the loudly fall event that scared many people. There are also reports of meteorites, which were kept in the homes till the 60's of the last century. In Poland, there are few specimens of the meteorite – only one sample (4 grams) is in the collection of Museum of Earth in Warsaw, the others are just a few but with not really known origin.

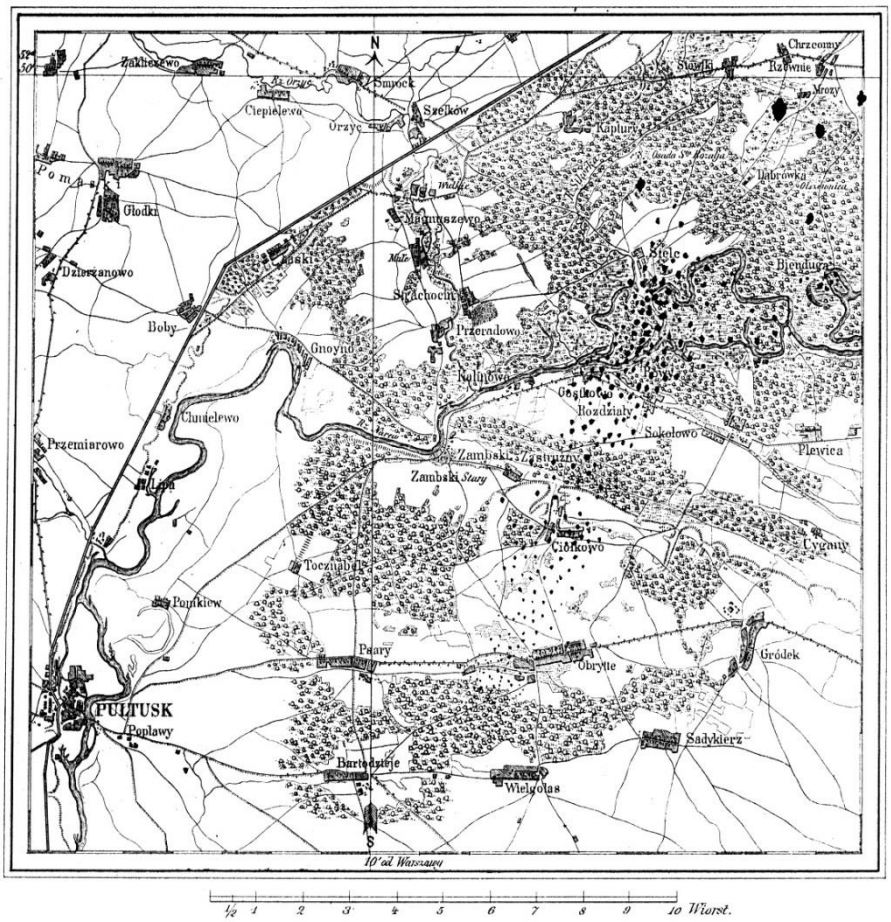

Figure 1 – The map of strewn field of Pułtusk taken from the pamphlet published by Central School in Warsaw few years after the fall.

Figure 2 – The Pułtusk 580g-specimen just after it was digged out from the soil (photo by M. Stolarz).

The meteorite is part of the Vesta asteroid group as eucrite. The Białystok strewn field is a place to which one would be happy to come back. Some people are convinced that meteorites can still be found around the Supraśl river but the effort of meteorite hunters didn't bring any positive results yet.

Łowicz, mesosiderite fall 1935

Mesosiderites, the type of meteorites that contains a similar amount of achondritic material rock and iron, most of them come from Vesta. Isotopic studies indicate their impact origin and indeed the results of the analysis made by the DOWN mission confirmed this assumption (as revealed the presence of diogenites, eucrites and howardites in the mantle of this asteroid). These are widely recognized among the Polish collectors of meteorites due to the rarity of their occurrence, and probably also due to the Łowicz meteorite, which is the representative of this group. In contrast to Bialystok this meteorite is commonly known in the site of fall. The systematic search led to the discovery of 49 kg from an estimated 110 kg – two biggest were 10 and 8 kg and the searchers noticed some craters produced by impacts. There are also documented meteorites held by the local people long after the World War II. For this reason the area of the Łowicz meteorite fall is visited by meteorite hunters and apparently even one specimen was found after years of searching. Unfortunately nothing more about this find is known.

3 Most famous meteorite finds

Świecie, IIIAB iron meteorite, 1850

The meteorite Schwetz (Świecie) has been excavated in 1850 on the left bank of the Wda river during the works on the construction of the railway line leading to East Prussia. Information from some sources mentions that 21.5 kg meteorite has been excavated at the flattening of the hill-top for the railway line from the depth of 3–4 feet and that it broke up into three parts after excavation. There is ambiguous information about the location of the meteorite find – one report describes the excavation close to the bridge girders, another one says a meteorite was found next to the Konopat town. A couple of searching campaigns were organized in this area but due to the unknown location of this find they failed.

Przełazy, iron IAB-MG iron meteorite

In the middle of the seventeenth century a local farmer in the village of Przełazy (Seeläsgen) found a lump of iron while digging a trench – it weighted 102 kg. In 1847 the stone was recognized as a meteorite and taken to Wroclaw. In 1852, Clark Smith described the meteorite as an oval body covered by a thin layer of weathered iron (0.5–1.5 mm). There were no signs of fragmentation and the meteorite was covered with regmaglypts. Today, a number of attempts were made to find any remaining fragments. Some specimens were found on the eastern side of the lake by Mr. Henryk Nowacki. There are more explorations planned to confirm the findings.

Morasko, IAB-MG iron meteorite, 1914

The Morasko represents one of the biggest iron meteorite falls in Europe. The strewn field was discovered by World War I soldiers, digging trenches in 1914 near Poznań. A mass of rock weighing approximately 77.5 kg was first extracted. Then more masses were discovered in 1936, 1956, 1992, 1995 and up to 2015 totaling about 1 ton of known meteorites. The meteorite is classified as an octahedrite IAB-MG – the most popular iron type but is distinctive from the other meteorites by the low iridium while gallium content is high. Among the Polish meteorites the Morasko is the easiest to find. It can be done using the simplest type of metal detector. There is a group of depressions associated with the fall. They were found by Jerzy Pokrzywnicki as craters. In recent years, prospectors found near them an impressive specimen of Morasko, as big as: 164 kg (Socha, 2006), 261 kg (Smuła and Skirzewska, 2012), 174 kg (Owczarzak and Nebelski, 2015).

Zakłodzie, enstantite achondrite-ungrupped

At the end of September 1998 Mr Stanisław Jachymek - collector of minerals found a "strange", heavy and rusty stone. The stone was lying on the road near the forest between the villages "Zakłodzie Dół" and "Zakłodzie Góra". After examining the find it turned out to be a rare specimen of a meteorite, weighing 8.68 kg. Further research (noble gases) showed that the meteorite (despite weathering) is a relatively fresh fall. Under the layer of the weathering a fusion crust is visible. It has been discovered that most probably the meteorite felt in April 1898 (one hundred years earlier). At this time a very bright fireball was seen from the south-east of Poland and this was described in local newspapers. Unfortunately, further explorations by Mr Jachymek and other meteorite hunters were unsuccessful.

4 Unclassified meteorite

Siewierz meteorite

The last Polish find is meteorite Siewierz, not registered yet. The meteorite sparked debate in the Polish meteorite world, because is shrouded in mystery since the story of its discovery is unknown. Meteorite Paris was recorded in 2010. It probably does not come from Paris, but was rediscovered in 2001 in a box with various objects belonging to a mining engineer working in the French Colonies. These items, together with the meteorite were purchased on sale in Paris, hence the name of the meteorite. The meteorite was registered as "unknown location". We have now a similar case – a meteorite, Siewierz, was recognized in the collectibles of the grandfather of the finder, deceased 20 years ago. A photo of the specimen and later a fragment was handed over to check by some jeweler and collector of meteorites, who confirmed its cosmic origin. In this way the finders proved this as suspicion and we have a chance for a 23th Polish meteorite. There are some investigators trying to find out the history of the meteorite either in libraries searching local archives or by scientific research.

5 Conclusion

There are relatively few meteorites discovered in Poland (22). Most of them are described by the pioneer of Polish Meteoritics Jerzy Pokrzywnicki who identified also the meteorite fall locations. Those known meteorite strewn fields can be still successfully exploited. The fields where meteorites dropped from huge bolides such as Pułtusk or Morasko can still bring additional material for research and for collections. For this reason many prospectors try to find meteorites there. In recent years meteorite hunters found impressive specimens of meteorites in Morasko: 34 kg, 50 kg, 164 kg, 174 kg and 261 kg. The pieces found last years in Pułtusk field were still smaller then known museum specimens, weighting: 1578 g, 1576 g, 1510 g, 610 g and 580 g.

The classification and description of Polish meteorites can be found on the Meteoritical Bulletin site[1].

Acknowledgment

We are thankful to the NCN for research funds – Grant no. 2013/09/B/ST9/02168.

References

Borovička J., Spurný P., Brown P., Wiegert P., Kalenda P., Clark D. and Shrbený L. (2013). "The trajectory, structure and origin of the Chelyabinsk asteroidal impactor". *Nature*, **503**, 235–237.

Buchwald V. F. (1975). "Handbook of Iron Meteorites. Their History". Distribution, Composition, and Structure, University of California Press, Berkeley.

Hanczke T. (1995). "Meteoryty i tektyty w zbiorach Muzeum Ziemi. Katalog". Muzeum Ziemi, Warszawa (*in Polish*).

Kosiński J. and Kamińska E. (2011). "The Fall and Distribution of Fragments Pułtusk Meteorite". *Acta Socientatis Metheoriticae Polonorum*, **2**, 57–66 (*in Polish*).

Krzesińska A. and Fritz J. (2014). "Weakly shocked and deformed CM microxenoliths in the Pułtusk H chondrite". *Meteoritics and Planetary Science*, **49**, 595–610.

Krzesińska A., Gattacceca J., Friedrich J. M. and Rochette P. (2015). "Impact-related noncoaxial deformation in the Pułtusk H chondrite inferred from petrofabric analysis". *Meteoritics and Planetary Science*, **50**, 401–417.

Lang B. and Kowalski M. (1971). "On possible number and mass of fragments from Pułtusk meteorite shower". *Meteoritics*, **6**, 149–158.

Lang B. (1972). "On the mass distribution of fragments from Lowicz meteorite shower 1935". *Earth and Planetary Science Letters*, **14**, 245–248.

Norton O. R. (2002). "The Cambridge Encyclopedia of Meteorites". Cambridge.

Norton O. R. and Chitwood L. (2008). "Field Guide to Meteors and Meteorites". Cambridge.

Pokrzywnicki J. (1964). "I. Meteoryty Polski. II. Katalog meteorytów w zbiorach polskich". *Studia Geologica Polonica*, **XV**, 114–115.

Pilski Andrzej S. (1995). "The Białystok meteorite shower". *Meteorite!*, **1**, 22–23.

Pilski A. S. (1999). "Nieziemskie skarby, Prószyński i S-ka". Warszawa (*in Polish*).

Pilski A. S., Wasson J. T., Muszyński A., Kryza R., Karwowski Ł. and Nowak M. (2013). "Low-Ir IAB irons from Morasko and other locations in central Europe: One fall, possibly distinct from IAB-MG". *Meteoritics and Planetary Science*, **48**, 2531–2541.

Przylibski T. A., Zagożdżon P., Kryza R. and Pilski A. S. (2005). "The Zakłodzie enstatite meteorite: Mineralogy, petrology, origin and classification". *Meteoritics and Planetary Science*, **40**, 185–200.

Rose G. (1852). "On the Meteoric mass discovered at Schwetz". *American Journal of Science and Arts*, **13**, 142.

Rose G. (1863). "Systematisches Verzeichniss der Meteoriten in dem mineralogischen Museum der Universität zu Berlin". *Annalen der Physik*, **118**, 419–423.

Samsonowicz J. (1952). "The age, origin, presumed number and mass of Pułtusk meteorite". *Wiadomości Muzeum Ziemi*, **VI**, 57–68 (*in Polish*).

Stankowski W. (2001). "The geology and morphology of the natural reserve 'Meteoryt Morasko'". *Planetary and Space Science*, **49**, 749–753.

Tymiński Z. and Brachaniec T. (2015). "Łowicz Meteorite - Mesosiderite from Vesta". *Meteoritics and Planetary Science*, **49**, 5426.

Tymiński Z., Stolarz M., Żołądek P., Wiśniewski M., Olech A., Kubalczak T., Zaręba P., Myszkiewicz M., Polakowski K. and Kosiński J. W (2015). "Meteorite search campaigns of the Polish Fireball Network". In Rault J.-L. and Roggemans P., editors, *Proceedings of the International Meteor Conference*, Mistelbach, Austria, 27-30 August 2015. IMO, pages 143–146.

[1] http://www.lpi.usra.edu/meteor and furthermore at: http://wiki.meteoritica.pl (in Polish).

A (revised) confidence index for the forecasting of meteor showers

Jeremie Vaubaillon

IMCCE, Paris Observatory, univ-PSL, Paris, France
vaubaill@imcce.fr

A confidence index for the forecasting of meteor showers is presented. The goal is to provide users with information regarding the way the forecasting is performed, so several degrees of confidence is achieved. This paper presents the meaning of the index coding system.

1 Introduction

The prediction of meteor showers has seen great success (McNaught and Asher, 1999), as well as deep disappointment in the past (Vaubaillon et al., 2014). Every year IMO publishes the calendar of the coming meteor showers, on the basis of forecasting performed by several authors. Comments included in the text allow one to decide whether or not such and such shower is worth travelling to the end of the world to observe. I believe every shower is worth observation, but of course in a practical sense everyone needs to choose how much effort to put in a given event. For this reason, the goal of this paper is to provide the meteor community with an explanation of the confidence index presented during the IMC.

2 The confidence index

How the index is built

The confidence index is basically a code providing information on how the ephemeris of a given meteor shower was performed.

The *first* letter informs us with the trail(s) the Earth (or any planet) is encountering. An encounter with a single trail is noted "**S**" (as in single), whereas an encounter with several trails is labelled "**G**" (as in global). Usually, single trail encounters are more accurate than multiple (Global) trails.

The *second* letter tells us about the year the forecasting is performed. Most of the time the prediction is made by taking into account only the simulated particles crossing the planet at a given year. In this case we label it "**Y**" (as in year). In other cases, there are not enough particles to really compute the location of the stream. As a consequence, we take into account all the particles crossing the planet concatenated over several years. In such a case we label it "**B**" (as in background).

The *third* element of the index tells how many perihelion passage of the parent body were observed, as well as how many passages were simulated. In short, the more observations, the better the confidence. The index is this built as: "O no/ns" with no: number of observed passages and ns: number of simulated passages.

The *fourth* element provides information regarding the stability of the orbit of the parent body. Orbits are usually best perturbed by close encounters with giant planets. The effect of such an encounter can be measured thanks to the mass of the planet, the distance of closest encounter and the velocity at the minimum distance. The index is the sum of all the contributions of the close encounters of a given trail (or sum of trails). The higher this number the less confident the forecasting can be, unless the parent body was observed before and after the encounter. If a single trail is considered the label starts with "**CE**" (as in close encounter), otherwise with "**CU**" (as in cumulative close encounters). Then the number (3 digits or more) of the sum of the close encounters is provided.

3 Example of confidence index

LEO in 2001: SYO0/1CE0.00 => single trail, single year, and passage not observed, no close encounter.

PER in 2017: GYO3/17CU0.00 => global trail, single year, 3 passages observed out of 17 simulated, no close encounter whatsoever during the whole duration of the simulations.

209P in 2014: GYO3/75CU46 => global trail, single year, 3 passages observed out of 75 simulated, cumulative encounter sum up to 46, which is quite a big number.

QUA in 2017: GYO1/57CU1500 => global trail, single year, one passage observed out of 75 simulated, cumulative encounter sum up to 1500, suggesting that the exact origin is unknown and the forecasting provides only statistical results. Note: my forecasting of the QUA is systematically offset by a few hours. In other words, the close encounter index tells us that one should not really rely on such a forecasting.

4 Conclusion

This confidence index is certainly not perfect, but it is better than nothing.

Acknowledgment

I am thankful to the IMC2016 team for such a terrific conference, as well as to G. Valsecchi for insights regarding the close encounters.

References

McNaught R. and Asher D. (1999). "Leonid Dust Trails and Meteor Storms". *WGN, Journal of the IMO*, **27**, 85–102.

Vaubaillon J., Maquet L. and Soja R. (2014). "Meteor hurricane at Mars on 2014 October 19 from comet C/2013". *Monthly Notices of the Royal Astronomical Society*, **439**, 3294–3299.

Nagatoshi Nogami and Eva Bojurova on the boat to the Waddenzee.

Software for Analysis of Visual Meteor Data: R package MetFns – Workshop report

Kristina Veljković

Petnica Meteor Group, Valjevo, Serbia
mackikac@gmail.com

New version of the package MetFns for analysis of visual meteor data, written in statistical software R, was presented on the workshop.

1 Introduction

New version of the package *MetFns* for analysis of visual meteor data (Veljković and Ivanović, 2014; 2015), written in statistical software R, was presented on the workshop. At the beginning, we downloaded the newest version of R from the site[1]. After that, a short introduction to R was made containing its history, advantages, few words about *GUI* (graphical user interface), text editors. We talked about types of objects, in R, giving more attention to vectors, factors, data frames and functions, necessary for better understanding and using the functions from the package. Note that both the package *MetFns* and statistical software R are open source and free.

2 Topics discussed and examples covered

We downloaded the package from the site[2]. In order to understand how its functions can be used, we checked the manual, which can be downloaded[3].

An overview of the package was made. It contains visual meteor data (yearly rate data, yearly magnitude data and accompanying data) and functions for data manipulation. In the current version, only data for selected years are part of the package, due to the limitation of the package capacity. But, there is also a possibility to read yearly rate or magnitude data directly from the IMO web site using provided functions. Package *MetFns* consists of 12 filter functions for data selection: by shower code, by period of days or months, by IMO observer code, by observer's first and last name, by geographical coordinates of observing site, by name of the observing site, by country, by solar longitudes, by correction factor(s) for field-of-view obstruction, by limiting magnitude(s), by radiant elevation(s) and by total correction factor. Also, there is a global filter function that combines previously mentioned filters in order to perform data selection by more than given in the manual, to the R command line. Then, we discussed the following functions for data calculations, provided in the package:

- function for calculation of solar longitude;
- function for calculation of calendar date and time corresponding to given value of solar longitude;
- function for calculation of the table and graphical representation of the summarized magnitude distribution of the meteor shower;
- function for calculation and graphical representation of the population index based on the method of linear regression that incorporates the probabilities of meteor perception;
- function for calculation and graphical representation of population index based on the method of the average distance from the limiting magnitude which uses an adaptive-bin size algorithm;
- function for calculation of the zenithal hourly rate of a meteor shower that uses an adaptive-bin size algorithm, with a population index being constant or calculated from the magnitude data.

Again, we copied the examples given in the manual to R, to illustrate how to use previously mentioned functions. Also, we made some changes to the parameter values of the functions, in order to show how the user can make adjustments for performing different analyses.

3 Conclusion

Participants of the workshop gave a lot of comments and suggestions, what to add and change in the package *MetFns*. All of these will lead to the new package version which is expected in the near future.

Reference

Veljković K. and Ivanović I. (2014). “Software for analysis of visual meteor data”. In Rault J.-L. and Roggemans P., editors, *Proceedings of the International Meteor Conference*, Giron, France, 18-21 September 2014. IMO, pages 104–108.

Veljković K. and Ivanović I. (2015). “Improvement of software for analysis of visual meteor data”. In Rault J.-L. and Roggemans P., editors, *Proceedings of the International Meteor Conference*, Mistelbach, Austria, 27-30 August 2015. IMO, pages 27–29.

[1] https://cran r-project.org/
[2] https://cran r-project.org/web/packages/MetFns/
[3] https://cran r-project.org/web/packages/MetFns/MetFns.pdf

Summary of the Open Session at the IMC 2016

Cis Verbeeck[1], Megan Argo[2], Peter Brown[3], Sirko Molau[4], Jürgen Rendtel[5] and Antonio Martínez Picar[6]

[1] **Royal Observatory of Belgium, Avenue Circulaire 3, 1180 Uccle, Belgium**
cis.verbeeck@oma.be

[2] **Jodrell Bank Centre for Astrophysics, School of Physics and Astronomy, The University of Manchester, Oxford Road, Manchester, M13 9PL, U.K.**
megan.argo@gmail.com

[3] **Dept. of Physics and Astronomy, University of Western Ontario, London, Ontario, N6A 3K7, Canada**
pbrown@uwo.ca

[4] **Abenstalstr. 13b, 84072 Seysdorf, Germany**
sirko@molau.de

[5] **Leibniz-Institut für Astrophysik Potsdam (AIP) An der Sternwarte 16, 14482 Potsdam, Germany**
jrendtel@web.de

[6] **Solar–Terrestrial Centre of Excellence – Royal Observatory of Belgium, Brussels, Belgium**
antonio.martinez@observatory.be

The Open Session at the IMC 2016 took place on Friday, June 3rd 2016 evening (21:30-22:30) and was intended to accommodate beginners' questions about meteor astronomy. Megan Argo moderated a panel of experts, consisting of Peter Brown, Sirko Molau, Jürgen Rendtel, and Antonio Martínez Picar.

1 Introduction

15 persons attended the Open Session. With only two questions received via the IMC 2016 website, the Open Session did not take the format of Q&A for beginners. Instead, the moderator asked the panel where and how amateurs can help meteor science best. The answers from the panel drew several comments from the audience, yielding a lively discussion. Here, we describe the basic recommendations from the experts.

2 Fireball shock waves

Peter Brown encourages amateurs to observe fireball shock waves with infrasound systems (a few hundred Hz to 0.01 Hz). It is easy to build a system but you need a lot of space. You can buy a system for a few hundred dollars, and it is recommended to add water hoses to protect against noise. By looking at the period of the sound, you get an idea of the energy. If you've got many microphones, you can do more. Software is typically included.

3 High resolution video

Sirko Molau points out that it is most interesting to go for new techniques like high resolution video and lunar impacts (which should be possible e.g., with a C8 telescope).

Sirko would start with a Watec camera if he would start now as a video observer. If you are hunting for fireballs, you use a large field of view (FOV). If you are going for good meteor statistics, you go for an intermediate FOV. You can then observe the visual showers which you cannot observe by radar.

There are a lot of geographical regions which are underrepresented in video observations, e.g., the Southern hemisphere, the large Asiatic region between Europe and China/Japan, and Hawaii.

4 Radio meteor astronomy

Sumio Nakane asks how amateurs can contribute to radio meteor astronomy. *Antonio Martínez Picar* is convinced that simplest is best. The continuous wave technique exists for many years, and is still his recommendation since it is simpler than other techniques.

Gaetano Brando asks which kind of antenna to use for meteor astronomy: a directional one or a dipole? Antonio suggests that a simple dipole may be best, unless your transmitter is so distant that you need a high (directional) gain to detect the signal. Also, he prefers a zenithal direction for the antenna since then you know the geometry better. The CMOR radar in London, Ontario also has a rather broad, zenithal gain pattern, and has about half of its maximal gain at 45 degrees zenith distance.

5 Visual observations

What can visual observers do? Visual observations are still important and complement video and radio observations. Visual observations provide first hand experiential impressions, rather than just looking at data on your screen. Observing together creates collaboration

between individuals, and IMO was created because of the ensuing collaboration between groups.

There are still really old and reliable visual datasets, which means that visual observations enable long term studies. For instance when the resonance in the Orionids 2006-2007 was found, *Jürgen Rendtel* went back to old observations back to 1913-1914 and did find a periodicity. Visual observations have a low threshold for beginners.

Sirko remarks that a good video observer should first do some visual observations for a better understanding about what meteors are all about.

Alejandro Sánchez de Miguel suggests developing an app to record visual observations, but the screen should not be too bright.

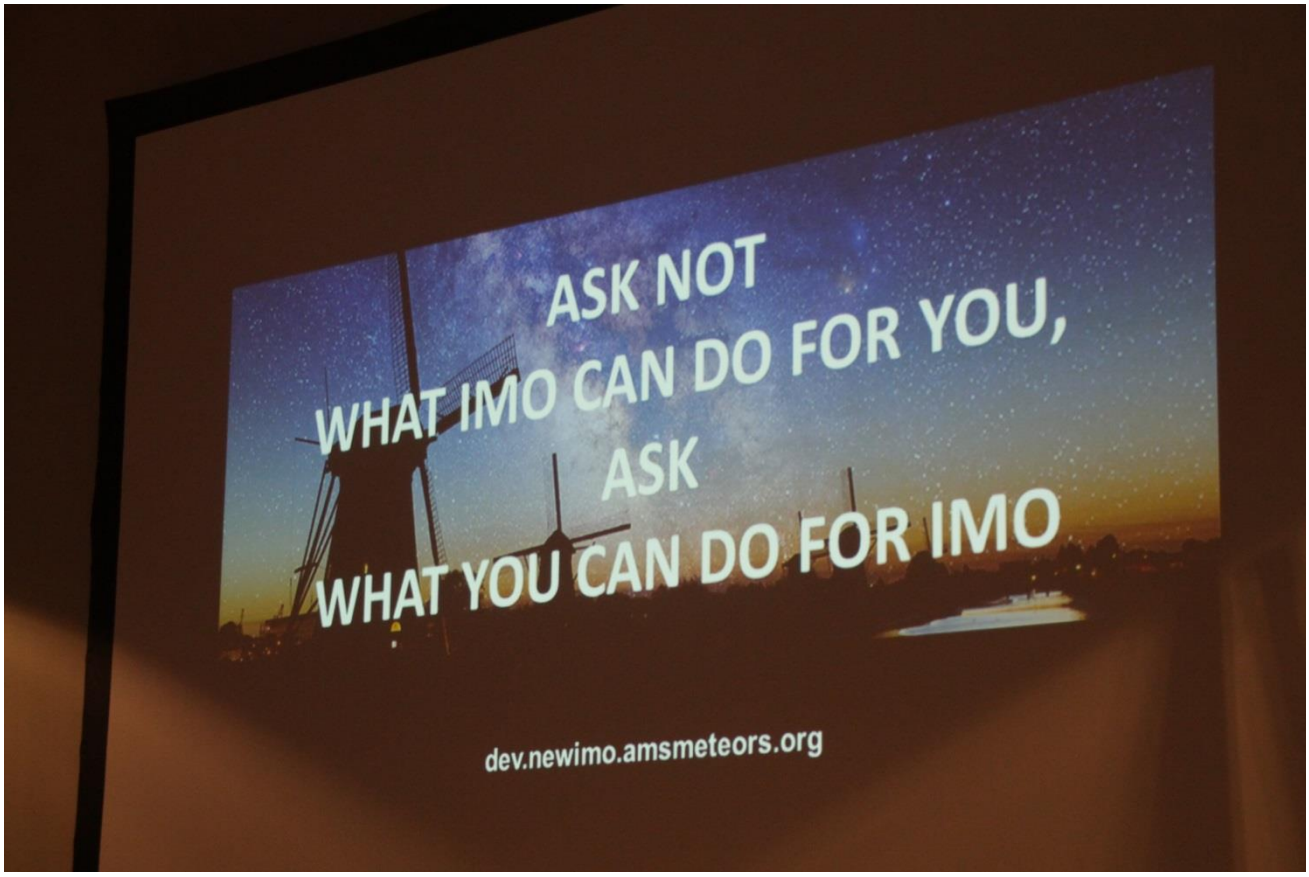

Presentation of the new IMO website: help with the IMO website is much appreciated!

Open-source meteor detection software for low-cost single-board computers

Denis Vida[1], Dario Zubović[2], Damir Šegon[3], Peter Gural[4] and Robert Cupec[5]

[1] **Astronomical Society "Anonymus", B. Radić 34, 31550 Valpovo, Croatia**
Faculty of Electrical Engineering, University of Osijek, Kneza Trpimira 2B, 31000 Osijek, Croatia
denis.vida@gmail.com

[2] **Croatian Meteor Network**
dario@zubovic.email

[3] **Astronomical Society Istra Pula, Park Monte Zaro 2, 52100 Pula, Croatia**
damir.segon@pu.htnet.hr

[4] **Gural Software Development, 351 Samantha Drive, Sterling, Virginia, USA 20164**
peter.s.gural@leidos.com

[5] **Faculty of Electrical Engineering, University of Osijek, Kneza Trpimira 2B, 31000 Osijek, Croatia**
rcupec@etfos.hr

This work aims to overcome the current price threshold of meteor stations which can sometimes deter meteor enthusiasts from owning one. In recent years small card-sized computers became widely available and are used for numerous applications. To utilize such computers for meteor work, software which can run on them is needed. In this paper we present a detailed description of newly-developed open-source software for fireball and meteor detection optimized for running on low-cost single board computers. Furthermore, an update on the development of automated open-source software which will handle video capture, fireball and meteor detection, astrometry and photometry is given.

1 Introduction

With the advent of low-cost sensitive video security cameras, amateur meteor enthusiasts quickly embraced this technology and noted its potential for meteor surveillance (Gural and Šegon, 2009). The technology has proven capable of delivering quality data, such that a meteorite recovery was possible based on an amateur meteor network (Borovička et al., 2015) using such cameras. As the price of these cameras has continued to decline, falling below 50 USD (Samuels et al., 2014), the main price component of a meteor station became the computer for recording and processing the data. As the computer's price is an order of magnitude larger than that of a single camera, the question of replacing it with a cheaper alternative naturally arises. The possible candidates were found in the form of low-cost single-board computers. A set of these computers were tested in (Zubović et al., 2015) and it was concluded that a viable alternative exists, namely the *Raspberry Pi 2* device which seemed affordable and powerful enough to serve the purpose. Furthermore, it was concluded that a low-cost meteor station using the *Raspberry Pi 2* computer could be built for about 150 USD, including all components. While the hardware is not the main topic of this paper, it is worth mentioning that a new generation of the *Raspberry Pi* has recently been released, the *Raspberry Pi 3* which offers up to 50% more computing power[1] than the previous generation. Although the hardware options are plentiful, there were no software solutions capable of running on such devices. Their ARM CPU architecture and the Unix-based operating system create a unique problem, where to successfully compile and use meteor processing pipeline software, one needs to obtain its source code and adapt it to run under such a system configuration. The work in (Zubović et al., 2015) presented software which works on *Raspberry Pi 2* devices, records video from the camera, compresses it into the CAMS FTP format (Gural, 2011) and performs a rudimentary real-time fireball detection.

In this paper new and improved algorithms are presented which include complete procedures for real-time fireball detection, meteor detection, star extraction and data calibration. All software is open-source and available on the project's GitHub page[2]. The authors believe that meteor surveillance is a matter of great importance, and as such it should be available to all. By making the software open-source, anyone can use the code, contribute to it and more experienced contributors can improve it significantly. The *Python* programming language was chosen as the main development language, while the computationally intensive parts of the code are written in *C++*. The choice of this combination of programming languages is common for astronomical purposes[3] in the recent years.

[1] https://www raspberrypi.org/magpi/raspberry-pi-3-specs-benchmarks/

[2] https://github.com/CroatianMeteorNetwork/RMS

[3] http://python-in-astronomy.github.io/

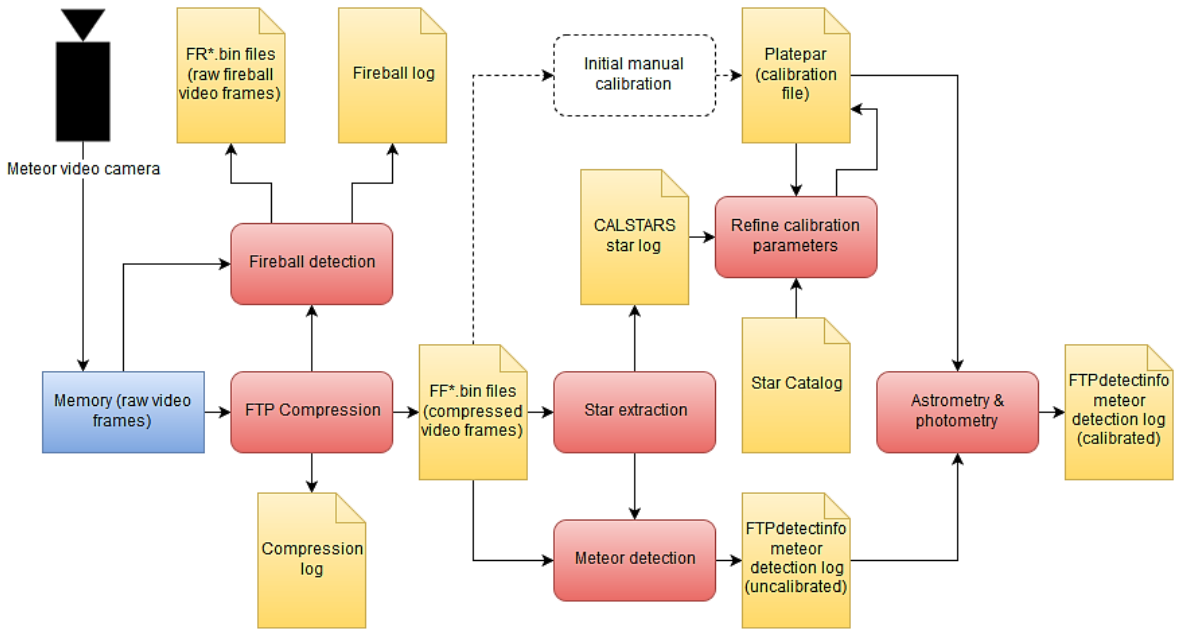

Figure 1 – A block diagram of the developed software.

2 Software overview

An overview of the developed software is shown on *Figure 1*.

The raw frames from the grabber are compressed in the CAMS FTP compression format (Gural, 2011). The compression procedure compresses 256 raw video frames into 4 images: maximum pixel value image (maxpixel), average pixel value image excluding the maximum (avepixel), standard deviation pixel value image excluding the maximum (stdpixel) and an image which tracks the time of the occurrence of the maximum pixel value (maxframe). The time, i.e. the frame number of the maximum pixel value is encoded as a byte valued image level. If a certain pixel has several maximum values occurring at different frames, the frame number which is stored in the maxframe image is randomly chosen to distribute noise peaks uniformly in time.

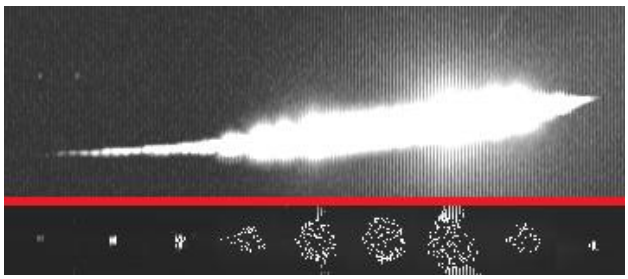

Figure 2 – Fireball maxpixel image (top) and several reconstructed frames showing compression artifacts (below).

While the aforementioned compression procedure works sufficiently enough to preserve meteors of moderate brightness, certain problems can occur with very bright fireballs. As the fireball saturates the CCD sensor and leaves a path of saturated values along its track, the compression algorithm only takes a single saturated value encoded in time. The effect of this is visible in *Figure 2*. The top of the figure shows the maxpixel image, while the bottom shows several reconstructed video frames. It can be seen that the reconstructed frames suffer from compression artifacts which can impair the precision of the centroid determination as information about the real position of the fireball is lost.

To counter this problem a real-time fireball detector was developed to enable saving the raw video frames while they are still in the temporary memory buffer. Fireballs have orders of magnitude higher signal-to-noise ratio in respect to the background than meteors of moderate brightness, and thus the authors believe that a dedicated fireball detector provides more consistent results than a combined approach. Furthermore, a fireball detection algorithm is simpler and faster, thus satisfying the real-time requirement. Fainter and moderate brightness meteors are detected on the compressed data with more elaborated methods offline, as they generally do not suffer from compression artifacts.

Besides fireball detection, to make a low-cost meteor station competitive with the existing solutions, an option to detect fainter meteors is highly desirable. As there are constraints on the computing power, the algorithm needs to be fast, reasonably robust and sensitive enough to detect meteors not detected by the fireball detector. To consider how fast the algorithm actually must be, Worst Case Execution Time and the maximum average time which can be spent per each image for meteor detection must be calculated.

To use the full power of the *RPi* computer, all 4 of its cores are employed. The capturing process has the highest priority and it needs to run in real-time, thus one core is completely dedicated to this task. Two cores are dedicated to video compression and real-time fireball detection. The compression and fireball detection process is serial, meaning that fireball detection is run after the compression. Thus each of these two cores run the same serial process, but the input data stream is alternated

between the two, to double the available processing time per single serial procedure. The one remaining core runs star extraction and meteor detection. Once the capture process is finished, all 4 cores run star extraction and meteor detection procedures. Finally, after the detection procedures finishes, astrometry and photometry procedures are performed.

With the core utilization laid out, the total available processing time for star extraction and meteor detection can be calculated. The longest night of the year at latitude 50° north is about 16 hours, which translates into 5625 CAMS format FF files at 25FPS and 256 frames per file. With the proposed core utilization, during the longest night the algorithm will have 16 hours available during the night on one core, and the remaining 8 hours on 4 cores. Thus the total computation available is 48 hours (not taking into account system housekeeping and post-processing). This translates to the maximum average time which the algorithm can spend on one FF file of about 30 seconds. Furthermore, taking into account that the *Raspberry Pi 2* is at least an order of magnitude less powerful than contemporary normal-sized computers, the average maximum time the algorithm running on a normal-sized computer can spend on each image is around 3 second. As this time is quite short, the algorithm should make an effort to reduce the number of analyzed files early on.

3 Fireball detector

An initial version of the fireball detection algorithm was presented in (Zubović et al., 2015). In this paper an improved version of the algorithm is presented - the algorithm was re-implemented in *Cython*[4] for faster execution and input parameters were fine tuned. Furthermore, the algorithm is discussed in more detail below.

The input data to the detector are the FTP compressed file and raw video frames. To detect significant rises in image intensity over the background, image thresholding is performed with the following operation:

$$Threshold(max, avg, stddev) = \begin{cases} white, & (\max > avg + K_1 \cdot sttdev) \ \& \ (\max > 40) \\ black, & otherwise \end{cases}$$

The K_1 parameters determines how many standard deviations above the background level the maximum intensity must be to be considered to be part of the fireball, i.e. a white pixel. The chosen value was $K_1 = 4$, based on numerous experiments on fireball images. Furthermore, the minimum intensity level of the pixel must be 40. *Figure 3* shows the influence of the varying value of the K_1 parameter. As it can be seen on the given figure, values of K_1 below 4 produce too many white pixels. Values above 4 can produce black regions in the middle of the fireball – these are caused by the very high standard deviation values in the middle of the fireball. When these high values are multiplied by the K_1 parameter of a higher value, the $avg + K_1 \cdot sttdev$ expression can exceed the maximum digitization value of 255, thus making the maximum image value unable to pass this threshold. If one requires such a high threshold, it is possible to clip the calculated value to 254 and thus ensure saturated pixels get through. As this would introduce a slight overhead in computation time, this feature was not implemented.

Following this procedure, the image pixels are now either white (pixels of interest) or black (background). As the CAMS FTP format image contains information about the occurrence of every maximum pixel value, the thresholded image can be shown as a 3D point cloud, XY components representing the image axes, and Z component representing the time axis. The resulting 3D point cloud can be seen in inset *a) of Figure 4*. To further reduce the noise and reduce the total number of points of interest, a subsampling procedure is performed. The point cloud is sampled by $16 \times 16 \times 256$ bins. A secondary thresholding is performed which is based on counting the number of points in each bin. If the number of points is less than 8, the bin is rejected. The result is shown in inset *b) of Figure 4*. As fireballs can often have bright flashes, an algorithm which removes the flashes (i.e. slices at the time axis which have considerably more points than average) is applied to the 3D point cloud. An example of such 3D point cloud is given on the inset *b) of Figure 4*, where a plane of points at frame 90 can be noticed. The flash filter looks for such planes in the data, i.e. the frames when the fireball 3D point cloud has at least 10x more points than the median number of points per frame. The frame is removed and the result is shown in inset *c) of Figure 4*.

After the described preprocessing, it is obvious from *Figure 4 inset c)* that the fireball is represented as a line segment in 3D space. Thus a new line segment detection algorithm has been independently developed and implemented in *Cython*. First, the points are sorted by their respective frames. Then the algorithm pairs each point with each other to hypothesize a line. Each hypothesized line is tested for the number of points in its neighborhood. The neighborhood is defined as cylinder around the hypothesized line (with a fixed radius). The algorithm evaluates each hypothesized line by the number of points and their distances from the line by producing a weighted score. The closer the point is to the line, the higher the score it has. Furthermore, if the algorithm determines that there is a discontinuity in the concentration of points, that particular hypothesized line is rejected as the goal is to find compact line segments. The line with the best cumulative score is chosen, its points are removed from the point cloud and the algorithm runs recursively until all acceptable lines are found. The pseudo code of the algorithm, as well as the description of the input parameters, are given in Code segment A. The line segment detection algorithm has a time complexity of $O(N^3)$ in the worst case, and given

[4] http://cython.org/

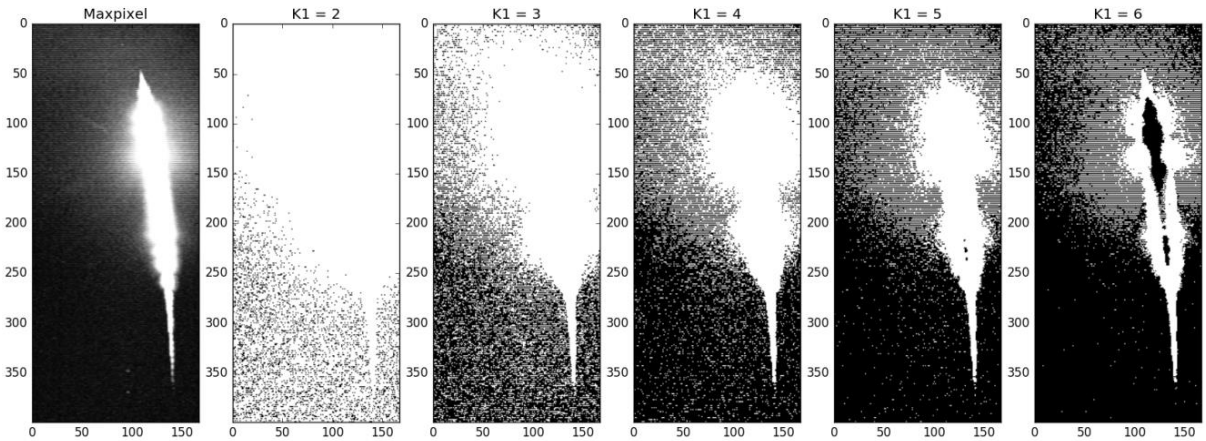

Figure 3 – Thresholding the fireball with various values of K_1.

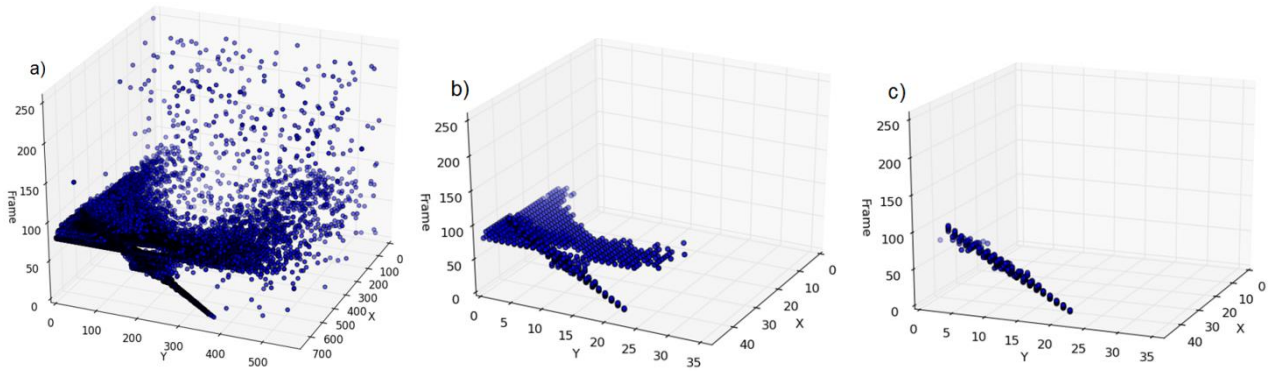

Figure 4 – Steps in the fireball detection thresholding procedure.

the restrictions on the computing time available, the total number of points which are fed into the algorithm was limited to 1000. If the point cloud contains more points, 1000 points are randomly chosen. In principle, the newly developed line segment detector is very similar to *RANSAC* (Fischler and Bolles, 1981), although it contains several key differences which enable it to search specifically for line segments, in contrast to unbounded lines. After the fireball is located, raw video frames containing the fireball are pulled from memory and are stored on disk for later use.

The performance of the fireball detector was evaluated on about a hundred examples of fireball images from the Croatian Meteor Network archives. The brightness of successfully detected events ranges from fireballs which saturated half the image, to 0th magnitude meteors. After examining the results, the authors have concluded that the fireball detector is robust and suitable its purpose.

4 Meteor detector

To reduce the total processing time, the star extraction procedure (described in the next section) is run before meteor detection. If the number of detected stars is too low, meaning that the sky is not clear, the meteor detection algorithm will not be run at all on the given image. When the skies are clear, the processing flow will include the detection procedure.

As the CAMS compression format saves the maximum and the average value of each pixel during 256 frames, as well as its standard deviation, thresholding the image to find events brighter than the average is done by applying the following operation on the image:

$$Threshold(max, avg, stddev) = \begin{cases} white, & \max > avg + K_1 \cdot sttdev + J_1 \\ black, & otherwise \end{cases}$$

K_1 is a scaling factor which determines how many standard deviations above average the event should be, while J_1 is an absolute factor which adds to the total level threshold by adding a minimum background level. The combination of factors K_1 = 1.7, J_1 = 9 proved to be optimal for discriminating meteors from the background noise.

After the image is thresholded, the algorithm checks the ratio between the thresholded and the total area of the image. If the thresholded part covers more than 5% of the image, the image is rejected. The reason for this is that moonlit clouds can often cause many above average pixel exceedances, which in turn slows down the algorithm.

As one compressed image contains information of about 256 frames, this allows reconstructing the whole video from the compressed file. To reduce noise, the whole 256-frame block is not analyzed at once, but only a 64 frame “window” is reconstructed from the FF file. The

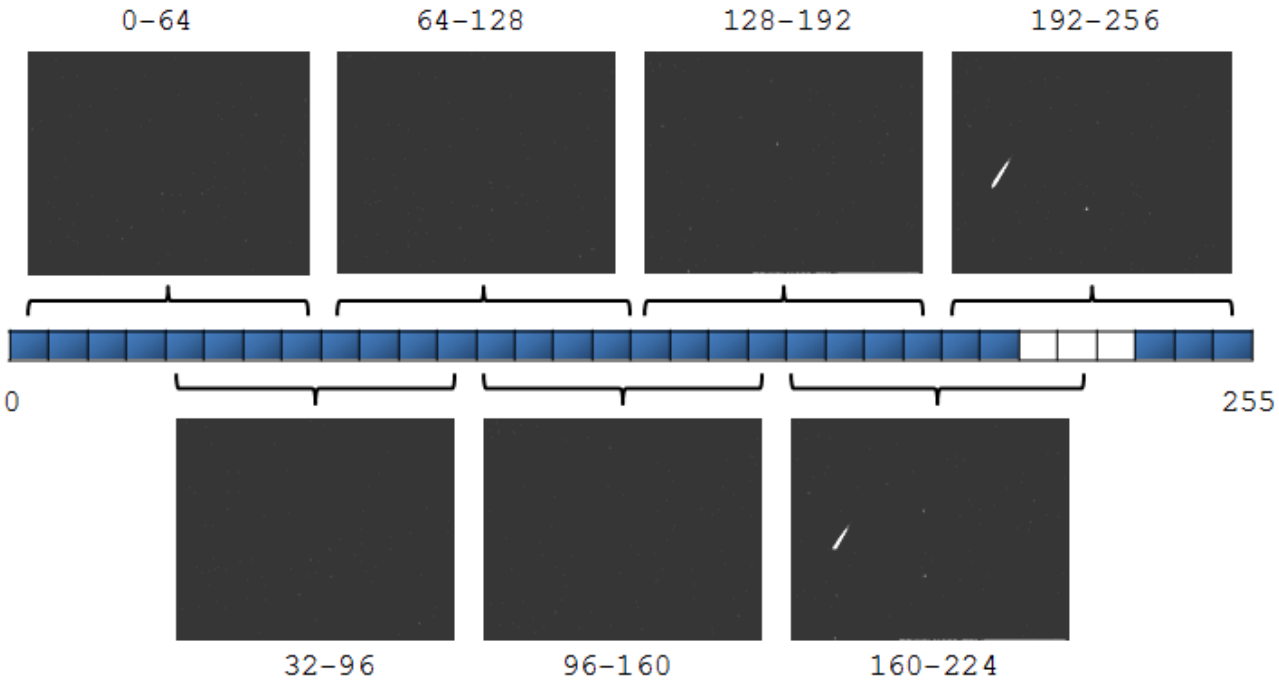

Figure 5 – Frame reconstruction and frame "windows". The meteor appears on frames from 211 to 228.

starting frame of each reconstructed window is shifted by 32 frames, producing 7 such windows covering frame ranges of 1–64, 32–96, 64–128, 96–160, 128–192, 160–224, and 192–256, thus the windows are overlapped in time to avoid "leakage" of meteors spanning processing windows. The mentioned "window" is not a set of 64 actual frames, but the maxpixel of the short window block. *Figure 5* illustrates the described procedure and shows individual frame "windows".

On each such window a set of image morphological operations (Gonzales and Woods, 2008) is performed. First, morphological cleaning is performed; a process which removes isolated pixels. This operation removes most of the noise on the image. *Figure 6* illustrates the described procedure.

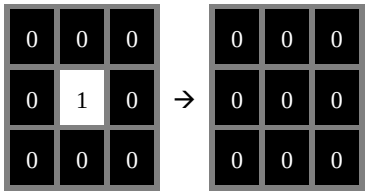

Figure 6 – Morphological cleaning.

Then a morphological bridging operation is performed which connects pixels which are on the opposite sides and all other pixels are 0. This operation helps to connect disconnected features on the image, such as broken lines. *Figure 7* illustrates the described procedure for 1 of 4 possible pixel orientations.

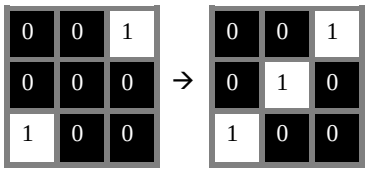

Figure 7 – Morphological bridging.

After that, a morphological closing is performed. Closing is a structured filling in of hollow image features which consists of two sub-operations: morphological dilation followed by erosion, using the same structuring element for both operations. This operation helps to fill in all the possible gaps in the thresholded meteor.

To prepare the image for line identification, all possible lines must be as thin as possible. Thus a *Zhan-Suen thinning algorithm* (Zhang and Suen, 1984) is applied to the image which skeletonizes the image i.e. makes all possible meteors on the image to appear as long thin lines.

Finally, a morphological cleaning is performed again to remove all noise on the image remaining after thinning. Now the image is ready to run the line detection algorithm. *Figure 8* shows an example of the maxpixel image (left), the image after thresholding (middle) and the image after the complete pre-processing procedure (right).

The image pre-processing procedure was implemented due to the peculiar operation of the chosen line finding algorithm. After a period of experimentation, it was decided to settle on the *Kernel-Based Hough Transform* (KHT) (Fernandes and Oliveira, 2008) due to its superior speed and performance, which was necessary due to the low computation power of single board computers. The authors of the *KHT* made it open-source which perfectly aligned with our needs and software development philosophy. The preprocessed images are fed into the algorithm and it returns all line candidates on the image.

After all lines have been retrieved on all 64-frame "windows", similar lines are identified using the *Discrete*

Figure 8 – Maxpixel image of a meteor (left), thresholded image (middle), image after preprocessing (right).

Fréchet distance (Eiter and Mannila, 1994) as the similarity measure and are averaged. During the line segment merging, the exact "windows" on which the line appears are tracked, thus the approximate time of the line appearance is known. In this point the algorithm has a list of candidate lines which need to be confirmed as meteors. If this list is empty, meaning no lines satisfying the given parameters were found, the procedure is aborted and the image is rejected and it is considered to not contain any meteors. On the other hand, if there are lines in the list, the algorithm proceeds to confirm that the found lines could be meteors.

The next phase of the algorithm determines if the candidate line contains a possible meteor by determining if the line propagates through time. First, as the approximate time of the line appearance is known as a range of frames between which the candidate line appeared, this fact is used to reconstruct the "window" image using the given frame range. Then a strip of about 50 pixels in width is extracted around the line. In CAMS FTP format, each pixel has an assigned time component of its maximum value during the 256 frame period, meaning that each pixel in the strip is given a time component. Thus a 3D point cloud is obtained - a line propagating through time should be a compact line in this point cloud, thus the same algorithm as the one in fireball detection is used, although with a different set of parameters to allow for smaller lines to be detected. The algorithm determines the exact starting and ending frames of the propagating line, as well as the true orientation of the line. Any event shorter than 4 frames (i.e. 0.16 seconds at 25 frames per second) is rejected due to a large number of such short events detected during cloudy weather, which can considerably slow down the algorithm. This also means that all meteors shorter than 4 frames are not detected. In the case of future improvements in available computational power, this restriction can be easily lifted.

After the algorithm determines the exact duration (i.e. the beginning and ending frames) of the event, centroiding is performed by reconstructing each frame of the event and again extracting a strip around the event. A center-of-mass calculation is performed, using pixel intensities as weights (Berry and Burnell, 2005). As the video camera employed produces an interlaced signal, a deinterlacing procedure is performed beforehand – centroiding is done separately on odd and even image rows, thus giving a half-frame time resolution. Finally, the obtained centroids are filtered by rejecting those which considerably deviate from the fitted trend line. *Figure 9* shows the marked centroids of the meteor shown on *Figure 8*. The results of the detection procedure are written out as a CAMS *FTPdetectinfo* file format, so that the results can be processed with the existing (although proprietary) CAMS procedures.

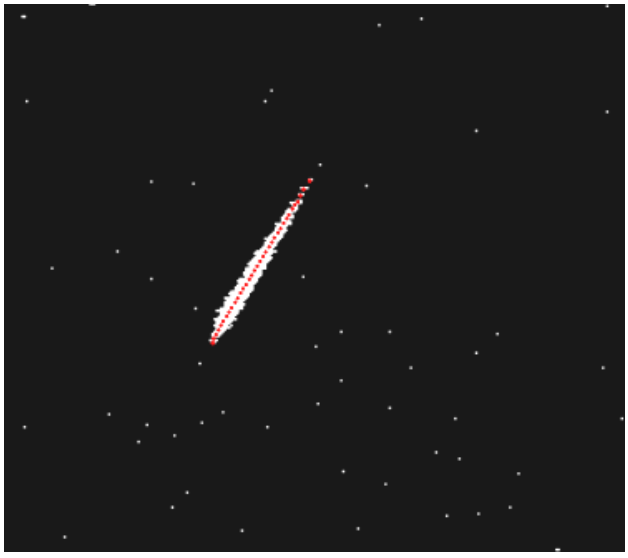

Figure 9 – A detected meteor with marked centroids.

The performance of the meteor detector was evaluated on about a hundred carefully chosen meteor images. The

Table 1 – Comparison of meteor detection performance between the new detector and the CAMS detector.

Type	Night ID	No. files	Total proc. time (sec)	Time per file (sec)	Meteors detected		False positives	
					New	CAMS	New	CAMS
1	VIB_20160419	3211	29390	9.15	14	11	53	18
2	OSE_20160417	3269	7770	2.37	0	2	9	61
3	VID_20160417	3263	37100	11.36	0	0	1679	304
4	OSO_20160419	3233	9430	2.91	2	4	36	2941
5	OSE_20160501	2950	2590	0.87	0	0	0	318
				TOTAL	16	17	1777	3642

goal was to sample a wide variety of meteors of varying brightness, duration and velocity to test the algorithm's detection performance. The algorithm's parameters were tuned until all chosen meteors were successfully detected.

Furthermore, the detector was tested on 5 full nights, each containing about 3000 individual image files. The night types were chosen to be representative of the conditions encountered during the year:

1. A clear and Moonless night with several meteors;
2. A cloudy night with the presence of the Moon with very few meteors;
3. A night with fast moving clouds with the presence of the Moon;
4. A rainy night in a light polluted environment, resulting in visible falling raindrops;
5. A cloudy and stormy night with the presence of lightning.

The goal of these data was to test the algorithms robustness and false positive rate. The results were compared to those obtained by the *MeteorScan detector* employed as a part of the CAMS processing pipeline (Jenniskens et al., 2011) in *FTP_CaptureAndDetect version 1.6* software. The results of comparison for full nights are given in *Table 1*.

Compared to the CAMS detector, the total number of false positives was considerably smaller. It was discovered that this was caused by the condition that the detection procedure is run only when a minimum number of stars is present on the image, thus eliminating most of the detections on clouds and during daytime. On the other hand, the new detector produced lots of false positives when part of the image contained fast moving moonlit clouds while the other part was clear. This behavior will be addressed in the future by introducing cloud mitigation techniques.

The total number of detected meteors was also smaller. After careful comparison, it was determined that the missing detections are those meteors shorter than 4 frames in duration (which are automatically rejected by the new detector) and meteors between the clouds. On the other hand, during clear nights the new detector performed similar to the CAMS detector. Real differences cannot be determined without a detailed comparison, but it is worth mentioning that in several cases the new detector detected more meteors than the CAMS detector (with the detection parameters used by the Croatian Meteor Network). Furthermore, on all tested data the algorithm never exceeded the maximum average processing time per image. The maximum average processing time per image for the tested nights on the *Raspberry Pi 2* device was about 11.5 seconds, including both the star extraction and meteor detection.

Although the detection rate was similar to the CAMS detection procedure, further analysis is needed. But based on these early results, it can be concluded that under the circumstances and the given computational power the newly developed detector is performing satisfactory for the needs of an amateur meteor enthusiast. Room for improvement still exists and it is hoped that a more successful algorithm will be implemented in the future, most probably the one given in (Gural, 2016). Furthermore, the algorithm should be tested on even more data to confirm its performance.

As the system is fully automated by design, a manual meteor confirmation procedure is not a part of the processing pipeline. False meteor detections will be rejected during orbit estimation as they will not form realizable orbit solutions. Nevertheless, as the results are CAMS compatible, it is possible to perform manual confirmation using the available software solutions, such as the *CMN_binViewer* (Vida et al., 2014).

5 Star extraction

To astrometrically calibrate the intrinsic (field distortion) and extrinsic (coordinate transformations) parameters of the camera, a set of stars from each recorded image is needed. Thus a robust algorithm for detecting stars on the recorded FF files was developed. The algorithm takes the "average pixel" image from the FF file and first calculates the mean intensity of the image. To quickly check if the algorithm should proceed at all, the mean image value is compared to a predefined threshold. If the image is too bright (e.g. an image recorded during the day), it is rejected. If the image passes this test, the inverse hyperbolic sine function is applied to all pixels on the image to adjust levels of the image so that the stars become more prominent. The maximum image filter (i.e. morphological erosion) is applied to the image; while on a copy of the original image a minimum image filter (i.e. morphological dilation) is applied. The difference of the 2

images thresholded by a fixed threshold value leaves only the areas of the image which are considerably brighter than their background. These peaks are detected and the center of mass is calculated for each on the original average pixel image, giving the approximate coordinates of the candidate stars.

To refine the results, and to better determine if the candidate is really a star or not, *point spread function (PSF) fitting* is performed by fitting a 2D Gaussian function to an area of 9 × 9 pixels centered around each candidate star using the least squares regression. The authors are aware that a 2D Gaussian does not perfectly represent the real *PSF* of the star, but for the purposes in video meteors which have a lower photometric resolution, a pure Gaussian *PSF* is assumed. Initial *PSF* parameters are approximated beforehand so that real stars converge quickly to a solution. Thus if the fitting does not converge in a limited number of iterations, the candidate is rejected. This procedure has proven to be a good discriminator between real stars and spurious detections. Furthermore, if the *PSF* fitting procedure is completed successfully, the covariance matrix of the *PSF* is evaluated. If the *PSF* is too narrow, the candidate star is rejected as a hot pixel (i.e. bright dot defect). Finally, as a consequence of fitting the *PSF*, the location of each star is known very accurately and its precision is on a subpixel level. The intensity of each star is calculated as a volume under the fitted *PSF*.

Finally, the stars found are written in the CAMS *CALSTARS* format, so that the calibration procedure can be done using CAMS-compatible procedures if needed.

The results of the new algorithm were compared to the results of the *CAMS FTP_CalStarExtractor* software. It was concluded that the newly developed algorithm yields very little false positives, only about 5%, while the *FTP_CalStarExtractor* often detects more false positives than real stars. Furthermore, the proposed algorithm yields virtually no detections during cloudy weather, thus its results can be used to determine weather conditions in the time of recording. When comparing the number of true positives between the two algorithms, the new algorithm detects about 90% of stars present in the CAMS data. The average number of detected stars per image during the periods of clear skies in the sample moderate field of view data was about 30. Combining frames from the same camera over the course of the night yields an average total number of detected stars in the tens of thousands.

6 Astrometry and photometry procedures

To transform the image coordinates of the meteor detection to celestial coordinates, an astrometric plate solution of the associated camera is needed. The initial plate constants (field center, scale, field distortion parameters) are first manually estimated by knowing the pointing direction of the camera and its optical properties. To further refine the plate constants, the detected stars need to be matched with stars from a star catalog. For this purpose, the Yale Bright Star Catalog[5] is used. To have a better quality of the solution and to cover a larger part of the focal plane, stars detected on images all throughout the night are used. As the total number of all stars in a single night can be in the tens of thousands, which can be hazardous for the computational time needed to calculate an astrometric solution, a random sample of images is taken where images with more stars have a greater probability of being chosen. At least 500 stars are needed to continue with the calibration, the number being chosen on the basis of findings in (Šegon, 2009).

The image coordinates of the chosen stars are transformed to celestial coordinates using the initial calibration parameters. The transformed coordinates are then matched to their nearest neighbors among the catalog values in celestial coordinates, but only if the coordinates are closer than a predefined angular distance threshold. The distance and the direction of the shift between each of the matched stars are recorded, the median values are calculated and the correction is applied to the plate constants. The procedure is repeated by reducing the angular distance threshold during each iteration, until the desired match is achieved. The matching metric is evaluated as a quotient of the standard deviation of the shift between the detected and catalog stars and the total number of matched stars. Thus a better solution is one that yields a smaller value.

Once the initial parameter refinement is complete, a more elaborate refining of the field center position is performed using the *Nelder-Mead method* (Nelder and Mead, 1965). Right ascension and declination of the center is adjusted until the algorithm converges to a stable solution – the same evaluation method is used as in the initial refinement procedure. Next, the distortion parameters are also refined using the same above-mentioned procedures. The image distortion is estimated by 3rd order polynomials with 2 extra "radial distortion" terms in both *X* and *Y* directions, albeit with different coefficient values:

$$\begin{aligned} f_x(x,y) = x + \ & a_1 + a_2 x + a_3 y + a_4 x^2 + a_5 xy + a_6 y^2 \\ & + a_7 x^3 + a_8 x^2 y + a_9 x y^2 + a_{10} y^3 \\ & + a_{11} x\sqrt{x^2+y^2} + a_{12} y\sqrt{x^2+y^2} \end{aligned}$$

$$\begin{aligned} f_y(x,y) = y + \ & b_1 + b_2 x + b_3 y + b_4 x^2 + b_5 xy + b_6 y^2 \\ & + b_7 x^3 + b_8 x^2 y + b_9 x y^2 + b_{10} y^3 \\ & + b_{11} x\sqrt{x^2+y^2} + b_{12} y\sqrt{x^2+y^2} \end{aligned}$$

The extra terms in the polynomials were first used as a part of the Croatian Meteor Network calibration procedures, but have been unpublished until now. During the initial development of the CMN procedures it was found that the modified polynomials produce smaller residuals compared to the ordinary 3rd order polynomials. This hypothesis has been tested again before the final implementation in this software and it was found that the

[5] http://tdc-www.harvard.edu/catalogs/bsc5 html

proposed equations produce significantly smaller standard deviations in the fitted star positions than the ordinary third order polynomials. The theoretical background behind the reasons of such behavior was not explored, that will be a topic of some future work.

After the astrometry parameter estimation is done and if the calibration was successful, a photometric calibration procedure is performed. Instrumental intensities of matched stars are compared to the apparent visual magnitude catalog values of said stars. A regression procedure is performed to fit the well-known intensity vs. magnitude function (Berry and Burnell, 2005):

$$m_1 = -2.5 \log_{10} C_1 + 2.5 \log_{10} C_2 + m_2$$

where m_1 is the calculated magnitude, C_1 is the input intensity, while C_2 and m_2 parameters are fitted from the abovementioned data. It is worth noting that the photometric procedures are very basic and with no regard to spectral sensitivity of the camera. Furthermore, no correction for saturated pixel values is performed. This part of the calibration procedure requires further work and improvement, which is hoped to be done in the future. Finally, meteor detections are converted from the image plane coordinates to celestial coordinates using the estimated plate constants and intensities are converted to apparent magnitudes.

The results of the proposed astrometric calibration procedure were compared to the results of the existing CMN calibration procedure. The new algorithm produced an order of magnitude better results, although results of the subsequent runs on the same dataset varied slightly because of the random sampling of the images from which the stars are used.

7 Discussion

The authors believe it is worth discussing the benefits that an automated low-cost meteor station could provide. Lowering the starting price of a meteor surveillance system would mean that existing networks could be easily expanded, as the human resources and a certain level of expertise exists among already organized groups. Furthermore, new networks could be easily formed with very little financial investment, meaning that meteor science would be available to a wider audience, especially in less than well-off nations. The total effect would be a considerable rise in the atmospheric collecting area and longitudinal coverage. An educational aspect should also be considered – students could be introduced to astronomy, computer and data science by installing such a system on their school and make them involved in every step of its operation. Moreover, scientists from other fields could recognize the practicality of a self-contained system with a video camera and repurpose it for their needs, such as bird watching or monitoring atmospheric phenomena.

If the project is favorably seen by a larger audience willing to set up a network of such systems, the authors believe that data produced by this hypothetical network using open-source software should be publically available. The usual arguments for keeping the data closed, such as the cost of the developed system, no longer justifies not publishing detailed data in this case, and no time is spent on manual processing as the system is fully automated. A similar open database exists in the form of the IMO Fireball Report (Hankey and Perlerin, 2014) and the authors hope that in the future more video meteor data will be open and the methods of its generation will become more transparent.

Finally, the benefits of a wide-spread meteor network to actual meteor science could be immense. Most meter-scale impactors are not observed optically, as the existing fireball and meteor networks cover only a fraction of the sky and most are only detected with non-optical methods which lack astrometric precision and show certain biases towards faster objects (Brown et al., 2016). In the recent years there have been reports of short meteor shower outbursts which were observed only by one or two meteor networks, namely the February Eta Draconds (Jenniskens and Gural, 2011) and April alpha Capricornids (SonotaCo et al., 2014). These occurrences lead to the question whether some meteor shower outbursts were not noticed due to overcast weather or the nonexistence of a meteor network beneath the skies where the outburst was visible.

8 Conclusion

A complete open-source software solution for video meteor capture and detection on the *RaspberryPi 2* single-board computer has been developed and described in detail. First, a set of requirements were set which such a station should meet. Next, real-time compression to CAMS FTP format and a fireball detection algorithm were described. Also, a newly-developed meteor detection algorithm was described and evaluated with the conclusion that it suits the needs of a low-cost meteor station. The pseudo code of a line segment detector in a 3D point cloud used by both fireball and meteor detectors was given. Furthermore, a star extraction algorithm which uses a Gaussian *PSF* fitting to stars was developed and tested with very positive results. Finally, the astrometry and photometry procedures were implemented and discussed.

While the individual segments of software described in this paper performed within the requirements on sample data, system tests during an actual night of meteor recording still need to be performed. Also, the software needs to be made more user-friendly and the documentation is to be expanded. It is the hope of the authors that the number of contributors to this project will rise in the future and that the developed system will find its place among meteor enthusiasts.

References

Berry R. and Burnell J. (2005). "The Handbook of Astronomical Image Processing", Willmann-Bell, 2nd edition.

Borovička J., Spurný P., Šegon D., Andreić Ž., Kac J., Korlević K., Atanackov J., Kladnik G., Mucke H., Vida D. and Novoselnik F. (2015). "The instrumentally recorded fall of the Križevci meteorite, Croatia, February 4, 2011". *Meteoritics and Planetary Science*, **50**, 1244–1259.

Brown P., Wiegert P., Clark D. and Tagliaferri E. (2016). "Orbital and physical characteristics of meter-scale impactors from airburst observations". *Icarus*, **266**, 96–111.

Eiter T. and Mannila H. (1994). "Computing discrete Fréchet distance". Technical Report CD-TR 94/64, Christian Doppler Laboratory for Expert Systems, TU Vienna, Austria.

Fernandes L. A. F. and Oliveira M. M. (2008). "Real-time line detection through an improved Hough transform voting scheme". Pattern Recognition (PR), Elsevier, 41:1, 2008. Pages 299–314.

Fischler M. A. and Bolles R. C. (1981). "Random Sample Consensus: A Paradigm for Model Fitting with Applications to Image Analysis and Automated Cartography". *Communications of the ACM;* **24,** 381–395.

Gonzalez R. and Woods R. (2008). "Digital Image Processing". Pearson, Third Edition, pages 627–676.

Gural P. S. (2011). "The California All-sky Meteor Surveillance (CAMS) System". In Asher D. J., Christou A. A., Atreya P. and Barentsen G., editors, *Proceedings of the International Meteor Conference*, Armagh, Northern Ireland, 16-19 September, 2010. IMO, pages 28–31.

Gural P. (2016). "A Fast Meteor Detection Algorithm". In Roggemans A. and Roggemans P., editors, *Proceedings of the International Meteor Conference*, Egmond, the Netherlands, 2-5 June 2016. Pages 96–104.

Gural P. and Šegon D. (2009). "A new meteor detection processing approach for observations collected by the Croatian Meteor Network (CMN)". *WGN, Journal of the IMO*, **37**, 28–32.

Hankey M. and Perlerin V. (2014). "IMO Fireball Reports". In Rault J.-L. and Roggemans P., editors, *Proceedings of the International Meteor Conference*, Giron, France, 18-21 September 2014. IMO, pages 160–162.

Jenniskens P., Gural P. S., Dynneson L., Grigsby B. J., Newman K. E., Borden M., Koop M. and Holman D. (2011). "CAMS: Cameras for Allsky Meteor Surveillance to establish minor meteor showers". *Icarus*, **216**, 40–61.

Jenniskens P. and Gural P. S. (2011). "Discovery of the February Eta Draconids (FED, IAU#427): the dust trail of a potentially hazardous long-period comet". *WGN, Journal of the IMO*, **39**, 93–97.

Nelder J. A. and Mead R. (1965). "A simplex method for function minimization". *Computer Journal*, **7**, 308–313.

Samuels D., Wray J., Gural P. S. and Jenniskens P. (2014). "Performance of new low-cost 1/3" security cameras for meteor surveillance". In Rault J.-L. and Roggemans P., editors, *Proceedings of the International Meteor Conference*, Giron, France, 18-21 September 2014. IMO, pages 66–73.

Šegon D. (2009). "How many stars are needed for a good camera calibration?". *WGN, The Journal of the IMO*, **37**, 80–83.

SonotaCo, Shimoda C., Inoue H., Masuzawa T. and Sato M. (2014). "Observation of April alpha Capricornids (IAU#752 AAC)". *WGN, Journal of the IMO*, **42**, 222–226.

Vida D., Šegon D., Gural P. S., Martinović G. and Skokić I. (2014). "CMN_ADAPT and CMN_binViewer software". In Rault J.-L. and Roggemans P., editors, *Proceedings of the International Meteor Conference*, Giron, France, 18-21 September 2014. IMO, pages 59–63.

Zhang T. Y. and Suen C. Y., (1984). "A Fast Parallel Algorithm for Thinning Digital Patterns". *Communications of the ACM*, **27**, 236–239.

Zubović D., Vida D., Gural P. and Šegon D. (2015). "Advances in the development of a low-cost video meteor station". In Rault J.-L. and Roggemans P., editors, *Proceedings of the International Meteor Conference*, Mistelbach, Austria, 27-30 August 2015. IMO, pages 94–97.

Code segment A. 3D line detector pseudo code

```
Function FindLines(Point_cloud, Lines_found){

  // Check if the previously found lines exceed the maximum number of lines to be found
  If (Length(Lines_found) >= Max_lines){
    Return Lines_found;
    }

  Results_list = [];

  For each point P1 in Point_cloud{
    For each point P2 in Point_cloud{
      Line = Line defined by P1 and P2;
      Distance_sum = 0;
      Point_counter = 0;
      Previous_P3 = P1;

      For each point P3 in Point_cloud{
        // Check if the point is close enough to the line
        If (Distance(Line, P3) < Distance_threshold){

          // Check if the point is too far away from the previous point
          If (Distance(Previous_P3, P3) > Gap_threshold){
            // Reject the hypothesized line if the previous point
            // was too far away from the second point that defines the line
            If (Distance(Previous_P3, P2) > Gap_threshold){
              Point_counter = 0;
              }
            Break loop;
          }
          Point_counter++;
          Distance_sum += Distance(Line, P3);
          Previous_P3 = P3;
        }
      }

      // Reject the hypothesized line if it envelops too few points
      If (Point_counter < Minimum_points)
        Continue loop;

      Average_distance = Distance_sum / Point_counter;
      Quality = Point_counter - Distance_weight * Average_distance;

      Add Line in Results_list;
    }
  }

  // Choose the best hypothesized line
  Best_line = Line with the largest Quality in Results_list;
  Point_ratio = (Number of points in Best_line) / (Number of points in Point_cloud);

  // Remove the points of the best line from the point cloud
  Point_cloud = Point_cloud \ Points(Best_line);

  // Add the best line to results only if it covers a minimum number of frames
  If (Frame_range(Best_line) >= Minimum_frame_range)
    Add Best_line in Lines_found;

  // Iteratively find lines on the point cloud until most of points
  // in the cloud have been covered, the remaining number of points is not too low,
  // and the flag for returning just one line was not set
  If ((Point_ratio < Ratio_threshold) & (Number of points in Point_cloud > 10)
       & NOT Return_one_line)
    FindLines(Point_cloud, Lines_found);

  Return Lines_found;
```

Table 2 – 3D line segment detector input parameters.

Name	Data type	Description
Point_cloud	list	a list of points in the point cloud, each point is defined by the (X, Y, Z) tuple
Max_lines	integer	the maximum number of lines which the algorithm should find
Distance_threshold	float	the radius of the cylinder around the hypothesized line
Gap_threshold	float	the maximum distance between subsequent points which make the line
Minimum_points	integer	the minimum number of points a line should have to be accepted
Distance_weight	float	the weight by which the point-line distance will be multiplied, a larger value of the parameter yields compact lines with a smaller amount of points, while a smaller value yields dispersed lines with more points
Minimum_frame_range	integer	minimum length of the Z axis component, i.e. the minimum number of frames the line segment covers
Ratio_threshold	float	minimum ratio between the found and the total points in the point cloud until the algorithm is stopped, e.g. if the ratio is 0.7, the algorithm will run until at least 70% of points are joined to a certain line, or no line satisfies the minimum requirements to be accepted
Return_one_line	boolean	if True, the algorithm will not do an iterative search, but return only one line

Table 3 – 3D line segment detector output description.

Name	Data type	Description
Lines_found	list	a list of lines found in the point cloud

Queuing to get some speaking time with Korado Korlević (left). Sirko Molau waiting for Denis Vida to finish…

Big data era in meteor science

Dejan Vinković[1,2], Maria Gritsevich[3,4,5], Vladimir Srećković[6], Bojan Pečnik[7], Gyula Szabó[8,9], Victor Debattista[10], Petr Škoda[11], Ashish Mahabal[12], Jouni Peltoniemi[3,13], Sanna Mönkölä[14], Areg Mickaelian[15], Esa Turunen[16], Jakub Kákona[17], Jarkko Koskinen[3] and Victor Grokhovsky[4]

[1] **Physics Department, University of Split, Nikole Tesle 12, 21000 Split, Croatia**
dejan@iszd.hr

[2] **Science and Society Synergy Institute, Bana J. Jelacica 22, 40000 Cakovec, Croatia**

[3] **Finnish Geospatial Research Institute (FGI), Geodeetinrinne 2, FI-02430 Masala, Finland**
maria.gritsevich@nls.fi

[4] **Institute of Physics and Technology, Ural Federal University, Mira street 19, 620002 Ekaterinburg, Russia**

[5] **Extraterrestrial Laboratory (MExLab), Moscow State University of Geodesy and Cartography (MIIGAiK), Gorokhovsky pereulok 4, 105064 Moscow, Russia**

[6] **Institute of Physics, University of Belgrade, P.O. Box 57, 11001 Belgrade, Serbia**
vlada@ipb.ac.rs

[7] **HiperSfera Ltd. Ilica 36, Zagreb, Croatia**
bpecnik@hipersfera.hr

[8] **ELTE Gothard Astrophysical Observatory, H-9704, Szombathely, Szent Imre herceg út 112**
szgy@gothard.hu

[9] **Konkoly Observatory, Research Centre for Astronomy and Earth Sciences, Hungarian Academy of Sciences, H- 1121 Budapest, Konkoly Thege Miklós út 15-17, Hungary**

[10] **Jeremiah Horrocks Institute, University of Central Lancashire, Preston, PR1 2HE, UK**
vpdebattista@uclan.ac.uk

[11] **Astronomical Institute of the Czech Academy of Sciences, Fričova 298, Ondřejov, 25165 Czech Republic**
skoda@sunstel.asu.cas.cz

[12] **California Institute of Technology, 1200 E California Bl., Pasadena, CA 91125, USA**
aam@astro.caltech.edu

[13] **Department of Physics, P.O. Box 64, FI-00014 University of Helsinki, Finland**
jouni.peltoniemi@helsinki.fi

[14] **Department of Mathematical Information Technology, P.O. Box 35, FI-40014 University of Jyväskylä, Finland**
sanna.monkola@jyu.fi

[15] **Byurakan Astrophysical Observatory (BAO), Byurakan 0213, Aragatzotn Province, Armenia**
aregmick@yahoo.com

[16] **Sodankylä Geophysical Observatory, University of Oulu, Tähteläntie 62, FI-99600 Sodankylä**
esa.turunen@sgo.fi

[17] **Czech Institute of Informatics, Robotics and Cybernetics, Czech Technical University, Prague, Czech Republic**
kakonjak@fel.cvut.cz

Over the last couple of decades technological advancements in observational techniques in meteor science have yielded drastic improvements in the quality, quantity and diversity of meteor data, while even more ambitious instruments are about to become operational. This empowers meteor science to boost its experimental and theoretical horizons and seek more advanced science goals. We review some of the developments that push meteor science into the big data era that requires more complex methodological approaches through interdisciplinary collaborations with other branches of physics and computer science. We argue that meteor science should become an integral part of large surveys in astronomy, aeronomy and space physics, and tackle the complexity of micro-physics of meteor plasma and its interaction with the atmosphere.

1 Introduction

Exploration of meteor physics and meteor related phenomena has reached the level of complexity that requires new experimental and theoretical advancements. There is a clear demand on more reliable data on meteor plasma and meteor-atmosphere interaction, as our current understanding of these physics is not comprehensive. The recent increased interest in meteor science triggered by the Chelyabinsk airburst (Borovička et al., 2013; Brown et al., 2013; Popova et al., 2013; Proud, 2013; Antolik et al., 2014; Kohout et al., 2014) helps in building the case for technologically and logistically more ambitious meteor projects. This requires developing new methodological approaches in meteor research, with Big Data science and close collaboration between geoscience and astronomy as critical elements. We discuss possibilities for improvements and promote an opportunity for collaboration in meteor science within the BigSkyEarth[1] network.

2 Big Data I

High-resolution and high-sensitivity meteor detections with high-precision photometry exist on images from big telescopes that resolve the meteors. For example, Iye et al. (2007) used the 8.2 meter Subaru telescope's 80 mega-pixel SuprimeCam camera and observed 13 faint meteors in 5 days. This proves that meteors are quite common stochastic feature in such images, but they are treated as a noise and stay untouched and unexplored. Finding them requires an automatic search for meteors in large astronomical databases. A recent example is an ongoing search for meteors in the SDSS database[2] (Bektešević, 2015), which required a development of a new machine recognition procedure for linear feature detection (Bektešević et al., 2016). Many other databases can be targeted by that approach, but this requires techniques in the domain of Big Data methodologies, where a small number of events has to be detected within terabytes or petabytes of imaging data. The upcoming big surveys covering the time domain in addition to large sky coverage will also have a daily stream of transient events alerts (e.g., LSST). Many current surveys too have such streams, either public (e.g. CRTS) or private (e.g. iPTF and Pan-STARRS). In fact searches on PTF data have been carried out to look for comets (using extendedness, Waszczack et al., 2013), and similar searches are on for asteroids (using streakiness), and a program has begun to get the missed ones using machine-learning. The meteor science community could be actively involved in these big sky survey collaborations and make an effort to put meteor detection into the surveys' automatic image recognition pipeline.

[1] http://bigskyearth.eu/
[2] http://vinkovic.org/Projects/MindExercises/radnje/2015_Dino.pdf

3 Big Data II

A recent discovery of MHz emission from meteors in the VHF radio band (Obenberger, 2014) demonstrates the need for monitoring possible meteor signals in sky surveys outside the traditional visual bands and comfort zone of meteor astronomers. The nature of this emission is not understood, but it shows the richness of meteor plasma physics. The ongoing and upcoming radio sky surveys will produce petabytes and soon exabytes of data (LOFAR, SKA). The meteor science community could pursue projects that combine meteor detection with different types of sensors simultaneously to extract more complex science from the data and to obtain precise timing of meteor appearance required for extracting data from big sky survey databases.

4 Big Data III

A search for dark energy and large-scale structure of the Universe as well as investigation of Galactic structure has motivated the development of specialized massively multi-object spectrographs equipped with several thousands of rapidly fixable fibres or Integral Field Unit spectrographs (IFUs). While some of them have very small field of view (e.g. 1 arcmin for ESO MUSE), other have several degrees, e.g. LAMOST[3] survey contains 4000 fibres of over 5°, the planned HETDEX survey even 33600 spectra in 22 arcmin (Adams et al., 2011) . Those systems are running wide-field spectroscopic surveys with an exposure time of tens of minutes to several hours. As the observation is continuously running for months or years, there is a high probability that many meteoric spectra were registered by them, which are, however hidden in the noise. Serendipitous observations of meteors with such instruments are of a great value, since the individual spectra can reveal differences in emission from various parts of the resolved defocused meteor image.

The spectra are reduced by automatic pipelines, with automatic matching of significant features like strong emission (for redshift estimation) and/or global matching with a library of templates (for stellar classification), but always individually, one spectrum independently of others. As the targets are usually faint, the signal-to-noise ratios are low and so the meteoric spectrum will be hidden in the noise. However, the potential of the astroinformatics approach is in finding the correlations in intensity of noise among all fibre spectra exposed during the same exposure, which are in addition correlated with position of fibres on the sky. So the data have a character of a sparse data cube – looking like an image, where every point contains a whole spectrum (the spatial coverage is regular grid in case of IFUs).

Finding such correlations is a challenge for advanced statistics and big data processing. The probability of such a detection requires analyzing of an enormous amount of data (of the order of hundreds of TB), which must have a

[3] http://www.lamost.org/public/?locale=en

unified metadata description. The great advantage of such a novel approach is in the possibility of observing changes of spectra of the meteor along the orbit while passing over different fibres or IFU elements.

This type of meteor astronomy requires new algorithms for meteor detection and analysis of their multispectral data as well as involvement of experts on advanced statistics and informatics understanding scientific Big Data processing.

Enormous potential, yet unexploited, presents the cross-matching of all such surveys in a global manner, with an aim to find observations of the same regions of the sky at the same time with different instruments, namely at the moment of a bright meteor detection in the wide field surveys. This may be feasible, if all the surveys follow the standards of the International Virtual Observatory Alliance (IVOA), namely the Table Access Protocol (Nandrekar-Heinis et al., 2014) operating on Observation Data Model Core Components (Louys et al., 2011) designed for temporal, spectral and spatial description of virtually all types of astronomical data.

We also suggest considering dedicated observation projects with middle class telescopes, with the telescope focus set onto the meteors. From SDSS statistics we see that the distribution diverges from the prediction from major meteor storms. I.e., there are a number of telescopic meteor storms with a small size distribution, which can dominate the optical groups in the telescopic magnitude range. The optimal strategy might be to make predictions from sky surveys and other detections, and to allocate the telescope time to the peaks of telescopic meteors. Even with a Schmidt telescope with 180 cm focal length, the sharp picture of a meteor at 110 km distance is 3 millimeters behind the sharp images of stars, leading to a blurred image by approximately 3 arcsec. The blurring keeps worsening heavily with the increasing focal length. A well-focused telescope can, on the other hand, reach a few 10 cm resolution, which is a solid observational basis for studying the plasma trail.

5 New meteor plasma physics

There is mounting evidence that our understanding of the meteor plasma physics is not adequate to explain various meteor related phenomena. High altitude meteors at about 130 km altitude have been explained by sputtering (Popova et al., 2007; Vinković, 2007), but some images show jets and structures that require additional explanations (Spurný, 2000). Similar fast jets have been detected at lower altitudes too (LeBlanc et al., 2000), and a complex plasma dynamics in the rarefied magnetized ionospheric environment might be the reason. Maybe this physics has some connection to the phenomenon of electrophonic sounds, which had been detected instrumentally, but their explanation is still missing (Zgrablić et al., 2002). The main problem is that this sound seems to originate from strong electric fields on the ground, but created at ionospheric altitudes. However, such strong quasi-electrostatic disturbances should not be able to propagate to the ground. Also, fragmentation above 100 km altitude can explain some radar or imaging data, but there is no explanation for detected high speed fragments at these altitudes (Stokan and Campbell-Brown, 2014). Similarly, fast (millisecond) high-amplitude flickering of light curves (Spurný and Ceplecha, 2008) and stationary oscillations of radar cross section (Kero et al., 2008) are still not explained. A large halo around a meteor detected in a high-speed recording (Stenbaek-Nielsen and Jenniskens, 2004) is probably connected to the same type of physics. A new theoretical model (Šiljić et al., 2016) seeks explanation for many of these phenomena in electromagnetic coupling between meteors and their surrounding ionosphere, where the Earth's magnetic field plays an important role.

The most up-to-date papers detailing radiation physics of meteors are still the works by Öpik (1933, 1955), though of course there exist many studies, where not yet well-known processes are simply modelled using a heavily increased number of free parameters. The use of scaling laws to formulate a well-posed inverse problem helps in finding some key meteor parameters (Gritsevich, 2009; Gritsevich and Koschny, 2011), but there is still room for improvement. The meteor trails are also a complex topic.

The magnetization of trail electrons results in their faster drift along the direction of the magnetic field, which has been detected by radars and simulated recently in 3D (Oppenheim and Dimant, 2015). Theory also shows that strong electric fields could be induced with the trail, which can drastically increase the complexity of meteor plasma dynamics (Dimant et al., 2009). Such a long list of unexplained meteor related phenomena suggests that our understanding of meteor plasma and hypervelocity shock physics in rarefied partially ionized and partially magnetized ionospheric plasma is not complete. The variety of detection techniques required for measuring these phenomena argues for a highly interdisciplinary approach with a combination of astronomical and geophysical techniques.

6 Numerical simulations

The recent development of numerical simulation methods and enhanced computational resources provide possibilities to forecast the meteor plasma dynamics and to test how changes in the atmospheric conditions affect the meteor radar reflections and explain unexpected results in the observations. Computer simulations, built by using modern and computationally efficient methods (see, e.g., Marshall and Close, 2015; Sansom et al., 2015; Räbinä et al., 2016), are reasonable tools to test new meteor plasma models and consider, e.g., the fragmentation of a meteoroid into smaller pieces (e.g. Kero et al., 2008; Zhu et al., 2016). However, when it comes to simulations of hypersonic meteor flight, numerical simulations are often scarce and simplified. These simulations can reveal details of the meteor non-equilibrium plasma formation and its properties and composition, but it is a highly complex problem. The meteor plasma physics includes a plethora of phenomena

– collisional processes between various charged and neutral plasma species; processes of atomic and molecular excitation, dissociation, ionization and recombination; evaporation (ablation) of the meteoroid surface; thermal radiative processes and transfer; chemical and charge exchange reactions; dusty plasma effects; etc. – and all that coupled with internal and external electric and magnetic field dynamics that influence election and ion mobility in different ways, depending on the ratio between their collision and cyclotron frequency. Not surprisingly, the meteor hypersonic flight simulations have been simplified to include only basic kinetics of atmospheric and meteor vapor species (Boyd, 2000; Vinković, 2007; Dyrud et al., 2008) or, in its most advanced version, a radiative gas dynamic model of physically and chemically non-equilibrium flow at lower meteor heights (70 km) where the atmosphere is dense enough to fulfil conditions for ignoring external electric and magnetic fields and for applying simulation methods developed for modelling the re-entry of space vehicles (Surzhikov, 2014). Hence, we still do not have numerical simulations that can address the issues of meteor plasma at typical heights between 70 and 130km, where: the flow is in a transition regime from free-molecule to continuous flow (Popova et al., 2000); electrons react to the external magnetic field while the ion mobility is still collisional dominated; we expect a self-induced electric field within the meteor's diffuse shock front (Farbar and Boyd, 2010). These new simulation frontiers are required to test the latest theoretical attempts of exploring the impact of the ionospheric electric and magnetic field on the meteor plasma dynamics (Dimant et al., 2009; Šiljić et al., 2016).

7 Complex connection with other atmospheric phenomena

Although the majority of meteors are sub-millimeter in size, they still have a great importance for the Earth's atmosphere. They are the main source of metallic ions for the ionospheric Sporadic E layers -– thin layers of metallic ion plasma which form mostly between 100 and 125 km (Haldoupis, 2012). Meteor airbursts create a plethora of large scale atmospheric and ionospheric disturbances. Meteor storms can significantly disturb the ionosphere and its ionization levels (e.g. Baumann et al., 2013; Pellinen-Wannberg et al., 2014). Nanometer size smoke particles from meteor ablation influence ion chemistry at altitudes from 80 to 120 km and are most likely nucleation sites for ice particles that make up noctilucent clouds (Hervig et al., 2012). It is also confirmed now that meteors can trigger sprites (large-scale electrical discharges high above thunderstorms), although the exact physical mechanism enabling this phenomenon is not understood (Qin et al., 2014). These examples demonstrate the complexity of the meteor-atmosphere interaction that goes far beyond meteor ablation physics.

8 Three dimensional radar observations

Radars play a critical role in the exploration of meteor plasma properties – from meteor head to meteor trails. A new dimension of meteor plasma exploration has been reached with a simultaneous usage of three radars. The potential observing capabilities of a radar system are evaluated by McCrea et al. (2015), McKay-Bukowski et al. (2015) and Pellinen-Wannberg et al. (2016). The authors address an important topic of improving the estimates for the flux of extraterrestrial matter to the Earth based on the data obtained using a high-power radar system. EISCAT_3D (Europe's Next-Generation Radar for Atmospheric and Geospace Science) is incoherent scatter radar and it is expected to be one of the most advanced instruments to investigate plasma physics phenomena in the terrestrial atmosphere. The multi-beaming capability makes it possible to perform three or more tri-static observations at different heights simultaneously, while the lower operating frequency makes head echoes observable at heights up to 115 km.

9 Meteorite fall location using weather radar imagery

This is a recently proven approach to locate fresh meteorite fall (Fries and Fries, 2010; Fries et al., 2014). Weather radars are operated by national weather bureaus worldwide and have assisted in the recovery of several meteorites in the United States within the past years, including the Sutter's Mill and Battle Mountain meteorites. Up to now the search for the specific signatures within the data acquired by weather radar has been performed manually and was initiated due to the existence of the other fireball records indicating a possible meteorite fall (i.e. by having the time and tentative location constrains available from the other observation means). However dedicated automatic software may be developed to recognize the 'meteorite signature' in the whole set of weather radar data and to calculate timely the locations and create immediate alerts for detected meteorite falls.

10 Emission and/or scattering of VLF

Very low frequency (VLF) radio waves have been occasionally explored in relation to meteors. The interest for this topic initially emerged from theoretical predictions of VLF being the cause of electrophonic sounds. However, their relation to meteors has not been firmly established and they have not been detected concurrently with electrophonic sounds. Instead, even lower radio frequencies (in the range of quasi-electrostatic fields) are suspected as the source of these sounds (Zgrablić et al., 2002). Two types of possible correlations between VLF and meteors have been implied: meteors emitting VLF waves (*case a*) or their perturbed surrounding simply scatter the atmospheric VLF waves (*case b*) producing the variations of amplitudes and a phase of kHz VLF signals. With a VLF receiver or network of receivers (Šulić et al., 2016) we

can continuously monitor and later analyze these meteors correlated VLF radio waves.

Case a

First we consider the electromagnetic detection of meteors. Recently, it was reported that a meteor shower produces ELF/VLF waves which propagate and reach the ground. It has been shown that 35% of observed meteors and corresponding VLF events are in correlations. However, more data with a statistical approach and further investigations are needed to confirm the statement that the process of possible detecting meteors with the help of an electromagnetic spectrum has potential to become a widely useful tool. In spite that it is at a very noisy frequency band (lot of EM waves produced in this band by other sources like lightning, electrical circuits, power supplies) this possible technique would have the advantage over the visual detection because it can be applicable at any time day/night and in almost all weather conditions. A dynamic VLF spectrum with broadband data is shown in *Figure 1*. With the help of this spectrum we can get all frequencies between 5 kHz and 13 kHz (possible emitted by meteors) compare and process them. This kind of data, i.e. a large volume of spectral images with spectral wavelengths, takes up a few GB per hour and requires complex processing and analysis.

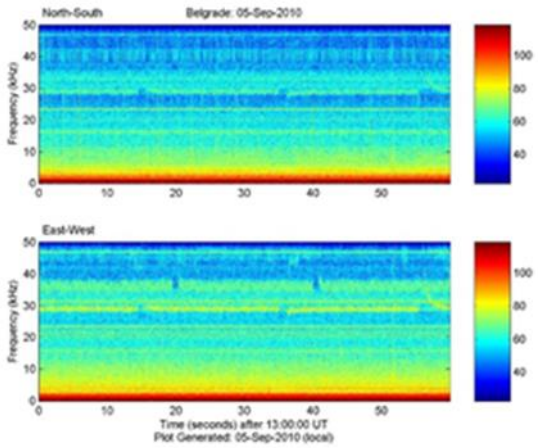

Figure 1 – Broadband data includes information at all frequencies between the systems cutoffs (few Hz – 47 kHz) recorded at receiver site.

Case b

Possible detection of meteors can be done by simply taking the amplitude and phase, separately (of a single narrow frequency range, specified in the software, and usually corresponding to the frequency of a VLF transmitter which can be seen from the map in *Figure 2*) and compared to the non-perturbed level. This can be quite improved with a simultaneous usage of different transmitters i.e. the usage of signals from different directions (path dependent) in order to really collect correlation between signal perturbation and meteor detection.

The physical explanation-mechanism for case b demonstrates the complexity of the meteor-atmosphere interaction (meteor plasma, ionization, triggering sprites, etc.). Meteor particles, due to collisions and perturbation of the surrounding ionosphere (neutral molecules), pass the kinetic energy and convert into potential energy of ionization with the production of extra ionization in the ionosphere. Meteors and this extra ionization produced by them during their passage through the lower ionosphere may have been the cause of high variation of signal level of amplitudes /phase of VLF signals in the Earth–ionosphere waveguide (recorded after their journey through a long distance), which is few times its normal value (De et al., 2012).

Figure 2 – Worldwide VLF transmitters.

It would be very useful for VLF researchers to make effort and implement some new solutions which are already used in other fields of astro- and geoscience, such as events alerts (e.g., CRTS). It was with the Palomar-QUEST, and CRTS that the VOEvent protocol was developed and implemented under the aegis of the US Virtual Observatory (NVO, VAO). The VOEvent (Williams and Seaman, 2006) is a simple and small packet describing the what/where/when/how/why of an event and can be conveyed as a variety of inter-transferable structured data-formats such that humans as well as machines that can make decisions and automated telescopes can receive them. CRTS, for instance, has made extensive use of it (Drake et al., 2009; Djorgovski et al., 2011; Mahabal et al., 2011). Recent systems like Gaia are using variations on the theme, and LSST plans to use an extended version to also include small image cutouts. We propose to the meteor science community more networked VLF observatories for a better understanding of this phenomenon and we propose a highly interdisciplinary approach utilizing the infrastructural developments in optical astronomy as mentioned above. The VLF event alerts can be combined with alerts of meteor detection coming from meteor networks. Such networks of video cameras are now established in many countries and often operated by amateur astronomers. The networks detect meteors and their trajectories and provide invaluable data for meteor activity and their origin exploration. But they can be further utilized as targets of meteor VLF events. A network observing the sky on the path of VLF signals from transmitters can feed the VLF observer with meteor detection alerts. In case ionization from a meteor shower or from bright individual meteors creates disturbances in the VLF signal, the cross-correlation between meteor and VLF alerts would reveal details of the physics behind this connection. However, such a coordinated work is not

challenging only from logistical point of view, but also from a Big Data perspective.

There is also an active radio observation of meteors ongoing in the VHF range using the French military satellite tracking radar system GRAVES at 143.05 MHz. An example of such VHF activity is the Czech radio meteor detection network Bolidozor (Pinter et al., 2013; Kákona et al., 2015). The primary goal of this network is calculation of meteor trajectories from multi-station meteor radio echoes. Bolidozor stations' and receivers' configuration is shown on *Figure 3a and 3b*.

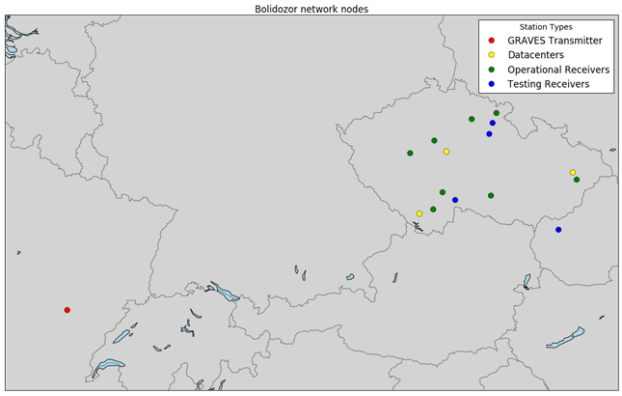

Figure 3a – Czech VHF meteor detection network Bolidozor. The red dot in France is the VHF transmitter GRAVES.

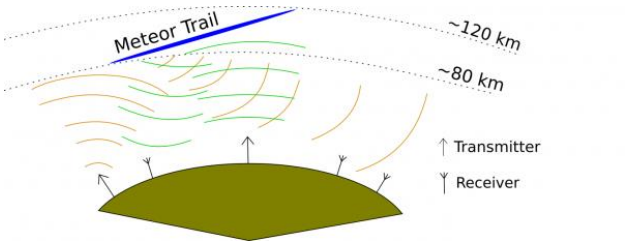

Figure 3b – The core of the system is made of a network of meteor radio detectors that are gradually upgraded and extended to contain new measurement methods.

The network is technically limited mainly by signal processing algorithm implementation because the multi-static systems require numerically demanding statistical calculations, which are furthermore being done in real-time and with a signal containing a high proportion of interference. Each station currently generates 1GB of pre-filtered data per day. The data are accumulated in a central data server located at the Ondřejov observatory. In order to effectively use the multi-static signal, there have to exist algorithms able to detect objects covered by interference and using the data from multiple stations, but the data processing complexity requires a high amount of computing power which is usually in the form of distributed computing power in modern scientific experiments, e.g. BOINC[4]. Such computing methods require data distribution on multiple nodes, which means the distributed storage of a big data amount, is necessary for such system. One of the promising, less computationally demanding methods seems to be an application of artificial neural networks (Roman and Buiu, 2014). However the research is just at the beginning and therefore there are many tasks open from the informatics point of view.

11 Solar migration

The study of meteors can also help inform the study of the Galaxy we live in. There is a growing consensus that the Milky Way has experienced significant levels of stellar radial migration, with stars having changed their orbital radius within the Milky Way significantly while retaining nearly circular orbits (Roskar et al., 2008; Hayden et al., 2015; Loebman et al., 2016). However the exact extent to which stars have migrated, particularly in the Solar neighborhood, is not well known. In much the same way as stars migrate, interstellar meteoroids will also have. A small, but not negligible, fraction of meteors reaching the Earth will originate from across the Milky Way, giving us direct access to conditions across the Milky Way. Properties, such as the relative abundance of alpha-elements (for instance, carbon, oxygen, magnesium, and calcium) compared with iron-peak elements, vary across the Milky Way, providing a means by which the origin within the Milky Way of meteors can be recognized. Such meteors at the Earth are therefore particularly useful for helping to constrain the extent to which migration has been taking place in the solar neighborhood.

12 Detection of meteors from orbit and stratosphere

Certain aspects of meteor science require observations outside the atmosphere, or at least above the majority of the atmosphere (Bouquet et al., 2014; Vaubaillon et al., 2015). For example, observations from satellites enable detection of meteor UV spectra and infrared signatures (Rambaux et al., 2014). In comparison with existing ground-based observations, a space-based optical system for meteor detection would escape dependency on weather and atmospheric conditions, critical not only for detectability, but also for subsequent data analysis (Lyytinen and Gritsevich, 2016). It is also the easiest way to set up meteor observations on other planets (Christou et al., 2012, 2014). Bouquet et al. (2014) recently evaluated potential performance by such systems as a function of observation parameters (optical system capabilities, orbital parameters) and considering a reasonable range of meteoroid properties (mass, velocity, composition) determining their luminosity. The authors developed a numerical tool called SWARMS (Simulator for Wide Area Recording of Meteors from Space) and calculated optimistic meteor detection rates for two different systems: the SPOSH (Smart Panoramic Optical Sensor Head) camera optimized for the observation of transient luminous events (Oberst et al., 2011; Christou et al., 2012), and the JEM-EUSO (Japanese Experiment Module – Extreme Universe Space Observatory) experiment on the International Space Station (ISS).

We also propose the creation of a stratospheric platform for meteor observations put on an autonomous unmanned airship. This would enable observations in a rarefied

[4] http://boinc.berkley.edu

atmosphere, above the majority of water vapor. Under such conditions meteors can be observed close to the horizon and with infrared detectors. Airborne meteor observations have a long history (Clifton, 1971; Millman, 1976), but it was the NASA MAC campaigns targeting Leonid showers that transformed airborne meteor science into a mainstream science (Jenniskens and Butow, 1999). This campaign has expanded in its scope and it is now using various types of aircraft[5] for observing meteor showers and it recently helped organize the first European airborne meteor observation campaign (Vaubaillon et al., 2015). The airborne platforms have an advantage of avoiding clouds and have access to a reduced air-mass of water vapor. This enables sampling of a large volume of atmosphere in search for meteors closer to the horizon. It also enables observations of meteor light-curves and spectra in wavelength regions typically inaccessible due to atmospheric water vapor.

A stratospheric airship would provide an entirely new direction in airborne meteor observations. Unlike airplane campaigns that last for a few days, such an airship would provide a continuous service over the year. It would also reach higher altitudes, nominally about 20 km above the sea level. And it would be much cheaper to operate it and maintain. Its science case would not be just meteor observations, but also a multitude of other topics in astronomy (e.g. infrared astronomy, where the need is already demonstrated by the SOFIA airborne telescope (Gehrz et al., 2009)), aeronomy (e.g. transient light phenomena above thunderclouds), Earth observation and remote sensing (e.g. continuous high resolution ground monitoring of about 4000 km^2 not possible with the current drone, airplane or satellite observations) and meteorology (e.g. continuous measurements of atmospheric conditions at high altitudes and during landing/rising maneuver). Such a stratospheric platform would be also ideal for testing various new technologies/instruments aimed for future deployment on satellites.

The key technical characteristics of the proposed airship are already provided by Hipersfera Ltd.[6], a company uniquely specialized for this type of autonomous unmanned aerial vehicles. The airship would host a stable payload platform for about 12 hours (during night time in case of astronomical observations), followed by a landing maneuver and just a few hours for maintenance, repair and overhaul procedures. This makes the airship ready for a new mission every day. The payload capacity would be 100 kg, with 5 kW of continuous and 7-10 kW peak electric power supply. The airship design allows mounting of useful payload either on the bottom or on the top side of the airship. Instruments of a small weight (simple sensors) can be attached on a side. The airship has a rigid structure with attached vectored thrust for attitude and position control. The stabilized payload platform (e.g. designed as a Stewart platform) is connected to the airship through passive vibration isolation, which improves on the default 0.2–0.5 deg/s stability achieved with the vector thrust. The vibration isolation can be further improved on request (e.g. with 3- or 5-axial gimbal). The airship design is scalable, which means that a larger payload can be achieved simply by scaling up the airship volume.

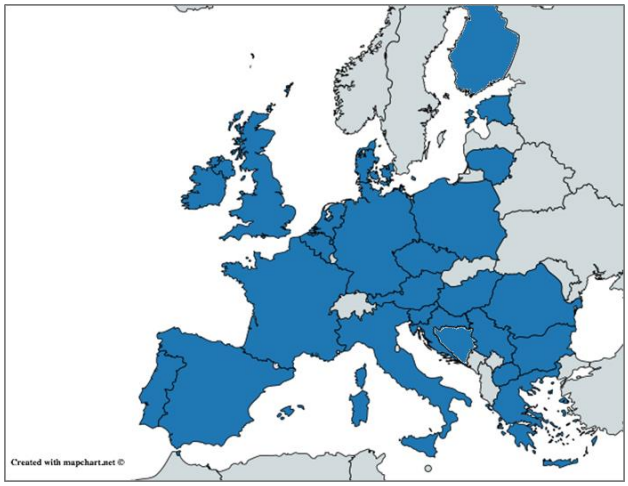

Figure 4 – The map showing COST member countries participating in the COST Action BigSkyEarth (as of June 2016). Further information on BigSkyEarth and its activities are given at http://bigskyearth.eu/.

The TD COST Action TD1403 "Big Data Era in Sky and Earth Observation" (BigSkyEarth, *Figure 4*) network offers an excellent platform to develop the stated big ideas for possible future advances in meteor science, as well as it provides suitable environment for efficient collaboration and joint research studies.

Acknowledgment

This review article is based upon a collaborative work from the COST Action TD1403 "Big Data Era in Sky and Earth Observation", supported by the COST (European Cooperation in Science and Technology, http://www.cost.eu/).

[5] http://airborne.seti.org
[6] http://www hipersfera.hr

References

Adams J. J., Blanc G. A., Hill G. J., Gebhardt K., Drory N., Hao L., Bender R., Byun J., Ciardullo R., Cornell M. E., Finkelstein S. L., Fry A., Gawiser E., Gronwall C., Hopp U., Jeong D., Kelz A., Kelzenberg R., Komatsu E., MacQueen P. J., Murphy J., Odoms P. S., Roth M., Schneider D. P., Tufts J. R. and Wilkinson C. P. (2011). "The HETDEX Pilot Survey. I. Survey Design, Performance, and Catalog of Emission-line Galaxies". *The Astrophysical Journal Supplement*, **192**, id 5, 34 pages.

Antolik M., Ichinose G., Creasey J. and Clauter D. (2014). "Seismic and Infrasonic Analysis of the Major Bolide Event of 15 February 2013". *Seismological Research Letters*, **85**, 334–343.

Baumann C., Rapp M., Kero A. and Enell C.-F. (2013). "Meteor smoke influences on the D-region charge balance - review of recent in situ measurements and one-dimensional model results". *Annales Geophysicae*, **31**, 2049–2062.

Bektešević D. (2015). "Linear feature detection in SDSS images". Master Thesis, University of Split.

Bektešević D., Cikota S., Jevremović D. and Vinković D. (2016). "Linear feature detection algorithm for astronomical surveys II. Parameter optimization". In preparation.

Borovička J., Spurný P., Brown P., Wiegert P., Kalenda P., Clark D. and Shrbený L. (2013). "The trajectory, structure and origin of the Chelyabinsk asteroidal impactor". *Nature*, **503**, 235–237.

Bouquet A., Baratoux D., Vaubaillon J., Gritsevich M. I., Mimoun D., Mousis O. and Bouley S. (2014). "Simulation of the capabilities of an orbiter for monitoring the entry of interplanetary matter into the terrestrial atmosphere". *Planetary and Space Science*, **103**, 238–249. doi: 10.1016/j.pss.2014.09.001.

Boyd I. D. (2000). "Computation of Atmospheric Entry Flow about a Leonid Meteoroid". *Earth, Moon, and Planets*, **82/83**, 93–108.

Brown P., Assink J. D., Astiz A., Blaauw R., Boslough M. B., Borovička J., Brachet N., Brown D., Campbell-Brown M., Ceranna L., Cooke W., de Groot-Hedlin C., Drob D. P., Edwards W., Evers L. G., Garces M., Gill J., Hedlin M., Kingery A., Laske G., Le Pichon A., Mialle P., Moser D. E., Saffer A., Silber E., Smets P., Spalding R. E., Spurný P., Tagliaferri E., Uren D., Weryk R. J., Whitaker R. and Krzeminski Z. (2013). "A 500-kiloton airburst over Chelyabinsk and an enhanced hazard from small impactors". *Nature*, **503**, 238–241.

Christou A. A., Oberst J., Elgner S., Flohrer J., Margonis A., McAuliffe J. P. and Koschny D. (2012). "Orbital observations of meteors in the Martian atmosphere using the SPOSH camera". *Planetary and Space Science*, **60**, 229–235.

Christou A. A., Oberst J., Lupovka V., Dmitriev V. and Gritsevich M. (2014). "The meteoroid environment and impacts on Phobos". *Planetary and Space Science*, **102**, 164–170.

Clifton K. S. (1971). "Airborne meteor observations at high latitudes". *NASA Technical Note D-6303*.

De S. S., Bandyopadhyay B., Barui S., Paul S., Haldar D. K., De D., De B. K., Chattopadhyay S. and Kundu A. K. (2012). "Studies on the Effects of 2009 Leonid Meteor Shower on Subionospheric Transmitted VLF Signals and Vertical Electric Potential Gradient". *Earth, Moon, and Planets*, **108**, 111–121.

Dimant Y. S., Oppenheim M. M. and Milikh G. M. (2009). "Meteor plasma trails: effects of external electric field". *Annales Geophysicae*, **27**, 279–296.

Djorgovski S. G., Drake A. J., Mahabal A. A., Graham M. J., Donalek C., Williams R., Beshore E. C., Larson S. M., Prieto J., Catelan M., Christensen E. and McNaught R. H. (2011). "The Catalina Real-Time Transient Survey (CRTS)". arXiv:1102.5004.

Drake A.J., Djorgovski S. G., Mahabal A., Beshore E., Larson S., Graham M. J., Williams R., Christensen E., Catelan M., Boattini A., Gibbs A., Hill R. and Kowalski R. (2009). "First Results from the Catalina Real-Time Transient Survey". *The Astrophysical Journal*, **696**, 870–884.

Dyrud L., Wilson D., Boerve S., Trulsen J., Pecseli H., Close S., Chen C. and Lee Y. (2008). "Plasma and electromagnetic wave simulations of meteors". *Advances in Space Research*, **42**, 136–142.

Farbar E. D. and Boyd I. D. (2010). "Modeling of the plasma generated in a rarefied hypersonic shock layer". *Physics of Fluids*, **22**, 106101–106101–12.

Fries M. and Fries J. (2010). "Doppler weather radar as a meteorite recovery tool". *Meteoritics and Planetary Science*, **45**, 1476–1487.

Fries M., Le Corre L., Hankey M., Fries J., Matson R., Schaefer J. and Reddy V. (2014). "Detection and rapid recovery of the Sutter's Mill meteorite fall as a model for future recoveries worldwide". *Meteoritics and Planetary Science*, **49**, 1989–1996.

Gehrz R. D., Becklin E. E., de Pater I., Lester D. F., Roellig T. L. and Woodward C. E. (2009). "A new window on the cosmos: The Stratospheric

Observatory for Infrared Astronomy (SOFIA)". *Advances in Space Research*, **44**, 413–432.

Gritsevich M. and Koschny D. (2011). "Constraining the luminous efficiency of meteors". *Icarus*, **212**, 877–884. doi: 10.1016/j.icarus.2011.01.033.

Gritsevich M. I. (2009). "Determination of parameters of meteor bodies based on flight observational data". *Advances in Space Research*, **44**, 323–334. doi: 10.1016/j.asr.2009.03.030.

Haldoupis C. (2012). "Midlatitude Sporadic E. A Typical Paradigm of Atmosphere-Ionosphere Coupling". *Space Science Reviews*, **168**, 441–461.

Hayden M. R., Bovy J., Holtzman J. A., Nidever D. L., Bird J. C., Weinberg D. H., Andrews B. H., Majewski S. R., Allende Prieto C., Anders F., Beers T. C., Bizyaev D., Chiappini C., Cunha K., Frinchaboy P., García-Herńandez D. A., García Pérez A. E., Girardi L., Harding P., Hearty F. R., Johnson J. A., Mészáros S., Minchev I., O'Connell R., Pan K., Robin A. C., Schiavon R. P., Schneider D. P., Schultheis M., Shetrone M., Skrutskie M., Steinmetz M., Smith V., Wilson J. C., Zamora O. and Zasowski G. (2015). "Chemical Cartography with APOGEE: Metallicity Distribution Functions and the Chemical Structure of the Milky Way Disk". *The Astrophysical Journal*, **808**, 132.

Hervig M. E., Deaver L. E., Bardeen C. G., Russell J. M., Bailey S. M. and Gordley L. L. (2012). "The content and composition of meteoric smoke in mesospheric ice particles from SOFIE observations". *Journal of Atmospheric and Solar-Terrestrial Physics*, **84**, 1–6.

Iye M., Tanaka M., Yanagisawa M., Ebizuka N., Ohnishi K., Hirose C., Asami N., Komiyama Y. and Furusawa H. (2007). "SuprimeCam Observation of Sporadic Meteors during Perseids 2004". *Publications of the Astronomical Society of Japan*, **59**, 841–855.

Jenniskens P. and Butow S. J. (1999). "The 1998 Leonid multi-instrument aircraft campaign – an early review". *Meteoritics and Planetary Science*, **34**, 933–943.

Kákona J., Kákona M., Povišer M., Milík J., Dvořák R., Štrobl J., Kovář P., Szylar J., Bednář P., Křivský L. and Chroust J. (2015). "Bolidozor radio meteor detection network". In Rault J.-L. and Roggemans P., editors, *Proceedings of the International Meteor Conference*, Mistelbach, Austria, 27-30 August 2015. IMO, pages 157–160.

Kero J., Szasz C., Pellinen-Wannberg A., Wannberg G., Westman A. and Meisel D. D. (2008). "Three-dimensional radar observation of a submillimeter meteoroid fragmentation". *Geophysical Research Letters*, **35**, CiteID L04101.

Kohout T., Gritsevich M., Grokhovsky V., Yakovlev G., Haloda J., Halodova P., Michallik R., Penttilä A. and Muinonen K. (2014). "Mineralogy, reflectance spectra, and physical properties of the Chelyabinsk LL5 chondrite – Insight into shock-induced changes in asteroid regoliths". *Icarus*, **228**, 78–85. doi: 10.1016/j.icarus.2013.09.027.

LeBlanc A. G., Murray I. S., Hawkes R. L., Worden P., Campbell M. D., Brown P., Jenniskens P., Correll R. R., Montague T. and Babcock D. D. (2000). "Evidence for transverse spread in Leonid meteors". *Monthly Notices of the Royal Astronomical Society*, **313**, L9–L13.

Loebman S. R., Debattista V. P., Nidever D. L., Hayden M. R., Holtzman J. A., Clarke A. J., Roskar R. and Valluri M. (2016). "Imprints of Radial Migration on the Milky Way's Metallicity Distribution Functions". *The Astrophysical Journal Letters*, **818**, L6.

Louys M., Bonnarel F., Schade D., Dowler P., Micol A., Durand D., Tody D., Michel L., Salgado J., Chilingarian I., Rino B., Santander-Vela J. D. and Škoda P. (2011). "IVOA Recommendation: Observation data model core components and its implementation in the table access protocol version 1.0". arXiv: 1111.1758.

Lyytinen E. and Gritsevich M. (2016). "Implications of the atmospheric density profile in the processing of fireball observations". *Planetary and Space Science*, **120**, 35–42. doi: 10.1016/j.pss.2015.10.012.

Mahabal A. A., Djorgovski S. G., Drake A. J., Donalek C., Graham M. J., Williams R. D., Chen Y., Moghaddam B., Turmon M., Beshore E. and Larson S. (2011). "Discovery, classification, and scientific exploration of transient events from the Catalina Real-time Transient Survey". *Bulletin of the Astronmical Society of India*, **39**, 387–408. http://arxiv.org/pdf/1111.0313.pdf

Marshall R. A. and Close S. (2015). "An FDTD model of scattering from meteor head plasma". *Journal of Geophysical Research*, **120**, 5931–5942.

McCrea I., Aikio A., Alfonsi L., Belova E., Buchert S., Clilverd M., Engler N., Gustavsson B., Heinselman C., Kero J., Kosch M., Lamy H., Leyser T., Ogawa Y., Oksavik K., Pellinen-Wannberg A., Pitout F., Rapp M., Stanislawska I. and Vierinen J. (2015). "The science case for the EISCAT_3D radar". *Progress in Earth and Planetary Science*, **1**, 1–63.

McKay-Bukowski D., Vierinen J., Virtanen I. I., Fallows R., Postila M., Ulich T., Wucknitz O.,

Brentjens M., Ebbendorf N., Enell C.-F., Gerbers M., Grit T., Gruppen P., Kero A., Iinatti T., Lehtinen M., Meulman H., Norden M., Orispää M., Raita T., de Reijer J. P., Roininen L., Schoenmakers A., Stuurwold K. and Turunen E. (2015). "KAIRA: The Kilpisjärvi Atmospheric Imaging Receiver Array-System Overview and First Results". *IEEE Transactions on Geoscience and Remote Sensing*, **53**, 1440–1451.

Millman P. M. (1976). "Quadrantid meteors from 41,000 feet". *Sky and Telescope*, **51**, 225–228.

Nandrekar-Heinis D., Michel L., Louys M. and Bonnarel F. (2014). "The Table Access Protocol: Providing standard access to astronomical data". *Astronomy and Computing*, **7–8**, 37–44.

Obenberger K. S., Taylor G. B., Lin C. S., Dowell J., Schinzel F. K. and Stovall K. (2015). "Dynamic radio spectra from two fireballs". *Journal of Geophysical Research: Space Physics*, **120**, 9916–9928. doi:10.1002/2015JA021229.

Oberst J., Flohrer J., Elgner S., Maue T., Margonis A., Schrödter R., Tost W., Buhl M., Ehrich J., Christou A. and Koschny D. (2011). "The smart panoramic optical sensor head (SPOSH) – A camera for observations of transient luminous events on planetary night sides". *Planetary and Space Science*, **59**, 1–9.

Öpik E. J. (1933). "Atomic Collisions and Radiation of Meteors". *Harvard Reprint Series*, **100**, Is. 100, 1–39.

Öpik E. J. (1955). "Meteor Radiation, Ionization and Atomic Luminous Efficiency". *Proceedings of the Royal Society of London. Series A, Mathematical and Physical Sciences*, **230**, Is. 1183, 463–501.

Oppenheim M. M. and Dimant Y. S. (2015). "First 3-D simulations of meteor plasma dynamics and turbulence". *Geophysical Research Letters*, **42**, 681–687.

Pellinen-Wannberg A., Häggström I., Carrillo Sánchez J. D., Plane J. M. C. and Westman A. (2014). "Strong E region ionization caused by the 1767 trail during the 2002 Leonids". *Journal of Geophysical Research*, **119**, 7880–7888.

Pellinen-Wannberg A., Kero J., Häggström I., Mann I. and Tjulin A. (2016). "The forthcoming EISCAT_3D as an extra-terrestrial matter monitor". *Planetary and Space Science*, **123**, 33–40. http://dx.doi.org/10.1016/j.pss.2015.10.009.

Pinter T., Kákona J., Kákona M. and Křivský L. (2013). "Radio meteor scattering with Software Defined Radio based on Open Hardware". In Gyssens M. and Roggemans P., editors, *Proceedings of the International Meteor Conference*, La Palma, Canary Islands, 20-23 September 2012. IMO, pages 213–217. doi: 10.5281/zenodo.53085.

Popova O. P., Sidneva S. N., Shuvalov V. V. and Strelkov A. S. (2000). "Screening of Meteoroids by Ablation Vapor in High-Velocity Meteors". *Earth, Moon, and Planets*, **82/83**, 109–128.

Popova O. P., Strelkov A. S. and Sidneva S. N. (2007). "Sputtering of fast meteoroids' surface". *Advances in Space Research*, **39**, 567–573.

Popova O. P., Jenniskens P., Emel'yanenko V., Kartashova A., Biryukov E., Khaibrakhamanov S., Shuvalov V., Rybnov Y., Dudorov A., Grokhovsky V. I., Badyukov D. D., Yin Q.-Z., Gural P. S., Albers J., Granvik M., Evers L. G., Kuiper J., Kharlamov V., Solovyov A., Rusakov Y. S., Korotkiy S., Serdyuk I., Korochantsev A. V., Larionov M., Y., Glazachev D., Mayer A. E., Gisler G., Gladkovsky S. V., Wimpenny J., Sanborn M. E., Yamakawa A., Verosub K. L., Rowland D. J., Roeske S., Botto N. W., Friedrich J. M., Zolensky M. E., Le L., Ross D., Ziegler K., Nakamura T., Ahn I., Lee J. I., Zhou Q., Li X.-H., Li Q.-L., Liu Y., Tang G.-Q., Hiroi T., Sears D., Weinstein I. A., Vokhmintsev A. S., Ishchenko A. V., Schmitt-Kopplin P., Hertkorn N., Nagao K., Haba M. K., Komatsu M. and Mikouchi T. (2013). "Chelyabinsk Airburst, Damage Assessment, Meteorite Recovery, and Characterization". *Science*, **342**, 1069–1073.

Proud S. R. (2013). "Reconstructing the orbit of the Chelyabinsk meteor using satellite observations". *Geophysical Research Letters*, **40**, 3351–3355. doi:10.1002/grl.50660.

Qin J., Pasko V. P., McHarg M. G. and Stenbaek-Nielsen H. C. (2014). "Plasma irregularities in the D-region ionosphere in association with sprite streamer initiation". *Nature Communications*, **5**, id. 3740.

Räbinä J., Mönkölä S., Rossi T., Markkanen J., Gritsevich M. and Muinonen K. (2016). "Controlled time integration for the numerical simulation of meteor radar reflections". *Journal of Quantitative Spectroscopy and Radiative Transfer*, **178**, 295–305.

Rambaux N., Galayko D., Mariscal J. F., Breton M. A., Vaubaillon J., Birlan M., Colas F. and Fouchet T. (2014). "Detection of spectral UV from meteors by a nanosatellite". In Rault J.-L. and Roggemans P., editors, *Proceedings of the International Meteor Conference*, Giron, France, 18-21 September 2014. IMO, pages 182–184.

Roman V. S. and Buiu C. (2014). "Automatic detection of meteors using artificial neural networks". In Rault J.-L. and Roggemans P., editors,

Proceedings of the International Meteor Conference, Giron, France, 18-21 September 2014. IMO, pages 122–125.

Roskar R., Debattista V. P., Quinn T. R., Stinson G. S. and Wadsley J. (2008). “Riding the Spiral Waves: Implications of Stellar Migration for the Properties of Galactic Disks”. *The Astrophysical Journal*, **684**, L79.

Sansom E. K., Bland P., Paxman J. and Towner M. (2015). “A novel approach to fireball modeling: The observable and the calculated”. *Meteoritics and Planetary Science*, **50**, 1423–1435. doi: 10.1111/maps.12478.

Šiljić A., Lunić F., Teklić J. and Vinković D. (2016). “Proton-induced halo formation in charged meteors”. In preparation.

Spurný P., Betlem H., Jobse K., Koten P. and van't Leven J. (2000). “New type of radiation of bright Leonid meteors above 130 km”. *Meteoritics and Planetary Science*, **35**, 1109–1115.

Spurný P. and Ceplecha Z. (2008). “Is electric charge separation the main process for kinetic energy transformation into the meteor phenomenon?”. *Astronomy and Astrophysics*, **489**, 449–454.

Stenbaek-Nielsen H. C. and Jenniskens P. (2004). “A "shocking" Leonid meteor at 1000 fps”. *Advances in Space Research*, **33**, 1459–1465.

Stokan E. and Campbell-Brown M. D. (2014). “Transverse motion of fragmenting faint meteors observed with the Canadian Automated Meteor Observatory”. *Icarus*, **232**, 1–12.

Šulić D. M., Srećković V. A. and Mihajlov A. A. (2016). “A study of VLF signals variations associated with the changes of ionization level in the D-region in consequence of solar conditions”. *Advances in Space Research*, **57**, 1029–1043.

Surzhikov S. T. (2014). “Non-Equilibrium Radiative Gas Dynamics of Small Meteor”. 44th AIAA Fluid Dynamics Conference, AIAA Aviation, 16-20 June 2014, Atlanta, AIAA 2014-2636.

Vaubaillon J., Koten P., Margonis A., Toth J., Rudawska R., Gritsevich M., Zender J., McAuliffe J., Pautet P. D., Jenniskens P., Koschny D., Colas F., Bouley S., Maquet L., Leroy A., Lecacheux J., Borovicka J., Watanabe J. and Oberst J. (2015). “The 2011 Draconids: the first European airborne meteor observation campaign”. *Earth, Moon, and Planets*, **114**, 137–157. doi: 10.1007/s11038-014-9455-5.

Vinković D. (2007). “Thermalization of sputtered particles as the source of diffuse radiation from high altitude meteors”. *Advances in Space Research*, **39**, 574–582.

Waszczakl A., Ofek E. O., Aharonson O., Kulkarni S. R., Polishook D., Bauer J. M., Levitan D., Sesar B., Laher R., Surace J., and the PTF Team (2013). “Main-belt comets in the Palomar Transient Factory survey – I. The search for extendedness”. *Monthly Notices of the Royal Astronomical Society*, **433**, 3115–3132.

Williams R. and Seaman R. (2006). “VOEvent: Information Infrastructure for Real-Time Astronomy”. *Astronomical Data Analysis Software and Systems XV ASP Conference Series*. Proceedings of the Conference Held 2-5 October 2005 in San Lorenzo de El Escorial, Spain. Edited by Carlos Gabriel, Christophe Arviset, Daniel Ponz, and Enrique Solano. San Francisco: Astronomical Society of the Pacific, 2006. **351**, 637–640.

Zgrablić G., Vinković D., Gradečak S., Kovačić D., Biliškov N., Grbac N., Andreić Ž. and Garaj S. (2002). “Instrumental recording of electrophonic sounds from Leonid fireballs”. *Journal of Geophysical Research*, **107**, SIA 11-1–SIA 11-9. DOI: 10.1029/2001JA000310.

Zhu Q., Dinsmore R., Gao B. and Mathews J. D. (2016). “High-resolution radar observations of meteoroid fragmentation and flaring at the Jicamarca Radio Observatory”. *Monthly Notices of the Royal Astronomical Society*, **457**, 1759–1769.

Statistical approach to meteoroid shape estimation

Vladimir Vinnikov[1], Maria Gritsevich[1,2,3], Daria Kuznetsova[1,4], Olga Krivonosova[5], Dmitry Zhilenko[5] and Leonid Turchak[1]

[1] **Dorodnicyn Computing Centre, Federal Research Center "Computer Science and Control" of the Russian Academy of Sciences, 119333 Moscow, Russia**
vinnikov@ccas.ru

[2] **Finnish Geospatial Research Institute, Department of Geodesy and Geodynamics, FI-02431 Masala, Finland**
maria.gritsevich@nls.fi

[3] **Ural Federal University, Institute of Physics and Technology, 620002 Ekaterinburg, Russia**
gritsevich@list.ru

[4] **Laboratoire d'Aérologie, Observatoire Midi-Pyrénées, 14 av. Edouard Belin, 31400 Toulouse, France**
daria.kuznetsova@aero.obs-mip.fr

[5] **Institute of Mechanics, Lomonosov Moscow State University, Michyrinskiy prospect 1, 119192 Moscow, Russia**
olga@imec.msu.ru

This paper describes a statistically-based technique for meteoroid shape estimation. The idea to obtain the pre-entry shape from a distribution of fragment masses is derived from the experiments on brittle fracturing, that produce multiple fragments of sizes less than or equal to the least dimension of the body. The fragment masses determine the number of fragments as a power law with exponential cutoff. The initial form of the fragmented body is essentially indicated by the value of this scaling exponent.

1 Introduction to the mathematical model

We explore the possibility of determining the proportions of a pre-fragmented meteoroid for the cases with large number of recovered meteorite fragments. The method follows the concepts proposed in (Oddershede et al., 1993; 1998; Vinnikov et al., 2015; 2016) and it is based on the following assumptions:

- The meteoroid material is assumed to be brittle. The common definition of brittleness involves the practical absence of plastic deformation prior to fracturing. We also assume that the crack propagation speed is comparable to the speed of sound through a brittle media and is at least one order higher than the acoustic speed of the surrounding environment. However, we do not completely address the issue of supersonic fracture (Buehler et al., 2003);
- The masses of the fragments recovered within one meteorite fall can be fitted via the power law (which is a special case of a *Weibull* distribution) with relatively small least squares error;
- A complementary cumulative distribution function (CCDF) can be constrained by the scaling exponent B_0, which accounts for the largest recovered fragment mass via an exponential cutoff:

$$F_c(m) = Cm^{-B_0} e^{-\frac{m}{m_U}}, \qquad (1)$$

- For the value of B_0^* obtained by fitting *Equation 1* to the masses of recovered fragments, we can estimate a dimensionless shape parameter, d (its definition is based on size proportions a_x, a_y, a_z) from the empirical equation

$$0.13d^2 - 0.21d + (1.1 - B_0^*) = 0 \qquad (2)$$

In formula (1) C is a normalization constant, $m_U > m_L$ is the upper cutoff fragment mass, m_U corresponds to the threshold where the exponential decay starts to dominate over the power law, and $m_L > 0$ is an arbitrary lower mass limit acting as an additional constraint for undersampled tiny unrecoverable particles resulting from the fragmentation. These mass constraints are also among the sought parameters.

We have applied the technique of the described scaling analysis to the empirical data on the mass distributions for the *Košice*, *Sutter's Mill* and *Bassikounou* meteorites. Each studied meteorite sample consists of N fragments ranging in mass from m_0 to m_{N-1}. In our analysis we arrange the fragment masses m_i in the ascending order and the values m_L and m_U are intermediate in the initial range. If two or more fragments possess equal masses, then we add a small value corresponding to the fragment mass measurement error (e.g. 0.001 g) to one of them, to disambiguate the masses. The fragment mass distribution for the *Košice* meteorite was additionally studied in further detail (Gritsevich et al., 2014; 2016). These mass distributions manifest undersampling for small fragments and an exponential cutoff due to a finite size effect. We apply methods of numerical optimization to estimate the best-fit values for the scaling exponent, the lower and upper constraints as well as the dimensionless shape parameter. Next, the shape parameter is converted into the triad of relative sizes along respective Cartesian axes. Therefore, the obtained triad yields one of the three distinct options of the estimated shape: rod-like, plate-like and sphere-like.

2 Results and discussion

The obtained power-law fits to the empirical fragment mass distributions of the considered meteoroids are presented on *Figure 1*.

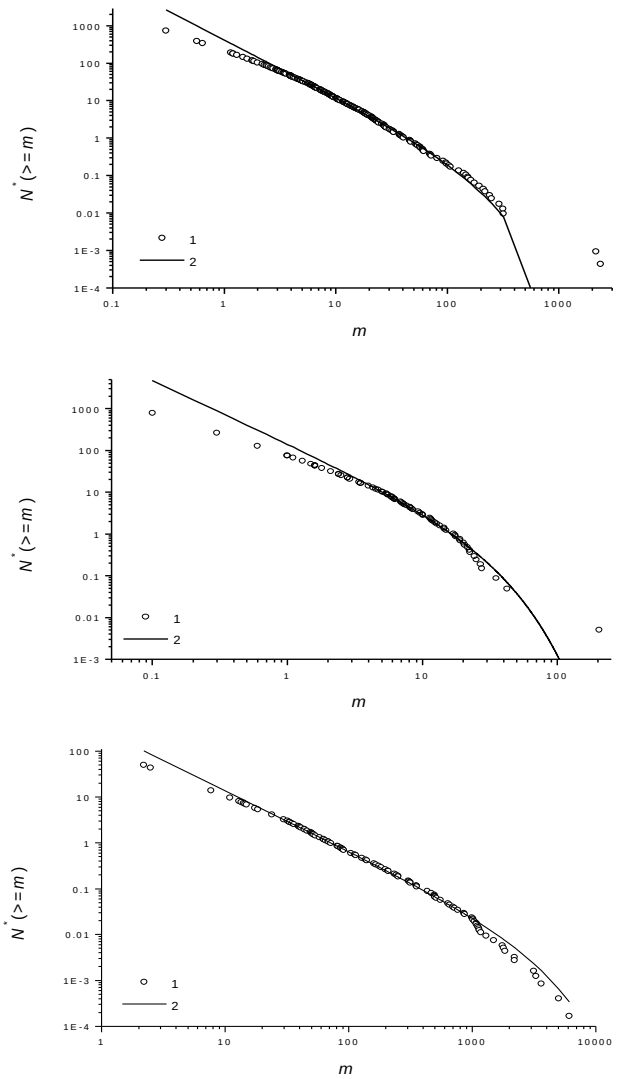

Figure 1 – Complementary cumulative number of fragments $N^*(\geq m)$ vs m. 1 – Observed data, 2 – Power law distribution with exponential cutoff.

Košice (*Figure 1 Top*)

$B_0 = 1.53$, $m_L = 5.64$, $m_U = 155.17$, $d = 2.8$, (a : b : c) = (2.0 : 1.69 : 1.0);

Sutter's Mill (*Figure 1 Middle*)

$B_0 = 1.51$, $m_L = 5.0$, $m_U = 21.0$, $d = 2.76$, (a : b : c) = (2.13 : 1.58 : 1.0);

Bassikounou (*Figure 1 Bottom*)

$B_0 = 1.32$, $m_L = 29.9$, $m_U = 2839.42$, $d = 2.34$, (a : b : c) = (2.98 : 1.13 : 1.0);

a, b, c are the linear dimensions of the fragment.

We emphasize that the applicability of the described meteoroid shape estimation technique is limited to non-prestrained homogeneous brittle solids. The prestrained solids respond differently to the external load due to the stress points with concentrated internal energy and their fragments do not comply to a power law mass distribution. However, we consider that the scaling analysis is suitable for the shape estimation, since the mass distribution of the asteroid belt formed by multiple fragmentations follows a power law (Hughes et al., 1994).

The scaling analysis of Oddershede et al. (1993) is subjected to criticism by Meibom and Balslev (1996), who performed fragmentation experiments with thick plates of dry clay. The experiments revealed different exponents for fragments larger and smaller than the plate thickness, so Meibom made implications denying scale and material invariance and expressed the opinion that "*the measured mass distribution tells little about the mechanisms of the fragmentation process*". On the second thought, this reasoning can be ruled out by the following facts. The speed of sound for clay is about 1–2.8 km/s, in contrast the respective values for gypsum are 2.3 km/s for transverse S-waves and 5 km/s for longitudinal P-waves. In comparison, the speed of sound for chondrites is about 3.5 km/s as stated by Rivkin and Bottke (1996). This leads to the question if the clay really exhibits brittle behavior. Indeed, the universal scaling was not observed for thick large plates of dry clay, but the masses of these plates (540–920 g) were an order of magnitude greater than those of small gypsum plates (58–77 g). We believe that the experiments with thick clay plates failed to provide energy sufficient for brittle fracture conditions. The brittle fracture is a dissipative process, which disperses locally supplied energy over the whole bulk via crack propagation. When all initially channeled energy dissipates, then in absence of internal strains the cracks cease to spread further. The results of experiments with small thin clay plates (237–393 g) by Meibom and Balslev (1996) exactly confirm the ideas and results of Oddershede et al. (1993). There is a theory of an additional fracturing mechanism for thin plates as stated in Linna et al. (2005). However, recent studies by Renshaw et al. (2001) and by Aström (2009) cast a doubt on the existence of the separate scaling law fragmentation models for thin plates and volumetric bodies. Anyway, for meteoroid applications the buildup of energy flux from the atmosphere drag (via ram pressure) is usually sufficient for fragmentation at all scales (with the exception of the top heaviest iron meteorites).

Recent studies provide increasing evidence to support the theory of power law distributions for fragment masses. For example, papers of Sotolongo-Costa et al. (2000; 2007) assume that high energy experiments with violent fragmentation processes produce power law distributions. On the contrary, low energy processes generate classical statistical functions like *log-normal* or *Rosin-Ramler*. The direct experiment on the Murchison CM2 chondrite with a high velocity impactor also yields a simple power law distribution (Flynn et al., 2007). Computational experiments considered in Domokos et al. (2015) show that the calculated mass distribution is best fitted by a

power law with an exponential cutoff. In addition, the transition from low energy distributions to a high energy power law is studied numerically in a paper of Hernández (2001) via a *random stopping mathematical model* as well as in a paper of Spahn et al. (2014) via a *random-walk model*. Considering these findings, we assume that meteoroid shapes can be estimated from the value of a power law exponent.

3 Conclusions

In the outcome of the study we obtained the following conclusions. The number of meteorite fragments depends on the fragment masses as a power law with an exponential cutoff. The scaling exponent essentially indicates the initial form of the fragmented body. The application of the scaling analysis to the meteorite cases with a large number of recovered fragments is feasible and can form a solid basis for future theoretical and experimental studies on this subject.

Acknowledgments

This work was supported by the Russian Foundation for Basic Research, project Nos 14-08-00204, 16-05-00004 and 16-07-01072.

References

Aström J. A. (2009). “Difference between fracture of thin brittle sheets and two-dimensional fracture”. *Physical Review E*, **80** (4 Pt 2), 046113.

Buehler M. J., Abraham F. F. and Gao H. (2003). “Hyperelasticity governs dynamic fracture at a critical length scale”. *Nature*, **426**, 141–146.

Domokos G., Kun F., Sipos A. Á. and Szabó T. (2015). “Universality of fragment shapes”. *Scientific reports*, **5**, 9147.

Flynn G. J., Durda D. D., Kreft J. W., Sitnitsky I. and Strait M. (2007). “Catastrophic disruption experiments on the murchison hydrous meteorite”. *Lunar and Planetary Science Conference*, **38**, 1744.

Gritsevich M., Dmitriev V., Vinnikov V., Kuznetsova D., Lupovka V., Peltoniemi J., Mönkölä S., Brower J. and Pupyrev Y. (2016). “Constraining the pre-atmospheric parameters of large meteoroids: Košice, a case study”. *Assessment and Mitigation of Asteroid Impact Hazards*, Springer, New York. In print.

Gritsevich M., Vinnikov V., Kohout T., Tóth J., Peltoniemi J., Turchak L. and Virtanen J. (2014). “A comprehensive study of distribution laws for the fragments of Košice meteorite”. *Meteoritics and planetary science*, **49**, 328–345.

Hernández G. (2001). “Discrete model for fragmentation with random stopping”. *Physica A: Statistical Mechanics and its Applications*, **300**, issues 1-2, 13–24.

Hughes D. W. and Harris N. W. (1994). “The distribution of asteroid sizes and its significance”. *Planetary and space science*, **42**, 291–295.

Linna R. P., Åström J. A. and Timonen J. (2005). “Dimensional effects in dynamic fragmentation of brittle materials”. *Physical Review E*, **72**, 015601(R).

Meibom A. and Balslev I. (1996). “Composite power laws in shock fragmentation”. *Physical Review Letters*, **76**, 2492.

Oddershede L., Dimon P. and Bohr J. (1993). “Self-organized criticality in fragmenting”. *Physical Review Letters*, **71**, 3107–3110.

Oddershede L., Meibom A. and Bohr J. (1998). “Scaling analysis of meteorite shower mass distributions”. *Europhysics Letters*, **43**, 598–604.

Renshaw C. E. and Schulson E. M. (2001). “Universal behaviour in compressive failure of brittle materials”. *Nature*, **412**, 897–900.

Rivkin A. S. and Bottke W. F. (1996). “Hypovelocity impacts in the asteroid belt”. *Lunar and Planetary Science*, **27**, 1077–1078.

Sotolongo-Costa O., Gamez R., Luzon F., Posadas A. and Weigandt Beckmann P. (2007). “Non Extensivity in Meteor Showers”. http://arxiv.org/abs/0710.4963.

Sotolongo-Costa O., Rodriguez A. H. and Rodgers G. J. (2000). “Tsallis entropy and the transition to scaling in fragmentation”. *Entropy*, **2**, 172–177.

Spahn F., Vieira Neto E., Guimaraes A. H. F., Gorban A. N. and Brilliantov N. V. (2014). “A statistical model of aggregate fragmentation”. *New Journal of Physics*, **16**, 013031.

Vinnikov V. V., Gritsevich M. I., Kuznetsova D. V. and Turchak L. I. (2016). “Estimation of the initial shape of meteoroids based on statistical distributions of fragment masses”. *Doklady Physics*, **61**, 305–308. DOI:10.1134/S1028335816060021

Vinnikov V., Gritsevich M. and Turchak L. (2015). “Shape estimation for Košice, Almahata Sitta and Bassikounou meteoroids”. In Heavens A. F., Starck J.-L. and Krone-Martins A., editors, *Proceedings of the International Astronomical Union (Cambridge Journals UK)*, Symposium S306, May 2014, volume 10, pages 394–396. http://dx.doi.org/10.1017/S1743921314013519

Catalogue of representative meteor spectra

Vlastimil Vojáček[1,2], Jiří Borovička[2], Pavel Koten[2], Pavel Spurný[2] and Rostislav Štork[2]

[1] **Astronomical Institute of the CAS, Ondřejov, Fričova 298, Czech Republic**
vojacek@asu.cas.cz, borovicka@asu.cas.cz

[2] **Astronomical Institute of the Charles University in Prague, V Holešovičkách 2, Czech Republic**

We present a library of low-resolution meteor spectra that includes sporadic meteors, members of minor meteor showers, and major meteor showers. These meteors are in the magnitude range from +2 to −3, corresponding to meteoroid sizes from 1 mm to10 mm. This catalogue is available online at the CDS for those interested in video meteor spectra.

1 Introduction

Despite the long history of meteor spectroscopy, very few general surveys of meteor spectra have been presented. Harvey (Harvey, 1973) published statistics of visual inspection of 500 photographic meteor spectra. Borovička et al. (Borovička et al., 2005) presented a survey of 97 spectra of mainly sporadic meteors mostly in the magnitude range from +3 to 0. Because of increasing popularity of the meteor spectra video observations, we present a catalogue of 84 video spectra of both sporadic and shower meteors. The catalogue of representative meteor spectra intends to serve as a reference work for future spectral surveys of meteors.

The full catalogue can be found in Vojáček et al. (2015).

2 Instruments and observations

All meteors were captured by our sensitive video technique. Double station observations were performed during the periods of activity of major meteor showers between the years 2006 and 2012.

Each station was equipped with S-VHS-C camcorders with the second-generation image intensifiers *Mullard XX1332*. One direct camera and one spectral camera were operated from one station and one direct camera was operated from the other station.

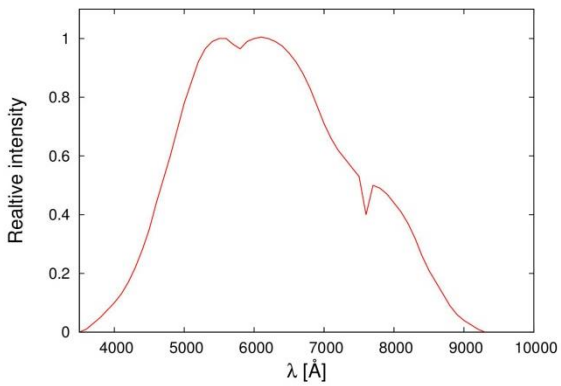

Figure 1 – Sensitivity curve of the system.

The uncompressed AVI files from cameras have a resolution of 768 × 576 pixels × 8 bit.

The spectral grating with 600 grooves/mm and the *Arsat 1.4/50 mm* lens was used for most spectral observations. The resulting dispersion was 30 Å pixel−1 for the Arsat lens. The spectral sensitivity extends from 3800 Å to 9000 Å. The sensitivity curve for the whole system (camera, image intensifier, and lens) is given in *Figure 1*.

3 Description and classification of the spectra

Description of the spectra

The observed spectrum usually consists of the continuum, the emission from the heated atmosphere (specifically the oxygen and nitrogen lines and the nitrogen molecular bands) and the emission that originated in the evaporated material of the meteoroid: the meteoritic lines.

The low-temperature lines of this three meteoric elements can be recognized in the video spectrum:

- Mg I : 5182 Å
- Na I: 5892 Å
- Fe I: 5269 – 5449 Å

Another group is formed by the lines from the meteor wake emitted just behind the meteoroid. In the last group, there is only one line, the forbidden green oxygen line at 5577 Å.

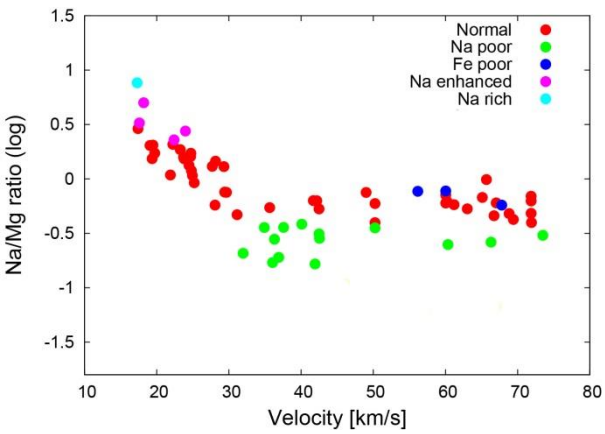

Figure 2 – Intensity ratio of the Na/Mg lines in meteor spectra as a function of the meteor speed.

The appearance of the spectrum can depend on the

velocity of the meteor (*Figure 2*). We observed that the dependence of the Na/Mg ratio on the velocity is valid for speeds below ≈ 35 km/s. The excitation and the evaporation temperatures are lower for smaller velocities and therefore the more volatile sodium has a brighter line for the given speed. There is no velocity dependence for speeds higher than ≈ 35 km/s.

In *Figure 3* we show the O/Mg ratio as a function of the velocity. The ratio of the O to Mg line intensities increases with the velocity. Fast meteors are characterized by more dominant atmospheric lines. For speeds below 30 km s^{-1} the scatter is large, mainly due to the faintness of the O line.

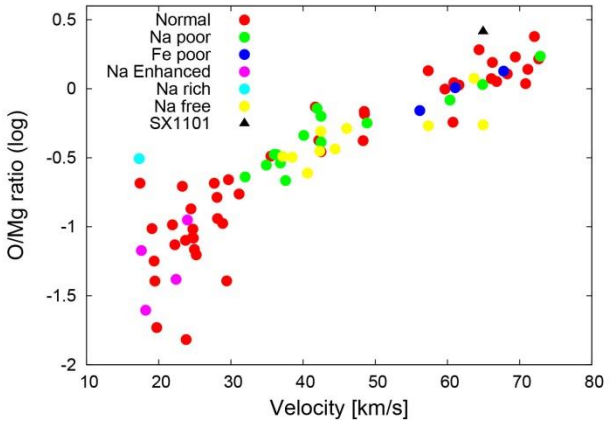

Figure 3 – Intensity ratio of the O/Mg lines in meteor spectra as a function of the meteor speed.

Classification of spectra

The contributions of individual multiplets were summed along the meteor path, so we worked with total line intensities. To visualize the spectral classification we used the Mg-Na-Fe ternary diagram (*Figures 4 and 5*) and the diagram of the dependence of the Mg/Na ratio on the velocity (*Figure 2*).

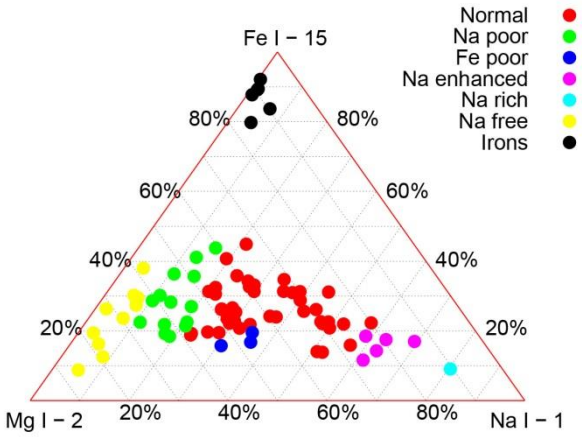

Figure 4 – Classification of spectra. Relative intensities of lines Mg I, Na I, Fe I.

We used the spectral classification of meteor populations suggested by Borovička et al. (2005). The meteoroids were divided as follows:

- Iron meteoroids;
- Na-free meteoroids;
- Na-rich meteoroids;
- Mainstream meteoroids;
    - Normal meteoroids;
    - Na-poor meteoroids;
    - Na-enhanced meteoroids;
- Fe-poor meteoroids.

The approach for the classification of spectra that we use was developed only for small meteoroids in the 1–10 mm size range.

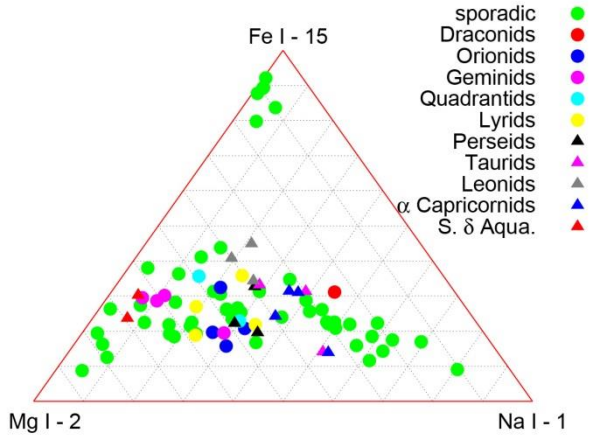

Figure 5 – Classification of spectra: meteor showers positions.

Figure 5 shows the Na-Mg-Fe ternary graph as well, but symbols of individual meteors represent the association with the shower. Most of the major shower meteoroids have been classified as normal. The only exceptions are the Geminids and two Southern δ Aquariids. Both Southern δ Aquariids meteoroids were classified as Na-free.

The Geminids have members of the Na-free, Na-poor, and normal spectral groups. The reason of Na depletion in both showers is solar heating at low perihelion distances (Čapek and Borovička, 2009). The perihelion distance of Geminids is somewhat larger and the degree of Na depletion probably depends on the meteoroid size and structure, especially porosity (Borovička, 2010).

The intensities of the spectral lines correspond to different meteoroid compositions (with the speed dependence taken into account). It is well known that different strength categories of meteoroids in the millimeter-size range have different beginnings of the meteor luminous path (Ceplecha, 1988). For a given speed, a meteoroid composed of stronger material has a lower beginning height than the meteoroid formed by weaker material. As we can see in *Figure 6*, the iron meteoroids and the Na-free meteoroids started to ablate at lower heights compared to most meteoroids, while the Fe-poor meteoroids started higher.

4 Meteoroid orbits

The heliocentric orbits are known for all 84 meteors from double-station observations. The catalogue has a representative sample of orbits with a wide variety of orbital elements.

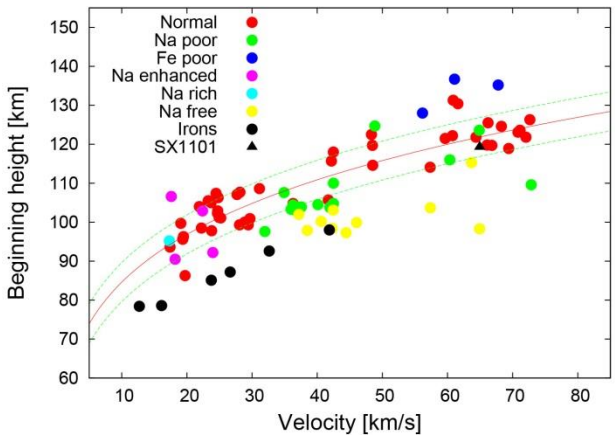

Figure 6 – Beginning height of meteor as a function of speed.

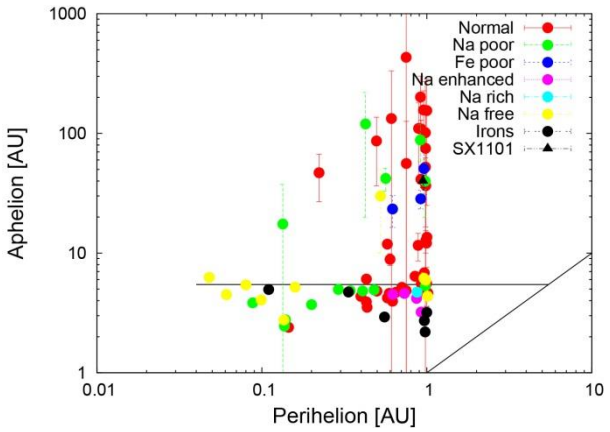

Figure 7– Aphelion and perihelion of meteoroids from the catalogue.

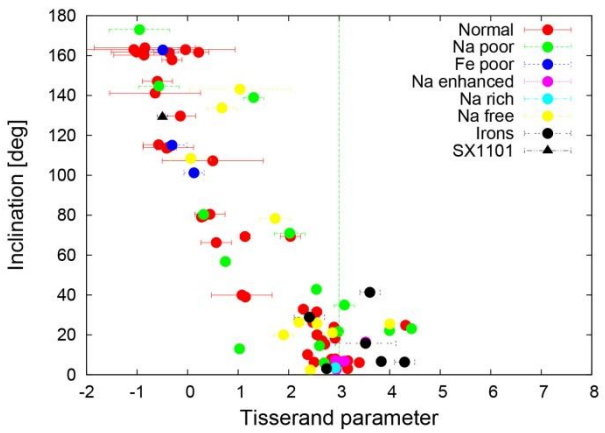

Figure 8– Tisserand parameter relative to Jupiter and the inclination of orbits for meteoroids from the catalogue.

4.1 Relation of meteor orbit to spectral classification

Five classes of meteoroid orbits were defined by Borovička et al. (2005):

- (SA) Sun-approaching orbits: $q < 0.2$ AU. Orbits with small perihelion distances are defined as a separate class.
- (ES) Ecliptic shower orbits: Members of ecliptical meteor showers. For example, the Taurid meteors derived from the comet 2P/Encke.
- (HT) Halley-type orbits: $TJ < 2$ or $2 < TJ < 3$ and $i > 45°$.
- (JF) Jupiter-family orbits: $2 < TJ < 3$ and $i < 45°$and $Q > 4.5$ AU.
- (A-C) Asteroidal-chondritic orbits: $TJ > 3$ or $Q < 4.5$ AU.

Spectral classes of meteoroids from the catalogue and their positions within the orbit classification schemes are shown in *Figures 7 and 8*.

4.2. Iron meteoroids

Six meteors were classified as iron meteoroids. The orbits of four of them satisfy the condition for the asteroidal-chondritic class. One meteoroid with a perihelion of only 0.11 AU can be classified as a Sun-approaching meteoroid. The orbit of one meteoroid can be classified as a Jupiter-family orbit, but asteroidal origin cannot be excluded, since the inclination is only 3 degrees and the aphelion of 4.7 AU is not particularly large.

4.3. Na-free meteoroids

We can clearly distinguish two different populations in the Na-free-meteoroids: the Sun-approaching population with small perihelia and the Halley-type population with high inclinations.

4.3.1. Sun-approaching meteoroids

Most of meteoroids with a perihelion distance $q < 0.2$ are Na-free or Na-poor.

The material of Na-free meteoroids also tends to have a greater strength (see *Figure 6*).

4.3.2. Cometary Na-free meteoroids

The close approach to the Sun is not the only process that causes depletion of Na in meteoroids. In our sample we have three meteoroids without a Na line in their spectra, but their orbits are different from those of Sun approaching meteoroids. Their perihelion distances are closer to 1 AU, and they have high inclinations or even retrograde orbits.

These orbits are of Halley type. According to Borovička et al. (2005), the reason for Na depletion in these types of orbits might be the long exposure to cosmic rays on the comet surface during their residence in the Oort cloud. This process can lead to the formation of a Na free refractory crust. The gradual or sudden disintegration of the crust during the cometary passage through the inner solar system then produces millimeter-sized compact Na free meteoroids.

4.4. Na-rich meteoroids

There is only one Na-rich meteoroid in our catalogue. The body has a Jupiter-family orbit.

4.5. Normal meteoroids

Both cometary and asteroidal orbits are found among meteoroids classified as normal. But only a part of these meteoroids have a typically chondritic composition, many of them show somewhat fainter Fe lines. The sample of meteoroids classified as normal is a mixture of normal chondritic material and cometary material similar to the

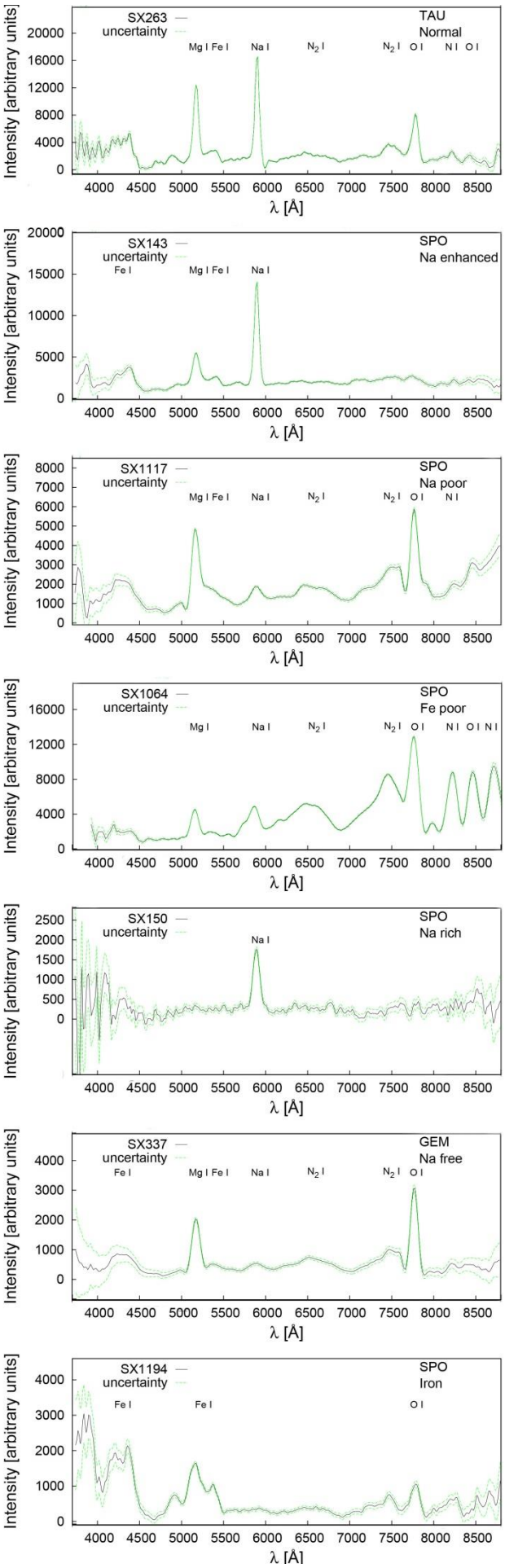

Figure 9 – Examples of typical spectrum for each spectral class.

Leonids. Three Taurid meteors with ecliptic shower orbits have a normal composition.

4.6. Fe-poor meteoroids

Three of the meteoroids in the catalogue were classified as Fe-poor. The iron lines were too faint to classify the meteoroids as normal, although the boundary is somewhat arbitrary. All of the Fe-poor meteoroids have cometary Halley-type orbits. Fe-poor meteoroids have low material strength, their beginning heights of ablation are usually high (see *Figure 6*).

4.7. Na-poor meteoroids

Na-poor meteoroids are the transition between normal and Na-free meteoroids. Like the Na-free meteoroids, some of them have low perihelia, others have cometary orbits. Thus they probably have the same two origins as the Na-free meteoroids.

4.8. Enhanced-Na meteoroids

Five meteoroids were classified as enhanced-Na meteoroids. One has a typical asteroidal-chondritic orbit. The other four meteoroids can be classified as ecliptical or Jupiter-family meteoroids. Their orbits were similar to the Na-rich meteoroid.

5 The catalogue

The full catalogue was published in Vojáček et al. (2015). The atmospheric trajectories and orbital elements for all meteors of the catalogue are at the CDS. Heliocentric orbits are known for all meteors, they are also available at the CDS.

Illustrative examples of typical spectra from each class are available in *Figure 9*. Calibrated and uncalibrated spectra of all 84 meteors are available at the CDS. The total intensities of the multiplets Mg1-2, Na1-1, and Fe1-15 are given explicitly in a separate file.

The catalogue is available online at the CDS via anonymous ftp[1] or via the website[2].

6 Conclusions

We presented a survey of 84 meteors in the magnitude range from +2 to −3, corresponding to meteor sizes from 1 mm to 10 mm. We also computed heliocentric orbits. We classified the meteor spectra according to the classification suggested by Borovička et al. (2005). Only a part of the meteoroids were found to have a typical chondritic composition. We found a variety of Na depletion, Fe depletion, or Na enhancement. Approximately 20% of the whole sample was found to contain no sodium in the spectra. Three populations can be distinguished among the Na free meteoroids: the iron meteoroids with an asteroidal origin, the Sun-approaching meteoroids with Na depleted by frequent approaches within ≈ 0.2 AU to the Sun, and the cometary Na free meteoroids with Na depletion that might be caused by

[1] cdsarc.u-strasbg fr (130.79.128.5)
[2] http://cdsarc.u-strasbg.fr/viz-bin/qcat?J/A+A/580/A67

long exposure to cosmic rays of the surface of comets in the Oort cloud.

Most of the major shower meteors have been classified as normal. Some members of the Geminid shower and two members of Southern δ Aquariids were classified as Na-free.

Most of the meteoroids on the asteroidal-chondritic orbits were found to be iron meteoroids. One iron meteoroid has a typical sun-approaching orbit. Meteoroids with cometary origin had a heterogonous composition, from Na-free, Na-poor, and Fe-poor for Halley-type orbits to Na-rich and enhanced-Na for Jupiter-family orbits.

Acknowledgments

This work was supported by grant No. P209/11/1382 from GA ČR and by the project SVV-260089 by the Charles University in Prague.

References

Borovička J., Koten P., Spurný P., Boček J. and Štork R. (2005). "A survey of meteor spectra and orbits: evidence for three populations of Na-free meteoroids". *Icarus*, **174**, 15–30.

Borovička J., Koten P., Spurný P., Shrbený L. and Štork R. (2010). "Material properties of transition objects 3200 Phaethon and 2003 EH_1". *Icy Bodies of the Solar System, Proceedings of the International Astronomical Union*, IAU Symposium, **263**, 218–222.

Čapek D. and Borovička J. (2009). "Quantitative model of the release of sodium from meteoroids in the vicinity of the Sun: Application to Geminids". *Icarus*, **202**, 361–370.

Ceplecha Z. (1988). "Earth's influx of different populations of sporadic meteoroids from photographic and television data". *Bulletin Astronomical Institutes of Czechoslovakia*, **39**, 221–236.

Harvey G. A. (1973). "Elemental abundance determinations for meteors by spectroscopy". *Journal of Geophysical Research*, **78**, 3913–3926.

Vojáček V., Borovička J., Koten P., Spurný P. and Štork R. (2015). "Catalogue of representative meteor spectra". *Astronomy and Astrophysics*, **580**, id. A67, 31 pp.

Arnold Tukkers busy with preparation of the lunchboxes for the excursion on Saturday afternoon.

2014 Southern δ-Aquariid observing campaign – carried out from Crete

Thomas Weiland

Ospelgasse 12-14/6/19, 1200 Wien, Austria
thomas.weiland@aon.at

With a peak ZHR of 15–20 at the end of July, the Southern δ-Aquariids rank as a major annual shower, but observation is often neglected in favor of the much more active Perseids of August, mainly as a consequence of their southerly radiant, which makes the stream a prominent target from low latitudes and the southern hemisphere. The extended activity period of more than a month, lacking a distinctive peak, and the paucity of bright meteors does not enhance interest of most observers, either. Nevertheless, one has not to go too far south in order to monitor the stream properly to gain scientific results. The Greek island of Crete, at the southernmost tip of Europe, is such a place, offering sufficiently dark skies and a 90 % probability of clear weather in July and August. Encouraged by a New Moon on July 26th an eight-night-long visual observing campaign was carried out in 2014. As a consequence, I managed to record nearly 250 Southern δ-Aquariids within 40 hours of effective observing time. An impression of the campaign together with a summary of the results is presented.

1 Why observing the Southern δ-Aquariids from Crete?

With a radiant declination of δ = -16°, the Southern δ-Aquariid meteor shower (SDA) is best observable from low latitudes and the southern hemisphere. Nevertheless, at the southernmost tip of Europe, the Greek Island of Crete (~35° North), the radiant culminates at a height of ~40°, making it a suitable place in order to monitor the stream properly and gain scientific results.

Even at sea level many parts of Crete, especially in the southwest, offer sufficiently dark skies (limiting magnitudes 6.10 to 6.50 on average) and in case of hazy weather one has only to move to the nearby mountains (500 to 1000 m altitude) to be rewarded with nearly unspoiled, pristine skies (limiting magnitudes > 6.20, but very often close to the standard sky). In addition to this, with a 90 % probability of clear weather in July and August, successful observing is almost guaranteed.

To make it short, the benefits of observing from Crete during the northern hemisphere summer months can be summarized as "African climate combined with European comfort"!

2 The 2014 observing campaign

With respect to New Moon on July 26th my visual observing campaign in 2014 started out on July 25th–26th and lasted until August 01st–02nd (8 nights).

As expected, the weather stayed quite cooperative. Very few isolated clouds at the end of the campaign did not hamper anyway, and transparent skies prevailed.

As a consequence, limiting magnitudes (averaged over each night) were ranging between 6.10 and 6.50 (direct view method, averted vision), averaging on 6.32 (see *Table 1*).

Finally I managed to record 242 SDA (counting method) within 40.26 hours of effective observing time (see *Table 1*).

3 Results

3.1 Magnitude distribution / Population index

From the overall magnitude distribution (see *Table 1*; *Figure 1*) it can be deduced that the SDA mainly yielded faint meteors (48 % of magnitudes +4 to +5), and only 12 % of all SDA reached at least magnitude 0, less than other major annual streams.

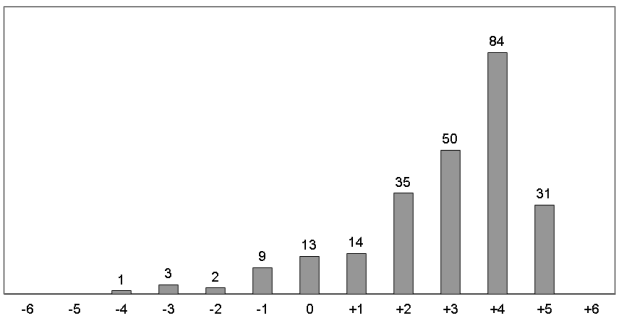

Figure 1 – Magnitude distribution for the Southern Delta-Aquariids 2014, July 25th–26th until August 01st–02nd (242 SDA).

Fireballs (≥ magnitude –3) were quite scarce (4 SDA), the brightest one of them matched magnitude –4 (July 29th, $21^h35^m50^s$ UT).

Interestingly, the number of bright SDA was increasing during the maximum and post-maximum period (Johannink and Miskotte, 2012). For comparison, the two brightest SDA ever recorded by the author (both of magnitude –5) occurred during the post-maximum period, too (2009, August 01st, $23^h48^m05^s$ UT; 2015, August 10th, $23^h32^m25^s$ UT).

Table 1 – Limiting magnitudes, magnitude distribution and meteor numbers.

Shower	Date	lm	**-6**	**-5**	**-4**	**-3**	**-2**	**-1**	**0**	1	2	3	4	5	6	Σ
SDA	25/26	6.1	0	0	0	0	0	0	0	0	3	0	4	0	0	7
SDA	26/27	6.3	0	0	0	0	0	0	**1**	1	1	3	9	3	0	18
SDA	27/28	6.17	0	0	0	0	**1**	**2**	0	1	3	3	10	7	0	27
SDA	28/29	6.5	0	0	0	**1**	**1**	**2**	**3**	3	8	14	12	11	0	55
SDA	29/30	6.38	0	0	**1**	0	0	**1**	**2**	5	4	6	21	1	0	41
SDA	30/31	6.2	0	0	0	0	0	**1**	**4**	3	5	10	8	2	0	33
SDA	31/01	6.44	0	0	0	**2**	0	**2**	0	0	8	4	8	5	0	29
SDA	01/02	6.5	0	0	0	0	0	**1**	**3**	1	3	10	12	2	0	32
Σ			0	0	**1**	**3**	**2**	**9**	**13**	14	35	50	84	31	0	242
Mean	6.32															

In a further step the mean population index for the SDA was derived, using the magnitude difference between the meteors and the limiting stellar magnitude, based on table 7.2, p. 122 in the Handbook for Meteor Observers (Rendtel and Arlt, 2014).

This yielded a mean r-value of 2.39 ± 0.14, which is significantly lower than the value given by IMO (r = 2.8; Rendtel, 2015). However, compared to the mean r obtained for the sporadic background (2.78 ± 0.12; based on 648 SPO), the mean population index for the SDA during the given period can be regarded as real.

3.2 Zenithal hourly rates

ZHR calculation followed the procedure given in the Handbook for Meteor Observers (Rendtel and Arlt, 2014). Due to the fact that limiting magnitudes were close to or even matching the standard sky of 6.50, using individual population indices would have a minor impact on ZHR calculation. Nevertheless, I took the individual r–value of 2.39 (cf. *3.1*) and considered only time frames with a mean radiant height ≥ 15°. The zenith exponent was assumed to be γ = 1.0. No perception coefficient was applied.

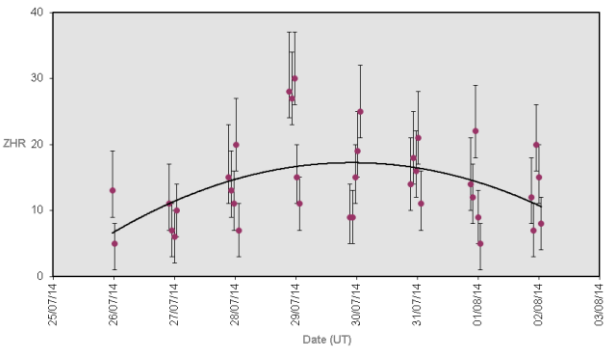

Figure 2 – ZHR profile with polynomial trend function for the Southern Delta-Aquariids 2014 (r = 2.39).

As expected, ZHR-values show a flat, skew profile with large fluctuations (see *Figure 2*). They started out with ~10 on July 25th–26th and reached their maximum (~30) on July 28th–29th. After that they were slowly declining to ~10 on August 01st–02nd again. This is quite in agreement with the corresponding IMO live ZHR profile.

However, an Excel-generated polynomial trend function yielded a broader maximum one day later, around July 29th–30th, with a peak ZHR of ~17, which fits better the parameters given in the Meteor Shower Calendar (ZHR 16; maximum July 30th; Rendtel, 2015).

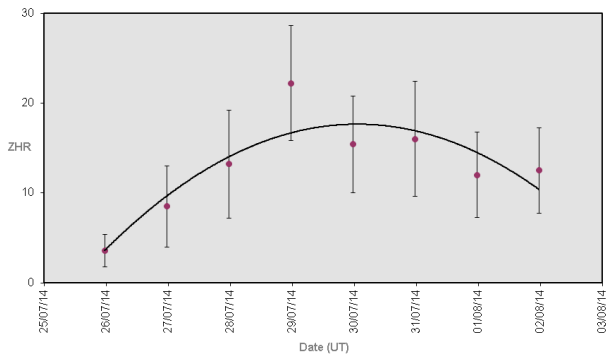

Figure 3 – Mean ZHR profile with polynomial trend function for the Southern Delta-Aquariids 2014 (r = 2.39).

Averaging ZHR-values over each night did not affect the date of the maximum (July 28th–29th), but rather their height (peak ZHR 22 ± 6; see *Figure 3*). In any case, the polynomial trend function was not altered, only becoming slightly more skew.

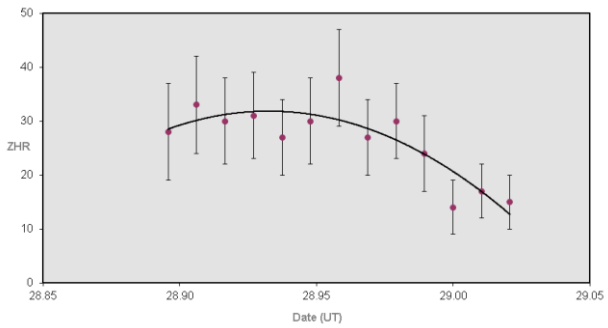

Figure 4 – ZHR profile around maximum with polynomial trend function for the Southern Delta-Aquariids 2014, Maximum July 28th–29th (r = 2.39).

In order to smooth the profile and to get the peak out more clearly, ZHR values were averaged using a sliding mean of 5 bins per step (A5), shifted by 15 minutes. This puts the time of the maximum to July 28th, 23^{h}00^{m} ± 15^{m} UT (ZHR 38 ± 9; see *Figure 4*). The polynomial trend function gives July 28th, 22^{h}30^{m} ± 15^{m} UT, with a peak ZHR ~32.

3.3 General Appearance

A typical feature of the SDA meteors is the scarcity of trains, similar to the Geminids. According to that, only 1 % of all SDA logged showed a prominent train (+2 and +4 magnitude class) and additional 18 % produced a short one (–4 to +4 magnitude class).

Flares were not observed at all.

Color estimates yielded mainly orange and yellow hues, with white and blue tints to a much lesser extent.

3.4 Conclusion

The 2014 observational results can be summarized as follows:

- The mean population index found in 2014 (r = 2.39) is significantly lower than the value given by IMO (r = 2.8).
- A higher percentage of bright meteors during the maximum and post-maximum period indicates mass-sorting within the stream (Johannink and Miskotte, 2012).
- The peak ZHR found in 2014 (~30) is significantly higher than the value given by IMO (16).
- The (almost complete) absence of prominent trains and flares indicates a high mean bulk density and low porosity of the meteoroids (Babadzhanov and Kokhirova, 2009). Taking the extremely small perihelion distance (q = ~0.09 AU) into account, one may assume a sintered surface of the meteoroids, similar to the Geminids.
- Despite the extremely small q the predominance of orange and yellow colors suggests an incomplete loss of volatile elements, like sodium.

4 Future Work

Due to the fact that there are still open questions about the observational stream parameters, visual meteor work should be focused on the following items:

- A complete r-profile over the whole activity period in order to prove mass-sorting within the stream (Johannink and Miskotte, 2012).
- Complete ZHR-profiles of moonless returns in order to prove whether peak ZHR-values are subject to variability (Johannink and Miskotte, 2012; Molau et al., 2015).

Favorable observing conditions in 2016, 2017 and 2019 offer good opportunities to follow up the performance of the stream!

References

Babadzhanov P. B. and Kokhirova G. I. (2009). “Densities and Porosities of Meteoroids”. *Astronomy and Astrophysics*, **495**, 353–358.

Johannink C. and Miskotte K. (2012). “Results for the Aquariid-expedition to Namibia, July 2011”. *WGN, Journal of the IMO*, **40**, 65–68.

Molau S., Crivello S., Goncalves R., Saraiva C., Stomeo E. and Kac J. (2015). “Results of the IMO Video Meteor Network – August 2015”. *WGN, Journal of the IMO*, **43**, 188–191.

Rendtel J. (editor) (2015). 2016 Meteor Shower Calendar. IMO.

Rendtel J. and Arlt R. (editors) (2014). Handbook for Meteor Observers. International Meteor Organization, Potsdam.

Current status of Polish Fireball Network

Mariusz Wiśniewski[1,2], Przemysław Żołądek[1], Arkadiusz Olech[1,3], Zbigniew Tyminski[1,4], Maciej Maciejewski[1], Karol Fietkiewicz[1], Mariusz Gozdalski[1], Marcin Przemysław Gawroński[1,5], Tomasz Suchodolski[1,6], Maciej Myszkiewicz[1], Marcin Stolarz[1] and Krzysztof Polakowski[1]

[1] **Polish Fireball Network, Comets and Meteors Workshop, ul. Bartycka 18, 00-716 Warsaw, Poland**
brahi@op.pl, mazziek@gmail.com, parmo.pfn@gmail.com, ma.gozdalski@gmail.com, spammer.m@gmail.com, marcin.stolarz@gmail.com, krzysiek-pol20@o2.pl

[2] **Central Office of Measures, ul. Elektoralna 2, 00-139 Warsaw, Poland**
marand.w@gmail.com

[3] **Nicolaus Copernicus Astronomical Center, ul. Bartycka 18, 00-716 Warsaw, Poland**
olech@camk.edu.pl

[4] **National Centre of Nuclear Research RC POLATOM, Soltan 7, Otwock-Świerk, Poland**
zbyszek.tyminski@gmail.com

[5] **Faculty of Physics, Astronomy and Informatics, Nicolaus Copernicus University, Grudziądzka 5, 87-100 Toruń, Poland**
motylek@astro.uni.torun.pl

[6] **Space Research Centre, Polish Academy of Sciences, ul. Bartycka 18A, 00-716 Warszawa, Poland**
tomasz.suchodolski@ptma.pl

The PFN started in March 2004. Most of its observers are amateurs, members of the Comets and Meteors Workshop. The network consists of 40 continuously working stations, where nearly 80 sensitive CCTV video and digital cameras operate. During the years 2011–2015 PFN cameras recorded 215049 single events. Using this data 34608 trajectories and orbits have been calculated.

1 Introduction

Since 2004 the Polish sky has been patrolled by cameras of the Polish Fireball Network (PFN). Most of PFN observers are amateurs, members of the Comets and Meteors Workshop performing observations from their homes. Some stations are located in astronomy clubs and schools. The network consists of 40 continuously working stations, where nearly 80 sensitive CCTV video and digital cameras operate (Olech et al., 2006). The PFN team published a number of papers with detailed analyzes of interesting events like the Leonids 2002 outburst (Wiśniewski et al., 2003), EN200204 "Łaskarzew" fireball (Spurny et al., 2004), PF030405a "Krzeszowice" fireball (Żołądek et al., 2007), PF191012 "Myszyniec" - highest Orionid meteor ever recorded (Olech et al., 2013), PF131010 Ciechanow fireball possible related to Near Earth Asteroids 2010 TB54 and 2010 SX11 (Olech et al., 2015).

2 Cameras of PFN

The network consists of 40 continuously working stations with nearly 80 cameras. The PFN cameras patrol the sky over entire Poland (see *Figure 1*). In Most stations we use low cost sensitive CCTV analog video cameras equipped with lenses with 65.6 × 49.2° field of view. We use MetRec (Molau, 1999) and UFOCapture (SonotaCo, 2005)[1] software for meteor detection. The *UFOAnnalyzer* software is used for the astrometric reduction of video recordings.

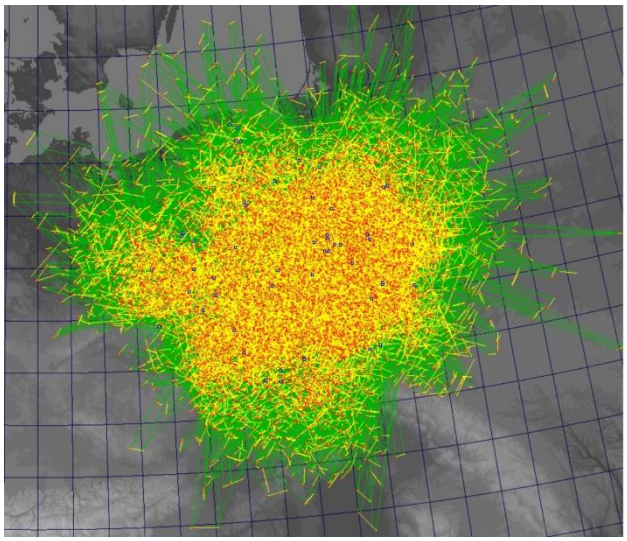

Figure 1 – Calculated trajectories of meteoroids in 2011-2015.

Part of the stations is equipped with high sensitive Mintron 12v6 cameras with fast lenses. These cameras detected up to 4 times more meteors than low cost cameras. Due to a higher sensitivity and smaller fields of view we can record a large number of fainter meteors.

New "Meteor Digital Cameras" (MDC) are based on the sensitive *DMK 33GX236*. These cameras have a

[1] http://sonotaco.com/soft/UFO2/help/english/index html
"UFCaptureV2 Users Manual".

Table 1 – Types of camera working in PFN.

Parameter	Low cost setup	Sensitive setup	HD digital setup
Camera type	Tayama C3102-01A1	Mintron 12v6	DMK 33GX 236
Image resolution	480 x 576 pixels Interlaced	768 x 576 pixels Interlaced	1920 x 1200 pixels Progressive
Time resolution	25/50 fps 8 bit	25/50 fps 8 bit	50/25 fps 8/12 bit
Lens	1.2/4 mm	0,8/6 mm - 0,8/12 mm	1.2/2.4 mm
FOV	66x50 degrees	<66x50 degrees	130x80 deg
Pixel size	5'/pixel	<5'/pixel	4'/pixel

resolution of 1920 x 1200 pixels. The new cameras are working with lenses with a focal length of 2.4 mm which gives 130 x 80° field of view. The new cameras offer images with much better quality compared to analog cameras.

Detections from all PFN cameras are automatically transmitted via internet to a central server where double station events are detected, analyzed and then a trajectory and obit is determined. All calculations are checked by manual inspection. We create the PyFN software for trajectory and orbit calculation. PyFN (Żołądek, 2012) utilizing the *Celpeha* method (Ceplecha, 1987).

Comparison of low cost setup, sensitive setup and new digital HD setup was presented in *Table 1*.

3 Results of PFN in years 2011–2015

In years 2011–2015 PFN cameras recorded 215049 single events. Using this data 34608 trajectories and orbits have been calculated. Detailed numbers of meteors were presented in *Table 2*. A special spike in the amount of registered meteors occurred in 2015. This was due to the launch of a number of new sets of sensitive cameras. During the next year, we are planning an extensive modernization of the PFN network, equipping it with dozens of new sensitive and digital HD cameras.

With the development of the network increases the number of registered detection of multiple stations (see *Figure 2*). This has a significant impact on improving the quality of the orbits.

Table 2 – Results of PFN in last 5 years.

Year	Detections	Orbits
2011	24099	3430
2012	28471	4186
2013	36347	6114
2014	46936	7351
2015	79083	13528

Acknowledgment

This work was supported by the National Science Center (decision No. DEC-2013/09/B/ST9/02168).

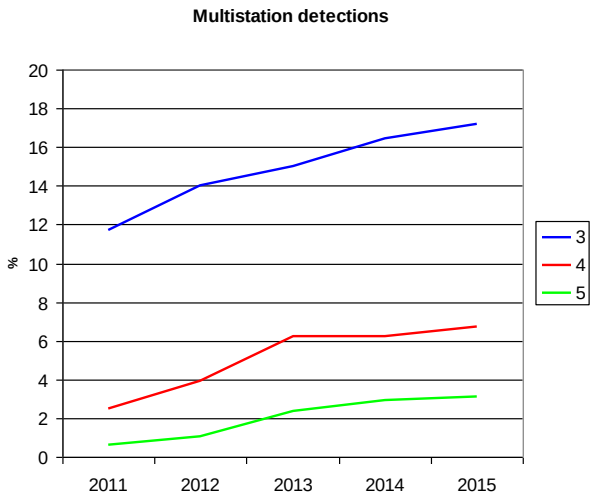

Figure 2 – Percentages of multistation detections in 2011–2015.

References

Ceplecha Z. (1987). "Geometric, dynamic, orbital and photometric data on meteoroids from photographic fireball networks". *Bulletin of the Astronomical Institutes of Czechoslovakia*, **38**, 222–234.

Molau S. (1999). "The meteor detection software MetRec". In Baggaley W. J. and Porubcan V., editors,. *Meteoroids 1998*, Proceedings of the International Conference held at Tatranska Lomnica, Slovakia, August 17-21, 1998. Astronomical Institute of the Slovak Academy of Sciences, pages 131–134.

Olech A., Żołądek P., Wiśniewski M., Kransowski M., Kwinta M., Fajfer T., Fietkiewicz K., Dorosz D., Kowalski Ł., Olejnik J., Mularczyk K. and Złoczewski K. (2006). "Polish Fireball Network". In Bastiaens L., Verbert J., Wislez J.-M. and Verbeeck C., editors, *Proceedings of the International Meteor Conference*, Oostmalle, Belgium, 15-18 September, 2005. IMO, pages 53–62.

Olech A., Żołądek P., Wiśniewski M., Fietkiewicz K., Maciejewski M., Tyminski Z., Krzyzanowski T., Krasnowski M., Kwinta M., Myszkiewicz M., Polakowski K. and Zaręba P. (2013). "PF191012

Myszyniec - highest Orionid meteor ever recorded". *Astronomy and Astrophysics*, **557**, A89.

Olech A., Żołądek P., Wiśniewski M., Rudawska R., Laskowski J., Polakowski K., Maciejewski M., Kransowski M., Krzyżanowski T., Fajfer T. and Tymiński Z. (2015). "PF131010 Ciechanow fireball - the body possible related to Near Earth Asteroids 2010 TB54 and 2010 SX11". *Monthly Notices of the Royal Astronomical Society*, **454**, 2965–2971.

Spurny P., Olech A. and Kedzierski P. (2004). "Trajectory and orbit of the EN200204 Łaskarzew fireball". *WGN, Journal of the IMO*, **32**, 48–50.

Wiśniewski M., Kędzierski P., Mularczyk K. and Złoczewski K. (2003). "Polish Automated Video Observations (PAVO)". *WGN, Journal of the IMO*, **31**, 33–34.

Żołądek P., Olech A., Wiśniewski M. and Kwinta M. (2007). "The PF030405a "Krzeszowice" fireball". *Earth, Moon, and Planets*, **100**, 215–224.

Żołądek P. (2012). "PyFN - multipurpose meteor software". In Gyssens M. and Roggemans P., editors, *Proceedings of the International Meteor Conference*, Sibiu, Romania, 15-18 September, 2011. IMO, pages 53–55.

Ad-hoc LOC meeting at the reception with Arnold Tukkers, Elise Ijland, Joost Hartman: 'what do we do if we run out of drinking tokens?'.

Space fireworks for upper atmospheric wind measurements by sounding rocket experiments

Masa-yuki Yamamoto

School of Systems Engineering, Kochi University of Technology, Kami, Japan
Yamamoto.masa-yuki@kochi-tech.ac.jp

Artificial meteor trains generated by chemical releases by using sounding rockets flown in upper atmosphere were successfully observed by multiple sites on ground and from an aircraft. We have started the rocket experiment campaign since 2007 and call it "Space fireworks" as it illuminates resonance scattering light from the released gas under sunlit/moonlit condition. By using this method, we have acquired a new technique to derive upper atmospheric wind profiles in twilight condition as well as in moonlit night and even in daytime. Magnificent artificial meteor train images with the surrounding physics and dynamics in the upper atmosphere where the meteors usually appear will be introduced by using fruitful results by the "Space firework" sounding rocket experiments in this decade.

1 Introduction

Meteor trains have been studied as one of luminescence events in upper atmosphere just after a large meteoroid entered into the upper atmosphere. Imaging of the meteor trains is difficult because it is a statistically rare event and has never been predicted when and where it occurs in the sky. However, just at the occasion of the maximum of the Leonids with its 33-years revolution, many meteor observers tried to figure out many unknown but principal parameters of the meteor trains with their imaging observations concentrated at a time of the maximum Leonid storm encounter (*Figure 1 – left*). Most recently, based on some fruitful results obtained during 1998–2002, morphology, details of the luminescence process, spectroscopic studies, height distributions and three-dimensional (3-D) spatial evolutions of meteor trains are studied (Higa et al., 2005; Borovicka and Koten, 2003; Abe et al., 2005; Yamamoto et al., 2003; 2005). Moreover, due to the enhancement of imaging devices of CCD and CMOS in these days, meteor train imaging with high temporal resolution has been realized, revealing the earliest stage of the meteor train process in the upper atmosphere. When we can obtain information about temporal evolution of the long-lasting faint emission of meteor trains by multiple-site observation, it can reveal the 3-D structures of meteor trains as well as a possible wind profile in the upper atmosphere within a height range of about 80 km up to 105 km by using the luminous cloud as a tracer. However, such effort for obtaining information about the neutral wind by using the natural meteor trains is limited only at an occasion of the peak period of a meteor storm which provides fireball-class bright meteors.

After becoming the space era in human history, as for the purpose of determining the neutral wind profiles in the upper atmosphere, many trials are devoted for atmospheric studies by using sounding rockets with developing so-called chemical release technique that produces artificial meteor trains in the sky at an exact place and height range at a precise time and date on demand. Since the early date of space era in 1950's, the chemical release technique has gradually been established, resulting in some beneficial chemical species of making long-lasting luminous trails in the sky (Davis, 1979). One luminous mechanism is the resonance-scattering illuminations of atomic metallic particles such as, Lithium, Sodium, Barium and Strontium by getting the energy of projecting light from the Sun mainly at the local time zone of twilight, namely under sunlit upper atmosphere with dark sky condition on the ground. Another mechanism is using a light-emitting chemical reaction process with releasing organo-aluminum molecules like tri-methyl-aluminum (TMA) that can effectively recombine with the oxygen and water vapor (or OH molecule) in the upper atmosphere, thus it means TMA is a kind of danger items on the ground. Luminescence of the TMA is not so bright that it has only been used for nighttime wind measurements (Larsen, 2002). The nature of daytime wind profiles in the Earth's thermosphere has rarely been investigated before the present days because its extremely severe environment to measure with high background luminescence of the daytime blue sky, however the trials of using Lithium vapor released by sounding rockets have been carried out

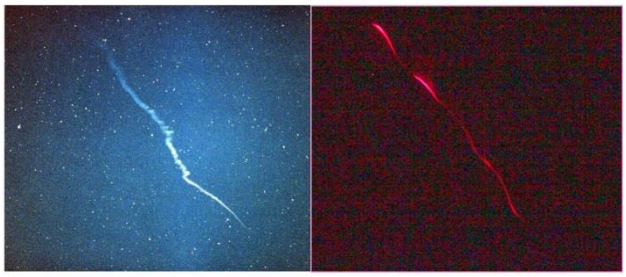

Figure 1 – A natural meteor train (left) and an artificial Lithium trails (right). The meteor train of a Leonid in 1997 was photographed by M. Toda (Toda et al., 2004). The Lithium trails consist of three parts of chemical releases during the down-leg of the rocket (Habu et al., 2013). Height ranges of both luminescence are almost the same for each.

by some teams of atmospheric scientists since the 1960's. The technique of the Lithium release was once suspended because of the great success of TMA chemical release method established and no one continued the development after the 1980's and unfortunately it gradually disappeared in the 1990's.

2 Visualization of upper atmosphere by "Space Fireworks" technique

After gathering a few documents written at that time in the U.S.A., India and Japan, we decided to create a new Lithium Ejection System (LES) to restart the trials of daytime wind measurements in 2005. Then, a comprehensive observation campaign using the JAXA S-520 type sounding rocket was successfully carried out on Sep. 2, 2007 with releasing three Lithium vapor clouds in the thermosphere in the summer evening sky over the Pacific Ocean along the southern coast of Japan (Yamamoto et al., 2014). The artificial clouds that were introduced as "Space Fireworks" at that time greatly illuminated with its resonance-scattering light of 670.8 nm emission of Lithium and were successfully imaged at 4 camera sites on the southern coast simultaneously at an exact synchronized time frame continuously for at least 45 minutes after the first release. Comparison between onboard plasma measuring sensors and the 3-D triangulation results of the Lithium clouds was also established (Uemoto et al., 2010).

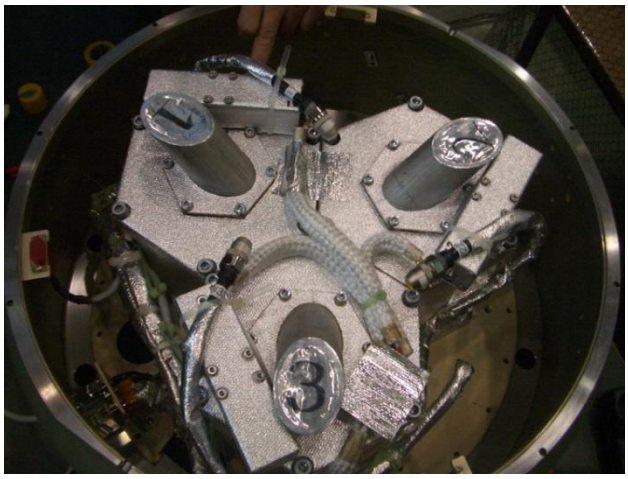

Figure 2 – Lithium Ejection System (LES).

The structures of LES are shown in *Figure 2*, where 125 g metallic Lithium was installed in each cylindrical pod in each LES canister and typical ingredients of the termite reaction were also installed at a torus-like region around the Lithium pod for a heat source required for vaporizing the metallic Lithium to the gaseous one in several seconds. The termite reaction is shown as:

$$Fe_2O_3 + 2Al \rightarrow Al_2O_3 + 2Fe \qquad (1)$$

Finally, the vaporized Lithium can be released by its thermal pressure (initial speed) into the space (Yamamoto et al., 2014).

As in the WINDs (Wind measurement for Ionized and Neutral atmospheric Dynamics study) campaign, we conducted two rocket experiments in the summer evening in 2007 as well as in winter dawn in 2012. In the second experiment, 2 of 3 planned releases were not successful; however, we could measure the neutral wind profile in the twilight thermosphere within a height range between 76 km and 400 km only using three Lithium releases with 125 g for each. As for the imaging of 670.8 nm Lithium emission, we developed new optics with a tele-centric lens with a narrow band-pass-filter (BPF) in order to obtain a 12 nm limitation in passing wavelength for high S/N ratio with a wide field of view of about 100 degrees. The tele-centric optics enable us to put a BPF between the lens and an imaging sensor. Imaging devices of usual single-reflex digital cameras (Canon, EOS Kiss Digital N and EOS Kiss X4) were used with the optics but with removing their IR-cut filters on the CMOS sensors. Due to the high sensitivity of the recent digital devices, the imaging of the faint Lithium clouds was successful even in the situation of the shaded region of the lower part of the third-released cloud in the case of the 2007 experiment (*Figure 3 – lower part of left image*), thus suggesting the possibilities of using the technique in daytime or nighttime under Full Moon condition after the two experiments of the WINDs campaign.

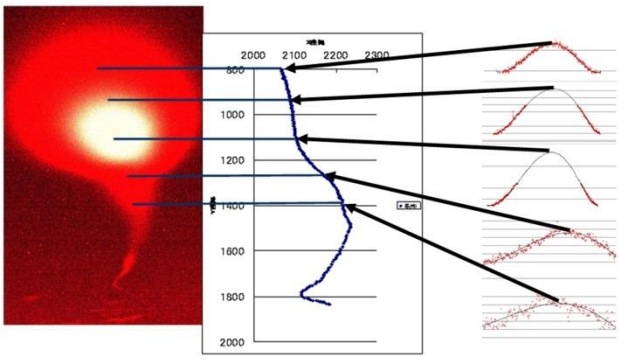

Figure 3 – Lithium clouds and image processing method to get a central position curve on diffusive fireworks. (Yamamoto et al., 2014).

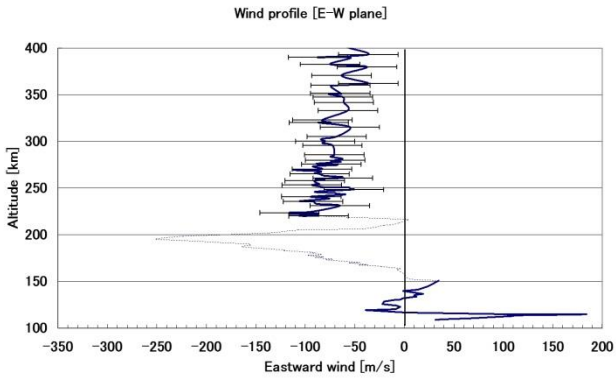

Figure 4 – Neutral wind profile on zonal plane (Yamamoto et al., 2014).

The image processing method can be used for determining the precise coordinates on each snapshot even in a case of rapid diffusion by a rarefied background atmospheric pressure level at the altitude of over about 160 km. It is noteworthy that the observed Lithium clouds showed a great diffusion feature very clearly at the middle/upper thermosphere in comparison with the lower

thermospheric case, usually seen for the natural meteor trains in an altitude range between 80 km and 105 km, whereas the artificial vapor clouds shows almost the same feature as the natural ones under the same altitude condition (*Figure 1*).

It can suggest the principal physical process of rapid diffusion in the upper atmosphere is the same although these luminous mechanisms are different from each other. It means that the error bars above 220 km shown in *Figure 4* are depending on the diffusion rate at each bin, whereas the error bars for the lower part of the profile is within the width of the plotted solid curve. A dotted curve between them shows the profile with some ambiguity because of a superimposed situation of two independent Lithium clouds at the same altitude range by rapid vertical diffusion. Wind shear structures are clearly observed in the profile at about 115 km and 200 km. The lower one is usually seen at the altitude range when we use a TMA chemical release, however the wind shear found at about 200 km might be an important feature at the environment which we usually cannot see without having the chemical release of Lithium.

The transition region of the diffusion process from a viscosity-dependent collisional region to a molecule-dependent collision-less region is usually considered as the turbo-pause height. Such environmental change in altitude might be connected with the strong wind shear regions. Thus the artificial chemical release clearly visualized the diffusion process in the upper atmosphere and it is a significant technique for calibrating some environmental parameters in the surrounding media of the Earth's atmosphere and it is almost the same region of the meteor phenomena.

3 Ongoing experiments for unknown fields of upper atmospheric study

After establishing the LES instrumentations onboard a sounding rocket, daytime and moonlit-midnight Lithium release experiments by using NASA/JAXA sounding rocket facilities were carried out in 2011 and 2013. As the first trial was not successful in 2011, we need to figure out the faced problems and solve them in those years, but finally, we could obtain faint images of the artificial Lithium clouds under the extremely severe S/N ratio conditions. Because of the bright blue-sky background in daytime by rayleigh scattering of the sunlight as well as the very faint moonlight source for the resonance-scattering of Lithium that is almost 1/500000 of sunlit Lithium clouds, the same brightness ratio between the Full Moon (-12.7 magnitude) and the Sun (-26.7 mag.) as well.

After the unsuccessful experiment in 2011, we conducted careful calibration of the absolute intensity of the Lithium emission as well as the background sky intensity level by using integral sphere facilities in Japan (NIPR and JAXA) for a given absolute light source in a unit of Rayleigh (R: 10^6 photons/m^2/s/sr). The calibration was achieved by applying image sequences of the dawn experiment in 2012, where we experienced the condition of enhancing the background sky level due to the sunrise, getting into the daytime condition. At the time of these experiments with very severe S/N ratio condition, we concluded to use an airplane to reduce the background rayleigh scattering by flying into the lower stratosphere at about 13 km in the sky reducing the background intensity into 1/10 or less than the observation on ground.

Another approach using few limited opportunities of artificial reentries of a capsule and/or spacecraft has also been carried out. In these experiments, artificial meteor trains due to the ablation and/or fragmentation process were successfully imaged (Yamamoto et al., 2011).

4 Conclusion

During the decade of 2005–2015, many kinds of experiments to acquire/improve the chemical release technique using sounding rockets have been carried out in Japan and the U.S. with a deep collaboration with each other, resulting in some fruitful outputs for both scientific and engineering aspects. This article is only an introduction of such a field of study for the readers of meteor science. The region of interests is almost similar, however the relationship between both fields is still limited mainly because the fields of studies are, in recent days, divided into many fractions of societies of scientific study. Human interaction between such adjacent fields looks important to open new significant studies of science we have never met before. In the near future, artificial experiments concerning the meteor and meteorite studies will be realized in some contexts in physics and technology. Such studies would probably provide us new knowledge about the interaction between the meteoroids and the Earth's atmosphere.

Acknowledgment

Technical information was provided at the initial stage of the development by Vikram Sarabhai Space Center, ISRO. Observation of the rocket campaign was carried out with Prof. Shigeto Watanabe (Hokkaido University), Prof. Miguel Larsen (Clemson University), Dr. Takumi Abe (ISAS/JAXA), Dr. Hiroto Habu (ISAS/JAXA), Prof. Mamoru Yamamoto (RISH, Kyoto University), Dr. Robert Pfaff (GSFC/NASA), partly supported by Dr. Yuichi Otsuka (STEL, Nagoya University), Dr. Akinori Saito (Kyoto University) and Prof. Takayuki Ono (Tohoku University) and their colleagues and students. The author and his colleagues wish to express their sincere thanks to the rocket team of ISAS/JAXA as well as of WFF/NASA and Andoya Rocket Range (ARR), Norway. They are also grateful to the Aeronautical Technology Directorate of JAXA, National Institute of Polar Research (NIPR) as well as many collaborators and supporters who provided their facilities to use for the observations and calibrating experiments. The meteor train image in *Figure 1* was provided by Masayuki Toda (Nippon Meteor Society).

References

Abe S., Ebizuka N., Murayama H., Ohtsuka K., Sugimoto S., Yamamoto M.-Y., Yano H., Watanabe J.-I. and Borovicka J. (2005). "Video and photographic spectroscopy of 1998 and 2001 Leonid persistent trains from 300 to 930 nm". *Earth, Moon, and Planets*, **95**, 265–277.

Borovicka J. and Koten P. (2003). "Three phases in the evolution of Leonid meteor trains". In Yano H., Abe S. and Yoshikawa M., editors, *Proceedings of the 2002 International Science Symposium on the Leonid Meteor Storms*, Inst. Space Astronaut. Sci., Sagamihara, Japan, ISAS Report SP 15, pages 165–173.

Davis T. N. (1979). "Chemical releases in the ionosphere". *Rep. Prog. Phys*., **42**, 1565–1595.

Habu H., Yamamoto M.-Y., Watanabe S. and Larsen M. F. (2013). "Rocket-borne Lithium ejection system for neutral wind measurement". In Oyama K. and Cheng C. Z., editors, *An introduction to space instrumentation*. TERAPUB, 53–61.

Higa Y., Yamamoto M.-Y., Toda M., Maeda K. and Watanabe J.-I. (2005). "Catalogue of Persistent Trains II: Images of Leonid Meteor Trains during the METRO campaign 1998-2002". *Publ. Natl. Astron. Obs. Japan*, **7**, 67–131.

Larsen M. F. (2002). "Winds and shears in the mesosphere and lower thermosphere: Results from four decades of chemical release wind measurements". *Journal of Geophysical Research*, **107**, Issue A8, 10.1029/2001JA000218.

Toda M., Yamamoto M.-Y., Higa Y. and Watanabe J.-I. (2004). "Catalogue of persistent trains I: Meteor train images during 1988-1997 and development of optimum observing technique". *Publ. Natl. Astron. Obs. Japan*, **7**, 53–66.

Uemoto J., Ono T., Yamada Y., Suzuki T., Yamamoto M.-Y., Watanabe S., Kumamoto A. and Iizima M. (2010). "Impact of lithium releases on ionospheric electron density observed by impedance probe during WIND campaign". *Earth Planets Space*, **62**, 589–597.

Yamamoto M.-Y., Toda M., Higa Y., Fujita M. and Suzuki S. (2003). "METRO campaign in Japan II: Three-dimensional structures of two Leonids meteor trains in early stage". In Yano H., Abe S. and Yoshikawa M., editors, *Proceedings of the 2002 International Science Symposium on the Leonid Meteor Storms*, Inst. Space Astronaut. Sci., Sagamihara, Japan, ISAS Report SP, 16, 237–244.

Yamamoto M.-Y., Toda M., Higa Y., Maeda K. and Watanabe J.-I. (2005). "Altitudinal Distribution of 20 Persistent Meteor Trains: Estimates Derived from METRO Campaign Archives". *Earth, Moon, and Planets*, **95**, 279–287.

Yamamoto M.-Y., Ishihara Y., Hiramatsu Y., Kitamura K., Ueda M., Shiba Y., Furumoto M. and Fujita K. (2011). "Detection of Acoustic/Infrasonic/Seismic Waves Generated by Hypersonic Re-Entry of the HAYABUSA Capsule and Fragmented Parts of the Spacecraft". *Publications of the Astronomical Society of Japan*, **63**, 971–978.

Yamamoto M.-Y., Kakinami Y., Kihara D., Watanabe S., Habu H., Abe T., Yamamoto M. and Larsen M. F. (2014). "Measurement of neutral wind profile in nighttime and daytime by Lithium releases and airborne observations". *Proc. of ISAS/JAXA Atmosphere Symposium*, 4-3 (*in Japanese*).

Exploring the relationship between meteor parameters based on photographic data

Yulia Yancheva[1], Simona Hristova[2] and Eva Bojurova[3]

[1] **Astroclub Canopus, Astronomical Observatory and Planetarium Nicholas Copernicus, Varna, Bulgaria**
methenarwhal@gmail.com

[2] **High school of mathematics Baba Tonka, Ruse, Bulgaria**
simona.hristowa@abv.bg

[3] **Astronomical observatory and Planetarium Nicholas Copernicus, Varna, Bulgaria**
eva.bojurova@gmail.com

The paper presents an attempt to investigate the relationship between the luminosity and the linear length of the meteors, based on photographic observations of the Geminid meteor shower during the night of maximum in December 2015.

1 Introduction

The luminosity of the meteors depends on a number of factors, including the masses and chemical composition of the meteoric particles, their linear velocities and the angles at which they enter the Earth's atmosphere. The same is true for the linear lengths of the luminous paths of the ablating meteoroids through the atmosphere. One can easily suppose that the two parameters – the luminosity of the meteors and their linear lengths – should be related in some way, i.e. the more massive meteor particles should produce brighter and longer meteors, and therefore brighter meteors should be longer. As obvious as it is, it could be still interesting to explore this relationship, bearing in mind that the masses of the meteors, which are fundamental to it, cannot be measured directly, but the luminosities and the lengths of the meteors can be derived from observations. For our investigation we use meteors belonging to one meteor shower – the Geminids. We can consider that all meteor particles from the Geminid stream have very similar linear velocities and chemical composition. Therefore the influence of these two factors on the relationship we study can be excluded. Looking to the future, a similar exploration would allow us to make an interesting comparison between the distinctive characteristics of this relationship for different meteor showers.

2 The observations

The photographic observations were carried out during the night of 14–15 December 2015 on the Plana Mountain near Sofia, Bulgaria. The photographer was Lyubomir Simeonov, a student in the Physics Department of Sofia University, who kindly provided the images to us. On them we found 11 Geminid meteors that were suitable for our measurements. The images were taken by a Nikon 3100 D camera with a 18-55mm lens and the exposure time for each image was 30 sec.

3 The linear paths of the meteors

We first used *Stellarium* software to define the angular length of every Geminid meteor in our series. The position of the meteor was found by comparing the star positions in the images with those on the *Stellarium* computer map. In this approximate method, we used the nearest stars to the beginning and to the end point of a meteor and found its angular length. We used the data shown by *Stellarium* to determine the height above the horizon of the beginning and end point of each meteor and the zenithal elongation of the shower radiant at the time of observation. We then measured the angular distance of the beginning and the end point of each meteor from the radiant.

Table 1 – The heights h_b and h_e of the beginning and the end point of each meteor above the horizon and the distances ψ_b and ψ_e of the beginning and the end point of each meteor from the Geminid radiant.

Meteor	h_b	h_e	ψ_β	ψ_ε
1	26.0°	24.2°	25.7°	29.8°
2	37.3°	36.9°	17.8°	20.9°
3	25.3°	21.6°	55.5°	61.6°
4	55.1°	53.8°	42.3°	46.8°
5	43.2°	41.8°	30.1°	34.7°
6	38.4°	36.6°	33.0°	36.6°
7	25.1°	20.4°	26.8°	32.1°
8	62.7°	62.2°	31.2°	35.2°
9	49.2°	44.8°	36.4°	44.5°
10	41.0°	39.1°	26.6°	29.2°
11	21.3°	17.5°	39.2°	43.3°

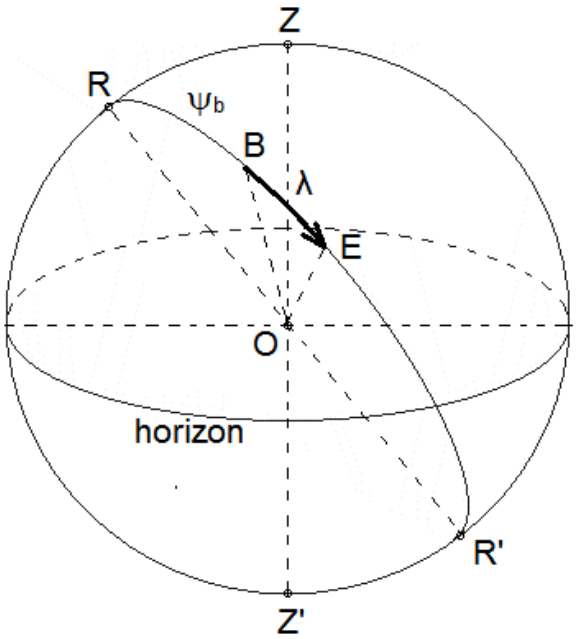

Figure 1 – The celestial sphere centered on the observer O with the positions of the radiant and anti-radiant R and R´, and a shower meteor with its beginning and end points B and E.

First we calculate the angular length of the meteor:

$$\lambda = \psi_b - \psi_e$$

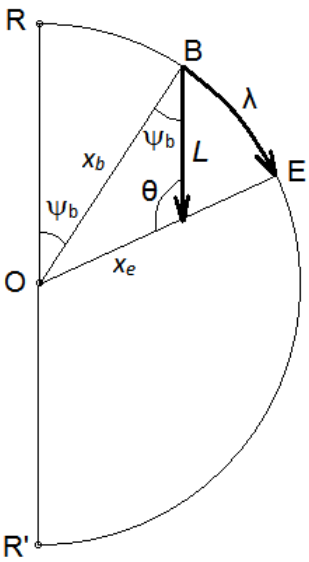

Figure 2 – The observer O, the radiant of the shower R, the angular length λ and the linear length L of the meteor.

In *Figure 2* we can see a representation of the apparent angular length λ and the linear length L of the meteor which is actually parallel to the radiant direction from the observer.

We assume that the Geminid meteors start to glow at a height of $H \approx 80$ km above the Earth's surface[1]. Of course the height will not be equal for all meteors and will depend on their masses and the angles at which they enter the Earth's atmosphere. That is why our investigation will be quite approximate. We then use the Earth's radius R and the sine theorem to calculate first the angles α and β, and then the distance x_b from the observer O to the beginning point B of the meteor:

$$\alpha = \arcsin\left(\sin(180° - z_b) \cdot \frac{R}{R+H}\right)$$

where $z_b = 90° - h_b$ is the zenithal distance of point B.

$$\beta = z_b - \alpha$$

$$x_b = R \cdot \frac{\sin\beta}{\sin\alpha}$$

Now we go back to *Figure 2* and, once again using the sine theorem, we finally find the length L of the meteor in kilometers:

$$L = x_b \cdot \frac{\sin\lambda}{\sin\theta}$$

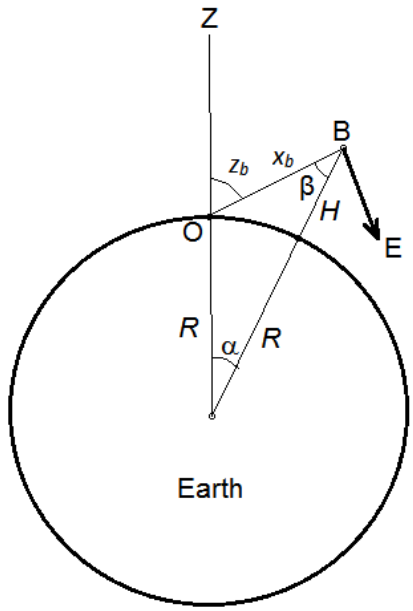

Figure 3 – The position O of the observer on the Earth and the meteor.

We calculated the linear lengths of all the meteors and then we tried to verify our results. We used the linear velocity of the Geminids $v = 35$ km/s and determined the duration of each meteor:

$$\Delta t = \frac{L}{v}$$

Then we used the angular length of each meteor to find its apparent angular velocity:

$$\omega = \frac{\lambda}{\Delta t}$$

There is a relationship between the angular velocities of the meteors and their distances from the radiant. We compared our results with the values given in the tables about Geminids in the Handbook for Visual Meteor

[1] http://earthsky.org/space/at-what-altitude-do-meteors-become-incandescent

Observations (Roggemans et al., 1992). We could see that there is a good agreement.

Table 2 – Apparent angular velocities of the meteors calculated using the results for their linear lengths.

Meteor	L [km]	t [s]	λ	ω [°/s]
1	25.6	0.73	4.13°	5.7
2	19.5	0.56	2.96°	5.3
3	22.1	0.63	6.14°	9.7
4	10.5	0.30	4.43°	14.8
5	16.4	0.47	4.38°	9.4
6	13.4	0.38	4.86°	12.67
7	31.9	0.91	5.26°	5.8
8	10.7	0.31	3.78°	12.4
9	21.12	0.60	8.07°	13.4
10	11.5	0.33	2.73°	8.3
11	22.0	0.63	4.15°	6.6

4 The brightness of the meteors

In order to find the meteor's brightness, we used the IRIS software. We measured the brightness at six points on the trajectory of each meteor, subtracting the background level of illumination. We then calculated the average value for the meteor E. In addition, we had to take into account the different distance of each meteor from the observer. To eliminate this factor we determined the brightness which the meteor would have had if it had appeared in the zenith – E_z . First we found the distance of the end point of the meteor from the observer (*Figure 2*):

$$x_e = L \cdot \frac{\sin\psi_b}{\sin\lambda}$$

We calculated a kind of "average" distance from the observer to the meteor:

$$x = \frac{x_b + x_e}{2}$$

And after that we reduced the observed meteor brightness to a zenithal position of the meteor:

$$E_z = E \cdot \frac{x^2}{H^2}$$

5 The results

Finally, we combined the two characteristics and built a graph representing the relationship between a meteor's luminosity and its linear length.

As it can be seen from the graph in *Figure 4*, the relationship between the two parameters is obvious as we expected. Further development of the method could improve the accuracy of the data. We applied a quite primitive method to obtain the apparent angular parameters of the meteors, by comparison between the images and stellar maps. We could instead use the astrometric options of the IRIS software. Nevertheless, some parameters will still remain not very accurate. For instance, it is difficult to define a brightness of a meteor – it has a different brightness at each point of its trajectory. It is also difficult to determine the positions of the beginning and the end point of a meteor on a photograph because the glow of the meteor does not begin and end abruptly. A major problem is the influence of the angle at which the meteors enter the Earth's atmosphere, or in other words, the altitude of shower radiant above the horizon. This influence should be significant but taking it into account requires quite complicate modeling of the behavior of the meteor particles in the atmosphere. Another source of inaccuracy is that for those meteors more distant from the observer, less of the meteor path would be bright enough to be visible to the observer, which would lead to underestimation of the length of the meteor.

Table 3 – Brightness of the Geminids (reduced to zenithal position) and their linear length.

Meteor	E_z instr. units	L km
1	572.9	25.6
2	129.0	19.5
3	665.5	22.1
4	71.5	10.5
5	85.3	16.4
6	134.8	13.4
7	1715.0	31.9
8	56.4	10.7
9	192.8	21.1
10	186.4	11.5
11	811.0	22.0

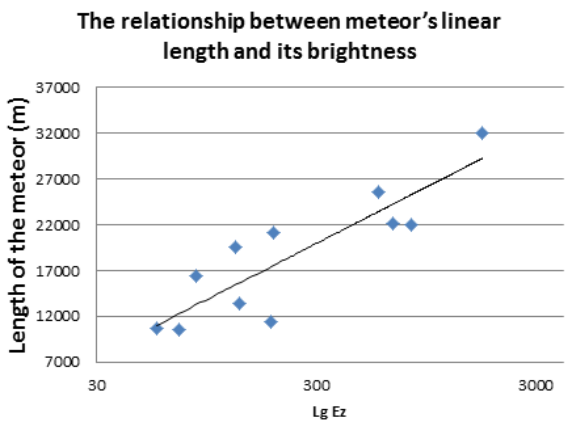

Figure 4 – Relationship between the brightness of the Geminids and their linear lengths.

6 Conclusions

We applied a simple and approximate method to determine the linear lengths and the brightness of a series of Geminid meteors and produced a graph showing the relationship between the two parameters.

The accuracy of the method could be increased by using more precise methods of measurement. However, there are natural limitations that ensue from the stochastic character of the meteor phenomenon itself. So another way to improve the results of this investigation would be to use a much greater amount of data so as to achieve more statistically significant results.

An interesting option for future work would be to explore the relationship between the brightness and the linear length for other meteor showers and to compare the parameters of this relationship.

References

Roggemans P., Gyssens M., Steyaert C. and Vanmunster T. (1992). “Handbook Visual Meteor Observations”. NATURELLA, Sofia (*in Bulgarian*).

Vivid discussion between Vincent Perlerin (in the center, ‘did I overlook something?’), Sirko Molau, Javor Kac and Cis Verbeeck. In the background Hans-Georg Schmidt and Bernd Gährken.

Radar observations of the Volantids meteor shower

Joel Younger[1,2], Iain Reid[1,2], Damian Murphy[3]

[1] **ATRAD Pty Ltd, Thebarton, Australia**
jyounger@atrad.com.au, ireid@atrad.com.au

[2] **School of Physical Sciences, The University of Adelaide, Adelaide, Australia**

[3] **Australian Antarctic Division, Kingston, Australia**
damian.murphy@aad.gov.au

A new meteor shower occurring for the first time on 31 December 2015 in the constellation Volans was identified by the CAMS meteor video network in New Zealand. Data from two VHF meteor radars located in Australia and Antarctica have been analyzed using the great circle method to search for Volantids activity. The new shower was found to be active for at least three days over the period 31 December 2015 – 2 January 2016, peaking at an apparent radiant of R.A. = 119.3 ± 3.7, dec. = –74.5 ± 1.9 on January 1st. Measurements of meteoroid velocity were made using the Fresnel transform technique, yielding a geocentric shower velocity of 28.1 ± 1.8 km s^{-1}. The orbital parameters for the parent stream are estimated to be a = 2.11 AU, e = 0.568, i = 47.2°, with a perihelion distance of q = 0.970 AU.

1 Introduction

The Camera for Allsky Meteor Surveillance (CAMS) video network in New Zealand reported the first detections of a meteor shower originating from a radiant of R.A. = 120.6, dec. = –72.0 in the constellation Volans on New Year's Eve 2015 (Jenniskens and Baggaley, 2016). A review of previous CAMS data indicated that the shower had not occurred in the previous year. In total, cameras recorded the trajectories of 21 Volantids meteors on December 31 and two on January 1, 2016, with activity peaking around 10^h15^m UT on 31 December. Shower meteors had a geocentric velocity of 28.4 km s^{-1} and visual magnitudes ranging from +3 to –2 (Jenniskens et al., 2016).

Existing VHF meteor radars, which are primarily used to study winds and plasma diffusion rates in the mesosphere/lower thermosphere (MLT) region of the atmosphere, can also be applied to the detection of meteor showers, with the advantage of being able to detect meteors during daylight hours and in inclement weather. Analysis of meteor radar echoes enables meteoroid velocity to be inferred, which, combined with the radiant of a detected shower, allows for orbital parameters of meteoroid streams to be calculated. Data collected in the course of unrelated atmospheric studies by two meteor radars in Australia and Antarctica were successfully searched for evidence of the new Volantids shower.

2 Meteor radar

Detection of meteor trails by radar

As a meteoroid enters Earth's atmosphere, kinetic energy is converted to thermal energy through collisions with atmospheric molecules. Once meteoroids are heated to the point of evaporation, atoms leave the meteoroid still traveling at similar geocentric velocities to the parent body. Subsequent collisions between atmospheric constituents and evaporated meteoric material can be energetic enough to ionize one or both of the colliding particles. This results in a trail of plasma behind the ablating meteoroid, comprised of a mixture of ions and electrons embedded in a background of neutral atmospheric molecules.

Meteoric plasma scatters incident radio waves, making it possible to detect meteor trails using the reflection of transmitted signals. The motion of meteor trails as they

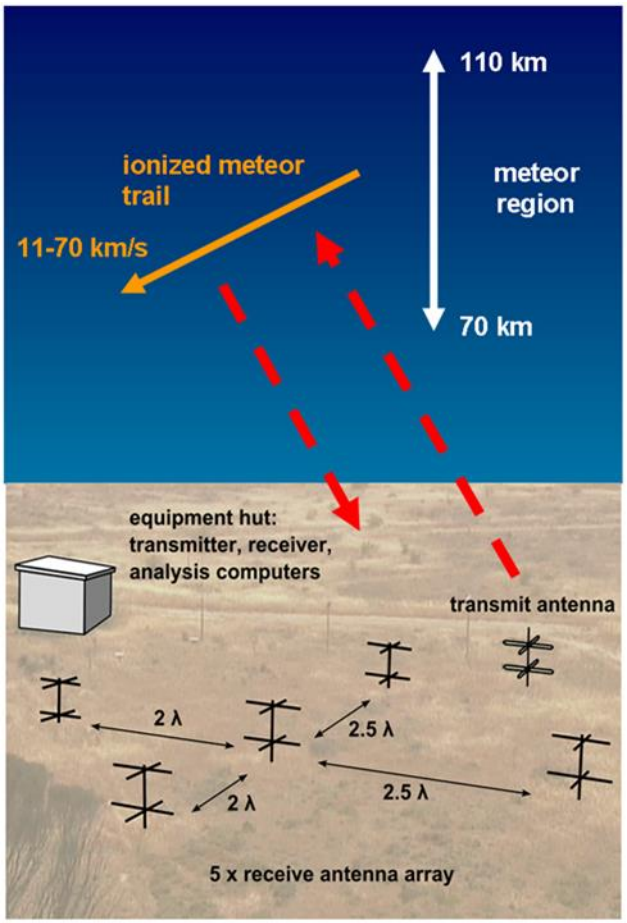

Figure 1 – Typical meteor radar configuration.

drift with background winds produces measurable Doppler shifts along the detection vector that can be combined across detections in different directions to infer the wind speed and direction in the meteor region. For small meteoroids (O(1 mm) diameter and smaller) that constitute the majority of the meteoroid flux, the meteoric plasma may be less than 2.4×10^{14} electrons m^{-1}, which classifies the trail as underdense (McKinley, 1961).

Radio waves can fully penetrate underdense plasmas, which produce specular echoes. Scatter from different points along the trail combines to produce the strongest echoes when the trail is perpendicular to the line of sight to the radar. Furthermore, meteoric plasma undergoes diffusion once formed, as the ions and electrons execute random walks away from the trail axis. The movement of meteoric plasma away from the trail axis reduces the intensity of observed radar backscatter through destructive interference. For underdense meteor trails, this results in a distinctive exponential decay in echo intensity over time. Hence, the duration of underdense meteor radar echoes can be used to infer the rate of plasma diffusion in the MLT, which can be used to estimate atmospheric temperature (Hocking, 1999; Cervera and Reid, 2000) and density (Younger et al., 2015a).

The radar backscatter produced during the passage of a meteoroid with a plasma trail across the field of view of a radar is analogous to a knife-edge diffraction pattern. The recording of echo phase in addition to intensity by a radar enables the diffraction pattern to be deconvolved through a process known as the Fresnel transform. The result is a profile of the scattering intensity along the trail, but an estimate of meteoroid speed is a fortunate byproduct of the process (Elford, 2004). Thus, radars can provide the three dimensional position of the perpendicular scattering point of a meteor trail and the instantaneous speed of the meteoroid as it passed that point.

Radar configuration

VHF meteor radars are a common tool for monitoring the atmosphere at heights between 70–110 km using frequencies in the range of 30–60 MHz. Modern meteor radars generally conform to similar configurations, consisting of a single all-sky transmit antenna and a five-element receive array (Jones et al., 1998), as shown in *Figure 1*.

The five antennas of the receive array form an interferometer, arranged in a T, L, or cross shape of two baselines sharing a common antenna. Antennas along the two perpendicular baselines are spaced at 2 and 2.5 times the radar wavelength, λ. The direction of incident backscatter is determined by comparing the phase differences of the different antenna pairs. The combination of the 2 and 2.5 λ allows for the construction of a virtual 0.5 λ antenna spacing, which provides unambiguous angle of arrival estimates, in addition to a higher precision 4.5 λ antenna pair. The minimum spacing of 2 λ ensures that mutual coupling between antennas is minimized.

Radars used in this study

Two ATRAD meteor radars were used for detection of Volantids shower activity in this study: a 40 kW 55 MHz radar at Buckland Park (34.6 S, 138.5 E) near Adelaide, Australia operated by The University of Adelaide and a 6.8 kW 33 MHz radar at Davis Station, Antarctica (68.6 S, 78.0 E) operated by the Australian Antarctic Division (Holdsworth et al., 2008). Both radars have a cross-shape receive array and transmit a 4-bit coded complimentary pulse at a pulse repetition frequency of 430 Hz. Signal to noise is improved using four-pulse coherent integration, which provides an effective sampling rate of 107.5 Hz. Details of meteor detection and classification criteria are given in (Holdsworth et al., 2004).

The Davis Station radar detects significantly more meteors than the Buckland Park radar. This is due in part to the polar location of the Davis Station radar and the higher radio noise in Buckland Park's metropolitan

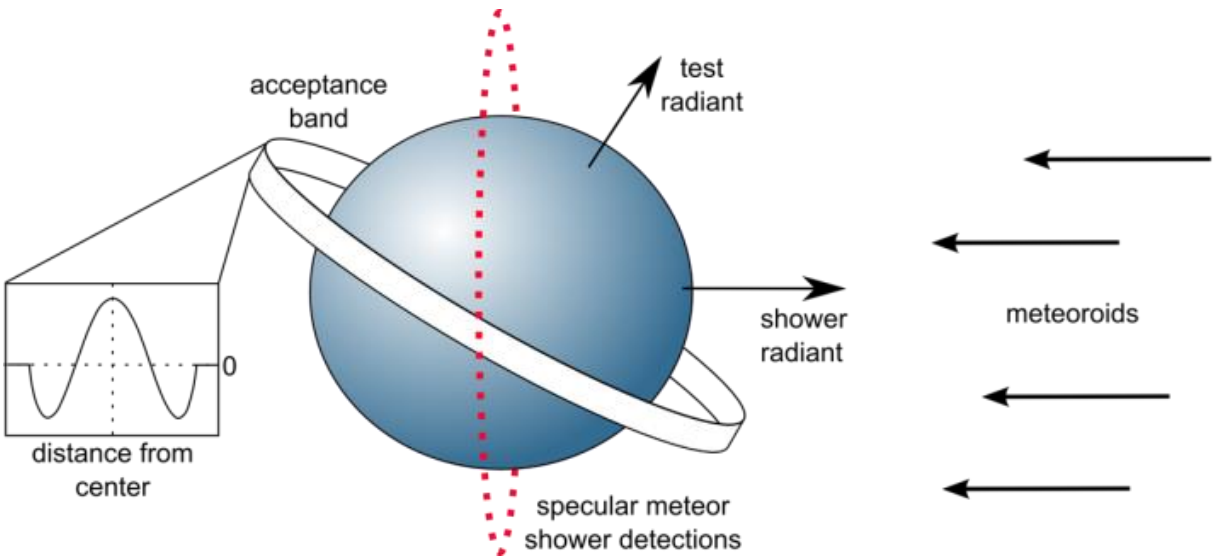

Figure 2 – Geometry of the great circle technique used to estimate shower activity using perpendicular detections. Possible radar detections resulting from a shower incident from the right are shown as a red dotted line. Earth rotates inside of the shaded celestial sphere. The inset plot depicts the weighting function as given by (1).

environment, but also to the lower transmitting frequency. As the minimum detectable plasma density is proportional to $\lambda^{3/2}$, where λ is the wavelength of the radar (Ceplecha et al., 1998), the minimum detectable trail density for the Buckland Park radar is more than double the minimum detectable density for the Davis Station radar at the same transmitting power levels. Additionally, during the Volantids observation period, the Buckland Park radar was operated as a passive radiometer for five out of every 15 minutes as part of an unrelated astrophysics experiment, which resulted in the array being used as a radar for only 2/3 of the time. Hence, while the Davis Station radar recorded an average of approximately 14000 meteor detections per day, the Buckland Park radar only recorded an average detection rate of about 4000 meteors per day.

3 Great circle method

General technique

The specular scatter of radio waves by underdense meteor trails produces the condition that meteors are detected when the line of sight to a meteor is perpendicular to the trail axis. This means that the trajectory of individual meteors cannot be determined by a single-station meteor radar. Thus, knowledge of the trajectory of single meteoroids is limited to a plane of ambiguity. This condition can, however, be exploited through a statistical analysis of large numbers of meteor detections.

If a well-defined filament of debris is in an orbit that

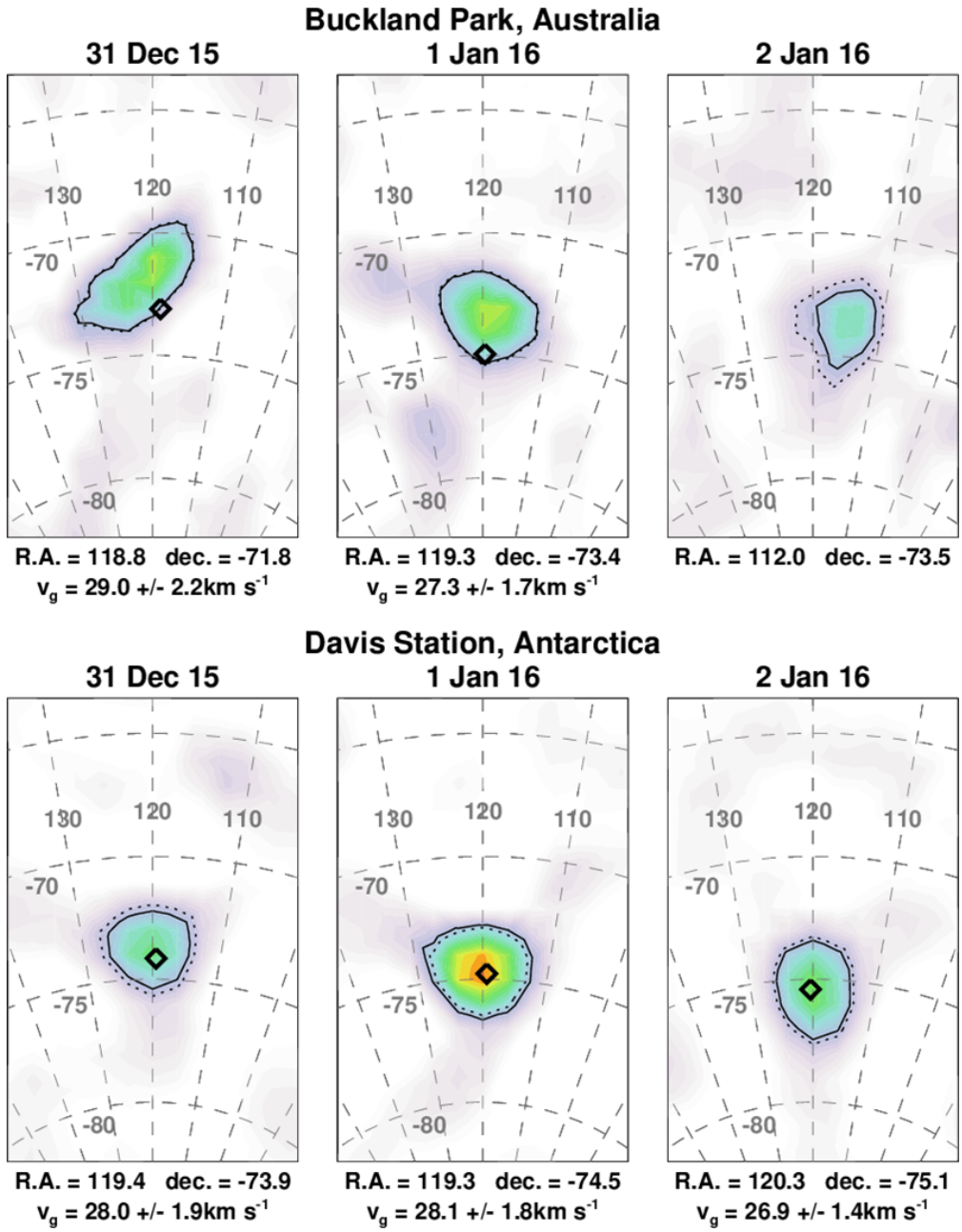

Figure 3 – Radiant activity maps showing daily detections of the Volantids shower in galactic-equatorial coordinates (J2000). Diamonds denote the position of the radiant after adjustment for zenith attraction. Dotted lines follow the full width at half maximum (FWHM) of the radiant activity peaks. Solid lines are the SNR = 5 contours used to flag possible shower activity. Data collected at Buckland Park on 2 January were insufficient to produce an estimate of shower velocity.

intersects the path of Earth, a meteor shower will occur. The perpendicular radar detections that result from a shower will lie in a ring on the celestial sphere, with the ring located perpendicular to the shower radiant, as depicted in *Figure 2*. Hence, radiants with shower activity can be found by counting the number of meteor detections in bands perpendicular to all possible radiants and searching for radiants with significantly elevated rates of perpendicular detections (Jones and Jones, 2006).

Application to this study

The great circle method has been applied previously by the authors to meteor radar data as part of a survey of Southern hemisphere shower activity (Younger et al., 2009) and for a detailed study of the predicted Camelopardalids shower in 2014 (Younger et al., 2015). To summarize the search process, the celestial sphere is first divided into discrete test radiants, separated by approximately one degree of solid angle. Radiant activity is quantified by a weighted count of meteors perpendicular to each radiant.

To reduce the blurring of narrow showers on the radiant activity map due to the overlap of perpendicular detection rings with misaligned acceptance bands, a weighting function,

$$w(\theta) = \begin{cases} 1 - 6\left(\frac{\theta}{\delta\theta}\right)^2 + 5\left(\frac{\theta}{\delta\theta}\right)^4 & \text{for } |\theta| \le \delta\theta \\ 0 & \text{for } |\theta| > \delta\theta \end{cases} \quad (1)$$

is applied, where θ is the distance from the center of the acceptance band. The width of the weighting function, δθ, is dependent on the width of showers being searched for and the angular accuracy of the radar. For this application, a value of four degrees has been found to work best.

Once activity values have been calculated for every possible radiant, an algorithm searches for discrete peaks corresponding to active showers. Radiant activity values are found to adhere to a normal distribution, so noise is defined as the standard deviation of non-zero radiant activity levels. The radiant activity map is searched for peaks that exceed the defined noise level by a factor of five. Shower activity peaks are characterized by fitting an ellipse to the noise threshold boundary on the map, which provides an estimate of the extent of the shower peak in right ascension and declination. Shower velocity is initially estimated by fitting a Gaussian curve to the velocities of meteors in a four degree wide band perpendicular to the peak centroid. Only meteors above the median detection height in the band are used to minimize the effects of deceleration (Younger et al., 2012).

Velocity distributions were further refined by subtracting an estimate of the sporadic background velocity distribution. The background velocity distribution was constructed by collecting candidate meteors from the average radiant of the detected Volantids shower in apex-centered solar coordinates on days to either side of shower activity. The background distribution was then subtracted from the detected shower candidate velocity distribution, with the resultant peak used to infer the apparent velocity of shower meteoroids.

4 Volantids shower detections

Initial detection

The great circle method as described was applied to single-day sets of meteor radar detections for each radar, peaking on January 1st at R.A. = 119.3 ± 3.7, dec. = –74.5 ± 1.9, as seen from Davis Station. Combined estimates of the apparent radiant at each location were used to construct the background velocity distribution as described. Summaries of the daily detection SNR values are given in *Table 1* and radiants locations are listed in *Figure 3*.

Table 1 – Daily signal to noise ratio of detections from each radar.

	signal to noise ratio	
	Buckland Park	Davis Station
31 Dec	9.7	8.3
1 Jan	9.5	11.7
2 Jan	7.3	8.8

Detailed estimates of the behavior of the detection rate over time are difficult, as the shower radiant passes close to the zenith of the Davis Station radar, which places shower trails' perpendicular reflection points on the horizon, where detection is impossible. This produces a detection distribution with a gap during what would otherwise be the time of the peak detection rate. Radiant analysis of a moving window of eight hour data subsets spaced two hours apart, shown in *Figure 4*, indicates that the Volantids shower occurred at least as early as 00^h00^m UT, 31 December 2015 and finished no earlier than 22^h00^m UT, 2 January 2016. Shower activity peaked at approximately 1300 UT, 1 January 2016. Volantids activity displays a gradual increase over the first three days, with a comparatively abrupt end. The Buckland Park radar, while more favorably located, did not achieve sufficient detection rates for a detailed analysis of radiant activity.

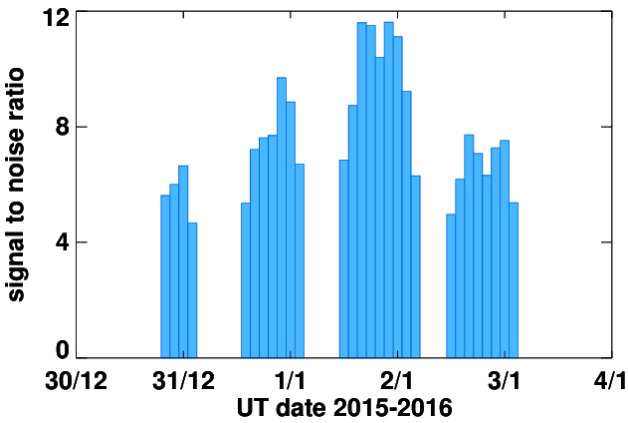

Figure 4 – 8-hour smoothed Volantids radiant activity at Davis Station, Antarctica.

Correction of apparent radiant

Earth's gravity affects the observed shower properties in two ways. Firstly, meteoroids are accelerated from their initial geocentric orbital velocity by the gravitational pull of Earth. Secondly, the gravitational pull towards Earth's barycenter causes meteoroid trajectories to be pulled towards the local zenith.

The geocentric velocity, v_g, of meteoroids can be calculated from the apparent velocity, v_a, that is observed on Earth via the equation

$$v_g = \sqrt{v_a^2 - \frac{GM_\oplus}{r_a}}, \qquad (2)$$

Where G is the gravitational constant, $M_\oplus$, is the mass of Earth, and r_a is the distance from the center of Earth to the meteor detections. The last term was determined by calculating the radius of Earth at each observing site using the WGS84 ellipsoid (Decker, 1986) and adding a nominal meteor detection height of 90 km.

The change in meteoroid trajectory zenith angle due to zenith attraction, $\Delta\varphi$, is given by

$$\Delta\varphi = 2\tan^{-1}\left(\frac{v_a - v_g}{v_a + v_g}\tan\frac{\varphi}{2}\right), \qquad (3)$$

where φ is the observed zenith angle. This correction was applied to the observed radiant of the Volantids to determine the radiant of the shower prior to the influence of Earth's gravity as shown as diamonds in *Figure 3*.

5 Orbit of the Volantid stream

The direction of the shower radiant can be combined with the speed of the shower meteoroids to estimate the orbital parameters of the parent stream (for equations, see e.g. Younger et al., 2009), the results of which are shown in *Table 2*. Uncertainties in the input variables were handled by using a Monte Carlo simulation, assuming normal statistics. 50000 calculations of orbital parameters were performed using randomized, normally distributed uncertainties centered on the measured values of right ascension, declination, and velocity. The widths of the randomized distributions were taken from the estimates of the standard deviations of the measured parameters.

Orbital parameter statistics

Estimation of uncertainty is problematic for some of the calculated values of the orbital elements. Eccentricity, inclination, and the argument of the perihelion all maintain normal or close to normal distribution following the propagation of input Gaussian uncertainty through orbital calculations, but the distributions of the calculated values of semi-major axis and perihelion distance exhibit substantial asymmetry, as can be seen in *Figure 5*.

To provide an estimate of the most likely value of a and q, the peak values of probability were used. A proxy for the 1-sigma uncertainty in each direction was determined by calculating the cumulative probability of the distribution moving away from the peak probability. The 1-sigma value was then assigned to the value for which the cumulative probability in each direction is equal to 0.34, which provides upper and lower uncertainty estimates for a and q.

Table 2 – Volantids orbital parameters determined from Monte Carlo simulation.

element	symbol	estimate	uncertainty
semi-major axis	a	2.11 AU	+ 0.50 - 0.18
eccentricity	e	0.568	± 0.069
inclination	i	47.2°	± 2.6
ascending node	Ω	100.3°	
perihelion arg.	ω	343.4°	± 3.4
perihelion distance	q	0.970 AU	+ 0.004 - 0.009

No uncertainty is provided for the argument of the ascending node, as the shower was observed at the ascending passage of the stream. The given value of the ascending node was determined from the solar longitude of Earth at the estimated time of maximum shower activity.

Comparison with CAMS derived orbit

The calculated values of a and q are slightly less than those given by Jenniskens and Baggaley in the initial announcement. This is likely due to the underestimation of meteoroid velocity by the radars. As meteor radars are specifically configured to detect faint meteor trails, radar detections are biased towards smaller meteoroids, which are strongly decelerated during ablation. By comparison, video detections necessarily correspond to larger meteoroids.

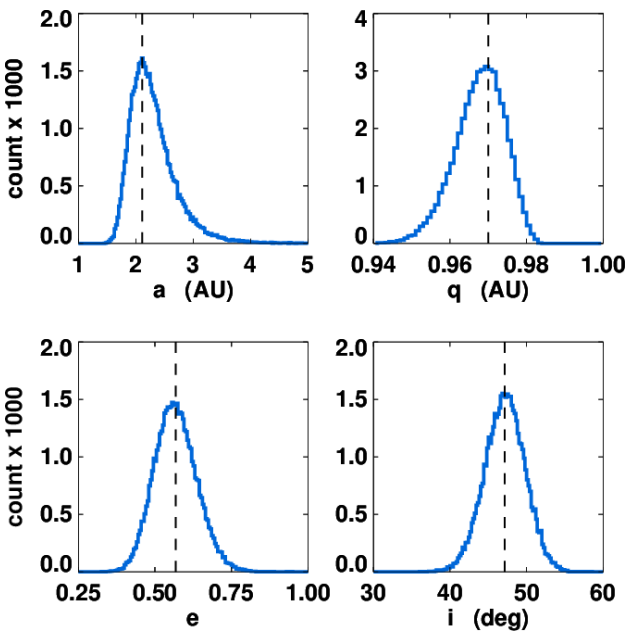

Figure 4 – Distributions of orbital parameters calculated in Monte Carlo simulation. Dashed lines show the final values listed in *Table 2*.

6 Conclusion

The Volantids shower of 2015/2016 has been detected by two meteor radars in the southern hemisphere, with results in good agreement with those of the CAMS video network that provided the initial detection. The use of radar enabled the monitoring of Volantid shower activity through daylight hours and in the absence of meteoroids sufficiently large enough to produce visible trails.

This study represents the first time that the Buckland Park meteor radar was used for astronomical purposes, which was done while the receive array was being periodically occupied by other experiments. This demonstrates the ability of the great circle method to successfully detect shower activity even from modestly performing meteor radars. The source of the Volantids is still unknown, but the stream is already well characterized after a single occurrence of the shower.

Acknowledgments

This project was made possible by generous financial support from ATRAD Pty Ltd. Radar observations were conducted with financial support from Australian Research Council grants DP0878144 and DP1096901 and ASAC grant 2325.

References

Ceplecha Z., Borovička J., Elford W. G., Revelle D. O., Hawkes R. L., Porubčan V. and Šimek M. (1998). "Meteor phenomena and bodies". *Space Science Reviews.*, **84**, 327–471.

Cervera M. A. and Reid I. M. (2000). "Comparison of atmospheric parameters derived from meteor observations with CIRA". *Radio Science*, **35**, 833–843.

Decker B. L. (1986). "World geodetic system 1984". Defense Mapping Agency Aerospace Center St Louis Afs Mo.

Elford W. G. (2004). "Radar observations of meteor trails, and their interpretation using Fresnel holography: a new tool in meteor science". *Atmos. Chem. Phys.*, **4**, 695–729.

Hocking W. K. (1999). "Temperatures using radar-meteor decay times". *Geophysical Research Letters*, **26**, 3297–3300.

Holdsworth D. A., Murphy D. J., Reid I. M. and Morris R. J. (2008). "Antarctic meteor observations using the Davis MST and meteor radars". *Advances in Space Research*, **42**, 143–154, doi:10.1016/j.asr.2007.02.037.

Holdsworth D. A., Reid I. M. and Cervera M. A. (2004). "Buckland Park all-sky interferometric meteor radar". *Radio Science*, **39**, 1–12, doi:10.1029/2003RS003014.

Jenniskens P. and Baggaley J. (2016). "Volantid meteor shower outburst on New Year's Eve 2015". CBET 4261, Central Bureau for Astronomical Telegrams.

Jenniskens P., Baggaley J., Crumpton I., Aldous P., Gural P. S., Samuels D., Albers J. and Soja R. (2016). "A surprise southern hemisphere meteor shower on New-Year's Eve 2015: the Volantids (IAU#758, VOL)". *WGN, Journal of the IMO*, **44**, 35–41.

Jones J. and Jones W. (2006). "Meteor radiant activity mapping using single-station radar observations". *Monthly Notices of the Royal Astronomical Society*, **367**, 1050–1056, doi:10.1111/j.1365-2966.2006.10025.x.

Jones J., Webster A. R. and Hocking W. K. (1998). "An improved interferometer design for use with meteor radars". *Radio Science*, **33**, 55–65.

McKinley D. W. R. (1961). *Meteor Science and Engineering*, McGraw-Hill, New York.

Younger J. P., Reid I. M., Vincent R. A., Holdsworth D. A. and Murphy D. J. (2009). "A southern hemisphere survey of meteor shower radiants and associated stream orbits using single station radar observations". *Monthly Notices of the Royal Astronomical Society*, **398**, 350–356, doi:10.1111/j.1365-2966.2009.15142.x.

Younger J. P., Reid I. M., Vincent R. A. and Murphy D. J. (2012). "Meteor shower velocity estimates from single-station meteor radar: accuracy and precision". *Monthly Notices of the Royal Astronomical Society*, **425**, 1473–1478, doi:10.1111/j.1365-2966.2012.21632.x.

Younger J. P., Reid I. M., Li G., Ning B. and Hu L. (2015). "Observations of the new Camelopardalids meteor shower using a 38.9 MHz radar at Mohe, China". *Icarus*, **253**, 25–30, doi: 10.1016/j.icarus.2015.02.021

Younger J. P., Reid I. M., Vincent R. A. and Murphy D. J. (2015a). "A method for estimating the height of a mesospheric density level using meteor radar". *Geophysical Research Letter.*, **42**, 1–6, doi:10.1002/2015GL065066.

Taurids 2015

Przemysław Żołądek[*1], Arkadiusz Olech[2], Mariusz Wiśniewski[3,1], Regina Rudawska[4], Marcin Bęben[1], Tomasz Krzyżanowski[1], Maciej Myszkiewicz[8,1], Marcin Stolarz[1], Marcin Gawroński[5], Mariusz Gozdalski[1], Tomasz Suchodolski[6], Walburga Węgrzyk[1] and Zbigniew Tymiński[7,1]

[1] **Comets and Meteors Workshop, ul. Bartycka 18 00-716 Warszawa, Poland**
*brahi@op.pl

[2] **Nicolaus Copernicus Astronomical Center, Polish Academy of Science ul. Bartycka 18 00-716 Warszawa, Poland**

[3] **Central Office of Measures, ul. Elektoralna 2 00-139 Warszawa, Poland**

[4] **ESA European Space Agency Research and Technology Centre, Noordwijk, The Netherlands**

[5] **Toruń Centre for Astronomy, Faculty of Physics, Astronomy and Applied Informatics, Nicolaus Copernicus University, ul. Grudziądzka 5, 87-100 Toruń, Poland**

[6] **Space Research Centre, Polish Academy of Science, ul. Bartycka 18A 00-716 Warszawa, Poland**

[7] **National Centre for Nuclear Research, POLATOM, ul. Sołtana 7 05-400 Otwock, Poland**

[8] **Warsaw University Observatory, Al. Ujazdowskie 4 00-478 Warszawa, Poland**

Enhanced activity of the Southern Taurids has been detected in the evening of 31 October 2015. Polish Fireball Network cameras detected several bright meteors and fireballs including extremely bright events at 18^h05^m UT and 23^h13^m UT. Trajectories and orbital elements have been calculated, the orbits of both fireballs have been compared with the NEO orbital database. Three asteroids on very similar orbits have been found – 2015TX24, 2005UR and 2015TF50. All these bodies have orbital periods close to a 7:2 resonance with Jupiter.

1 Introduction

The Northern and Southern Taurids are well known autumn meteor showers. Observed during several decades by visual observers and presently by modern equipment, the Taurids look to be a meteor shower with many interesting features. This is an ecliptic meteor stream divided in two branches known as the Northern Taurids (NTA) and the Southern Taurids (STA). Both Taurid streams usually produce rather low visual rates, typical activity doesn't exceed a ZHR = 5. According to the IMO visual data Northern Taurids are active from October 10 to December 20 with a barely visible maximum close to November 12. Southern Taurids are active from September 10 to November 20 with a maximum close to October 10. Both streams produce also daylight meteor showers. The Northern branch of the Taurids encounters the Earth again at the end of June producing the daytime Beta Taurids, the Southern branch meets the Earth in the beginning of June producing the daytime Zeta Perseids. Various authors described the complex structure of the Taurids which is detectable using modern observing techniques. There is a large number of streams which can be connected with comet 2P/Encke (Porubčan et al., 2006), all these streams create a widely dispersed complex of meteor showers. For most of these showers NEO asteroids on similar orbits were found.

Some data suggests that the Taurids are responsible for some unusual activity outbursts with enhanced numbers of bright fireballs observed. All these observations have been analyzed (Asher and Clube, 1993). The authors found traces of the high activity in October 1951, November 1978, November 1981 and November 1988. There are also observations of transient lunar phenomena in June 1931 and June 1975 probably caused by meteoroids hitting the moon during daytime encounters with the stream. Authors pointed out that such activity may be connected with a Taurid filament which is in a resonance of 7:2 with Jupiter. Further possible enhancements of activity were predicted for 1995, 1998 and 2005. Higher ZHR's were observed in 1998 and 2005 (Dubietis and Arlt, 2007). Especially the 2005 maximum was spectacular, with a higher overall activity and enhanced number of very bright STA fireballs. Between 28 October and 10 November the Polish Fireball Network observed five bright Taurid fireballs, the brightest one, a –15 magnitude fireball was observed on November 4, 2005.

A new prediction of the outburst has been published after the 2005 maximum with a possible enhanced activity in 2015.

2 Observations

During the evening of 31 October 31 the sky over Poland was clear. Shortly after sunset video cameras of the Polish Fireball Network started to observe. It is worth to mention that this evening many amateur astronomers photographed the northern sky trying to register the 2015 TB145 asteroid visible at the same time. An extremely bright fireball appeared over Northern horizon on 18^h05^m UT reaching a magnitude much brighter than the Full Moon. Casual observers describe the fireball as a

Figure 1 – The "Okonek" fireball, 31 October 2015 18^h05^m UT. Image taken in Czernice Borowe, 80 km north of Warsaw.

moderate speed, blue-green fireball with multiple flashes which completely lightened the sky and surrounding landscape. Some observers located exactly below the trajectory reported electrophonic sounds exactly in the moment of brightest flare, they didn't notice any other sound effects. The persistent trail left by this fireball has been visible for at least 50 minutes drifting slowly to the west.

The 18^h05^m fireball was registered by multiple stations of the Polish Fireball Network, most of recordings were only partially usable due to strong image saturation. A very precise fireball image has been obtained by a casual photographer from Czernice Borowe (former PFN22 station), 80km north of Warsaw. The fireball trail visible on this image is almost complete and the terminal part of the trajectory is clearly visible. The same photographer also registered a very detailed image of the persistent trail.

After the fireball, during the next few hours a significant rise in the Taurids activity has been observed. Dozens of Taurids have been observed by the whole network resulting in 14 calculated trajectories and orbits. This activity was concentrated between 20^h UT and 21^h UT.

The second very bright fireball appeared at 23^h13^m UT and was not so widely noticed by casual observers. This fireball saturated cameras located in the north-western part of Poland, the more distant stations recorded quite usable video material. This event was a bit fainter and had a shorter duration than the fireball observed on 18^h05^m UT. The fireball appeared over the western part of Poland, and was located higher at the sky in most of the fireball stations.

During the second half of the night the Southern Taurid activity decreased and only two Southern Taurids have been observed before the sunrise.

3 Results

All meteors and fireballs from the 31 October 2015 night have been measured and after that the trajectories and orbital elements have been calculated using the *PyFN* software (Żołądek, 2012). Most of the coordinates used for calculations come directly from the *MetRec* software while the brightest fireballs have been measured manually due to possible errors caused by image saturation.

The fireball which occurred at 18^h05^m UT reached an absolute magnitude of –16 over the town Okonek in north-western Poland. The east-west oriented trajectory of this fireball was located close to the cities Chojnice, Drawsko Pomorskie and Szczecinek. The fireball appeared at a height of 118 km and terminated its luminous patch at the height of 60 km after a 181 km long flight.

The second fireball reached a brightness of –14.5 magnitude 82 kilometers above the town Ostrowite, 80 km east of Poznań. The trajectory was steep, with the beginning at 108 kilometers and the terminal point at 58 kilometers.

In total 64 orbits have been calculated for this particular night, among which 20 orbits belong to the Southern Taurids, 4 orbits belong to the Northern Taurids and the remaining 40 orbits are sporadics and minor showers.

The orbits of the Okonek and Ostrowite fireballs are very similar, with Drummond similarity criterion D' = 0.011. The semimajor axis of the Okonek fireball is 2.25 AU and for Ostrowite fireball 2.27 AU. The resulting orbital periods are 1234 days and 1282 days respectively while the orbital period of the 7:2 resonance stream is 1238 days. Both fireballs were caused by meteoroids orbiting the Sun close to the 7:2 resonance, this is in good agreement with model published by Asher and Clube (1993).

Orbital elements of these two meteoroids have been compared with the NEODYS database using the Drummond criterion. We found three NEO objects on similar orbits, with an orbital period close to a 7:2 resonance with Jupiter. The most similar object is 2015TX24 – this NEO asteroid orbiting the Sun on an almost identical orbit as the "Ostrowite" fireball (D' = 0.0056), moreover this quite big, few hundred meters sized body has been discovered on 8 October 2015 and encountered the Earth on 29 October 2015, just two days before the "Okonek" and "Ostrowite" fireballs. The orbital period of 2015TX24 perfectly fits the 7:2 resonance with Jupiter (1248 days). The second body is 2005UR, with an orbital period of 1241 days and D' = 0.036 (if compared to the Ostrowite fireball). It is interesting that also this body has encountered the Earth during the previous Southern Taurid maximum in 2005, the closest encounter was observed on 30 October 2005 at 13^h UT. The third body is the 2005TF50 (D' = 0.042 with the Ostrowite fireball). This body has an orbital period of 1251 days and is previously recognized as a body associated with one of the Taurid filaments (Porubčan et al., 2006).

4 Conclusion

The 2015 Taurid maximum occurred as expected, with a noticeable enhancement in stream activity. Two very bright, spectacular fireballs appeared in the evening of 31 October 2015, both significantly brighter than the Full Moon. The orbital elements of the fireballs have been calculated and compared to the orbital elements from the NEODYS database. Three bodies orbiting the Sun on very similar orbits have been found, especially one of these asteroids – 2015TX24 orbiting the Sun on an almost identical orbit like the second observed fireball. The orbital periods of both fireballs and all three NEO asteroids are very close to the 7:2 resonance with Jupiter which is in good agreement with the existing model. These NEO objects shouldn't be treated as parent bodies of the 7:2 filament, it is more correct to treat them as the most massive remnants of the larger body fragmented in the past. It's worth to mention that larger numbers of such bodies may exist in the Southern Taurid stream creating a kind of asteroidal core of the 7:2 stream.

Acknowledgment

This work was supported by the NCN grant number 2013/09/B/ST9/02168.

References

Asher D. J. and Clube S. V. M. (1993). "An Extraterrestrial Influence during the Current Glacial-Interglacial". *Quarterly Journal of the Royal Astronomical Society*, **34**, 481–511.

Dubietis A. and Arlt R. (2007). "Taurid resonant-swarm encounters from two decades of visual observations". *Monthly Notices of the Royal Astronomical Society*, **376**, 890–894.

Porubčan V., Kornoš L. and Williams I. P. (1993). "The Taurid complex meteor showers and asteroids". *Contributions of the Astronomical Observatory Skalnaté Pleso*, **36**, 103–117.

Żołądek P. (2012). "PyFN – multipurpose meteor software". In Gyssens M. and Roggemans P., editors, *Proceedings of the International Meteor Conference*, Sibiu, Romania, 15-18 September 2011. IMO, pages 53–55.

International Meteor Conference 2017 Petnica, Serbia, September 21–24, 2017

Dušan Pavlović, Snežana Todorović and Miroslav Živanović

Petnica Science Center, Petnica, Valjevo, Serbia
dusan.pavlovicc@gmail.com, pmg.todsn@gmail.com, miroslavzivanovic6@gmail.com

The International Meteor Conference 2017 will be hosted by Petnica Science Center in Petnica, a village near the city of Valjevo, Serbia, from September 21 to September 24, 2017. Here we present some basic information about this conference, as presented at the International Meteor Conference 2016 in Egmond, the Netherlands.

1 Introduction

In 1997 the International Meteor Conference was held in Petnica Science Center, in Serbia. At that time, one of the most interesting experiences was the fact that there was a *large number of very active young meteor observers*.

Now, exactly 20 years after the previous IMC in Serbia, Petnica Science Center will host once more an IMC in 2017.

In the meantime, Petnica Meteor Group, the group which works within the Petnica Science Center since 1993, continued to bring together meteor observers and those interested in other fields of meteor science (not only the high school students but people from all disciplines and of all professions). The Petnica Meteor Group experienced a significant boost by hosting the IMC in 1997. The visual observations were enriched by video and all-sky observations, a little bit of theoretical work and data analysis, and greatly by the School of Meteor Astronomy, a week-long seminar teaching the high school students the basics of meteor science. Those are all the reasons to bring the IMC back to Petnica next year.

2 Date and location

The International Meteor Conference 2017 will be hosted by Petnica Science Center from Thursday evening, September 21, till Sunday lunch time, September 24, 2017, in Petnica Science Center, near the city of Valjevo, Serbia.

The PSC is an extracurricular science education center for high school students from all countries of former Yugoslavia. It is located in Petnica, the small village near the city of Valjevo, about 100 km southwest from Belgrade.

3 Accommodation

The PSC campus has undergone a significant expansion since the IMC 1997. Today, the PSC has a campus with separate buildings hosting lecture halls and classrooms, a library, laboratories, dormitories, a restaurant, etc. The IMC 2017 participants will be accommodated on-campus. Since all conference events will be hosted on-campus, there will be plenty of opportunity for the meteor community to interact at the conference, both formally and informally.

Figure 1 – The dormitory building.

There will be 14 single, 20 double and 28 triple bedrooms (138 beds in total) available in the dormitory building, which is connected to the main conference building by a covered walkway.

Figure 2 – The night sky at Petnica over the restaurant and cafe.

The talks and poster sessions will be held in the nearby main building. The talks will be presented in an amphitheater (150 seats) and the posters will be displayed

Figure 3 – A part of the Petnica Science Center campus, Petnica, Serbia.

Figure 4 – An airial view at Petnica Science Center campus.

in the hallway and two small classrooms (50 seats per classroom) across the hall and at the lower floor of the building. Also, there is an open amphitheater with 500 seats which can be used for the evening activities.

The campus is covered by free WiFi internet and all bedrooms also have LAN connections.

The campus includes a restaurant (350 seats), a café, and a small shop. The restaurant and café open up to a nice terrace overlooking the area. Special food requirements can be arranged in advance.

4 Program and social events

As usual at the IMCs, the main part of the program will consist of talks and poster sessions. The exact schedule of those activities will be determined after the end of the registration period, when we get a clear picture of the number of registered speakers and topics. There will be short talks and extended sessions, as well as workshops organized by the prominent specialists in various fields of meteor science.

All presentations, both talks and posters, will be included in the IMC 2017 Proceedings as full-length papers or abstracts.

Also, there will be a contest for the best poster and the best meteor photo.

Social events include evening activities, an excursion to points of interest in and around Valjevo and a visit to one of the local wineries in the evening after the excursion.

5 Registration

Registration opens in January 2017. This will be announced in the IMO journal WGN and on the IMO and IMC 2017 web sites. The early-bird registration deadline is June 30, 2017. The final deadline will be August 15, 2017, but mind that registration may have to be closed earlier if full capacity is reached before that date.

The early-bird registration fee is 130 EUR per person for accommodation in a triple bedroom, 170 EUR per person for accommodation in a double bedroom and 240 EUR for accommodation in a single bedroom. After June 30th, 2017 an extra fee of 20 EUR is charged.

The standard registration fee includes full board (accommodation, breakfast, lunch, and dinner) from Thursday evening September 21 (dinner included) till Sunday noon September 24 (lunch included), IMC lectures, coffee breaks and the excursion. Accompanying persons older than 12 years sharing a room with a participant must also register as a participant. T-shirts and printed proceedings can be purchased separately upon registering. An electronic version of the proceedings will be made available to all participants for no additional charge.

More detailed information will be announced when the registration is opened.

6 Travel information

As Petnica is a small village, there is no bus connection, but a shuttle will be available from the Valjevo bus and train stations located 7 km from Petnica. So, participants (if not arriving by car directly to Petnica Science Center) should come to Valjevo, from where an organized free shuttle bus will bring them to Petnica Science Center. The GPS location of the Petnica Science Center is 44° 14' 48" N, 19° 55' 52" E.

Detailed travel information and instructions for car drivers will be published in due time on the IMC 2017 web pages. Here, we limit ourselves to some general information.

If you travel by plane, the best way is to fly to Belgrade (Airport “Nikola Tesla”), then go to the Belgrade central bus or train station, and from there to Valjevo by bus or train (there is a connection approximately every hour). You can also rent a car at the airport – you will find the car rental agencies at the arrivals terminal.

If you travel by bus or train, the best way is to go to Belgrade and from the Belgrade central bus or train station to Valjevo by bus or train (there is a connection approximately every hour).

If you travel by car, you can use the E70 and E75 Motorways connecting Zagreb, Novi Sad, Belgrade and Niš. Or simply drive to Belgrade and from Belgrade to Valjevo.

We encourage the participants to consider carpooling. The Local Organizing Committee (LOC) will provide assistance once the registration is closed. By encouraging carpooling we want to reduce the number of cars, lower the cost by sharing cars and promote socializing while traveling to the IMC.

7 Contact

Detailed information will be posted at the IMC 2017 web pages as they become available. (As usual, a link to these pages will be provided on the homepage of the IMO website as soon as they are active.) Meanwhile, you may contact the LOC at imc2017@imo.net.

See you next year at the IMC 2017 in Petnica!

Acknowledgments

We want to thank Vladimir Lukić, Marc Gyssens, Dragana Okolić and Branislav Savić for useful comments on this text and the presentation of the IMC 2017.

List of participants

The alphabetical list below contains all participants of the 35th International Meteor Conference. Numbers serve to identify positions in the group photographs, if applicable. You can find the group photograph on page 369.

Abe Shinsuke, Japan (127)
Abedin Abedin, Canada (Not on the photo)
Albin Thomas, Germany (118)
Argo Megan, United Kingdom (124)
Asher David, United Kingdom (125)
Bagrov Alexander, Russia (21)
Barbieri Lorenzo, Italy (52)
Bastiaens Luc, Belgium (48)
Bettonvil Uros, Netherlands ()
Bettonvil Dusan, Netherlands (6)
Bettonvil Eduard, Netherlands (53)
Bettonvil Felix, Netherlands (71)
Biondić Jakov, Croatia (109)
Biondić Damir, Croatia (110)
Birlan Mirel, France (19)
Bojurova Eva, Bulgaria (41)
Bonino Donata, Italy (137)
Borovička Jiří, Czech Republic (141)
Brando Gaetano, Italy (47)
Bronikowska Malgorzata, Poland (Not on the photo)
Brown Peter, Canada (1)
Calders Stijn, Belgium (79)
Campbell-Brown Margaret, Canada (2)
Čapek David, Czech Republic (34)
Colas Francois, France (93)
Çubuk Kerem Osman, Turkey (Not on the photo)
Currie Malcolm, United Kingdom (51)
De Queiroz José, Switzerland (Not on the photo)
de Vet Sebastiaan, Netherlands (3)
Devillepoix Hadrien, Australia (8)
Dolinský Peter, Slovakia (Not on the photo)
Drolshagen Esther, Germany (87)
Dubs Martin, Switzerland (46)
Egal Auriane, France (7)
Fujiwara Yasunori, Japan (98)
Gährken Bernd, Germany (70)
Gardiol Daniele, Italy (90)
Georgescu Ana, Romania (82)
Georgescu Tudor, Romania (80)
Gostinski David, Croatia (78)
Grašić Ljubica, Serbia (128)
Gritsevich Maria, Finland (42)
Guliyev Ayyub, Azerbaijan (89)
Gural Pete, United States (5)
Gyssens Marc, Belgium (58)
Haas Robert, Netherlands (Not on the photo)
Hajduková Mária, Slovakia (83)
Hankey Michael, United States (32)
Hartman Joost, Netherlands (106)
Hillestad Eli Fugelsoe, Norway (62)
Hillestad Trond Erik, Norway (60)
Hristova Simona, Bulgaria (126)
Ibhi Abderrahmane, Morocco (54)
Igaz Réka, Hungary (13)
Igaz Antal, Hungary (12)
IJland Elise, Netherlands (121)
Jacobs Lars, Belgium (86)
Jenniskens Peter, United States (117)
Jobse Klaas, Netherlands (38)
Kac Javor, Slovenia (92)
Kákona Jakub, Czech Republic (36)
Kartashova Anna, Russia (133)
Kastinen Daniel, Sweden (116)
Keeris Roy, Netherlands (120)
Kero Johan, Sweden (115)
Klemt Bernd, Germany (96)
Knöfel André, Germany (69)
Koelers Selma, Netherlands (101)
Kokkeler Ben, Netherlands (Not on the photo)
Korec Matej, Slovakia (123)
Korlević Korado, Croatia (16)
Koschny Gabi, Netherlands (64)
Koschny Detlef, Netherlands (66)
Koten Pavel, Czech Republic (10)
Koukal Jakub, Czech Republic (140)
Kurtović Goran, Croatia (114)
Lamy Hervé, Belgium (Not on the photo)
Lesanu Cezar, Romania (95)
Maciejewski Maciej, Poland (23)
Madkour Waleed, Japan (119)
Malarić Mirjana, Croatia (112)
Markham Tony, United Kingdom (104)
Marshall Robert, United States (18)
Martínez Picar Antonio, Belgium (14)
Mizumoto Satoshi, Japan (103)
Molau Sirko, Germany (73)
Moreno-Ibáñez Manuel, Spain (22)
Nakane Sumio, Japan (Not on the photo)
Neijts Marc, Netherlands (122)
Netjes Gert Jan, Netherlands (Not on the photo)

Nijland Jos, Netherlands (65)
Nogami Nagatoshi, Japan (102)
Novoselnik Filip, Croatia (111)
Ocaña González Francisco, Spain (94)
O'Connell Michael, Ireland (75)
Okolić Dragana, Netherlands (134)
Ott Theresa, Germany (85)
Ozeren Ferhat Fikri, Turkey (Not on the photo)
Pavela Debora, Serbia (29)
Pavlović Dušan, Serbia (129)
Perlerin Vincent, France (31)
Peterson Chris, United States (15)
Pittich Eduard, Slovakia (138)
Poerink Urijan, Netherlands (17)
Polakowski Krzysztof, Poland (63)
Polfliet Tim, Belgium (59)
Popescu Miruna, United Kingdom (55)
Rault Jean-Louis, France (25)
Reid Iain, Australia (37)
Rendtel Juergen, Germany (33)
Roelandts Tom, Belgium (27)
Roggemans Paul, Belgium (39)
Roggemans Adriana, Belgium (44)
Rudawska Regina, Netherlands (135)
Ryabova Galina, Russia (Not on the photo)
Sánchez de Miguel Alejandro, Spain (49)
Sansom Eleanor, Australia (35)
Schenker Jonas, Switzerland (91)
Schmidt Irmgard, Germany (97)
Schmidt Hans-Georg, Germany (105)
Šegon Damir, Croatia (4)
Shrbený Lukáš, Czech Republic (68)
Shuttleworth Alan, United Kingdom (Not on the photo)
Skokić Ivica, Croatia (108)
Skunca Gordan, Croatia (77)
Slagter Daan, Netherlands (76)
Smeets Nastassia, Belgium (30)
Soja Rachel Halina, Germany (132)
Solovaya Nina, Slovakia (88)
Spurný Pavel, Czech Republic (56)
Stewart Peter, United Kingdom (113)
Steyaert Chris, Belgium (57)
Stolarz Marcin, Poland (20)
Sutherland Paul, United Kingdom (45)
ter Kuile Casper, Netherlands (Not on the photo)
Theiler Laura, Germany (43)
Theiler Carina, Germany (72)
Todorović Snežana, Serbia (131)
Tomezzoli Giancarlo, Germany (Not on the photo)
Tóth Juraj, Slovakia (139)
Tukkers Arnold, Netherlands (11)
Vaubaillon Jeremie, France (24)
Veljković Kristina, Slovenia (Not on the photo)
Verbeeck Cis, Belgium (67)
Verbert Jan, Belgium (81)
Vida Denis, Croatia (107)
Vojáček Vlastimil, Czech Republic (9)
Ward Bill, United Kingdom (28)
Weatherley Gillian, United Kingdom (50)
Weiland Thomas, Austria (61)
Wiśniewski Mariusz, Poland (100)
Wrigley Nick, United Kingdom (130)
Yamamoto Masa-yuki, Japan (99)
Yancheva Yulia, Bulgaria (136)
Younger Joel, Australia (40)
Zender Joe, Netherlands (Not on the photo)
Zigo Pavol, Slovakia (74)
Živanović Miroslav, Serbia (26)
Żołądek Przemysław, Poland (84)

If you wish to locate a particular person on the group photo on the adjacent page, search for his or her name in the alphabetical list above, and find the face corresponding to the number mentioned using the key under the group photo.

Conversely, if you wish to identify a face on the group photo, find the corresponding number in the key, and find his or her name in the numerically ordered list below:

(1) Brown Peter; (2) Campbell-Brown Margaret; (3) de Vet Sebastiaan; (4) Šegon Damir; (5) Gural Pete; (6) Bettonvil Dusan; (7) Egal Auriane; (8) Devillepoix Hadrien; (9) Vojáček Vlastimil; (10) Koten Pavel; (11) Tukkers Arnold; (12) Igaz Antal; (13) Igaz Réka; (14) Martínez Picar Antonio; (15) Peterson Chris; (16) Korlević Korado; (17) Poerink Urijan; (18) Marshall Robert; (19) Birlan Mirel; (20) Stolarz Marcin; (21) Bagrov Alexander; (22) Moreno-Ibáñez Manuel; (23) Maciejewski Maciej; (24) Vaubaillon Jeremie; (25) Rault Jean-Louis; (26) Živanović Miroslav; (27) Roelandts Tom; (28) Ward Bill; (29) Pavela Debora; (30) Smeets Nastassia; (31) Perlerin Vincent; (32) Hankey Michael; (33) Rendtel Juergen; (34) Čapek David; (35) Sansom Eleanor; (36) Kákona Jakub; (37) Reid Iain; (38) Jobse Klaas; (39) Roggemans Paul; (40) Younger Joel; (41) Bojurova Eva; (42) Gritsevich Maria; (43) Theiler Laura; (44) Roggemans Adriana; (45) Sutherland Paul; (46) Dubs Martin; (47) Brando Gaetano; (48) Bastiaens Luc; (49) Sánchez de Miguel Alejandro; (50) Weatherley Gillian; (51) Currie Malcolm; (52) Barbieri Lorenzo; (53) Bettonvil Eduard; (54) Ibhi Abderrahmane; (55) Popescu Miruna; (56) Spurný Pavel; (57) Steyaert Chris; (58) Gyssens Marc; (59) Polfliet Tim; (60) Hillestad Trond Erik; (61) Weiland Thomas; (62) Hillestad Eli Fugelsoe; (63) Polakowski Krzysztof; (64) Koschny Gabi; (65) Nijland

Jos; (66) Koschny Detlef; (67) Verbeeck Cis; (68) Shrbený Lukáš; (69) Knöfel André; (70) Gährken Bernd; (71) Bettonvil Felix; (72) Theiler Carina; (73) Molau Sirko; (74) Zigo Pavol; (75) O'Connell Michael; (76) Slagter Daan; (77) Skunca Gordan; (78) Gostinski David; (79) Calders Stijn; (80) Georgescu Tudor; (81) Verbert Jan; (82) Georgescu Ana; (83) Hajduková Mária; (84) Żołądek Przemysław; (85) Ott Theresa; (86) Jacobs Lars; (87) Drolshagen Esther; (88) Solovaya Nina; (89) Guliyev Ayyub; (90) Gardiol Daniele; (91) Schenker Jonas; (92) Kac Javor; (93) Colas Francois; (94) Ocaña González Francisco; (95) Lesanu Cezar; (96) Klemt Bernd; (97) Schmidt Irmgard; (98) Fujiwara Yasunori; (99) Yamamoto Masa-yuki; (100) Wiśniewski Mariusz; (101) Koelers Selma; (102) Nogami Nagatoshi; (103) Mizumoto Satoshi; (104) Markham Tony; (105) Schmidt Hans-Georg; (106) Hartman Joost; (107) Vida Denis; (108) Skokić Ivica; (109) Biondić Jakov; (110) Biondić Damir; (111) Novoselnik Filip; (112) Malarić Mirjana; (113) Stewart Peter; (114) Kurtović Goran; (115) Kero Johan; (116) Kastinen Daniel; (117) Jenniskens Peter; (118) Albin Thomas; (119) Madkour Waleed; (120) Keeris Roy; (121) IJland Elise; (122) Neijts Marc; (123) Korec Matej; (124) Argo Megan; (125) Asher David; (126) Hristova Simona; (127) Abe Shinsuke; (128) Grašić Ljubica; (129) Pavlović Dušan; (130) Wrigley Nick; (131) Todorović Snežana; (132) Soja Rachel Halina; (133) Kartashova Anna; (134) Okolić Dragana; (135) Rudawska Regina; (136) Yancheva Yulia; (137) Bonino Donata; (138) Pittich Eduard; (139) Tóth Juraj; (140) Koukal Jakub; (141) Borovička Jiří.

Missing in the group photo: Abedin Abedin;. Bettonvil Uros; Çubuk Kerem Osman; De Queiroz José, Dolinský Peter; Haas Robert; Kokkeler Ben; Lamy Hervé; Nakane Sumio; Netjes Gert Jan; Ozeren Ferhat Fikri; Ryabova Galina; Shuttleworth Alan; ter Kuile Casper; Tomezzoli Giancarlo; Veljković Kristina and Zender Joe.

The group photo has been made by Casper ter Kuile.

Due to a lack of identification, the names of the photographers of some of the photographs included in these Proceedings could not be mentioned with each photo. We apologize for this.

Next year the IMC will be in Petnica, Serbia!

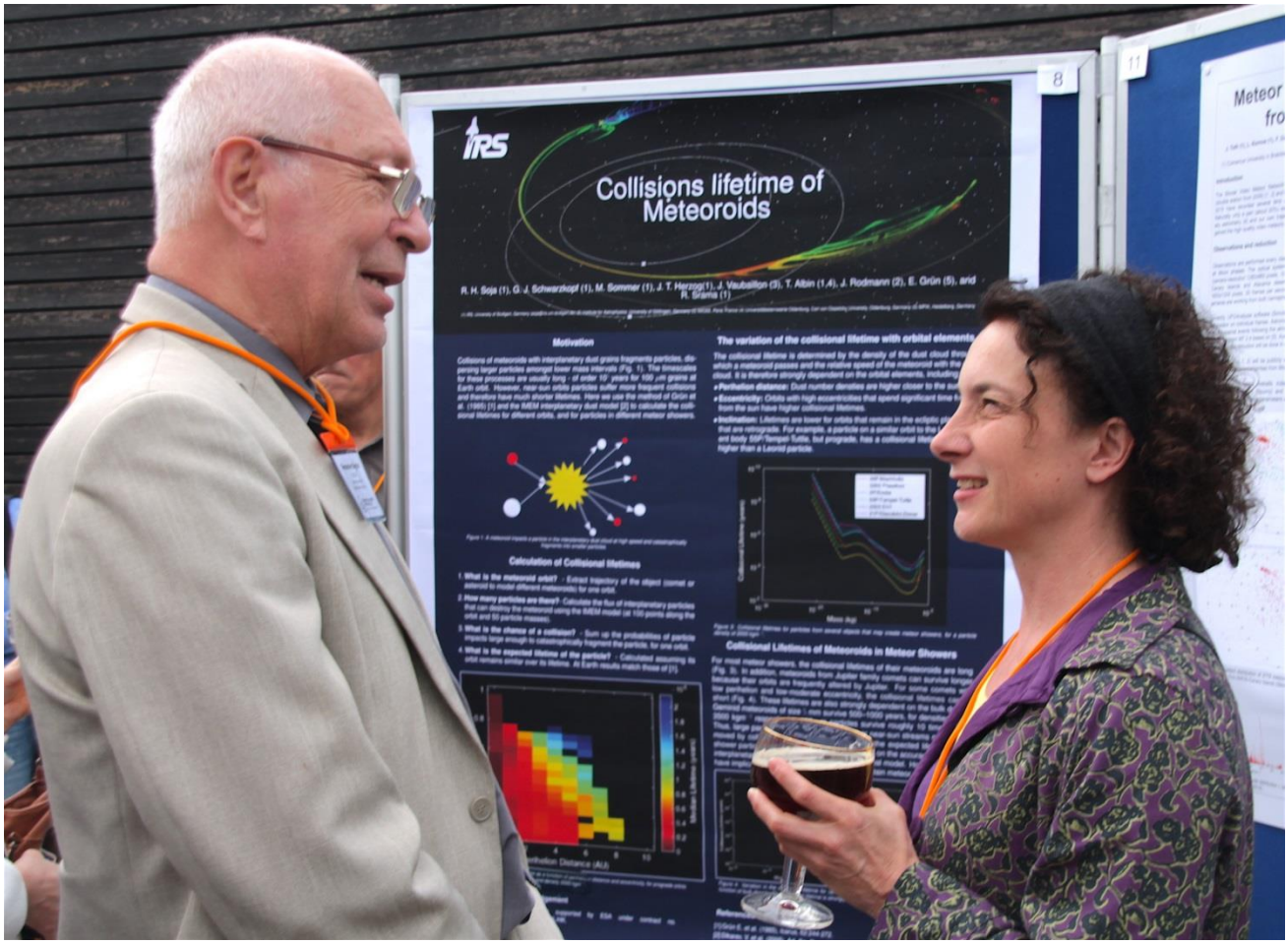

Alexander Bagrov and Maria Hajduckova at the poster session.

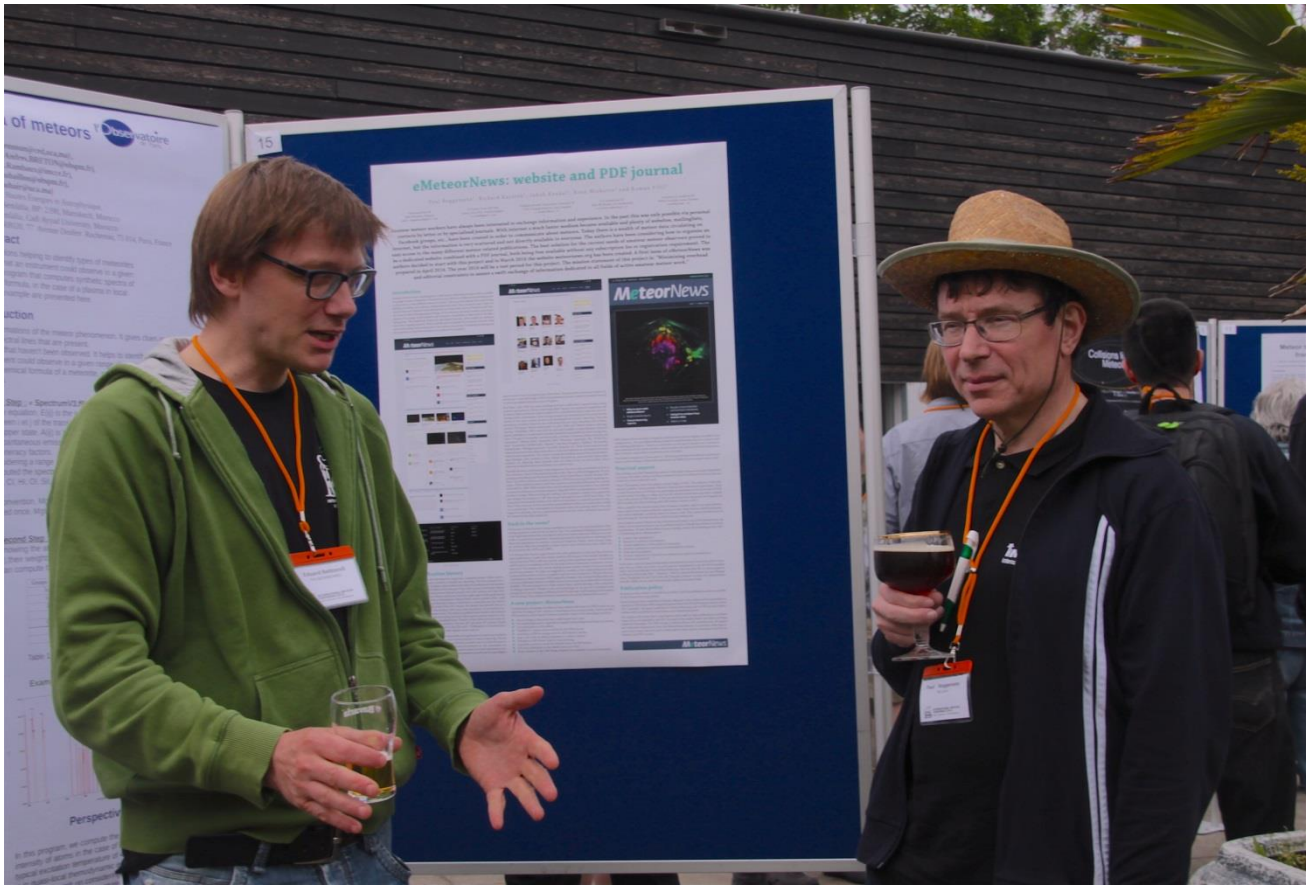

Eduard Bettonvil enthusiastically prizes his ideas on meteors to Paul Roggemans.

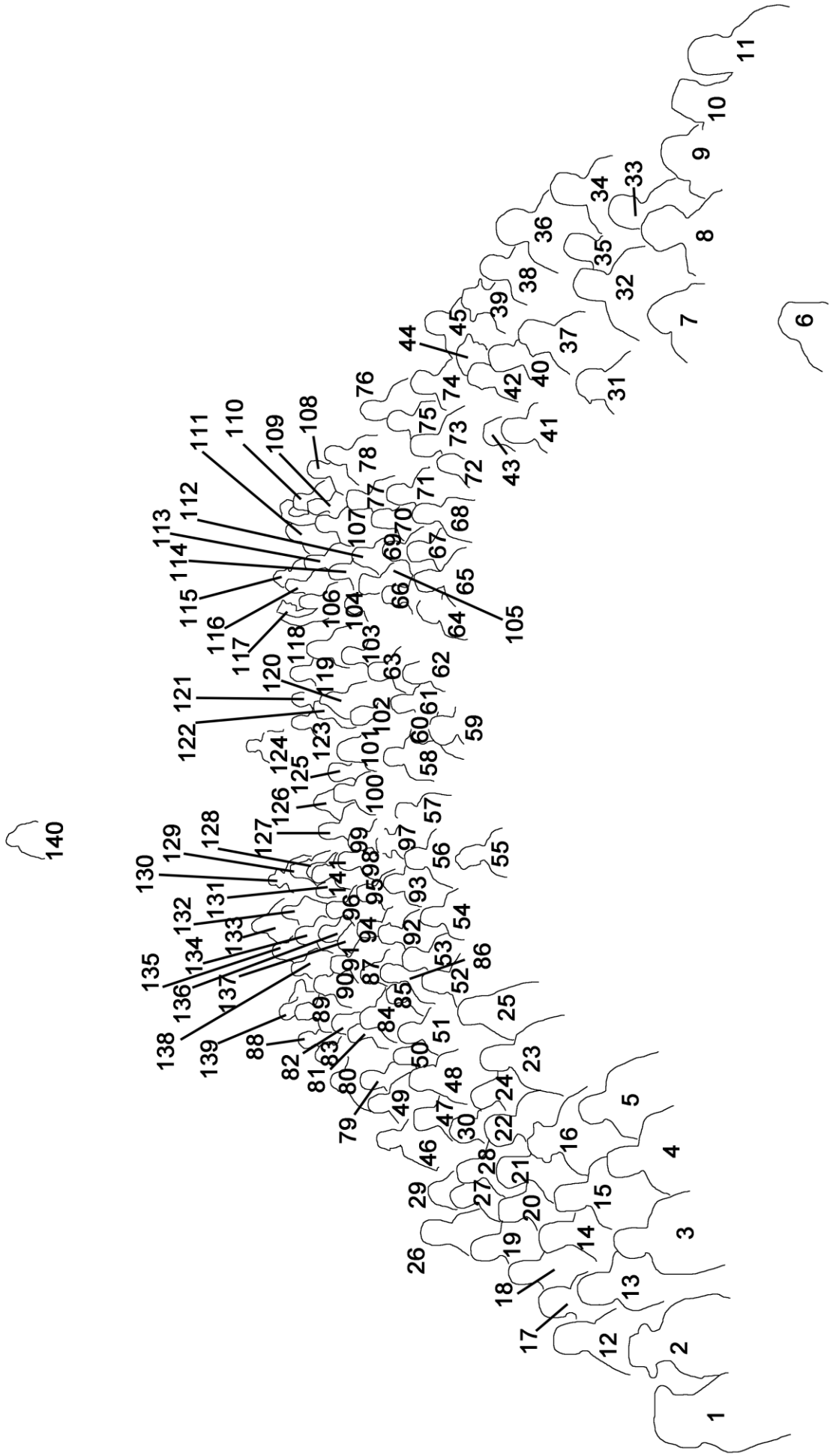
1
2
3
4
5
6
7
8
9
10
11
12
13
14
15
16
17
18
19
20
21
22
23
24
25
26
27
28
29
30
31
32
33
34
35
36
37
38
39
40
41
42
43
44
45
46
47
48
49
50
51
52
53
54
55
56
57
58
59
60
61
62
63
64
65
66
67
68
69
70
71
72
73
74
75
76
77
78
79
80
81
82
83
84
85
86
87
88
89
90
91
92
93
94
95
96
97
98
99
100
101
102
103
104
105
106
107
108
109
110
111
112
113
114
115
116
117
118
119
120
121
122
123
124
125
126
127
128
129
130
131
132
133
134
135
136
137
138
139
140
141

The girls from Petnica (Serbia) in a row: Ljubica Grašić, Debora Pavela, Snežana Todorović and Dragana Okolić.

Felix and Dušan Bettonvil: father and son, and as almost always both at the IMC.

The song of the IMC – 2016

- Jérémie Vaubaillon -

Don't ask me where is the IMC
I can't say the name but it's close to the sea
the crew is dressed all in orange
as a result they are a bit strange

(chorus)

You're very welcome,
You're very welcome to the IMC

At the bar I was doing so well
but someone ring me the Dutch bell
I had to talk about the stream
when all I wanted was to have a shrimp

(Chorus)

You're very welcome,
You're very welcome to the IMC

I was looking for the tulip
but all I found was a big ship
next to the bow we took a photo
and to the seagull we throw nemo

(Chorus)

You're very welcome,
You're very welcome to the IMC!
You're very welcome,
You're very welcome to the IMC!!!

Author index

Abe S. 17, 18
Abedin A. 19
Albin T. 20, 284
Anciaux M. 175
Andreić Ž. 270
Argo M. 305
Audureau Y. 55
Bagrov A.V. 148, 151
Barbieri L. 26, 291
Bęben M. 358
Benkhaldoun Z. 91
Bettonvil F. 6, 31
Birlan M. 55, 69
Birnbaum C. 55
Bland P.A. 60, 267, 275
Blanpain C. 55
Bojurova E. 348
Bolgova G. 120
Borovička J. 34, 53, 287, 333
Bouley S. 55
Brando G. 39
Breton M.-A. 91
Brown P. 19, 42, 171, 305
Buček M. 294
Calders S. 46, 175
Camargo J. 55
Caminade S. 55
Campbell-Brown 50
Čapek D. 53
Cellino A. 55, 76
Civiš S. 137
Close S. 171
Colas F. 55, 73
Cupák M. 60
Cupec R. 307
de Vet S. 56, 205, 222
Debattista V. 319
Delcourt J.-J. 235
Devillepoix H.A.R. 60
Di Martino M. 55, 76
Dimant Y. 171
Dolinský P. 63
Droldhagen E. 209
Dubs M. 65
Dumitru B.A. 69
Ďuriš F. 294
Efimov A. 202
Egal A. 55, 73
Ferrière L. 55
Ferus M. 137
Fietkiewicz K. 341
Fliegel K. 133
Fujiwara Y. 18, 167
Gajdoš S. 294
Gamby E. 175
Gardiol D. 55, 76
Gattacceca J. 55
Gawroński M.P. 341, 358
Georgescu A. 80
Georgescu. T. 80
Glazachev D. 120
Gorková S. 137
Gozdalski M. 341, 358
Grašić L. 83
Gritsevich M. 87, 159, 192, 197, 227, 230, 319, 330
Grokhovsky V. 319
Grün E. 284
Guennoun M. 91
Gulliyev A. 94
Gural P. 96, 307
Hajdukova M. jr. 105
Haloda J. 287
Hankey M. 111
Hartig B.A.D. 60
Hashiguchi H. 18
Howie R.M. 60
Hristova S. 348
Ibhi A. 127
Jansen-Sturgeon T. 60
Jenniskens P. 113
Jorda L. 55

Kaiserová T. 137
Kákona J. 114, 117
Kákona J. 319
Kalmančok D. 294, 297
Kaniansky S. 295
Kartashova A. 120
Kastinen D. 18, 123
Kero J. 18, 123, 288
Khiri F. 127
Knížek A. 137
Korlević K. 270
Kornoš L. 294
Koschny D. 20, 131, 209, 265
Koskinen J. 319
Koten P. 133, 333
Koukal J. 137
Krivonosova O. 330
Krzyżanowski T. 358
Kubelík P. 137
Kurtović G. 280
Kuznetsova D. 330
Kwon M.-K. 55, 73
Lamy H. 46, 143, 175
Lecubin J. 55
Lenža L. 137
Leonov V.A. 148, 151
Lesanu C.E. 80, 155
Licandro J. 294
Loizeau D. 55
Lyytinen E. 159, 192, 230
Maciejewski M. 341
Madkour W. 164, 179
Maeda K. 65, 167
Mahabal A. 319
Malgoyre A. 55
Maquet L. 55
Markkanen J. 227
Marmo C. 55, 73
Marqué C. 175
Marshall R.A. 171
Martínez Picar A. 46, 175, 305
Matlovič P. 297
Medjkane M. 127
Mickaelian A. 319
Milanović N. 83
Mizumoto S. 179
Molau S. 185, 305
Mönkölä S. 227, 319
Moreno-Ibáñez M. 192, 197, 230
Muinonen K. 227
Murphy D. 352
Murtazov A. 202
Myszkiewicz M. 341, 358
Nakamura T. 18
Näränen Y. 230
Nedelcu A. 69
Netjes G.J. 205
Nishizono T. 17
Nitschelm C. 55
Nojiri Y. 17
Okajima L. 17
Olech A. 298, 341, 358
Ott T. 209
Ouknine L. 127
Páta P. 133
Pavlović D. 83, 361
Paxman J. 60, 267
Pečnik B. 319
Peltoniemi J. 230, 319
Perez J.C. 294
Perlerin V. 111
Peterson C. 214
Pittich E. 217
Poerink U. 222
Pokorny P. 19
Polakowski K. 341
Popescu M. 55, 69
Popova O. 120
Poppe B. 20, 209
Poutanen M. 230
Räbinä J. 227
Raja-Halli A. 230
Rambaux N. 91
Ranvier S. 175
Rault J.-L. 55, 235
Reid I.M. 242, 352
Rendtel J. 247, 294, 305
Ridgewell J. 267
Rodmann J. 284
Roelandts T. 250
Roggemans P. 8, 254, 261
Rossi T. 227
Rotaru M. 55
Rudawska R. 265, 266, 297, 258

Rybnov Y. 120
Sahara H. 17
Saint-Gerant T. 127
Sansom E.K. 60, 267
Schwarzkopf G.J. 284
Šegon D. 270, 280, 307
Serra-Ricart M. 294
Shrbený L. 275, 287
Šimon J. 294
Škoda P. 319
Skokić I. 280
Soja R.H. 20, 284
Solovaya N. 217
Sommer M. 284
Spurný P. 275, 287, 333
Srama R. 20, 284
Srba J. 137
Srećković V. 319
Stempels E. 288
Stolarz M. 298, 341, 358
Štork R. 133, 333
Suchodolski T. 341, 358
Szabó G. 319
Tétard C. 143, 175
Todorović S. 361
Tomezzoli G. 291
Tóth J. 294, 295, 297
Towner M.C. 60
Trigo-Rodríguez J.M. 192, 197
Turchak L. 330
Turunen E. 319
Tymiński Z. 298, 341, 358
Vaduvescu O. 294
Valenzuela M. 55
Váňa P. 137
Vaubaillon J. 55, 73, 91, 284, 302
Veljković K. 304
Verbeeck C. 46, 175, 305
Vernazza P. 55
Vida D. 270, 307
Világi J. 294
Vinković D. 319
Vinnikov V. 330
Virtanen J. 230
Vítek S. 133
Vojáček V. 333
Watanabe J. 18
Watanabe T. 17
Węgrzyk W. 358
Weiland T. 338
Wiegert P. 19
Wiśniewski M. 298, 341, 358
Yamamoto M. 164, 179, 344
Yancheva Y. 348
Younger J. 242, 352
Zanda B. 55
Zender J. 265
Zhilenko D. 330
Zigo P. 294, 297
Zikmund T. 287
Živanović M. 361
Żołądek P. 298, 341, 358
Zubko N. 230
Zubović D. 307

ACKNOWLEDGEMENT TO SPONSORS

We are sincerely grateful to our Sponsors whose generous contributions helped greatly in organizing this IMC. The Local Organization Committee of the IMC along with the conference organizers, in particular acknowledge the following companies and organizations:

Thank you all!